Reverse cholesterol transport : a potential therapeutic target for atherosclerosis

Zhao, Y.

Reverse Cholesterol Transport

a potential therapeutic target for atherosclerosis

Ying Zhao

赵颖

ISBN: 978-90-8570-840-7

Printed by Wöhrmann Print Service – Zutphen

Reverse Cholesterol Transport

a potential therapeutic target for atherosclerosis

PROEFSCHRIFT

ter verkrijging van
de graad Doctor aan de Universiteit Leiden,
op gezag van de Rector Magnificus Prof. mr. P.F. van der Heijden,

volgens besluit van het College voor Promoties
te verdedigen op dinsdag 1 november 2011
klokke 15.00 uur

door

Ying Zhao

Geboren te Nanjing, P.R. China
in 1978

PROMOTIECOMMISSIE

Promotor:	Prof. Dr. Th.J.C. van Berkel
Co-promotor:	Dr. M. van Eck
Overige leden:	Prof. Dr. M. Danhof (Leiden/Amsterdam Center for Drug Research)
	Prof. Dr. M.J. Chapman (INSERM, Paris, France)
	Prof. L.M. Havekes (Leiden University Medical Center)
	Dr. J.A. Kuivenhoven (Academic Medical Center, Amsterdam)

The studies described in this thesis were performed at the Division of Biopharmaceutics, Leiden/Amsterdam Center for Drug Research, Leiden University.

The research described in this thesis was supported by a grant of the Dutch Heart Foundation (DHF-2011T4101).

Financial support by the Dutch Heart Foundation for the publication of this thesis is gratefully acknowledged.

The printing of this thesis was financially supported by:

Leiden/Amsterdam Center for Drug Research

J.E. Jurriaanse Stichting

TABLE OF CONTENTS

Abbreviations

Chapter 1 General introduction;

Chapter 2 Hypocholesterolemia, foam cell accumulation, but no atherosclerosis in mice lacking ABC-transporter A1 and scavenger receptor class B type I (*Atherosclerosis.* 2011, 218: 314-322)

Chapter 3 ABC-transporter A1 deficiency induces macrophage foam cell formation and leukocytosis but inhibits early atherosclerotic lesion development in scavenger receptor class B type I knockout mice

Chapter 4 Relative roles of various efflux pathways in net cholesterol efflux from macrophage foam cells in atherosclerotic lesions (*Curr. Opin. Lipidol.* 2010, 21: 441-453)

Chapter 5 Enhanced foam cell formation, atherosclerotic lesion development, and inflammation by combined deletion of ABC-transporter A1 and scavenger receptor class B type I in bone marrow-derived cells in LDL receptor knockout mice on Western-type diet (*Circ. Res.* 2010, 107: e20-31)

Chapter 6 Leukocyte ABC-transporter A1 and LDL receptor play independent roles in atherosclerosis: the potential contribution of T cells

Chapter 7 Leukocyte ABC-transporter A1 is atheroprotective in absence of apolipoprotein AI

Chapter 8 Stage-specific remodeling of atherosclerotic lesions upon cholesterol lowering in LDL receptor knockout mice (*Am. J. Pathol.* 2011, 179: 1522-32)

Chapter 9 The dynamics of macrophage infiltration into the arterial wall during atherosclerotic lesion development in LDL receptor knockout mice (*Am. J. Pathol.* 2011, 178:413-33)

Chapter 10 High-dose phosphatidylcholine particles mobilize free cholesterol and rapidly stabilize initial and advanced atherosclerotic lesions

Chapter 11 Summaries and perspectives

Curriculum Vitae

Publications

ABBREVIATIONS

RCT: reverse cholesterol transport
ABC: ATP-binding cassette
ABCA1: ABC-transporter A1
SR-BI: scavenger receptor class B type 1
ABCG1: ABC-transporter G1
VLDL: very low-density lipoprotein
LDL: low-density lipoprotein
Ox-LDL: oxidized LDL
Ac-LDL: acetylated LDL
HDL: high-density lipoprotein
apoAI: apolipoprotein AI
apoE: apolipoprotein E
PC: phosphatidylcholine
LDLr: LDL receptor
LRP-1: LDL-related protein 1
WT: wild-type
KO: knockout
-/-: KO
dKO: double KO
BMT: bone marrow transplantation
WTD: Western-type diet
ATD: atherogenic diet
FC: free cholesterol
TC: total cholesterol
CE: cholesteryl ester
TG: triglycerides
PL: phospholipids
ID: injected dose
MCP-1: monocyte chemotactic protein-1
ICAM-1: inter-cellular adhesion molecule 1
KC: keratinocyte-derived chemokine
IL-12: interleukin 12
α-NT: α-nitrotyrosine
8-OHdG: α-8-hydroxy-2'-deoxyguanosine
LXR: liver X receptor
SREBP: sterol regulatory element binding protein

CHAPTER 1

General Introduction

1.1 Lipoproteins, Lipoprotein receptors, and lipid metabolism

1.2 Atherosclerosis

1.3 ABCA1 and atherosclerosis: cholesterol homeostasis, reverse cholesterol transport, and inflammation

1.4 SR-BI and atherosclerosis: beyond HDL metabolism

1.5 Macrophage reverse cholesterol transport: potential therapeutic target for atherosclerosis

1.6 Outline of the thesis

1.7 References

1.1 Lipoproteins, Lipoprotein receptors, and lipid metabolism

1.1.1 Lipoproteins

Lipoproteins are macromolecular complexes of lipids and proteins that are essential for the transport of cholesterol, triglycerides (TG), and fat-soluble vitamins in the blood. Lipoproteins are composed of a hydrophobic lipid core containing triglycerides (TG) and cholesteryl esters (CE) surrounded by an amphipatic monolayer of phospholipids (PL), free cholesterol (FC), and specific proteins (Figure 1). Proteins associated with lipoproteins, called apolipoproteins, are required for the assembly, structure, and the function of lipoproteins. Apolipoproteins activate enzymes important in lipid metabolism and act as ligands for cell surface receptors (Table 1). Based on the relative densities of the lipoproteins upon density-gradient ultracentrifugation, five major classes of lipoproteins can be distinguished, including chylomicrons (CM), very-low-density lipoproteins (VLDL), intermediate-density lipoproteins (IDL), low-density lipoproteins (LDL), and high-density lipoproteins (HDL) [4]. CM and VLDL are the major carriers of TG in the blood, while plasma cholesterol is mainly transported as CE in LDL and HDL. As shown in Table 2, each lipoprotein class comprises a family of particles that vary slightly in density, size, electrophoretic mobility, and protein composition. Generally, HDL can be classified into lipid-poor discoidal nascent pre-β HDL and lipid-rich spherical mature α-HDL, based on their difference in electrophoretic mobility [5]. Preβ-HDL contains mainly apoAI and phospholipids with small amounts of cholesterol. Preβ-HDL has been resolved into $preβ_1$, $preβ_2$, and $preβ_3$ HDL particles according to increasing size by two-dimensional gel electrophoresis [5]. α-HDL encompasses two main density classes, namely large cholesteryl ester (CE) -rich HDL_2 (d: 1.063-1.125g/mL) and small CE-poor HDL_3 (d: 1.125-1.21 g/mL). They can be further subdivided by increasing size into HDL_{3c}, $_{3b}$, $_{3a}$ and HDL_{2a}, $_{2b}$ [5]. The heterogeneity in lipoprotein size and composition induces changes in interaction with different tissues, thereby influencing lipoprotein metabolism.

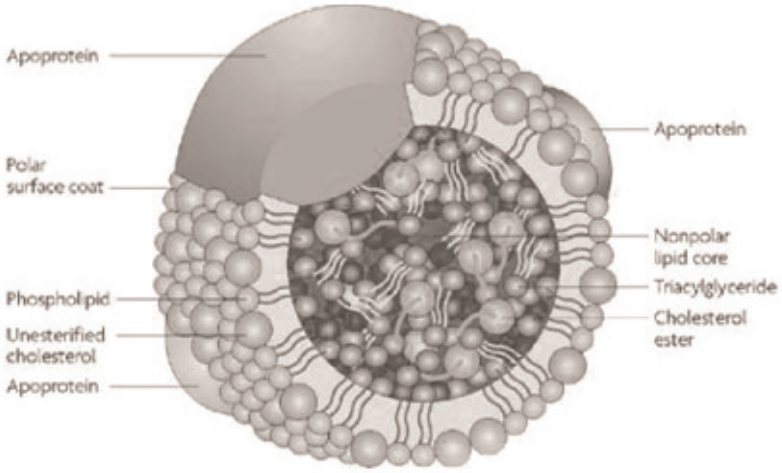

Figure 1. Molecular compositions of lipoprotein. See text for explanation. Adapted from Wasan *et al.* [3]

Table 1. The function of apolipoproteins.

Apolipo-protein	Source	Lipoprotein association	Function
ApoAI	Intestine, liver	CM, HDL	Structure protein for HDL Activation of LCAT [6]
ApoAII	Liver	CM, HDL	Structure protein for HDL Enhancement of HL activity [7]
ApoAIV	Intestine	CM, HDL	TG-rich lipoprotein/HDL metabolism Facilitation of CETP activity [8]
ApoAV	Liver	CM, VLDL	Promotion of LPL-mediated TG lipolysis [9]
ApoB48	Intestine, Liver*	CM	Structure protein for CM [7]
ApoB100	Liver	VLDL, IDL, LDL, Lp(a)	Structure protein for VLDL, IDL, LDL, Lp(a) Ligand for binding to LDL receptor [10]
ApoCI	Liver	CM, VLDL, HDL	Activation of LCAT [11], inhibition of CETP [12], HL [13], and SR-BI [14], inhibition of remnant uptake [13]
ApoCII	Liver	CM, VLDL, HDL	Cofactor for LPL [15]
ApoCIII	Liver	CM, VLDL, HDL	Inhibition of LPL [16], inhibition of remnant uptake [17]
ApoD	Spleen, brain, testes, adrenals	HDL	Transport of multiple ligands, including arachidonic acid, progesterone, and phosphorylated MAPK [18, 19]
ApoE	Liver	CM remnants, IDL, HDL	Ligand for binding to LDL receptor and LRP1 [20]
ApoH	Liver	CM, VLDL, LDL, HDL	Antigen target for antiphospholipid antibody [21]
ApoJ	Liver	HDL	Binding and transport of Aβ [22]
ApoL	Liver	HDL	Unknown [23]
ApoM	Liver	HDL	Formation of preβ HDL [24]
Apo(a)	Liver	Lp(a)	Unknown [25]

Abbreviations: CM, chylomicron; VLDL, very-low-density lipoprotein; IDL, intermediate-density lipoprotein; LDL, low-density lipoprotein; HDL, high-density lipoprotein; LCAT, lectin-cholesterol acyltransferase; HL, hepatic lipase; CETP, cholesterol ester transfer protein; SR-BI, scavenger receptor BI; LPL, lipoprotein lipase; MAPK, mitogen-activated protein kinase; LRP, LDL receptor-related protein; Aβ, amyloid beta. *: only for mice and rat, not for human

Table 2. Physical properties and composition of human plasma lipoproteins [4].

	CM	VLDL	IDL	LDL	HDL
Density (g/mL)	<0.95	0.95-1.006	1.006-1.019	1.019-1.063	1.063-1.210
Diameter (nm)	75-1200	30-80	25-35	18-25	5-12
Mw (x 10^6 Da)	400	10-80	5-10	2.3	0.17-0.36
Mobility*	origin	Pre-β	Pre-β/β	β	Pre-β/α
Lipid composition (weight%)					
TG	80-95	55-80	20-50	5-15	5-10
Total cholesterol	2-7	5-15	20-40	40-50	15-25
PL	3-9	10-20	15-25	20-25	20-30
Apolipoproteins	A-I, A-II, A-IV, B48 C-I, C-II, C-III E	- B100 C-I, C-II, C-III E	- B100 C-I, C-II, C-III E	- B100 - -	A-I, A-II, A-IV, - C-I, C-II, C-III E

* According to the mobility of plasma α- and β-globulin on agarose gel electrophoresis.

1.1.2 Lipoprotein receptors

Lipoprotein receptors play a crucial role in lipid metabolism. The main lipoprotein receptors include the LDL receptor (LDLr), LDLr-related protein 1 (LRP1), VLDL receptor (VLDLr), and several types of scavenger receptors. With respect to the scope of this thesis, the roles of the LDL receptor, LRP1, and scavenger receptor class B type I (SR-BI) in lipoprotein metabolism will be discussed in more detail in the following paragraphs.

1.1.2.1 Low-density lipoprotein receptor

The LDL receptor is a membrane-spanning glycoprotein containing five functional domains: the ligand-binding domain, the epidermal growth factor (EGF) repeats domain, the O-linked polysaccharide domain, the transmembrane domain, and the cytoplasmic domain [26, 27] (Figure 2). The LDL receptor is expressed in most mammalian cells, including lymphocytes and macrophages [28, 29]. The highest expression level is found in the liver and the adrenals [30, 31], where the LDL receptor is involved in lipid metabolism and hormone production.

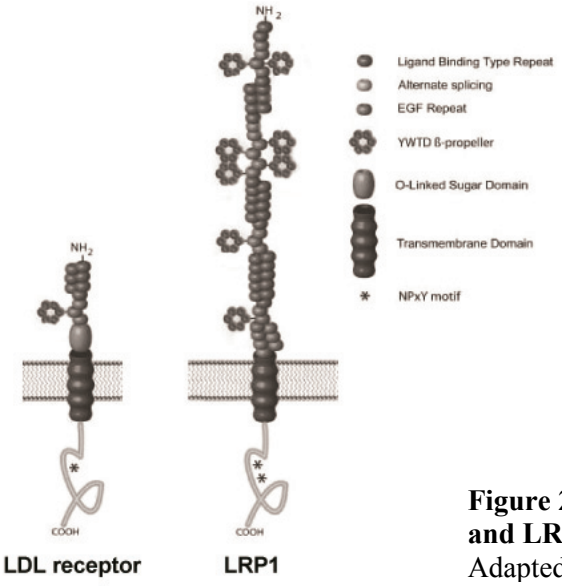

Figure 2 Structure of LDL receptor and LRP1. See text for explanation. Adapted from Rebeck *et al*. [1]

Regulation of the LDL receptor expression

The expression of the LDL receptor gene is under complex regulation at both transcriptional and posttranscriptional levels via a variety of signaling pathways. Cholesterol and cholesterol derivatives, and nonsterol mediators, like cytokines, growth factors, and some hormones, are able to regulate LDL receptor expression [32, 33]. The sterol regulatory element-binding protein (SREBP) pathway is crucial for the transcriptional regulation of LDL receptor gene expression by cholesterol and its derivatives [34]. In mammalian cells, there are three types of SREBP, namely SREBP-1a, SREBP-1c, and SREBP-2. Among them, SREBP-2 is the major activator of the LDL receptor gene [35]. SREBPs are synthesized as inactive precursors in the endoplasmic reticulum (ER) [36]. The SREBP precursor needs the escort of another ER membrane protein named SREBP cleavage-activating protein (SCAP) to get to the Golgi apparatus for cleavage [37]. The cleavage of the SREBP precursor results in the release of nuclear SREBP, which enters the nucleus and activates transcription. When cholesterol or its derivatives are abundant in

cells, cholesterol can bind to SCAP and inhibit the dissociation of SCAP from a pair of ER membrane proteins named insulin-induced genes (Insig) 1 and 2, thereby trapping SREBP/SCAP in the ER and suppressing the SREBP-mediated transcription of the LDL receptor [38-42]. On the contrary, when cells lack sterols, SCAP does not interact with the Insig proteins and the SREBP/SCAP complex is free to reach the Golgi apparatus for the generation of nSREBP. Statins, inhibitors of 3-hydroxy-3-methylglutaryl coenzyme A (HMG-CoA) reductase, upregulate the expression of the LDL receptor via the SREBP pathway secondary to shutting down cholesterol biosynthesis [43]. Furthermore, activation of extracellular signal-regulated kinase (ERK) is also crucial for the expression of LDL receptor. ERK activation induces the transcription of the LDL receptor through nSREBP [44] and/or transcriptional factor Egr1 and c/EBPβ [45]. A number of cytokines, such as tumor factor (TNF) α, interleukin (IL)-1, IL-6, and oncostatin M (OM) are able to activate the transcription of the LDL receptor gene in hepatocytes via activation of ERK [46]. Interestingly, inflammation disrupts the cholesterol-sensitive feedback regulation of LDL receptor and cause statin resistance [47].

Mechanisms for post-translational modulation of LDL receptor expression include proprotein convertase subtilisin/kexin type 9 (PCSK9) [48] and the E3 ubiquitin ligase Idol [49]. PCSK9 is a secreted protein predominantly expressed in the liver, small intestine, and kidney [50]. In plasma, PCSK9 directly binds to the EGF-A extracellular domain of the LDL receptor in the liver [51, 52]. This binding and the subsequent internalization of the PCSK9-LDL receptor complex lead to the intracellular degradation of LDL receptor in lysosomes. In humans, gain-of-function mutations in PCSK9 result in autosomal hypercholesterolemia [53]. On the contrary, loss-of-function mutations within PCSK9 are associated with a reduction in plasma LDL cholesterol levels [54, 55]. Interestingly, PCSK9 is also a target gene of SREBPs [56]. In line, statins induce the expression of PCSK9. However, activation of janus kinase1 (JAK1), JAK2, and the downstream ERK suppresses the expression of PCSK9 [57]. In contrast, Idol triggers ubiquitination of the LDL receptor on conserved residues in its intracellular tail, leading to degradation of the receptor [49]. Consistent with this mechanism, overexpression of Idol effectively inhibits LDL uptake by downregulation of the LDL receptor protein levels in vitro and in vivo. Conversely, knockdown of Idol results in an increase in LDL receptor expression and LDL uptake. Of note, Idol is a transcriptional target of liver X receptors (LXR) but not regulated by SREBPs.

LDL receptor function in lipid metabolism and cellular cholesterol homeostasis

LDL receptors on the cell surface bind and take up apoB- and/or apoE-containing lipoproteins (especially LDL). Seven cysteine-rich repeats (R1-R7) (Figure 2), the so-called LDL receptor class A (LA) repeats at the amino-terminal end of the receptor are responsible for binding to apoB and apoE in lipoproteins [26]. Whereas binding of apoB-100 in LDL depends on the presence of R3-R7, only R5 appears essential for interaction with apoE in VLDL [58, 59]. After endocytosis, the LDL receptor uncouples from its ligand and returns to the cell surface for recycling, while the LDL particle undergoes further metabolism [60].

In the liver the LDL receptor is crucial for clearance of LDL from the circulation. In humans, the hepatic LDL receptor accounts for more than 70% of the total LDL clearance from plasma [61]. Thus, LDL receptor gene mutations often result in highly increased LDL-cholesterol levels in the circulation, a disease called familial hypercholesterolemia (FH) [62]. The binding of apoB-100 to the LDL receptor is required for clearance of LDL. Naturally occurring mutants of apoB-100, including R3500Q, R3840W,

and W4369Y, have been unequivocally linked to defective LDL receptor binding and hypercholesterolemia [63]. In addition, endocytosis is also required for the clearance of LDL [64]. ARH1, an adaptor protein is required for internalization. Mutations in ARH1 lead to a rare autosomal recessive form of hypercholesterolemia (ARH) [65]. Importantly, retroviral expression of normal human ARH1 rescues LDL receptor internalization in cells from patients with ARH [66].

Uptake of LDL via the LDL receptor is an important pathway in supplying peripheral cells with cholesterol, which is required for the buildup and maintenance of membranes and the synthesis of biomolecules such as bile salts, vitamin D and the steroid hormones. However, excessive intracellular cholesterol accumulation inhibits the synthesis of the LDL receptor. This leads to the limited contribution of the macrophage LDL receptor to foam cell formation and atherogenesis [67, 68].

1.1.2.2 Low-density lipoprotein receptor-related protein 1

LRP1 is the largest receptor of the LDL receptor family. The modular structures within LRP1 include cysteine-rich ligand-binding domain, EGF repeats, β-propeller domains, a transmembrane domain, and a cytoplasmic domain [69] (Figure 2). Although LRP1 is structurally related to the LDL receptor, the function of LRP1 is more complex than the LDL receptor. LRP1 interacts with a number of functional diverse ligands, including apoE-enriched lipoproteins, lipoprotein lipase (LPL), α2-macroglobulin-protease complexes [70]. Also LRP1 can engage a variety of adaptor molecules in endocytosis, phagocytosis, and cell signaling via its cytoplasmic domain [71]. LRP1 is expressed in various mammalian cell types, most highly in hepatocytes, neurons and fibroblasts [69, 72]. Studies using mice in which LRP1 is selectively disrupted in neurons [73], hepatocytes [74], adipocytes [75], vascular smooth muscle cells [76], and macrophages [77, 78] have revealed tissue-specific functions of LRP1 and their roles in the pathogenesis of Alzheimer's disease, hypercholesterolemia, atherosclerosis, and inflammation.

Regulation of LRP1 expression

Biosynthesis and maturation of LRP1 involves interaction with receptor-associated protein (RAP) and proteolytic processing into two receptor subunits. RAP is a molecular chaperone that is required for the proper folding and export of receptors from ER to the Golgi apparatus. Interaction with RAP also prevents premature association of LRP1 with ligands, ER retention, and subsequent degradation [79, 80]. RAP deficiency thus results in intracellular accumulation and degradation of most of the synthesized LRP1 molecules [80]. In the post-Golgi secretary compartment, furin, a proprotein-converting enzyme cleaves a 600 kDa precursor protein into two subunits, namely a 515 kDa N-terminal subunit and an 85 kDa C-terminal subunit [81, 82]. Interestingly, studies using furin deficient cells indicate that the proteolytic processing of the LRP1 precursor is not required for transport of the receptor to the cell surface but may increase its endocytic activity [81].

So far, the understanding of the regulation of LRP1 is still limited. Studies on the sequence and structure of the promoter region of LRP1 isolated from blood leukocytes indicate that it has no sterol regulatory element [83]. However, at the transcriptional level, SREBPs do downregulate the expression of LRP1 in smooth muscle cells and macrophages after incubation with normal LDL or aggregated LDL [84-87]. LRP1 is thus distinct from the LDL receptor in response to cholesterol loading. Also the proinflammatory cytokine interferon γ (IFNγ) dose-dependently decreases LRP1 mRNA and protein expression in

RAW 264.7, a macrophage cell line [88]. In contrast, transforming growth factor-β1 (TGFβ1) has no effect on LRP1 expression. However, pretreatment of TGFβ1 does rescue the LRP1 expression that is suppressed by IFNγ [88]. In addition, insulin affects the expression of LRP1 largely at post-translational level. It stimulates recycling of LRP1 in 3T3-L1 adipocytes from an endosomal pool to the plasma membrane in a PI3K-dependent manner [89, 90]. However, in J774 macrophages, insulin induces a significant reduction in the LRP1 protein content by activation of the proteasomal system [91].

LRP1 Function in lipid metabolism and cellular cholesterol homeostasis

When LRP1 was originally identified, its structural similarity to the LDL receptor and its expression in the liver suggested a role in lipoprotein metabolism. LRP1 binds apoE-rich βVLDL [92, 93] and chylomicron remnants [94] *in vitro*. However, no accumulation of remnant lipoproteins is evident in the circulation of wild-type mice with selective disruption of hepatic LRP1 [74]. Interestingly, liver-specific inactivation of LRP1 in LDL receptor knockout mice does lead to the accumulation of remnant lipoproteins in the circulation [74]. The function of LRP1 in hepatic remnant metabolism is thus in concert with the LDL receptor. In addition, as LRP1 binds apoE, lipoprotein lipase (LPL), and hepatic lipase (HL), which facilitate the uptake of CE of HDL by the liver [95-97], LRP1 is also implicated in HDL metabolism.

In addition, it participates in the uptake of matrix-retained LDL and aggregated LDL by macrophages [98] and smooth muscle cells [99, 100]. Importantly, LRP1 also promotes the translocation of 12/15 lipoxygenase (LO) from the cytosol to the plasma membrane [101] and thereby facilitates LDL oxidation [102] in J774A.1 macrophages. Overproduction of oxidized LDL can subsequently lead to macrophage foam cell formation [103]. In adipocytes and neurons, the expression of LRP1 regulates cellular cholesterol levels primarily via uptake of apoE-containing lipoproteins [104, 105]. In addition, the deletion of LRP1 is associated with downregulation of the ABC transporter A1 (ABCA1) expression, which might subsequently affect intracellular cholesterol trafficking and cellular cholesterol efflux [106].

1.1.2.3 Scavenger receptor BI

Scavenger receptors, first described by Brown and Goldstein [107, 108], are membrane glycoproteins that are involved in the cellular uptake of a broad range of polyanionic ligands including modified lipoproteins, collagen, apoptotic cells, and bacterial components. Scavenger receptors thus play important roles in foam cell formation, atherosclerosis, adhesion, and inflammation [109, 110]. Table 3 summarizes the different types of scavenger receptors identified and their respective ligands.

The scavenger receptor class B type I (SR-BI), a member of the CD36 superfamily, is a 82 kDa cell surface glycoprotein comprising two transmembrane and two cytoplasmic domains as well as a large extracellular loop with several N-glycosylation sites [111] (Figure 3). SR-BI is expressed in various mammalian tissues and cells, including brain, kidney, intestine, heart, placenta, macrophages, endothelial cells, smooth muscle cells, and various epithelial cells [112]. The highest expression of SR-BI, however, is in organs with critical roles in cholesterol metabolism (liver) and steroidogenesis (adrenal, ovary, testis) [113]. It is the first molecularly well defined receptor for HDL.

Table 3: Major ligands of scavenger receptors [109, 122, 123]

Scavenger receptor		Lipid and lipoprotein ligands							Other ligands
		FC	FA	LDL	HDL	oxLDL	acLDL	agLDL	
A	SR-A I/II					+	+	+	AP, LPS, bacteria
	MARCO					+	+		LPS, LTA, bacteria
B	CD36		+		+	+	+		collagen, erythrocytes, AP, bacteria
	SR-BI	+	+	+	+	+	+		AP, hepatitic C virus
C	dSR-C1						+		
D	Macrosialin					+	+		
	CD68					+	+		AP
E	LOX-1					+			
F	SREC					+	+	+	calreticulin, avillin
N*	SR-PSOX					+			bacteria
	CD163								hemoglobin, bacteria
	CL-P1								bacteria
	FEEL-1						+		AGE-modified proteins, bacteria
	FEEL-2						+		AGE-modified proteins, bacteria
	SCARA5								bacteria

Abbreviation: FC: free cholesterol, FA: fatty acid, oxLDL: oxidized LDL, acLDL: acetylated LDL, agLDL: aggregated LDL, LPS: lipopolysaccharide, LTA: lipoteichoic acid, AP: apoptotic cells, AGE: advanced glycation end-products.
*newly identified scavenger receptors capable of specifically binding modified LDL in non-macrophage cell types

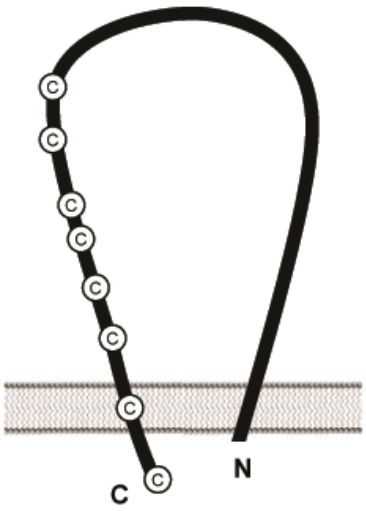

Figure 3. Structure of SR-BI. See text for explanation. Adapted from Krieger *et al.* [2]. ©: cysteine.

Regulation of SR-BI expression

The transcription of SR-BI can be regulated by SREBPs [114, 115], steroidogenic factor-1 (SF-1) [114, 116], liver receptor homolog 1 (LRH-1) [117], and the peroxisome proliferator-activated receptor-α (PPAR-α) [118-120]. The stability of SR-BI proteins is modulated by Ras/mitogen-activated protein kinase (MAPK) [121]. Interestingly, SR-BI is regulated differently in liver

and in steroidogenic tissues. Overexpression of SREBP1a downregulates the transcription of hepatic SR-BI but induces its expression in ovaries [114, 115]. Moreover, fibrates, PPAR-α agonists, reduce SR-BI in liver while they upregulate SR-BI in macrophages and have no effect on SR-BI in adrenals [118-120]. Of note, the expression of SR-BI is also regulated differently in different types of cells at post-translational level. In hepatocytes as well as epithelial cells of the intestine, an adaptor protein, PDZK1 is essential for the expression of SR-BI on the cell surface as PDZK1 KO mice showed a ~95% and ~50% reduction in the protein levels of SR-BI in the liver and the small intestine, respectively [124]. Also atherogenic diet-induced downregulation of SR-BI protein expression in the liver and intestine is associated with a reduction of PDZK1 [115]. Interestingly, in PDZK1 KO mice, the expression of SR-BI in adrenals and macrophages is unchanged [124]. Moreover, small PDZK1-associated protein (SAAP) decreases PDZK1 in a liver-specific fashion, thereby resulting in downregulation of hepatic SR-BI, but again has no effect on the levels of SR-BI in the adrenals or peritoneal macrophages [125]. All these findings indicate that SR-BI is regulated in a cell type specific fashion.

SR-BI Functions in lipid metabolism and cellular cholesterol metabolism

Evidence for the physiological importance of SR-BI in HDL metabolism was obtained from studies in genetically engineered mice. Hepatic overexpression of SR-BI increased the selective uptake of HDL-CE by liver [126, 127], resulting in the virtual absence of plasma HDL-C [128, 129]. On the contrary, impaired hepatic uptake of HDL-CE in mice with attenuated expression of SR-BI expression or complete SR-BI deficiency led to the accumulation of abnormally large HDL particles and increased plasma HDL-C levels [130-132]. In humans, a clear association between mutations in the coding and promoter regions of human SR-BI and increased plasma HDL-C has been shown in several populations [133-135]. Recent genome-wide association studies (GWAS) also demonstrated that single nucleotide polymorphism (SNPs) in and near SR-BI are significantly associated with plasma levels of HDL-C in humans [136]. However, only very recently conclusive evidence was provided by Vergeer *et al* on the importance of SR-BI in controlling HDL cholesterol levels in humans. They identified a family in which heterozygous carriers of a unique mutation (P297S) in the extracellular domain of SR-BI showed a 37% elevation in plasma HDL-C levels. Importantly, hepatocytes that expressed the P297S mutant SR-BI displayed a reduced capacity to take up HDL-CE, thereby explaining the observed increase in HDL-C in the circulation in carriers of the mutant SR-BI [137]. By comparing the uptake of HDL-CE with holo-particle uptake in SR-BI knockout (KO) mice and wild-type (WT) mice, SR-BI is identified as the sole molecule responsible for the selective uptake of CEs from HDL in mice [138, 139]. The extracellular domain of SR-BI and the proper orientation of apoAI molecules on the HDL particles are crucial for efficient lipid uptake via SR-BI [140-145]. The selective uptake of HDL-CE is considered as a two-step process: the first step is the binding of the lipoprotein to the extracellular domain of SR-BI, followed by internalization of its CEs without net internalization and degradation of the lipoprotein itself [146]. Moreover, HDL binding and CE uptake are independent processes [140, 147]. High affinity HDL binding to SR-BI is not sufficient for efficient HDL-CE selective uptake [148, 149]. Interestingly, SR-BI reconstituted into liposomes is still capable to avidly bind lipoproteins and selectively take up CEs, indicating that specific cellular structures and compartments are not required for SR-BI-mediated HDL-CEs uptake [150]. In addition, several recent studies have indicated that a so-called retro-endocytosis pathway involving holo-particle uptake of HDL followed by re-secretion of CE-poor HDL could also contribute to the selective uptake of HDL-CE via SR-BI [151, 152]. Upon selective uptake via SR-BI, HDL-CEs

are delivered into an extra-lysosomal metabolically active membrane pool and subsequently hydrolyzed by neutral cholesteryl ester hydrolase [153-155], which is different from LDL-CEs which are hydrolyzed in the lysosomes by acidic cholesteryl ester hydrolase after endocytosis via LDL receptor [156, 157].

SR-BI has also been implicated in the metabolism of apoB-containing lipoproteins, including LDL and VLDL. Wiersma et al demonstrated that the expression level of hepatic SR-BI is correlated with the production rate of VLDL by affecting the hepatic cholesterol content and the activity of microsomal triglyceride transfer protein (MTP) [158]. Moreover, *in-vitro* studies clearly demonstrated that SR-BI binds apoB lipoproteins and facilitates the subsequent uptake of cholesterol from these lipoproteins [159-163]. *In vivo*, SR-BI attenuation or deficiency led to increased VLDL and LDL cholesterol levels in WT [162], LDL receptor KO [164], and apoE KO mice [132], while mice overexpressing SR-BI displayed reduced levels of apoB-containing lipoproteins [126, 129, 165]. In addition, SR-BI is also involved in chylomicron metabolism as evidenced by higher postprandial TG levels in the plasma of SR-BI KO mice and reduced association of chylomicron-like emulsion particles to freshly isolated hepatocytes lacking SR-BI [166]. Béaslas et al recently demonstrated that postprandial micelles supplied to Caco2/TC7 enterocytes induced the clustering of SR-BI at the apical brush border membrane and movement from non-raft to raft domains [167]. Importantly, competition, inhibition, or knockdown of SR-BI impairs the trafficking of apoB from apical towards secretory domains, indicating the involvement of SR-BI in the secretion of intestinal TG-rich lipoproteins [167]. Moreover, overexpression of intestinal SR-BI results in accelerated lipid absorption [168]. Several studies on common polymorphisms of CLA-1, the human homologue of SR-BI, also suggested its role in the metabolism of apoB lipoproteins [133, 169-171] and postprandial lipoproteins in humans [172].

The role of SR-BI in cellular cholesterol homeostasis is complex. Apart from selective uptake of CEs from HDL, like CD36, SR-BI binds modified lipoproteins and mediates their uptake by macrophages [173, 174][. Also SR-BI stimulates the bi-directional flux of free cholesterol (FC) between cells and mature HDL down the concentration gradient [175]. In addition, SR-BI is also expressed in the late endo/lysosomes and might be involved in the intracellular cholesterol trafficking as SR-BI deficiency is associated with accumulation of lysosomal cholesterol in hepatocytes [176].

The SR-BI mediated cholesterol efflux pathway has been shown to be crucial for prevention of macrophage foam cell formation, especially in the absence of ABCA1 [177, 178]. The mechanisms underlying SR-BI mediated bi-directional flux of cholesterol are largely unclear. Although not proven, it is often assumed that SR-BI accelerates aqueous diffusion of FC between cells and mature HDL. Binding to SR-BI will tether potential cholesterol acceptors in close proximity to the plasma membrane, thereby facilitating aqueous diffusion [179]. The extracellular domain of SR-BI is crucial for mediating the bi-directional flux of FC [180]. However, high-affinity binding alone is not sufficient to stimulate FC flux [181]. Interestingly, SR-BI also facilitates FC efflux by increasing the fraction of membrane cholesterol available for efflux [182]. Cholesterol in this faction of the membrane is not available for lipid-free/poor apoAI, although apoAI can bind to SR-BI. One study, using mutated forms of SR-BI, suggests that low efficiency export of FC to HDL is related to low cholesterol availability in the plasma membrane rather than impaired binding of acceptors to the mutated forms of SR-BI [180]. In addition, SR-BI mediated HDL retro-endocytosis, i.e. the uptake of whole HDL particles followed by re-secretion of CE-poor HDL, has also been implicated in SR-BI mediated cholesterol efflux [183, 184]. This process appears independent of cholesterol transport out of the lysosome [183].

1.1.3 Lipid metabolism

The plasma lipid levels depend on the integrated balance of the exogenous and endogenous pathways of lipid metabolism.

1.1.3.1 Exogenous lipid transport

The exogenous pathway of lipid metabolism permits efficient transport of dietary lipids (Figure 4). Dietary TG and CE are hydrolyzed by the pancreatic lipase and cholesteryl esterase and absorbed by the epithelium in the proximal small intestine. Subsequently, TG, FC, PL, and apoB48, apoAI, apoAII, and apoAIV are packaged to form CMs. Nascent CMs are secreted into the intestinal lymph and delivered via the thoracic duct directly to the systemic circulation. Meanwhile, CMs loose apoAI and partly apoAIV and acquire apoCI, apoCII, apoCIII, and apoE. Upon entering the blood circulation, the TGs in the core of CMs are hydrolyzed by lipoprotein lipase (LPL) [185] and released fatty acids are taken up by peripheral tissues such as adipose tissue (for storage as TG), skeletal muscle and heart (as energy source), and the liver (as storage or generation of lipoproteins). As TGs are hydrolyzed and FC, PL and apoAI and apoC's on the surface of CMs are in part transferred to HDL, CMs progressively shrink in size and turn into CM remnants. CM remnants are rapidly removed from the circulation by the liver via an apoE-specific recognition site on hepatocytes [186], including the LDL receptor, LRP1, heparan sulphate proteoglycans (HSPG), and as recently demonstrated SR-BI [166].

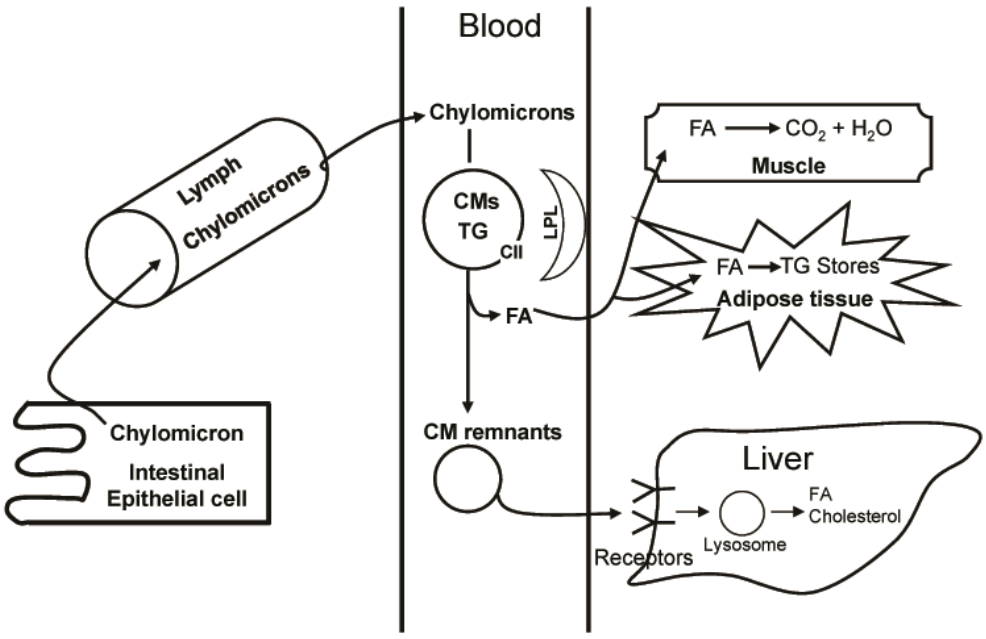

Figure 4. Exogenous lipid transport. See text for explanation. CMs, chylomicrons; FA, fatty acid; TG, triglycerides; LPL, lipoprotein lipase.

1.1.3.2 Endogenous lipid transport

The endogenous pathway of lipoprotein metabolism refers to the hepatic secretion of TG-rich VLDL and their metabolism (Figure 3). The TGs and cholesterol of VLDL are derived from either de novo synthesis or lipoprotein uptake. Nascent VLDL contains a single copy of apoB-100 as well as newly synthesized apoE and apoC's. The packaging of nascent VLDL particles requires the action of the enzyme MTP. Once secreted into the circulation,

VLDL acquires multiple copies of apoE and apoC's from HDL. The TGs of VLDL undergo lipolysis by LPL and PLs are transferred to HDL by phospholipid transfer protein (PLTP), leading to the formation of VLDL remnants or IDLs. The liver removes approximately 40-60% of the IDLs by receptor-mediated endocytosis via apoE. The remaining IDLs further loose TG, PL, apoE, and apoCs as a result of the action of hepatic lipase (HL), leading to the formation of LDL. The formed LDL particle contains apoB-100 as the sole apolipoprotein, which is recognized by the LDL receptor for the clearance from the circulation. Cholesterol in LDL is the important source for the maintenance of membranes in cells and the production of steroids in steroidogenic tissues. In addition, LDL can be retained in the intima of arteries, where it can be modified and subsequently taken up by macrophages via scavenger receptors.

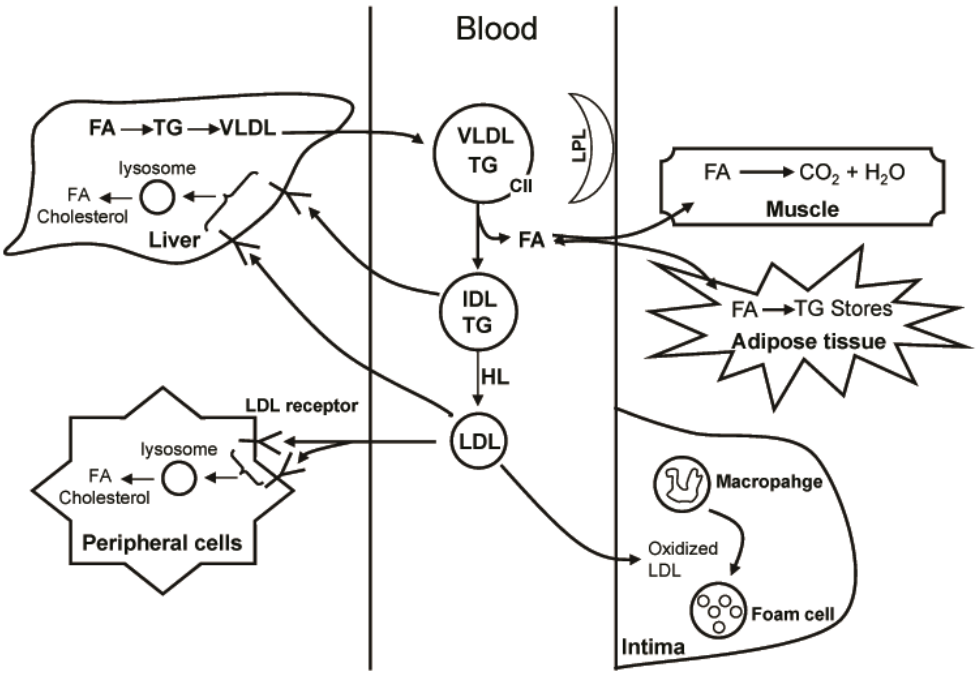

Figure 5. Endogenous lipid transport. See text for explanation. VLDL, very-low-density lipoprotein; IDL, intermediate-density lipoprotein; LDL, low-density lipoprotein; FA, fatty acid; TG, triglycerides; LPL, lipoprotein lipase; HL, hepatic lipase.

1.1.3.3 Reverse cholesterol transport

All nucleated cells synthesize cholesterol. However, only hepatocytes and enterocytes can efficiently excrete cholesterol from the body into feces. In the classical view, reverse cholesterol transport (RCT) is a process that describes the HDL-mediated transport of excess cholesterol from peripheral tissues to the liver for biliary secretion as bile acids or biliary cholesterol [187] (Figure 4). For a long time, this removal via hepatobiliary secretion was considered as the sole route in the RCT process. Of note, a novel non-biliary RCT pathway, transintestinal cholesterol efflux (TICE) has been recently identified [188].

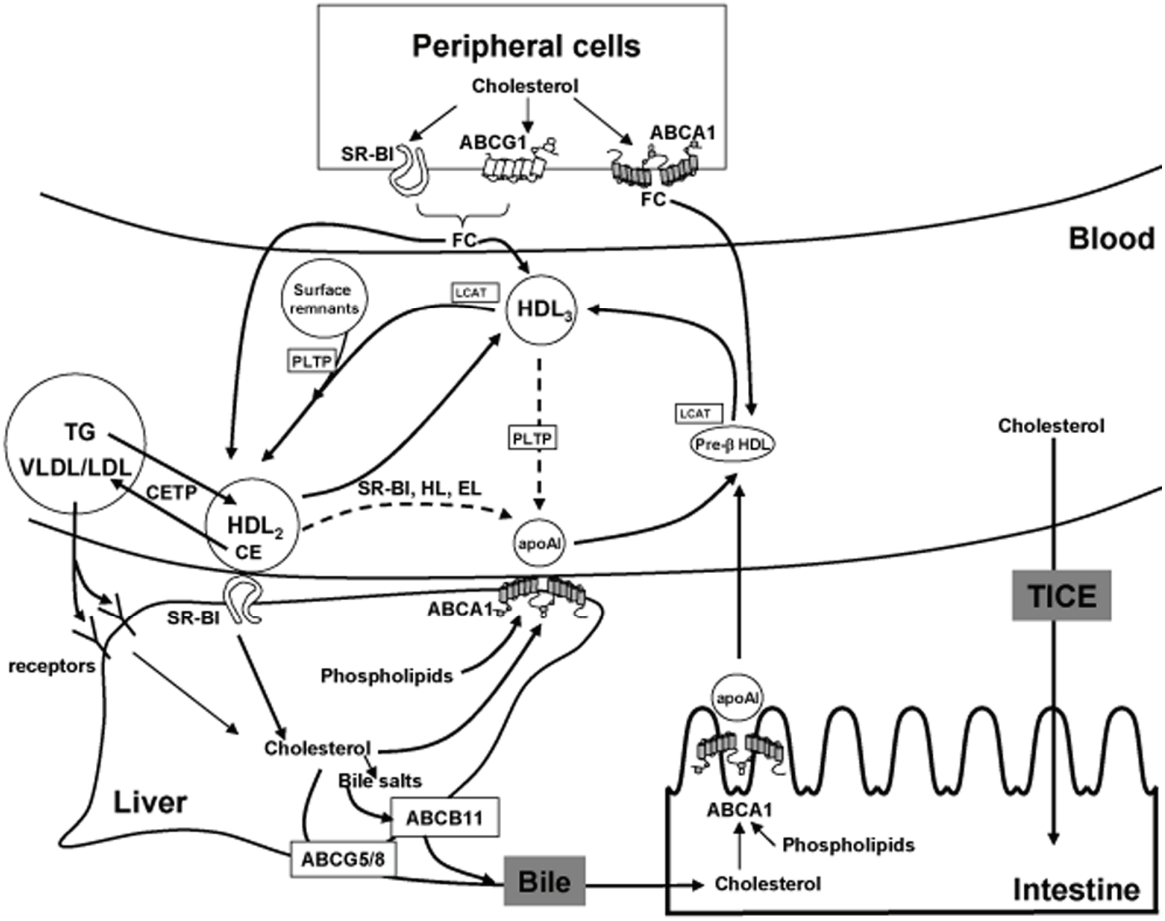

Figure 6. Reverse cholesterol transport. See text for explanation. HDL, high-density lipoprotein; apoAI, apolipoprotein AI; ABCA1, ABC-transporter A1; ABCG1, ABC-transporter G1; SR-BI, scavenger receptor class B type 1; FC, free cholesterol; TG, triglycerides; LCAT, lecithin: cholesterol acyltransferase; CETP, cholesterol ester transfer protein; PLTP, phospholipid transfer protein; VLDL, very-low-density lipoprotein; LDL, low-density lipoprotein; HL, hepatic lipase; EL, endothelial lipase; ABCG5/8, ABC-transporter G5 and G8; ABCB11, ABC-transporter B11, TICE, transintestinal cholesterol efflux.

HDL metabolism and reverse cholesterol transport

HDL is a universal plasma acceptor for cholesterol efflux from both peripheral tissues and the liver by passive diffusion or cholesterol transporters, such as ABC-transporter A1 (ABCA1), ABC-transporter G1 (ABCG1), and SR-BI [189, 190]. As an important mediator in RCT, HDL metabolism is more complex than that of other major lipoprotein fractions, in that the individual lipid and apolipoprotein components of HDL are mostly acquired after secretion of the nascent particle, frequently exchanged with or transferred to other lipoproteins, actively remodeled within the plasma compartment, and cleared at least in part independent from one another [191]. ApoAI, the main apolipoprotein of HDL, is synthesized by liver and intestine. Lipidation of apoAI with PL and FC via ABCA1 in the liver and intestine leads to the generation of pre-β HDL particles [192-195]. Pre-β HDL is present as minor components in plasma. However, it is believed to play a role as initial acceptor of FC from cells [196]. Lipidation of pre-β HDL constrains the conformation of apoAI and reduces its subsequent binding to ABCA1 [197]. Furthermore, esterification of FC

into CE in pre-β HDL by lecithin-cholesterol acyltransferase (LCAT) generates spherical mature α-HDL [198].

HDL particles undergo extensive remodeling within the plasma compartment by a variety of lipid transfer proteins and lipases. LCAT mediated FC esterification, and PLTP mediated particle fusion and surface remnant transfer convert HDL_3 into HDL_2 [199-201], in which lipid-free or -poor apoAI is liberated [202]. Conversely, HDL_2 are converted into HDL_3 and in turn lipid-free or -poor apoAI by cholesteryl ester transfer protein (CETP) mediated CE and triglycerides (TG) exchange with apoB containing lipoproteins [203]. Also hepatic lipase (HL) and endothelial lipase (EL) mediated hydrolysis of PL and TG [204, 205] and SR-BI mediated selective uptake of CE into liver and steroidogenic organs [2, 206] are involved in the conversion of HDL_2 to HDL_3. It has been shown that apoAI conformation and HDL particle size influence the interaction of the HDL particle with SR-BI [143, 207]. The remodeling of HDL thus plays the critical role in determining the ultimate metabolic fate of HDL.

HDL cholesterol is transported to the liver by both a direct and an indirect pathway. HDL cholesterol can be taken up by liver via SR-BI-mediated selective cholesterol uptake [112]. Also, apoE-enriched HDL can be taken up as a whole particle by the liver [208]. In addition, CE of HDL can be transferred to apoB-containing lipoproteins in exchange for TG by CETP and then taken up by the liver through their lipoprotein receptors, such as LDL receptor and LRP1 [203]. Upon delivery of HDL cholesterol to the liver, the CEs are hydrolyzed for either lipoprotein assembly or sterol secretion into the bile via ABCG5/8 (half-transporters that work together as heterodimers) and ABCB11 (BSEP)-mediated pathways [209, 210].

Transintestinal cholesterol efflux and reverse cholesterol transport

Several mouse models with diminished hepatobiliary cholesterol secretion show normal fecal sterol loss [211-216], indicating a non-biliary RCT route in addition to classical pathway through biliary secretion. Increasing evidence shows that the proximal part of the small intestine is able to secrete cholesterol actively, a pathway named TICE [188]. Of note, in mice, TICE is sensitive to pharmacological manipulation. Activation of the liver X receptor (LXR) [214] and the peroxisome proliferator activated receptor δ (PPAR-δ) [217] promotes TICE. Strikingly, TICE accounts for up to 70% of fecal neutral sterol excretion in mice [188]. However, the understanding of the process of TICE is still limited. The origin of intestinally secreted cholesterol and the components involved in TICE remain to be elucidated. Moreover, the importance of TICE in humans still needs to be determined.

1.1.4 Dyslipidemia as a major risk factor for atherosclerosis

Dyslipidemia is a broad term that refers to a number of lipid disorders. The majority of the disorders (80%) are related to diet and lifestyle, although familial disorders (20%) are important as well. The basic categories of dyslipidemias include: elevated LDL-C, low HDL-C, excess lipoprotein(a), hypertriacylglycerolemia, atherogenic dyslipidemia, and mixed lipid disorders (Table 4) [218]. A clear direct relationship exists between dyslipidemia and cardiovascular risk [103]. Normalization of dyslipidemia is thus important for prevention of atherosclerosis and its clinical manifestations such as myocardial infarction and cerebrovascular accidents.

Table 4. Primary hyperlipidemia caused by known single gene mutation.

Genetic disorder	Mutated gene	Elevated Lipoproteins	Clinical complications
LPL deficiency	LPL	CM	Xanthomas, hepatosplenomegaly, pancreatitis [219]
Familiar apoCII deficiency	apoCII	CM	Xanthomas, hepatosplenomegaly, pancreatitis [15]
ApoAV deficiency	apoAV	CM, VLDL	Xanthomas, hepatosplenomegaly, pancreatitis [220]
Familiar HL deficiency	HL	VLDL remnant	Premature atherosclerosis, pancreatitis [221]
Familiar dysbetalipoproteinemia	apoE	CM, VLDL remnant	Xanthomas, CHD, PVD [20]
Familiar hypercholesterolemia	LDLr	LDL	Xanthomas, CHD [222]
Familiar defective apoB-100	apoB100	LDL	Xanthomas, CHD [63]
Autosomal dominant hypercholesterolemia	PCSK9	LDL	Xanthomas, CHD [222]
Autosomal recessive hypercholesterolemia	ARH	LDL	Xanthomas, CHD [223]
Sitosterolemia	ABCG5/8	LDL	Xanthomas, CHD [224]

Abbreviations: LPL, lipoprotein lipase; CM, chylomicron; VLDL, very-low-density lipoprotein; HL, hepatic lipase; CHD, coronary heart disease; PVD, peripheral vascular disease; ARH, autosomal recessive hypercholesterolemia; ABCG5/8, ABC-transporter G5/8

1.2 Atherosclerosis

Atherosclerosis is a progressive disease characterized by the accumulation of lipids and fibrous elements in large arteries. As the primary cause of myocardial infarction and cerebral stroke, atherosclerosis is the underlying cause of about 50% of all deaths in westernized societies. Epidemiological studies have revealed several important environmental (i.e. diet, smoking, and exercise) and genetic risk factors (e.g. dyslipidemia, hypertension, systemic inflammation, diabetes, and obesity) associated with atherosclerosis [103].

1.2.1 Pathogenesis of atherosclerosis

Atherosclerosis is now appreciated to represent a chronic inflammatory reaction of the vascular wall in response to dyslipidemia and endothelial distress involving the inflammatory recruitment of leukocytes and the activation of resident vascular cells [225]. Pathological studies have revealed a defined series of changes in the vessel during atherogenesis and suggested possible pathways of disease initiation and progression (Figure 7).

Several hypotheses have been proposed on the initiation of atherosclerosis. According to the generally accepted "response-to-injury" hypothesis, atherogenesis is initiated by injury to the endothelial lining of the arterial wall and the underlying smooth muscle cells [226]. Various risk factors such as hypertension and oxidized lipids, induce changes in the permeability of the arterial wall, expression of adhesion molecules, and the production of cytokines and chemokines, thereby leading to the migration of inflammatory cells including monocytes, T and B lymphocytes, neutrophils and mast cells from the circulation into the intima of the arterial wall. The "response-to-retention" hypothesis is based on the finding that lipoproteins can pass through endothelium by endothelial cell (EC) junctions or transcytosis, bind to subendothelial matrix, and accumulate in the intima

of the arterial wall [227]. Oxidation of the lipoproteins in the subendothelial matrix results in dysfunction of the endothelium and subsequent recruitment of inflammatory cells.

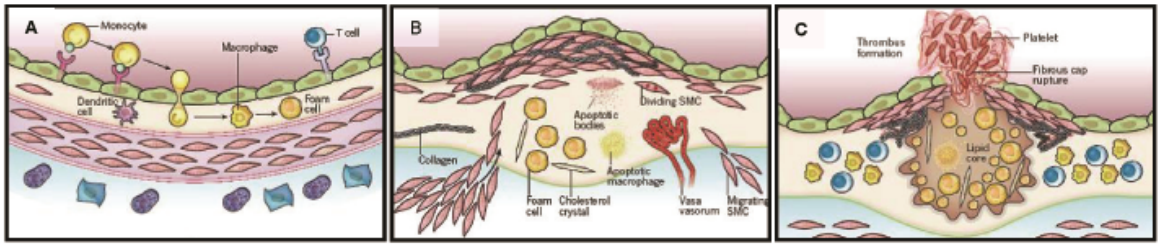

Figure 7. Development of atherosclerosis. See text for explanation. A. Initiation of atherosclerosis due to endothelial dysfunction. B. Lesion progression. C. Lesion rupture and thrombosis. Adapted from Libby *et al*. [228]

Bifurcations and branches of the arteries are the most vulnerable sites for atherosclerosis [229]. This might be due to hypoxia [230] and increased hemodynamic forces [231] at these locations, which could induce endothelium dysfunction and create a proinflammatory environment with low-grade recruitment and accumulation of monocytes into the intima. Upon induction of hypercholesterolemia, these resident intimal monocyte-derived cells initiate atherosclerosis by rapidly engulfing lipid and becoming the first foam cells in the nascent lesion [231] (Figure 7A).

Macrophage foam cell formation is the hallmark of the early atherosclerotic lesion called the fatty streak [232, 233] (Figure 7A). LDL must be extensively modified before it can be taken up rapidly by macrophages to form foam cells. This modification presumably involves reactive oxygen species produced by ECs and macrophages, and several enzymes including myeloperoxidase (MPO) [234], sphingomyelinase [235, 236], and a secretory phospholipase [237, 238]. Two scavenger receptors, SR-A and CD36 are of primary importance for the uptake of modified LDL by macrophages as mice lacking either receptor show a modest reduction in atherosclerotic lesions [239, 240]. Also macrophages can release their cholesterol via various efflux pathways (described in detail in Chapter 4). Since macrophages cannot limit the uptake of cholesterol, functional cholesterol efflux pathways are crucial for prevention of foam cell formation and atherosclerosis. In line, impaired macrophage cholesterol efflux pathways, including facilitated transport via ABCA1, ABCG1, and SR-BI, promote the development of atherosclerosis [178, 241-243].

As the early atherosclerotic lesions progress, additional inflammatory cells are recruited with the further accumulation of extracellular lipids. The inflammatory response in the lesions induces the transformation of smooth muscle cells (SMCs) from the quiescent “contractile” phenotype state to the active “synthetic” state. Vascular SMCs thereafter can proliferate and migrate from the media into the intima. SMCs can take up lipids, thereby contributing to foam cell accumulation. Also, they start to cover the core of the lesions constituted of extracellular lipids, foam cells, T cells and a poorly developed matrix of connective tissue [103]. Further progression of the lesion results in the formation of the advanced lesion characterized by a fibrous cap and a cell-free lipid core [244] (Figure 7B). The fibrous cap is formed by migrated SMCs and their secreted extracellular matrix such as collagen. A uniformly thick fibrous cap provides stability to the atherosclerotic lesion. On the contrary, thinning of the fibrous cap due to the apoptosis of SMCs or increased production of matrix metalloproteinases (MMPs) by macrophages may lead to rupture of

the lesion. A complicated lesion is formed when the fissured atherosclerotic lesion induces secondary hemorrhage and thrombosis (Figure 7C), which may lead to occlusion of the artery and become clinically symptomatic as a myocardial infarction or cerebral stroke [245, 246].

1.2.2 Cells in atherosclerotic lesions

A variety of cells have been found in human atherosclerotic lesions, including monocytes/macrophages/dendritic cells, T and B lymphocytes, smooth muscle cells, neutrophils, and mast cells. Studies in mice have revealed their respective roles in the pathogenesis of atherosclerosis.

1.2.2.1 Monocytes, macrophages, and dendritic cells

Monocytes are widely regarded as key cellular protagonists of atherosclerosis as in the absence of macrophages, severe hypercholesterolemia is not sufficient to drive the pathologic process [246, 247]. Monocytes can differentiate into macrophages and dendritic cells and become foam cells after excessive accumulation of lipids in the intima, thereby initiating atherosclerosis. Monocyte accumulation in atherosclerotic lesions is progressive and correlates to the lesion size [248]. The deficiency of monocyte chemoattrant protein-1 (MCP-1) [249] or its receptor CC-chemokine receptor 2 (CCR2) [250] provides dramatic protection from monocyte recruitment and atherosclerotic lesion formation. However, when the fibrous cap is formed, further recruitment of monocytes is inhibited [247, 251]. Subsets of monocytes with distinct patterns of surface markers and behaviors during inflammation have recently been characterized and shown to have complementary roles during progression of atherosclerosis [252, 253]. In the mouse, one subset of monocytes with high expression of Ly6C ($Ly6C^{high}$) promotes inflammation while the other subset with low expression of Ly6C ($Ly6C^{low}$) attenuates inflammation and promotes angiogenesis and granulation tissue formation in models of tissue injury [254]. $Ly6C^{high}$ monocytes expand in hypercholesterolemic conditions, infiltrate into the intima via CCR2, CCR5 and C-X(3)-C motif chemokine receptor 1 (CX3CR1), and selectively give rise to macrophages in atheroma [252, 253]. In contrast, $Ly6C^{low}$ monocytes enter the atherosclerotic lesion less frequently and employ CX3CR1 and CCR5 to accumulate in the lesion and differentiate into cells expressing the dendritic cell-associated marker CD11c [253]. Interestingly, the expression of MCP-1 in atherosclerotic lesions rises quickly after the initiation of lesion formation, while CX3CL3 only appears later and in more advanced lesions [255, 256], indicating that the two monocyte subsets may recruit sequentially during lesion development.

Different environmental signals, including microbial products and cytokines activate macrophages diversely, leading to macrophage heterogeneity. Gordon and Taylor summarized evidence for the existence of two macrophage phenotypes, widely known as classically activated (M1) and alternatively activated (M2) macrophages [257]. LPS or IFN-γ activated M1 macrophages have enhanced capacity in phagocytosis and produce proinflammatory mediators such as TNF-α and IL-6 [257]. Incubation of M-CSF-differentiated macrophages with IL-4 or IL-13 induces the polarization of macrophages into M2 with increased expression of anti-inflammatory cytokines such as IL-10 and TGF-β [258]. Moreover, inducible nitric oxide synthase (iNOS) is upregulated during classical M1 activation while arginase-1 that competes with iNOS for substrate is induced during alternative M2 activation. The balance of M1-M2 may thus greatly affect lesion development by regulating not only the immune response but also the production of nitric

oxide. Interestingly, oxidized LDL increases the expression of markers of both classical activation (MMP-1 and iNOS) and alternative activation (arginase-I) [259, 260]. In line, foam cells isolated from atherosclerotic lesions express MMP-1 and reduced arginase-I, a feature of classical activation, and increased MMP-12, a feature of alternative activation [261]. Of note, the phenotype of macrophages is plastic and reversible [262]. However, whether modulation of M1-M2 can become a therapeutic target requires further investigation.

Dendritic cells (DCs), as the most potent professional antigen-presenting cells (APC), are essential for the priming of adaptive immune responses and involved in maintaining immune tolerance to self antigens [263]. DCs originate from bone marrow progenitors, penetrate peripheral tissues from the circulation, and give rise to immature DCs. In the peripheral tissues, DCs monitor the microenvironment and, when the cells encounter 'danger' signals, DCs undergo differentiation and maturation [264]. The identification of DCs in the arterial walls of animal models [265, 266] facilitated the investigation of the impact of DCs in atherosclerosis. The significance of DCs in atherogenesis is evident in mice overexpressing hBcl-2 [267]. Expansion of the DC population in these animals alleviates atherosclerosis. However, this reduction of lesion size is correlated with decreased levels of plasma cholesterol. Conversely, depletion of DCs results in increased plasma cholesterol levels and accelerated atherosclerosis, indicating that DCs may act on lipid metabolism and thereby inhibit lesion development [267]. More importantly, vaccination using mature DCs pulsed with oxidized LDL induced oxidized-specific T cells with a lowered T-helper 1 (Th1) response, increases the levels of ox-LDL-specific antibodies and reduces lesion development in LDLr KO mice [268]. Likewise, the development of atherosclerosis in human apoB-100 transgenic LDLr KO mice is attenuated by treatment with apoB-100 loaded tolerogenic dendritic cells [269]. However, treatment with DCs pulsed with malondialdehyde modified LDL in apoE KO mice aggravates atherosclerosis [270]. Therefore, the potential of DC-based therapy in atherosclerosis needs further investigation.

1.2.2.2 Lymphocytes

The antigen-specific adaptive immune system is involved in the development of atherosclerosis [271]. Deficiency in both B and T cells inhibits the development of the early lesions rather than advanced lesions [272]. Different B and T cell subsets can be distinguished with different effects on atherosclerosis.

B lymphocytes

B lymphocytes, essential players in humoral immunity, are mainly present in the adventitia rather than in the lesion [273, 274]. The atheroprotective role of B lymphocytes was evidenced by the finding that B cell deficiency results in increased atherosclerotic lesion development in LDLr KO mice [275], while adoptive transfer of splenic B cells protects against atherosclerosis in apoE KO mice [276]. In mice, several B cell subsets, including B1, B2, and B10 have been described [277]. B1 cells, preferentially localized in the peritoneal cavity, have been recognized as producers of antibodies that mainly are immunoglobulins (Ig)M. IgM protects against atherosclerosis via clearance of apoptotic cells and oxidized LDL [278]. Deficiency of IL-5, a cytokine that promotes the expansion of B1 cells, leads to reduced levels of IgM and concomitantly increased atherosclerosis. Therefore, B1 cells are atheroprotective. In contrast, B2 cells are conventional B cells and constitute the major B cell population in spleen and lymph nodes. They produce low levels of IgM and high amounts of IgD. Recent studies indicated that B2 cells are pro-

atherogenic [279, 280]. Depletion of B2 cells using a CD20-specific monoclonal antibody ameliorates, while adoptive transfer of B2 cells aggravates atherosclerosis. The atherogenic effect of B2 cells may be mediated by promoting T cells to secrete IFNγ and reduce IL-17 production [279, 281]. Recently, a third subset called B10 cells have been identified as IL-10 producing B cells [282]. Since IL-10 is anti-inflammatory and atheroprotective [283, 284], B10 cells might protect against atherosclerosis.

T lymphocytes

CD4+ T helper cells

T cells in atherosclerotic lesions are mostly CD4+ T cells [285]. Adoptive transfer of CD4+ T helper cells into severe combined immune deficient (*scid*) apoE KO mice revealed their pro-atherogenic role [286]. The majority of the pathogenic CD4+ T cells in atherosclerosis are Th1 cells. Atherosclerosis-prone mice that are deficient in T-bet, a Th1-associated transcription factor, show attenuated atherosclerosis [287]. Th1 cells secrete IFNγ as a signature cytokine which promotes atherosclerosis [288, 289]. IL-12 is important in Th1 cell differentiation and IL-18 synergizes with IL-12 to induce IFNγ production [290]. IL-12 or IL-18 deletion results in a significant reduction in atherosclerotic lesion development [291, 292], while exogenous administration of IL-12 or IL-18 clearly accelerates lesion progression [234, 293, 294]. In contrast, Th2 cells are proposed to antagonize the pro-atherogenic Th1 effects and thereby confer atheroprotection. In mouse models that are relatively resistant to atherosclerosis, a Th2-bias has been shown to protect against early fatty streak development [295]. IL-33, a powerful inducer of Th2 responses, results in less atherosclerosis in apoE KO mice [296]. Th2 cells secrete IL-4, IL-5, and IL-10 and provide help for antibody production by B cells. IL-4 drives Th2 cell differentiation and downregulates IFNγ. Strikingly, IL-4 deficiency in bone marrow-derived cells results in attenuation of atherosclerosis in the aortic arch and the thoracic aorta [297]. IL-5 drives production of IgM by B1 cells and inhibits atherogenesis [287]. The protective effect of IL-10 in atherosclerosis is evidenced by the finding that IL-10 deficiency leads to increased lesion development [298-300]. Thus, the Th1/2 balance greatly influences atherosclerotic lesion development.

Th17 cells represent a newly identified subset of CD4+ T helper cells producing IL-17. The role of Th17 cells and IL-17 in atherosclerosis is emerging. In atherosclerotic arterial walls, Th17 cells are present in both the adventitia and the lesion [301]. Blockade of IL-17 by using a neutralizing antibody or the adenovirous producing IL-17A receptor results in reduced atherosclerosis while exogenous treatment of recombinant IL-17 or IL-17A promotes the formation of atherosclerotic lesions [301-303]. However, Taleb et al recently revealed that IL-17 might be atheroprotective as mice lacking a preponderance of Th17 cells due to deficiency of SOCS3, a suppressor of signaling from IL-17 and several other cytokines, show less atherosclerotic lesion development [281]. The function of IL-17 thus remains controversial and awaits more direct studies to further address the issue.

CD8+ T cells

In addition to CD4+ T cells, also CD8+ T cells are present in atherosclerotic lesions [285]. However, the exact role of CD8+ T cells in atherosclerosis is still unknown. Activation and infiltration of CD8+ T cells seems to correlate with larger lesions in apoE KO mice treated with an agonist to the tumor necrosis factor-like surface protein CD137 [304] and LDLr KO mice deficient in the inhibitory molecules PD-L1 and PD-L2 [305].

Regulatory T cells

Regulatory T (Treg) cells are identified as a group of T cells that can suppress immune responses. *In-vitro* studies showed that naturally occurring Tregs, characterized by the expression of CD4, high levels of CD25 and the transcriptional factor Foxp3, steer macrophage differentiation towards M2 and inhibit macrophage foam cell formation by cell-to-cell contact and cytokine IL-10 and TGF-β [306]. Evidence for the atheroprotective effects of Treg cells has been provided using mice with fewer Treg cells due to the deficiency of CD80-86 or CD28. Leukocyte deficiency in CD80-86 or CD28 results in more atherosclerosis [307]. Interestingly, in apoE KO mice, the number and suppressive property of naturally occurring Tregs are decreased. Importantly, adoptive transfer of Tregs from WT into apoE KO mice inhibits lesion development [308]. Moreover, induction of Tregs by oral administration of oxLDL or HSP60 results in less atherosclerosis [309, 310]. Likewise, *in vivo* expansion of Tregs using a complex of IL-2 and anti-IL-2 mAb (monoclonal antibody), reduced atherosclerotic lesion formation in LDLr KO mice [311]. On the contrary, vaccination against Foxp3, a transcriptional factor instrumental in mediating the suppressive functions of natural Treg cells, aggravates atherosclerosis [312]. The cytokines secreted by Treg cells, such as TGF-β and IL-10, also have profound atheroprotective effects [313]. Of note, oxidized LDL attenuates the suppressive function of Tregs [308]. Therefore, therapeutic strategies aiming to induce Tregs may be more effective in the presence of anti-oxidants.

1.2.2.3 Smooth muscle cells

It is generally accepted that transition of SMCs from a contractile state to a proliferative and migratory state contributes to the growth of the atherosclerotic lesion. The first evidence is provided by one study on SMC-specific deletion of LRP1 in LDLr KO mice [76]. Aggravation of atherosclerosis was shown to be correlated with increased expression of platelet-derived growth factor (PDGF) receptor-β on SMC and enhanced proliferation and migration of SMC due to the deletion of LRP1 [76]. Conversely, inhibition of SMC proliferation and migration due to the deficiency of β-arrestins, multifunctional adaptor proteins, reduces atherosclerosis in LDLr KO mice [314]. SMCs are also responsible for the formation of the fibrotic cap that can stabilize and prevent the lesion from rupture [315]. Using transgenic mice with selective induction of SMC apoptosis, Clark et al demonstrated the crucial role of SMC apoptosis for lesion vulnerability [316]. Interestingly, histological studies of autopsy specimens of human coronary arteries ranging from infants to adults provide evidence that regions prone to the development of atherosclerosis contain abundant SMCs in the intima while regions that are more resistant to atherosclerosis contain few [317-319], indicating the potential role of SMCs in the lesion development. The underlying mechanisms might involve: 1) Atherogenic stimuli such as oxidized LDL stimulate SMCs to secrete larger and more highly sulfated proteoglycans, thereby altering the composition of extracellular matrix (ECM) and in turn increasing lipoprotein retention [320]. 2) Atherogenic stimuli such as hypercholesterolemia and proinflammatory cytokines increase the expression of receptors involved in cholesterol uptake, including LDL receptor, VLDL receptor, and scavenger receptors, thereby promoting SMCs transformation into foam cells [321, 322]. 3) SMCs in the lesion express a variety of adhesion molecules including intercellular adhesion molecule-1 (ICAM-1), vascular cell adhesion molecule-1 (VCAM-1), and fractalkine, thereby leading to the retention of monocytes and macrophages inside the lesion [323-326]. 4) Interaction of macrophages and lymphocytes with SMCs via ICAM-1 and VCAM-1 protects these cells against apoptosis, thus contributing to the cellularity of the lesion [327]. 5) SMCs can produce many cytokines such as PDGF,

transforming growth factor-β (TGF−β), interferon γ (IFNγ), and monocyte chemoattractant protein (MCP-1), all of which contribute to the initiation and propagation of the inflammatory response to lipid [328].

1.2.2.4 Neutrophils

In contrast to lymphocytes and monocytes/macrophages, neutrophils are not detected in high numbers in atherosclerotic lesions. Since neutrophils are primarily found at sites of lesion rupture and erosion or in thrombi [329], neutrophils were believed to be important only in the late-stage of atherosclerosis. However, neutrophils are present in atherosclerotic lesions of all stages and the surrounding adventitia in apoE KO and LDLr KO mice [330, 331]. The low frequency of neutrophils found in the atherosclerotic lesions might be due to their short life span and rapid apoptosis upon activation [332]. The functional importance of neutrophils for the initiation and development of atherosclerotic lesions was recently demonstrated by Zernecke et al [330] and Drechsier et al [333]. Hypercholesterolemia enhances granulopoiesis and mobilization from bone marrow, thereby leading to neutrophilia [333]. The degree of neutrophilia is correlated to the extent of early atherosclerotic lesions. Importantly, depletion of neutrophils in the circulation significantly inhibits early lesion development [330, 333]. However, the development of advanced lesions was not affected by neutropenia [333], suggesting an important role of neutrophils in the initiation of atherosclerosis.

Neutrophils can affect atherosclerosis through its granule proteins such as myeloperoxidase (MPO), elastase, and cathepsin G. First, deposition of neutrophil granule proteins on the endothelium may induce endothelial dysfunction, thereby triggering the retention of lipoproteins and the recruitment of leukocytes [334-338]. Second, neutrophil granule proteins may also activate macrophages to produce and release proinflammatory cytokines such as TNFα and IFNγ to promote lesion development [339, 340]. Third, neutrophil granule proteins induce apoptosis of endothelial cells, thereby contributing to the vulnerability and rupture of the lesion [341, 342]. In addition, oxygen radicals produced by neutrophils via MPO, lipoxygenases, and NADPH oxidase also affect atherosclerosis by inducing lipid oxidation, endothelial dysfunction, and apoptosis of endothelial cells [343].

1.2.2.5 Mast cells

Activated mast cells are found in human atherosclerotic lesions and have a wide range of functions in the pathogenesis of atherosclerosis [263, 344]. The recent studies by Sun et al. [345] and Bot et al. [346-348] highlight the importance of mast cells in atherosclerosis. In atherosclerotic lesions, mast cells can be activated by oxidized LDL-IgG immune complexes [349] and neuropeptide substance P [347]. Proinflammatory cytokines including IFNγ and IL-6 [345] and chymase [348] secreted by activated mast cells promote lesion development and vulnerability. Moreover, mast cells can secrete several chemokines, including IL-8 and MCP-1, leading to the recruitment of other leukocytes [349]. In addition, mast cells may play roles in lipid metabolism [350] and macrophage foam cell formation [351, 352], thereby influencing the susceptibility to atherosclerosis.

1.3 ABCA1 and atherosclerosis: cholesterol homeostasis, reverse cholesterol transport, and inflammation

ABCA1 is a plasma membrane protein which functions as a major regulator of cellular cholesterol and phospholipid homeostasis [353, 354]. ABCA1 mediates cholesterol and phospholipid efflux to lipid-free and lipid-poor apoAI [355]. Loss-of-function mutations of

ABCA1 cause Tangier's disease characterized by low plasma HDL, macrophage accumulation and deposition of CEs, and premature atherosclerosis [356-358]. Animal studies demonstrate that hepatic and intestinal ABCA1 are crucial for the biogenesis of HDL [194, 195, 359], while macrophage ABCA1 promotes cholesterol efflux and thereby protects against foam cell formation [241, 360, 361]. The atheroprotective effects of ABCA1 are primarily attributed to its role in promotion of reverse cholesterol transport from macrophages via HDL to the liver [362-364].

In addition, effects of ABCA1 on the immune-inflammation response [365] might also influence the development of atherosclerosis. Leukocyte ABCA1 deficiency promotes macrophage infiltration into different tissues [241, 360], probably due to the increased chemotactic response of macrophages [366]. Moreover, ABCA1 deficient macrophages show enhanced proinflammatory response to lipopolysaccharide (LPS) [367-369]. Interestingly, ABCA1 is absent in the inflammatory monocyte subsets that are more apt to the proinflammatory effects induced by LPS/IFN-γ [370]. The potent anti-inflammatory properties of ABCA1 can be directly attributed to its cholesterol export activity. ABCA1 deficiency increases FC and lipid rafts in the membrane of macrophages and subsequently induces trafficking of MyD88-dependent Toll-like receptors to lipid rafts. Of note, Tang et al recently provide evidence that macrophage ABCA1 also functions as a direct anti-inflammatory receptor, which is independent of its lipid transport function [371]. The interaction between apoAI and ABCA1 in macrophage activates Janus kinase 2 (JAK2)/STAT3 pathway and suppresses LPS-induced inflammation. In addition, ABCA1 deficiency is associated with increased immune complex accumulation in the kidney, a phenotype of systemic lupus erythematosus (SLE) [372]. Deranged apoptosis is implicated in the pathogenesis of SLE [373]. Therefore, the SLE phenotype in ABCA1 KO mice might be related to a role of ABCA1 in prevention of apoptosis and clearance of apoptotic cells. First, due to its lipid transport function, ABCA1 protects against FC loading, ER stress, and oxidized lipid-mediated apoptosis [374]. Second, ABCA1 is important for the efficient exposure of phosphatidylserine on apoptotic cells, which is necessary to guarantee recognition by phagocytes [375]. Last, ABCA1 interacts with syntaxin 13 and flotillin-1 in Lubrol WX-insoluble raft microdomains in macrophages which participate in the formation of phagosomes [376]. Therefore, the role of ABCA1 in apoptosis and clearance of apoptotic cells might also contribute to its immunosuppressive function.

It is conceivable that ABCA1 is atheroprotective based on its role in the prevention of foam cell formation and inflammation. However, manipulation of ABCA1 expression in mouse models has yielded conflicting results. Mice lacking ABCA1 globally do not show increased susceptibility to atherosclerosis in LDLr KO and apoE KO mice [360]. Overexpression of ABCA1 in both liver and macrophages even results in more atherosclerotic lesion formation in apoE KO [377] and LDLr KO [378] mice, although plasma HDL-C levels and biliary cholesterol secretion are upregulated [379]. These might be due to the fact that manipulation of ABCA1 expression affects not only HDL-C levels but also cholesterol levels in apoB-containing lipoproteins. Bone marrow transplantation studies showed that leukocyte ABCA1 is atheroprotective as deletion of ABCA1 in bone marrow-derived hematopoietic cells resulted in increased atherosclerosis [178, 241, 243, 360, 380] while overexpression of leukocyte ABCA1 reduced atherosclerosis [381]. However, Brunham et al found that specific knockdown of macrophage ABCA1 in LDLr KO mice did not modulate the initiation and development of atherosclerosis [382]. Interestingly, this study also demonstrated that liver-specific inactivation of ABCA1 leads to reduced HDL-C levels and accelerated atherosclerosis while overexpression of ABCA1 in the liver alleviates the atherosclerosis [382], indicating that the liver is an important site at which ABCA1 plays an

anti-atherogenic role. In addition, modest overexpression of human ABCA1 on endothelial cells (EC) also protects the atherosclerotic lesion development in wild-type mice [383]. Strikingly, EC-specific overexpression of human ABCA1 did not influence the atherosclerotic lesion development in ABCA1 KO or apoE KO mice, suggesting that the protective effect of ABCA1 on endothelium is conditional. The effects of ABCA1 on other cell types, such as T cells, B cells, and mast cells, on the development of atherosclerosis remain to be elucidated.

1.4 SR-BI and atherosclerosis: beyond HDL metabolism

Experiments using transgenic and KO mice have established that SR-BI protects against atherosclerosis. Disruption of SR-BI in wild-type as well as LDLr KO mice increases atherosclerosis [384, 385]. Tissue-specific inactivation of SR-BI has dissected the discrete role of SR-BI in different cell types on atherosclerosis susceptibility. Liver-specific knockdown of SR-BI results in the accumulation of abnormally large HDL particles and accelerated atherosclerosis [384]. Increased oxidative stress in SR-BI KO mice suggests that the abnormally large HDL particles are dysfunctional, which may also potentially promote atherogenesis [386]. Normalization of HDL levels by CETP cannot reverse the oxidative stress and reduce atherosclerosis in SR-BI KO mice [387]. Transgene or adenovirus-mediated hepatic overexpression of SR-BI markedly reduced atherosclerosis [165, 388, 389]. The atheroprotective effect of hepatic SR-BI is thus largely attributed its role in HDL-mediated RCT. Of note, hepatic SR-BI is also involved in the clearance of VLDL [162] and CM [166], which might affect atherosclerotic lesion development.

Extrahepatic SR-BI is also protective against atherosclerosis, as evidenced by the finding that knockout of hepatic SR-BI results in less lesion formation as compared to total-body SR-BI deficiency [384]. Bone marrow transplantation studies indicate that macrophage SR-BI plays a unique dual role in the pathogenesis of atherosclerosis, depending on the stage of lesion development [390]. The development of early fatty streak lesions is facilitated by macrophage SR-BI [177], while SR-BI on macrophages reduces the development of advanced atherosclerotic lesions [177, 385]. This unique dual role is likely a direct effect of the multi-functional and multi-ligand qualities of SR-BI, which binds a wide array of native and modified lipoproteins and mediates the bi-directional flux of cholesterol between HDL and cells [390]. Moreover, SR-BI is also expressed on ECs. Overexpression of SR-BI on ECs leads to decreased en face aortic lesion area in wild-type mice [391]. Several lines of evidence have indicated that SR-BI on ECs is important for the atheroprotective effects of HDL. Endothelial SR-BI transports HDL through the endothelium by transcytosis to get access to the cells in the intima [392]. Importantly, during the transcytosis, the size of HDL is reduced, but the protein moiety remained intact, which might increase the capacity of HDL as a cholesterol acceptor. Moreover, HDL prevents against apoptosis of EC [393], promotes EC migration to maintain the integrity of the endothelium [394], and induces the activation of endothelial nitric oxide synthase (eNOS) via SR-BI [395, 396].

The atheroprotective effects of SR-BI might also be attributed to its role in inflammation. SR-BI-mediated cholesterol uptake by the adrenal is essential for optimal glucocorticoid production [397]. Also SR-BI can bind to and internalize LPS [398]. Therefore, enhanced immune response to LPS in SR-BI KO mice is largely the consequence of defective glucocorticoid production and hepatic LPS clearance [399]. Importantly, overexpression of SR-BI reduces septic death [400]. Interestingly, SR-BI on macrophage also suppresses TLR-4-mediated nuclear factor-κB (NF-κB) activation, thereby alleviating the

inflammatory response to LPS [400]. In addition, interaction of HDL with SR-BI on EC can inhibit expression of adhesion molecules VCAM-1 and ICAM-1 [401], which may prevent the activation and infiltration of inflammatory cells.

1.5 Macrophage reverse cholesterol transport: potential therapeutic target for atherosclerosis

Reverse cholesterol transport is important for the removal of excessive cholesterol from peripheral tissues. Macrophage-derived foam cells, as major cellular components of early and advanced lesions, contribute to the initiation, development, and rupture of atherosclerotic lesions. Macrophage RCT, removal of cholesterol from macrophage foam cells in the atherosclerotic lesions, is thus crucial for the treatment of atherosclerosis. However, the mass of cholesterol derived from macrophage foam cells is only a tiny fraction of the overall flux of cholesterol from peripheral tissues. Mass-based methods cannot be used to trace such a small amount of cholesterol derived from macrophage foam cells. For this reason, the group of Dr. Rader developed a method to trace cholesterol efflux and reverse cholesterol transport specifically from macrophage foam cells to the feces [402]. Macrophages are labeled with [^{3}H]cholesterol in the presence of acetylated LDL and injected into the peritoneal cavity of mice. The tracer can be detected in the plasma, liver, bile, and feces. Although this assay has limitations, this method helps us to increase the understanding of the molecular regulation of RCT. More importantly, the rate of macrophage RCT predicts atherosclerosis better than the level of HDL-C in mice [403]. Specific cellular cholesterol transporters including ABCA1, ABCG1, and SR-BI [362-364, 404] and the quantity and quality of HDL-based acceptors [362, 405] greatly influence macrophage RCT *in vivo*. Therapeutic targeting of macrophage reverse cholesterol transport may potentially prevent progression or even induce regression of atherosclerosis. Overexpression of hepatic apoAI increases HDL levels and enhances macrophage RCT [406]. LXR agonists increase cholesterol efflux by induction of ABCA1 and ABCG1 and promotes biliary cholesterol secretion by upregulation of ABCG5 and ABCG8, thereby facilitating macrophage RCT [407]. Furthermore, induction of HDL by overexpression of hepatic apoAI [408, 409] and activation of LXR [410] is required for regression of atherosclerotic lesions. In addition, PPAR-α agonists could promote macrophage RCT and reduce atherosclerosis [411]. Therefore, determination of the role of RCT, especially macrophage-specific RCT in atherosclerosis are of essential importance for the treatment of atherosclerosis.

1.6 Outline of the thesis

ABCA1 and SR-BI are important mediators in RCT. To study the putative synergistic role of ABCA1 and SR-BI in RCT, ABCA1/SR-BI double knockout (dKO) mice were generated. In **Chapter 2**, the phenotype of dKO mice with respect to plasma lipid levels, HDL metabolism, blood cell counts, macrophage RCT, and tissue cholesterol homeostasis was characterized. Due to the lack of atherogenic lipids in the circulation, enhanced macrophage foam cell formation but no atherosclerosis was observed in ABCA1/SR-BI dKO mice. DKO mice were thus challenged with high fat/high cholesterol diet containing 0.05% cholate to determine the effects of combined deficiency of ABCA1 and SR-BI on atherosclerosis in **Chapter 3**.

Macrophage cannot limit the lipid uptake and depend on the cholesterol efflux mechanisms to prevent their transformation into foam cell formation. Several cholesterol efflux pathways have been identified including aqueous diffusion, SR-BI mediated efflux, and active transport via ABCA1 and ABCG1. The contribution of these pathways to foam

cell formation in the atherosclerotic lesion is reviewed in **Chapter 4**. In **Chapter 5**, bone marrow cells from ABCA1/SR-BI dKO mice and respective control mice were transplanted into female LDLr KO mice to specifically investigate the effects of combined deficiency of ABCA1 and SR-BI in bone marrow-derived cells on atherosclerosis. Deletion of the macrophage LDL receptor impairs sterol-induced upregulation of ABCA1 expression [412]. To investigate the interaction of the LDL receptor and ABCA1 on leukocytes and the consequences for atherosclerotic lesion development *in vivo*, bone marrow transplantation experiments were performed using LDLr/ABCA1 dKO mice as donors in **Chapter 6**. In **Chapter 7**, bone marrow from ABCA1 KO mice was transplanted into LDLr/apoAI dKO mice to investigate whether leukocyte ABCA1 is atheroprotective in the absence of circulating apoAI.

Different strategies, including dietary lipid lowering, overexpression of macrophage ABCA1, and infusion of synthetic cholesterol-free phosphatidylcholine (PC) particles, were used to induce cholesterol efflux from macrophages in established atherosclerotic lesions. The effect of dietary lipid lowering on the remodeling of established atherosclerotic lesions in LDLr KO mice was studied in **Chapter 8**. In **Chapter 9**, the dynamics of macrophage infiltration into the established lesions and the effect of macrophage ABCA1 overexpression were studied in LDLr KO mice. The beneficial effects of reconstituted HDL (composed of human apoAI and PC) infusion on atherosclerosis might be attributed to both its capacities to induce cholesterol efflux from macrophage foam cells and its anti-inflammatory actions. The effects of induction of macrophage cholesterol efflux by solely infusion of PC particle on established atherosclerotic lesions were investigated in **Chapter 10**.

Finally, all the results obtained in this thesis and future perspectives are summarized and discussed in **Chapter 11**.

1.7 Reference

(1) Rebeck GW, LaDu MJ, Estus S, Bu G, Weeber EJ. The generation and function of soluble apoE receptors in the CNS. *Mol Neurodegener* 2006;1:15.

(2) Krieger M. Charting the fate of the "good cholesterol": identification and characterization of the high-density lipoprotein receptor SR-BI. *Annu Rev Biochem* 1999;68:523-58.

(3) Wasan KM, Brocks DR, Lee SD, Sachs-Barrable K, Thornton SJ. Impact of lipoproteins on the biological activity and disposition of hydrophobic drugs: implications for drug discovery. *Nat Rev Drug Discov* 2008 January;7(1):84-99.

(4) Ginsberg HN. Lipoprotein physiology. *Endocrinol Metab Clin North Am* 1998 September;27(3):503-19.

(5) Rothblat GH, Phillips MC. High-density lipoprotein heterogeneity and function in reverse cholesterol transport. *Curr Opin Lipidol* 2010 June;21(3):229-38.

(6) Frank PG, Marcel YL. Apolipoprotein A-I: structure-function relationships. *J Lipid Res* 2000 June;41(6):853-72.

(7) Boucher J, Ramsamy TA, Braschi S, Sahoo D, Neville TA, Sparks DL. Apolipoprotein A-II regulates HDL stability and affects hepatic lipase association and activity. *J Lipid Res* 2004 May;45(5):849-58.

(8) Verges B. Apolipoprotein A-IV in diabetes mellitus. *Diabete Metab* 1995 April;21(2):99-105.

(9) Lookene A, Beckstead JA, Nilsson S, Olivecrona G, Ryan RO. Apolipoprotein A-V-heparin interactions: implications for plasma lipoprotein metabolism. *J Biol Chem* 2005 July 8;280(27):25383-7.

(10) Davidson NO, Shelness GS. APOLIPOPROTEIN B: mRNA editing, lipoprotein assembly, and presecretory degradation. *Annu Rev Nutr* 2000;20:169-93.

(11) Jonas A, Sweeny SA, Herbert PN. Discoidal complexes of A and C apolipoproteins with lipids and their reactions with lecithin: cholesterol acyltransferase. *J Biol Chem* 1984 May 25;259(10):6369-75.

(12) Gautier T, Masson D, de Barros JP, Athias A, Gambert P, Aunis D, Metz-Boutigue MH, Lagrost L. Human apolipoprotein C-I accounts for the ability of plasma high density lipoproteins to inhibit the cholesteryl ester transfer protein activity. *J Biol Chem* 2000 December 1;275(48):37504-9.

(13) Conde-Knape K, Bensadoun A, Sobel JH, Cohn JS, Shachter NS. Overexpression of apoC-I in apoE-null mice: severe hypertriglyceridemia due to inhibition of hepatic lipase. *J Lipid Res* 2002 December;43(12):2136-45.

(14) De HW, Out R, Berbee JF, van der Hoogt CC, van Dijk KW, Van Berkel TJ, Romijn JA, Jukema JW, Havekes LM, Rensen PC. Apolipoprotein CI inhibits scavenger receptor BI and increases plasma HDL levels in vivo. *Biochem Biophys Res Commun* 2008 December 26;377(4):1294-8.

(15) Fojo SS, Brewer HB. Hypertriglyceridaemia due to genetic defects in lipoprotein lipase and apolipoprotein C-II. *J Intern Med* 1992 June;231(6):669-77.

(16) Gerritsen G, Rensen PC, Kypreos KE, Zannis VI, Havekes LM, Willems van DK. ApoC-III deficiency prevents hyperlipidemia induced by apoE overexpression. *J Lipid Res* 2005 July;46(7):1466-73.

(17) Ebara T, Ramakrishnan R, Steiner G, Shachter NS. Chylomicronemia due to apolipoprotein CIII overexpression in apolipoprotein E-null mice. Apolipoprotein CIII-induced hypertriglyceridemia is not mediated by effects on apolipoprotein E. *J Clin Invest* 1997 June 1;99(11):2672-81.

(18) Rassart E, Bedirian A, Do CS, Guinard O, Sirois J, Terrisse L, Milne R. Apolipoprotein D. *Biochim Biophys Acta* 2000 October 18;1482(1-2):185-98.

(19) Soiland H, Soreide K, Janssen EA, Korner H, Baak JP, Soreide JA. Emerging concepts of apolipoprotein D with possible implications for breast cancer. *Cell Oncol* 2007;29(3):195-209.

(20) Smelt AH, de BF. Apolipoprotein E and familial dysbetalipoproteinemia: clinical, biochemical, and genetic aspects. *Semin Vasc Med* 2004 August;4(3):249-57.

(21) Valesini G, Shoenfeld Y. A new player in the antiphospholipid syndrome: the beta 2 glycoprotein I cofactor. *Autoimmunity* 1992;14(2):105-10.

(22) Zlokovic BV. Cerebrovascular transport of Alzheimer's amyloid beta and apolipoproteins J and E: possible anti-amyloidogenic role of the blood-brain barrier. *Life Sci* 1996;59(18):1483-97.

(23) Vanhollebeke B, Pays E. The function of apolipoproteins L. *Cell Mol Life Sci* 2006 September;63(17):1937-44.

(24) Dahlback B, Nielsen LB. Apolipoprotein M--a novel player in high-density lipoprotein metabolism and atherosclerosis. *Curr Opin Lipidol* 2006 June;17(3):291-5.

(25) Erqou S, Thompson A, Di AE, Saleheen D, Kaptoge S, Marcovina S, Danesh J. Apolipoprotein(a) isoforms and the risk of vascular disease: systematic review of 40 studies involving 58,000 participants. *J Am Coll Cardiol* 2010 May 11;55(19):2160-7.

(26) Sudhof TC, Goldstein JL, Brown MS, Russell DW. The LDL receptor gene: a mosaic of exons shared with different proteins. *Science* 1985 May 17;228(4701):815-22.

(27) Defesche JC. Low-density lipoprotein receptor--its structure, function, and mutations. *Semin Vasc Med* 2004 February;4(1):5-11.

(28) Ho YK, Brown S, Bilheimer DW, Goldstein JL. Regulation of low density lipoprotein receptor activity in freshly isolated human lymphocytes. *J Clin Invest* 1976 December;58(6):1465-74.

(29) Wintergerst ES, Jelk J, Asmis R. Differential expression of CD14, CD36 and the LDL receptor on human monocyte-derived macrophages. A novel cell culture system to study macrophage differentiation and heterogeneity. *Histochem Cell Biol* 1998 September;110(3):231-41.

(30) Huettinger M, Schneider WJ, Ho YK, Goldstein JL, Brown MS. Use of monoclonal anti-receptor antibodies to probe the expression of the low density lipoprotein receptor in tissues of normal and Watanabe heritable hyperlipidemic rabbits. *J Clin Invest* 1984 September;74(3):1017-26.

(31) Gherardi E, Bowyer DE, Fitzsimmons C, Le CT, Hutchings A, Butcher G. Probing of the expression of the low-density lipoprotein receptor in vivo using an anti-receptor monoclonal antibody. *Biochem J* 1991 November 15;280 (Pt 1):1-7.

(32) Soutar AK, Knight BL. Structure and regulation of the LDL-receptor and its gene. *Br Med Bull* 1990 October;46(4):891-916.

(33) Catapano AL. The low density lipoprotein receptor: structure, function and pharmacological modulation. *Pharmacol Ther* 1989;43(2):187-219.

(34) Rawson RB. The SREBP pathway--insights from Insigs and insects. *Nat Rev Mol Cell Biol* 2003 August;4(8):631-40.

(35) Horton JD, Goldstein JL, Brown MS. SREBPs: activators of the complete

program of cholesterol and fatty acid synthesis in the liver. *J Clin Invest* 2002 May;109(9):1125-31.

(36) Hua X, Sakai J, Ho YK, Goldstein JL, Brown MS. Hairpin orientation of sterol regulatory element-binding protein-2 in cell membranes as determined by protease protection. *J Biol Chem* 1995 December 8;270(49):29422-7.

(37) Nohturfft A, DeBose-Boyd RA, Scheek S, Goldstein JL, Brown MS. Sterols regulate cycling of SREBP cleavage-activating protein (SCAP) between endoplasmic reticulum and Golgi. *Proc Natl Acad Sci U S A* 1999 September 28;96(20):11235-40.

(38) Yang T, Espenshade PJ, Wright ME, Yabe D, Gong Y, Aebersold R, Goldstein JL, Brown MS. Crucial step in cholesterol homeostasis: sterols promote binding of SCAP to INSIG-1, a membrane protein that facilitates retention of SREBPs in ER. *Cell* 2002 August 23;110(4):489-500.

(39) Yabe D, Brown MS, Goldstein JL. Insig-2, a second endoplasmic reticulum protein that binds SCAP and blocks export of sterol regulatory element-binding proteins. *Proc Natl Acad Sci U S A* 2002 October 1;99(20):12753-8.

(40) Radhakrishnan A, Sun LP, Kwon HJ, Brown MS, Goldstein JL. Direct binding of cholesterol to the purified membrane region of SCAP: mechanism for a sterol-sensing domain. *Mol Cell* 2004 July 23;15(2):259-68.

(41) Brown AJ, Sun L, Feramisco JD, Brown MS, Goldstein JL. Cholesterol addition to ER membranes alters conformation of SCAP, the SREBP escort protein that regulates cholesterol metabolism. *Mol Cell* 2002 August;10(2):237-45.

(42) Adams CM, Goldstein JL, Brown MS. Cholesterol-induced conformational change in SCAP enhanced by Insig proteins and mimicked by cationic amphiphiles. *Proc Natl Acad Sci U S A* 2003 September 16;100(19):10647-52.

(43) Corsini A, Bellosta S, Baetta R, Fumagalli R, Paoletti R, Bernini F. New insights into the pharmacodynamic and pharmacokinetic properties of statins. *Pharmacol Ther* 1999 December;84(3):413-28.

(44) Arito M, Horiba T, Hachimura S, Inoue J, Sato R. Growth factor-induced phosphorylation of sterol regulatory element-binding proteins inhibits sumoylation, thereby stimulating the expression of their target genes, low density lipoprotein uptake, and lipid synthesis. *J Biol Chem* 2008 May 30;283(22):15224-31.

(45) Liu J, Briggs MR, Kraemer FB. Elucidation of an SRE-1/SREBP-independent cellular pathway for LDL-receptor regulation: from the cell surface to the nucleus. *Future Cardiol* 2006 September;2(5):605-12.

(46) Kong WJ, Liu J, Jiang JD. Human low-density lipoprotein receptor gene and its regulation. *J Mol Med (Berl)* 2006 January;84(1):29-36.

(47) Chen Y, Ruan XZ, Li Q, Huang A, Moorhead JF, Powis SH, Varghese Z. Inflammatory cytokines disrupt LDL-receptor feedback regulation and cause statin resistance: a comparative study in human hepatic cells and mesangial cells. *Am J Physiol Renal Physiol* 2007 September;293(3):F680-F687.

(48) Abifadel M, Varret M, Rabes JP, Allard D, Ouguerram K, Devillers M, Cruaud C, Benjannet S, Wickham L, Erlich D, Derre A, Villeger L, Farnier M, Beucler I, Bruckert E, Chambaz J, Chanu B, Lecerf JM, Luc G, Moulin P, Weissenbach J, Prat A, Krempf M, Junien C, Seidah NG, Boileau C. Mutations in PCSK9 cause autosomal dominant hypercholesterolemia. *Nat Genet* 2003 June;34(2):154-6.

(49) Zelcer N, Hong C, Boyadjian R, Tontonoz P. LXR regulates cholesterol uptake through Idol-dependent ubiquitination of the LDL receptor. *Science* 2009 July 3;325(5936):100-4.

(50) Seidah NG, Benjannet S, Wickham L, Marcinkiewicz J, Jasmin SB, Stifani S, Basak A, Prat A, Chretien M. The secretory proprotein convertase neural apoptosis-regulated convertase 1 (NARC-1): liver regeneration and neuronal differentiation. *Proc Natl Acad Sci U S A* 2003 February 4;100(3):928-33.

(51) Zhang DW, Lagace TA, Garuti R, Zhao Z, McDonald M, Horton JD, Cohen JC, Hobbs HH. Binding of proprotein convertase subtilisin/kexin type 9 to epidermal growth factor-like repeat A of low density lipoprotein receptor decreases receptor recycling and increases degradation. *J Biol Chem* 2007 June 22;282(25):18602-12.

(52) McNutt MC, Kwon HJ, Chen C, Chen JR, Horton JD, Lagace TA. Antagonism of secreted PCSK9 increases low density lipoprotein receptor expression in HepG2 cells. *J Biol Chem* 2009 April 17;284(16):10561-70.

(53) Timms KM, Wagner S, Samuels ME, Forbey K, Goldfine H, Jammulapati S, Skolnick MH, Hopkins PN, Hunt SC, Shattuck DM. A mutation in PCSK9 causing autosomal-dominant hypercholesterolemia in a Utah pedigree. *Hum Genet* 2004 March;114(4):349-53.

(54) Cohen JC, Boerwinkle E, Mosley TH, Jr., Hobbs HH. Sequence variations in PCSK9, low LDL, and protection against coronary heart disease. *N Engl J Med* 2006 March 23;354(12):1264-72.

(55) Cohen J, Pertsemlidis A, Kotowski IK, Graham R, Garcia CK, Hobbs HH. Low LDL cholesterol in individuals of African descent resulting from frequent nonsense mutations in PCSK9. *Nat Genet* 2005 February;37(2):161-5.

(56) Jeong HJ, Lee HS, Kim KS, Kim YK, Yoon D, Park SW. Sterol-dependent regulation of proprotein convertase subtilisin/kexin type 9 expression by sterol-regulatory element binding protein-2. *J Lipid Res* 2008 February;49(2):399-409.

(57) Cao A, Wu M, Li H, Liu J. Janus kinase activation by cytokine oncostatin M decreases PCSK9 expression in liver cells. *J Lipid Res* 2011 March;52(3):518-30.

(58) Russell DW, Brown MS, Goldstein JL. Different combinations of cysteine-rich repeats mediate binding of low density lipoprotein receptor to two different proteins. *J Biol Chem* 1989 December 25;264(36):21682-8.

(59) Esser V, Limbird LE, Brown MS, Goldstein JL, Russell DW. Mutational analysis of the ligand binding domain of the low density lipoprotein receptor. *J Biol Chem* 1988 September 15;263(26):13282-90.

(60) Soutar AK. Intracellular transport of the low-density lipoprotein receptor. *Biochem Soc Trans* 1996 May;24(2):547-52.

(61) Spady DK. Hepatic clearance of plasma low density lipoproteins. *Semin Liver Dis* 1992 November;12(4):373-85.

(62) Hobbs HH, Russell DW, Brown MS, Goldstein JL. The LDL receptor locus in familial hypercholesterolemia: mutational analysis of a membrane protein. *Annu Rev Genet* 1990;24:133-70.

(63) Whitfield AJ, Barrett PH, van Bockxmeer FM, Burnett JR. Lipid disorders and mutations in the APOB gene. *Clin Chem* 2004 October;50(10):1725-32.

(64) Jeon H, Blacklow SC. Structure and physiologic function of the low-density lipoprotein receptor. *Annu Rev Biochem* 2005;74:535-62.

(65) Garcia CK, Wilund K, Arca M, Zuliani G, Fellin R, Maioli M, Calandra S, Bertolini S, Cossu F, Grishin N, Barnes R, Cohen JC, Hobbs HH. Autosomal recessive hypercholesterolemia caused by mutations in a putative LDL receptor adaptor protein. *Science* 2001 May 18;292(5520):1394-8.

(66) Eden ER, Patel DD, Sun XM, Burden JJ, Themis M, Edwards M, Lee P, Neuwirth C, Naoumova RP, Soutar AK. Restoration of LDL receptor function in cells from patients with autosomal recessive hypercholesterolemia by retroviral expression of ARH1. *J Clin Invest* 2002 December;110(11):1695-702.

(67) German J, Bloom D, Passarge E. Bloom's syndrome. V. Surveillance for cancer in affected families. *Clin Genet* 1977 September;12(3):162-8.

(68) Herijgers N, Van EM, Groot PH, Hoogerbrugge PM, Van Berkel TJ. Effect of bone marrow transplantation on lipoprotein metabolism and atherosclerosis in LDL receptor-knockout mice. *Arterioscler Thromb Vasc Biol* 1997 October;17(10):1995-2003.

(69) Herz J, Hamann U, Rogne S, Myklebost O, Gausepohl H, Stanley KK. Surface location and high affinity for calcium of a 500-kd liver membrane protein closely related to the LDL-receptor suggest a physiological role as lipoprotein receptor. *EMBO J* 1988 December 20;7(13):4119-27.

(70) Lillis AP, Van Duyn LB, Murphy-Ullrich JE, Strickland DK. LDL receptor-related protein 1: unique tissue-specific functions revealed by selective gene knockout studies. *Physiol Rev* 2008 July;88(3):887-918.

(71) Herz J, Strickland DK. LRP: a multifunctional scavenger and signaling receptor. *J Clin Invest* 2001 September;108(6):779-84.

(72) Beisiegel U, Weber W, Ihrke G, Herz J, Stanley KK. The LDL-receptor-related protein, LRP, is an apolipoprotein E-binding protein. *Nature* 1989 September 14;341(6238):162-4.

(73) May P, Rohlmann A, Bock HH, Zurhove K, Marth JD, Schomburg ED, Noebels JL, Beffert U, Sweatt JD, Weeber EJ, Herz J. Neuronal LRP1 functionally associates with postsynaptic proteins and is required for normal motor function in mice. *Mol Cell Biol* 2004 October;24(20):8872-83.

(74) Rohlmann A, Gotthardt M, Hammer RE, Herz J. Inducible inactivation of hepatic LRP gene by cre-mediated recombination confirms role of LRP in clearance of chylomicron remnants. *J Clin Invest* 1998 February 1;101(3):689-95.

(75) Hofmann SM, Zhou L, Perez-Tilve D, Greer T, Grant E, Wancata L, Thomas A, Pfluger PT, Basford JE, Gilham D, Herz J, Tschop MH, Hui DY. Adipocyte LDL receptor-related protein-1 expression modulates postprandial lipid transport and glucose homeostasis in mice. *J Clin Invest* 2007 November;117(11):3271-82.

(76) Boucher P, Gotthardt M, Li WP, Anderson RG, Herz J. LRP: role in vascular wall integrity and protection from atherosclerosis. *Science* 2003 April 11;300(5617):329-32.

(77) Hu L, Boesten LS, May P, Herz J, Bovenschen N, Huisman MV, Berbee JF, Havekes LM, van Vlijmen BJ, Tamsma JT. Macrophage low-density lipoprotein receptor-related protein deficiency enhances atherosclerosis in ApoE/LDLR double knockout mice. *Arterioscler Thromb Vasc Biol* 2006 December;26(12):2710-5.

(78) Overton CD, Yancey PG, Major AS, Linton MF, Fazio S. Deletion of macrophage LDL receptor-related protein increases atherogenesis in the mouse. *Circ Res* 2007 March 16;100(5):670-7.

(79) Bu G, Geuze HJ, Strous GJ, Schwartz AL. 39 kDa receptor-associated protein is an ER resident protein and molecular chaperone for LDL receptor-related protein. *EMBO J* 1995 May 15;14(10):2269-80.

(80) Willnow TE, Rohlmann A, Horton J, Otani H, Braun JR, Hammer RE, Herz J. RAP, a specialized chaperone, prevents ligand-induced ER retention and degradation of LDL receptor-related endocytic receptors. *EMBO J* 1996 June 3;15(11):2632-9.

(81) Willnow TE, Moehring JM, Inocencio NM, Moehring TJ, Herz J. The low-density-lipoprotein receptor-related protein (LRP) is processed by furin in vivo and in vitro. *Biochem J* 1996 January 1;313 (Pt 1):71-6.

(82) Herz J, Kowal RC, Goldstein JL, Brown MS. Proteolytic processing of the 600 kd low density lipoprotein receptor-related protein (LRP) occurs in a trans-Golgi compartment. *EMBO J* 1990 June;9(6):1769-76.

(83) Kutt H, Herz J, Stanley KK. Structure of the low-density lipoprotein receptor-related protein (LRP) promoter. *Biochim Biophys Acta* 1989 December 22;1009(3):229-36.

(84) Llorente-Cortes V, Otero-Vinas M, Sanchez S, Rodriguez C, Badimon L. Low-density lipoprotein upregulates low-density lipoprotein receptor-related protein expression in vascular smooth muscle cells: possible involvement of sterol regulatory element binding protein-2-dependent mechanism. *Circulation* 2002 December 10;106(24):3104-10.

(85) Llorente-Cortes V, Costales P, Bernues J, Camino-Lopez S, Badimon L. Sterol regulatory element-binding protein-2 negatively regulates low density lipoprotein receptor-related protein transcription. *J Mol Biol* 2006 June 16;359(4):950-60.

(86) Llorente-Cortes V, Royo T, Otero-Vinas M, Berrozpe M, Badimon L. Sterol regulatory element binding proteins downregulate LDL receptor-related protein (LRP1) expression and LRP1-mediated aggregated LDL uptake by human macrophages. *Cardiovasc Res* 2007 June 1;74(3):526-36.

(87) Costales P, Aledo R, Vernia S, Das A, Shah VH, Casado M, Badimon L, Llorente-Cortes V. Selective role of sterol regulatory element binding protein isoforms in aggregated LDL-induced vascular low density lipoprotein receptor-related protein-1 expression. *Atherosclerosis* 2010 December;213(2):458-68.

(88) Hussaini IM, LaMarre J, Lysiak JJ, Karns LR, VandenBerg SR, Gonias SL. Transcriptional regulation of LDL receptor-related protein by IFN-gamma and the antagonistic activity of TGF-beta(1) in the RAW 264.7 macrophage-like cell line. *J Leukoc Biol* 1996 May;59(5):733-9.

(89) Ko KW, Avramoglu RK, McLeod RS, Vukmirica J, Yao Z. The insulin-stimulated cell surface presentation of low density lipoprotein receptor-related protein in 3T3-L1 adipocytes is sensitive to phosphatidylinositide 3-kinase inhibition. *Biochemistry* 2001 January 23;40(3):752-9.

(90) Zhang H, Links PH, Ngsee JK, Tran K, Cui Z, Ko KW, Yao Z. Localization of low density lipoprotein receptor-related protein 1 to caveolae in 3T3-L1 adipocytes in response to insulin treatment. *J Biol Chem* 2004 January 16;279(3):2221-30.

(91) Ceschin DG, Sanchez MC, Chiabrando GA. Insulin induces the low density lipoprotein receptor-related protein 1 (LRP1) degradation by the proteasomal system in J774 macrophage-derived cells. *J Cell Biochem* 2009 February 15;106(3):372-80.

(92) Kowal RC, Herz J, Goldstein JL, Esser V, Brown MS. Low density lipoprotein receptor-related protein mediates uptake of cholesteryl esters derived from apoprotein E-enriched lipoproteins. *Proc Natl Acad Sci U S A* 1989 August;86(15):5810-4.

(93) Kuchenhoff A, Harrach-Ruprecht B, Robenek H. Interaction of apo E-containing lipoproteins with the LDL receptor-related protein LRP. *Am J Physiol* 1997 February;272(2 Pt 1):C369-C382.

(94) Beisiegel U, Weber W, Bengtsson-Olivecrona G. Lipoprotein lipase enhances the binding of chylomicrons to low density lipoprotein receptor-related protein. *Proc Natl Acad Sci U S A* 1991 October 1;88(19):8342-6.

(95) Kadowaki H, Patton GM, Robins SJ. Metabolism of high density lipoprotein lipids by the rat liver: evidence for participation of hepatic lipase in the uptake of cholesteryl ester. *J Lipid Res* 1992 November;33(11):1689-98.

(96) Schorsch F, Malle E, Sattler W. Selective uptake of high density lipoprotein-associated cholesterylesters by differentiated Ob1771 adipocytes is modulated by endogenous and exogenous lipoprotein lipase. *FEBS Lett* 1997 September 15;414(3):507-13.

(97) Arai T, Rinninger F, Varban L, Fairchild-Huntress V, Liang CP, Chen W, Seo T, Deckelbaum R, Huszar D, Tall AR. Decreased selective uptake of high density lipoprotein cholesteryl esters in apolipoprotein E knock-out mice. *Proc Natl Acad Sci U S A* 1999 October 12;96(21):12050-5.

(98) Morita SY, Kawabe M, Sakurai A, Okuhira K, Vertut-Doi A, Nakano M, Handa T. Ceramide in lipid particles enhances heparan sulfate proteoglycan and low density lipoprotein receptor-related protein-mediated uptake by macrophages. *J Biol Chem* 2004 June 4;279(23):24355-61.

(99) Llorente-Cortes V, Martinez-Gonzalez J, Badimon L. LDL receptor-related protein mediates uptake of aggregated LDL in human vascular smooth muscle cells. *Arterioscler Thromb Vasc Biol* 2000 June;20(6):1572-9.

(100) Llorente-Cortes V, Otero-Vinas M, Camino-Lopez S, Costales P, Badimon L. Cholesteryl esters of aggregated LDL are internalized by selective uptake in human vascular smooth muscle cells. *Arterioscler Thromb Vasc Biol* 2006 January;26(1):117-23.

(101) Zhu H, Takahashi Y, Xu W, Kawajiri H, Murakami T, Yamamoto M, Iseki S, Iwasaki T, Hattori H, Yoshimoto T. Low density lipoprotein receptor-related protein-mediated membrane translocation of 12/15-lipoxygenase is required for oxidation of low density lipoprotein by macrophages. *J Biol Chem* 2003 April 11;278(15):13350-5.

(102) Xu W, Takahashi Y, Sakashita T, Iwasaki T, Hattori H, Yoshimoto T. Low density lipoprotein receptor-related protein is required for macrophage-mediated oxidation of low density lipoprotein by 12/15-lipoxygenase. *J Biol Chem* 2001 September 28;276(39):36454-9.

(103) Lusis AJ. Atherosclerosis. *Nature* 2000 September 14;407(6801):233-41.

(104) Vassiliou G, McPherson R. A novel efflux-recapture process underlies the mechanism of high-density lipoprotein cholesteryl ester-selective uptake mediated by the low-density lipoprotein receptor-related protein. *Arterioscler Thromb Vasc Biol* 2004 September;24(9):1669-75.

(105) Liu Q, Zerbinatti CV, Zhang J, Hoe HS, Wang B, Cole SL, Herz J, Muglia L, Bu G. Amyloid precursor protein regulates brain apolipoprotein E and cholesterol metabolism through lipoprotein receptor LRP1. *Neuron* 2007 October 4;56(1):66-78.

(106) Zhou L, Choi HY, Li WP, Xu F, Herz J. LRP1 controls cPLA2 phosphorylation, ABCA1 expression and cellular cholesterol export. *PLoS One* 2009;4(8):e6853.

(107) Goldstein JL, Ho YK, Basu SK, Brown MS. Binding site on macrophages that mediates uptake and degradation of acetylated low density lipoprotein, producing massive cholesterol deposition. *Proc Natl Acad Sci U S A* 1979 January;76(1):333-7.

(108) Brown MS, Goldstein JL, Krieger M, Ho YK, Anderson RG. Reversible accumulation of cholesteryl esters in macrophages incubated with acetylated lipoproteins. *J Cell Biol* 1979 September;82(3):597-613.

(109) Dhaliwal BS, Steinbrecher UP. Scavenger receptors and oxidized low density lipoproteins. *Clin Chim Acta* 1999 August;286(1-2):191-205.

(110) Zingg JM, Ricciarelli R, Azzi A. Scavenger receptor regulation and atherosclerosis. *Biofactors* 2000;11(3):189-200.

(111) Babitt J, Trigatti B, Rigotti A, Smart EJ, Anderson RG, Xu S, Krieger M. Murine SR-BI, a high density lipoprotein receptor that mediates selective lipid uptake, is N-glycosylated and fatty acylated and colocalizes with plasma membrane caveolae. *J Biol Chem* 1997 May 16;272(20):13242-9.

(112) Acton S, Rigotti A, Landschulz KT, Xu S, Hobbs HH, Krieger M. Identification of scavenger receptor SR-BI as a high density lipoprotein receptor. *Science* 1996 January 26;271(5248):518-20.

(113) Rigotti A, Miettinen HE, Krieger M. The role of the high-density lipoprotein receptor SR-BI in the lipid metabolism of endocrine and other tissues. *Endocr Rev* 2003 June;24(3):357-87.

(114) Lopez D, McLean MP. Sterol regulatory element-binding protein-1a binds to cis elements in the promoter of the rat high density lipoprotein receptor SR-BI gene. *Endocrinology* 1999 December;140(12):5669-81.

(115) Niemeier A, Kovacs WJ, Strobl W, Stangl H. Atherogenic diet leads to posttranslational down-regulation of murine

hepatocyte SR-BI expression. *Atherosclerosis* 2009 January;202(1):169-75.

(116) Martin G, Pilon A, Albert C, Valle M, Hum DW, Fruchart JC, Najib J, Clavey V, Staels B. Comparison of expression and regulation of the high-density lipoprotein receptor SR-BI and the low-density lipoprotein receptor in human adrenocortical carcinoma NCI-H295 cells. *Eur J Biochem* 1999 April;261(2):481-91.

(117) Schoonjans K, Annicotte JS, Huby T, Botrugno OA, Fayard E, Ueda Y, Chapman J, Auwerx J. Liver receptor homolog 1 controls the expression of the scavenger receptor class B type I. *EMBO Rep* 2002 December;3(12):1181-7.

(118) Chinetti G, Gbaguidi FG, Griglio S, Mallat Z, Antonucci M, Poulain P, Chapman J, Fruchart JC, Tedgui A, Najib-Fruchart J, Staels B. CLA-1/SR-BI is expressed in atherosclerotic lesion macrophages and regulated by activators of peroxisome proliferator-activated receptors. *Circulation* 2000 May 23;101(20):2411-7.

(119) Mardones P, Pilon A, Bouly M, Duran D, Nishimoto T, Arai H, Kozarsky KF, Altayo M, Miquel JF, Luc G, Clavey V, Staels B, Rigotti A. Fibrates down-regulate hepatic scavenger receptor class B type I protein expression in mice. *J Biol Chem* 2003 March 7;278(10):7884-90.

(120) Fu T, Kozarsky KF, Borensztajn J. Overexpression of SR-BI by adenoviral vector reverses the fibrateinduced hypercholesterolemia of apolipoprotein E-deficient mice. *J Biol Chem* 2003 December 26;278(52):52559-63.

(121) Wood P, Mulay V, Darabi M, Chan KC, Heeren J, Pol A, Lambert G, Rye KA, Enrich C, Grewal T. Ras/Mitogen-activated Protein Kinase (MAPK) Signaling Modulates Protein Stability and Cell Surface Expression of Scavenger Receptor SR-BI. *J Biol Chem* 2011 July 1;286(26):23077-92.

(122) Greaves DR, Gough PJ, Gordon S. Recent progress in defining the role of scavenger receptors in lipid transport, atherosclerosis and host defence. *Curr Opin Lipidol* 1998 October;9(5):425-32.

(123) Greaves DR, Gordon S. Thematic review series: the immune system and atherogenesis. Recent insights into the biology of macrophage scavenger receptors. *J Lipid Res* 2005 January;46(1):11-20.

(124) Kocher O, Yesilaltay A, Cirovic C, Pal R, Rigotti A, Krieger M. Targeted disruption of the PDZK1 gene in mice causes tissue-specific depletion of the high density lipoprotein receptor scavenger receptor class B type I and altered lipoprotein metabolism. *J Biol Chem* 2003 December 26;278(52):52820-5.

(125) Silver DL, Wang N, Vogel S. Identification of small PDZK1-associated protein, DD96/MAP17, as a regulator of PDZK1 and plasma high density lipoprotein levels. *J Biol Chem* 2003 August 1;278(31):28528-32.

(126) Ueda Y, Royer L, Gong E, Zhang J, Cooper PN, Francone O, Rubin EM. Lower plasma levels and accelerated clearance of high density lipoprotein (HDL) and non-HDL cholesterol in scavenger receptor class B type I transgenic mice. *J Biol Chem* 1999 March 12;274(11):7165-71.

(127) Ji Y, Wang N, Ramakrishnan R, Sehayek E, Huszar D, Breslow JL, Tall AR. Hepatic scavenger receptor BI promotes rapid clearance of high density lipoprotein free cholesterol and its transport into bile. *J Biol Chem* 1999 November 19;274(47):33398-402.

(128) Kozarsky KF, Donahee MH, Rigotti A, Iqbal SN, Edelman ER, Krieger M. Overexpression of the HDL receptor SR-BI alters plasma HDL and bile cholesterol levels. *Nature* 1997 May 22;387(6631):414-7.

(129) Wang N, Arai T, Ji Y, Rinninger F, Tall AR. Liver-specific overexpression of scavenger receptor BI decreases levels of very low density lipoprotein ApoB, low density lipoprotein ApoB, and high density lipoprotein in transgenic mice. *J Biol Chem* 1998 December 4;273(49):32920-6.

(130) Varban ML, Rinninger F, Wang N, Fairchild-Huntress V, Dunmore JH, Fang Q, Gosselin ML, Dixon KL, Deeds JD, Acton SL, Tall AR, Huszar D. Targeted mutation reveals a central role for SR-BI in hepatic selective uptake of high density lipoprotein cholesterol. *Proc Natl Acad Sci U S A* 1998 April 14;95(8):4619-24.

(131) Rigotti A, Trigatti BL, Penman M, Rayburn H, Herz J, Krieger M. A targeted mutation in the murine gene encoding the high density lipoprotein (HDL) receptor scavenger receptor class B type I reveals its key role in HDL metabolism. *Proc Natl Acad Sci U S A* 1997 November 11;94(23):12610-5.

(132) Trigatti B, Rayburn H, Vinals M, Braun A, Miettinen H, Penman M, Hertz M, Schrenzel M, Amigo L, Rigotti A, Krieger M. Influence of the high density lipoprotein receptor SR-BI on reproductive and cardiovascular pathophysiology. *Proc Natl Acad Sci U S A* 1999 August 3;96(16):9322-7.

(133) Acton S, Osgood D, Donoghue M, Corella D, Pocovi M, Cenarro A, Mozas P, Keilty J, Squazzo S, Woolf EA, Ordovas JM. Association of polymorphisms at the SR-BI gene locus with plasma lipid levels and body mass index in a white population. *Arterioscler Thromb Vasc Biol* 1999 July;19(7):1734-43.

(134) Hsu LA, Ko YL, Wu S, Teng MS, Peng TY, Chen CF, Chen CF, Lee YS. Association between a novel 11-base pair deletion mutation in the promoter region of the scavenger receptor class B type I gene and plasma HDL cholesterol levels in Taiwanese Chinese. *Arterioscler Thromb Vasc Biol* 2003 October 1;23(10):1869-74.

(135) Roberts CG, Shen H, Mitchell BD, Damcott CM, Shuldiner AR, Rodriguez A. Variants in scavenger receptor class B type I gene are associated with HDL cholesterol levels in younger women. *Hum Hered* 2007;64(2):107-13.

(136) Teslovich TM, Musunuru K, Smith AV, Edmondson AC, Stylianou IM, Koseki M, Pirruccello JP, Ripatti S, Chasman DI, Willer CJ, Johansen CT, Fouchier SW, Isaacs A, Peloso GM, Barbalic M, Ricketts SL, Bis JC, Aulchenko YS, Thorleifsson G, Feitosa MF, Chambers J, Orho-Melander M, Melander O, Johnson T, Li X, Guo X, Li M, Shin CY, Jin GM, Jin KY, Lee JY, Park T, Kim K, Sim X, Twee-Hee OR, Croteau-Chonka DC, Lange LA, Smith JD, Song K, Hua ZJ, Yuan X, Luan J, Lamina C, Ziegler A, Zhang W, Zee RY, Wright AF, Witteman JC, Wilson JF, Willemsen G, Wichmann HE, Whitfield JB, Waterworth DM, Wareham NJ, Waeber G, Vollenweider P, Voight BF, Vitart V, Uitterlinden AG, Uda M, Tuomilehto J, Thompson JR, Tanaka T, Surakka I, Stringham HM, Spector TD, Soranzo N, Smit JH, Sinisalo J, Silander K, Sijbrands EJ, Scuteri A, Scott J, Schlessinger D, Sanna S, Salomaa V, Saharinen J, Sabatti C, Ruokonen A, Rudan I, Rose LM, Roberts R, Rieder M, Psaty BM, Pramstaller PP, Pichler I, Perola M, Penninx BW, Pedersen NL, Pattaro C, Parker AN, Pare G, Oostra BA, O'Donnell CJ, Nieminen MS, Nickerson DA, Montgomery GW, Meitinger T, McPherson R, McCarthy MI, McArdle W, Masson D, Martin NG, Marroni F, Mangino M, Magnusson PK, Lucas G, Luben R, Loos RJ, Lokki ML, Lettre G, Langenberg C, Launer LJ, Lakatta EG, Laaksonen R, Kyvik KO, Kronenberg F, Konig IR, Khaw KT, Kaprio J, Kaplan LM, Johansson A, Jarvelin MR, Janssens AC, Ingelsson E, Igl W, Kees HG, Hottenga JJ, Hofman A, Hicks AA, Hengstenberg C, Heid IM, Hayward C, Havulinna AS, Hastie ND, Harris TB, Haritunians T, Hall AS, Gyllensten U, Guiducci C, Groop LC, Gonzalez E, Gieger C, Freimer NB, Ferrucci L, Erdmann J, Elliott P, Ejebe KG, Doring A, Dominiczak AF, Demissie S, Deloukas P, de Geus EJ, de FU, Crawford G, Collins FS, Chen YD, Caulfield MJ, Campbell H, Burtt NP, Bonnycastle LL, Boomsma DI, Boekholdt SM, Bergman RN, Barroso I, Bandinelli S, Ballantyne CM, Assimes TL, Quertermous T, Altshuler D, Seielstad M, Wong TY, Tai ES, Feranil AB, Kuzawa CW, Adair LS, Taylor HA, Jr., Borecki IB, Gabriel SB, Wilson JG, Holm H, Thorsteinsdottir U, Gudnason V, Krauss RM, Mohlke KL, Ordovas JM, Munroe PB, Kooner JS, Tall AR, Hegele RA, Kastelein JJ, Schadt EE, Rotter JI, Boerwinkle E, Strachan DP, Mooser V, Stefansson K, Reilly MP, Samani NJ, Schunkert H, Cupples LA, Sandhu MS, Ridker PM, Rader DJ, van Duijn CM, Peltonen L, Abecasis GR, Boehnke M, Kathiresan S. Biological, clinical and population relevance of 95 loci for blood lipids. *Nature* 2010 August 5;466(7307):707-13.

(137) Vergeer M, Korporaal SJ, Franssen R, Meurs I, Out R, Hovingh GK, Hoekstra M, Sierts JA, Dallinga-Thie GM, Motazacker MM, Holleboom AG, Van Berkel TJ, Kastelein JJ, Van EM, Kuivenhoven JA. Genetic variant of the scavenger receptor BI in humans. *N Engl J Med* 2011 January 13;364(2):136-45.

(138) Out R, Hoekstra M, Spijkers JA, Kruijt JK, Van EM, Bos IS, Twisk J, Van Berkel TJ. Scavenger receptor class B type I is solely responsible for the selective uptake of cholesteryl esters from HDL by the liver and the adrenals in mice. *J Lipid Res* 2004 November;45(11):2088-95.

(139) Brundert M, Ewert A, Heeren J, Behrendt B, Ramakrishnan R, Greten H, Merkel M, Rinninger F. Scavenger receptor class B type I mediates the selective uptake of high-density lipoprotein-associated cholesteryl ester by the liver in mice. *Arterioscler Thromb Vasc Biol* 2005 January;25(1):143-8.

(140) Gu X, Trigatti B, Xu S, Acton S, Babitt J, Krieger M. The efficient cellular uptake of high density lipoprotein lipids via scavenger receptor class B type I requires not only receptor-mediated surface binding but also receptor-specific lipid transfer mediated by its extracellular domain. *J Biol Chem* 1998 October 9;273(41):26338-48.

(141) Temel RE, Walzem RL, Banka CL, Williams DL. Apolipoprotein A-I is necessary for the in vivo formation of high density lipoprotein competent for scavenger

receptor BI-mediated cholesteryl ester-selective uptake. *J Biol Chem* 2002 July 19;277(29):26565-72.

(142) Temel RE, Parks JS, Williams DL. Enhancement of scavenger receptor class B type I-mediated selective cholesteryl ester uptake from apoA-I(-/-) high density lipoprotein (HDL) by apolipoprotein A-I requires HDL reorganization by lecithin cholesterol acyltransferase. *J Biol Chem* 2003 February 14;278(7):4792-9.

(143) Thuahnai ST, Lund-Katz S, Dhanasekaran P, Llera-Moya M, Connelly MA, Williams DL, Rothblat GH, Phillips MC. Scavenger receptor class B type I-mediated cholesteryl ester-selective uptake and efflux of unesterified cholesterol. Influence of high density lipoprotein size and structure. *J Biol Chem* 2004 March 26;279(13):12448-55.

(144) Papale GA, Nicholson K, Hanson PJ, Pavlovic M, Drover VA, Sahoo D. Extracellular hydrophobic regions in scavenger receptor BI play a key role in mediating HDL-cholesterol transport. *Arch Biochem Biophys* 2010 April 15;496(2):132-9.

(145) Papale GA, Hanson PJ, Sahoo D. Extracellular disulfide bonds support scavenger receptor class B type I-mediated cholesterol transport. *Biochemistry* 2011 July 19;50(28):6245-54.

(146) Rigotti A, Trigatti B, Babitt J, Penman M, Xu S, Krieger M. Scavenger receptor BI--a cell surface receptor for high density lipoprotein. *Curr Opin Lipidol* 1997 June;8(3):181-8.

(147) Connelly MA, Klein SM, Azhar S, Abumrad NA, Williams DL. Comparison of class B scavenger receptors, CD36 and scavenger receptor BI (SR-BI), shows that both receptors mediate high density lipoprotein-cholesteryl ester selective uptake but SR-BI exhibits a unique enhancement of cholesteryl ester uptake. *J Biol Chem* 1999 January 1;274(1):41-7.

(148) Vinals M, Xu S, Vasile E, Krieger M. Identification of the N-linked glycosylation sites on the high density lipoprotein (HDL) receptor SR-BI and assessment of their effects on HDL binding and selective lipid uptake. *J Biol Chem* 2003 February 14;278(7):5325-32.

(149) Nieland TJ, Penman M, Dori L, Krieger M, Kirchhausen T. Discovery of chemical inhibitors of the selective transfer of lipids mediated by the HDL receptor SR-BI. *Proc Natl Acad Sci U S A* 2002 November 26;99(24):15422-7.

(150) Liu B, Krieger M. Highly purified scavenger receptor class B, type I reconstituted into phosphatidylcholine/cholesterol liposomes mediates high affinity high density lipoprotein binding and selective lipid uptake. *J Biol Chem* 2002 September 13;277(37):34125-35.

(151) Silver DL, Wang N, Xiao X, Tall AR. High density lipoprotein (HDL) particle uptake mediated by scavenger receptor class B type 1 results in selective sorting of HDL cholesterol from protein and polarized cholesterol secretion. *J Biol Chem* 2001 July 6;276(27):25287-93.

(152) Rhainds D, Bourgeois P, Bourret G, Huard K, Falstrault L, Brissette L. Localization and regulation of SR-BI in membrane rafts of HepG2 cells. *J Cell Sci* 2004 July 1;117(Pt 15):3095-105.

(153) Sparrow CP, Pittman RC. Cholesterol esters selectively taken up from high-density lipoproteins are hydrolyzed extralysosomally. *Biochim Biophys Acta* 1990 April 2;1043(2):203-10.

(154) Shimada A, Tamai T, Oida K, Takahashi S, Suzuki J, Nakai T, Miyabo S. Increase in neutral cholesteryl ester hydrolase activity produced by extralysosomal hydrolysis of high-density lipoprotein cholesteryl esters in rat hepatoma cells (H-35). *Biochim Biophys Acta* 1994 November 17;1215(1-2):126-32.

(155) Delamatre JG, Carter RM, Hornick CA. Evidence that a neutral cholesteryl ester hydrolase is responsible for the extralysosomal hydrolysis of high-density lipoprotein cholesteryl ester in rat hepatoma cells (Fu5AH). *J Cell Physiol* 1993 October;157(1):164-8.

(156) Brown MS, Goldstein JL. A receptor-mediated pathway for cholesterol homeostasis. *Science* 1986 April 4;232(4746):34-47.

(157) Goldstein JL, Brown MS, Anderson RG, Russell DW, Schneider WJ. Receptor-mediated endocytosis: concepts emerging from the LDL receptor system. *Annu Rev Cell Biol* 1985;1:1-39.

(158) Wiersma H, Nijstad N, Gautier T, Iqbal J, Kuipers F, Hussain MM, Tietge UJ. Scavenger receptor BI facilitates hepatic very low density lipoprotein production in mice. *J Lipid Res* 2010 March;51(3):544-53.

(159) Calvo D, Gomez-Coronado D, Lasuncion MA, Vega MA. CLA-1 is an 85-kD plasma membrane glycoprotein that acts as a high-affinity receptor for both native (HDL, LDL, and VLDL) and modified (OxLDL and AcLDL) lipoproteins. *Arterioscler Thromb Vasc Biol* 1997 November;17(11):2341-9.

(160) Stangl H, Hyatt M, Hobbs HH. Transport of lipids from high and low density

lipoproteins via scavenger receptor-BI. *J Biol Chem* 1999 November 12;274(46):32692-8.

(161) Gu X, Lawrence R, Krieger M. Dissociation of the high density lipoprotein and low density lipoprotein binding activities of murine scavenger receptor class B type I (mSR-BI) using retrovirus library-based activity dissection. *J Biol Chem* 2000 March 31;275(13):9120-30.

(162) Van EM, Hoekstra M, Out R, Bos IS, Kruijt JK, Hildebrand RB, Van Berkel TJ. Scavenger receptor BI facilitates the metabolism of VLDL lipoproteins in vivo. *J Lipid Res* 2008 January;49(1):136-46.

(163) Rohrl C, Fruhwurth S, Schreier SM, Lohninger A, Dolischka A, Huttinger M, Zemann N, Hermann M, Strobl W, Stangl H. Scavenger receptor, Class B, Type I provides an alternative means for beta-VLDL uptake independent of the LDL receptor in tissue culture. *Biochim Biophys Acta* 2010 February;1801(2):198-204.

(164) Huszar D, Varban ML, Rinninger F, Feeley R, Arai T, Fairchild-Huntress V, Donovan MJ, Tall AR. Increased LDL cholesterol and atherosclerosis in LDL receptor-deficient mice with attenuated expression of scavenger receptor B1. *Arterioscler Thromb Vasc Biol* 2000 April;20(4):1068-73.

(165) Kozarsky KF, Donahee MH, Glick JM, Krieger M, Rader DJ. Gene transfer and hepatic overexpression of the HDL receptor SR-BI reduces atherosclerosis in the cholesterol-fed LDL receptor-deficient mouse. *Arterioscler Thromb Vasc Biol* 2000 March;20(3):721-7.

(166) Out R, Kruijt JK, Rensen PC, Hildebrand RB, de VP, Van EM, Van Berkel TJ. Scavenger receptor BI plays a role in facilitating chylomicron metabolism. *J Biol Chem* 2004 April 30;279(18):18401-6.

(167) Beaslas O, Cueille C, Delers F, Chateau D, Chambaz J, Rousset M, Carriere V. Sensing of dietary lipids by enterocytes: a new role for SR-BI/CLA-1. *PLoS One* 2009;4(1):e4278.

(168) Bietrix F, Yan D, Nauze M, Rolland C, Bertrand-Michel J, Comera C, Schaak S, Barbaras R, Groen AK, Perret B, Terce F, Collet X. Accelerated lipid absorption in mice overexpressing intestinal SR-BI. *J Biol Chem* 2006 March 17;281(11):7214-9.

(169) Perez-Martinez P, Ordovas JM, Lopez-Miranda J, Gomez P, Marin C, Moreno J, Fuentes F, Fernandez de la Puebla RA, Perez-Jimenez F. Polymorphism exon 1 variant at the locus of the scavenger receptor class B type I gene: influence on plasma LDL cholesterol in healthy subjects during the consumption of diets with different fat contents. *Am J Clin Nutr* 2003 April;77(4):809-13.

(170) Osgood D, Corella D, Demissie S, Cupples LA, Wilson PW, Meigs JB, Schaefer EJ, Coltell O, Ordovas JM. Genetic variation at the scavenger receptor class B type I gene locus determines plasma lipoprotein concentrations and particle size and interacts with type 2 diabetes: the framingham study. *J Clin Endocrinol Metab* 2003 June;88(6):2869-79.

(171) Morabia A, Ross BM, Costanza MC, Cayanis E, Flaherty MS, Alvin GB, Das K, James R, Yang AS, Evagrafov O, Gilliam TC. Population-based study of SR-BI genetic variation and lipid profile. *Atherosclerosis* 2004 July;175(1):159-68.

(172) Perez-Martinez P, Lopez-Miranda J, Ordovas JM, Bellido C, Marin C, Gomez P, Paniagua JA, Moreno JA, Fuentes F, Perez-Jimenez F. Postprandial lipemia is modified by the presence of the polymorphism present in the exon 1 variant at the SR-BI gene locus. *J Mol Endocrinol* 2004 February;32(1):237-45.

(173) Acton SL, Scherer PE, Lodish HF, Krieger M. Expression cloning of SR-BI, a CD36-related class B scavenger receptor. *J Biol Chem* 1994 August 19;269(33):21003-9.

(174) Calvo D, Vega MA. Identification, primary structure, and distribution of CLA-1, a novel member of the CD36/LIMPII gene family. *J Biol Chem* 1993 September 5;268(25):18929-35.

(175) Yancey PG, Llera-Moya M, Swarnakar S, Monzo P, Klein SM, Connelly MA, Johnson WJ, Williams DL, Rothblat GH. High density lipoprotein phospholipid composition is a major determinant of the bi-directional flux and net movement of cellular free cholesterol mediated by scavenger receptor BI. *J Biol Chem* 2000 November 24;275(47):36596-604.

(176) Ahras M, Naing T, McPherson R. Scavenger receptor class B type I localizes to a late endosomal compartment. *J Lipid Res* 2008 July;49(7):1569-76.

(177) Van EM, Bos IS, Hildebrand RB, Van Rij BT, Van Berkel TJ. Dual role for scavenger receptor class B, type I on bone marrow-derived cells in atherosclerotic lesion development. *Am J Pathol* 2004 September;165(3):785-94.

(178) Zhao Y, Pennings M, Hildebrand RB, Ye D, Calpe-Berdiel L, Out R, Kjerrulf M, Hurt-Camejo E, Groen AK, Hoekstra M, Jessup W, Chimini G, Van Berkel TJ, Van EM. Enhanced foam cell formation, atherosclerotic lesion development, and

inflammation by combined deletion of ABCA1 and SR-BI in Bone marrow-derived cells in LDL receptor knockout mice on western-type diet. *Circ Res* 2010 December 10;107(12):e20-e31.

(179) Gu X, Kozarsky K, Krieger M. Scavenger receptor class B, type I-mediated [3H]cholesterol efflux to high and low density lipoproteins is dependent on lipoprotein binding to the receptor. *J Biol Chem* 2000 September 29;275(39):29993-30001.

(180) Connelly MA, Llera-Moya M, Monzo P, Yancey PG, Drazul D, Stoudt G, Fournier N, Klein SM, Rothblat GH, Williams DL. Analysis of chimeric receptors shows that multiple distinct functional activities of scavenger receptor, class B, type I (SR-BI), are localized to the extracellular receptor domain. *Biochemistry* 2001 May 1;40(17):5249-59.

(181) Favari E, Calabresi L, Adorni MP, Jessup W, Simonelli S, Franceschini G, Bernini F. Small discoidal pre-beta1 HDL particles are efficient acceptors of cell cholesterol via ABCA1 and ABCG1. *Biochemistry* 2009 November 24;48(46):11067-74.

(182) Llera-Moya M, Rothblat GH, Connelly MA, Kellner-Weibel G, Sakr SW, Phillips MC, Williams DL. Scavenger receptor BI (SR-BI) mediates free cholesterol flux independently of HDL tethering to the cell surface. *J Lipid Res* 1999 March;40(3):575-80.

(183) Pagler TA, Neuhofer A, Laggner H, Strobl W, Stangl H. Cholesterol efflux via HDL resecretion occurs when cholesterol transport out of the lysosome is impaired. *J Lipid Res* 2007 October;48(10):2141-50.

(184) Pagler TA, Rhode S, Neuhofer A, Laggner H, Strobl W, Hinterndorfer C, Volf I, Pavelka M, Eckhardt ER, van der Westhuyzen DR, Schutz GJ, Stangl H. SR-BI-mediated high density lipoprotein (HDL) endocytosis leads to HDL resecretion facilitating cholesterol efflux. *J Biol Chem* 2006 April 21;281(16):11193-204.

(185) Goldberg IJ. Lipoprotein lipase and lipolysis: central roles in lipoprotein metabolism and atherogenesis. *J Lipid Res* 1996 April;37(4):693-707.

(186) Mahley RW, Ji ZS. Remnant lipoprotein metabolism: key pathways involving cell-surface heparan sulfate proteoglycans and apolipoprotein E. *J Lipid Res* 1999 January;40(1):1-16.

(187) Eisenberg S. High density lipoprotein metabolism. *J Lipid Res* 1984 October;25(10):1017-58.

(188) van der Velde AE, Brufau G, Groen AK. Transintestinal cholesterol efflux. *Curr Opin Lipidol* 2010 June;21(3):167-71.

(189) Gotto AM, Jr. High-density lipoproteins: biochemical and metabolic factors. *Am J Cardiol* 1983 August 22;52(4):2B-4B.

(190) Zannis VI, Chroni A, Krieger M. Role of apoA-I, ABCA1, LCAT, and SR-BI in the biogenesis of HDL. *J Mol Med (Berl)* 2006 April;84(4):276-94.

(191) Lewis GF, Rader DJ. New insights into the regulation of HDL metabolism and reverse cholesterol transport. *Circ Res* 2005 June 24;96(12):1221-32.

(192) Timmins JM, Lee JY, Boudyguina E, Kluckman KD, Brunham LR, Mulya A, Gebre AK, Coutinho JM, Colvin PL, Smith TL, Hayden MR, Maeda N, Parks JS. Targeted inactivation of hepatic Abca1 causes profound hypoalphalipoproteinemia and kidney hypercatabolism of apoA-I. *J Clin Invest* 2005 May;115(5):1333-42.

(193) Brunham LR, Kruit JK, Pape TD, Parks JS, Kuipers F, Hayden MR. Tissue-specific induction of intestinal ABCA1 expression with a liver X receptor agonist raises plasma HDL cholesterol levels. *Circ Res* 2006 September 29;99(7):672-4.

(194) Singaraja RR, Van EM, Bissada N, Zimetti F, Collins HL, Hildebrand RB, Hayden A, Brunham LR, Kang MH, Fruchart JC, Van Berkel TJ, Parks JS, Staels B, Rothblat GH, Fievet C, Hayden MR. Both hepatic and extrahepatic ABCA1 have discrete and essential functions in the maintenance of plasma high-density lipoprotein cholesterol levels in vivo. *Circulation* 2006 September 19;114(12):1301-9.

(195) Brunham LR, Kruit JK, Iqbal J, Fievet C, Timmins JM, Pape TD, Coburn BA, Bissada N, Staels B, Groen AK, Hussain MM, Parks JS, Kuipers F, Hayden MR. Intestinal ABCA1 directly contributes to HDL biogenesis in vivo. *J Clin Invest* 2006 April;116(4):1052-62.

(196) Fielding CJ, Fielding PE. Molecular physiology of reverse cholesterol transport. *J Lipid Res* 1995 February;36(2):211-28.

(197) Mulya A, Lee JY, Gebre AK, Thomas MJ, Colvin PL, Parks JS. Minimal lipidation of pre-beta HDL by ABCA1 results in reduced ability to interact with ABCA1. *Arterioscler Thromb Vasc Biol* 2007 August;27(8):1828-36.

(198) Miida T, Kawano M, Fielding CJ, Fielding PE. Regulation of the concentration of pre beta high-density lipoprotein in normal plasma by cell membranes and lecithin-cholesterol acyltransferase activity. *Biochemistry* 1992 November 17;31(45):11112-7.

(199) Dieplinger H, Zechner R, Kostner GM. The in vitro formation of HDL2 during the action of LCAT: the role of triglyceride-rich lipoproteins. *J Lipid Res* 1985 March;26(3):273-82.

(200) Jiang XC, Bruce C, Mar J, Lin M, Ji Y, Francone OL, Tall AR. Targeted mutation of plasma phospholipid transfer protein gene markedly reduces high-density lipoprotein levels. *J Clin Invest* 1999 March;103(6):907-14.

(201) Lusa S, Jauhiainen M, Metso J, Somerharju P, Ehnholm C. The mechanism of human plasma phospholipid transfer protein-induced enlargement of high-density lipoprotein particles: evidence for particle fusion. *Biochem J* 1996 January 1;313 (Pt 1):275-82.

(202) Jiang X, Francone OL, Bruce C, Milne R, Mar J, Walsh A, Breslow JL, Tall AR. Increased prebeta-high density lipoprotein, apolipoprotein AI, and phospholipid in mice expressing the human phospholipid transfer protein and human apolipoprotein AI transgenes. *J Clin Invest* 1996 November 15;98(10):2373-80.

(203) Tall AR. Plasma cholesteryl ester transfer protein. *J Lipid Res* 1993 August;34(8):1255-74.

(204) Patsch JR, Prasad S, Gotto AM, Jr., Bengtsson-Olivecrona G. Postprandial lipemia. A key for the conversion of high density lipoprotein2 into high density lipoprotein3 by hepatic lipase. *J Clin Invest* 1984 December;74(6):2017-23.

(205) Rader DJ, Jaye M. Endothelial lipase: a new member of the triglyceride lipase gene family. *Curr Opin Lipidol* 2000 April;11(2):141-7.

(206) Trigatti B, Rigotti A, Krieger M. The role of the high-density lipoprotein receptor SR-BI in cholesterol metabolism. *Curr Opin Lipidol* 2000 April;11(2):123-31.

(207) de Beer MC, Durbin DM, Cai L, Jonas A, de Beer FC, van der Westhuyzen DR. Apolipoprotein A-I conformation markedly influences HDL interaction with scavenger receptor BI. *J Lipid Res* 2001 February;42(2):309-13.

(208) Wilson HM, Patel JC, Russell D, Skinner ER. Alterations in the concentration of an apolipoprotein E-containing subfraction of plasma high density lipoprotein in coronary heart disease. *Clin Chim Acta* 1993 November 15;220(2):175-87.

(209) Yu L, Gupta S, Xu F, Liverman AD, Moschetta A, Mangelsdorf DJ, Repa JJ, Hobbs HH, Cohen JC. Expression of ABCG5 and ABCG8 is required for regulation of biliary cholesterol secretion. *J Biol Chem* 2005 March 11;280(10):8742-7.

(210) Wakabayashi Y, Lippincott-Schwartz J, Arias IM. Intracellular trafficking of bile salt export pump (ABCB11) in polarized hepatic cells: constitutive cycling between the canalicular membrane and rab11-positive endosomes. *Mol Biol Cell* 2004 July;15(7):3485-96.

(211) Voshol PJ, Havinga R, Wolters H, Ottenhoff R, Princen HM, Oude Elferink RP, Groen AK, Kuipers F. Reduced plasma cholesterol and increased fecal sterol loss in multidrug resistance gene 2 P-glycoprotein-deficient mice. *Gastroenterology* 1998 May;114(5):1024-34.

(212) Kruit JK, Plosch T, Havinga R, Boverhof R, Groot PH, Groen AK, Kuipers F. Increased fecal neutral sterol loss upon liver X receptor activation is independent of biliary sterol secretion in mice. *Gastroenterology* 2005 January;128(1):147-56.

(213) Temel RE, Sawyer JK, Yu L, Lord C, Degirolamo C, McDaniel A, Marshall S, Wang N, Shah R, Rudel LL, Brown JM. Biliary sterol secretion is not required for macrophage reverse cholesterol transport. *Cell Metab* 2010 July 4;12(1):96-102.

(214) Temel RE, Tang W, Ma Y, Rudel LL, Willingham MC, Ioannou YA, Davies JP, Nilsson LM, Yu L. Hepatic Niemann-Pick C1-like 1 regulates biliary cholesterol concentration and is a target of ezetimibe. *J Clin Invest* 2007 July;117(7):1968-78.

(215) Brown JM, Bell TA, III, Alger HM, Sawyer JK, Smith TL, Kelley K, Shah R, Wilson MD, Davis MA, Lee RG, Graham MJ, Crooke RM, Rudel LL. Targeted depletion of hepatic ACAT2-driven cholesterol esterification reveals a non-biliary route for fecal neutral sterol loss. *J Biol Chem* 2008 April 18;283(16):10522-34.

(216) Yu L, Hammer RE, Li-Hawkins J, Von BK, Lutjohann D, Cohen JC, Hobbs HH. Disruption of Abcg5 and Abcg8 in mice reveals their crucial role in biliary cholesterol secretion. *Proc Natl Acad Sci U S A* 2002 December 10;99(25):16237-42.

(217) Vrins CL, van der Velde AE, van den Oever K, Levels JH, Huet S, Oude Elferink RP, Kuipers F, Groen AK. Peroxisome proliferator-activated receptor delta activation leads to increased transintestinal cholesterol efflux. *J Lipid Res* 2009 October;50(10):2046-54.

(218) Fiorucci S, Cipriani S, Baldelli F, Mencarelli A. Bile acid-activated receptors in the treatment of dyslipidemia and related disorders. *Prog Lipid Res* 2010 April;49(2):171-85.

(219) Rahalkar AR, Giffen F, Har B, Ho J, Morrison KM, Hill J, Wang J, Hegele RA, Joy T. Novel LPL mutations associated

with lipoprotein lipase deficiency: two case reports and a literature review. *Can J Physiol Pharmacol* 2009 March;87(3):151-60.

(220) Priore OC, Pisciotta L, Li VG, Sambataro MP, Cantafora A, Bellocchio A, Catapano A, Tarugi P, Bertolini S, Calandra S. Inherited apolipoprotein A-V deficiency in severe hypertriglyceridemia. *Arterioscler Thromb Vasc Biol* 2005 February;25(2):411-7.

(221) Connelly PW. The role of hepatic lipase in lipoprotein metabolism. *Clin Chim Acta* 1999 August;286(1-2):243-55.

(222) Soutar AK, Naoumova RP. Mechanisms of disease: genetic causes of familial hypercholesterolemia. *Nat Clin Pract Cardiovasc Med* 2007 April;4(4):214-25.

(223) Soutar AK, Naoumova RP. Autosomal recessive hypercholesterolemia. *Semin Vasc Med* 2004 August;4(3):241-8.

(224) Tsubakio-Yamamoto K, Nishida M, Nakagawa-Toyama Y, Masuda D, Ohama T, Yamashita S. Current therapy for patients with sitosterolemia--effect of ezetimibe on plant sterol metabolism. *J Atheroscler Thromb* 2010 September 30;17(9):891-900.

(225) Weber C, Schober A, Zernecke A. MicroRNAs in arterial remodelling, inflammation and atherosclerosis. *Curr Drug Targets* 2010 August;11(8):950-6.

(226) Ross R. Atherosclerosis--an inflammatory disease. *N Engl J Med* 1999 January 14;340(2):115-26.

(227) Boren J, Olin K, Lee I, Chait A, Wight TN, Innerarity TL. Identification of the principal proteoglycan-binding site in LDL. A single-point mutation in apo-B100 severely affects proteoglycan interaction without affecting LDL receptor binding. *J Clin Invest* 1998 June 15;101(12):2658-64.

(228) Libby P, Ridker PM, Hansson GK. Progress and challenges in translating the biology of atherosclerosis. *Nature* 2011 May 19;473(7347):317-25.

(229) Gimbrone MA, Jr. Vascular endothelium, hemodynamic forces, and atherogenesis. *Am J Pathol* 1999 July;155(1):1-5.

(230) Jarvilehto M, Tuohimaa P. Vasa vasorum hypoxia: initiation of atherosclerosis. *Med Hypotheses* 2009 July;73(1):40-1.

(231) Cybulsky MI, Jongstra-Bilen J. Resident intimal dendritic cells and the initiation of atherosclerosis. *Curr Opin Lipidol* 2010 October;21(5):397-403.

(232) Munro JM, van der Walt JD, Munro CS, Chalmers JA, Cox EL. An immunohistochemical analysis of human aortic fatty streaks. *Hum Pathol* 1987 April;18(4):375-80.

(233) Walker LN, Reidy MA, Bowyer DE. Morphology and cell kinetics of fatty streak lesion formation in the hypercholesterolemic rabbit. *Am J Pathol* 1986 December;125(3):450-9.

(234) Podrez EA, Febbraio M, Sheibani N, Schmitt D, Silverstein RL, Hajjar DP, Cohen PA, Frazier WA, Hoff HF, Hazen SL. Macrophage scavenger receptor CD36 is the major receptor for LDL modified by monocyte-generated reactive nitrogen species. *J Clin Invest* 2000 April;105(8):1095-108.

(235) Marathe S, Kuriakose G, Williams KJ, Tabas I. Sphingomyelinase, an enzyme implicated in atherogenesis, is present in atherosclerotic lesions and binds to specific components of the subendothelial extracellular matrix. *Arterioscler Thromb Vasc Biol* 1999 November;19(11):2648-58.

(236) Pavoine C, Pecker F. Sphingomyelinases: their regulation and roles in cardiovascular pathophysiology. *Cardiovasc Res* 2009 May 1;82(2):175-83.

(237) Ivandic B, Castellani LW, Wang XP, Qiao JH, Mehrabian M, Navab M, Fogelman AM, Grass DS, Swanson ME, de Beer MC, de BF, Lusis AJ. Role of group II secretory phospholipase A2 in atherosclerosis: 1. Increased atherogenesis and altered lipoproteins in transgenic mice expressing group IIa phospholipase A2. *Arterioscler Thromb Vasc Biol* 1999 May;19(5):1284-90.

(238) Oorni K, Kovanen PT. Lipoprotein modification by secretory phospholipase A(2) enzymes contributes to the initiation and progression of atherosclerosis. *Curr Opin Lipidol* 2009 October;20(5):421-7.

(239) Suzuki H, Kurihara Y, Takeya M, Kamada N, Kataoka M, Jishage K, Ueda O, Sakaguchi H, Higashi T, Suzuki T, Takashima Y, Kawabe Y, Cynshi O, Wada Y, Honda M, Kurihara H, Aburatani H, Doi T, Matsumoto A, Azuma S, Noda T, Toyoda Y, Itakura H, Yazaki Y, Kodama T, . A role for macrophage scavenger receptors in atherosclerosis and susceptibility to infection. *Nature* 1997 March 20;386(6622):292-6.

(240) Febbraio M, Podrez EA, Smith JD, Hajjar DP, Hazen SL, Hoff HF, Sharma K, Silverstein RL. Targeted disruption of the class B scavenger receptor CD36 protects against atherosclerotic lesion development in mice. *J Clin Invest* 2000 April;105(8):1049-56.

(241) Van EM, Bos IS, Kaminski WE, Orso E, Rothe G, Twisk J, Bottcher A, Van Amersfoort ES, Christiansen-Weber TA, Fung-Leung WP, Van Berkel TJ, Schmitz G. Leukocyte ABCA1 controls

susceptibility to atherosclerosis and macrophage recruitment into tissues. *Proc Natl Acad Sci U S A* 2002 April 30;99(9):6298-303.

(242) Out R, Hoekstra M, Hildebrand RB, Kruit JK, Meurs I, Li Z, Kuipers F, Van Berkel TJ, Van EM. Macrophage ABCG1 deletion disrupts lipid homeostasis in alveolar macrophages and moderately influences atherosclerotic lesion development in LDL receptor-deficient mice. *Arterioscler Thromb Vasc Biol* 2006 October;26(10):2295-300.

(243) Out R, Hoekstra M, Habets K, Meurs I, de W, V, Hildebrand RB, Wang Y, Chimini G, Kuiper J, Van Berkel TJ, Van EM. Combined deletion of macrophage ABCA1 and ABCG1 leads to massive lipid accumulation in tissue macrophages and distinct atherosclerosis at relatively low plasma cholesterol levels. *Arterioscler Thromb Vasc Biol* 2008 February;28(2):258-64.

(244) Ross R, Wight TN, Strandness E, Thiele B. Human atherosclerosis. I. Cell constitution and characteristics of advanced lesions of the superficial femoral artery. *Am J Pathol* 1984 January;114(1):79-93.

(245) Davies MJ, Bland JM, Hangartner JR, Angelini A, Thomas AC. Factors influencing the presence or absence of acute coronary artery thrombi in sudden ischaemic death. *Eur Heart J* 1989 March;10(3):203-8.

(246) Smith JD, Trogan E, Ginsberg M, Grigaux C, Tian J, Miyata M. Decreased atherosclerosis in mice deficient in both macrophage colony-stimulating factor (op) and apolipoprotein E. *Proc Natl Acad Sci U S A* 1995 August 29;92(18):8264-8.

(247) Stoneman V, Braganza D, Figg N, Mercer J, Lang R, Goddard M, Bennett M. Monocyte/macrophage suppression in CD11b diphtheria toxin receptor transgenic mice differentially affects atherogenesis and established plaques. *Circ Res* 2007 March 30;100(6):884-93.

(248) Swirski FK, Pittet MJ, Kircher MF, Aikawa E, Jaffer FA, Libby P, Weissleder R. Monocyte accumulation in mouse atherogenesis is progressive and proportional to extent of disease. *Proc Natl Acad Sci U S A* 2006 July 5;103(27):10340-5.

(249) Gosling J, Slaymaker S, Gu L, Tseng S, Zlot CH, Young SG, Rollins BJ, Charo IF. MCP-1 deficiency reduces susceptibility to atherosclerosis in mice that overexpress human apolipoprotein B. *J Clin Invest* 1999 March;103(6):773-8.

(250) Boring L, Gosling J, Cleary M, Charo IF. Decreased lesion formation in CCR2-/- mice reveals a role for chemokines in the initiation of atherosclerosis. *Nature* 1998 August 27;394(6696):894-7.

(251) Ye D, Zhao Y, Hildebrand RB, Singaraja RR, Hayden MR, Van Berkel TJ, Van EM. The dynamics of macrophage infiltration into the arterial wall during atherosclerotic lesion development in low-density lipoprotein receptor knockout mice. *Am J Pathol* 2011 January;178(1):413-22.

(252) Swirski FK, Libby P, Aikawa E, Alcaide P, Luscinskas FW, Weissleder R, Pittet MJ. Ly-6Chi monocytes dominate hypercholesterolemia-associated monocytosis and give rise to macrophages in atheromata. *J Clin Invest* 2007 January;117(1):195-205.

(253) Tacke F, Alvarez D, Kaplan TJ, Jakubzick C, Spanbroek R, Llodra J, Garin A, Liu J, Mack M, van RN, Lira SA, Habenicht AJ, Randolph GJ. Monocyte subsets differentially employ CCR2, CCR5, and CX3CR1 to accumulate within atherosclerotic plaques. *J Clin Invest* 2007 January;117(1):185-94.

(254) Swirski FK, Weissleder R, Pittet MJ. Heterogeneous in vivo behavior of monocyte subsets in atherosclerosis. *Arterioscler Thromb Vasc Biol* 2009 October;29(10):1424-32.

(255) Cheng C, Tempel D, van HR, de Boer HC, Segers D, Huisman M, van Zonneveld AJ, Leenen PJ, van der Steen A, Serruys PW, de CR, Krams R. Shear stress-induced changes in atherosclerotic plaque composition are modulated by chemokines. *J Clin Invest* 2007 March;117(3):616-26.

(256) Kowala MC, Recce R, Beyer S, Gu C, Valentine M. Characterization of atherosclerosis in LDL receptor knockout mice: macrophage accumulation correlates with rapid and sustained expression of aortic MCP-1/JE. *Atherosclerosis* 2000 April;149(2):323-30.

(257) Gordon S, Taylor PR. Monocyte and macrophage heterogeneity. *Nat Rev Immunol* 2005 December;5(12):953-64.

(258) Martinez FO, Helming L, Gordon S. Alternative activation of macrophages: an immunologic functional perspective. *Annu Rev Immunol* 2009;27:451-83.

(259) Chase AJ, Bond M, Crook MF, Newby AC. Role of nuclear factor-kappa B activation in metalloproteinase-1, -3, and -9 secretion by human macrophages in vitro and rabbit foam cells produced in vivo. *Arterioscler Thromb Vasc Biol* 2002 May 1;22(5):765-71.

(260) Gallardo-Soler A, Gomez-Nieto C, Campo ML, Marathe C, Tontonoz P, Castrillo A,

Corraliza I. Arginase I induction by modified lipoproteins in macrophages: a peroxisome proliferator-activated receptor-gamma/delta-mediated effect that links lipid metabolism and immunity. *Mol Endocrinol* 2008 June;22(6):1394-402.

(261) Johnson JL, Newby AC. Macrophage heterogeneity in atherosclerotic plaques. *Curr Opin Lipidol* 2009 October;20(5):370-8.

(262) Khallou-Laschet J, Varthaman A, Fornasa G, Compain C, Gaston AT, Clement M, Dussiot M, Levillain O, Graff-Dubois S, Nicoletti A, Caligiuri G. Macrophage plasticity in experimental atherosclerosis. *PLoS One* 2010;5(1):e8852.

(263) Weber C, Zernecke A, Libby P. The multifaceted contributions of leukocyte subsets to atherosclerosis: lessons from mouse models. *Nat Rev Immunol* 2008 October;8(10):802-15.

(264) Bobryshev YV. Dendritic cells and their role in atherogenesis. *Lab Invest* 2010 July;90(7):970-84.

(265) Bobryshev YV, Taksir T, Lord RS, Freeman MW. Evidence that dendritic cells infiltrate atherosclerotic lesions in apolipoprotein E-deficient mice. *Histol Histopathol* 2001 July;16(3):801-8.

(266) Ozmen J, Bobryshev YV, Lord RS, Ashwell KW. Identification of dendritic cells in aortic atherosclerotic lesions in rats with diet-induced hypercholesterolaemia. *Histol Histopathol* 2002 January;17(1):223-37.

(267) Gautier EL, Huby T, Saint-Charles F, Ouzilleau B, Pirault J, Deswaerte V, Ginhoux F, Miller ER, Witztum JL, Chapman MJ, Lesnik P. Conventional dendritic cells at the crossroads between immunity and cholesterol homeostasis in atherosclerosis. *Circulation* 2009 May 5;119(17):2367-75.

(268) Habets KL, van Puijvelde GH, van Duivenvoorde LM, van Wanrooij EJ, de VP, Tervaert JW, Van Berkel TJ, Toes RE, Kuiper J. Vaccination using oxidized low-density lipoprotein-pulsed dendritic cells reduces atherosclerosis in LDL receptor-deficient mice. *Cardiovasc Res* 2010 February 1;85(3):622-30.

(269) Hermansson A, Johansson DK, Ketelhuth DF, Andersson J, Zhou X, Hansson GK. Immunotherapy with tolerogenic apolipoprotein B-100-loaded dendritic cells attenuates atherosclerosis in hypercholesterolemic mice. *Circulation* 2011 March 15;123(10):1083-91.

(270) Hjerpe C, Johansson D, Hermansson A, Hansson GK, Zhou X. Dendritic cells pulsed with malondialdehyde modified low density lipoprotein aggravate atherosclerosis in Apoe(-/-) mice. *Atherosclerosis* 2010 April;209(2):436-41.

(271) Andersson J, Libby P, Hansson GK. Adaptive immunity and atherosclerosis. *Clin Immunol* 2010 January;134(1):33-46.

(272) Dansky HM, Charlton SA, Harper MM, Smith JD. T and B lymphocytes play a minor role in atherosclerotic plaque formation in the apolipoprotein E-deficient mouse. *Proc Natl Acad Sci U S A* 1997 April 29;94(9):4642-6.

(273) Ramshaw AL, Parums DV. Immunohistochemical characterization of inflammatory cells associated with advanced atherosclerosis. *Histopathology* 1990 December;17(6):543-52.

(274) Moos MP, John N, Grabner R, Nossmann S, Gunther B, Vollandt R, Funk CD, Kaiser B, Habenicht AJ. The lamina adventitia is the major site of immune cell accumulation in standard chow-fed apolipoprotein E-deficient mice. *Arterioscler Thromb Vasc Biol* 2005 November;25(11):2386-91.

(275) Major AS, Fazio S, Linton MF. B-lymphocyte deficiency increases atherosclerosis in LDL receptor-null mice. *Arterioscler Thromb Vasc Biol* 2002 November 1;22(11):1892-8.

(276) Caligiuri G, Nicoletti A, Poirier B, Hansson GK. Protective immunity against atherosclerosis carried by B cells of hypercholesterolemic mice. *J Clin Invest* 2002 March;109(6):745-53.

(277) Yanaba K, Bouaziz JD, Matsushita T, Magro CM, St Clair EW, Tedder TF. B-lymphocyte contributions to human autoimmune disease. *Immunol Rev* 2008 June;223:284-99.

(278) Lewis MJ, Malik TH, Ehrenstein MR, Boyle JJ, Botto M, Haskard DO. Immunoglobulin M is required for protection against atherosclerosis in low-density lipoprotein receptor-deficient mice. *Circulation* 2009 August 4;120(5):417-26.

(279) Ait-Oufella H, Herbin O, Bouaziz JD, Binder CJ, Uyttenhove C, Laurans L, Taleb S, Van VE, Esposito B, Vilar J, Sirvent J, Van SJ, Tedgui A, Tedder TF, Mallat Z. B cell depletion reduces the development of atherosclerosis in mice. *J Exp Med* 2010 August 2;207(8):1579-87.

(280) Kyaw T, Tay C, Khan A, Dumouchel V, Cao A, To K, Kehry M, Dunn R, Agrotis A, Tipping P, Bobik A, Toh BH. Conventional B2 B cell depletion ameliorates whereas its adoptive transfer aggravates atherosclerosis. *J Immunol* 2010 October 1;185(7):4410-9.

(281) Taleb S, Romain M, Ramkhelawon B, Uyttenhove C, Pasterkamp G, Herbin O, Esposito B, Perez N, Yasukawa H, Van SJ, Yoshimura A, Tedgui A, Mallat Z. Loss of SOCS3 expression in T cells reveals a

regulatory role for interleukin-17 in atherosclerosis. *J Exp Med* 2009 September 28;206(10):2067-77.

(282) Bouaziz JD, Yanaba K, Tedder TF. Regulatory B cells as inhibitors of immune responses and inflammation. *Immunol Rev* 2008 August;224:201-14.

(283) Zernecke A, Liehn EA, Gao JL, Kuziel WA, Murphy PM, Weber C. Deficiency in CCR5 but not CCR1 protects against neointima formation in atherosclerosis-prone mice: involvement of IL-10. *Blood* 2006 June 1;107(11):4240-3.

(284) Mallat Z, Taleb S, Ait-Oufella H, Tedgui A. The role of adaptive T cell immunity in atherosclerosis. *J Lipid Res* 2009 April;50 Suppl:S364-S369.

(285) Hansson GK, Robertson AK, Soderberg-Naucler C. Inflammation and atherosclerosis. *Annu Rev Pathol* 2006;1:297-329.

(286) Zhou X, Nicoletti A, Elhage R, Hansson GK. Transfer of CD4(+) T cells aggravates atherosclerosis in immunodeficient apolipoprotein E knockout mice. *Circulation* 2000 December 12;102(24):2919-22.

(287) Buono C, Binder CJ, Stavrakis G, Witztum JL, Glimcher LH, Lichtman AH. T-bet deficiency reduces atherosclerosis and alters plaque antigen-specific immune responses. *Proc Natl Acad Sci U S A* 2005 February 1;102(5):1596-601.

(288) Gupta S, Pablo AM, Jiang X, Wang N, Tall AR, Schindler C. IFN-gamma potentiates atherosclerosis in ApoE knock-out mice. *J Clin Invest* 1997 June 1;99(11):2752-61.

(289) Whitman SC, Ravisankar P, Elam H, Daugherty A. Exogenous interferon-gamma enhances atherosclerosis in apolipoprotein E-/- mice. *Am J Pathol* 2000 December;157(6):1819-24.

(290) Gerdes N, Sukhova GK, Libby P, Reynolds RS, Young JL, Schonbeck U. Expression of interleukin (IL)-18 and functional IL-18 receptor on human vascular endothelial cells, smooth muscle cells, and macrophages: implications for atherogenesis. *J Exp Med* 2002 January 21;195(2):245-57.

(291) Davenport P, Tipping PG. The role of interleukin-4 and interleukin-12 in the progression of atherosclerosis in apolipoprotein E-deficient mice. *Am J Pathol* 2003 September;163(3):1117-25.

(292) Elhage R, Jawien J, Rudling M, Ljunggren HG, Takeda K, Akira S, Bayard F, Hansson GK. Reduced atherosclerosis in interleukin-18 deficient apolipoprotein E-knockout mice. *Cardiovasc Res* 2003 July 1;59(1):234-40.

(293) Whitman SC, Ravisankar P, Daugherty A. Interleukin-18 enhances atherosclerosis in apolipoprotein E(-/-) mice through release of interferon-gamma. *Circ Res* 2002 February 8;90(2):E34-E38.

(294) Tenger C, Sundborger A, Jawien J, Zhou X. IL-18 accelerates atherosclerosis accompanied by elevation of IFN-gamma and CXCL16 expression independently of T cells. *Arterioscler Thromb Vasc Biol* 2005 April;25(4):791-6.

(295) Huber SA, Sakkinen P, David C, Newell MK, Tracy RP. T helper-cell phenotype regulates atherosclerosis in mice under conditions of mild hypercholesterolemia. *Circulation* 2001 May 29;103(21):2610-6.

(296) Miller AM, Xu D, Asquith DL, Denby L, Li Y, Sattar N, Baker AH, McInnes IB, Liew FY. IL-33 reduces the development of atherosclerosis. *J Exp Med* 2008 February 18;205(2):339-46.

(297) King VL, Szilvassy SJ, Daugherty A. Interleukin-4 deficiency decreases atherosclerotic lesion formation in a site-specific manner in female LDL receptor-/- mice. *Arterioscler Thromb Vasc Biol* 2002 March 1;22(3):456-61.

(298) Mallat Z, Besnard S, Duriez M, Deleuze V, Emmanuel F, Bureau MF, Soubrier F, Esposito B, Duez H, Fievet C, Staels B, Duverger N, Scherman D, Tedgui A. Protective role of interleukin-10 in atherosclerosis. *Circ Res* 1999 October 15;85(8):e17-e24.

(299) Caligiuri G, Rudling M, Ollivier V, Jacob MP, Michel JB, Hansson GK, Nicoletti A. Interleukin-10 deficiency increases atherosclerosis, thrombosis, and low-density lipoproteins in apolipoprotein E knockout mice. *Mol Med* 2003 January;9(1-2):10-7.

(300) Potteaux S, Esposito B, van OO, Brun V, Ardouin P, Groux H, Tedgui A, Mallat Z. Leukocyte-derived interleukin 10 is required for protection against atherosclerosis in low-density lipoprotein receptor knockout mice. *Arterioscler Thromb Vasc Biol* 2004 August;24(8):1474-8.

(301) Smith E, Prasad KM, Butcher M, Dobrian A, Kolls JK, Ley K, Galkina E. Blockade of interleukin-17A results in reduced atherosclerosis in apolipoprotein E-deficient mice. *Circulation* 2010 April 20;121(15):1746-55.

(302) Erbel C, Chen L, Bea F, Wangler S, Celik S, Lasitschka F, Wang Y, Bockler D, Katus HA, Dengler TJ. Inhibition of IL-17A attenuates atherosclerotic lesion development in apoE-deficient mice. *J Immunol* 2009 December 15;183(12):8167-75.

(303) Gao Q, Jiang Y, Ma T, Zhu F, Gao F, Zhang P, Guo C, Wang Q, Wang X, Ma C, Zhang Y, Chen W, Zhang L. A critical function of Th17 proinflammatory cells in the development of atherosclerotic plaque in mice. *J Immunol* 2010 November 15;185(10):5820-7.

(304) Olofsson PS, Soderstrom LA, Wagsater D, Sheikine Y, Ocaya P, Lang F, Rabu C, Chen L, Rudling M, Aukrust P, Hedin U, Paulsson-Berne G, Sirsjo A, Hansson GK. CD137 is expressed in human atherosclerosis and promotes development of plaque inflammation in hypercholesterolemic mice. *Circulation* 2008 March 11;117(10):1292-301.

(305) Gotsman I, Grabie N, Dacosta R, Sukhova G, Sharpe A, Lichtman AH. Proatherogenic immune responses are regulated by the PD-1/PD-L pathway in mice. *J Clin Invest* 2007 October;117(10):2974-82.

(306) Lin J, Li M, Wang Z, He S, Ma X, Li D. The role of CD4+CD25+ regulatory T cells in macrophage-derived foam-cell formation. *J Lipid Res* 2010 May;51(5):1208-17.

(307) Ait-Oufella H, Salomon BL, Potteaux S, Robertson AK, Gourdy P, Zoll J, Merval R, Esposito B, Cohen JL, Fisson S, Flavell RA, Hansson GK, Klatzmann D, Tedgui A, Mallat Z. Natural regulatory T cells control the development of atherosclerosis in mice. *Nat Med* 2006 February;12(2):178-80.

(308) Mor A, Planer D, Luboshits G, Afek A, Metzger S, Chajek-Shaul T, Keren G, George J. Role of naturally occurring CD4+ CD25+ regulatory T cells in experimental atherosclerosis. *Arterioscler Thromb Vasc Biol* 2007 April;27(4):893-900.

(309) van Puijvelde GH, Hauer AD, de VP, van den Heuvel R, van Herwijnen MJ, van der Zee R, van EW, Van Berkel TJ, Kuiper J. Induction of oral tolerance to oxidized low-density lipoprotein ameliorates atherosclerosis. *Circulation* 2006 October 31;114(18):1968-76.

(310) van Puijvelde GH, van ET, van Wanrooij EJ, Habets KL, de VP, van der Zee R, van EW, Van Berkel TJ, Kuiper J. Induction of oral tolerance to HSP60 or an HSP60-peptide activates T cell regulation and reduces atherosclerosis. *Arterioscler Thromb Vasc Biol* 2007 December;27(12):2677-83.

(311) Foks AC, Frodermann V, Ter BM, Habets KL, Bot I, Zhao Y, Van EM, Van Berkel TJ, Kuiper J, van Puijvelde GH. Differential effects of regulatory T cells on the initiation and regression of atherosclerosis. *Atherosclerosis* 2011 May 5.

(312) van ET, van Puijvelde GH, Foks AC, Habets KL, Bot I, Gilboa E, Van Berkel TJ, Kuiper J. Vaccination against Foxp3(+) regulatory T cells aggravates atherosclerosis. *Atherosclerosis* 2010 March;209(1):74-80.

(313) Hansson GK, Hermansson A. The immune system in atherosclerosis. *Nat Immunol* 2011 March;12(3):204-12.

(314) Kim J, Zhang L, Peppel K, Wu JH, Zidar DA, Brian L, DeWire SM, Exum ST, Lefkowitz RJ, Freedman NJ. Beta-arrestins regulate atherosclerosis and neointimal hyperplasia by controlling smooth muscle cell proliferation and migration. *Circ Res* 2008 July 3;103(1):70-9.

(315) Orr AW, Hastings NE, Blackman BR, Wamhoff BR. Complex regulation and function of the inflammatory smooth muscle cell phenotype in atherosclerosis. *J Vasc Res* 2010;47(2):168-80.

(316) Clarke MC, Figg N, Maguire JJ, Davenport AP, Goddard M, Littlewood TD, Bennett MR. Apoptosis of vascular smooth muscle cells induces features of plaque vulnerability in atherosclerosis. *Nat Med* 2006 September;12(9):1075-80.

(317) Stary HC, Blankenhorn DH, Chandler AB, Glagov S, Insull W, Jr., Richardson M, Rosenfeld ME, Schaffer SA, Schwartz CJ, Wagner WD, . A definition of the intima of human arteries and of its atherosclerosis-prone regions. A report from the Committee on Vascular Lesions of the Council on Arteriosclerosis, American Heart Association. *Arterioscler Thromb* 1992 January;12(1):120-34.

(318) Stary HC, Chandler AB, Glagov S, Guyton JR, Insull W, Jr., Rosenfeld ME, Schaffer SA, Schwartz CJ, Wagner WD, Wissler RW. A definition of initial, fatty streak, and intermediate lesions of atherosclerosis. A report from the Committee on Vascular Lesions of the Council on Arteriosclerosis, American Heart Association. *Arterioscler Thromb* 1994 May;14(5):840-56.

(319) Stary HC, Chandler AB, Dinsmore RE, Fuster V, Glagov S, Insull W, Jr., Rosenfeld ME, Schwartz CJ, Wagner WD, Wissler RW. A definition of advanced types of atherosclerotic lesions and a histological classification of atherosclerosis. A report from the Committee on Vascular Lesions of the Council on Arteriosclerosis, American Heart Association. *Circulation* 1995 September 1;92(5):1355-74.

(320) Chang MY, Potter-Perigo S, Tsoi C, Chait A, Wight TN. Oxidized low density lipoproteins regulate synthesis of monkey aortic smooth muscle cell proteoglycans

that have enhanced native low density lipoprotein binding properties. *J Biol Chem* 2000 February 18;275(7):4766-73.

(321) Wagsater D, Olofsson PS, Norgren L, Stenberg B, Sirsjo A. The chemokine and scavenger receptor CXCL16/SR-PSOX is expressed in human vascular smooth muscle cells and is induced by interferon gamma. *Biochem Biophys Res Commun* 2004 December 24;325(4):1187-93.

(322) Li H, Freeman MW, Libby P. Regulation of smooth muscle cell scavenger receptor expression in vivo by atherogenic diets and in vitro by cytokines. *J Clin Invest* 1995 January;95(1):122-33.

(323) Endres M, Laufs U, Merz H, Kaps M. Focal expression of intercellular adhesion molecule-1 in the human carotid bifurcation. *Stroke* 1997 January;28(1):77-82.

(324) O'Brien KD, Allen MD, McDonald TO, Chait A, Harlan JM, Fishbein D, McCarty J, Ferguson M, Hudkins K, Benjamin CD, . Vascular cell adhesion molecule-1 is expressed in human coronary atherosclerotic plaques. Implications for the mode of progression of advanced coronary atherosclerosis. *J Clin Invest* 1993 August;92(2):945-51.

(325) Barlic J, Zhang Y, Foley JF, Murphy PM. Oxidized lipid-driven chemokine receptor switch, CCR2 to CX3CR1, mediates adhesion of human macrophages to coronary artery smooth muscle cells through a peroxisome proliferator-activated receptor gamma-dependent pathway. *Circulation* 2006 August 22;114(8):807-19.

(326) Barlic J, Zhang Y, Murphy PM. Atherogenic lipids induce adhesion of human coronary artery smooth muscle cells to macrophages by up-regulating chemokine CX3CL1 on smooth muscle cells in a TNFalpha-NFkappaB-dependent manner. *J Biol Chem* 2007 June 29;282(26):19167-76.

(327) Cai Q, Lanting L, Natarajan R. Interaction of monocytes with vascular smooth muscle cells regulates monocyte survival and differentiation through distinct pathways. *Arterioscler Thromb Vasc Biol* 2004 December;24(12):2263-70.

(328) Raines EW, Ferri N. Thematic review series: The immune system and atherogenesis. Cytokines affecting endothelial and smooth muscle cells in vascular disease. *J Lipid Res* 2005 June;46(6):1081-92.

(329) Naruko T, Ueda M, Haze K, van der Wal AC, van der Loos CM, Itoh A, Komatsu R, Ikura Y, Ogami M, Shimada Y, Ehara S, Yoshiyama M, Takeuchi K, Yoshikawa J, Becker AE. Neutrophil infiltration of culprit lesions in acute coronary syndromes. *Circulation* 2002 December 3;106(23):2894-900.

(330) Zernecke A, Bot I, Djalali-Talab Y, Shagdarsuren E, Bidzhekov K, Meiler S, Krohn R, Schober A, Sperandio M, Soehnlein O, Bornemann J, Tacke F, Biessen EA, Weber C. Protective role of CXC receptor 4/CXC ligand 12 unveils the importance of neutrophils in atherosclerosis. *Circ Res* 2008 February 1;102(2):209-17.

(331) van LM, Gijbels MJ, Duijvestijn A, Smook M, van de Gaar MJ, Heeringa P, de Winther MP, Tervaert JW. Accumulation of myeloperoxidase-positive neutrophils in atherosclerotic lesions in LDLR-/- mice. *Arterioscler Thromb Vasc Biol* 2008 January;28(1):84-9.

(332) Soehnlein O, Weber C. Myeloid cells in atherosclerosis: initiators and decision shapers. *Semin Immunopathol* 2009 June;31(1):35-47.

(333) Drechsler M, Megens RT, van ZM, Weber C, Soehnlein O. Hyperlipidemia-triggered neutrophilia promotes early atherosclerosis. *Circulation* 2010 November 2;122(18):1837-45.

(334) Nicholls SJ, Hazen SL. Myeloperoxidase and cardiovascular disease. *Arterioscler Thromb Vasc Biol* 2005 June;25(6):1102-11.

(335) Soehnlein O, Zernecke A, Eriksson EE, Rothfuchs AG, Pham CT, Herwald H, Bidzhekov K, Rottenberg ME, Weber C, Lindbom L. Neutrophil secretion products pave the way for inflammatory monocytes. *Blood* 2008 August 15;112(4):1461-71.

(336) Gautam N, Olofsson AM, Herwald H, Iversen LF, Lundgren-Akerlund E, Hedqvist P, Arfors KE, Flodgaard H, Lindbom L. Heparin-binding protein (HBP/CAP37): a missing link in neutrophil-evoked alteration of vascular permeability. *Nat Med* 2001 October;7(10):1123-7.

(337) Di GA, Kenne E, Wan M, Soehnlein O, Lindbom L, Haeggstrom JZ. Leukotriene B4-induced changes in vascular permeability are mediated by neutrophil release of heparin-binding protein (HBP/CAP37/azurocidin). *FASEB J* 2009 June;23(6):1750-7.

(338) Soehnlein O, Lindbom L, Weber C. Mechanisms underlying neutrophil-mediated monocyte recruitment. *Blood* 2009 November 19;114(21):4613-23.

(339) Soehnlein O, Kai-Larsen Y, Frithiof R, Sorensen OE, Kenne E, Scharffetter-Kochanek K, Eriksson EE, Herwald H, Agerberth B, Lindbom L. Neutrophil primary granule proteins HBP and HNP1-3

boost bacterial phagocytosis by human and murine macrophages. *J Clin Invest* 2008 October;118(10):3491-502.

(340) Soehnlein O, Weber C, Lindbom L. Neutrophil granule proteins tune monocytic cell function. *Trends Immunol* 2009 November;30(11):538-46.

(341) Eliason JL, Hannawa KK, Ailawadi G, Sinha I, Ford JW, Deogracias MP, Roelofs KJ, Woodrum DT, Ennis TL, Henke PK, Stanley JC, Thompson RW, Upchurch GR, Jr. Neutrophil depletion inhibits experimental abdominal aortic aneurysm formation. *Circulation* 2005 July 12;112(2):232-40.

(342) Sugiyama S, Kugiyama K, Aikawa M, Nakamura S, Ogawa H, Libby P. Hypochlorous acid, a macrophage product, induces endothelial apoptosis and tissue factor expression: involvement of myeloperoxidase-mediated oxidant in plaque erosion and thrombogenesis. *Arterioscler Thromb Vasc Biol* 2004 July;24(7):1309-14.

(343) Harrison D, Griendling KK, Landmesser U, Hornig B, Drexler H. Role of oxidative stress in atherosclerosis. *Am J Cardiol* 2003 February 6;91(3A):7A-11A.

(344) Kovanen PT. Mast cells: multipotent local effector cells in atherothrombosis. *Immunol Rev* 2007 June;217:105-22.

(345) Sun J, Sukhova GK, Wolters PJ, Yang M, Kitamoto S, Libby P, MacFarlane LA, Mallen-St CJ, Shi GP. Mast cells promote atherosclerosis by releasing proinflammatory cytokines. *Nat Med* 2007 June;13(6):719-24.

(346) Bot I, de Jager SC, Zernecke A, Lindstedt KA, Van Berkel TJ, Weber C, Biessen EA. Perivascular mast cells promote atherogenesis and induce plaque destabilization in apolipoprotein E-deficient mice. *Circulation* 2007 May 15;115(19):2516-25.

(347) Bot I, de Jager SC, Bot M, van Heiningen SH, de GP, Veldhuizen RW, Van Berkel TJ, von der Thusen JH, Biessen EA. The neuropeptide substance P mediates adventitial mast cell activation and induces intraplaque hemorrhage in advanced atherosclerosis. *Circ Res* 2010 January 8;106(1):89-92.

(348) Bot I, Bot M, van Heiningen SH, van Santbrink PJ, Lankhuizen IM, Hartman P, Gruener S, Hilpert H, Van Berkel TJ, Fingerle J, Biessen EA. Mast cell chymase inhibition reduces atherosclerotic plaque progression and improves plaque stability in ApoE-/- mice. *Cardiovasc Res* 2011 January 1;89(1):244-52.

(349) Lappalainen J, Lindstedt KA, Oksjoki R, Kovanen PT. OxLDL-IgG immune complexes induce expression and secretion of proatherogenic cytokines by cultured human mast cells. *Atherosclerosis* 2011 February;214(2):357-63.

(350) Heikkila HM, Trosien J, Metso J, Jauhiainen M, Pentikainen MO, Kovanen PT, Lindstedt KA. Mast cells promote atherosclerosis by inducing both an atherogenic lipid profile and vascular inflammation. *J Cell Biochem* 2010 February 15;109(3):615-23.

(351) Lee-Rueckert M, Kovanen PT. Mast cell proteases: physiological tools to study functional significance of high density lipoproteins in the initiation of reverse cholesterol transport. *Atherosclerosis* 2006 November;189(1):8-18.

(352) Judstrom I, Jukkola H, Metso J, Jauhiainen M, Kovanen PT, Lee-Rueckert M. Mast cell-dependent proteolytic modification of HDL particles during anaphylactic shock in the mouse reduces their ability to induce cholesterol efflux from macrophage foam cells ex vivo. *Atherosclerosis* 2010 January;208(1):148-54.

(353) Oram JF, Lawn RM. ABCA1. The gatekeeper for eliminating excess tissue cholesterol. *J Lipid Res* 2001 August;42(8):1173-9.

(354) Attie AD, Kastelein JP, Hayden MR. Pivotal role of ABCA1 in reverse cholesterol transport influencing HDL levels and susceptibility to atherosclerosis. *J Lipid Res* 2001 November;42(11):1717-26.

(355) Lawn RM, Wade DP, Garvin MR, Wang X, Schwartz K, Porter JG, Seilhamer JJ, Vaughan AM, Oram JF. The Tangier disease gene product ABC1 controls the cellular apolipoprotein-mediated lipid removal pathway. *J Clin Invest* 1999 October;104(8):R25-R31.

(356) Bodzioch M, Orso E, Klucken J, Langmann T, Bottcher A, Diederich W, Drobnik W, Barlage S, Buchler C, Porsch-Ozcurumez M, Kaminski WE, Hahmann HW, Oette K, Rothe G, Aslanidis C, Lackner KJ, Schmitz G. The gene encoding ATP-binding cassette transporter 1 is mutated in Tangier disease. *Nat Genet* 1999 August;22(4):347-51.

(357) Brooks-Wilson A, Marcil M, Clee SM, Zhang LH, Roomp K, van DM, Yu L, Brewer C, Collins JA, Molhuizen HO, Loubser O, Ouelette BF, Fichter K, Ashbourne-Excoffon KJ, Sensen CW, Scherer S, Mott S, Denis M, Martindale D, Frohlich J, Morgan K, Koop B, Pimstone S, Kastelein JJ, Genest J, Jr., Hayden MR. Mutations in ABC1 in Tangier disease and familial high-density lipoprotein deficiency. *Nat Genet* 1999 August;22(4):336-45.

(358) Rust S, Rosier M, Funke H, Real J, Amoura Z, Piette JC, Deleuze JF, Brewer HB, Duverger N, Denefle P, Assmann G. Tangier disease is caused by mutations in the gene encoding ATP-binding cassette transporter 1. *Nat Genet* 1999 August;22(4):352-5.

(359) Singaraja RR, Stahmer B, Brundert M, Merkel M, Heeren J, Bissada N, Kang M, Timmins JM, Ramakrishnan R, Parks JS, Hayden MR, Rinninger F. Hepatic ATP-binding cassette transporter A1 is a key molecule in high-density lipoprotein cholesteryl ester metabolism in mice. *Arterioscler Thromb Vasc Biol* 2006 August;26(8):1821-7.

(360) Aiello RJ, Brees D, Bourassa PA, Royer L, Lindsey S, Coskran T, Haghpassand M, Francone OL. Increased atherosclerosis in hyperlipidemic mice with inactivation of ABCA1 in macrophages. *Arterioscler Thromb Vasc Biol* 2002 April 1;22(4):630-7.

(361) Oram JF, Heinecke JW. ATP-binding cassette transporter A1: a cell cholesterol exporter that protects against cardiovascular disease. *Physiol Rev* 2005 October;85(4):1343-72.

(362) Wang MD, Franklin V, Marcel YL. In vivo reverse cholesterol transport from macrophages lacking ABCA1 expression is impaired. *Arterioscler Thromb Vasc Biol* 2007 August;27(8):1837-42.

(363) Calpe-Berdiel L, Rotllan N, Palomer X, Ribas V, Blanco-Vaca F, Escola-Gil JC. Direct evidence in vivo of impaired macrophage-specific reverse cholesterol transport in ATP-binding cassette transporter A1-deficient mice. *Biochim Biophys Acta* 2005 December 30;1738(1-3):6-9.

(364) Wang X, Collins HL, Ranalletta M, Fuki IV, Billheimer JT, Rothblat GH, Tall AR, Rader DJ. Macrophage ABCA1 and ABCG1, but not SR-BI, promote macrophage reverse cholesterol transport in vivo. *J Clin Invest* 2007 August;117(8):2216-24.

(365) Aiello RJ, Brees D, Francone OL. ABCA1-deficient mice: insights into the role of monocyte lipid efflux in HDL formation and inflammation. *Arterioscler Thromb Vasc Biol* 2003 June 1;23(6):972-80.

(366) Francone OL, Royer L, Boucher G, Haghpassand M, Freeman A, Brees D, Aiello RJ. Increased cholesterol deposition, expression of scavenger receptors, and response to chemotactic factors in Abca1-deficient macrophages. *Arterioscler Thromb Vasc Biol* 2005 June;25(6):1198-205.

(367) Koseki M, Hirano K, Masuda D, Ikegami C, Tanaka M, Ota A, Sandoval JC, Nakagawa-Toyama Y, Sato SB, Kobayashi T, Shimada Y, Ohno-Iwashita Y, Matsuura F, Shimomura I, Yamashita S. Increased lipid rafts and accelerated lipopolysaccharide-induced tumor necrosis factor-alpha secretion in Abca1-deficient macrophages. *J Lipid Res* 2007 February;48(2):299-306.

(368) Zhu X, Lee JY, Timmins JM, Brown JM, Boudyguina E, Mulya A, Gebre AK, Willingham MC, Hiltbold EM, Mishra N, Maeda N, Parks JS. Increased cellular free cholesterol in macrophage-specific Abca1 knock-out mice enhances pro-inflammatory response of macrophages. *J Biol Chem* 2008 August 22;283(34):22930-41.

(369) Yvan-Charvet L, Welch C, Pagler TA, Ranalletta M, Lamkanfi M, Han S, Ishibashi M, Li R, Wang N, Tall AR. Increased inflammatory gene expression in ABC transporter-deficient macrophages: free cholesterol accumulation, increased signaling via toll-like receptors, and neutrophil infiltration of atherosclerotic lesions. *Circulation* 2008 October 28;118(18):1837-47.

(370) Pradel LC, Mitchell AJ, Zarubica A, Dufort L, Chasson L, Naquet P, Broccardo C, Chimini G. ATP-binding cassette transporter hallmarks tissue macrophages and modulates cytokine-triggered polarization programs. *Eur J Immunol* 2009 August;39(8):2270-80.

(371) Tang C, Liu Y, Kessler PS, Vaughan AM, Oram JF. The macrophage cholesterol exporter ABCA1 functions as an anti-inflammatory receptor. *J Biol Chem* 2009 November 20;284(47):32336-43.

(372) Christiansen-Weber TA, Voland JR, Wu Y, Ngo K, Roland BL, Nguyen S, Peterson PA, Fung-Leung WP. Functional loss of ABCA1 in mice causes severe placental malformation, aberrant lipid distribution, and kidney glomerulonephritis as well as high-density lipoprotein cholesterol deficiency. *Am J Pathol* 2000 September;157(3):1017-29.

(373) Dieker JW, van d, V, Berden JH. Deranged removal of apoptotic cells: its role in the genesis of lupus. *Nephrol Dial Transplant* 2004 February;19(2):282-5.

(374) Yvan-Charvet L, Pagler TA, Seimon TA, Thorp E, Welch CL, Witztum JL, Tabas I, Tall AR. ABCA1 and ABCG1 protect against oxidative stress-induced macrophage apoptosis during efferocytosis. *Circ Res* 2010 June 25;106(12):1861-9.

(375) Venegas V, Zhou Z. Two alternative mechanisms that regulate the presentation of apoptotic cell engulfment signal in

Caenorhabditis elegans. *Mol Biol Cell* 2007 August;18(8):3180-92.

(376) Bared SM, Buechler C, Boettcher A, Dayoub R, Sigruener A, Grandl M, Rudolph C, Dada A, Schmitz G. Association of ABCA1 with syntaxin 13 and flotillin-1 and enhanced phagocytosis in tangier cells. *Mol Biol Cell* 2004 December;15(12):5399-407.

(377) Joyce CW, Amar MJ, Lambert G, Vaisman BL, Paigen B, Najib-Fruchart J, Hoyt RF, Jr., Neufeld ED, Remaley AT, Fredrickson DS, Brewer HB, Jr., Santamarina-Fojo S. The ATP binding cassette transporter A1 (ABCA1) modulates the development of aortic atherosclerosis in C57BL/6 and apoE-knockout mice. *Proc Natl Acad Sci U S A* 2002 January 8;99(1):407-12.

(378) Joyce CW, Wagner EM, Basso F, Amar MJ, Freeman LA, Shamburek RD, Knapper CL, Syed J, Wu J, Vaisman BL, Fruchart-Najib J, Billings EM, Paigen B, Remaley AT, Santamarina-Fojo S, Brewer HB, Jr. ABCA1 overexpression in the liver of LDLr-KO mice leads to accumulation of pro-atherogenic lipoproteins and enhanced atherosclerosis. *J Biol Chem* 2006 November 3;281(44):33053-65.

(379) Vaisman BL, Lambert G, Amar M, Joyce C, Ito T, Shamburek RD, Cain WJ, Fruchart-Najib J, Neufeld ED, Remaley AT, Brewer HB, Jr., Santamarina-Fojo S. ABCA1 overexpression leads to hyperalphalipoproteinemia and increased biliary cholesterol excretion in transgenic mice. *J Clin Invest* 2001 July;108(2):303-9.

(380) Yvan-Charvet L, Ranalletta M, Wang N, Han S, Terasaka N, Li R, Welch C, Tall AR. Combined deficiency of ABCA1 and ABCG1 promotes foam cell accumulation and accelerates atherosclerosis in mice. *J Clin Invest* 2007 December;117(12):3900-8.

(381) Van EM, Singaraja RR, Ye D, Hildebrand RB, James ER, Hayden MR, Van Berkel TJ. Macrophage ATP-binding cassette transporter A1 overexpression inhibits atherosclerotic lesion progression in low-density lipoprotein receptor knockout mice. *Arterioscler Thromb Vasc Biol* 2006 April;26(4):929-34.

(382) Brunham LR, Singaraja RR, Duong M, Timmins JM, Fievet C, Bissada N, Kang MH, Samra A, Fruchart JC, McManus B, Staels B, Parks JS, Hayden MR. Tissue-specific roles of ABCA1 influence susceptibility to atherosclerosis. *Arterioscler Thromb Vasc Biol* 2009 April;29(4):548-54.

(383) Vaisman BL, Knapper CL, Demosky SJ, Stonik JA, Amar MJ, Remaley AT. Expression of Human ABCA1 in Endothelium Protects Against Diet-induced Atherosclerosis in Mice. *Circulation* 2008 October 28;118(18):S558.

(384) Huby T, Doucet C, Dachet C, Ouzilleau B, Ueda Y, Afzal V, Rubin E, Chapman MJ, Lesnik P. Knockdown expression and hepatic deficiency reveal an atheroprotective role for SR-BI in liver and peripheral tissues. *J Clin Invest* 2006 October;116(10):2767-76.

(385) Covey SD, Krieger M, Wang W, Penman M, Trigatti BL. Scavenger receptor class B type I-mediated protection against atherosclerosis in LDL receptor-negative mice involves its expression in bone marrow-derived cells. *Arterioscler Thromb Vasc Biol* 2003 September 1;23(9):1589-94.

(386) Van EM, Hoekstra M, Hildebrand RB, Yaong Y, Stengel D, Kruijt JK, Sattler W, Tietge UJ, Ninio E, Van Berkel TJ, Pratico D. Increased oxidative stress in scavenger receptor BI knockout mice with dysfunctional HDL. *Arterioscler Thromb Vasc Biol* 2007 November;27(11):2413-9.

(387) Hildebrand RB, Lammers B, Meurs I, Korporaal SJ, De HW, Zhao Y, Kruijt JK, Pratico D, Schimmel AW, Holleboom AG, Hoekstra M, Kuivenhoven JA, Van Berkel TJ, Rensen PC, Van EM. Restoration of high-density lipoprotein levels by cholesteryl ester transfer protein expression in scavenger receptor class B type I (SR-BI) knockout mice does not normalize pathologies associated with SR-BI deficiency. *Arterioscler Thromb Vasc Biol* 2010 July;30(7):1439-45.

(388) Arai T, Wang N, Bezouevski M, Welch C, Tall AR. Decreased atherosclerosis in heterozygous low density lipoprotein receptor-deficient mice expressing the scavenger receptor BI transgene. *J Biol Chem* 1999 January 22;274(4):2366-71.

(389) Ueda Y, Gong E, Royer L, Cooper PN, Francone OL, Rubin EM. Relationship between expression levels and atherogenesis in scavenger receptor class B, type I transgenics. *J Biol Chem* 2000 July 7;275(27):20368-73.

(390) Van EM, Pennings M, Hoekstra M, Out R, Van Berkel TJ. Scavenger receptor BI and ATP-binding cassette transporter A1 in reverse cholesterol transport and atherosclerosis. *Curr Opin Lipidol* 2005 June;16(3):307-15.

(391) Wang J, van DH, Scherer HU, Huizinga TW, Toes RE. Suppressor activity among CD4+,CD25++ T cells is discriminated by membrane-bound tumor necrosis factor

alpha. *Arthritis Rheum* 2008 June;58(6):1609-18.

(392) Rohrer L, Ohnsorg PM, Lehner M, Landolt F, Rinninger F, von EA. High-density lipoprotein transport through aortic endothelial cells involves scavenger receptor BI and ATP-binding cassette transporter G1. *Circ Res* 2009 May 22;104(10):1142-50.

(393) Li XA, Guo L, Dressman JL, Asmis R, Smart EJ. A novel ligand-independent apoptotic pathway induced by scavenger receptor class B, type I and suppressed by endothelial nitric-oxide synthase and high density lipoprotein. *J Biol Chem* 2005 May 13;280(19):19087-96.

(394) Seetharam D, Mineo C, Gormley AK, Gibson LL, Vongpatanasin W, Chambliss KL, Hahner LD, Cummings ML, Kitchens RL, Marcel YL, Rader DJ, Shaul PW. High-density lipoprotein promotes endothelial cell migration and reendothelialization via scavenger receptor-B type I. *Circ Res* 2006 January 6;98(1):63-72.

(395) Yuhanna IS, Zhu Y, Cox BE, Hahner LD, Osborne-Lawrence S, Lu P, Marcel YL, Anderson RG, Mendelsohn ME, Hobbs HH, Shaul PW. High-density lipoprotein binding to scavenger receptor-BI activates endothelial nitric oxide synthase. *Nat Med* 2001 July;7(7):853-7.

(396) Li XA, Titlow WB, Jackson BA, Giltiay N, Nikolova-Karakashian M, Uittenbogaard A, Smart EJ. High density lipoprotein binding to scavenger receptor, Class B, type I activates endothelial nitric-oxide synthase in a ceramide-dependent manner. *J Biol Chem* 2002 March 29;277(13):11058-63.

(397) Hoekstra M, Ye D, Hildebrand RB, Zhao Y, Lammers B, Stitzinger M, Kuiper J, Van Berkel TJ, Van EM. Scavenger receptor class B type I-mediated uptake of serum cholesterol is essential for optimal adrenal glucocorticoid production. *J Lipid Res* 2009 June;50(6):1039-46.

(398) Vishnyakova TG, Bocharov AV, Baranova IN, Chen Z, Remaley AT, Csako G, Eggerman TL, Patterson AP. Binding and internalization of lipopolysaccharide by Cla-1, a human orthologue of rodent scavenger receptor B1. *J Biol Chem* 2003 June 20;278(25):22771-80.

(399) Cai L, Ji A, de Beer FC, Tannock LR, van der Westhuyzen DR. SR-BI protects against endotoxemia in mice through its roles in glucocorticoid production and hepatic clearance. *J Clin Invest* 2008 January;118(1):364-75.

(400) Guo L, Song Z, Li M, Wu Q, Wang D, Feng H, Bernard P, Daugherty A, Huang B, Li XA. Scavenger Receptor BI Protects against Septic Death through Its Role in Modulating Inflammatory Response. *J Biol Chem* 2009 July 24;284(30):19826-34.

(401) Kimura T, Tomura H, Mogi C, Kuwabara A, Damirin A, Ishizuka T, Sekiguchi A, Ishiwara M, Im DS, Sato K, Murakami M, Okajima F. Role of scavenger receptor class B type I and sphingosine 1-phosphate receptors in high density lipoprotein-induced inhibition of adhesion molecule expression in endothelial cells. *J Biol Chem* 2006 December 8;281(49):37457-67.

(402) Cuchel M, Rader DJ. Macrophage reverse cholesterol transport: key to the regression of atherosclerosis? *Circulation* 2006 May 30;113(21):2548-55.

(403) Rader DJ, Alexander ET, Weibel GL, Billheimer J, Rothblat GH. The role of reverse cholesterol transport in animals and humans and relationship to atherosclerosis. *J Lipid Res* 2009 April;50 Suppl:S189-S194.

(404) Adorni MP, Zimetti F, Billheimer JT, Wang N, Rader DJ, Phillips MC, Rothblat GH. The roles of different pathways in the release of cholesterol from macrophages. *J Lipid Res* 2007 November;48(11):2453-62.

(405) Zhang Y, Da Silva JR, Reilly M, Billheimer JT, Rothblat GH, Rader DJ. Hepatic expression of scavenger receptor class B type I (SR-BI) is a positive regulator of macrophage reverse cholesterol transport in vivo. *J Clin Invest* 2005 October;115(10):2870-4.

(406) Zhang Y, Zanotti I, Reilly MP, Glick JM, Rothblat GH, Rader DJ. Overexpression of apolipoprotein A-I promotes reverse transport of cholesterol from macrophages to feces in vivo. *Circulation* 2003 August 12;108(6):661-3.

(407) Escola-Gil JC, Rotllan N, Julve J, Blanco-Vaca F. In vivo macrophage-specific RCT and antioxidant and antiinflammatory HDL activity measurements: New tools for predicting HDL atheroprotection. *Atherosclerosis* 2009 October;206(2):321-7.

(408) Tangirala RK, Tsukamoto K, Chun SH, Usher D, Pure E, Rader DJ. Regression of atherosclerosis induced by liver-directed gene transfer of apolipoprotein A-I in mice. *Circulation* 1999 October 26;100(17):1816-22.

(409) Feig JE, Rong JX, Shamir R, Sanson M, Vengrenyuk Y, Liu J, Rayner K, Moore K, Garabedian M, Fisher EA. HDL promotes rapid atherosclerosis regression in mice and alters inflammatory properties of plaque

monocyte-derived cells. *Proc Natl Acad Sci U S A* 2011 April 26;108(17):7166-71.

(410) Feig JE, Pineda-Torra I, Sanson M, Bradley MN, Vengrenyuk Y, Bogunovic D, Gautier EL, Rubinstein D, Hong C, Liu J, Wu C, van RN, Bhardwaj N, Garabedian M, Tontonoz P, Fisher EA. LXR promotes the maximal egress of monocyte-derived cells from mouse aortic plaques during atherosclerosis regression. *J Clin Invest* 2010 December 1;120(12):4415-24.

(411) Junichiro T, Tanigawa H, Snehal N, Billheimer JT, Reilly M, Millar JS, Fuki IV, Huet S, Jaye M, Rothblat GH, Rader DJ. PPAR alpha Agonism Promotes Reverse Cholesterol Transport in a Macrophage PPAR alpha and Liver X Receptor Dependent Manner. *Circulation* 2009 November 3;120(18):S529.

(412) Zhou X, He W, Huang Z, Gotto AM, Jr., Hajjar DP, Han J. Genetic deletion of low density lipoprotein receptor impairs sterol-induced mouse macrophage ABCA1 expression. A new SREBP1-dependent mechanism. *J Biol Chem* 2008 January 25;283(4):2129-38.

CHAPTER 2

Hypocholesterolemia, foam cell formation, but no atherosclerosis in mice lacking ABC-transporter A1 and scavenger receptor class B type I

Ying Zhao[1], Marieke Pennings[1], Carlos L.J. Vrins[2], Laura Calpe-Berdiel[1], Menno Hoekstra[1], J. Kar Kruijt[1], Roelof Ottenhoff[2], Reeni B. Hildebrand[1], Ronald van der Sluis[1], Wendy Jessup[3], Wilfried Le Goff[4], M. John Chapman[4], Thierry Huby[4], Albert K. Groen[5], Theo J.C. Van Berkel[1], Miranda Van Eck[1]

[1] Division of Biopharmaceutics, Leiden/Amsterdam Center for Drug Research, Leiden University, Einsteinweg 55, 2333 CC Leiden, The Netherlands
[2] Department of Medical Biochemistry, Academic Medical Center, Amsterdam, The Netherlands
[3] Centre for Vascular Research, University of New South Wales, Sydney, Australia
[4] INSERM U551, Paris, France; Universite´ Pierre et Marie Curie-Paris 06, UMRS 939 Paris, France
[5] Department of Pediatrics, University Medical Center Groningen, Groningen, The Netherlands

Abstract

High-density lipoprotein (HDL) mediated reverse cholesterol transport (RCT) is regarded to be crucial for prevention of foam cell formation and atherosclerosis. ABC-transporter A1 (ABCA1) and scavenger receptor BI (SR-BI) are involved in the biogenesis of HDL and the selective delivery of HDL cholesterol to the liver, respectively. In the present study, we phenotypically characterized mice lacking these two proteins essential for HDL metabolism. ABCA1xSR-BI double knockout (dKO) mice showed severe hypocholesterolemia mainly due to HDL loss, despite a 90% reduction of HDL cholesterol uptake by liver. VLDL production was increased in dKO mice. However, non-HDL cholesterol levels were reduced, probably due to enhanced clearance via LRP1. Hepatobiliary cholesterol transport and fecal sterol excretion were not impaired in dKO mice. In contrast, the macrophage RCT in dKO mice was markedly impaired as compared to WT mice, associated with the accumulation of macrophage foam cells in the lung and Peyer's patches. Strikingly, no atherosclerotic lesion formation was observed in dKO mice. In conclusion, both ABCA1 and SR-BI are essential for maintaining a properly functioning HDL-mediated macrophage RCT, while the potential anti-atherosclerotic functions of ABCA1 and SR-BI are not evident in dKO mice due to the absence of pro-atherogenic lipoproteins.

--- *Atherosclerosis.* 2011; 218: 314-322 ---

Introduction

Plasma HDL cholesterol levels are inversely correlated with the risk of atherosclerotic vascular disease [1]. HDL-mediated reverse cholesterol transport (RCT), a process in which excess peripheral cholesterol is removed and delivered to the liver for biliary secretion, has been regarded crucial for prevention of foam cell formation and atherosclerosis [2]. Two important genes recognized in RCT are the ATP-binding cassette transporter A1 (ABCA1) and the scavenger receptor class B type I (SR-BI) [2]. ABCA1 promotes the efflux of cholesterol and phospholipid to lipid-poor apolipoprotein AI (ApoAI), leading to HDL particle maturation, the first step in RCT [2]. In contrast, SR-BI facilitates the bi-directional flux of cholesterol between cells and mature HDL down a concentration gradient. Importantly, SR-BI is essential for the selective uptake of cholesteryl esters (CEs) from HDL by the liver for biliary secretion, the last step in RCT [2].

Recent genome-wide association studies (GWAS) have identified ABCA1 as a major gene influencing HDL levels in humans [3]. Targeted deletion of ABCA1 in the liver [4] and intestine [5] of mice has revealed the crucial roles of hepatic and intestinal ABCA1 for HDL biogenesis. In agreement, induction of hepatic and intestinal ABCA1 expression increases plasma HDL cholesterol (HDL-C) levels [4,6]. In contrast, macrophage ABCA1 minimally contributes to plasma HDL cholesterol [7]. Patients with functional mutations in ABCA1 have Tangier disease (TD), characterized by a marked reduction in plasma HDL-C and increased macrophage foam cell formation in several tissues [8]. Likewise, ABCA1 knockout (KO) mice display the similar pathophysiologic phenotype as TD patients [9]. Cells from patients with TD and ABCA1 KO mice are defective in the efflux of cholesterol and phospholipid to apoAI and partially to HDL [8]. Also, macrophage RCT is impaired in ABCA1 KO mice, mainly due to HDL deficiency [10-11].

In several population studies, a clear association between mutations in the coding and promoter regions of human SR-BI and increased plasma HDL-C has been shown [12,13]. Recent GWAS studies also demonstrated that single nucleotide polymorphism (SNPs) in and near SR-BI are significantly associated with plasma levels of HDL-C in humans [14]. However, only very recently conclusive evidence was provided on the importance of SR-BI for controlling HDL-C levels in humans. Vergeer et al identified a family in which heterozygous carriers of a unique mutation (P297S) in the extracellular domain of SR-BI showed 37% elevated HDL cholesterol levels [15]. Importantly, hepatocytes that expressed the P297S mutant SR-BI displayed a reduced capacity to take up CEs from HDL, thereby leading to the elevation in plasma HDL-C [15]. Also, SR-BI KO mice display increased HDL-C, due to impaired delivery of HDL-CEs to liver [16]. Interestingly, despite the high levels of HDL-C, SR-BI deficient mice have impaired macrophage RCT [17]. Conversely, overexpression of hepatic SR-BI decreases HDL-C and promotes macrophage RCT [17].

Given that ABCA1 and SR-BI are involved in the different steps of RCT, it is conceivable that ABCA1 and SR-BI might act synergistically in the process of RCT. To study the RCT process under conditions in which both of these key mediators are absent, ABCA1/SR-BI double knockout (dKO) mice were generated. In this study, we describe the characterization of ABCA1/SR-BI dKO mice with respect to plasma lipids, HDL metabolism, blood cell counts, bile secretion, macrophage RCT, tissue cholesterol homeostasis, and atherosclerosis susceptibility.

Materials and Methods:

For detailed methodology, please see the data supplement, available online at http://www.sciencedirect.com. Briefly, ABCA1/SR-BI dKO mice were generated by intercrossing double heterozygous offsprings obtained from crossbreeding of ABCA1 KO mice with SR-BI KO mice. Plasma cholesterol levels, the lipoprotein distribution, blood cell counts, and hepatic expression of lipoprotein receptors, including SR-BI, LDL receptor (LDLr), and LDLr related protein 1 (LRP1) were determined. Moreover, VLDL production, serum decay and liver uptake of [^{3}H]-cholesteryl ether-labeled HDL, hepatobiliary and fecal cholesterol secretion, and macrophage RCT were analyzed. In addition, tissue macrophage cholesterol homeostasis and atherosclerosis susceptibility were examined by Oil-red-O staining and immunohistochemical staining against Moma-2.

Results

Hypocholesterolemia and HDL loss in ABCA1/SR-BI dKO mice

To analyze the potential synergistic role of ABCA1 and SR-BI in the RCT process, we generated ABCA1/SR-BI dKO mice. The absence of ABCA1 and SR-BI in the dKO mice was verified at DNA level by performing PCR on genomic DNA (Supplementary Figure 1). From the crosses of ABCA1/SR-BI double heterozygous mice, 7.2%, 6.5%, and 6.2% of the offspring were ABCA1 KO, SR-BI KO, and dKO mice, which are close to the expected Mendelian inheritance rate of 6.25%. Homozygous dKO males are fertile while dKO females, similar to SR-BI KO females [18,19], are infertile, which could be reversed by administering the cholesterol-lowering drug probucol. However, as described for ABCA1 KO mice [20], also under these conditions a lower frequency of pregnancy and extensive neonatal death of pups born from dKO mothers was observed. No significant differences in body weight between wild-type (WT), ABCA1 KO, SR-BI KO, and dKO mice were observed at the age of 12 weeks (22.7±0.9 g, 20.3±0.3 g, 22.0±0.6 g, 21.3±0.3 g, respectively). Furthermore, dKO mice born from ABCA1 × SR-BI double heterozygous breedings did not appear to have a reduced life expectancy as they can reach ages of >1 year.

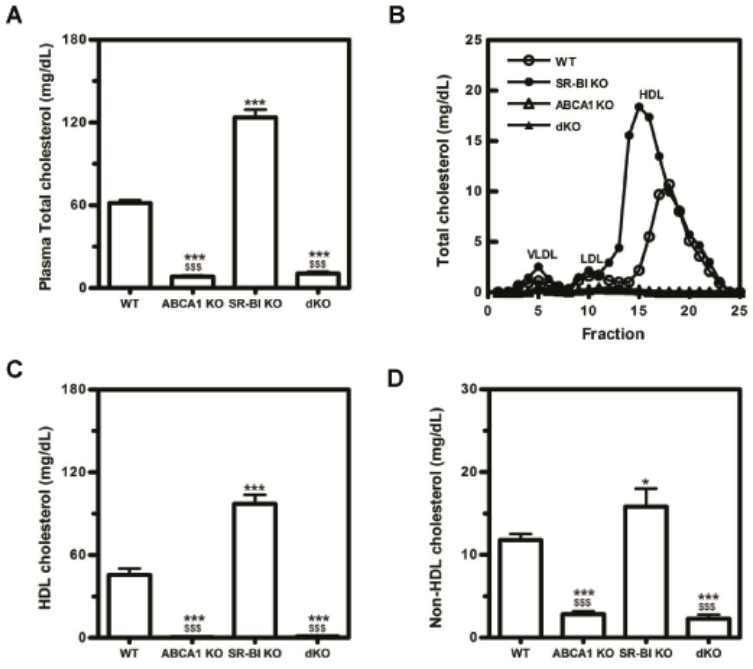

Figure 1. Hypocholesterolemia and HDL loss in ABCA1/SR-BI double knockout mice. Total plasma cholesterol levels (A), lipoprotein distribution of total cholesterol (B), HDL cholesterol levels (C), and non-HDL cholesterol levels (D) of WT, ABCA1 KO, SR-BI KO and ABCA1/SR-BI double KO mice (mixed male and female) at the age of 12-16 weeks old on chow. Bar graphs represent the means±SEM (n=8). Two hundred microliters of pooled mouse plasma from the different genotypes were fractioned by FPLC. Statistically significant difference $^{*}p<0.05$, $^{***}p<0.001$ *vs* WT mice; $^{\$\$\$}p<0.001$ *vs* SR-BI KO mice.

In line with previous studies [8-9,18,19], SR-BI KO mice showed increased plasma free (5.5-fold, p<0.001) and total cholesterol (2.0-fold, p<0.001) levels as compared to WT animals and accumulated abnormally large HDL particles. ABCA1 KO mice on the contrary were severely hypocholesterolemic and had a near complete absence of HDL (Figure 1A-1C and Supplementary Table 4). Mice with a combined deficiency of ABCA1 and SR-BI resembled single ABCA1 KO mice with a dramatic >80% and >99% decrease in the plasma TC and HDL-C levels, respectively (Figure 1A-1C). Of note, ABCA1 deficiency dramatically reduced the plasma free cholesterol levels (22-fold, p<0.001) in the SR-BI KO background (Supplementary Table 4). SR-BI deficiency also led to an increase in plasma levels of phospholipids (1.2-fold, p<0.001) and triglycerides (1.2-fold, p<0.05). In contrast, both ABCA1 KO and dKO mice showed comparably reduced plasma levels of phosholipids (3.0-fold, p<0.001 *vs* WT) and triglycerides (1.7-fold, p<0.001 *vs* WT) (Supplementary Table 4).

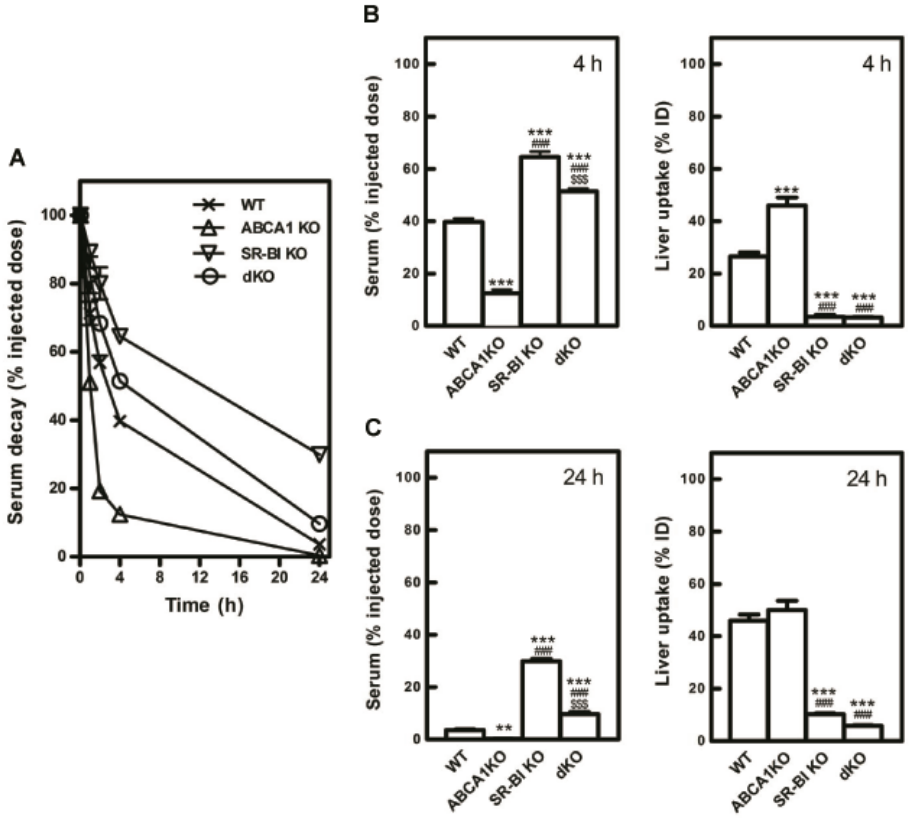

Figure 2. Reduced serum decay and liver uptake of [^{3}H]CEt-HDL in ABCA1/SR-BI double knockout mice. Serum decay and liver uptake was determined in 12-16 week old female animals on chow diet. (A) The clearance of [^{3}H]CEt-HDL from the circulation in WT (×), ABCA1 KO (Δ), SR-BI KO (∇) and ABCA1/SR-BI double KO (○) mice at 0, 1, 2, 4, and 24 hours after intravenous injection of 200 μg [^{3}H]CEt-HDL. (B) The amount of [^{3}H]CEt-HDL in the circulation and the liver at 4 hours after injection. (C) The amount of [^{3}H]CEt-HDL in the circulation and the liver at 24 hours after injection. Bar graphs represent the means±SEM (n=3/group). Statistically significant difference **p<0.01, ***p<0.001 *vs* WT mice; $^{\#\#\#}$p<0.001 *vs* ABCA1 KO mice; $^{\$\$\$}$ p<0.001 *vs* SR-BI KO mice.

Serum decay and hepatic uptake of HDL-CE in dKO mice were studied next. Upon injection of [^{3}H]CEt-HDL into WT mice, 60.3±1.3% of the injected label was removed from the blood during the first 4 h (Figure 2A and 2B). Consistent with previous findings [21], serum clearance was severely delayed upon deletion of SR-BI. At 4 h after injection only 35.4±1.9% (p<0.001) was removed from the circulation in SR-BI KO mice. Notably, in ABCA1 KO mice, 87.6±1.4% (p<0.001) of the injected label was removed from the

circulation at 4 h after injection. Combined disruption of ABCA1 and SR-BI led to a significantly delayed serum clearance of [^{3}H]CEt-HDL (48.6±1.1% removed at 4h, p<0.001 *vs* WT mice; p<0.001 *vs* ABCA1 KO mice). Importantly, these findings in the dKO mice for the first time show that SR-BI deficiency dramatically decreases HDL-CEt clearance in the absence of a circulation pool of HDL. At this time point, in WT mice, 26.5±1.5% of the injected dose (ID) was recovered in the liver while ABCA1 KO mice showed a 1.7-fold (46.0±3.1%, p<0.001) increase in uptake by the liver (Figure 2B). In contrast, only 3.5±0.6% (p<0.001 *vs* WT) and 3.2±0.3% (p<0.001 *vs* ABCA1 KO) of the ID accumulated in the liver of SR-BI KO and dKO mice, indicating that SR-BI is responsible for the majority (around 80-90%) of the removal of CEt from HDL in the circulation by liver. Moreover, the distribution of radioactivity over extrahepatic tissues was also analyzed at 4 hours after injection (Supplementary Table 3). It was found that the majority of the extrahepatic label was present in bone (6-9%), skin (4-9%), and the muscle (1-3%). The total recovery of label was between 79 to 82%. In line with previous study [21], SR-BI deficiency also led to an ~88% (p<0.001 *vs* WT) reduction of [^{3}H]CEt uptake by adrenal. Similarly, the adrenal upake of [^{3}H]CEt in dKO mice was also dramatically decreased 85% (p<0.001) and 97% (p<0.001) as compared to WT and ABCA1 KO mice, respectively (Supplementary Table 3). Interestingly, ABCA1 deficiency led to 6-fold (p<0.001 *vs* WT) more adrenal uptake of [^{3}H]CEt. Also a 3-fold (p<0.01) increase in skin uptake of [^{3}H]CEt was observed in ABCA1 KO mice as compared to WT mice. However, the absolute uptake by adrenal and skin in ABCA1 KO mice was only 3.5% and 2.6% of ID. Thus, increased clearance of [^{3}H]CEt-HDL from the circulation in ABCA1 KO mice as compared to WT animals was mainly due to enhanced uptake by the liver. After 24 h, above 90% of injected [^{3}H]CEt-HDL was removed from the circulation in WT, ABCA1 KO, and dKO mice whereas 30.0±0.8% (p<0.001) of the injected label remained in the circulation of SR-BI KO mice (Figure 2A and 2C). At this time point, 46.0±2.3% and 50.1±3.4% of ID were recovered in the liver of WT and ABCA1 KO mice. In contrast, only 10.2±0.3% (p<0.001 *vs* WT) and 5.9±0.2% (p<0.001 *vs* ABCA1 KO) of the ID had accumulated in livers of SR-BI KO and dKO mice, respectively (Figure 2C).

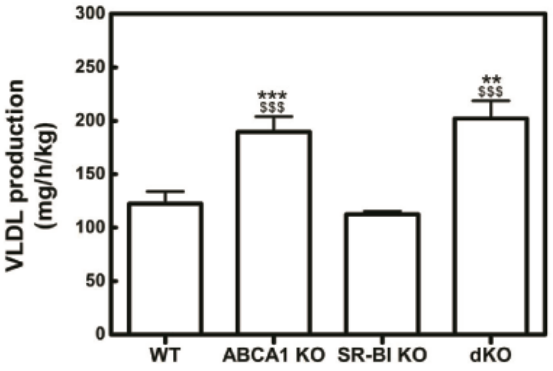

Figure 3. Increased VLDL production in ABCA1/SR-BI double knockout mice. VLDL production rate was determined in 12-16 week old female animals on chow diet. VLDL production was determined by calculating the accumulation rate (g/h/kg body weight) of triglycerides in the plasma after blocking VLDL clearance by Triton WR-1339. Data are expressed as mean±SEM (n=5/group). Statistically significant difference **p<0.01, ***p<0.001 *vs* WT mice; $^{\$\$\$}$p<0.001 *vs* SR-BI KO mice.

In line with previous findings [22], deletion of SR-BI also resulted in a 1.3-fold (p<0.05) increase in non-HDL-C levels (Figure 1D). Interestingly, non-HDL-C levels were reduced 4.2-fold (p<0.001) and 5.1-fold (p<0.001) in ABCA1 KO and dKO animals, respectively as compared to WT mice (Figure 1D). However, ABCA1 deficiency did lead to a 1.5-fold (P<0.001) and 1.8-fold (P<0.01) higher VLDL production rate against both the WT and SR-BI KO background, respectively (Figure 3A). The observed reduction in non-HDL-C in ABCA1 KO and dKO mice was thus not the result of an impaired hepatic VLDL secretion. Next, we analyzed the hepatic expression of ABCA1, SR-BI, LDLr, and

LRP1 at both the mRNA and the protein level. As anticipated, deletion of ABCA1 and/or SR-BI resulted in undetectable mRNA and protein expression of the respective proteins in the liver (Figure 4). ABCA1 deficiency did not affect the expression of hepatic SR-BI. Thus, the observed increased accumulation of [^{3}H]CEt-HDL in the liver of ABCA1 KO mice might be due to the lack of an endogenous HDL pool, which could compete with [^{3}H]CEt-HDL in binding with hepatic SR-BI. The mRNA levels of LDLr and LRP1 were increased 2.5-fold ($p<0.01$) and 2.0-fold ($p<0.01$), respectively in the liver of dKO mice as compared to WT and single KOs (Figure 4A). However, only the protein levels of hepatic LRP1 were significantly upregulated 1.7-fold ($p<0.05$) in the dKOs (Figure 4B). Strikingly, the protein levels of the LDLr in livers of the dKO mice were dramatically reduced (4-fold, $p<0.05$) (Figure 4B). Since dKO mice showed 3-fold ($p<0.01$) higher hepatic expression of PCSK9 protein as compared to WT mice and single KOs (Supplementary Figure 2A), the reduced LDLr protein levels in the liver might be due to enhanced degradation of the LDLr via PCSK9 [23] (Supplementary Figure 2A). In addition, the expression of P2Y13, an important player in HDL metabolism [24], was also analyzed by Western blot. As shown in Supplementary Figure 2B, single ABCA1 and SR-BI deficiency did not affect the expression of P2Y13 in the liver. In contrast, dKO mice showed slightly increased hepatic levels of P2Y13 (1.5-fold, $p<0.05$ *vs* WT mice and single KOs).

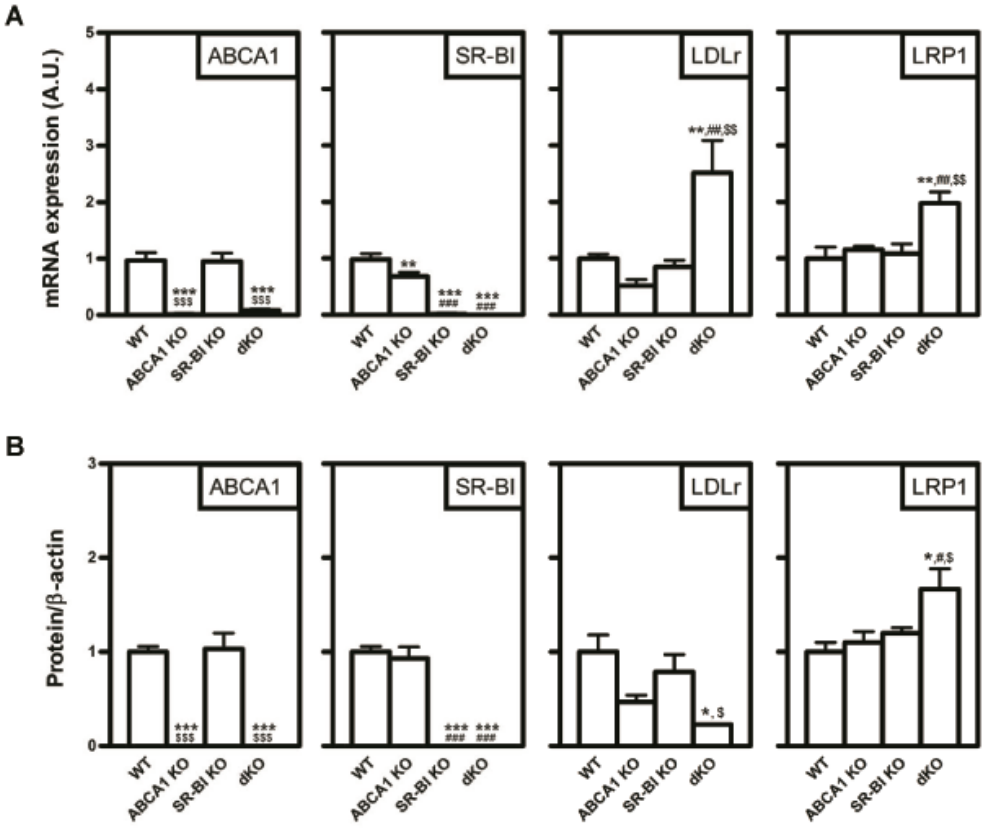

Figure 4. **Expression levels of ABCA1, SR-BI, LDLr, and LRP1 in livers of ABCA1/SR-BI dKO mice.** Livers were harvested from 16-week old chow-fed WT, ABCA1 KO, SR-BI KO, and dKO mice and total RNA and protein were isolated for real-time PCR analysis (A, n=6) and western blotting analysis (B, n=3), respectively as described in Materials and Methods. The expression levels in livers of WT animals were normalized to 1. Data are expressed as mean±SEM. Statistically significant difference $^{*}p<0.05$, $^{**}p<0.01$, $^{***}p<0.001$ *vs* WT mice; $^{\#}p<0.05$, $^{\#\#}p<0.01$, $^{\#\#\#}p<0.001$ *vs* ABCA1 KO mice; $^{\$}p<0.05$, $^{\$\$}p<0.01$, $^{\$\$\$}p<0.001$ *vs* SR-BI KO mice.

Normalized red blood cell and reticulocyte counts in ABCA1/SR-BI dKO mice

Circulating white and red blood cells were next analyzed. No significant differences in white blood cells, including lymphocytes, monocytes, and granulocytes were observed among the different strains of animals (Supplementary Table 5). In line with previous study [25, 26], SR-BI KO mice showed a slightly reduced red blood cell (RBC) count (10.0±0.1 x10^9/mL *vs* 11.1±0.2 x10^9/mL in WT mice, $p<0.01$) with an increased reticulocyte count (215±15‰ *vs* 34±1‰ in WT mice, $p<0.0001$) (Supplementary Table 5). No significant differences in the RBC (11.5±0.2 x10^9/mL) and reticulocyte (36±2‰) count were found in ABCA1 KO mice as compared to WT mice. Notably, ABCA1 deficiency normalized the RBC and reticulocyte counts in SR-BI KO mice (dKO mice: RBC, 10.8±0.3 x10^9/mL, $p<0.05$; reticulocyte, 38±5‰, $p<0.001$ *vs* SR-BI KO). This is most likely the consequence of the large reduction in FC levels in the dKO mice [25,26].

Unaltered hepatic lipid content and biliary and fecal sterol secretion in ABCA1/SR-BI dKO mice

Hepatic total cholesterol, phospholipids, and triglycerides levels were not changed in dKO mice as compared to WT and single KOs (Supplementary Table 6). In line with one previous study [27], ABCA1 deficiency did not influence biliary cholesterol secretion. Also, the biliary secretion rate of cholesterol was not impaired in dKO mice, although a slight but not significant decrease in biliary cholesterol secretion was observed in SR-BI KO mice. The expression of ABCG5 and ABCG8, important cholesterol transporters on hepatic canalicular membrane [28], was unaffected in SR-BI KO and dKO mice (Supplementary Figure 2C and 2D). Moreover, biliary secretion of phospholipid and bile salts were lower in dKO mice, but the differences were not statistically significant, which might be due to the high variation among the animals (Supplementary Table 6). Furthermore, dKO mice produced similar amount of feces (1.26±0.35 g/day) as compared to WT mice (1.13±0.08 g/day). Lipid analysis of fecal samples showed that combined deficiency of ABCA1 and SR-BI did not affect fecal cholesterol (2.34±0.04 *vs* 2.43±0.09 mmol/kg) and bile salt content (12.75±2.28 *vs* 10.30±0.65 mmol/kg) as compared to WT mice. Thus, despite the absence of HDL, ABCA1 deficiency did not alter the hepatic lipid content and biliary and fecal sterol secretion in either the WT or the SR-BI KO background.

Impaired macrophage RCT in ABCA1/SR-BI dKO mice

Next, we investigated the effect of combined deficiency of ABCA1 and SR-BI on macrophage-specific RCT. First, bone marrow-derived macrophages from WT, ABCA1 KO, SR-BI KO, and dKO mice were loaded with [^{3}H]-cholesterol and acetylated LDL (acLDL). The lipid-laden macrophages were subsequently injected intraperitoneally into WT mice, and the transport of labeled cholesterol to blood, liver, and feces was measured at 24 h after the injection. Consistent with previous findings [11], ABCA1 deficiency on macrophages did result in a ~20% reduction ($p<0.05$) in the amount of tracer excreted into feces. However, given that the expression of macrophage SR-BI was undetectable after cholesterol loading, we could not pick up the effect of macrophage SR-BI deficiency on RCT in this experimental setting (Supplementary Figure 3). Thus, we next quantified the release of [^{3}H]-cholesterol from acLDL-loaded WT macrophages to the plasma and their transport to the liver and ultimately the feces in WT, ABCA1 KO, SR-BI KO and dKO mice. In line with previous findings [10,11,17], at 24 hours after injection, the absence of HDL due to ABCA1 deficiency resulted in a significant reduction of ^{3}H-cholesterol in

plasma (13.5-fold, p<0.001), liver (1.5-fold, p<0.05), and feces (1.3-fold, p<0.05) (Figure 5). SR-BI KO mice with impaired hepatic uptake of HDL-CE had significantly increased ^{3}H-cholesterol (1.7-fold, p<0.001) in the plasma but reduced ^{3}H-cholesterol in the liver (1.4-fold, p<0.05) and feces (1.3-fold, p<0.05) (Figure 5). Combined deficiency of ABCA1 and SR-BI also led to a significant reduction of ^{3}H-cholesterol in the plasma (13.3-fold, p<0.001), liver (1.7-fold, p<0.05), and feces (1.4-fold, p<0.05). However, no added effect of ABCA1 and SR-BI on the reverse transport of cholesterol from WT macrophages was observed.

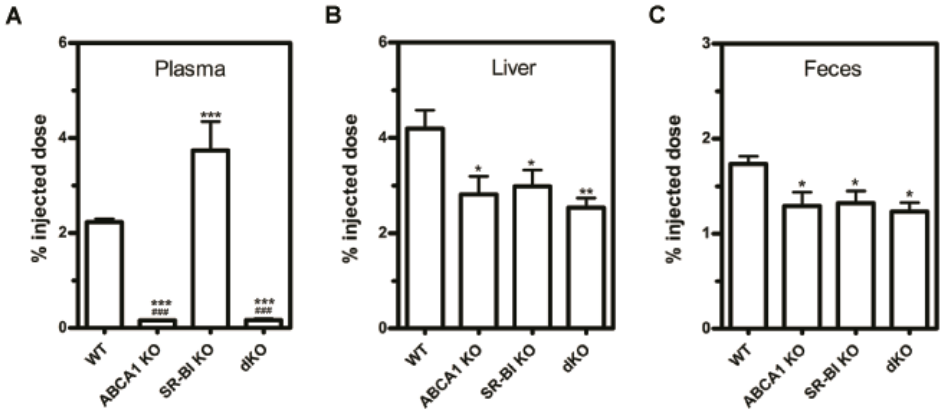

Figure 5. **Impaired macrophage-specific reverse cholesterol transport in ABCA1/SR-BI double knockout mice.** Peritoneal macrophages from WT mice were prepared and labeled with [^{3}H]-cholesterol and acetylated LDL (5 μCi/mL, 100 μg/mL) for 48 hours. After equilibration, [^{3}H]-cholesterol labeled macrophage foam cells were harvested and injected into male WT, ABCA1 KO, SR-BI KO and ABCA1/SR-BI double knockout mice at the age of 12-16 weeks old on chow. Blood (A), liver (B), and feces (C) were collected at 24 hours after injection and the tracer levels in various samples were measured. Data are expressed as percentage of the [^{3}H]-cholesterol tracer relative to total dpm tracer injected ±SEM (n=6). *p<0.05, **p<0.01, ***p<0.001 *vs* WT mice; $^{\#\#\#}$p<0.001 *vs* SR-BI KO mice.

Tissue cholesterol homeostasis in ABCA1/SR-BI dKO mice

To assess the morphological changes associated with combined ABCA1 and SR-BI deficiency, a necropsy of the mice at the age of 16 weeks old on chow diet was performed. No significant differences were observed in liver weight between WT, ABCA1 KO, SR-BI KO, and dKO mice (50.0±1.8 mg/g, 55.3±2.1 mg/g, 56.0±3.0 mg/g, 52.5±3.3 mg/g body weight, respectively). In line with previous findings [8,25,26], ABCA1 KO mice and SR-BI KO mice showed a 1.3-fold (4.4±0.2 mg/g, p<0.05) and a 3.3-fold (11.0±0.5 mg/g, p<0.001) increase in spleen weight, respectively as compared to WT mice (3.3±0.2 mg/g body weight). Interestingly, the spleen weight of dKO mice was increased 1.9-fold to 6.3±0.7 mg/g body weight (p<0.001 *vs* WT), which was significantly lower than the spleen weight of SR-BI KO mice (1.7-fold, p<0.001) and higher than the spleen weight of ABCA1 KO mice (1.4-fold, p<0.01). The splenomegaly observed in SR-BI KO mice was associated with enhanced erythropoiesis in the spleen and the accumulation of reticulocytes in the blood, due to the abnormally high plasma FC levels [25,26]. ABCA1 deficiency did lower plasma FC levels and normalized the counts of reticulocytes in the circulation of SR-BI KO mice (Supplementary Table 4 and 5). The splenomegaly observed in the dKO mice thus can not be the result of enhanced erythropoiesis.

To further determine the effect of combined deficiency of ABCA1 and SR-BI on tissue cholesterol homeostasis, cryostat sections of liver, spleen, lung, thymus, and Peyer's patches in mice at the age of 16 weeks old on chow were stained for neutral lipids with

Oil-red-O. Interestingly, no visible lipid accumulation was found in liver, spleen, and thymus in WT, single ABCA1 KO, single SR-BI KO, and dKO mice at the age of 16 weeks (data not shown). Thus, the splenomegaly observed in single and double KOs was also not due to lipid accumulation. Consistent with previous findings [9], neutral lipid accumulation was observed in the lung of the single ABCA1 KOs. Also, Peyer's patches of

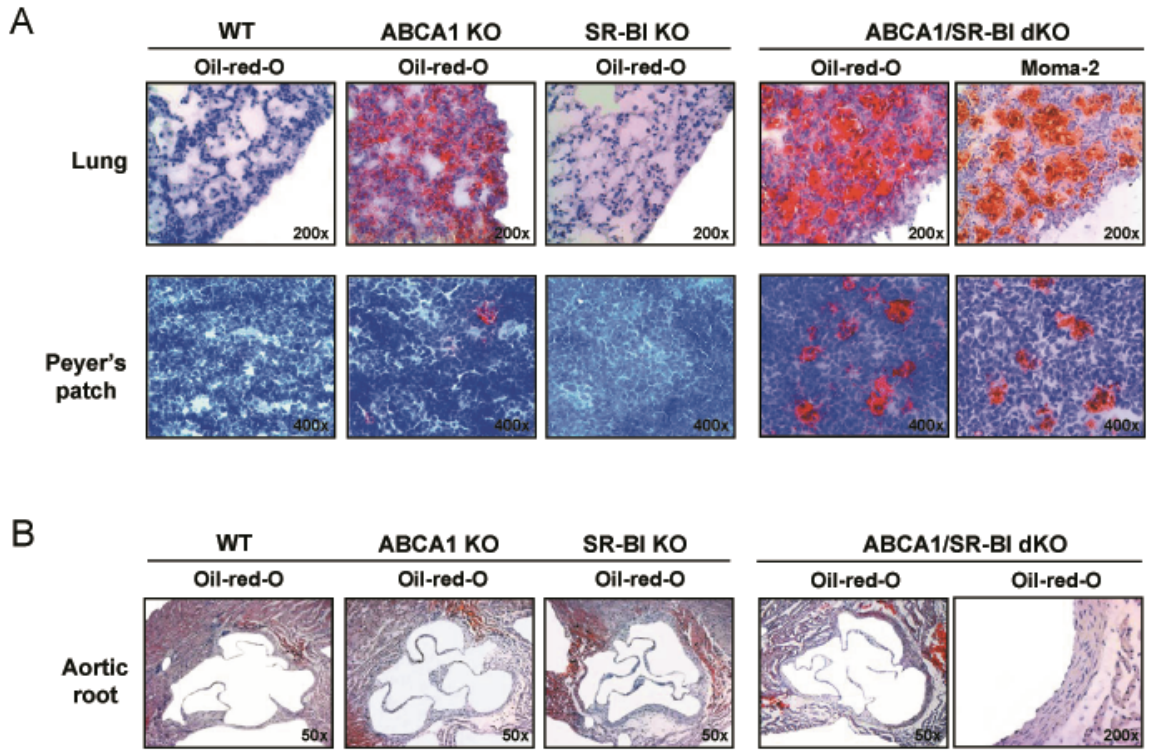

Figure 6. **Enhanced macrophage foam cell formation but no atherosclerosis in ABCA1/SR-BI double knockout mice.** (A and B) A necropsy was performed on mice at the age of 16 weeks on chow diet. Cryostat sections of lung and Peyer's patches were stained with Oil-red-O and a rat monoclonal antibody against Moma-2 to visualize lipid accumulation and macrophages, respectively by light microscopy. (C) Atherosclerosis was analyzed at the aortic root of mice at the age of 1 year old on chow diet. Representative photomicrographs from sections of the aortic root after Oil-red-O lipid staining.

ABCA1 KOs showed red staining with Oil-red-O, consistent with lipid accumulation. Strikingly, dKO mice displayed more extreme macrophage foam cell formation in the lung and Peyer's patches as evidenced by colocalization of Oil-red-O with Moma-2 macrophage staining (Figure 6A). Lipid quantification indicated that accumulated neutral lipid in the lung is cholesterol ester (dKO: 204.2±31.04 μg/mg protein *vs* WT: 1.8±1.2 μg/mg protein, $p<0.001$). Furthermore, atherosclerosis was analyzed at the aortic root of seperate mice at the age of 1 year old on chow diet. As shown in Figure 6B, no atherosclerotic lesions were evident in the WT, ABCA1 KO, and SR-BI KO mice. Despite enhanced macrophage foam cell formation in the lung and Peyer's patches, also dKO mice did not develop any atherosclerotic lesions, even at the age of 1 year. This is most likely due to the fact that the dKO mice lack the high plasma levels of atherogenic lipoproteins needed to trigger arterial wall accumulation of macrophages.

Discussion

In the current study, we for the first time phenotypically characterized ABCA1/SR-BI dKO mice, and studied the interrelationship between ABCA1 and SR-BI in macrophage RCT

using these unique dKO mice lacking both transporters essential for HDL metabolism. ABCA1/SR-BI dKO mice resembled single ABCA1 KO mice in HDL loss and hypocholesterolemia. Although the transport of cholesterol from WT macrophages to feces was impaired in dKO mice, combined deficiency of ABCA1 and SR-BI did not result in an additive effect as compared to the rate of cholesterol transport to feces in single ABCA1 KO and SR-BI KO mice. Interestingly, enhanced macrophage foam cell formation was evident in the lung and Peyer's patches of dKO mice, clearly illustrating the importance of both ABCA1 and SR-BI for macrophage cholesterol homeostasis in these organs. However, no atherosclerotic lesion development was observed in these dKOs, even at the age of 1 year, probably due to the low levels of non-HDL-C.

SR-BI mediated hepatic uptake of HDL cholesterol is nearly completely blocked in SR-BI KO and dKO mice, similar as in SR-BI KO mice. However, with respect to the lipid levels in the plasma and the lipoprotein distribution of cholesterol, our dKO mice resembled single ABCA1 KO mice. The HDL loss in the dKO mice is thus due to impaired HDL production, similarly as previously described for single ABCA1 KO mice [29]. Although ABCA1 deficiency did not affect the hepatic expression of SR-BI, ABCA1 KO mice did take up 2 times more [3H]-CEt from HDL by liver as compared to WT mice. This clearly indicates that endogenous HDL could compete with [3H]-CEt-HDL for uptake by the liver, thereby inhibiting the clearance of [3H]-CEt-HDL in wild-type mice. Importantly, the absence of the endogenous HDL pool in ABCA1 KO and dKO mice allowed us to study the role of SR-BI in HDL catabolism in absence of competition with endogenous HDL in the circulation. We hereby thus for the first time provide direct compelling *in vivo* evidence that SR-BI is the determining factor for the selective uptake CE from HDL by liver in the absence of the endogenous HDL pool.

Interestingly, dKO mice also resembled the single ABCA1 KOs in non-HDL-C levels, which were significantly lower than WT and SR-BI KO mice. VLDL production, however, was increased in dKO and single ABCA1 KO mice. Chung et al previously demonstrated that pre-β migrating nascent HDL generated by ABCA1 inhibits VLDL production through activation of phosphoinositide 3 (PI3)-kinase [30]. As a result, ABCA1 deficiency leads to increased VLDL production *in vivo* secondary to reduced PI3-kinase signaling [31]. Moreover, SR-BI has been shown to promote VLDL production through induction of microsomal triglyceride transfer protein (MTP) activity [32], which might also be regulated via PI3-kinase signaling [33]. In the present study and previous studies [22], we could not show the effect of SR-BI deficiency on VLDL production. SR-BI KO mice, however, do display increased non-HDL cholesterol levels which can be attributed to a direct role of SR-BI in the clearance of VLDL [22]. In the absence of competition with endogenous HDL, VLDL clearance via SR-BI thus might also contribute to the lower levels of non-HDL-C in ABCA1 KO mice. In contrast, the decreased non-HDL-C levels in the circulation of dKO mice are probably the consequence of compensatory upregulation of LRP1-mediated clearance pathway in the liver.

In agreement with a previous study showing that biliary cholesterol secretion is not affected by the absence of HDL [27], our single ABCA1 KO and dKO mice did not display impaired biliary cholesterol secretion. The reduced biliary cholesterol secretion in SR-BI KO mice was observed in previous studies [34,35,36], which could not be confirmed in the current study. Differences in the background of mice [34,35] and treatment of mice, e.g. dietary challenge[35] and viral exposure [36], between the present study and previous studies might account for this different observation. The low levels of basal biliary cholesterol secretion in our single SR-BI KO and dKO mice indicate that SR-BI might not be essential for the basal cholesterol secretion or that the other cholesterol secretion pathways such as ABCG5 and ABCG8 are redundant under this condition.

Although overexpression of SR-BI could increase biliary secretion in the absence of ABCG5 and ABCG8 [37], our results indicate that the contribution of SR-BI at the physiological level to the biliary cholesterol secretion still needs further investigation.

Despite being a tiny pool for RCT, macrophage RCT is crucial for the prevention of macrophage foam cell formation and atherosclerosis [38]. Inactivation of ABCA1 results in HDL deficiency, thereby impairing macrophage RCT [10-11]. Blocking the hepatic CE uptake from HDL by the deletion of SR-BI also impairs macrophage RCT [17]. In line, HDL deficiency in ABCA1/SR-BI dKO mice did lead to the reduced transport of the [^{3}H]-cholesterol tracer from WT macrophages to feces. SR-BI deficiency, however, did not further impair macrophage RCT in the dKO mice as compared to single ABCA1 KO mice. Thus, in dKO mice, the effect of ABCA1 on generation of HDL rather than the delivery of HDL-C to the liver via SR-BI is the rate limiting factor for macrophage RCT. Notably, in ABCA1/SR-BI dKO mice, a substantial amount of the [^{3}H]-cholesterol tracer could still be transferred from WT macrophages to the feces. [^{3}H]-Cholesterol from the macrophages is detected in plasma not only in the HDL pool but also in the non-HDL pool [10-11]. Therefore, non-HDL lipoproteins might also participate in macrophage RCT. Augmentation of the clearance of non-HDL lipoproteins by liver might be thus important for promoting macrophage RCT, thereby protecting against foam cell formation and atherosclerosis. In line, macrophage-derived apoE promotes both the clearance of non-HDL lipoproteins [39] and macrophage-specific reverse cholesterol transport in apoE KO mice [40]. Moreover, erythrocytes and albumin might also aid the transport of cholesterol through the circulation [41,42]. In addition, Van der Velde et al reported a novel reverse cholesterol transport pathway, namely transintestinal cholesterol transport (TICE) that directly transfers cholesterol from blood to the intestinal lumen via enterocytes. TICE can contribute for up to 70% of the daily total body neutral sterol secretion in mice [43]. Interestingly, TICE is not mediated through HDL particles because ABCA1 KO and our dKO mice show unaltered TICE (Vrins CLJ, unpublished data). How important TICE is for macrophage RCT, however, remains to be determined.

ABCA1/SR-BI dKO mice display enhanced macrophage foam cell formation in the lung and Peyer's patches. Macrophages cannot limit the uptake of cholesterol and thus depend on cholesterol efflux mechanisms to prevent foam cell formation. ABCA1, ABCG1, and SR-BI are important players in cholesterol efflux from macrophages [44]. ABCA1 and ABCG1 actively transfer cholesterol to lipid-free/poor apoAI and mature HDL, respectively while SR-BI induces cholesterol efflux to a phospholipid-containing acceptor like mature HDL down a concentration gradient. HDL deficiency and reduced macrophage RCT in single ABCA1 KO and dKO mice thus contribute to the macrophage foam cell formation observed in the lung and the Peyer's patches. Interestingly, However, since more extreme foam cell formation was observed in dKO mice as compared to ABCA1 KO mice, probably also absence of ABCA1 and SR-BI in the macrophages will have contribution to the observed foam cell formation. Wang et al recently demonstrated that macrophage SR-BI does not promote macrophage RCT [45]. In the present study, we also failed to pick up the effect of macrophage SR-BI on macrophage RCT. However, cholesterol loading *in vitro* does downregulate the expression of SR-BI on WT macrophages [46]. Importantly, in previous bone marrow transplantation studies, we have shown that combined deficiency of macrophage ABCA1 and SR-BI did lead to massive foam cell formation in the peritoneal cavity and spleen of LDLr KO mice transplanted with dKO bone marrow and challenged with a Western-type diet [47]. Thus, the combined role of ABCA1 and SR-BI in cholesterol efflux could account for the enhanced formation of macrophage foam cells in the lung and Peyer's patches of the dKO mice *in vivo*. Interestingly, ABCA1/ABCG1 dKO mice showed even more extreme foam cell formation

in the peritoneal cavity as well as other macrophage-rich tissues, including liver, spleen, lung, Peyer's patches and thymus [48]. Thus, despite the similarity in acceptor specificity of SR-BI and ABCG1, their relative *in vivo* importance could be affected by the biological environment of the macrophage and possibly the availability of substrates [47]. Interestingly, both ABCA1/ABCG1 dKO mice and ABCA1/SR-BI dKO mice show enhanced foam cell formation under hypocholesterolemia. The source of lipids for the observed foam cell formation is still elusive. Recent findings indicate that Toll-like receptor activation induces macrophage foam cell formation by promoting the lipid droplet formation in the absence of extracellular lipids [49]. Whether this mechanism contributes to the foam cell formation in our dKO mice warrants further investigation in future. Of note, like ABCA1/ABCG1 dKO mice [48], ABCA1/SR-BI dKO mice did not develop atherosclerotic lesions, further indicating the importance of high levels of atherogenic lipoproteins for the development of atherosclerosis.

In summary, by characterizing our unique ABCA1/SR-BI dKO mice, we have provided more insight into the important roles of ABCA1 and SR-BI in lipid metabolism and macrophage foam cell formation *in vivo*. Our data indicate that both ABCA1-mediated HDL generation and HDL-CE delivery to the liver via SR-BI are essential for macrophage RCT. Macrophage foam cells can be formed under hypocholesterolemia, while the presence of high levels of atherogenic lipoproteins is essential for the induction of atherosclerotic lesion formation.

Acknowledgements

This work was supported by grants from the Netherlands Heart Foundation (2001T4101 to M.V.E. and Y.Z., 2008T070 to M.H., and the Established Investigator grant 2007T056 to M.V.E.), Dutch Digestive Foundation (MLDS grant 04-55; CV), the Catalan University and Research Grants Management Agency (Beatriu de Pinós Postdoctoral Grant to L.C-B), and the Netherlands Organization for Scientific Research (VIDI grant 917.66.301 to M.V.E.).

References

1. Despres JP, Lemieux I, Dagenais GR, Cantin B, Lamarche B. HDL-cholesterol as a marker of coronary heart disease risk: the Quebec cardiovascular study. *Atherosclerosis.* 2000; **153**:263-272.
2. Van Eck M, Pennings M, Hoekstra M, Out R, Van Berkel TJ. Scavenger receptor BI and ATP-binding cassette transporter A1 in reverse cholesterol transport and atherosclerosis. *Curr Opin Lipidol.* 2005; **16**:307-315.
3. Kathiresan S, Melander O, Anevski D, Guiducci C, Burtt NP, Roos C, Hirschhorn JN, Berglund G, Hedblad B, Groop L, Altshuler DM, Newton-Cheh C, Orho-Melander M. Polymorphisms associated with cholesterol and risk of cardiovascular events. *N Engl J Med.* 2008; **358**:1240-1249.
4. Singaraja RR, Van Eck M, Bissada N, Zimetti F, Collins HL, Hildebrand RB, Hayden A, Brunham LR, Kang MH, Fruchart JC, Van Berkel TJ, Parks JS, Staels B, Rothblat GH, Fiévet C, Hayden MR. Both hepatic and extrahepatic ABCA1 have discrete and essential functions in the maintenance of plasma high-density lipoprotein cholesterol levels in vivo. *Circulation.* 2006; **114**:1301-1309.
5. Brunham LR, Kruit JK, Iqbal J, Fievet C, Timmins JM, Pape TD, Coburn BA, Bissada N, Staels B, Groen AK, Hussain MM, Parks JS, Kuipers F, Hayden MR. Intestinal ABCA1 directly contributes to HDL biogenesis in vivo. *J Clin Invest.* 2006; **116**:1052-1062.
6. Brunham LR, Kruit JK, Pape TD, Parks JS, Kuipers F, Hayden MR. Tissue-specific induction of intestinal ABCA1 expression with a liver X receptor agonist raises plasma HDL cholesterol levels. *Circ Res.* 2006; **99**:672-674.
7. Haghpassand M, Bourassa PA, Francone OL, Aiello RJ. Monocyte/macrophage expression of ABCA1 has minimal contribution to plasma HDL levels. *J Clin Invest.* 2001; **108**:1315-1320.

8. Orsó E, Broccardo C, Kaminski WE, Böttcher A, Liebisch G, Drobnik W, Götz A, Chambenoit O, Diederich W, Langmann T, Spruss T, Luciani MF, Rothe G, Lackner KJ, Chimini G, Schmitz G. Transport of lipids from golgi to plasma membrane is defective in tangier disease patients and Abc1-deficient mice. *Nat Genet.* 2000; **24**:192-196.
9. McNeish J, Aiello RJ, Guyot D, Turi T, Gabel C, Aldinger C, Hoppe KL, Roach ML, Royer LJ, de Wet J, Broccardo C, Chimini G, Francone OL. High density lipoprotein deficiency and foam cell accumulation in mice with targeted disruption of ATP-binding cassette transporter-1. *Proc Natl Acad Sci USA.* 2000; **97**:4245-4250.
10. Calpe-Berdiel L, Rotllan N, Palomer X, Ribas V, Blanco-Vaca F, Escolà-Gil JC. Direct evidence in vivo of impaired macrophage-specific reverse cholesterol transport in ATP-binding cassette transporter A1-deficient mice. *Biochim Biophys Acta.* 2005; **1738**:6-9.
11. Wang MD, Franklin V, Marcel YL. In vivo reverse cholesterol transport from macrophages lacking ABCA1 expression is impaired. *Arterioscler Thromb Vasc Biol.* 2007; **27**:1837-1842.
12. Acton S, Osgood D, Donoghue M, Corella D, Pocovi M, Cenarro A, Mozas P, Keilty J, Squazzo S, Woolf EA, Ordovas JM. Association of polymorphisms at the SR-BI gene locus with plasma lipid levels and body mass index in a white population. *Arterioscler Thromb Vasc Biol*. 1999; **19**:1734–1743.
13. Hsu LA, Ko YL, Wu S, Teng MS, Peng TY, Chen CF, CF Chen, Lee YS. Association between a novel 11-base pair deletion mutation in the promoter region of the scavenger receptor class B type I gene and plasma HDL cholesterol levels in Taiwanese Chinese. *Arterioscler Thromb Vasc Biol.* 2003; **23**:1869-1874.
14. Teslovich TM, Musunuru K, Smith AV, et al. Biological, clinical and population relevance of 95 loci for blood lipids. *Nature.* 2010; **466**:707-713.
15. Vergeer M, Korporaal SJ, Franssen R, Meurs I, Out R, Hovingh GK, Hoekstra M, Sierts JA, Dallinga-Thie GM, Motazacker MM, Holleboom AG, Van Berkel TJ, Kastelein JJ, Van Eck M, Kuivenhoven JA. Genetic variant of the scavenger receptor BI in humans. *N Engl J Med.* 2011; **364**:136-145
16. Varban ML, Rinninger F, Wang N, Fairchild-Huntress V, Dunmore JH, Fang Q, Gosselin ML, Dixon KL, Deeds JD, Acton SL, Tall AR. Huszar. Targeted mutation reveals a central role for SR-BI in hepatic selective uptake of high density lipoprotein cholesterol. *Proc Natl Acad Sci USA.* 1998; **95**:4619-4624.
17. Zhang Y, Da Silva JR, Reilly M, Billheimer JT, Rothblat GH, Rader DJ. Hepatic expression of scavenger receptor class B type I (SR-BI) is a positive regulator of macrophage reverse cholesterol transport in vivo. *J Clin Invest.* 2005; **115**:2870-2874.
18. Trigatti B, Rayburn H, Viñals M, Braun A, Miettinen H, Penman M, Hertz M, Schrenzel M, Amigo L, Rigotti A, Krieger M. Influence of the high density lipoprotein receptor SR-BI on reproductive and cardiovascular pathophysiology. *Proc Natl Acad Sci U S A.* 1999; **96**:9322-9327.
19. Miettinen HE, Rayburn H, Krieger M. Abnormal lipoprotein metabolism and reversible female infertility in HDL receptor (SR-BI)-deficient mice. *J Clin Invest.* 2001; **108**:1717-22.
20. Christiansen-Weber TA, Voland JR, Wu Y, Ngo K, Roland BL, Nguyen S, Peterson PA, Fung-Leung WP. Functional loss of ABCA1 in mice causes severe placental malformation, aberrant lipid distribution, and kidney glomerulonephritis as well as high-density lipoprotein cholesterol deficiency. *Am J Pathol*. 2000; **157**:1017–1029.
21. Out R, Hoekstra M, Spijkers JA, Kruijt JK, van Eck M, Bos IS, Twisk J, Van Berkel TJ. Scavenger receptor class B type I is solely responsible for the selective uptake of cholesteryl esters from HDL by the liver and the adrenals in mice. *J Lipid Res.* 2004; **45**:2088-2095.
22. Van Eck M, Hoekstra M, Out R, Bos IS, Kruijt JK, Hildebrand RB, Van Berkel TJ. Scavenger receptor BI facilitates the metabolism of VLDL lipoproteins in vivo. *J Lipid Res.* 2008; **49**:136-146.
23. Maxwell KN, Fisher EA, Breslow JL. Overexpression of PCSK9 accelerates the degradation of the LDLR in a post-endoplasmic reticulum compartment. *Proc Natl Acad Sci U S A.* 2005; **102**:2069-2074. 15677715
24. Fabre AC, Malaval C, Ben Addi A, Verdier C, Pons V, Serhan N, Lichtenstein L, Combes G, Huby T, Briand F, Collet X, Nijstad N, Tietge UJ, Robaye B, Perret B, Boeynaems JM, Martinez LO. P2Y13 receptor is critical for reverse cholesterol transport. *Hepatology.* 2010; **52**:1477-1483.
25. Meurs I, Hoekstra M, van Wanrooij EJ, Hildebrand RB, Kuiper J, Kuipers F, Hardeman MR, Van Berkel TJ, Van Eck M. HDL cholesterol levels are an important factor for determining the lifespan of erythrocytes. *Exp Hematol.* 2005; **33**:1309-19.

26. Holm TM, Braun A, Trigatti BL, Brugnara C, Sakamoto M, Krieger M, Andrews NC. Failure of red blood cell maturation in mice with defects in the high-density lipoprotein receptor SR-BI. *Blood.* 2002; **99**:1817-1824.
27. Groen AK, Bloks VW, Bandsma RH, Ottenhoff R, Chimini G, Kuipers F. Hepatobiliary cholesterol transport is not impaired in Abca1-null mice lacking HDL. *J Clin Invest.* 2001; **108**:843-850.
28. Yu L, Hammer RE, Li-Hawkins J, Von Bergmann K, Lutjohann D, Cohen JC, Hobbs HH. Disruption of Abcg5 and Abcg8 in mice reveals their crucial role in biliary cholesterol secretion. *Proc Natl Acad Sci U S A.* 2002; **99**:16237-16242.
29. Tsujita M, Wu CA, Abe-Dohmae S, Usui S, Okazaki M, Yokoyama S. On the hepatic mechanism of HDL assembly by the ABCA1/apoA-I pathway. *J Lipid Res.* 2005; **46**:154-62.
30. Chung S, Gebre AK, Seo J, Shelness GS, Parks JS. A novel role for ABCA1-generated large pre-beta migrating nascent HDL in the regulation of hepatic VLDL triglyceride secretion. *J Lipid Res.* 2010; **51**:729-742.
31. Chung S, Timmins JM, Duong M, Degirolamo C, Rong S, Sawyer JK, Singaraja RR, Hayden MR, Maeda N, Rudel LL, Shelness GS, Parks JS. Targeted deletion of hepatocyte ABCA1 leads to very low density lipoprotein triglyceride overproduction and low density lipoprotein hypercatabolism. *J Biol Chem.* 2010; **285**:12197-12209.
32. Wiersma H, Nijstad N, Gautier T, Iqbal J, Kuipers F, Hussain MM, Tietge UJ. Scavenger receptor BI facilitates hepatic very low density lipoprotein production in mice. *J Lipid Res.* 2010; **51**:544-553.
33. Qiu W, Federico L, Naples M, Avramoglu RK, Meshkani R, Zhang J, Tsai J, Hussain M, Dai K, Iqbal J, Kontos CD, Horie Y, Suzuki A, Adeli K. Phosphatase and tensin homolog (PTEN) regulates hepatic lipogenesis, microsomal triglyceride transfer protein, and the secretion of apolipoprotein B-containing lipoproteins. *Hepatology.* 2008; **48**:1799-1809.
34. Mardones P, Quiñones V, Amigo L, Moreno M, Miquel JF, Schwarz M, Miettinen HE, Trigatti B, Krieger M, VanPatten S, Cohen DE, Rigotti A. Hepatic cholesterol and bile acid metabolism and intestinal cholesterol absorption in scavenger receptor class B type I-deficient mice. *J Lipid Res.* 2001; **42**:170-180.
35. Van Eck M, Twisk J, Hoekstra M, Van Rij BT, Van der Lans CA, Bos IS, Kruijt JK, Kuipers F, Van Berkel TJ. Differential effects of scavenger receptor BI deficiency on lipid metabolism in cells of the arterial wall and in the liver. *J Biol Chem.* 2003; **278**:23699-23705.
36. Wiersma H, Gatti A, Nijstad N, Kuipers F, Tietge UJ. Hepatic SR-BI, not endothelial lipase, expression determines biliary cholesterol secretion in mice. *J Lipid Res.* 2009; **50**:1571-1580.
37. Wiersma H, Gatti A, Nijstad N, Oude Elferink RP, Kuipers F, Tietge UJ. Scavenger receptor class B type I mediates biliary cholesterol secretion independent of ATP-binding cassette transporter g5/g8 in mice. *Hepatology.* 2009; **50**:1263-1272.
38. Rader DJ, Alexander ET, Weibel GL, Billheimer J, Rothblat GH. The role of reverse cholesterol transport in animals and humans and relationship to atherosclerosis. *J Lipid Res.* 2009; **Suppl**:S189-S194.
39. Van Eck M, Herijgers N, Yates J, Pearce NJ, Hoogerbrugge PM, Groot PH, Van Berkel TJ. Bone marrow transplantation in apolipoprotein E-deficient mice. Effect of ApoE gene dosage on serum lipid concentrations, (beta)VLDL catabolism, and atherosclerosis. *Arterioscler Thromb Vasc Biol.* 1997; **17**:3117-3126.
40. Zanotti I, Pedrelli M, Potì F, Stomeo G, Gomaraschi M, Calabresi L, Bernini F. Macrophage, but not systemic, apolipoprotein E is necessary for macrophage reverse cholesterol transport in vivo. *Arterioscler Thromb Vasc Biol.* 2011; **31**:74-80.
41. Zhao Y, Marcel YL. Serum albumin is a significant intermediate in cholesterol transfer between cells and lipoproteins. *Biochemistry.* 1996; **35**:7174-7180
42. Nikolić M, Stanić D, Baricević I, Jones DR, Nedić O, Niketić V. Efflux of cholesterol and phospholipids derived from the haemoglobin-lipid adduct in human red blood cells into plasma. *Clin Biochem.* 2007; **40**:305-309.
43. Van der Velde AE, Brufau G, Groen AK. 2010. Transintestinal cholesterol efflux. *Curr Opin Lipidol.* **21**:167-171.
44. Zhao Y, Van Berkel TJ, Van Eck M. Relative roles of various efflux pathways in net cholesterol efflux from macrophage foam cells in atherosclerotic lesions. *Curr Opin Lipidol.* 2010; **21**:441-453.
45. Wang X, Collins HL, Ranalletta M, Fuki IV, Billheimer JT, Rothblat GH, Tall AR, Rader DJ. Macrophage ABCA1 and ABCG1, but not SR-BI, promote macrophage reverse cholesterol

transport in vivo. *J Clin Invest.* 2007; **117**:2216-2224.
46. Yu L, Cao G, Repa J, Stangl H. Sterol regulation of scavenger receptor class B type I in macrophages. *J. Lipid Res.* 2004; **45**:889-899.
47. Zhao Y, Pennings M, Hildebrand RB, Ye D, Calpe-Berdiel L, Out R, Kjerrulf M, Hurt-Camejo E, Groen AK, Hoekstra M, Jessup W, Chimini G, Van Berkel TJ, Van Eck M. Enhanced Foam Cell Formation, Atherosclerotic Lesion Development, and Inflammation by Combined Deletion of ABCA1 and SR-BI in Bone Marrow-Derived Cells in LDL Receptor Knockout Mice on Western-Type Diet. *Cir. Res.* 2010; **107**:e20-31.
48. Out R, Jessup W, Le Goff W, Hoekstra M, Gelissen IC, Zhao Y, Kritharides L, Chimini G, Kuiper J, Chapman MJ, Huby T, Van Berkel TJ, Van Eck M. Coexistence of foam cells and hypocholesterolemia in mice lacking the ABC transporters A1 and G1. *Cir. Res.* 2008; **102**:113-120.
49. Nicolaou G, Erridge C. Toll-like receptor-dependent lipid body formation in macrophage foam cell formation. *Curr Opin Lipidol.* 2010; **21**:427-433.

Supplementary methods and data

Materials and Methods

Animals

Both ABCA1 knockout (ABCA1 KO) and SR-BI knockout (SR-BI KO) mice, kindly provided by Dr. G. Chimini [1] and Dr. M. Krieger [2], respectively, were back-crossed onto a C57Bl/6 background for at least 8 generations. Double heterozygous offsprings generated by cross-breeding were subsequently intercrossed to obtain the ABCA1/SR-BI double knockout (dKO) mice. The genotypes were analyzed using the primers shown in supplementary table 1. Mice were maintained on sterilized regular chow, containing 4.3% fat and no added cholesterol (RM3; Special Diet Services, Witham, UK). Animal experiments were performed at the Gorlaeus Laboratories of the Leiden/Amsterdam Center for Drug Research in accordance with the National Laws. All experimental protocols were approved by Ethics Committee for Animal Experiments of Leiden University.

Plasma and hepatic lipid analyses

After an overnight fasting-period, 200 μL of blood was drawn from the mice by tail bleeding. Hepatic lipids were extracted according to the method of Bligh & Dyer [3] and dissolved in 2% Triton X-100. Triglycerides (TG) and Phospholipids (PL) in serum and liver were determined using a standard enzymatic colorimetric assay (TG: Roche Diagnostics, Mannheim, Germany; PL: Spinreact, Girona, Spain). The concentrations of cholesterol in serum and liver were determined by incubation with 0.025 U/mL cholesterol oxidase (Sigma), 0.065 U/mL peroxidise, and 15 μg/mL cholesteryl esterase (Roche Diagnostics, Mannheim, Germany) in reaction buffer (1.0 KPi buffer, pH=7.7 containing 0.01 M phenol, 1 mM 4-amino-antipyrine, 1% polyoxyethylene-9-laurylether, and 7.5% methanol). Absorbance was read at 490 nm. The hepatic lipids levels were normalized to their protein concentrations determined using the BCA^{TM} protein assay (Pierce Biotechnology, Rockford, USA). HDL cholesterol was measured after precipitation with phosphotungstic acid and magnesium ions (Boehringer GmbH). The distribution of cholesterol over the different lipoproteins in serum was determined by fractionation of 30 μL of serum of the individual mice using a Superpose 6 column (3.2 x 300 mm, Smart system; Pharmacia, Uppsala, Sweden).

Blood cell count

Blood was drawn from the tail vein of mice on chow diet at the age of 12-16 weeks old. White and Red blood cells were quantified using an automated Sysmex XT-2000iV Veterinary Hematology analyzer (Sysmex Corporation, Kobe, Japan).

Analysis of gene expression by real-time quantitative PCR

Total RNA was extracted from liver of male animals at the age of 16 weeks old on chow by the acid guanidium thiocyanate-phenol chloroform extraction method according to Chomczynski et al [4]. cDNA was synthesized from 1 μg of total RNA using RevertAid^{TM} M-MuLV Reverse Transcriptase according to manufacturer's instructions. mRNA levels were quantitatively determined on an ABI Prism® 7700 Sequence Detection System (Applied Biosystems, Foster City, CA) using SYBR-green technology. PCR primers (Supplementary Table 2) were designed using Primer Express 1.5 Software with the manufacturer's default settings (Applied Biosystems). mRNA expression levels are indicated relative to the average of the housekeeping genes hypoxanthine phosphoribosyltransferase (HPRT), glyceraldehyde-3-phosphate dehydrogenase (GAPDH), ribosomal protein 36B4, and β-actin.

Western blot Analysis

Livers from 16-week old chow-fed male animals were homogenized with T-PER tissue protein extraction reagent with added protease inhibitors (Pierce Biotechnology, Rockford, USA). Cell debris was removed by centrifugation at 12,000 rpm for 10 min, and the protein content was determined by the Bio-Rad protein assay (Pierce Biotechnology). Aliquots of 50 μg of protein were separated by 7.5% SDS-PAGE electrophoresis and transferred onto nitrocellulose membranes (Schleicher and Schnell, Dassel, Germany). Immunolabelling was performed using either the rabbit polyclonal antibody α-SR-BI (ab3; Abcam, Cambridge, UK), rabbit polyclonal α-LDL receptor-related protein type 1 (α-LRP-1) (H-80; Santa Cruz Biotechnology, CA), rabbit polyclonal α-LDL receptor (EP1553Y) and α-P2Y13 (Novus Biologicals, Cambridge, UK), rabbit polyclonal α-PCSK9 (ab31762, Abcam, Cambridge, UK), rabbit polyclonal α-ABCG5 and α-ABCG8 (H-300, Santa Cruz Biotechnology), mouse monoclonal antibody α-β-actin (C4; Santa Cruz Biotechnology), or mouse monoclonal α-ABCA1 (AC-10, kindly provided by Dr M. R. Hayden (Vancouver, Canada)) as primary antibodies and horseradish peroxidase-conjugated goat-anti-rabbit and goat-anti-mouse IgG (Jackson ImmunoResearch), respectively, as secondary antibodies. Finally, immunolabeling was detected using SuperSignal West Pico Chemiluminescent Substrate (Pierce Biotechnology).

Hepatic HDL cholesterol uptake assay

Human HDL was isolated from blood of healthy subjects by differential ultracentrifugation as described by Redgrave (1975). HDL (1.063 g/mL<d<1.21 g/mL) was labeled with [^{3}H]-Cholesteryl oleoyl ether (CEt) via exchange from donor particles as reported previously [5]. Unilamellar liposome donor particles were formed by sonication of egg yolk phosphatidylcholine supplemented with 50 μCi of [^{3}H-CEt]. A dose of 200 μg apolipoprotein (± 1.2 × 10^{6} dpm) of [^{3}H]CEt-HDL (total volume of 100 μL) was injected into the tail vein of the indicated types of female mice at the age of 12-16 weeks old on chow. At 3 min after injection, a blood sample was drawn to verify the injected dose. At 1h, 2h, 4h, and 24h after injection, blood samples were drawn to measure serum decay. For analysis of liver association, the liver was excised at 24 h after tracer injection, weighed, solubilized, and counted for [^{3}H] radioactivity in a Packard liquid scintillation unit. A correction was made for the radioactivity in the blood present in the liver at the time of sampling as determined by injection of screened [^{125}I]BSA (84.7 μL/g wet weight). Recovery of radioactivity in tissues is around 80% in all different strains of mice (Supplementary Table 3).

In-vivo VLDL production

Female animals at the age of 12-16 weeks old on chow were injected intravenously with 500 mg of Triton WR-1339 (Sigma) per kg body weight as a 15 g/dL solution in 0.9% NaCl after an overnight fast. Previous studies have shown that plasma VLDL clearance is virtually completely inhibited under these conditions [6]. Blood samples (50 μL) were taken at 0, 1, 2, and 3h after Triton WR-1339 injection. Plasma triglycerides were analyzed enzymatically as described above and were

related to the body mass of the animals. The hepatic VLDL production was calculated from the slope of the curve and expressed as g/h/kg body weight.

Bile sampling and biliary Lipid Content determination

Bile was collected from 12-16 weeks old chow-fed male mice by cannulation of the gallbladder under hypnorm (fentanyl/fluanisone; 1 mg/kg) and diazepam (10 mg/kg) anaesthesia, using a humidified incubator to maintain body temperature. Bile was collected at 15 min intervals, and production was determined gravimetrically. All collected bile samples were examined for bile salt and lipid content as described previously [7-8].

Fecal sterol secretion

The male animals at 12-16 weeks old on chow were placed individually in a metabolic cage with food and water available ad libitum. Feces were collected for 24 hours. Fecal samples were lyophilized, weighed and homogenized. Neutral sterols and bile salts were analyzed by gas liquid chromatographic procedures [8].

In-vivo macrophage-specific reverse cholesterol transport assay

Thioglycollate-elicited peritoneal macrophages (PMs) from wildtype mice were loaded with 5 μCi/mL [1α,2α(n)-^{3}H]-cholesterol (Amersham Biosciences Europe GmbH, Germany) and 100 μg/mL of acetylated LDL (acLDL) in DMEM/0.2% BSA for 48 hours, while bone marrow-derived macrophages (BMMs) from different genotypic mice were loaded with 50 μg/mL [3H]-cholesterol-labeled acLDL (5 μCi/mL) in fresh differentiation media containing 4 μg/mL 22-hydroxy-cholesterol and 1 μmol/L 9-cis retinoic acid for 48 hours. These cells were washed, equilibrated and harvested by treatment with accutase (PAA) for 15 min at 37^{o}C. Radioactivity incorporated in the macrophages was determined by lipid extraction and liquid scintillation counting (Beckman). To determine the effect of combined deletion of macrophage ABCA1 and SR-BI on RCT, 5x10^{6} ^{3}H-cholesterol labeled-BMMs in 0.5 mL PBS were injected intraperitoneallly into wildtype male mice on chow at the age of 12-16 weeks old. Next, the different genotypic male mice on chow at the age of 12-16 weeks old were injected intraperitoneallly with 2×10^{6} ^{3}H-cholesterol labeled-PMs in 0.5 mL PBS to determine the effect of combined hepatic ABCA1 and SR-BI deficiency on RCT. Blood was collected at 24 hours after injection via the vena cava and plasma was used for liquid scintillation counting (Beckman). Livers were removed, weighed, solubilized, and counted in a scintillation vial. Feces were collected, dried at 50^{o}C, weighed and rehydrated in 10 mL miliQ water overnight. Fecal samples were then homogenized and radioactivity was determined by liquid scintillation counting (Beckman). The amount of ^{3}H-tracer in plasma, liver, and feces was expressed as a percent of the injected dose.

Histological and tissue lipid analysis

Histological analyses were performed on 10-μm cryosections of lung, liver, spleen, thymus, and Peyer's patches from 16-week old chow-fed animals. Lipid accumulation was determined by oil red O staining, combined with hematoxylin to visualize nuclei. Macrophages were visualized by immunolabeling against Moma-2 (Research diagnostics). Novared was used as the substrate. The red color is the positive staining, visible with regular light microscropy. Atherosclerotic lesion development was quantified in the aortic root of dKO mice of 1 year old animals on chow as described before [9].

Statistical Analysis

Values are expressed as mean±SEM. A one way ANOVA and the Student Newman Keuls posttest were used to compare means after confirming normal distribution by the method Kolmogorov and Smirnov using Graphpad Instat Software (San Diego, USA). A p value of <0.05 was considered significant.

Supplementary data

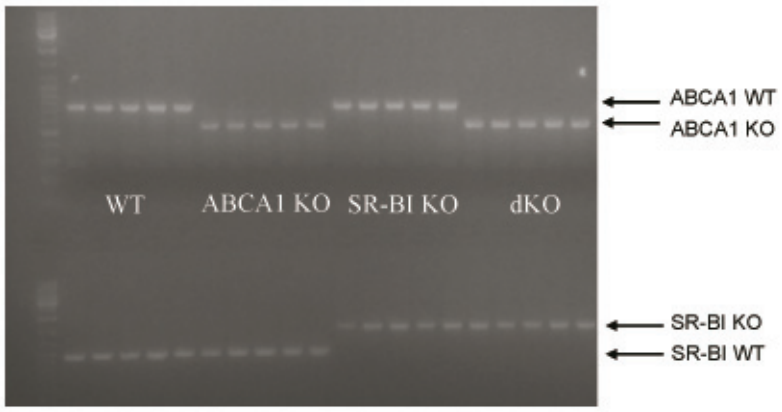

Supplementary Figure 1. Verification of the ABCA1/SR-BI dKO mice. PCR analysis of genomic DNA to verify the genotype of wildtype (WT), ABCA1 knockout (KO), SR-BI KO, and ABCA1/SR-BI double KO (dKO) mice.

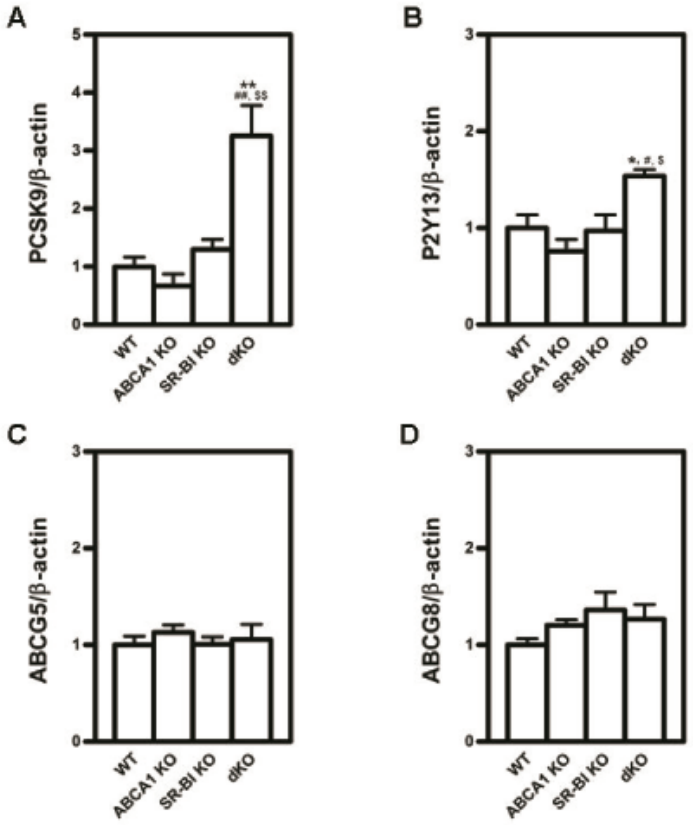

Supplementary Figure 2 Hepatic protein levels of PCSK9 (A), P2Y13 (B), ABCG5 (C), and ABCG8 (D) in ABCA1/SR-BI dKO mice. Livers were harvested from 16-week old chow-fed WT, ABCA1 KO, SR-BI KO, and dKO male mice and total protein was isolated for Western blot analysis as described in Materials and Methods. The expression levels in livers of WT animals were normalized to 1. Data are expressed as mean±SEM (n=3). Statistically significant difference $^{*}p<0.05$ and $^{**}p<0.01$ vs WT mice; $^{\#}p<0.05$ and $^{\#\#}p<0.01$ vs ABCA1 KO mice; $^{\$}p<0.05$ and $^{\$\$}p<0.01$ vs SR-BI KO mice.

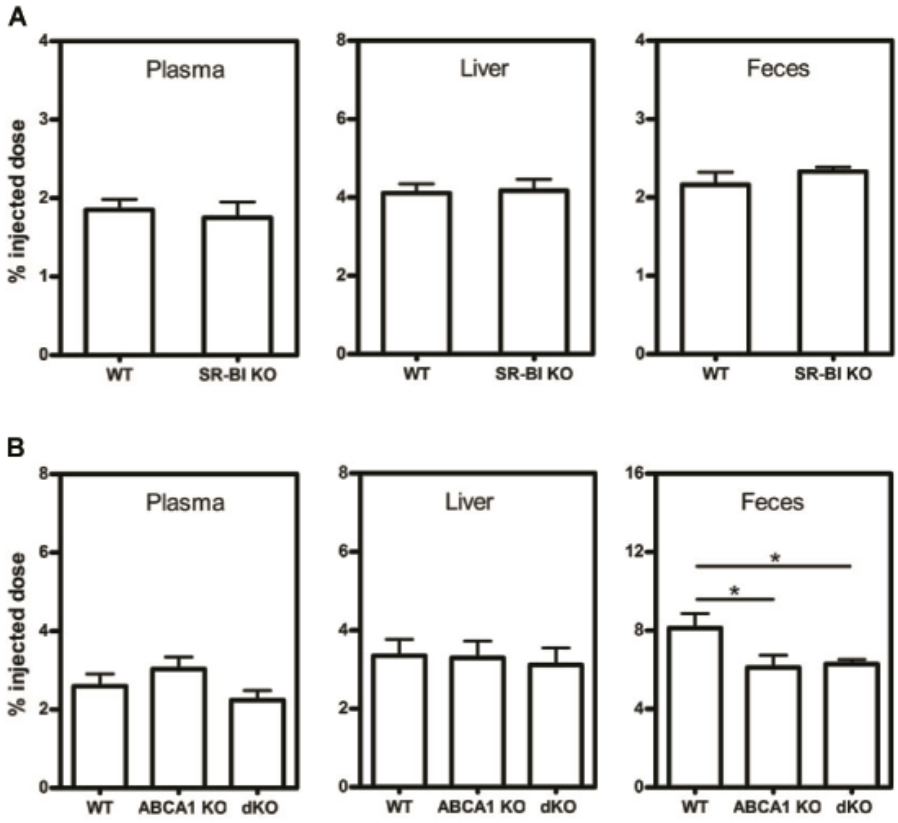

Supplementary Figure 3 Effect of combined deletion of macrophage ABCA1 and SR-BI on reverse cholesterol transport. (A) Macrophages from WT and SR-BI KO mice were labeled with 50 μg/mL [3H]-cholesterol-labeled acLDL before intraperitoneal injection into male WT mice on chow at the age of 12-16 weeks old. (B) Macrophages from WT, ABCA1 KO, and ABCA1/SR-BI dKO mice were labeled with 50 μg/mL [3H]-cholesterol-labeled acLDL in the presence of 4 μg/mL 22-hydroxy-cholesterol and 1 μmol/L 9-cis retinoic acid before intraperitoneal injection into male wildtype mice on chow at the age of 12-16 weeks old. Quantification of macrophage-specific RCT was determined at 24 hours after injection. Data are expressed as mean±SEM (n=4-6/group). Statistically significant difference $^{*}p<0.05$. Macrophage SR-BI deficiency did not affect macrophage-specific RCT, while macrophage ABCA1 deletion led to reduced macrophage-specific RCT. Combined deletion of ABCA1 and SR-BI led to a similar reduction of macrophage-specific RCT as single ABCA1 deficiency.

Supplementary Table 1: Primers for detection of both wild type and the disrupted ABCA1 and SR-BI gene

	Forward Primer	Reverse Primer	PCR products (bp)
ABCA1 WT	'5-TGGGAACTCCTGCTAAAAT-3'	'5-CCATGTGGTGTGTAGACA-3'	600
ABCA1 KO	'5-TTTCTCATAGGGTTGGTCA-3'	5'-TGCAATCCATCTTGTTCAAT-3'	800
SR-BI	'5-GATGGGACATGGGACACGAAGCCATTCT-3'	'5-TCTGTCTCCGTCTCCTTCAGGTCCTGA-3'	1000 for WT, 1200 for KO

Supplementary Table 2: Hepatic mRNA expression levels measured by quantitative real-time PCR in different genotypic mice

Gene	GenBank Accession No.	Forward Primer	Reverse Primer	Amplicon Size
ABCA1	NM013454	GGTTTGGAGATGGTTATACA ATAGTTGT	TTCCCGGAAACGCAAGT C	96
SR-BI	NM016741	GGCTGCTGTTTGCTGCG	GCTGCTTGATGAGGGAG GG	63
LDLR	Z19521	CTGTGGGCTCCATAGGCTAT CT	GCGGTCCAGGGTCATCT TC	68
LRP1	NM008512	TGGGTCTCCCGAAATCTGTT	ACCACCGCATTCTTGAA GGA	95
HPRT	J00423	TTGCTCGAGATGTCATGAAG GA	AGCAGGTCAGCAAAGAA CTTATAGC	91
GAPDH	NM008084	TCCATGACAACTTTGGCATT G	TCACGCCACAGCTTTCC A	103
36B4	NM007475	GGACCCGAGAAGACCTCCTT	GCACATCACTCAGAATT TCAATGG	85
β actin	X03672	AACCGTGAAAAGATGACCC AGAT	CACAGCCTGGATGGCTA CGTA	75

Supplementary Table 3. Recovery of radioactivity in tissues in ABCA1/SR-BI dKO mice

Organ	WT	ABCA1 KO	SR-BI KO	dKO
Serum	39.7±1.30	12.4±1.4	64.6±1.9	51.4±1.1
Liver	26.5±1.5	46.0±3.1	3.5±0.6	3.1±0.3
Spleen	0.22±0.02	0.85±0.26	nd	nd
Pancreas	nd	0.02±0.01	nd	0.01±0.01
Kidney	nd	0.03±0.02	nd	nd
Adrenal	0.59±0.06	3.48±0.11[a]	0.07±0.01[b]	0.09±0.01[b]
Stomach	0.15±0.09	0.29±0.10	0.35±0.14	0.42±0.19
Small intestine	nd	1.15±0.30	nd	0.09±0.09
Large intestine	0.04±0.02	0.69±0.11	nd	nd
Bladder	0.02±0.01	0.03±0.01	nd	0.06±0.01
thymus	0.02±0.01	0.06±0.01	nd	0.06±0.01
Lung	nd	0.25±0.02	nd	nd
Heart	0.13±0.03	0.13±0.01	0.28±0.03	0.29±0.03
fat	0.40±0.07	0.48±0.08	0.29±0.05	1.09±0.06
muscle	0.84±0.32	2.55±0.32[c]	1.03±0.20	3.41±0.21[d]
Bone	5.49±0.68	6.39±1.08	5.70±0.52	8.57±0.27
skin	4.42±0.39	3.96±0.67	6.40±0.25	8.78±0.19
Recovery	78.6%	78.7%	82.3%	77.4%

HDL labeled with [^{3}H]CEt was injected into the tail vein of female different genotypic mice at the age of 12-16 weeks old. At 4h after injection, the animals were sacrificed, serum was collected and tissues were removed. Tissues were assayed for [^{3}H] counts and a correction was made for the contribution of serum to the measured organ associated radioactivity (See Materials and methods). Values are presented as mean ± SEM of 3 female animals at the age of 12-16 weeks old in each group. n.d.: not detectable. Significant difference [a]$p<0.001$ *vs* WT, SR-BI KO, and dKO; [b]$p<0.001$ *vs* WT and ABCA1 KO; [c]$p<0.01$ and [d]$p<0.001$ *vs* WT and SR-BI KO mice.

Supplementary Table 4. Plasma lipid levels of ABCA1/SR-BI dKO mice

Genotype	WT	ABCA1 KO	SR-BI KO	dKO
Free cholesterol (mg/dL)	14.7±0.9	3.6±0.3[a]	80.5±2.0[a,c]	3.6±0.2[a,d]
Total cholesterol (mg/dL)	61.6±2.1	8.3±0.7[a]	123.7±5.7[a,c]	10.5±1.3[a,d]
Phospholipids (mg/dL)	136.9±3.5	46.3±4.8[a]	157.5±2.4[a,c]	47.5±2.0[a,d]
Triglycerides (mg/dL)	51.9±3.6	32.9±3.8[a]	63.7±4.0[b,c]	30.8±2.8[a,d]

Plasma was collected from mice (mixed male and female) at the age of 12-16 weeks old on chow after overnight fasting for lipid analysis. Values are presented as mean ± SEM for 8-13 animals in each group. Statistically significant difference [a]$p<0.001$ and [b]$p<0.05$ *vs* WT; [c]$p<0.001$ *vs* ABCA1 KO; [d]$p<0.001$ *vs* SR-BI KO.

Supplementary Table 5. Blood cell count of ABCA1/SR-BI dKO mice

Genotype	WT	ABCA1 KO	SR-BI KO	dKO
White blood cells ($x10^6$/mL)	12.6±1.0	11.7±0.6	11.2±0.4	10.9±0.7
Lymphocytes ($x10^6$/mL)	10.6±0.8	10.4±0.8	9.4±0.3	9.5±0.7
Monocytes ($x10^6$/mL)	0.45±0.10	0.32±0.04	0.37±0.05	0.35±0.03
Granulocytes ($x10^6$/mL)	1.54±0.25	1.03±0.12	1.17±0.11	0.91±0.12
Red blood cells ($x10^9$/mL)	11.0±0.2	11.5±0.2	10.0±0.1[a,c,d]	10.8±0.3
Reticulocytes ($x10^9$/mL)	0.51±0.02	0.49±0.03	2.12±0.10[b,c,e]	0.50±0.05
Reticulocytes (‰)	45.8±2.5	42.2±2.4	214.9±15.3[b,c,e]	46.3±4.6

Blood were drawn from the tail vein of mice (mixed male and female) at the age of 12-16 weeks old on chow without fasting for cell counting by Sysmex hematology analyzer. Values are presented as mean ± SEM for 6-8 animals in each group. Statistically significant difference [a]$p<0.01$ and [b]$p<0.001$ *vs* WT; [c]$p<0.001$ *vs* ABCA1 KO; [d]$p<0.05$ and [e]$p<0.001$ *vs* dKO.

Supplementary Table 6. Hepatic lipid content and biliary lipid and bile salt secretion in ABCA1/SR-BI dKO mice

Genotype	WT	ABCA1 KO	SR-BI KO	dKO
Hepatic total cholesterol (mg/g)	51.2±3.2	52.8±2.1	56.8±6.1	54.4±2.5
Hepatic Phospholipids (mg/g)	69.5±3.3	77.9±1.9	81.4±8.9	69.8±5.1
Hepatic triglycerides (mg/g)	64.3±5.6	51.7±2.1	68.7±7.5	67.3±10.5
Biliary cholesterol secretion (nmol/min/100 g BW)	0.92±0.15	0.93±0.38	0.79±0.04	0.86±0.18
Biliary phospholipid secretion (nmol/min/100 g BW)	26.5±3.7	21.4±6.9	24.6±1.5	17.0±3.3
Biliary bile salt secretion (nmol/min/100 g BW)	177.8±35.7	119.9±48.6	179.1±14.2	109.7±19.0

Values are presented as mean ± SEM for 5-6 male animals at the age of 12-16 weeks old on chow diet in each group. BW, body weight. No significant differences were found among different genotypic mice in hepatic lipid content and biliary lipid and bile salt secretion.

Supplemental References

1. McNeish, J., R. J. Aiello, D. Guyot, T. Turi, C. Gabel, C. Aldinger, K. L. Hoppe, M. L. Roach, L. J. Royer, J. de Wet, C. Broccardo, G. Chimini, O. L. Francone. 2000. High density lipoprotein deficiency and foam cell accumulation in mice with targeted disruption of ATP-binding cassette transporter-1. *Proc. Natl. Acad. Sci. U. S. A.* **97**:4245-4250.

2. Trigatti B, Rayburn H, Viñals M, Braun A, Miettinen H, Penman M, Hertz M, Schrenzel M, Amigo L, Rigotti A, Krieger M. Influence of the high density lipoprotein receptor SR-BI on reproductive and cardiovascular pathophysiology. *Proc Natl Acad Sci U S A.* 1999; **96**:9322-9327.

3. Bligh, E. G., W. J. Dyer. 1959. A rapid method of total lipid extraction and purification. *Can. J. Med. Sci.* **37**: 911-917.

4. Chomczynski, P., N. Sacchi. 1987. Single-step method of RNA isolation by acid guanidinium thiocyanate-phenol-chloroform extraction. *Anal. Biochem.* **162**:156-159.

5. Fluiter, K, T. J. van Berkel. 1997. Scavenger receptor B1 (SR-B1) substrates inhibit the selective uptake of high-density-lipoprotein cholesteryl esters by rat parenchymal liver cells. *Biochem. J.* **326**:515-519.

6. Aalto-Setälä, K., E. A. Fisher, X. Chen, T. Chajek-Shaul, T. Hayek, R. Zechner, A. Walsh, R. Ramakrishnan, H. N. Ginsberg, J. L. Breslow. 1992. Mechanism of hypertriglyceridemia in human apolipoprotein (apo) CIII transgenic mice. Diminished very low density lipoprotein fractional catabolic rate associated with increased apo CIII and reduced apo E on the particles. *J. Clin. Invest.* **90**:1889-900.

7. Frijters, C. M., R. Ottenhoff, M. J. van Wijland, C. M. van Nieuwkerk, A. K. Groen, R. P. Oude Elferink. 1997. Regulation of mdr2 P-glycoprotein expression by bile salts. *Biochem. J.* **321**:389-395.

8. Voshol, P. J., R. Havinga, H. Wolters, R. Ottenhoff, H. M. Princen, R. P. Oude Elferink, A. K. Groen, F. Kuipers. 1998. Reduced plasma cholesterol and increased fecal sterol loss in multidrug resistance gene 2 P-glycoprotein-deficient mice. *Gastroenterology.* **114**:1024-1034.

10. Zhao, Y., M. Pennings, R. B. Hildebrand, D. Ye, L. Calpe-Berdiel, R. Out, M. Kjerrulf, E. Hurt-Camejo, A. K. Groen, M. Hoekstra, W. Jessup, G. Chimini, T. J. Van Berkel, M. Van Eck. 2010. Enhanced Foam Cell Formation, Atherosclerotic Lesion Development, and Inflammation by Combined Deletion of ABCA1 and SR-BI in Bone Marrow-Derived Cells in LDL Receptor Knockout Mice on Western-Type Diet. *Circ. Res.* **107**:e20-31.

CHAPTER 3

ABC-transporter A1 deficiency induces macrophage foam cell formation and leukocytosis but attenuates atherosclerosis in scavenger receptor class B type I knockout mice

Ying Zhao[1], Jun Wang[2], Ruud Out [1], Dan Ye[1], Theo J.C. Van Berkel[1], Miranda Van Eck[1]

[1] Division of Biopharmaceutics, Leiden/Amsterdam Center for Drug Research, Leiden University, Einsteinweg 55, 2333 CC Leiden, The Netherlands

[2] Department of Human Genetics, Leiden University Medical Center, Leiden, The Netherlands

Abstract

Objective: The aim of this study is to investigate the effect of combined deletion of ABCA1 and SR-BI, important facilitators of reverse cholesterol transport, on atherosclerosis.

Methods and Results: ABCA1xSR-BI double knockout (dKO) mice and respective controls were challenged with an atherogenic diet (ATD) for 10 weeks to induce atherosclerosis. Upon challenge with ATD, dKO mice showed substantially lower cholesterol levels, mainly due to the absence of HDL. The levels of non-HDL cholesterol in dKO mice were similar to WT mice, higher than ABCA1 KO mice, but much lower than SR-BI KO mice. However, dKO mice accumulated more extreme foam cells in the peritoneal cavity. Also, combined deletion of ABCA1 and SR-BI led to enhanced $Ly6C^{high}$ monocytosis in the circulation. Strikingly, despite more susceptible to atherosclerosis than WT animals, dKO mice, similar to ABCA1 KO mice, developed smaller lesions than SR-BI KO mice. This was associated with reduced recruitment of monocytes, probably due to lower levels of the adhesion molecule ICAM-1 in the arterial wall and the monocyte chemoattractant MCP-1 in plasma.

Conclusion: ABCA1 and SR-BI are essential for prevention of macrophage foam cell formation and leukocytosis. ABCA1 deficiency, however, attenuates atherosclerosis in SR-BI KO mice, probably by lowering the circulating levels of atherogenic lipoproteins and reducing the recruitment of monocytes from the circulation into the arterial wall.

--- submitted ---

Introduction

Reverse cholesterol transport (RCT) is important for macrophages to get rid of excess cholesterol, thereby inhibiting foam cell formation and atherosclerosis. Macrophage cholesterol efflux pathways, the first step of RCT, include passive diffusion, and transporter-mediated efflux via ABC-transporter A1 (ABCA1), ABC-transporter G1 (ABCG1), and scavenger receptor class B type I (SR-BI) [1]. ABCA1 and ABCG1 actively transport cholesterol to lipid-free apolipoprotein AI (apoAI) and HDL, respectively, while SR-BI promotes cholesterol efflux to HDL down the gradient [1]. Recently, we showed that macrophage ABCA1 and SR-BI synergistically protect against macrophage foam cell formation and atherosclerotic lesion development in LDL receptor knockout (LDLr KO) mice upon challenge with Western-type diet (WTD) [2]. In addition to macrophages, also hepatocytes of the liver express ABCA1 and SR-BI, where they play a role in the generation of HDL and clearance of HDL cholesterol by selective uptake of cholesteryl ester (CE), respectively. Total-body ABCA1 x SR-BI double knockout (dKO) mice showed enhanced foam cell formation in the lung and Peyer's patches [3]. However, no atherosclerotic lesion development was evident in these dKO mice even when fed WTD for 20 weeks (Zhao Y et al. unpublished data). This might be due to the lack of circulating atherogenic lipoproteins. To investigate the putative synergistic effect of ABCA1 and SR-BI on atherosclerosis, we fed dKO mice a high fat/high cholesterol atherogenic diet (ATD) for 10 weeks. Interestingly, our data demonstrate that ABCA1 deficiency induces macrophage foam cell formation and leukocytosis but inhibits atherosclerotic lesion development in SR-BI KO mice.

Materials and Methods:

Animals

Both ABCA1 KO mice, a kind gift of Dr. G. Chimini [4], and SR-BI KO mice obtained from Dr. M. Krieger [5] were back-crossed onto a C57Bl/6 background for at least 8 generations. Subsequently the mice were cross-bred to generate double heterozygous offspring, which were further intercrossed to obtain the ABCA1/SR-BI double knockout (dKO) mice, and single ABCA1 KO, SR-BI KO, and wild-type (WT) littermates. All mice were maintained on sterilized regular chow containing 4.3% (w/w) fat and no added cholesterol (RM3, Special Diet Services). At 12-16 weeks of age, female animals were fed a semisynthetic atherogenic diet (ATD), containing 15% (w/w) fat, 1% (w/w) cholesterol, and 0.5% (w/w) cholate (Diet N, Abdiets) for 10 weeks. Animal experiments were performed at the Gorlaeus Laboratories of the Leiden/Amsterdam Center for Drug Research in accordance with the National Laws. All experimental protocols were approved by Ethics Committee for Animal Experiments of Leiden University.

Lipid Analyses

After an overnight fasting-period, 100 μL of blood was drawn from the mice by tail bleeding. The concentrations of cholesterol in serum were determined as described before [2]. The distribution of cholesterol over the different lipoproteins in serum was determined by fractionation of 200 μL of pooled serum using a Superose 6 column (3.2 x 300 mm, Smart system; Pharmacia, Uppsala, Sweden).

Serum Atherogenicity Assay

RAW 264.7 (mouse leukaemic monocyte/macrophage cell line) cells were incubated with 3% mouse serum from each group of mice at 37^{o}C for 24 hours. Cells were then stained with Oil-red-O for detection of lipid accumulation and counterstained with hematoxylin.

Blood and Peritoneal Leukocyte Analysis

Upon sacrifice the blood was collected by retro-orbital puncture under anesthesia. The peritoneal cavity of the mice was lavaged with 10 mL cold PBS to collect peritoneal leukocytes. Total white blood cells, neutrophil, lymphocyte, and monocyte counts in the blood and macrophage foam cells in the peritoneal cavity were analyzed using an automated Sysmex XT-2000iV Veterinary Heamatology analyzer (Sysmex Corporation). Corresponding samples were cytospun for manual confirmation and stained with Oil-red-O for detection of lipid accumulation, and counterstained with hematoxylin.

Flow cytometry

Cell surface immunolabelling was performed according to the manufacturer's instructions (eBioscience & BD Biosciences). At sacrifice, blood, spleen, and mediastinal lymph nodes near the heart (HLN) were isolated. Single cell suspensions were obtained by squeezing the organs through a 70 μm cell strainer. Red blood cells were removed from blood and splenocytes using erythrocyte lysis buffer. Subsequently, cells were stained for the surface markers CD11b, CD8, CD44, CD62L (eBiosciences), CD4, Ly6G, and Ly6C (BD Biosciences) for 30 min at 4^{o}C in labeling buffer (1% mouse serum in PBS). Flow cytometric analysis was performed with FacsCalibur and then analyzed with CellQuest software (Becton Dickinson, San Jose), correcting for nonspecific staining with isotype antibody controls.

Histological Analysis of the Aortic Root

On sacrifice the arterial tree was perfused *in situ* with PBS and the heart was excised and stored in 3.7% neutral-buffered formalin (Formal-fixx; Shandon Scientific) until use. Atherosclerotic lesion development was quantified in the aortic root from Oil-red-O/hematoxylin-stained cryostat sections using the Leica image analysis system, consisting of a Leica DMRE microscope coupled to a video camera and Leica Qwin Imaging software (Leica Ltd). Mean lesion area (in μm^2) was calculated from 10 Oil-red-O/hematoxylin-stained sections, starting at the appearance of tricuspid valves. Sections were immunolabeled against MOMA-2 (monoclonal rat IgG2b, dilution 1:50, Research diagnostics), Ly6G (monoclonal rat IgG2b, dilution 1:100, eBioscience), and CD3 (polyclonal Rabbit IgG, dilution 1:150, Neomarkers) for detection of macrophages, neutrophils, and T cells. ICAM-1 expression was visualized using purified anti-mouse CD54 (monoclonal rat IgG2a, dilution 1:100, eBiosciences). All analyses were performed blinded.

Statistical Analysis

Values are expressed as mean±SEM. One way ANOVA and the Student Newman Keuls posttest were used to compare means after confirming normal distribution by the method Kolmogorov and Smirnov using Graphpad Instat Software (San Diego, USA). A p value of <0.05 was considered significant.

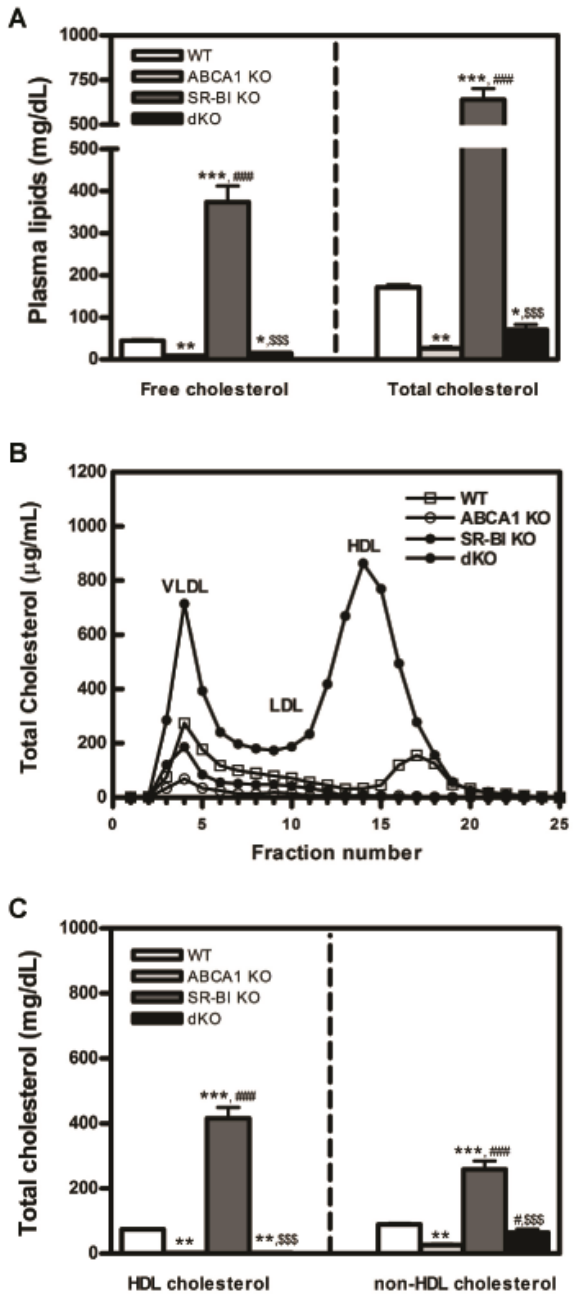

Figure 1. Effect of combined ABCA1 and SR-BI deficiency on plasma cholesterol levels under an atherogenic diet. Plasma free and total cholesterol levels (A), lipoprotein distribution of total cholesterol (B), HDL cholesterol levels and non-HDL cholesterol levels (C) of WT (open bar/open square), ABCA1 KO (light gray bar/close square), SR-BI KO mice (dark gray bar/close circle), and ABCA1/SR-BI dKO mice (dark bar/open circle) at 10 weeks on an atherogenic diet. Bar graphs represent the means±SEM (n=9-15). Two hundred microliters of pooled mouse plasma from the different genotypes were fractioned by FPLC. Statistically significant difference $^{*}p<0.05$, $^{**}p<0.01$, and $^{***}p<0.001$ *vs* WT mice; $^{\#\#\#}p<0.001$ *vs* ABCA1 KO mice; $^{\$\$\$}p<0.001$ *vs* SR-BI KO mice.

Results

Plasma cholesterol levels in ABCA1/SR-BI dKO mice upon challenge with ATD

On a chow diet containing 4.3% fat and no added cholesterol, as reported previously [3], inactivation of SR-BI increased plasma total cholesterol (TC) (137±3 mg/dL *vs* 59±2 mg/dL in WT mice, $p<0.001$) due to the impaired hepatic uptake of HDL-cholesterol (HDL-C). Hypocholesterolemia was evident in both ABCA1 KO (9±1 mg/dL, $p<0.001$) and ABCA1/SR-BI dKO (12±1 mg/dL, $p<0.001$) mice as a result of impaired HDL production. To induce atherosclerotic lesion formation, WT, ABCA1 KO, SR-BI KO and dKO mice were fed ATD containing 15% fat, 1% cholesterol, and 0.5% cholate for 10 weeks. Upon sacrifice, plasma cholesterol levels were determined. Upon challenge with ATD, plasma TC levels were increased 2.9-fold and 4.7-fold, respectively in WT mice (172±6 mg/dL) and SR-BI KO mice (640±62 mg/dL) (Figure 1A). In SR-BI KO mice, around 60% of TC in the plasma is free cholesterol (374±38 mg/dL, $p<0.001$ *vs* WT mice).

Moreover, in agreement with previous findings [12, 13] , the largely elevated TC in SR-BI KO mice on ATD was mainly due to increased cholesterol levels in both large HDL and VLDL (Figure 1B). As compared to WT mice, SR-BI KO mice displayed 5.6-fold ($p<0.001$) and 2.9-fold ($p<0.001$) higher cholesterol levels in HDL-C and non-HDL-C, respectively (Figure 1C). When fed ATD, ABCA1 KO mice showed a 3.0-fold increase in plasma total cholesterol levels (27±4 mg/dL), which were, however, 6.4-fold ($p<0.01$) lower than the levels in WT mice. As shown in Figure 1B and 1C, absence of HDL-C and lower levels of non-HDL-C (3.2-fold, $p<0.01$ *vs* WT mice) accounted for the lower levels of plasma total cholesterol observed in ABCA1 KO mice. DKO mice fed ATD showed a 5.9-fold elevation in plasma TC levels (71±12 mg/dL). TC levels in dKO mice, however, also remained substantially lower than the levels in WT mice (2.4-fold, $p<0.05$) and SR-BI KO mice (9.0-fold, $p<0.001$). Given the absence of HDL-C, plasma cholesterol in dKO mice accumulated in the non-HDL fraction (Figure 1B). Interestingly, dKO mice showed similar levels of non-HDL-C as WT mice, which, notably, were 2.5-fold ($p<0.05$) higher than the levels in ABCA1 KO mice but 4.0-fold ($p<0.001$) lower than the levels in SR-BI KO mice (Figure 1C).

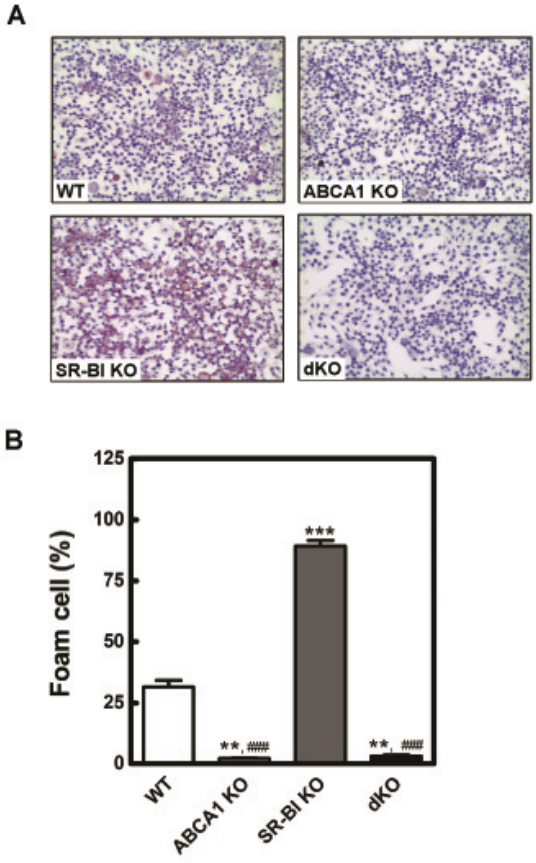

Figure 2. **Effect of combined ABCA1 and SR-BI deficiency on the serum atherogenicity under an atherogenic diet.** (A) Photomicrographs of oil-red-O-stained RAW cells at 24 after incubation with 3% serum from separate mice. (B) Bar graph showing the quantification of the foam cell formation. Values are mean±SEM. Statistically significant difference $^{**}p<0.01$ and $^{***}p<0.001$ *vs* WT mice; $^{###}p<0.001$ *vs* SR-BI KO mice.

ABCA1 deficiency reduced the atherogenicity of serum in the SR-BI KO mice

Macrophage foam cell formation by uptake of atherogenic lipoproteins is the hallmark of atherosclerosis [6]. The serum atherogenicity was tested by determination of foam cell formation after incubation of RAW cells with 3% serum of the different types of mice. As compared to serum from WT mice, serum from SR-BI KO mice induced extreme foam cell formation (2.9-fold, $p<0.001$) (Figure 2A and 2B), while ABCA1 deficiency dramatically reduced the serum atherogenicity against both WT (13-fold, $p<0.001$) and SR-BI KO (10-

fold, p<0.001) background. The atherogenicity of the serum in the different groups of animals is thus SR-BI>WT>dKO>ABCA1 KO and corresponds to the TC levels in serum.

Combined ABCA1 and SR-BI disruption enhances macrophage foam cell formation in the peritoneal cavity upon challenge with ATD

Next, *in vivo* foam cell formation was examined in the peritoneal cavity. The percentage of foam cells was increased 3-fold (p<0.05 *vs* WT) in the peritoneum of ABCA1 KO mice (Figure 3A). Despite more atherogenic lipids in serum, almost no foam cells were observed in peritoneal cavity of SR-BI KO mice. Strikingly, in dKO mice, lipid-laden peritoneal cells were even more numerous (6-fold, p<0.001) as compared to single ABCA1 KO mice (Figure 3A), which were also evident in Oil-red-O stained cytospins of the peritoneal cells (Figure 3B). These data indicate that not only serum lipids, but also the combined action of ABCA1 and SR-BI in macrophages determines the susceptibility to macrophage foam cell formation.

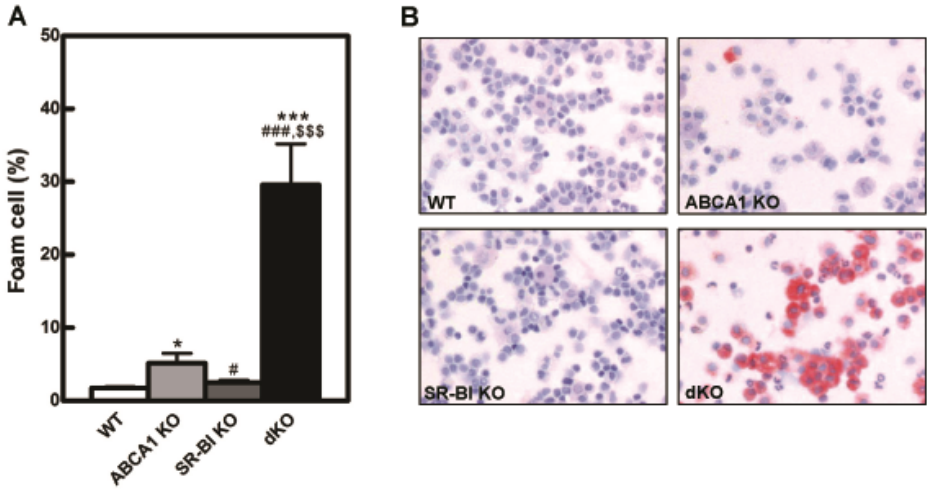

Figure 3. Effect of combined ABCA1 and SR-BI deficiency on macrophage foam cell formation in the peritoneal cavity under an atherogenic diet. (A) Macrophage foam cell formation in the peritoneal cavity of WT (open bar), ABCA1 KO (light gray bar), SR-BI KO (dark gray bar), and ABCA1/SR-BI dKO (dark bar) mice at 10 weeks on an atherogenic diet was quantified as percentage of total leukocytes in the peritoneal cavity. (B) Photomicrographs of Oil-red-O-stained cytospins of peritoneal cells. Values are mean±SEM. Statistically significant difference *p<0.05 and ***p<0.001 *vs* WT mice; $^{\#}$p<0.05 and $^{\#\#\#}$p<0.001 *vs* ABCA1 KO mice; $^{\$\$\$}$p<0.001 *vs* SR-BI KO mice.

Combined ABCA1 and SR-BI disruption increased leukocytosis upon challenge with ATD

Leukocytosis, particularly monocytosis [7] and neutrophilia [8] has been implicated in the development of atherosclerosis. Therefore, circulating leukocytes were analyzed using a hematology analyzer and flow cytometry. As compared to WT mice, SR-BI KO mice displayed a trend towards a larger amount of white blood cells (5.9±0.8 x10^6/mL *vs* 3.8±0.7 x10^6/mL, p=0.09) in the circulation (Figure 4A), mainly due to the elevation of circulating lymphocytes (1.8-fold, p<0.05) (Figure 4B). ABCA1 deficiency resulted in an increase in total white blood cell counts on both the WT (2.6-fold, p<0.001) and SR-BI KO (2.9-fold, p<0.001) background (Figure 4A). Not only lymphocyte counts, but also neutrophil and monocyte counts were elevated in ABCA1 KO mice (lymphocytes: 2.6-fold, p<0.001; neutrophils: 3.8-fold, p<0.05; monocytes: 9.0-fold, p<0.05) and dKO mice

(lymphocytes: 2.1-fold, p<0.01; neutrophils: 5.6-fold, p<0.01; monocytes: 30.7-fold, p<0.01) (Figure 4B, 4C, and 4D). Of note, dKO mice displayed even higher levels of circulating monocytes (3.5-fold, p<0.01) compared to single ABCA1 KO mice. This was associated with a ~2-fold increase in the percentage of Ly6C^{high} monocytes (Figure 2E). Thus, on ATD, combined deletion of ABCA1 and SR-BI resulted in enhanced Ly6C^{high} monocytosis.

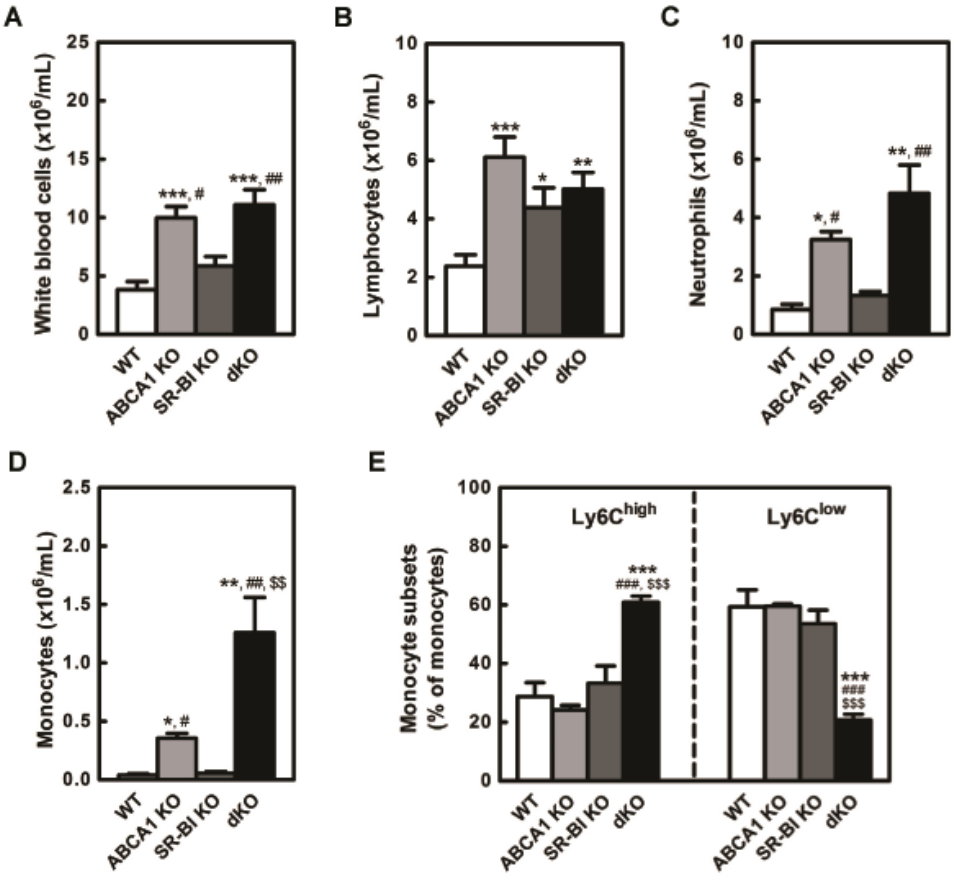

Figure 4. Effect of combined ABCA1 and SR-BI deficiency on circulating leukocyte counts under an atherogenic diet. Circulating total white blood cells (A), lymphocytes (B), neutrophils (C), and monocytes (D) in WT (open bar), ABCA1 KO (light gray bar), SR-BI KO (dark gray bar), and ABCA1/SR-BI dKO (dark bar) mice at 10 weeks on an atherogenic diet were analyzed using a hematology analyzer. Monocyte ($CD11b^+ly6G^-$) subsets expressing different levels of Ly6C were quantified using flow cytometry. Values represent the mean±SEM. Statistically significant difference *p<0.05, **p<0.01, and ***p<0.001 *vs* WT mice; $^{\#}$p<0.05, $^{\#\#}$p<0.01, and $^{\#\#\#}$p<0.001 *vs* ABCA1 KO mice; $^{\$\$}$p<0.01 and $^{\$\$\$}$p<0.001 *vs* SR-BI KO mice.

Next, the peritoneal leukocyte counts were analyzed. The total amount of leukocytes was not changed in the peritoneal cavity of ABCA1 KO or SR-BI KO mice (Supplementary Figure 1A). Interestingly, leukocyte counts were increased ~2-fold in the peritoneal cavity of dKO mice. This was mainly due to elevation of the amount of neutrophils (>=5-fold, p<0.001) and monocytes/macrophages (~2-fold, p<0.01) (Supplementary Figure 1C and 1D). In line with the observed increased Ly6C^{high} monocytosis, the percentage of Ly6C^{high} monocyte-derived macrophages in the peritoneal cavity of dKO mice was also significantly increased (~25-fold, p<0.001) (Supplementary Figure 1E).

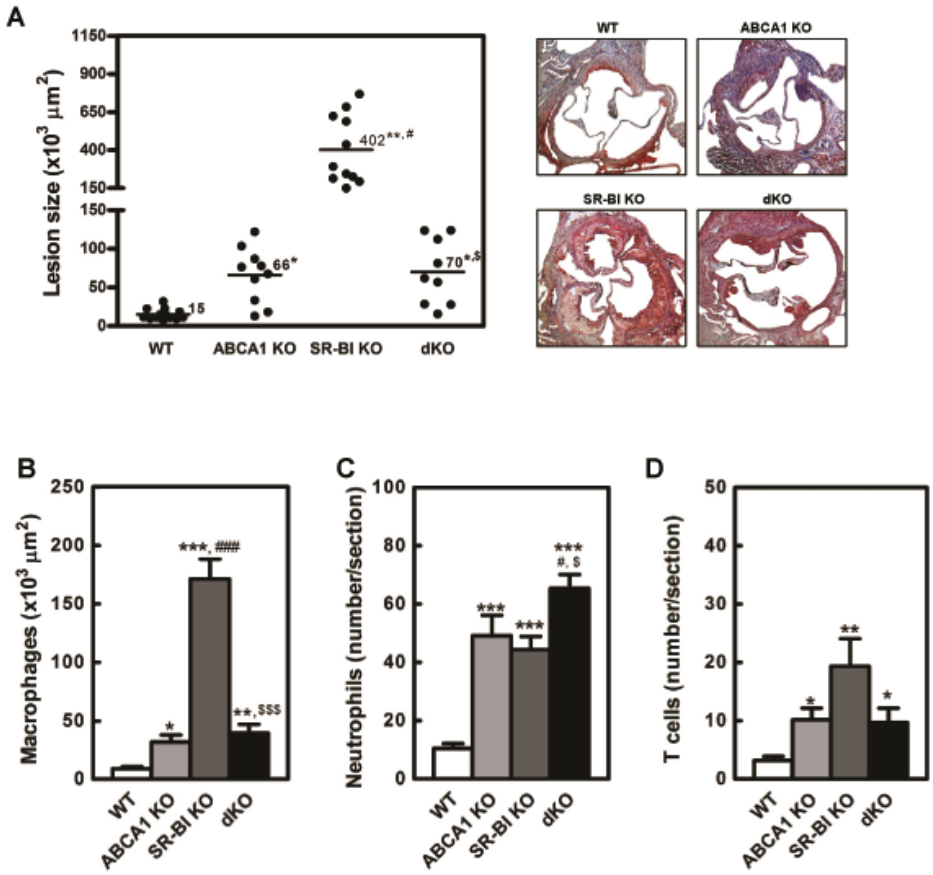

Figure 5. Effect of combined ABCA1 and SR-BI deficiency on the development of atherosclerotic lesions. (A) Photomicrographs showing a scatter dot plot of atherosclerotic lesion quantification (left panel) and representative Oil-red-O stained sections (right panel, original magnification 40x). Each symbol represents the mean lesion area in a single mouse. The horizontal line represents the mean of the group. Bar graphs showing the amount of neutrophils (B), T cells (C), and macrophages (D) in the lesion visualized by immunohistochemical staining with antibodies against Ly6G, CD3, and Moma-2, respectively. Statistically significant difference $^{*}P<0.05$, $^{**}P<0.01$, and $^{***}P<0.001$ *vs* WT mice; $^{\#}P<0.05$ and $^{\#\#\#}P<0.001$ *vs* ABCA1 KO mice; $^{\$}P<0.05$ and $^{\$\$\$}P<0.001$ *vs* SR-BI KO mice.

ABCA1 deficiency attenuated atherosclerotic lesion development in SR-BI KO mice

Atherosclerotic lesion development was quantified at the aortic root of mice challenged with ATD for 10 weeks. The lesion size of ABCA1 KO mice and SR-BI KO mice was increased 4.4-fold ($p<0.05$) and 27-fold ($p<0.01$), respectively as compared to the lesion size of WT mice (Figure 5A). Strikingly, despite enhanced foam cell formation and leukocytosis, dKO mice, similar to ABCA1 KO mice, displayed only 4.7-fold larger lesions than WT mice. Of note, the lesion size of dKO mice was 5.7-fold smaller ($p<0.05$) than SR-BI KO mice (Figure 5A). As the main component of lesions, the amount of macrophages was increased 3.5-fold ($p<0.05$) and 18-fold ($p<0.001$), respectively in lesions of ABCA1 KO and SR-BI KO mice as compared to WT mice (Figure 5B). Despite enhanced Ly6C^{high} monocytosis, dKO mice displayed only 4.3-fold more macrophages in lesions as compared to WT mice. Of note, the amount of macrophages in lesions of dKO mice was 4.3-fold ($p<0.001$) lower than in lesions of SR-BI KO mice (Figure 5B). The reduced lesion formation in dKOs compared to SR-BI KOs might thus be attributed to reduced recruitment of monocytes from circulation.

Next, neutrophils and T cells in lesions and adventitias were quantified. The amount of neutrophils was increased ~5-fold ($p<0.001$) in lesions of single ABCA1 KOs and SR-BI KOs as compared to WT mice (Figure 5C). Interestingly, combined deletion of ABCA1 and SR-BI deficiency led to an additional ~1.4-fold ($p<0.05$) induction of neutrophil infiltration into the lesion (Figure 5C). Furthermore, ABCA1 deficiency also resulted in increased infiltration of T cells (~3-fold, $p<0.05$) into lesions on both the WT and SR-BI KO background (Figure 5C). Interestingly, SR-BI KO mice showed a trend to an increased amount of T cells (2-fold, $p=0.10$) in lesions as compared to ABCA1 KO and dKO mice. However, neutrophils and T cells in the adventitia underlying lesions were comparably increased ~4-fold ($p<0.01$ *vs* WT) and ~3-fold ($p<0.01$ *vs* WT), respectively in all single and double KOs (Supplementary Figure 2A and 2B).

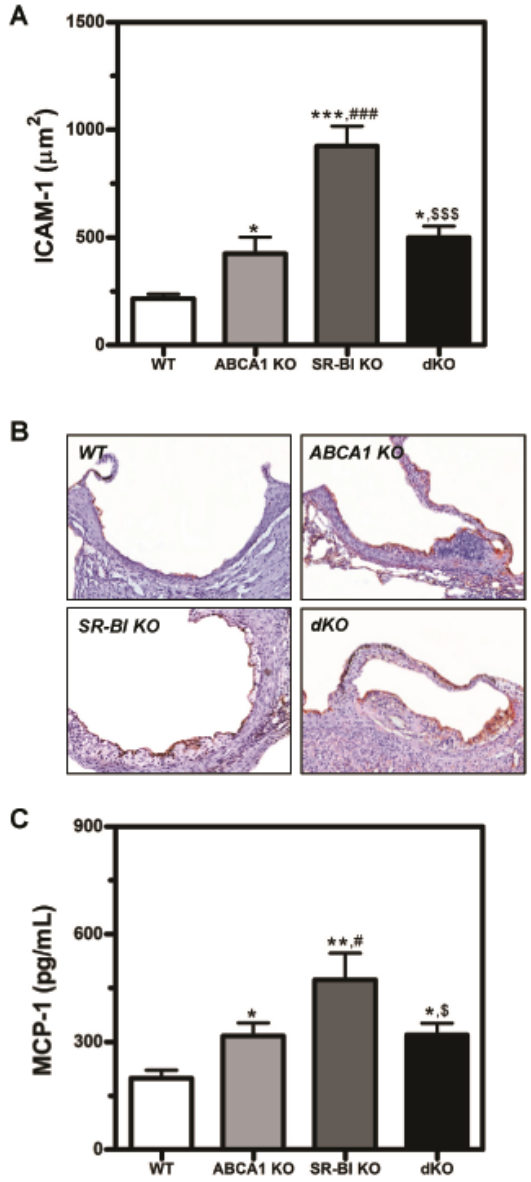

Figure 6. Effect of combined ABCA1 and SR-BI deficiency on the expression of ICAM-1 in the vascular wall under an atherogenic diet. (A) ICAM-1 in the arterial wall at the aortic root of the WT (open bar), ABCA1 KO (light gray bar), SR-BI KO (dark gray bar), and ABCA1/SR-BI dKO (dark bar) mice was detected by immunohistochemistry using a monoclonal rat anti-mouse ICAM-1 antibodies. (B) Representative photomicrographs showing the expression of ICAM-1 in the arterial wall at the aortic root of separate mice. Values are mean±SEM. Statistically significant difference $^{*}p<0.05$and $^{***}p<0.001$ *vs* WT mice; $^{\#\#\#}p<0.001$ *vs* ABCA1 KO mice; $^{\$\$\$}p<0.001$ *vs* SR-BI KO mice.

ABCA1 deficiency attenuates the induction of ICAM-1 in the vascular wall and reduced the plasma MCP-1 levels of SR-BI KO mice

Adherence of leukocytes, especially monocytes to the endothelial layer is required before migration into the intima, thereby promoting atherogenesis [9]. The expression of the

adhesion molecule, ICAM-1 on the vascular wall was thus determined. ICAM-1 expression was upregulated 2.0-fold ($p<0.05$) and 4.3-fold ($p<0.001$), respectively in the endothelial layer overlying lesions of ABCA1 KO and SR-BI KO mice as compared to WT mice (Figure 6A and 6B). Also, dKO mice showed a 2.3-fold ($p<0.05$ vs WT mice) increase in expression of ICAM-1 in the endothelium overlying lesions. In line with the observed effects on lesion size and macrophage content of lesions, the expression of ICAM-1 in the endothelium of lesions of dKO mice was 1.8-fold ($p<0.001$) lower than of lesions of SR-BI KO mice (Figure 6A and 6B).

In addition, the plasma levels of MCP-1, a potent chemoattractant for monocyte migration were also determined. MCP-1 levels were increased 1.6-fold ($p<0.05$) in plasma of both ABCA1 KO and dKO mice. Again, consistent with the lesion size and the amount of macrophage in lesions, dKO mice showed 1.5-fold lower levels of MCP-1 as compared to single SR-BI KO mice.

Discussion

In the current study, we investigated the effects of combined deletion of ABCA1 and SR-BI, important transporters in HDL metabolism, on atherogenesis. Disruption of ABCA1 in SR-BI KO mice led to increased foam cell formation in the peritoneal cavity despite lower levels of pro-atherogenic lipids upon challenge with ATD. Also, $Ly6C^{high}$ monocytosis was enhanced by ABCA1 deficiency in SR-BI KO mice. Despite these apparent pro-atherogenic conditions, ABCA1 deficiency attenuated atherosclerotic lesion development in SR-BI KO animals, probably by lowering the circulating levels of atherogenic lipoproteins and reducing the recruitment of monocytes from the circulation into the arterial wall.

HDL-mediated reverse cholesterol transport is hypothesized to be crucial for prevention of atherosclerotic lesion development. Indeed, impairment of HDL production via ABCA1, disruption of SR-BI-mediated delivery of HDL-C to the liver, or both was associated with increased atherosclerosis. Impaired delivery of HDL-C to the liver in single SR-BI KO mice, however, led a more dramatic increase in atherosclerosis susceptibility as compared to virtual absence of HDL in the circulation due to ABCA1 deficiency on both WT and SR-BI KO background. Combined deletion of ABCA1 and SR-BI on the other hand led to the highest level of foam cell formation in the peritoneal cavity. Enhanced foam cell formation in the peritoneal cavity thus not necessarily correlates with the development of atherosclerotic lesions, especially under hypocholesterolemic conditions.

Previously, we showed that *in vivo* RCT was impaired to a similar degree upon injection of WT macrophages into ABCA1 KO mice, SR-BI KO mice, and dKO mice [3]. This seems to be in contrast to a recent study by Yamamoto et al showing that suppression of hepatic ABCA1 activity by probucol promotes *in vivo* RCT in SR-BI KO mice [10]. Of note, in contrast to ABCA1/SR-BI dKO mice, SR-BI KO animals treated with probucol still transported a substantial amount of their cholesterol in HDL which might be required for the enhancement of RCT by probucol. Importantly, the similar impairment of RCT in ABCA1 KO, SR-BI KO, and dKO mice cannot explain the observed differences in macrophage foam cell in vivo formation nor atherosclerosis susceptibility. Macrophage foam cell formation is determined by the balance between cholesterol influx and efflux. Furthermore, animal studies have shown that a concentration of 250 mg/dL total cholesterol in serum is required for the induction of atherosclerosis [11]. Consistent with previous studies [12], single SR-BI KO mice also displayed a dramatic elevation of plasma

cholesterol levels upon challenge with ATD due to the accumulation of large HDL as well as VLDL. This is because SR-BI also plays an important physiological role in the clearance of VLDL [13]. Due to the increased content of pro-atherogenic lipoproteins, plasma of SR-BI KO mice had a high capacity to induce foam cell formation upon incubation with RAW cells, which also corresponded to the increased susceptibility to atherosclerotic lesion development of these animals. Furthermore, HDL that accumulates in SR-BI KO mice has reduced anti-oxidant properties, as evidenced by increased oxidative stress in these animals [14]. Oxidative modification of HDL by myeloperoxidase (MPO) induces the expression of adhesion molecules on aortic endothelial cells [15]. In agreement, SR-BI KO mice showed increased expression of ICAM-1 in the endothelial layer overlying atherosclerotic lesions.

Single ABCA1 KO and ABCA1/SR-BI dKOs, when fed ATD, displayed a total cholesterol concentration of only ~25 mg/dL and ~70 mg/dL. This is because disruption of ABCA1 in SR-BI KO mice not only diminished HDL but also greatly reduced the amount of cholesterol transported by VLDL. ABCA1 deficiency increases VLDL production in mice on chow [3]. However, the absence of apoE-rich HDL, which accumulates in plasma of SR-BI KO mice, might result in less competition with VLDL for uptake via the LDLr and LDLr-related protein 1 (LRP1) in dKO mice. Of note, the non-HDL cholesterol levels of dKO mice were higher than single ABCA1 KO mice, stressing the importance of SR-BI for the clearance of VLDL. However, plasma of ABCA1 KO and ABCA1/SR-BI dKO mice had a similarly low capacity to induce foam cell formation upon incubation with RAW cells, which was substantially lower than the capacity of plasma from single SR-BI KO mice. Furthermore, ICAM-1 expression in the endothelial layer overlying the atherosclerotic lesions of single ABCA1 KO and ABCA1/SR-BI dKO mice was reduced as compared to single SR-BI KO mice. It is interesting to speculate that this might be the result of the absence of dysfunctional HDL particles and the reduction of pro-atherogenic lipoproteins due to inactivation of ABCA1 in SR-BI KO mice. Nevertheless, ABCA1 KO and dKO mice did develop moderate atherosclerotic lesions when challenged with ATD for 10 weeks. The atherosclerosis susceptibility of single ABCA1 KO and dKO mice is thus likely the consequence of other pro-atherogenic factors than lipids in the plasma.

Epidemiological observations showed that leukocytosis, especially monocytosis and neutrophilia, is strongly associated with the progression of atherosclerosis [16]. Hypercholesterolemia induces leukocytosis, in particular neutrophilia and monocytosis [7, 8]. Of note, even under hypocholesterolemia increased amounts of neutrophils and monocytes were evident in single ABCA1 KO and ABCA1/SR-BI dKO mice on ATD. Yvan-Charvet et al recently showed that HDL is essential to suppress the proliferation of hematopoietic stem cells (HSC) [17]. The observed increase in circulating neutrophils and monocytes might thus be due to lack of suppression by HDL [17]. HDL-mediated cholesterol efflux mechanisms are crucial for inhibiting the proliferation of HSC [17]. The large HDL that accumulates in SR-BI KO mice has enhanced cholesterol efflux capacity [18]. In line, no induction of monocytosis and neutrophilia was observed in SR-BI KO mice despite hypercholesterolemia. Moreover, the cholesterol efflux transporters ABCA1 and ABCG1 are important for cholesterol homeostasis of HSC [17]. Currently, it is unknown if SR-BI is expressed on HSC and might be involved in HSC cholesterol homeostasis. DKO mice on ATD showed increased monocytosis as compared with single ABCA1 KO mice. This suggests that SR-BI might indeed be involved in maintaining HSC cholesterol homeostasis.

Circulating monocytes, the precursors of macrophages, are a heterogenous population of cells which can be distinguished based on the expression level of Ly6C [7].

Ly6C^{high} monocytosis is promoted by hypercholesterolemia [7]. Enhanced Ly6C^{high} monocytosis in dKO mice as compared to single ABCA1 KO mice might thus also be attributed to elevated levels of non-HDL cholesterol. Ly6C^{high} monocytes selectively populate sites of experimentally induced inflammation, while their Ly6C^{low} counterparts can enter lymphoid and nonlymphoid tissues under homeostatic conditions [19]. In line, the major population of monocytes/macrophages in the peritoneal cavity of WT, single ABCA1 KO, and SR-BI KO mice was Ly6C^{low}. Increased accumulation of Ly6C^{high} monocytes/macrophages in the peritoneal cavity of dKO mice might be attributed to enhanced Ly6C^{high} monocytosis in the circulation. In addition, macrophage foam cells in the peritoneal cavity of the dKO mice, as a source of pro-inflammatory factors, might preferentially attract Ly6C^{high} monocytes from circulation.

Drechsler et al. has elegantly shown that hypercholesterolemia-induced neutrophilia and subsequent infiltration of neutrophils promotes the development of early atherosclerotic lesions in apoE KO mice [8]. Upon activation, these neutrophils can secrete oxygen which induces endothelial dysfunction and initiates lesion development [20]. Despite lack of atherogenic lipoproteins, single ABCA1 KO and dKO mice showed a dramatic increase of neutrophils in lesions. Accelerated lesion development of single ABCA1 KOs and dKOs might thus be a consequence of the observed neutrophilia in these animals and enhanced recruitment of neutrophils into the arterial wall. In contrast to the neutrophilia, Ly6C^{high} monocytosis, particularly in the dKO mice, did not lead to a further enhancement of atherosclerosis. Recruitment of monocytes into atherosclerotic lesions involves several adhesion molecules, including ICAM-1 and VCAM-1, and chemokines [9]. As indicated above, ICAM-1 expression in the endothelial layer overlying the atherosclerotic lesions of single ABCA1 KO and ABCA1/SR-BI dKO mice was reduced as compared to single SR-BI KO mice. Furthermore, the attenuated atherosclerosis in dKO mice (as compared to single SR-BI KO mice) was associated with lower levels of MCP-1, an important chemoattractant for monocytes. Deletion of monocyte chemoattractant MCP-1 or ICAM-1 inhibits the development of atherosclerotic lesions [21, 22], indicating that these are essential factors for recruitment of monocytes into the subendothelial space of the arterial wall. The reduced levels of MCP-1 in the blood and lower level of ICAM-1 expression in the endothelium might thus explain why the enhanced Ly6C^{high} monocytosis in the dKO mice did not lead to larger lesions as compared with ABCA1 KO mice with less extreme monocytosis.

In summary, by using our unique ABCA1/SR-BI dKO mice, we have provided more insights into roles of facilitators of reverse cholesterol transport in atherogenesis *in vivo*. Our data indicate that ABCA1-mediated HDL generation and HDL-C delivery to the liver via SR-BI are essential for prevention of atherosclerosis. Despite more foam cell formation and leukocytosis, ABCA1 deficiency inhibits the recruitment of monocytes from the circulation and attenuated atherosclerotic lesion development in SR-BI KO mice. This is probably due to the reduction of proatherogenic lipoproteins, including VLDL and dysfunctional HDL by inactivation of ABCA1. Therefore, lowering cholesterol levels of non-HDL and elevating levels of functional HDL are both important for prevention of atherosclerosis.

Acknowledgements

This work was supported by grants from the Netherlands Heart Foundation (2001T4101 to M.V.E. and Y.Z., 2008T070 to M.H., and the Established Investigator grant 2007T056 to M.V.E.).

References

1. Zhao Y, Van Berkel TJ, Van Eck M. Relative roles of various efflux pathways in net cholesterol efflux from macrophage foam cells in atherosclerotic lesions. *Curr Opin Lipidol.* 2010; 21(5):441-53.
2. Zhao Y, Pennings M, Hildebrand RB, Ye D, Calpe-Berdiel L, Out R, Kjerrulf M, Hurt-Camejo E, Groen AK, Hoekstra M, Jessup W, Chimini G, Van Berkel TJ, Van Eck M. Enhanced foam cell formation, atherosclerotic lesion development, and inflammation by combined deletion of ABCA1 and SR-BI in Bone marrow-derived cells in LDL receptor knockout mice on western-type diet. *Circ Res.* 2010; 107(12):e20-31.
3. Zhao Y, Pennings M, Vrins CL, Calpe-Berdiel L, Hoekstra M, Kruijt JK, Ottenhoff R, Hildebrand RB, van der Sluis R, Jessup W, Le Goff W, Chapman MJ, Huby T, Groen AK, Van Berkel TJ, Van Eck M. Hypocholesterolemia, foam cell accumulation, but no atherosclerosis in mice lacking ABC-transporter A1 and scavenger receptor BI. *Atherosclerosis*. 2011; in press
4. Orsó E, Broccardo C, Kaminski WE, Böttcher A, Liebisch G, Drobnik W, Götz A, Chambenoit O, Diederich W, Langmann T, Spruss T, Luciani MF, Rothe G, Lackner KJ, Chimini G, Schmitz G. Transport of lipids from golgi to plasma membrane is defective in tangier disease patients and Abc1-deficient mice. Nat Genet. 2000; 24(2):192-6.
5. Miettinen HE, Rayburn H, Krieger M. Abnormal lipoprotein metabolism and reversible female infertility in HDL receptor (SR-BI)-deficient mice. *J Clin Invest.* 2001; 108(11):1717-22.
6. van Berkel TJ, Out R, Hoekstra M, Kuiper J, Biessen E, van Eck M. Scavenger receptors: friend or foe in atherosclerosis? *Curr Opin Lipidol.* 2005; 16(5):525-35.
7. Swirski FK, Libby P, Aikawa E, Alcaide P, Luscinskas FW, Weissleder R, Pittet MJ. Ly-6Chi monocytes dominate hypercholesterolemia-associated monocytosis and give rise to macrophages in atheromata. *J Clin Invest.* 2007; 117(1):195-205.
8. Drechsler M, Megens RT, van Zandvoort M, Weber C, Soehnlein O. Hyperlipidemia-triggered neutrophilia promotes early atherosclerosis. *Circulation.* 2010; 122(18):1837-45.
9. Dong ZM, Wagner DD. Leukocyte-endothelium adhesion molecules in atherosclerosis. *J Lab Clin Med.* 1998; 132(5):369-75.
10. Yamamoto S, Tanigawa H, Li X, Komaru Y, Billheimer JT, Rader DJ. Pharmacologic Suppression of Hepatic ATP-Binding Cassette Transporter 1 Activity in Mice Reduces High-Density Lipoprotein Cholesterol Levels but Promotes Reverse Cholesterol Transport. *Circulation.* 2011; in press
11. Getz GS, Reardon CA. Diet and murine atherosclerosis. *Arterioscler Thromb Vasc Biol.* 2006; 26(2):242-9.
12. Huby T, Doucet C, Dachet C, Ouzilleau B, Ueda Y, Afzal V, Rubin E, Chapman MJ, Lesnik P. Knockdown expression and hepatic deficiency reveal an atheroprotective role for SR-BI in liver and peripheral tissues. *J Clin Invest.* 2006; 116(10):2767-76.
13. Van Eck M, Hoekstra M, Out R, Bos IS, Kruijt JK, Hildebrand RB, Van Berkel TJ. Scavenger receptor BI facilitates the metabolism of VLDL lipoproteins in vivo. *J Lipid Res.* 2008; 49(1):136-46.
14. Van Eck M, Hoekstra M, Hildebrand RB, Yaong Y, Stengel D, Kruijt JK, Sattler W, Tietge UJ, Ninio E, Van Berkel TJ, Praticò D. Increased oxidative stress in scavenger receptor BI knockout mice with dysfunctional HDL. *Arterioscler Thromb Vasc Biol.* 2007; 27(11):2413-9.
15. Undurti A, Huang Y, Lupica JA, Smith JD, DiDonato JA, Hazen SL. Modification of high density lipoprotein by myeloperoxidase generates a pro-inflammatory particle. *J Biol Chem.* 2009; 284(45):30825-35.
16. Loimaala A, Rontu R, Vuori I, Mercuri M, Lehtimäki T, Nenonen A, Bond MG. Blood leukocyte count is a risk factor for intima-media thickening and subclinical carotid atherosclerosis in middle-aged men. *Atherosclerosis.* 2006; 188(2):363-9.
17. Yvan-Charvet L, Pagler T, Gautier EL, Avagyan S, Siry RL, Han S, Welch CL, Wang N, Randolph GJ, Snoeck HW, Tall AR. ATP-binding cassette transporters and HDL suppress hematopoietic stem cell proliferation. *Science.* 2010; 328(5986):1689-93.
18. Brundert M, Heeren J, Bahar-Bayansar M, Ewert A, Moore KJ, Rinninger F. Selective uptake of HDL cholesteryl esters and cholesterol efflux from mouse peritoneal macrophages independent of SR-BI. *J Lipid Res.* 2006; 47(11):2408-21.

19. Sunderkötter C, Nikolic T, Dillon MJ, Van Rooijen N, Stehling M, Drevets DA, Leenen PJ. Subpopulations of mouse blood monocytes differ in maturation stage and inflammatory response. *J Immunol.* 2004; 172(7):4410-7.

20. Harrison D, Griendling KK, Landmesser U, Hornig B, Drexler H. Role of oxidative stress in atherosclerosis. *Am J Cardiol.* 2003; 91(3A):7A-11A.

21. Gosling J, Slaymaker S, Gu L, Tseng S, Zlot CH, Young SG, Rollins BJ, Charo IF. MCP-1 deficiency reduces susceptibility to atherosclerosis in mice that overexpress human apolipoprotein B. *J Clin Invest.* 1999; 103(6):773-8.

22. Kitagawa K, Matsumoto M, Sasaki T, Hashimoto H, Kuwabara K, Ohtsuki T, Hori M. Involvement of ICAM-1 in the progression of atherosclerosis in APOE-knockout mice. *Atherosclerosis.* 2002; 160(2):305-10.

Supplementary data

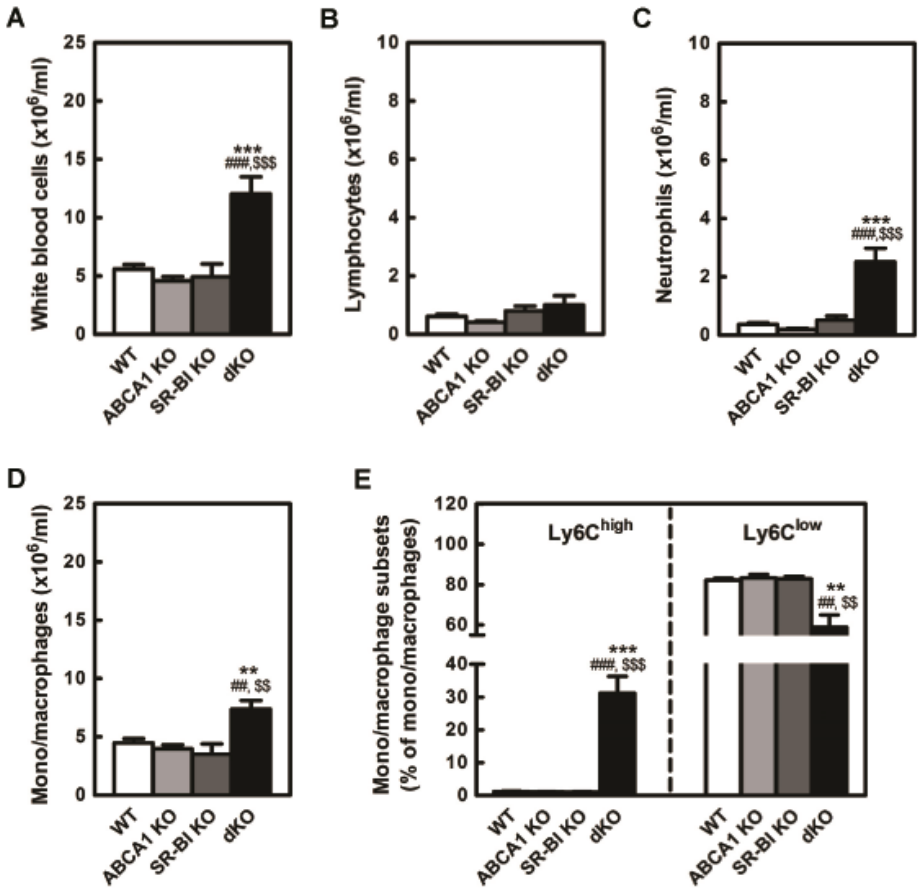

Supplementary Figure 1. Effect of combined ABCA1 and SR-BI deficiency on peritoneal leukocytes under an atherogenic diet. Total white blood cells (A), lymphocytes (B), neutrophils (C), and monocytes (D) in the peritoneal cavity of WT (open bar), ABCA1 KO (light gray bar), SR-BI KO (dark gray bar), and ABCA1/SR-BI dKO (dark bar) mice at 10 weeks on an atherogenic diet were analyzed using a hematology analyzer. Monocyte ($CD11b^+ly6G^-$) subsets expressing different levels of Ly6C were quantified using flow cytometery. Values represent the mean±SEM. Statistically significant difference $^{**}p<0.01$ and $^{***}p<0.001$ *vs* WT mice; $^{\#\#}p<0.01$, and $^{\#\#\#}p<0.001$ *vs* ABCA1 KO mice; $^{\$\$}p<0.01$ and $^{\$\$\$}p<0.001$ *vs* SR-BI KO mice.

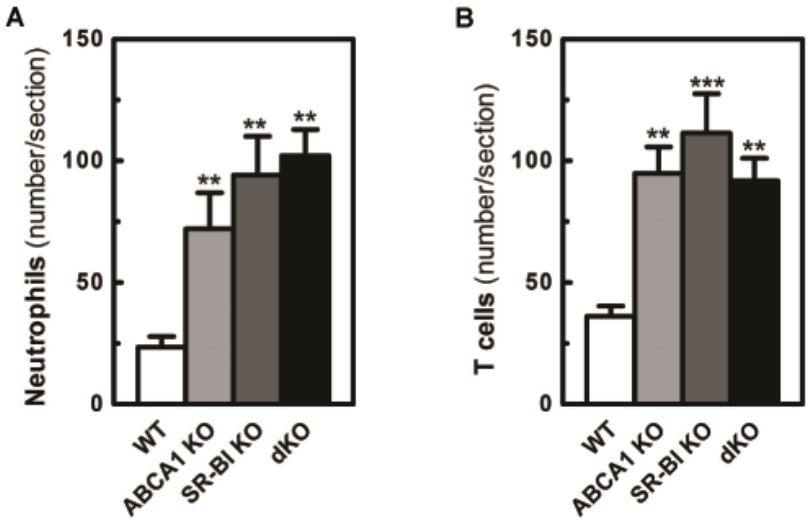

Supplementary Figure 2. Effect of combined ABCA1 and SR-BI deficiency on the recruitment of neutrophils and T cells into the adventitia underlying atherosclerotic lesions under an atherogenic diet. Bar graphs showing the amount of neutrophils (A) and T cells (B) in the adventitia visualized by immunohistochemical staining with antibodies against Ly6G and CD3, respectively. Statistically significant difference $^{**}P<0.01$ and $^{***}P<0.001$ *vs* WT mice.

CHAPTER 4

Relative roles of various efflux pathways in net cholesterol efflux from macrophage foam cells in atherosclerotic lesions

Ying Zhao, Theo J.C. Van Berkel, and Miranda Van Eck

Division of Biopharmaceutics, Leiden/Amsterdam Center for Drug Research, University of Leiden, Leiden, The Netherlands

Purpose of this review
Cholesterol efflux mechanisms are essential for macrophage cholesterol homeostasis. HDL, an important cholesterol efflux acceptor, comprises a class of heterogeneous particles that induce cholesterol efflux via distinct pathways. This review focuses on the understanding of the different cholesterol efflux pathways and physiological acceptors involved, and their regulation in atherosclerotic lesions.

Recent findings
The synergistic interactions of ATP-binding cassette A1 (ABCA1) and G1 (ABCG1) as well as ABCA1 and scavenger receptor class B type I (SR-BI) are essential for cellular cholesterol efflux and the prevention of macrophage foam cell formation. However, the importance of aqueous diffusion should also not be underestimated. Significant progress has been made in understanding the mechanisms underlying ABCA1-mediated cholesterol efflux and regulation of its expression and trafficking. Conditions locally in the atherosclerotic lesion, e.g. lipids, cytokines, oxidative stress, and hypoxia, as well as systemic factors, including inflammation and diabetes, critically influence the expression of cholesterol transporters on macrophage foam cells. Furthermore, HDL modification and remodeling in atherosclerosis, inflammation, and diabetes impairs its function as an acceptor for cellular cholesterol.

Summary
Recent advances in the understanding of the regulation of cholesterol transporters and their acceptors in atherosclerotic lesions indicate that HDL-based therapies should aim to enhance the activity of cholesterol transporters and improve both the quantity and quality of HDL.

***--- Curr. Opin. Lipidol.* 2010; 21(5): 441-453 ---**

Introduction

Cholesterol efflux pathways are pivotal for prevention of macrophage foam cell formation as macrophages cannot limit the uptake of excessive cholesterol. The efficiency of cholesterol efflux from macrophage foam cells in atherosclerotic lesions is determined by the quantity and quality of the extracellular acceptors, the activity of cholesterol transporters, and the availability of cholesterol for efflux. Significant progress has been made in the understanding of the mechanisms involved in cellular cholesterol efflux from macrophage foam cells in atherosclerotic lesions. In this review we will focus on the current view of the various cellular cholesterol efflux pathways and the physiological acceptors involved, and discuss their relative contributions to the prevention of macrophage foam cell formation in atherosclerotic lesions.

Macrophage cholesterol efflux pathways and their physiological acceptors

An important cholesterol efflux acceptor and facilitator of reverse cholesterol transport (RCT) from macrophage foam cells in the arterial wall to liver is high-density lipoprotein (HDL) [1]. Transport of HDL across the endothelium is essential for removal of the excess cholesterol from macrophage foam cells in atherosclerotic lesions. Two studies from the group of Von Eckardstein recently showed that transcytosis of apoAI through the endothelial layer occurs via ABC-transporter A1 (ABCA1), while ABC-transporter G1 (ABCG1) and scavenger receptor class B type I (SR-BI) mediate the transcytosis of HDL [2,3•].

HDL comprises a heterogeneous class of particles with a density (d) higher than 1.063 g/mL. HDL heterogeneity has recently been carefully reviewed by Rothblat and Phillips [4]. Generally, HDL can be classified into lipid-poor discoidal nascent pre-β HDL and lipid-rich spherical mature α-HDL, based on their difference in electrophoretic mobility [5,6]. Mature α-HDL functions as an acceptor for free cholesterol (FC) that dissociates from the cell membrane by aqueous diffusion [7,8]. Aqueous diffusion is a passive process driven by the FC gradient between cells and acceptors. It is thus thought that aqueous diffusion is inefficient. In contrast, scavenger receptor class B type I (SR-BI) and ATP-binding cassette G1 (ABCG1) facilitate FC efflux to mature α-HDL [9,10]. Furthermore, pre-β HDL induces phospholipid (PL) and FC efflux via ATP-binding cassette A1 (ABCA1) [11].

SR-BI facilitates passive transport of cholesterol to mature α-HDL

SR-BI is a multi-functional cell surface receptor [12,13]. One of its functions is to stimulate the bi-directional flux of FC between cells and α-HDL down the concentration gradient [10]. Interestingly, SR-BI is also found in the late endo/lysosomes and SR-BI deficiency is associated with accumulation of lysosomal cholesterol [14]. Thus, SR-BI may be involved in intracellular cholesterol trafficking from late endo/lysosomes.

Although not proven, it is often assumed that SR-BI accelerates aqueous diffusion of FC between cells and α-HDL. Binding to SR-BI will tether α-HDL in close proximity to the plasma membrane, thereby probably facilitating aqueous diffusion [15]. However, high-affinity binding alone is not sufficient to stimulate FC flux [16]. Moreover, SR-BI increases the fraction of membrane cholesterol available for efflux to α-HDL but not lipid-

free apoAI, although apoAI can bind to SR-BI [16,17]. Thus, the efficiency of SR-BI-mediated cholesterol efflux is related to its ability to enrich the membrane with cholesterol for efflux rather than to its binding to α-HDL[18]. In addition, SR-BI mediated HDL retro-endocytosis, i.e. the uptake of HDL whole particles followed by re-secretion of CE-poor HDL, has been implicated in SR-BI mediated cholesterol efflux [19,20]. This process appears independent of cholesterol transport out of the lysosome [20]. Currently, however, the importance for mass cholesterol efflux and prevention of macrophage foam cell formation is unclear.

Regulation of SR-BI expression in macrophages

SR-BI is undetectable in human monoytes, but its expression increases upon differentiation into macrophages [21,22]. Furthermore, the expression of SR-BI in macrophages is under control of peroxisome proliferator-activated receptor (PPAR) α and γ [23]. In liver, SR-BI stability and expression are posttranscriptionally regulated by PDZK1, a multi-PDZ domain containing adaptor protein [24]. Interestingly, targeted deletion of PDZK1 in mice reduced SR-BI expression in liver by 95%, but did not affect SR-BI expression in macrophages [25], indicating that macrophages have different posttranscriptional regulatory mechanisms.

Regulation of SR-BI expression in atherosclerosis

SR-BI is expressed in macrophages of atherosclerotic lesions [21,23,26] and regulated by lesional factors such as lipid, oxidative stress, and hypoxia (Figure 1). Cholesterol loading of macrophages reduces the mRNA levels of SR-BI through mechanisms independent of liver-X-receptor (LXR) and sterol regulatory element binding proteins (SREBPs) [22]. Interestingly, induction of atherosclerotic lesion regression by transplantation of plaque-containing arterial segments from apoE knockout (KO) mice into WT animals is associated with increased SR-BI expression in macrophages of atherosclerotic lesions [27]. Moreover, there is evidence that oxidative stress dampens the expression of SR-BI. Depletion of paraoxonase 1 (PON1), a major HDL-associated anti-oxidant enzyme, reduces mRNA and protein levels of SR-BI in peritoneal macrophages [28•]. SR-BI transcription is also suppressed by 7-ketocholesterol (7-KC), a major oxysterol in atherosclerotic lesions [29]. In addition, exposure of macrophages to hypoxic conditions decreased SR-BI transcription [26].

ABCG1 actively transports sterols to mature α-HDL

ABCG1 is an ABC half-transporter that actively transports sterols, including FC and 7-KC to α-HDL [9,30,31]. In non-cholesterol loaded macrophages, ABCG1 locates intracellularly [32]. Cholesterol loading or activation of LXR leads to the trafficking of ABCG1 from intracellular organelles, principally the Golgi, to the plasma membrane [32]. This ABCG1 redistribution is associated with increased cholesterol efflux to HDL.

Several lines of evidence have suggested that aqueous diffusion is involved in ABCG1-mediated cholesterol efflux. First, binding of HDL to ABCG1 is not required for induction of cholesterol efflux [30,33••]. Second, induction of ABCG1-mediated cholesterol efflux is linked to its capacity to enrich the membrane cholesterol pool for removal [34]. Cholesterol in ABCG1 generated lipid domains can only be removed by HDL but not lipid-free apoAI [34]. Third, only minimal amounts of PL are exported to

HDL [33••], which is in line with the fact that PL has a lower aqueous solubility as compared to FC. Some studies have suggested that ABCG1-mediated cholesterol efflux is

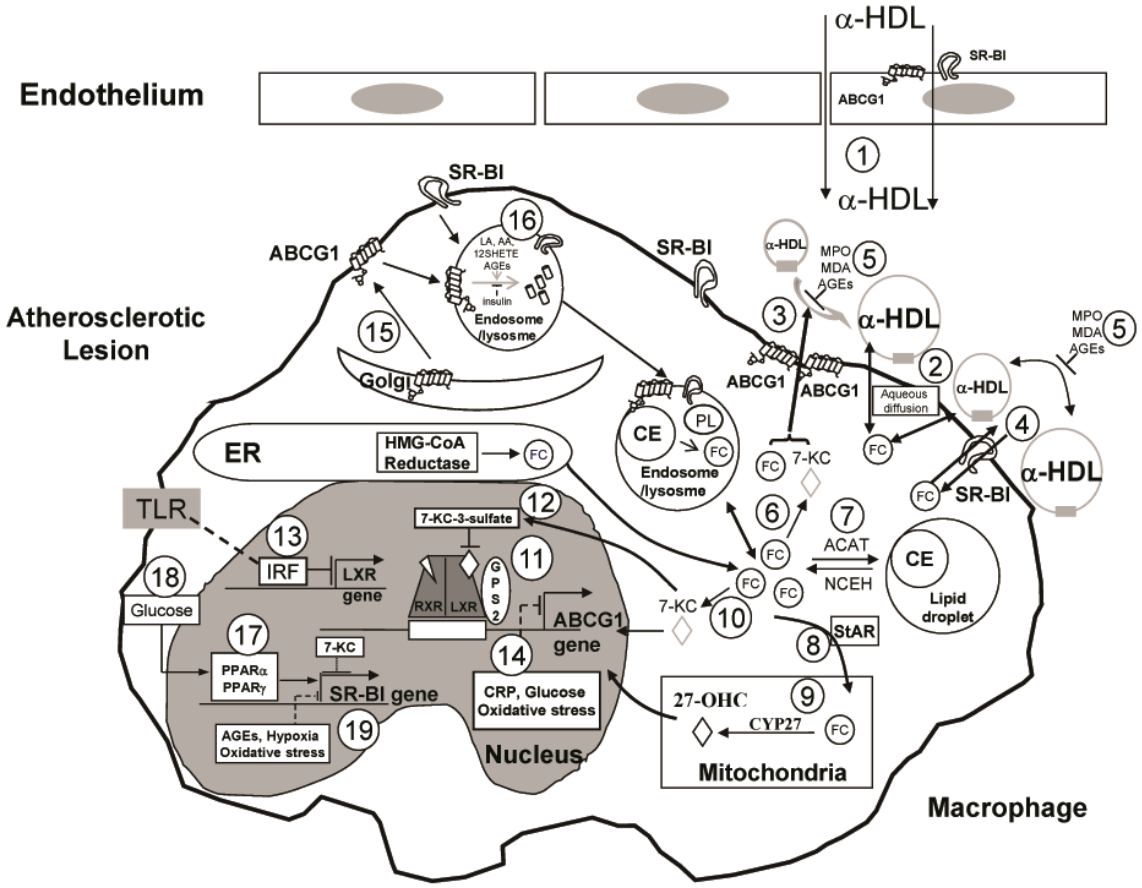

Figure1. Regulation of cholesterol efflux from macrophage foam cells to α-HDL in atherosclerotic lesions. (1) Two pathways for the infiltration of α-HDL into subendothelial space can be distinguished: paracellular transfer and ABCG1- and SR-BI-mediated transcytosis. Subsequently, α-HDL can induce efflux of free cholesterol (FC) from macrophages by aqueous diffusion (2) as well as via ABCG1 (3) and SR-BI (4). (5) In atherosclerotic lesions, MPO (myeloperoxidase)- and MDA (malondialdehyde)-mediated oxidation as well as AGEs (advanced glycation end products)-mediated glycation of HDL decrease its acceptor capacities to remove cholesterol by all these pathways. (6) Cholesterol traffics among different organelles. (7) FC can be esterified into cholesteryl ester (CE) by acyl-CoA:cholesterol acyltransferase (ACAT) while neutral cholesterol ester hydrolase (NCEH) hydrolyzes CE into FC. (8) Steroidogenic acute regulatory protein (StAR) transfers FC into mitochondrion where (9) FC is converted into 27-hydroxycholesterol (27-HOC) by sterol 27-hydroxylase (Cyp27). (10) 7-ketocholesterol (7-KC) is generated from FC and becomes the main sterol in atherosclerotic lesions. ABCG1 also exports 7-KC to HDL (3). The expression of ABCG1 and SR-BI in macrophages in lesions is regulated by different factors, thereby influencing their capacity to facilitate FC efflux. (11) ABCG1 transcription is induced by 27-HOC-mediated activation of liver-X-receptor (LXR) and recruitment of G protein suppressor 2 (GPS2). LXR heterodimerises with the retinoid-X-receptor (RXR) and induces transcription. (12) 7-KC-3-sulfate derived from 7-KC in lesions is an antagonist of LXR. (13) Activation of Toll-like receptor (TLR) can inhibit the expression of LXR through interferon regulatory factor (IRF) and indirectly decrease the ABCG1 expression. (14) In addition, the expression of ABCG1 can be downregulated by C-reactive peptide (CRP), glucose and oxidative stress. (15) After translation, ABCG1 is transported to the plasma membrane. (16) Fatty acids LA (linoleate acid) and AA (arachidonic acid) as well as 12SHETE (12S-hydroxyeicosatetranoic acid) and AGEs promote ABCG1 degradation, while insulin might increase the protein levels of ABCG1 by inhibition its degradation. (17) SR-BI transcription is under control of peroxisome proliferator-activated receptor alpha and gamma (PPARα and PPARγ). (18) Glucose might upregulate SR-BI expression through PPAR. (19) The transcription of SR-BI can be decreased by AGEs, hypoxia, and oxidative stress.

sphingomyelin-dependent [35,36]. Reduced cellular sphingomyelin levels due to a mutation of the ceramide transfer protein (CERT) are associated with a reduction of cholesterol efflux via ABCG1 [36]. Conversely, overexpression of CERT enhances ABCG1-mediated cholesterol efflux [36]. Different from SR-BI, ABCG1-mediated cholesterol transport is uni-directional from cells to HDL [33••].

Regulation of ABCG1 expression in macrophages

ABCG1 expression is highly regulated by LXR [37,38]. 27-hydroxycholesterol (27-HOC), an endogenous LXR ligand in macrophages, increases the expression of ABCG1 [39]. Activation of LXR by GW3965, an LXR agonist, triggers the recruitment of G protein suppressor 2 (GPS2), LXR, and the coactivator complex to the promoter for induction of ABCG1 transcription in THP-1 cells [40••]. Furthermore, knockdown of GPS2 by siRNA specifically decreases GW3965 induced ABCG1 expression. In addition, superoxide anions in macrophages, induced by C-reactive peptide (CRP), decrease the expression of ABCG1 in THP-1 cells, which can be abolished by the anti-oxidant selenon-L-methionine [45].

Regulation of ABCG1 expression in atherosclerotic lesions

In atherosclerotic lesions, ABCG1 co-localizes with macrophage foam cells [41]. Sterols, fatty acids (FAs), and oxidative stress regulate ABCG1 expression in macrophages (Figure 1). Cholesterol loading increases the accumulation of oxysterols, which activate LXR and induce the transcription of ABCG1 [37,39]. In contrast, the unsaturated FAs (uFAs) linoleic and arachidonic acid that accumulated in lesions promote the degradation of ABCG1 [42].

Oxidative stress in atherosclerotic lesions is also a negative regulator for ABCG1 expression. 12/15-lipoxygenase, highly expressed in macrophages of early atherosclerotic lesions [43], destabilizes ABCG1 through generation of an uFA metabolite named 12S-hydroxyeicosatetranoic acid (12SHETE) [42,44•]. 12SHETE promotes the serine phosphorylation of ABCG1 through p38- and JNK2-dependent pathways, thereby increasing proteasome-mediated ABCG1 degradation [44•].

Interestingly, ABCG1 is undetectable in macrophages from patients with diabetes, leading to a 30% decrease in cholesterol efflux to HDL [46]. High glucose levels in these patients reduce the mRNA and protein levels of ABCG1 in macrophages [47]. Importantly, insulin treatment increases the protein but not mRNA levels of ABCG1 [47].

ABCA1 mediated phospholipid and cholesterol efflux to lipid-free/poor apoAI

ABCA1 is an ABC full transporter that facilitates the efflux of PL and FC to lipid-free/poor apolipoproteins [11,48,49]. ABCA1 localizes to the plasma membrane and intracellular compartments, including the Golgi apparatus and endo/lysosomes [50]. Deletion of the C-terminal VFVNFA and PDZ motifs of ABCA1 inhibits the exit of ABCA1 from the endoplasmic reticulum (ER) [51], while palmitoylation of the cysteines of ABCA1 promotes its trafficking to the plasma membrane [52••]. Interestingly, in macrophages, SPTLC1, a subunit of the serine palmitoyltransferase enzyme, can bind to ABCA1 and trap it in the ER [51]. In addition, Rab8, a Rab GTPase was recently suggested to regulate ABCA1 trafficking to the plasma membrane in macrophages from human atherosclerotic lesions [53••]. Depletion of Rab8 keeps ABCA1 in recycling

organelles containing β1 integrin and transferrin, while overexpression of Rab8 increases ABCA1 levels at the cellular membrane and reduces cholesterol deposition in foam cells [53••].

Several different models for ABCA1-mediated cholesterol efflux have been suggested. According to the simplest model, ABCA1 acts as an apoAI receptor that induces the transfer of PL and FC upon binding [54,55]. ABCA1 expression, however, changes the cellular membrane lipid microenvironment [56-58]. Furthermore, the ATPase activity of ABCA1 is necessary for apoAI binding to the cell surface [59]. Therefore, another view is that apoAI interacts with specialized lipid domains in the plasma membrane formed by ABCA1 and subsequently induces lipid removal. In addition, a hybrid model has been proposed [60-62]. ApoAI first interacts with ABCA1 to activate janus kinase 2 (JAK2), which in turn increases binding of apoAI to ABCA1. This latter binding facilitates the interaction of apoAI to the lipid domains generated by ABCA1, thereby promoting apoAI lipidation. By using various ABCA1 mutants, Vaughan et al. recently further revealed the interdependency between JAK2 activation, apoAI binding and lipid export via ABCA1 [63•].

ApoAI binding to ABCA1 can lead to internalization of the ABCA1/apoAI complex [64]. It has been proposed that apoAI enters the cell and is re-secreted as a lipidated particle during ABCA1-mediated cholesterol efflux from macrophages [64,65]. However, other groups showed that apoAI lipidation occurs on the cell surface and that apoAI is degraded in the lysosome after internalization [66,67]. Recently, Lu et al. provided evidence that binding of apoAI to ABCA1 prevents ABCA1 degradation after internalization and promotes rapid recycling of ABCA1 to the cell surface in non-cholesterol loaded THP-1 cells [68]. Under this condition, blockade of clathrin-mediated ABCA1 endocytosis by cytochalasin D increased ABCA1 expression on the cell surface and subsequently enhanced apoAI lipidation, indicating that endocytic recycling of ABCA1/apoAI is not required for lipid efflux to apoAI. In contrast, blockade of clathrin-mediated endocytosis by monodansyl cadaverine leads to increased ABCA1 expression on the cell surface of acetylated LDL (acLDL) loaded THP-1 cells, but reduces cholesterol efflux to apoAI, indicating that intracellular trafficking of ABCA1/apoAI is important for cholesterol efflux under conditions that macrophages have accumulated excess cholesterol [69••].

In human serum, pre-β1 HDL generated by ABCA1 is characterized as a 67 kDa subspecies of HDL, containing two apoAI molecules with several molecules of PL and FC [70]. Similar to lipid-free apoAI, preβ1 HDL can interact with ABCA1 for further cholesterol efflux. Although pre-β1 HDL only comprises around 5% of the amount of apoAI in the circulation, it is suggested that the levels and function of pre-β1 HDL are important for prevention of atherosclerosis. Llera-Moya et al. recently demonstrated that the concentration of pre-β1 HDL in serum of healthy individuals significantly correlates to the serum efflux capacity via ABCA1, and is negatively associated with the carotid intima thickness [71••].

Regulation of ABCA1 in macrophages

ABCA1 is preferentially expressed on ly6C^{low} tissue macrophages [72•]. The transcription of ABCA1 is upregulated through 27-HOC-induced activation of LXR [39,73]. In line, increasing 27-HOC by enhancement of cholesterol delivery to mitochondrial sterol 27-hydroxylase (Cyp27) by steroidogenic acute regulatory protein (StAR) increases the expression of ABCA1 [74•]. LXR has two isoforms, namely LXRα and LXRβ. While

LXRα is primarily involved in the transcriptional regulation of ABCA1, LXRβ regulates ABCA1 protein expression posttranslationally [75••]. In absence of cholesterol loading, LXRβ binds to the C-terminus of ABCA1 and stabilizes it on the cellular membrane. Interestingly, this stabilization is associated with reduced ABCA1-mediated cholesterol efflux, thereby preventing excessive elimination of cholesterol. Upon cholesterol loading, increased oxysterols bind to LXRβ, leading to dissociation of LXRβ from ABCA1 and a rapid restoration of ABCA1 activity in cholesterol efflux. This interaction between ABCA1 and LXRβ thus provides a novel regulatory mechanism for cells to quickly respond to cholesterol loading.

ApoAI stabilizes ABCA1 by inhibition of thiol protease-mediated and calpain-mediated proteolysis [76-78]. Phosphorylation of a PEST sequence, rich in proline, glutamic acid, serine, and threonine at the cytoplasmic region of ABCA1 directs calpain-mediated degradation [77]. Iwamoto et al. recently demonstrated that calmodulin directly binds to a motif of ABCA1 near the PEST sequence in a Ca2+ dependent manner and protects ABCA1 from calpain-mediated degradation [79•]. Since binding of apoAI to ABCA1 quickly induces Ca2+ influx [80], it is conceivable that Ca2+/calmodulin contributes to the apoAI-increased ABCA1 stability. In addition, activation of Ras homolog family member A (RhoA) is involved in the apoAI-induced ABCA1 stabilization [81•]. The binding of apoAI to ABCA1 transiently activates RhoA, whereas inhibition of RhoA activation by pharmaceutical inhibitors or expression of a negative RhoA mutant block the ability of apoAI to stabilize ABCA1.

Regulation of ABCA1 in atherosclerotic lesions

In atherosclerotic lesions, ABCA1 co-localizes with macrophage foam cells [82,83]. Below important factors, known to regulate the expression of ABCA1 in atherosclerotic lesions and thus are expected to influence the net transfer of cholesterol out of lesions, are described (Figure 2).

Sterols and fatty acid

ABCA1 expression in atherosclerotic tissue correlates with LXRα mRNA levels [83]. 7-KC, a highly toxic oxysterol found in atherosclerotic lesions [84], induces ABCA1 transcription by activation of LXR [85]. In agreement, overexpression of LXRα in macrophages increases ABCA1-mediated cholesterol efflux to apoAI and prevents the development of atherosclerosis [86]. In advanced atherosclerotic lesions, accumulation of FC in macrophages decreases the expression of ABCA1 protein by proteasome-mediated degradation [87]. Moreover, uFA linoleic acid decreases the transcription of ABCA1 [47]. Like ABCG1, ABCA1 is destabilized by unsaturated fatty acids (uFAs) that accumulate in atherosclerotic lesions [88-90]. In line, deletion of macrophage fatty acid synthase increases cellular cholesterol efflux to apoAI [91•].

Inflammation

Atherosclerotic lesions are inflammatory sites containing various cytokines [92,93]. The balance between pro- and anti-inflammatory cytokines in atherosclerotic lesions is an important determinant for macrophage foam cell formation by regulation of ABCA1 expression. The pro-inflammatory cytokines IFNγ and TNFα downregulate ABCA1 transcription in macrophage foam cells [94,95]. Interestingly, the anti-inflammatory cytokines IL-10 and TGFβ can reverse the TNFα and IFNγ induced downregulation of

ABCA1, respectively [95,96]. In agreement, overexpression of macrophage IL-10 reduces CE accumulation in atherosclerotic lesions and inhibits atherogenesis [97].

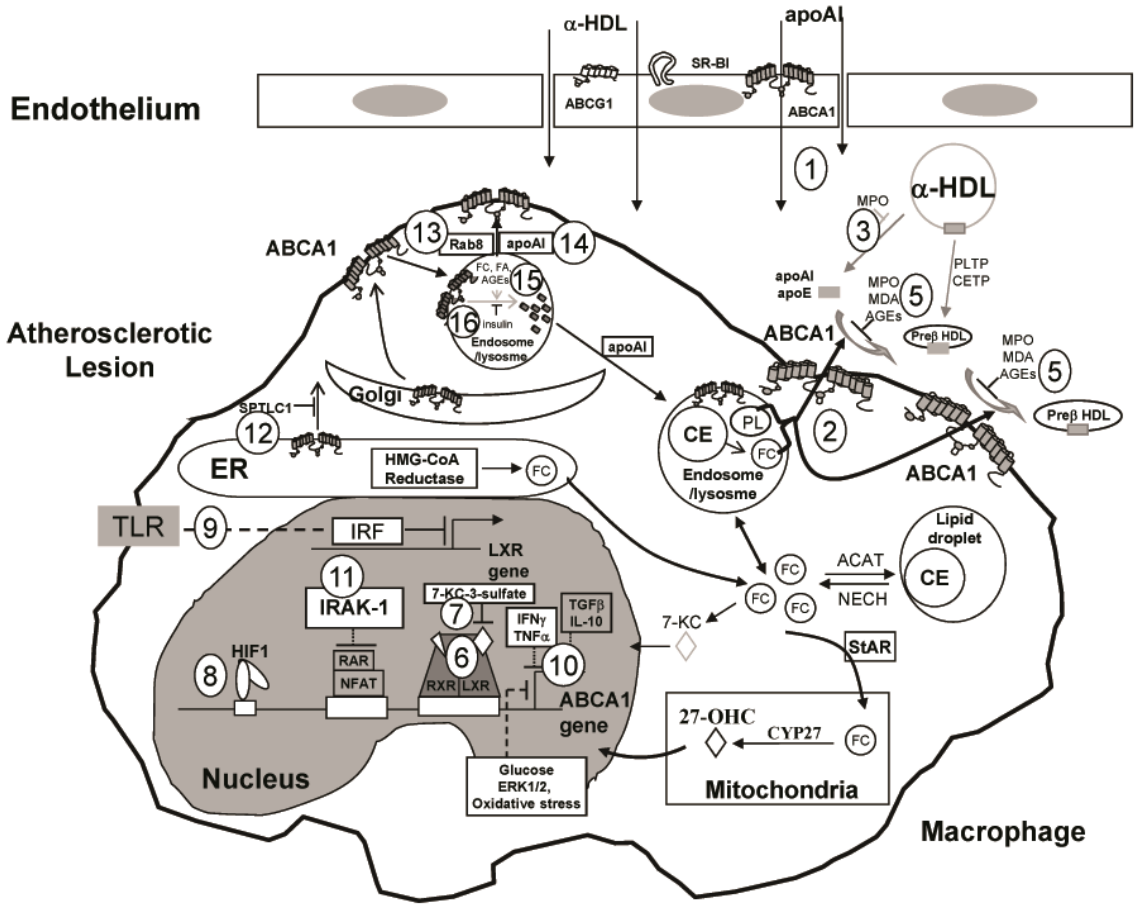

Figure 2. Regulation of cholesterol efflux from macrophage foam cells to lipid-free/poor apolipoproteins in atherosclerotic lesions. (1) Macrophages do not produce apoAI. Therefore, transport of apoAI across endothelium is pre-requisite for apoAI-mediated removal of cholesterol from macrophage foam cells in lesions. ABCA1 on endothelial cells is involved in transcytosis of apoAI. (2) ApoAI and macrophage-derived apoE induce ABCA1-mediated PL and FC efflux to form preβ HDL, which can further remove phospholipid (PL) and FC via ABCA1. (3) MPO inhibits the dissociation of apoAI from α-HDL. (4) Phospholipid and cholesteryl ester transfer protein (PLTP and CETP) can generate preβ HDL from α-HDL. (5) MPO- and MDA-mediated oxidation as well as AGEs-mediated glycation of lipid-free/poor apoAI impair its function as cholesterol acceptor. The expression of ABCA1 can be regulated by several factors locally in the atherosclerotic lesion. (6) LXR activation by the oxysterols 27-HOC and 7-KC induce the transcription of ABCA1. (7) In atherosclerotic lesions, 7-KC can be converted into 7-KC-3-sulfate, which decrease the transcription of ABCA1 by inhibiting the activation of LXR. (8) In hypoxic regions of lesions, hypoxia-inducible factor 1 (HIF1) induces the expression of ABCA1. (9) Activation of TLR during inflammation decreases the gene expression of LXR through IRF, thereby indirectly decreasing the expression of ABCA1. Inflammation can also downregulate the expression of ABCA1 through (10) the proinflammatory cytokines IFNγ and TNFα as well as (11) a key innate immunity signaling kinase (IRAK-1). IRAK-1 reduces the levels of nuclear factor of activated T-cells (NFAT) as well as retinoid acid receptor (RAR), thereby downregulating the expression of ABCA1. The trafficking of ABCA1 to the plasma membrane is important for its function. (12) SPTLC1 (a subunit of the serine palmitoyltransferase enzyme) binds ABCA1 and inhibits the exit of ABCA1 from the endoplasmic reticulum (ER), while (13) Rab8 participates in the trafficking of ABCA1 from recycling organelles to the plasma membrane. (14) Binding of apoAI to ABCA1 inhibits ABCA1 degradation and facilitates the recycling of ABCA1 back to the plasma membrane. Furthermore, (15) FC, FA (fatty acid), and AGEs promote the protein degradation of ABCA1. (16) Insulin increases the protein levels of ABCA1 probably by increasing the protein stability of ABCA1.

Viral and bacterial pathogens have long been suspected to be modulators of atherosclerosis. Microbial ligands activate toll-like receptor (TLR) signaling, which blocks LXR activation by interferon regulatory factors, thereby decreasing the expression of ABCA1 and increasing lipid accumulation in macrophages [98,99]. Conversely, LXR activation reduces TLR-mediated macrophage foam cell formation [99,100]. Importantly, Maitra et al. recently provided a novel connection between innate immunity signaling and the regulation of ABCA1 expression in macrophages [101•]. This study identified binding sites for retinoic acid receptor (RAR) and nuclear factor of activated T-cells (NFAT) in the promoter of ABCA1, and revealed that IRAK-1, a key innate immunity signaling kinase, suppressed ABCA1 transcription by downregulation of RARα and NFATc2.

In addition, CRP, an acute phase (AP) protein of inflammation, inhibits ABCA1 expression and cholesterol efflux in macrophage foam cells by activation of extracellular signal regulated kinase 1 and 2 (ERK1/2) [45]. In line, Zhou et al. demonstrated that inhibition of ERK1/2 increases the mRNA and protein levels of ABCA1 in macrophages independent of LXR [102•]. Interestingly, inhibition of ERK1/2 and activation of LXR synergistically induce ABCA1 expression and macrophage cholesterol efflux [102•]. Thus, combined targeting of ERK1/2 and LXR might be a potent therapeutic strategy for inhibition of atherosclerosis.

Oxidative stress

Induction of oxidative stress by iron/ascorbate or CRP in THP-1 cells decreases the mRNA and protein expression of ABCA1 [45,103]. Importantly, anti-oxidant treatment can rescue the oxidative stress-induced attenuation of ABCA1 expression and cholesterol efflux [45,103].

Hypoxia

Hypoxia-inducible factor 1 (HIF1), activated under hypoxic conditions [104,105], is a heterodimer composed of HIF1α and HIF1β [106]. Importantly, in macrophages isolated from human atherosclerotic lesions, ABCA1 expression showed a strong correlation with HIF1β expression [107••], indicating that HIF1β is a major regulator of macrophage ABCA1 transcription in atherosclerotic lesions. However, hypoxia also promotes the secretion of inflammatory mediators, fatty acid biosynthesis, ATP depletion and lipid droplet formation [108]. Thus, hypoxia is associated with increased macrophage foam cell formation despite HIF1-mediated induction of macrophage ABCA1 transcription.

Diabetes

In diabetes, high levels of glucose decrease the mRNA and protein levels of ABCA1 in macrophages [47]. In line, macrophages in diabetic mice show a reduced expression of ABCA1 [109]. Moreover, glyoxal and glycoaldehyde acutely and severely destabilize the ABCA1 protein [110].

Interestingly, ABCA1 expression on beta-cells of pancreatic islets influences insulin secretion and glucose homeostasis [111, 112•]. Like ABCG1, the protein levels of ABCA1 are elevated by insulin treatment [47]. Macrophages have a functional insulin receptor signaling pathway, and downregulation of this pathway due to insulin resistance has been implicated in the progression of advanced atherosclerotic lesions [113]. Thus, macrophage insulin resistance might favor increased foam cell formation in atherosclerosis by inhibiting insulin-mediated ABCA1 and ABCG1 induction.

The relative role of each pathway for net cholesterol efflux from macrophage foam cells in atherosclerotic lesions

The relative contribution of aqueous diffusion and the ABCA1-, ABCG1-, and SR-BI-mediated pathways for the net cholesterol efflux from macrophage foam cells to serum has been evaluated *in vitro* by using cholesterol-loaded macrophages isolated from ABCA1, ABCG1, and SR-BI KO mice [114,115]. The studies indicate that ABCA1, ABCG1 and SR-BI are responsible for approximately 35%, 21%, and 9%, respectively of the efflux capacity of the cells. Interestingly, a staggering 35% of the cholesterol is effluxed simply via aqueous diffusion. Moreover, data from *in vivo* RCT assays, in which *in vitro* ^{3}H-cholesterol/acLDL laden macrophages are injected into the peritoneal cavity of WT mice and the excretion of the ^{3}H-label into the feces is followed, suggest a similar contribution of the different pathways [114,115]. However, it must be noted that the following limitations in the experimental setups of these studies might impede an accurate evaluation of the relative roles of the different cholesterol efflux pathways. 1) *In vitro* cell culture might change the expression of the transporters studied; 2) Most studies use acLDL, which is not an endogenous modified lipoprotein, to induce macrophage foam cell formation. In relation to this it is important to be aware that acLDL-laden macrophages exhibit a different phenotype from oxidized LDL-laden cells [116]; Moreover, acLDL loading increases the cellular cholesterol poor for efflux to apoAI via the ABCA pathway while cells loaded with native LDL preferentially efflux cholesterol to HDL [117]; 13) Nonlipidemic serum as acceptor used for *in vitro* cholesterol efflux studies and WT mice used as recipients for the macrophage foam cells in the *in vivo* RCT assays are not likely to accurately reflect the conditions in atherosclerotic lesions *in vivo*.

The net cholesterol efflux from macrophage foam cells in atherosclerotic lesions is not simply a sum of the amount cholesterol removed via each individual pathway. Competitive and synergistic interactions of different efflux pathways can result in more or less net cholesterol efflux. Lipidation of apoAI via ABCA1 generates the substrates for ABCG1-mediated cholesterol efflux, suggesting that ABCA1 and ABCG1 work in sequence and in synergy to export cholesterol [118]. Combined deletion of ABCA1 and ABCG1 on macrophages results in a dramatic decrease in net cholesterol mass efflux to HDL *in vitro* and largely reduced macrophage RCT *in vivo* [115,119-121]. Accordingly, massive macrophage foam cell accumulation was observed in the peritoneal cavity as well as various organs such as spleen, lymph nodes, liver, Peyer's patches, and lung in total body ABCA1/ABCG1 double KO (dKO) mice on chow [119]. In contrast, single ABCA1 KO and ABCG1 KO mice only displayed a relatively small number of foam cells in the lung. In bone marrow transplanted LDLr KO mice on either chow or Western-type diet (WTD), single ABCA1 deficiency leads to a slight increase in the percentage of foam cells in the peritoneal cavity. Also a small number of foam cells were observed in the lung of ABCG1 KO transplanted animals. In contrast, combined deletion of ABCA1 and ABCG1 leads to massive foam cell accumulation in various tissues and the peritoneal cavity [120,121] (Out R, unpublished data), further illustrating the importance of ABCA1 and ABCG1 in preventing macrophage foam cell formation. As ABCA1/ABCG1 dKO mice do express SR-BI, the ABCA1- and ABCG1-mediated pathways have been thought to account for the majority of the cholesterol effluxed from macrophage foam cells *in vivo*, while SR-BI seems to be only a minor contributor. In line, SR-BI KO macrophages exhibit a small decrease in cholesterol efflux to HDL *in vitro* as compared to WT macrophages [114,122]. Also, SR-BI deficiency in macrophages does not influence *in vivo* RCT in WT mice [115]. SR-BI is a multifunctional receptor that can influence macrophage foam cell formation via different mechanisms. First, SR-BI facilitates cholesterol efflux from macrophages to α-

HDL, which will limit foam cell formation. Second, SR-BI promotes the uptake of atherogenic ligands like βVLDL and oxidized LDL [12,13,122], thereby promoting macrophage foam cell formation. Third, SR-BI mediates selective uptake of CE from HDL will promote CE accumulation in macrophages [123], but also may generate CE-depleted/PL-rich HDL particles that are efficient acceptors for cholesterol efflux. Thus, the net effect of SR-BI on macrophage foam cell formation *in vivo* is difficult to predict and may vary with conditions studied. Consistently, SR-BI on macrophages accelerates the development of small fatty streak lesions in LDLr KO mice [122], whereas the development of advanced atherosclerotic lesions in LDLr KO and apoE KO mice is inhibited by macrophage SR-BI [122,124,125]. In line, Yancey et al. showed dramatically increased FC and CE accumulation in peritoneal macrophages of apoE/SR-BI dKO mice as compared to those of apoE KO mice [126]. Interestingly, Cuchel et al. recently showed that FC mobilization *in vivo* in response to rHDL infusion is primarily mediated by SR-BI but not ABCA1 or ABCG1 [127••]. Moreover, Yvan-Charvet et al. demonstrated that overexpression of apoAI in heterozygous LDLr KO mice can protect against atherosclerosis in the absence of macrophage ABCG1 and ABCA1 [128••]. Thus, SR-BI might be more important for controlling cellular cholesterol homeostasis *in vivo* than was initially anticipated. In agreement, we found that combined deletion of macrophage ABCA1 and SR-BI resulted in massive foam cell formation in the peritoneal cavity and spleen of LDLr KO mice on WTD (Zhao Y, unpublished data). These data indicate that, at least under severe hypercholesterolemia, the synergistic action of ABCA1 and SR-BI-mediated cholesterol efflux from macrophage foam cells, similarly as the combined function of ABCA1 and ABCG1, is important for preventing excessive macrophage foam cell formation *in vivo*.

Importantly, a recent study demonstrated that in human cholesterol-loaded macrophages, ABCA1 and Cla-1, the human ortholog of SR-BI, rather than ABCG1 are key mediators in cholesterol efflux to HDL [129••], suggesting distinguished differences in the relative roles of the ABCG1 and SR-BI pathway in net cholesterol efflux from human and mouse macrophages.

Aqueous diffusion might be underestimated [114,115]. Since mature α-HDL is an important acceptor for cholesterol released from macrophages via aqueous diffusion as well as for ABCG1 and SR-BI mediated cholesterol efflux, combined deletion of ABCG1 and SR-BI will be essential for determination of the relative importance of aqueous diffusion for the prevention of macrophage foam cell formation *in vivo*. In addition, ABCG1/SR-BI dKO mice will be a useful tool for studying the interaction between macrophage ABCG1 and SR-BI and the subsequent effects on macrophage foam cell formation *in vivo*.

HDL modification and remodeling in atherosclerosis

Epidemiological studies have consistently shown that high levels of HDL cholesterol (HDL-C) are associated with reduced susceptibility to cardiovascular disease (CVD) [130,131]. However, increasing evidence indicates that HDL functionality rather than HDL-C level is a good predictor of cardiovascular risk [131]. HDL has multiple functions, including cholesterol efflux induction, anti-inflammation, anti-oxidation, anti-thrombosis, and enhancement of endothelial function [131,132]. Many of these functions are linked to various proteins associated with HDL particles [131,133•]. Changes in the protein and/or lipid composition of HDL might lead to the formation of a dysfunctional HDL particle that is no longer protective against atherosclerosis. Several pathological states, including oxidative stress [134,135], inflammation [136,137], and diabetes [138-140], modify and

remodel the HDL, leading to a compromised function as a cellular lipid acceptor (Figure 1 & 2).

MPO, a potent oxidizing enzyme secreted by macrophages and neutrophils in atherosclerotic lesions [141,142], is regarded as a good *in vivo* biomarker, associated with dysfunctional HDL. MPO binds to apoAI and uses hydrogen peroxide to generate chlorinated and nitrated apoAI [143,144] that shows a reduced ABCA1-binding capacity and an impaired ability to promote cholesterol efflux [145•]. Importantly, human atherosclerotic lesions are enriched in chlorinated and nitrated apoAI and patients with CVD have higher circulating levels of chlorinated and nitrated apoAI [143,144]. Also MPO-modified HDL is no longer capable of interacting with SR-BI [146•]. Recently, Cavigiolio et al. provided evidence that MPO-mediated crosslinking of apoAI retards the spontaneous dissociation of apoAI from HDL, thereby limiting the availability of lipid-free apoAI for efflux [147••]. Oxidation of methionine in apoAI by MPO also inhibits its ability to activate LCAT, a critical step in HDL metabolism and RCT [148]. In line, overexpression of MPO impairs *in vivo* reverse cholesterol transport [149]. In addition, MPO-modified HDL is proinflammatory as these particles can activate NF-kappaB (nuclear factor kappa-light-chain-enhancer of activated B) and increase the expression of adhesion molecules in aortic endothelial cells [146•].

Malondialdehyde (MDA) is a product of lipid peroxidation [150,151]. In human atherosclerotic lesions, MDA-apoAI adducts are elevated [152•]. This modification is suggested to hinder the interaction of apoAI with lipids and ABCA1, thereby reducing cholesterol efflux via ABCA1.

In addition, *in-vitro* experiments have shown that lipid-free apoAI and pre-β–HDL are sensitive to proteolytic degradation by matrix metalloproteinases [153], cathepsins [154], and the mast cell-derived enzymes chymase and tryptase [155, 156], which are present in atherosclerotic lesions. Interestingly, in fatty streaks, mast cells are localized close to foam cells [157]. Thus, chymase and tryptase secreted by mast cells in the atherosclerotic lesions could promote macrophage foam cell formation by reducing the availability of extracellular acceptors for ABCA1-mediated cholesterol efflux. In line, systemic activation of mast cells by compound 48/80 results in an impaired capacity of serum and intraperitoneal fluid to promote cellular cholesterol efflux from macrophage foam cells in culture [158●].

Conclusion

The relative importance of the different pathways for cholesterol efflux from macrophage foam cells in atherosclerotic lesions is attributed to the activity of SR-BI, ABCA1, and ABCG1, the interaction between these transporters, as well as the quantity and quality of their respective acceptors. Conditions locally inside the atherosclerotic lesions, including the presence of lipids, cytokines, hypoxia, and oxidative stress as well as systemic factors (e.g. diabetes and inflammation) modulate cholesterol efflux from macrophages by influencing the activity of the transporters involved and modification of their acceptors (Figure 1 & 2). Thus, improvement of HDL quality as well as quantity will be an important clinical goal for atherosclerosis treatment. Hereto, international consensus is required on standardized methodologies for HDL isolation and protocols for evaluation of HDL function. HDL proteome analysis may lead to a more comprehensive understanding of the differential functions of individual HDL subclasses. Importantly, increased understanding of the various cholesterol efflux pathways and HDL functionality will promote the development of new HDL-based therapies.

Acknowledgement

This work was supported by The Netherlands Organization of Scientific Research (VIDI grant 917.66.301 (M.V.E.)) and The Netherlands Heart Foundation (2001T4101 (Y.Z)). M.V.E. is an Established Investigator of The Netherlands Heart Foundation (grant 2007T056).

References and recommended reading

Papers of particular interest, published within the annual period of review, have been highlighted as:

- • of special interest
- •• of outstanding interest

1. Fielding CJ, Fielding PE. Molecular physiology of reverse cholesterol tranport. J Lipid Res 1995; 36:211-228.
2. Cavelier C, Rohrer L, von EA. ATP-Binding cassette transporter A1 modulates apolipoprotein A-I transcytosis through aortic endothelial cells. Circ Res 2006, 99:1060-1066.
3. Rohrer L, Ohnsorg PM, Lehner M, Landolt F, Rinninger F, von EA. High-density lipoprotein transport through aortic endothelial cells involves scavenger receptor BI and ATP-binding cassette transporter G1. Circ Res 2009, 104:1142-1150.

• This study shows the involvement of ABCG1 and SR-BI in transcytosis of HDL through the endothelial layer, which is one way for HDL to get access to macrophage foam cells in atherosclerotic lesions.

4. Rothblat GH, Phillips MC. High-density lipoprotein heterogeneity and function in reverse cholesterol transport. Curr Opin Lipidol 2010; 21:229-238.
5. Davidson WS, Sparks DL, Lund-Katz S, Phillips MC. The molecular basis for the difference in charge between pre-beta- and alpha-migrating high density lipoproteins**.** J Biol Chem 1994; 269:8959-8965.
6. Kunitake ST, La Sala KJ, Kane JP. Apolipoprotein A-I-containing lipoproteins with pre-beta electrophoretic mobility. J Lipid Res 1985; 26:549-555.
7. Phillips MC, Johnson WJ, Rothblat GH. Mechanisms and consequences of cellular cholesterol exchange and transfer. Biochim Biophys Acta 1987; 906:223-276.
8. Rothblat GH, Phillips MC. Mechanism of cholesterol efflux from cells. Effects of acceptor structure and concentration. J Biol Chem 1982; 257:4775-4782.
9. Klucken J, Buchler C, Orso E, Kaminski WE, Porsch-Ozcurumez M, Liebisch G, Kapinsky M, Diederich W, Drobnik W, Dean M, Allikmets R, Schmitz G. ABCG1 (ABC8), the human homolog of the Drosophila white gene, is a regulator of macrophage cholesterol and phospholipid transport. Proc Natl Acad Sci U S A 2000; 97:817-822.
10. Yancey PG, Llera-Moya M, Swarnakar S, Monzo P, Klein SM, Connelly MA, Johnson WJ, Williams DL, Rothblat GH. High density lipoprotein phospholipid composition is a major determinant of the bi-directional flux and net movement of cellular free cholesterol mediated by scavenger receptor BI. J Biol Chem 2000; 275:36596-36604.
11. Mulya A, Lee JY, Gebre AK, Thomas MJ, Colvin PL, Parks JS. Minimal lipidation of pre-beta HDL by ABCA1 results in reduced ability to interact with ABCA1. Arterioscler Thromb Vasc Biol 2007; 27:1828-1836.
12. Van EM, Pennings M, Hoekstra M, Out R, Van Berkel TJ. Scavenger receptor BI and ATP-binding cassette transporter A1 in reverse cholesterol transport and atherosclerosis. Curr Opin Lipidol 2005; 16:307-315.
13. Calvo D, Gomez-Coronado D, Lasuncion MA, Vega MA. CLA-1 is an 85-kD plasma membrane glycoprotein that acts as a high-affinity receptor for both native (HDL, LDL, and VLDL) and modified (OxLDL and AcLDL) lipoproteins. Arterioscler Thromb Vasc Biol 1997; 17:2341-2349.
14. Ahras M, Naing T, McPherson R. Scavenger receptor class B type I localizes to a late endosomal compartment. J Lipid Res 2008; 49:1569-1576.
15. Gu X, Kozarsky K, Krieger M. Scavenger receptor class B, type I-mediated [3H]cholesterol efflux to high and low density lipoproteins is dependent on lipoprotein binding to the receptor. J Biol Chem 2000; 275:29993-30001.

16. De La Llera-Moya M, Rothblat GH, Connelly MA, Kellner-Weibel G, Sakr SW, Phillips MC, Williams DL. Scavenger receptor BI (SR-BI) mediates free cholesterol flux independently of HDL tethering to the cell surface. J Lipid Res 1999; 40:575-580.
17. Kellner-Weibel G, de LL-M, Connelly MA, Stoudt G, Christian AE, Haynes MP, Williams DL, Rothblat GH. Expression of scavenger receptor BI in COS-7 cells alters cholesterol content and distribution. Biochemistry 2000; 39:221-229.
18. Connelly MA, De La Llera-Moya M, Peng Y, Drazul-Schrader D, Rothblat GH, Williams DL. Separation of lipid transport functions by mutations in the extracellular domain of scavenger receptor class B, type I. J Biol Chem 2003; 278:25773-25782.
19. Pagler TA, Rhode S, Neuhofer A, Laggner H, Strobl W, Hinterndorfer C, Volf I, Pavelka M, Eckhardt ER, van der Westhuyzen DR, Schutz GJ, Stangl H. SR-BI-mediated high density lipoprotein (HDL) endocytosis leads to HDL resecretion facilitating cholesterol efflux. J Biol Chem 2006; 281:11193-11204.
20. Pagler TA, Neuhofer A, Laggner H, Strobl W, Stangl H. Cholesterol efflux via HDL resecretion occurs when cholesterol transport out of the lysosome is impaired. J Lipid Res 2007; 48:2141-2150.
21. Hirano K, Yamashita S, Nakagawa Y, Ohya T, Matsuura F, Tsukamoto K, Okamoto Y, Matsuyama A, Matsumoto K, Miyagawa J, Matsuzawa Y. Expression of human scavenger receptor class B type I in cultured human monocyte-derived macrophages and atherosclerotic lesions. Circ Res 1999; 85:108-116.
22 Yu L, Cao G, Repa J, Stangl H. Sterol regulation of scavenger receptor class B type I in macrophages. J Lipid Res 2004; 45:889-899.
23. Chinetti G, Gbaguidi FG, Griglio S, Mallat Z, Antonucci M, Poulain P, Chapman J, Fruchart JC, Tedgui A, Najib-Fruchart J, Staels B. CLA-1/SR-BI is expressed in atherosclerotic lesion macrophages and regulated by activators of peroxisome proliferator-activated receptors. Circulation 2000; 101:2411-2417.
24. Nakamura T, Shibata N, Nishimoto-Shibata T, Feng D, Ikemoto M, Motojima K, Iso O, Tsukamoto K, Tsujimoto M, Arai H. Regulation of SR-BI protein levels by phosphorylation of its associated protein, PDZK1. Proc Natl Acad Sci U S A 2005; 102:13404-13409.
25. Kocher O, Yesilaltay A, Cirovic C, Pal R, Rigotti A, Krieger M. Targeted disruption of the PDZK1 gene in mice causes tissue-specific depletion of the high density lipoprotein receptor scavenger receptor class B type I and altered lipoprotein metabolism. J Biol Chem 2003; 278:52820-52825.
26. Svensson PA, Englund MC, Snackestrand MS, Hagg DA, Ohlsson BG, Stemme V, Mattsson-Hulten L, Thelle DS, Fagerberg B, Wiklund O, Carlsson LM, Carlsson B. Regulation and splicing of scavenger receptor class B type I in human macrophages and atherosclerotic plaques. BMC Cardiovasc Disord 2005; 5:25.
27. Trogan E, Feig JE, Dogan S, Rothblat GH, Angeli V, Tacke F, Randolph GJ, Fisher EA. Gene expression changes in foam cells and the role of chemokine receptor CCR7 during atherosclerosis regression in ApoE-deficient mice. Proc Natl Acad Sci U S A 2006; 103:3781-3786.
28. Fuhrman B, Gantman A, Aviram M. Paraoxonase 1 (PON1) deficiency in mice is associated with reduced expression of macrophage SR-BI and consequently the loss of HDL cytoprotection against apoptosis. Atherosclerosis 2010; Jan 28. [Epub ahead of print]
- This study showed that SR-BI expression in macrophages decreased in PON1 deficient mice. Less HDL can bind to PON1-deficent macrophages as compared to WT macrophages. Moreover, HDL cannnot protect PON1-deficent macrophages against tunicamycin-induced apoptosis.
29. Han J, Nicholson AC, Zhou X, Feng J, Gotto AM, Jr., Hajjar DP. Oxidized low density lipoprotein decreases macrophage expression of scavenger receptor B-I. J Biol Chem 2001; 276:16567-16572.
30. Wang N, Lan D, Chen W, Matsuura F, Tall AR. ATP-binding cassette transporters G1 and G4 mediate cellular cholesterol efflux to high-density lipoproteins. Proc Natl Acad Sci U S A 2004; 101:9774-9779.
31. Terasaka N, Wang N, Yvan-Charvet L, Tall AR. High-density lipoprotein protects macrophages from oxidized low-density lipoprotein-induced apoptosis by promoting efflux of 7-ketocholesterol via ABCG1. Proc.Natl.Acad.Sci.U.S.A 2007, 104:15093-15098.
32. Wang N, Ranalletta M, Matsuura F, Peng F, Tall AR. LXR-induced redistribution of ABCG1 to plasma membrane in macrophages enhances cholesterol mass efflux to HDL. Arterioscler Thromb Vasc Biol 2006; 26:1310-1316.
33. Sankaranarayanan S, Oram JF, Asztalos BF, Vaughan AM, Lund-Katz S, Adorni MP, Phillips MC, Rothblat GH. Effects of acceptor composition and mechanism of ABCG1-mediated cellular free cholesterol efflux. J Lipid Res 2009; 50:275-284.

•• This study intensively investigated the compositions of acceptor particles for ABCG1-mediated efflux and provides evidence that aqueous diffusion is involved in this cholesterol efflux pathway. Different from aqueous diffusion, ABCG1 does not mediate cholesterol influx.

34. Vaughan AM, Oram JF. ABCG1 redistributes cell cholesterol to domains removable by high density lipoprotein but not by lipid-depleted apolipoproteins. J Biol Chem 2005; 280:30150-30157.
35. Kobayashi A, Takanezawa Y, Hirata T, Shimizu Y, Misasa K, Kioka N, Arai H, Ueda K, Matsuo M. Efflux of sphingomyelin, cholesterol, and phosphatidylcholine by ABCG1. J Lipid Res 2006; 47:1791-1802.
36. Sano O, Kobayashi A, Nagao K, Kumagai K, Kioka N, Hanada K, Ueda K, Matsuo M. Sphingomyelin-dependence of cholesterol efflux mediated by ABCG1. J Lipid Res 2007; 48:2377-2384.
37 Venkateswaran A, Repa JJ, Lobaccaro JM, Bronson A, Mangelsdorf DJ, Edwards PA. Human white/murine ABC8 mRNA levels are highly induced in lipid-loaded macrophages. A transcriptional role for specific oxysterols. J Biol Chem 2000; 275:14700-14707
38. Schmitz G, Langmann T, Heimerl S. Role of ABCG1 and other ABCG family members in lipid metabolism. J Lipid Res 2001; 42:1513-1520.
39. Fu X, Menke JG, Chen Y, Zhou G, MacNaul KL, Wright SD, Sparrow CP, Lund EG. 27-hydroxycholesterol is an endogenous ligand for liver X receptor in cholesterol-loaded cells. J Biol Chem 2001; 276:38378-38387.
40. Jakobsson T, Venteclef N, Toresson G, Damdimopoulos AE, Ehrlund A, Lou X, Sanyal S, Steffensen KR, Gustafsson JA, Treuter E. GPS2 is required for cholesterol efflux by triggering histone demethylation, LXR recruitment, and coregulator assembly at the ABCG1 locus. Mol Cell 2009; 34:510-518.

•• This study reveals the distinct transcriptional coregulators recruited for LXR-mediated gene expression of ABCG1 and ABCA1 and demonstrates the role of GPS2 in ABCG1 transcription in macrophage THP-1 cells. Knowdown of GPS2 blocks the GW3965 induced ABCG1-mediated cholesterol efflux to HDL.

41. Lorkowski S, Kratz M, Wenner C, Schmidt R, Weitkamp B, Fobker M, Reinhardt J, Rauterberg J, Galinski EA, Cullen P. Expression of the ATP-binding cassette transporter gene ABCG1 (ABC8) in Tangier disease. Biochem Biophys Res Commun 2001; 283:821-830.
42. Nagelin MH, Srinivasan S, Lee J, Nadler JL, Hedrick CC. 12/15-Lipoxygenase activity increases the degradation of macrophage ATP-binding cassette transporter G1. Arterioscler Thromb Vasc Biol 2008; 28:1811-1819.
43. Yla-Herttuala S, Rosenfeld ME, Parthasarathy S, Sigal E, Sarkioja T, Witztum JL, Steinberg D. Gene expression in macrophage-rich human atherosclerotic lesions. 15-lipoxygenase and acetyl low density lipoprotein receptor messenger RNA colocalize with oxidation specific lipid-protein adducts. J Clin Invest 1991; 87:1146-1152.
44. Nagelin MH, Srinivasan S, Nadler JL, Hedrick CC: Murine 12/15-lipoxygenase regulates ATP-binding cassette transporter G1 protein degradation through p38- and JNK2-dependent pathways. J Biol Chem 2009; 284:31303-31314.

• This study provides evidence that 12/15-lipoxygenase enhanced serine phosphorylation of ABCG1 by p38- and JNK2-dependent pathways and proteasome-mediated degradation of ABCG1.

45. Wang X, Liao D, Bharadwaj U, Li M, Yao Q, Chen C. C-reactive protein inhibits cholesterol efflux from human macrophage-derived foam cells. Arterioscler Thromb Vasc Biol 2008; 28:519-526.
46. Mauldin JP, Nagelin MH, Wojcik AJ, Srinivasan S, Skaflen MD, Ayers CR, McNamara CA, Hedrick CC. Reduced expression of ATP-binding cassette transporter G1 increases cholesterol accumulation in macrophages of patients with type 2 diabetes mellitus. Circulation 2008; 117:2785-2792.
47. Mauerer R, Ebert S, Langmann T. High glucose, unsaturated and saturated fatty acids differentially regulate expression of ATP-binding cassette transporters ABCA1 and ABCG1 in human macrophages. Exp Mol Med 2009; 41:126-132.
48. Higgins CF. ABC transporters: from microorganisms to man. Annu Rev Cell Biol 1992; 8:67-113.
49. Yancey PG, Bielicki JK, Johnson WJ, Lund-Katz S, Palgunachari MN, Anantharamaiah GM, Segrest JP, Phillips MC, Rothblat GH. Efflux of cellular cholesterol and phospholipid to lipid-free apolipoproteins and class A amphipathic peptides. Biochemistry 1995; 34:7955-7965.
50. Santamarina-Fojo S, Remaley AT, Neufeld EB, Brewer HB, Jr. Regulation and intracellular trafficking of the ABCA1 transporter. J Lipid Res 2001; 42:1339-1345.

51. Tamehiro N, Zhou S, Okuhira K, Benita Y, Brown CE, Zhuang DZ, Latz E, Hornemann T, von EA, Xavier RJ, Freeman MW, Fitzgerald ML. SPTLC1 binds ABCA1 to negatively regulate trafficking and cholesterol efflux activity of the transporter. Biochemistry 2008; 47:6138-6147.

52. Singaraja RR, Kang MH, Vaid K, Sanders SS, Vilas GL, Arstikaitis P, Coutinho J, Drisdel RC, El-Husseini AD, Green WN, Berthiaume L, Hayden MR. Palmitoylation of ATP-binding cassette transporter A1 is essential for its trafficking and function. Circ Res 2009; 105:138-147.

•• ABCA1 is located not only on the plasma membrane, but also in the intracellular organels. The trafficking of ABCA1 to the plasma membrane is important for its function as a cholesterol transporter. This study demonstrates the importance of palmitoylation of cysteines of ABCA1 for its localization to the plasma membrane.

53. Linder MD, Mayranpaa MI, Peranen J, Pietila TE, Pietiainen VM, Uronen RL, Olkkonen VM, Kovanen PT, Ikonen E. Rab8 regulates ABCA1 cell surface expression and facilitates cholesterol efflux in primary human macrophages. Arterioscler Thromb Vasc Biol 2009; 29:883-888.

•• The mechanisms of ABCA1 delivery to the plasma membrane are not well understood. This study shows the involvement of Rab8 in ABCA1 trafficking to the plasma membrane. Importantly, Rab8 is upregulated in macrophages from human atherosclerotic lesions. *In vitro* overexpression of Rab8 in macrophages increases ABCA1 protein levels on the cell surface and stimulates endosomal cholesterol efflux to apoAI.

54. Wang N, Silver DL, Costet P, Tall AR. Specific binding of ApoA-I, enhanced cholesterol efflux, and altered plasma membrane morphology in cells expressing ABC1. J Biol Chem 2000; 275:33053-33058.

55. Fitzgerald ML, Morris AL, Rhee JS, Andersson LP, Mendez AJ, Freeman MW. Naturally occurring mutations in the largest extracellular loops of ABCA1 can disrupt its direct interaction with apolipoprotein A-I. J Biol Chem 2002; 277:33178-33187.

56. Vaughan AM, Oram JF. ABCA1 redistributes membrane cholesterol independent of apolipoprotein interactions. J Lipid Res 2003; 44:1373-1380.

57. Landry YD, Denis M, Nandi S, Bell S, Vaughan AM, Zha X. ATP-binding cassette transporter A1 expression disrupts raft membrane microdomains through its ATPase-related functions. J Biol Chem 2006; 281:36091-36101.

58. Zarubica A, Plazzo AP, Stockl M, Trombik T, Hamon Y, Muller P, Pomorski T, Herrmann A, Chimini G. Functional implications of the influence of ABCA1 on lipid microenvironment at the plasma membrane: a biophysical study. FASEB J 2009; 23:1775-1785.

59. Chambenoit O, Hamon Y, Marguet D, Rigneault H, Rosseneu M, Chimini G. Specific docking of apolipoprotein A-I at the cell surface requires a functional ABCA1 transporter. J Biol Chem 2001; 276:9955-9960.

60. Tang C, Vaughan AM, Anantharamaiah GM, Oram JF. Janus kinase 2 modulates the lipid-removing but not protein-stabilizing interactions of amphipathic helices with ABCA1. J Lipid Res 2006; 47:107-114.

61. Vedhachalam C, Duong PT, Nickel M, Nguyen D, Dhanasekaran P, Saito H, Rothblat GH, Lund-Katz S, Phillips MC. Mechanism of ATP-binding cassette transporter A1-mediated cellular lipid efflux to apolipoprotein A-I and formation of high density lipoprotein particles. J Biol Chem 2007; 282:25123-25130.

62. Vedhachalam C, Ghering AB, Davidson WS, Lund-Katz S, Rothblat GH, Phillips MC. ABCA1-induced cell surface binding sites for ApoA-I. Arterioscler Thromb Vasc Biol 2007; 27:1603-1609.

63. Vaughan AM, Tang C, Oram JF. ABCA1 mutants reveal an interdependency between lipid export function, apoA-I binding activity, and Janus kinase 2 activation. J Lipid Res 2009; 50:285-292.

• This study determined the abilities of the different ABCA1 mutants in apoAI binding, JAK2 activation, and cellular cholesterol efflux induction. Linear regression analysis showed high correlations between these functions of ABCA1.

64. Hassan HH, Bailey D, Lee DY, Iatan I, Hafiane A, Ruel I, Krimbou L, Genest J. Quantitative analysis of ABCA1-dependent compartmentalization and trafficking of apolipoprotein A-I: implications for determining cellular kinetics of nascent high density lipoprotein biogenesis. J Biol Chem 2008; 283:11164-11175.

65. Takahashi Y, Smith JD. Cholesterol efflux to apolipoprotein AI involves endocytosis and resecretion in a calcium-dependent pathway. Proc Natl Acad Sci U S A 1999; 96:11358-11363.

66. Denis M, Landry YD, Zha X. ATP-binding cassette A1-mediated lipidation of apolipoprotein A-I occurs at the plasma membrane and not in the endocytic compartments. J Biol Chem 2008; 283:16178-16186.

67. Faulkner LE, Panagotopulos SE, Johnson JD, Woollett LA, Hui DY, Witting SR, Maiorano JN, Davidson WS. An analysis of the role of a retroendocytosis pathway in ABCA1-mediated cholesterol efflux from macrophages. J Lipid Res 2008; 49:1322-1332.

68. Lu R, Arakawa R, Ito-Osumi C, Iwamoto N, Yokoyama S. ApoA-I facilitates ABCA1 recycle/accumulation to cell surface by inhibiting its intracellular degradation and increases HDL generation. Arterioscler Thromb Vasc Biol 2008; 28:1820-1824.

69. Azuma Y, Takada M, Shin HW, Kioka N, Nakayama K, Ueda K. Retroendocytosis pathway of ABCA1/apoA-I contributes to HDL formation. Genes Cells 2009; 14:191-204.

•• Using overexpression of human ABCA1 constructs with either an extracellular hemaglutinin tag or an intracellular GFP tag, the internalization route of the ABCA1/apoAI complex is shown to be clathrin- and Rab5-dependent. Moreover, upon blockade of the clathrin-mediated internalization, ac-LDL-loaded THP-1 cells exhibited reduced cholesterol efflux to apoAI.

70. Miyazaki O, Kobayashi J, Fukamachi I, Miida T, Bujo H, Saito Y. A new sandwich enzyme immunoassay for measurement of plasma pre-beta1-HDL levels. J Lipid Res 2000; 41:2083-2088.

71. Llera-Moya M, Drazul-Schrader D, Asztalos BF, Cuchel M, Rader DJ, Rothblat GH. The ability to promote efflux via ABCA1 determines the capacity of serum specimens with similar high-density lipoprotein cholesterol to remove cholesterol from macrophages. Arterioscler Thromb Vasc Biol 2010; 30:796-801.

•• This study demonstrates that HDL, isolated from individuals with similar plasma levels of HDL-C and apoAI, exhibits different abilities to induce cholesterol efflux from acLDL-loaded J774 macrophages. These differences are due to variations in the serum concentrations of preβ1 HDL, indicating that preβ1 HDL is better biomarker than apoAI and HDL-C for serum cholesterol efflux capacity.

72. Pradel LC, Mitchell AJ, Zarubica A, Dufort L, Chasson L, Naquet P, Broccardo C, Chimini G. ATP-binding cassette transporter hallmarks tissue macrophages and modulates cytokine-triggered polarization programs. Eur J Immunol 2009; 39:2270-2280.

• In this study, ABCA1 expression was shown to be limited to “non-inflammatory” $Ly6C^{low}$ circulating monocytes and tissue-resident macrophages. Moreover, expression of ABCA1 on macrophages influences their immune response to LPS and cytokines.

73. Schmitz G, Langmann T. Transcriptional regulatory networks in lipid metabolism control ABCA1 expression. Biochim Biophys Acta 2005; 1735:1-19.

74. Taylor JM, Borthwick F, Bartholomew C, Graham A. Overexpression of steroidogenic acute regulatory protein increases macrophage cholesterol efflux to apolipoprotein AI. Cardiovasc Res 2010; 86:526-534.

• This study demonstrates that induction of 27-HOC generation by promotion of the transfer of cholesterol to mitochondrial sterol 27-hydroxylase increases the expression of ABCA1 and ABCA1 mediated cholesterol efflux.

75. Hozoji M, Munehira Y, Ikeda Y, Makishima M, Matsuo M, Kioka N, Ueda K. Direct interaction of nuclear liver X receptor-beta with ABCA1 modulates cholesterol efflux. J Biol Chem 2008; 283:30057-30063.

•• This study demonstrates that LXRβ can bind to ABCA1 and regulate the expression and activity of ABCA1 at the posttranslational level. Under non-cholesterol loading condition, the binding of LXRβ to ABCA1 stabilizes the expression of ABCA1 on the plasma membrane. This stabilization decreases the activity of ABCA1 and limits cholesterol efflux. Upon cholesterol loading, the dissociation of LXRβ from ABCA1 rapidly remove excessive cholesterol from the cell.

76. Arakawa R, Yokoyama S. Helical apolipoproteins stabilize ATP-binding cassette transporter A1 by protecting it from thiol protease-mediated degradation. J Biol Chem 2002; 277:22426-22429.

77. Martinez LO, Agerholm-Larsen B, Wang N, Chen W, Tall AR. Phosphorylation of a pest sequence in ABCA1 promotes calpain degradation and is reversed by ApoA-I. J Biol Chem 2003; 278:37368-37374.

78. Wang N, Chen W, Linsel-Nitschke P, Martinez LO, Agerholm-Larsen B, Silver DL, Tall AR. A PEST sequence in ABCA1 regulates degradation by calpain protease and stabilization of ABCA1 by apoA-I. J Clin Invest 2003; 111:99-107.

79. Iwamoto N, Lu R, Tanaka N, Abe-Dohmae S, Yokoyama S. Calmodulin Interacts With ATP Binding Cassette Transporter A1 to Protect From Calpain-Mediated Degradation and Upregulates High-Density Lipoprotein Generation. Arterioscler Thromb Vasc Biol 2010; Apr 15. [Epub ahead of print]

- This study showed that calmodulin inhibited calpain-mediated ABCA1 degradation by interfering with the phosphorylation of PEST sequence at the cytoplamic region of ABCA1. Interestingly, a increase in binding of calmodulin to ABCA1 enhances ABCA1-mediated cholesterol efflux to apoAI.

80. Karwatsky J, Ma L, Dong F, Zha X. Cholesterol efflux to apoA-I in ABCA1-expressing cells is regulated by Ca2+-dependent calcineurin signaling. J Lipid Res 2010; 51:1144-1156.

81. Okuhira K, Fitzgerald ML, Tamehiro N, Ohoka N, Suzuki K, Sawada JI, Naito M, Nishimaki-Mogami T. Binding of PDZ-RhoGEF to ATP-binding cassette transporter A1 (ABCA1) induces cholesterol efflux through RhoA activation and prevention of transporter degradation. J Biol Chem 2010; 285:16369-16377.

- This study demonstrated the importance of RhoA activation for apoAI-mediated stabilization of ABCA1. The PDZ protein RhoGEF stabilizes ABCA1 through activation of RhoA.

82. Lawn RM, Wade DP, Couse TL, Wilcox JN. Localization of human ATP-binding cassette transporter 1 (ABC1) in normal and atherosclerotic tissues. Arterioscler Thromb Vasc Biol 2001; 21:378-385.

83. Albrecht C, Soumian S, Amey JS, Sardini A, Higgins CF, Davies AH, Gibbs RG. ABCA1 expression in carotid atherosclerotic plaques. Stroke 2004; 35:2801-2806.

84. Brown AJ, Watts GF, Burnett JR, Dean RT, Jessup W. Sterol 27-hydroxylase acts on 7-ketocholesterol in human atherosclerotic lesions and macrophages in culture. J Biol Chem. 2000; 275:27627-27633.

85. Zhou X, He W, Huang Z, Gotto AM, Jr., Hajjar DP, Han J. Genetic deletion of low density lipoprotein receptor impairs sterol-induced mouse macrophage ABCA1 expression. A new SREBP1-dependent mechanism. J Biol Chem 2008; 283:2129-2138.

86. Teupser D, Kretzschmar D, Tennert C, Burkhardt R, Wilfert W, Fengler D, Naumann R, Sippel AE, Thiery J. Effect of macrophage overexpression of murine liver X receptor-alpha (LXR-alpha) on atherosclerosis in LDL-receptor deficient mice. Arterioscler Thromb Vasc Biol 2008; 28:2009-2015.

87. Feng B, Tabas I. ABCA1-mediated cholesterol efflux is defective in free cholesterol-loaded macrophages. Mechanism involves enhanced ABCA1 degradation in a process requiring full NPC1 activity. J Biol Chem 2002; 277:43271-43280.

88. Wang Y, Kurdi-Haidar B, Oram JF. LXR-mediated activation of macrophage stearoyl-CoA desaturase generates unsaturated fatty acids that destabilize ABCA1. J Lipid Res 2004; 45:972-980.

89. Wang Y, Oram JF. Unsaturated fatty acids phosphorylate and destabilize ABCA1 through a protein kinase C delta pathway. J Lipid Res 2007; 48:1062-1068.

90. Wang Y, Oram JF. Unsaturated fatty acids phosphorylate and destabilize ABCA1 through a phospholipase D2 pathway. J Biol Chem 2005; 280:35896-35903.

91. Schneider JG, Yang Z, Chakravarthy MV, Lodhi IJ, Wei X, Turk J, Semenkovich CF. Macrophage fatty acid synthase deficiency decreases diet-induced atherosclerosis. J Biol Chem 2010; May 17. [Epub ahead of print]

- This study provides evidence that fatty acids are proatherogenic. Inactivation of fatty acid synthase in macrophages increases cholesterol efflux to apoAI.

92. Kleemann R, Zadelaar S, Kooistra T. Cytokines and atherosclerosis: a comprehensive review of studies in mice. Cardiovasc Res 2008; 79:360-376.

93. Jiang X, Zeng HS, Guo Y, Zhou ZB, Tang BS, Li FK. The expression of matrix metalloproteinases-9, transforming growth factor-beta1 and transforming growth factor-beta receptor I in human atherosclerotic plaque and their relationship with plaque stability. Chin Med J (Engl) 2004; 117:1825-1829.

94. Hao XR, Cao DL, Hu YW, Li XX, Liu XH, Xiao J, Liao DF, Xiang J, Tang CK. IFN-gamma down-regulates ABCA1 expression by inhibiting LXRalpha in a JAK/STAT signaling pathway-dependent manner. Atherosclerosis 2009; 203:417-428.

95. Mei CL, Chen ZJ, Liao YH, Wang YF, Peng HY, Chen Y. Interleukin-10 inhibits the down-regulation of ATP binding cassette transporter A1 by tumour necrosis factor-alpha in THP-1 macrophage-derived foam cells. Cell Biol Int 2007; 31:1456-1461.

96. Panousis CG, Evans G, Zuckerman SH. TGF-beta increases cholesterol efflux and ABC-1 expression in macrophage-derived foam cells: opposing the effects of IFN-gamma. J Lipid Res 2001; 42:856-863.

97. Han X, Kitamoto S, Wang H, Boisvert WA. Interleukin-10 overexpression in macrophages suppresses atherosclerosis in hyperlipidemic mice. FASEB J 2010; Mar 30. [Epub ahead of print]

98. Castrillo A, Joseph SB, Vaidya SA, Haberland M, Fogelman AM, Cheng G, Tontonoz P. Crosstalk between LXR and toll-like receptor signaling mediates bacterial and viral antagonism of cholesterol metabolism. Mol Cell 2003; 12:805-816.

99. Chen S, Sorrentino R, Shimada K, Bulut Y, Doherty TM, Crother TR, Arditi M. Chlamydia pneumoniae-induced foam cell formation requires MyD88-dependent and -independent signaling and is reciprocally modulated by liver X receptor activation. J Immunol 2008; 181:7186-7193.

100. Sorrentino R, Morello S, Chen S, Bonavita E, Pinto A. The activation of liver X receptors inhibits toll-like receptor-9-induced foam cell formation. J Cell Physiol 2010; 223:158-167.

101. Maitra U, Parks JS, Li L. An innate immunity signaling process suppresses macrophage ABCA1 expression through IRAK-1-mediated downregulation of retinoic acid receptor alpha and NFATc2. Mol Cell Biol 2009; 29:5989-5997.

- In this study, the binding sites for nuclear factor of activated T-cells (NFAT) and retinoic acid receptors (RAR) were identified in the promoter region of ABCA1. Furthermore, evidence is provided that IRAK-1 downregulates ABCA1 expression during inflammation by reducing nuclear levels of NFATc2 and RARα.

102. Zhou X, Yin Z, Guo X, Hajjar DP, Han J. Inhibition of ERK1/2 and activation of liver X receptor synergistically induce macrophage ABCA1 expression and cholesterol efflux. J Biol Chem 2010; 285:6316-6326.

- This study demonstrates the synergistic effect of ERK1/2 inhibitors and LXR agonists for induction of ABCA1 expression and cholesterol efflux, which might be a potent therapeutic strategy for prevention of atherosclerosis.

103. Marcil V, Delvin E, Sane AT, Tremblay A, Levy E. Oxidative stress influences cholesterol efflux in THP-1 macrophages: role of ATP-binding cassette A1 and nuclear factors. Cardiovasc Res 2006; 72:473-482.

104. Semenza GL. HIF-1 and human disease: one highly involved factor. Genes Dev 2000; 14:1983-1991.

105. Semenza GL. Hypoxia-inducible factor 1: oxygen homeostasis and disease pathophysiology. Trends Mol Med 2001; 7:345-350.

106. Jiang BH, Rue E, Wang GL, Roe R, Semenza GL. Dimerization, DNA binding, and transactivation properties of hypoxia-inducible factor 1. J Biol Chem 1996; 271:17771-17778.

107. Ugocsai P, Hohenstatt A, Paragh G, Liebisch G, Langmann T, Wolf Z, Weiss T, Groitl P, Dobner T, Kasprzak P, Gobolos L, Falkert A, Seelbach-Goebel B, Gellhaus A, Winterhager E, Schmidt M, Semenza GL, Schmitz G. HIF-1beta determines ABCA1 expression under hypoxia in human macrophages. Int J Biochem Cell Biol. 2010; 42:241-252.

•• This paper demonstrates that the expression of ABCA1 in macrophages is correlated with the expression of HIF-1β under hypoxic conditions as well as atherosclerotic lesions.

108. Hulten LM, Levin M. The role of hypoxia in atherosclerosis. Curr Opin Lipidol 2009; 20:409-414.

109. Tang C, Kanter JE, Bornfeldt KE, LeBoeuf RC, Oram JF. Diabetes reduces the cholesterol exporter ABCA1 in mouse macrophages and kidneys. J Lipid Res 2009; Nov 23. [Epub ahead of print]

110. Passarelli M, Tang C, McDonald TO, O'Brien KD, Gerrity RG, Heinecke JW, Oram JF. Advanced glycation end product precursors impair ABCA1-dependent cholesterol removal from cells. Diabetes 2005; 54:2198-2205.

111. Brunham LR, Kruit JK, Pape TD, Timmins JM, Reuwer AQ, Vasanji Z, Marsh BJ, Rodrigues B, Johnson JD, Parks JS, Verchere CB, Hayden MR. Beta-cell ABCA1 influences insulin secretion, glucose homeostasis and response to thiazolidinedione treatment. Nat Med 2007; 13:340-347.

112. Vergeer M, Brunham LR, Koetsveld J, Kruit JK, Verchere CB, Kastelein JJ, Hayden MR, Stroes ES. Carriers of loss-of-function mutations in ABCA1 display pancreatic beta-cell dysfunction. Diabetes Care 2010; 33:869-874.

- This study indicates the importance of ABCA1 for the function of pancreatic beta-cells in secreting insulin in humans.

113. Tabas I, Tall A, Accili D. The impact of macrophage insulin resistance on advanced atherosclerotic plaque progression. Circ.Res. 2010, 106:58-67.

114. Adorni MP, Zimetti F, Billheimer JT, Wang N, Rader DJ, Phillips MC, Rothblat GH. The roles of different pathways in the release of cholesterol from macrophages. J Lipid Res 2007; 48:2453-2462.

115. Wang X, Collins HL, Ranalletta M, Fuki IV, Billheimer JT, Rothblat GH, Tall AR, Rader DJ. Macrophage ABCA1 and ABCG1, but not SR-BI, promote macrophage reverse cholesterol transport in vivo. J Clin Invest 2007; 117:2216-2224.

116. Ye D, Meurs I, Ohigashi M, Calpe-Berdiel L, Habets KL, Zhao Y, Kubo Y, Yamaguchi A, Van Berkel TJ, Nishi T, Van EM. Macrophage ABCA5 deficiency influences cellular cholesterol efflux and increases susceptibility to atherosclerosis in female LDLr knockout mice. Biochem Biophys Res Commun 2010; 395:387-394

117. Wang MD, Kiss RS, Franklin V, McBride HM, Whitman SC, Marcel YL. Different cellular traffic of LDL-cholesterol and acetylated LDL-cholesterol leads to distinct reverse cholesterol transport pathways. J Lipid Res 2007; 48:633-645.

118. Gelissen IC, Harris M, Rye KA, Quinn C, Brown AJ, Kockx M, Cartland S, Packianathan M, Kritharides L, Jessup W. ABCA1 and ABCG1 synergize to mediate cholesterol export to apoA-I. Arterioscler Thromb Vasc Biol 2006; 26:534-540.

119. Out R, Jessup W, Le GW, Hoekstra M, Gelissen IC, Zhao Y, Kritharides L, Chimini G, Kuiper J, Chapman MJ, Huby T, Van Berkel TJ, Van EM. Coexistence of foam cells and hypocholesterolemia in mice lacking the ABC transporters A1 and G1. Circ Res 2008; 102:113-120.

120. Out R, Hoekstra M, Habets K, Meurs I, de W, V, Hildebrand RB, Wang Y, Chimini G, Kuiper J, Van Berkel TJ, Van EM. Combined deletion of macrophage ABCA1 and ABCG1 leads to massive lipid accumulation in tissue macrophages and distinct atherosclerosis at relatively low plasma cholesterol levels. Arterioscler Thromb Vasc Biol 2008; 28:258-264.

121. Yvan-Charvet L, Ranalletta M, Wang N, Han S, Terasaka N, Li R, Welch C, Tall AR. Combined deficiency of ABCA1 and ABCG1 promotes foam cell accumulation and accelerates atherosclerosis in mice. J Clin Invest 2007; 117:3900-3908.

122. Van EM, Bos IS, Hildebrand RB, Van Rij BT, Van Berkel TJ. Dual role for scavenger receptor class B, type I on bone marrow-derived cells in atherosclerotic lesion development. Am J Pathol 2004; 165:785-794.

123. Yvan-Charvet L, Pagler TA, Wang N, Senokuchi T, Brundert M, Li H, Rinninger F, Tall AR. SR-BI inhibits ABCG1-stimulated net cholesterol efflux from cells to plasma HDL. J Lipid Res 2008; 49:107-114.

124. Covey SD, Krieger M, Wang W, Penman M, Trigatti BL. Scavenger receptor class B type I-mediated protection against atherosclerosis in LDL receptor-negative mice involves its expression in bone marrow-derived cells. Arterioscler Thromb Vasc Biol 2003; 23:1589-1594.

125. Zhang W, Yancey PG, Su YR, Babaev VR, Zhang Y, Fazio S, Linton MF. Inactivation of macrophage scavenger receptor class B type I promotes atherosclerotic lesion development in apolipoprotein E-deficient mice. Circulation 2003; 108:2258-2263.

126. Yancey PG, Jerome WG, Yu H, Griffin EE, Cox BE, Babaev VR, Fazio S, Linton MF. Severely altered cholesterol homeostasis in macrophages lacking apoE and SR-BI. J Lipid Res 2007; 48:1140-1149.

127. Cuchel M, Lund-Katz S, Llera-Moya M, Millar JS, Chang D, Fuki I, Rothblat GH, Phillips MC, Rader DJ. Pathways by which reconstituted high-density lipoprotein mobilizes free cholesterol from whole body and from macrophages. Arterioscler Thromb Vasc Biol 2010; 30:526-532.

•• This study demonstrated that rHDL induced free cholesterol mobilization was mediated by SR-BI but not ABCA1 and ABCG1.

128. Yvan-Charvet L, Pagler T, Gautier EL, Avagyan S, Siry RL, Han S, Welch CL, Wang N, Randolph GJ, Snoeck HW, Tall AR. ATP-Binding Cassette Transporters and HDL Suppress Hematopoietic Stem Cell Proliferation. Science 2010; May 20. [Epub ahead of print]

•• In hypercholesterolemic mice, combined deficiency of macrophage ABCA1 and ABCG1 leads to a transplantable myeloproliferative disorder. Interestingly, overexpression of apoAI can suppress this disorder and the accelerated atherosclerosis observed in these animals.

129. Larrede S, Quinn CM, Jessup W, Frisdal E, Olivier M, Hsieh V, Kim MJ, Van EM, Couvert P, Carrie A, Giral P, Chapman MJ, Guerin M, Le GW. Stimulation of cholesterol efflux by LXR agonists in cholesterol-loaded human macrophages is ABCA1-dependent but ABCG1-independent. Arterioscler Thromb Vasc Biol 2009; 29:1930-1936.

•• In this study, cholesterol efflux from human cholesterol-loaded THP-1 cells to HDL stimulated by LXR agonists was shown to be primarily dependent on ABCA1 expression. Interestinly, the induction of ABCG1 expression was not essential for cholesterol efflux. However, blocking of Cla-1, an human ortholog of SR-BI did inhibit cholesterol efflux.

130. Despres JP, Lemieux I, Dagenais GR, Cantin B, Lamarche B. HDL-cholesterol as a marker of coronary heart disease risk: the Quebec cardiovascular study. Atherosclerosis 2000; 153:263-272.

131. Movva R, Rader DJ. Laboratory assessment of HDL heterogeneity and function. Clin Chem 2008; 54:788-800.

132. Tall AR. Cholesterol efflux pathways and other potential mechanisms involved in the athero-protective effect of high density lipoproteins. J Intern Med 2008; 263:256-273.

133. Davidson WS, Silva RA, Chantepie S, Lagor WR, Chapman MJ, Kontush A. Proteomic analysis of defined HDL subpopulations reveals particle-specific protein clusters: relevance to antioxidative function. Arterioscler Thromb Vasc Biol 2009; 29:870-876

• In this study, the protein compositions of different HDL subpopulations separated by classical density gradient ultra-centrifugation, were analyzed. Specific HDL proteins, including apoL-I, PON1, and PON3 appear to be enriched in HDL3 particles and are correlated with its anti-oxidative function.

134. Smith JD. Dysfunctional HDL as a diagnostic and therapeutic target. Arterioscler Thromb Vasc Biol 2010; 30:151-155.

135. Feng H, Li XA. Dysfunctional high-density lipoprotein. Curr Opin Endocrinol Diabetes Obes 2009; 16:156-162

136. Van der Westhuyzen DR, de Beer FC, Webb NR. HDL cholesterol transport during inflammation. Curr Opin Lipidol 2007; 18:147-151

137. Jahanggiri A. High-density lipoprotein and the acute phase response. Curr Opin Endocrinol Diabetes Obes 2010; 17:156-160

138. Mastorikou M, Mackness B, Liu Y, Mackness M. Glycation of paraoxonase-1 inhibits its activity and impairs the ability of high-density lipoprotein to metabolize membrane lipid hydroperoxides. Diabet Med 2008; 25:1049-1055.

139. Verges B. Lipid modification in type 2 diabetes: the role of LDL and HDL. Fundam Clin Pharmacol 2009; 23:681-685.

140. Mooradian AD. Dyslipidemia in type 2 diabetes mellitus. Nat.Clin.Pract.Endocrinol.Metab 2009; 5:150-159.

141. Sugiyama S, Okada Y, Sukhova GK, Virmani R, Heinecke JW, Libby P. Macrophage myeloperoxidase regulation by granulocyte macrophage colony-stimulating factor in human atherosclerosis and implications in acute coronary syndromes. Am J Pathol 2001; 158:879-891.

142. van LM, Gijbels MJ, Duijvestijn A, Smook M, van de Gaar MJ, Heeringa P, de Winther MP, Tervaert JW. Accumulation of myeloperoxidase-positive neutrophils in atherosclerotic lesions in LDLR-/- mice. Arterioscler Thromb Vasc Biol 2008; 28:84-89.

143. Bergt C, Pennathur S, Fu X, Byun J, O'Brien K, McDonald TO, Singh P, Anantharamaiah GM, Chait A, Brunzell J, Geary RL, Oram JF, Heinecke JW. The myeloperoxidase product hypochlorous acid oxidizes HDL in the human artery wall and impairs ABCA1-dependent cholesterol transport. Proc Natl Acad Sci U S A 2004; 101:13032-13037.

144. Zheng L, Nukuna B, Brennan ML, Sun M, Goormastic M, Settle M, Schmitt D, Fu X, Thomson L, Fox PL, Ischiropoulos H, Smith JD, Kinter M, Hazen SL. Apolipoprotein A-I is a selective target for myeloperoxidase-catalyzed oxidation and functional impairment in subjects with cardiovascular disease. J Clin Invest 2004; 114:529-541.

145. Shao B, Tang C, Heinecke JW, Oram JF. Oxidation of apolipoprotein A-I by myeloperoxidase impairs the initial interactions with ABCA1 required for signaling and cholesterol export. J Lipid Res 2010; Jan 11. [Epub ahead of print]

• This study demonstrates that chlorination of apoAI by MPO impaires ABCA1-mediated cholesterol efflux through interference with the interaction of apoAI and ABCA1 and inhibition of activation of JNK2 signalling.

146. Undurti A, Huang Y, Lupica JA, Smith JD, Didonato JA, Hazen SL. Modification of high density lipoprotein by myeloperoxidase generates a pro-inflammatory particle. J Biol Chem 2009; 284:30825-30835.

• This paper shows that MPO modifed HDL is proinflammatory. The modified HDL particles can induce NF-κB activation and vascular cell adhesion molecule expression on aortic endothelial cells. Interestingly, MPO modified HDL loses the SR-BI binding ability.

147. Cavigiolio G, Geier EG, Shao B, Heinecke JW, Oda MN. The exchange of apolipoprotein A-I between the lipid-associated and the lipid-free states: a potential target for oxidative generation of dysfunctional HDL. J Biol Chem 2010; 285:18847-18857.

•• Fluorescently labeled apoAI was used in this study to establish the kinetics of apoAI transition between the lipid-associated and lipid-free states. Lipid-free apoAI exhibits a distict fluorescence emission

spectrum from lipid-rich apoAI. The authors demonstrate that MPO-mediated crosslinking of apoAI inhibited its dissociation from HDL.

148. Shao B, Cavigiolio G, Brot N, Oda MN, Heinecke JW. Methionine oxidation impairs reverse cholesterol transport by apolipoprotein A-I. Proc Natl Acad Sci U S A 2008; 105:12224-12229.
149. Annema W, Nijstad N, Tolle M, de Boer JF, Buijs RV, Heeringa P, van der Giet M, Tietge UJ. Myeloperoxidase and serum amyloid A contribute to impaired in vivo reverse cholesterol transport during the acute phase response but not group IIA secretory phospholipase A(2). J Lipid Res 2010; 51:743-754.
150. Esterbauer H, Schaur RJ, Zollner H. Chemistry and biochemistry of 4-hydroxynonenal, malonaldehyde and related aldehydes. Free Radic Biol Med 1991; 11:81-128.
151. Stadtman ER, Levine RL. Free radical-mediated oxidation of free amino acids and amino acid residues in proteins. Amino Acids 2003; 25:207-218.
152. Shao B, Pennathur S, Pagani I, Oda MN, Witztum JL, Oram JF, Heinecke JW. Dysfunctional HDL: Modifying apolipoprotein A-I by malondialdehyde, but not by an array of other reactive carbonyls, blocks cholesterol efflux by the abca1 pathway. J Biol Chem 2010; 285:18473-18484.

•• MDA mediated crosslinking of apoAI was shown to be elevated in the atherosclerotic lesions. This modification blocks the ability of apoAI to remove cellular cholesterol via ABCA1.

153. Lindstedt L, Saarinen J, Kalkkinen N, Welgus H, Kovanen PT. Matrix metalloproteinases-3, -7, and -12, but not -9, reduce high density lipoprotein-induced cholesterol efflux from human macrophage foam cells by truncation of the carboxyl terminus of apolipoprotein A-I. Parallel losses of pre-beta particles and the high affinity component of efflux. J Biol Chem. 1999;274:22627-34.
154. Lindstedt L, Lee M, Oörni K, Brömme D, Kovanen PT. Cathepsins F and S block HDL3-induced cholesterol efflux from macrophage foam cells. Biochem Biophys Res Commun. 2003;312:1019-24.
155. Lee M, von Eckardstein A, Lindstedt L, Assmann G, Kovanen PT. Depletion of pre beta 1LpA1 and LpA4 particles by mast cell chymase reduces cholesterol efflux from macrophage foam cells induced by plasma. Arterioscler Thromb Vasc Biol. 1999;19:1066-74.
156. Lee M, Sommerhoff CP, von Eckardstein A, Zettl F, Fritz H, Kovanen PT. Mast cell tryptase degrades HDL and blocks its function as an acceptor of cellular cholesterol. Arterioscler Thromb Vasc Biol. 2002;22:2086-91.
157. Kaartinen M, Penttilä A, Kovanen PT. Mast cells of two types differing in neutral protease composition in the human aortic intima. Demonstration of tryptase- and tryptase/chymase-containing mast cells in normal intimas, fatty streaks, and the shoulder region of atheromas. Arterioscler Thromb. 1994;14:966-72.
158. Judström I, Jukkola H, Metso J, Jauhiainen M, Kovanen PT, Lee-Rueckert M. Mast cell-dependent proteolytic modification of HDL particles during anaphylactic shock in the mouse reduces their ability to induce cholesterol efflux from macrophage foam cells ex vivo. Atherosclerosis. 2010;208:148-54.

• Mast cell derived enzymes chymase and tryptase has been shown to degrade apoAI and preβ HDL in vitro. This study uses an *ex-vivo* experiment to demonstrate that systemic activation of mast cells impairs the capacity of serum and intraperitoneal fluid to promote cellular cholesterol efflux.

CHAPTER 5

Enhanced foam cell formation, atherosclerotic lesion development, and inflammation by combined deletion of ABCA1 and SR-BI in bone marrow-derived cells in LDL receptor knockout mice on Western-type diet

Ying Zhao[1], Marieke Pennings[1], Reeni B. Hildebrand[1], Dan Ye[1], Laura Calpe-Berdiel[1], Ruud Out[1], Martin Kjerrulf[2], Eva Hurt-Camejo[2], Albert K. Groen[3], Menno Hoekstra[1], Wendy Jessup[4], Giovanna Chimini[5], Theo J.C. Van Berkel[1], Miranda Van Eck[1]

[1]Division of Biopharmaceutics, Leiden/Amsterdam Center for Drug Research, Leiden University, Einsteinweg 55, 2333 CC Leiden, The Netherlands
[2]Department of Molecular Pharmacology, AstraZeneca R&D, Mölndal, Sweden
[3]Department of Pediatrics, University Medical Center Groningen, Groningen, The Netherlands
[4]Centre for Vascular Research, University of New South Wales, Sydney, New South Wales, Australia
[5]Centre d'Immunologie de Marseille Luminy, Institut National de la Santé et la Recherche Médicale, Centre National de la Recherche Scientifique, Université de la Méditerranée, Marseille, France

Abstract

Rationale. Macrophages are incapable of limiting the uptake of lipids and therefore rely on cholesterol efflux mechanisms for maintaining cellular cholesterol homeostasis. Important mediators of macrophage cholesterol efflux are ABCA1, which mediates the efflux of cholesterol to lipid-poor apoAI, and SR-BI that promotes efflux to mature HDL.

Objective. The aim of the current study was to increase the insight into the putative synergistic roles of ABCA1 and SR-BI in foam cell formation and atherosclerosis,

Methods and Results. LDL receptor knockout (LDLr KO) mice were transplanted with bone marrow from ABCA1/SR-BI double knockout mice, the respective single knockouts, or wildtype littermates. Serum cholesterol levels were lower in ABCA1/SR-BI double knockout transplanted animals, as compared to the single knockout and wildtype transplanted animals on Western-type diet. Despite the lower serum cholesterol levels, massive foam cell formation was found in macrophages from spleen and the peritoneal cavity. Interestingly, ABCA1/SR-BI double knockout transplanted animals also showed a major increase in pro-inflammatory KC (murine IL-8) and IL-12p40 levels in the circulation. Furthermore, after 10 weeks Western-type diet feeding atherosclerotic lesion development in the aortic root was more extensive in the LDLr KO mice reconstituted with ABCA1/SR-BI double knockout bone marrow.

Conclusions. This study shows that deletion of ABCA1 and SR-BI in bone marrow-derived cells enhances in vivo macrophage foam cell formation and atherosclerotic lesion development in LDLr KO mice on Western diet, indicating that under high-dietary lipid conditions both macrophage ABCA1 and SR-BI contribute significantly to cholesterol homeostasis in the macrophage in vivo and are essential for reducing the risk for atherosclerosis.

--- *Cir. Res.* 2010; 107(12): e20-31 ---

Introduction

The hallmark of atherosclerotic lesion development is the accumulation of macrophage foam cells (1). Transporters implicated in cholesterol efflux from macrophages include the ATP-binding cassette (ABC) transporters ABCA1 and ABCG1, and scavenger receptor BI (SR-BI) (2,3). ABCA1 is a full-size ABC-transporter that facilitates cholesterol efflux to lipid-poor apoAI (2,3). Total-body ABCA1 knockout mice and Tangier disease patients with dysfunctional ABCA1 display a virtual absence of HDL, showing the essential role for ABCA1 in HDL metabolism (3). Targeted inactivation of ABCA1 in bone marrow-derived cells in mice leads to increased atherosclerotic lesion formation (4,5), whereas overexpression of ABCA1 inhibits the progression of atherosclerosis (6). Macrophages lacking ABCA1, however, still have substantial ability to efflux cholesterol to HDL despite impaired efflux to lipid-poor apoAI, suggesting that macrophages have additional pathways via which cellular cholesterol can be exported. In addition to ABCA1, macrophages also express the ABC half-transporter ABCG1. In contrast to ABCA1, ABCG1 facilitates cellular cholesterol efflux from macrophages to mature HDL, but not to lipid-free apolipoproteins (7,8). Furthermore, HDL levels are not affected in genetically-engineered mice lacking ABCG1 (8). Disruption of ABCG1 specifically in macrophages has only a moderate effect on atherosclerotic lesion development (9-11). Combined deletion of ABCA1 and ABCG1 on macrophages, however, led to a major impairment of cholesterol mass efflux to apoAI and HDL and a dramatic accumulation of foam cells in tissues (12-14). Transplantation of ABCA1/ABCG1 double KO bone marrow into LDL receptor knockout (LDLr KO) mice led only to modest atherosclerosis when challenged with a Western-type diet which was associated with markedly decreased plasma cholesterol levels (12). In heterozygous LDLr KO mice fed a high cholesterol/cholate diet disruption of ABCA1 and ABCG1 in bone marrow-derived cells, however, did not affect serum cholesterol levels and consequently led to markedly increased atherosclerotic lesion development as compared to mice receiving single ABCA1 KO or ABCG1 KO bone marrow (14). These studies clearly illustrate the importance of studying the effects of combined deficiency of cholesterol transporters to establish the importance of a specific transporter for preventing foam cell formation and atherosclerotic lesion development in vivo.

In addition to ABCA1 and ABCG1, also scavenger receptor class B type I (SR-BI) has been implicated in macrophage cholesterol efflux. SR-BI facilitates the transport of cholesterol from macrophages down a concentration gradient to mature HDL and mediates the selective uptake of cholesterol esters from HDL by the liver (2,3). Complete disruption of SR-BI function in mice is associated with the accumulation of abnormally large HDL particles in the circulation, reflecting impaired delivery of cholesteryl esters to the liver (3). Bone marrow-specific deletion of SR-BI did not affect serum HDL cholesterol levels and inhibited early atherosclerotic development (15), while the progression of advanced lesions was induced (15-17), indicating a unique dual role for macrophage SR-BI in the pathogenesis of atherosclerosis. Recent studies using macrophages from SR-BI knockout mice and inhibitors of SR-BI and ABCA1-mediated efflux showed that macrophage SR-BI does not promote cholesterol efflux from murine macrophages in culture (18). In addition, reverse transport of cholesterol from SR-BI KO macrophages to feces after transfer into wildtype C57BL/6 mice was not affected (19). Based on these studies the role of macrophage SR-BI for cellular cholesterol efflux was considered to be limited. However, studies from Yancey et al. demonstrated that macrophages with a combined deficiency of SR-BI and apoE display a reduced efflux capacity and accumulate free cholesterol in lysosomes (20). Moreover, recently Cuchel et al. showed that free cholesterol mobilization in vivo in response to reconstituted HDL infusion is primarily mediated by SR-BI and not

ABCA1 or ABCG1 (21). In addition, overexpression of apoAI in heterozygous LDLr KO mice can protect against atherosclerosis in the absence of macrophage ABCG1 and ABCA1 (22). Thus, SR-BI might be more important for controlling cellular cholesterol homeostasis in vivo than was initially anticipated.

In the present study, we investigated the putative synergistic effects of combined disruption of ABCA1 and SR-BI in bone marrow-derived cells and thus macrophages on lipoprotein metabolism and atherosclerosis. Our results indicate that both ABCA1 and SR-BI in macrophages have a significant protective role in foam cell formation and Western-type diet induced atherosclerotic lesion development in vivo.

Methods

For detailed methodology, please see the data supplement. Briefly, bone marrow transplantations were performed with ABCA1/SR-BI double KO mice as donors and LDLr KO mice as recipients. Plasma lipids were determined by enzymatic colorimetric assays and cytokines in serum by using the mouse Bio-Plex suspension array (Bio-Rad, Sweden). For histological analysis cryostat sections were routinely stained with oil-red-O. Peritoneal leukocytes were analyzed with a hematology cell analyzer. Atherosclerotic lesion areas in oil-red-O stained cryostat sections of the aortic root and coronary arteries and en face lesions in the aortic arch and thoracic aorta were quantified using the Leica image analysis system. Macrophage-cholesterol efflux studies were performed using bone marrow-derived macrophages (BMDM) and thioglycollate-elicited macrophages.

Results

Reduced VLDL/LDL cholesterol levels by combined deletion of ABCA1 and SR-BI in bone marrow-derived cells

To study the effects of combined macrophage ABCA1 and SR-BI deficiency on lipoprotein metabolism and atherosclerosis *in vivo,* LDLr KO recipient mice were transplanted with bone marrow from wildtype (WT), ABCA1 KO, SR-BI KO, or ABCA1/SR-BI double KO littermates. Deletion of ABCA1, SR-BI or both ABCA1 and SR-BI in bone marrow-derived cells did not affect total serum cholesterol concentrations at 8 weeks after transplantation when fed a regular chow diet (Figure 1A). Furthermore, no significant effects were observed of single ABCA1 or combined ABCA1/SR-BI deletion on the cholesterol lipoprotein distribution profile on chow diet (Figure 1B). Single SR-BI deletion resulted in 1.7-fold ($n=10$, $p<0.05$) lower HDL cholesterol levels, while VLDL and LDL cholesterol levels showed a tendency to increased values, but this failed to reach statistical significance. At 8 weeks after bone marrow transplantation the diet was switched from regular chow diet to a Western-type diet (WTD), containing 15% (w/w) total fat and 0.25% (w/w) cholesterol to induce atherosclerotic lesion development. After 10 weeks feeding WTD the effects on serum cholesterol levels and the lipoprotein-distribution profiles were analysed. The diet switch induced a large increase in serum cholesterol concentrations to 1856±111 mg/dL in the WT ($n=12$) and 1722±84 mg/dL in SR-BI KO ($n=9$) transplanted LDLr KO mice. In agreement with our previous studies (4,13), deletion of ABCA1 in bone marrow-derived cells resulted in lower serum cholesterol levels upon challenge with WTD (1429±78 mg/dL, $n=8$, $p<0.01$). Interestingly, more dramatically lower serum cholesterol levels were found in the ABCA1/SR-BI double KO transplanted animals upon challenge with WTD (812±84 mg/dL, $n=11$, $p<0.001$ as compared to WT transplanted animals) (Figure 1C). In the WT and SR-BI KO transplanted groups the increase in serum cholesterol was mainly due to increased VLDL and LDL levels (Figure 1D). Also in the mice reconstituted with ABCA1 KO bone marrow a clear increase in

VLDL and LDL levels was observed, although to a lower extent as compared to the mice transplanted with WT or SR-BI KO bone marrow. The increase in VLDL and LDL in the ABCA1/SR-BI double KO transplanted animals, however, was largely attenuated as compared to the other 3 groups (Figure 1D).

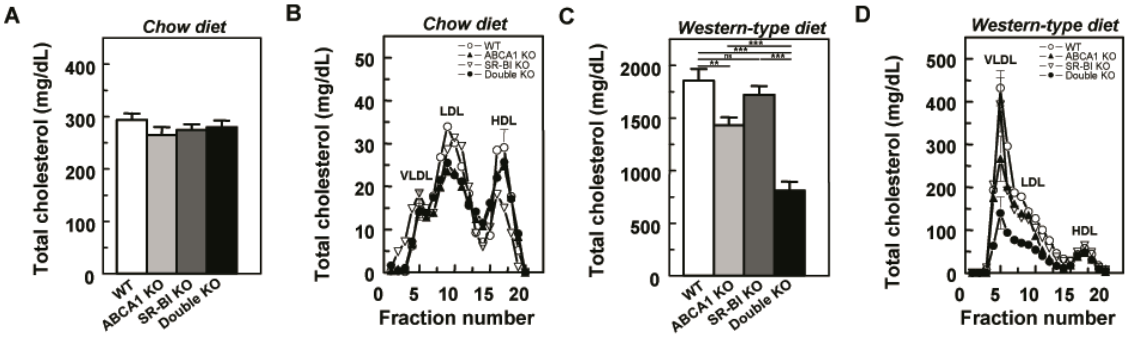

Figure 1. **Total serum cholesterol levels and lipoprotein cholesterol distribution profile in LDLr KO mice reconstituted with WT, ABCA1 KO, SR-BI KO and ABCA1/SR-BI double KO bone marrow at 8 weeks after transplantation (chow) and at 18 weeks after transplantation (Western-type diet).**

Total serum cholesterol concentrations on chow (**A**) and on Western-type diet (**C**) of LDLr KO mice transplanted with WT (open bars), ABCA1 KO (grey bars), SR-BI KO (dark grey bars), and ABCA1/SR-BI double KO (black bars) bone marrow. Lipoprotein distribution of total cholesterol of WT (○), ABCA1 KO (▲), SR-BI KO (Δ), and ABCA1/SR-BI double KO (●) reconstituted mice on chow (**B**) and Western-type diet (**D**). Values are means±SEM (n=8-12). Statistically significant difference **p<0.01, ***p<0.001.

To investigate the effects of combined deletion of ABCA1 and SR-BI in bone marrow-derived cells on cholesterol homeostasis, food intake and cholesterol absorption by the animals was analysed at 16 weeks post-transplant after 8 weeks WTD feeding. Food intake was reduced by 15% ($p<0.01$) in ABCA1/SR-BI double KO transplanted animals (2.16±0.13 g/day, n=6) as compared to WT transplanted mice (2.55±0.28 g/day, n=6). Moreover, the intestinal cholesterol absorption was mildly reduced by 27% ($p<0.05$, n=4) in ABCA1/SR-BI double KO transplanted animals as compared to controls, while triglyceride absorption was reduced by 43% ($p<0.05$, n=4). In addition, we tested whether combined ABCA1 and SR-BI deletion in bone marrow-derived cells affected VLDL synthesis by in vivo inactivation of lipolysis using Triton WR1339. The VLDL production rate was significantly lower in mice lacking ABCA1 and SR-BI in bone marrow-derived cells (1,814 ± 228 µg/mL/h, n=3) as compared to control transplanted animals (3,337 ± 570 µg/mL/h, n=3, $p<0.01$). In addition, a 1.8-fold reduction in hepatic HMGCoA reductase mRNA expression from 0.30±0.5 in WT to 0.17±0.2 in ABCA1/SR-BI double knockout transplanted animals (n=4, $p<0.05$) was observed. Hepatic lipase mRNA expression in the liver was not affected (data not shown). In summary, reduced food intake, impaired intestinal lipid absorption, and reduced VLDL production by the liver will have contributed to the observed reduction in serum cholesterol levels in de ABCA1/SR-BI double KO transplanted animals.

Enhanced atherosclerotic lesion development in the aortic root upon combined deletion of ABCA1 and SR-BI in bone marrow-derived cells

Atherosclerotic lesion development was analyzed in cryostat sections of the aortic root after 10 weeks WTD feeding (18 weeks post-transplant). As anticipated, deletion of ABCA1 and/or SR-BI in bone marrow-derived cells resulted in total erasure of the respective proteins in the lesions of the transplanted mice (Figure 2A). Selective disruption of either ABCA1 or SR-BI in bone marrow-derived cells induced a 1.4–fold ($p<0.001$) and

1.5–fold ($p<0.001$) increase in the mean atherosclerotic lesion size as compared to WT transplanted animals, respectively (Figure 2B). Thus, as previously demonstrated, both leukocyte ABCA1 (4,5) and SR-BI (16-18) have an important role in the protection against

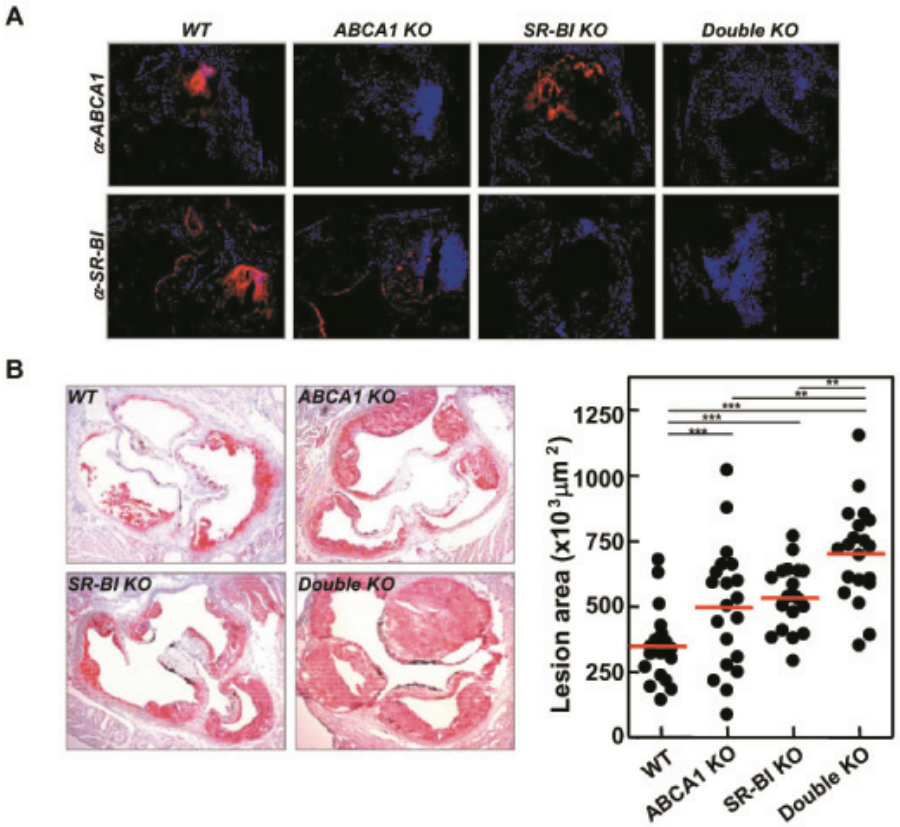

Figure 2. **Atherosclerotic lesion development in the aortic root of LDLr KO mice reconstituted with WT, ABCA1 KO, SR-BI KO, and ABCA1/SR-BI double KO bone marrow.**
(**A**) Expression of ABCA1 and SR-BI was immunofluorescently detected (red) in the aortic roots of WT, ABCA1 KO, SR-BI KO, or ABCA1/SR-BI double KO transplanted LDLr KO mice at 18 weeks post transplantation including a 10-week Western-type diet-feeding period. Nuclei were stained with DAPI (blue). Original magnification 10x10. (**B**) Photomicrographs showing representative oil-red-O stained sections (original magnification 10x5) and mean atherosclerotic lesion size in the aortic roots of mice, transplanted with WT (n=20), ABCA1 (n=20), SR-BI KO (n=20), or ABCA1/SR-BI double knockout (n=21) bone marrow. Each symbol represents the mean lesion area in a single mouse. The horizontal line represents the mean of the group (WT: $348\pm30*10^3$ µm^2; ABCA1 KO: $496\pm53*10^3$ µm^2; SR-BI KO $533\pm27*10^3$ µm^2; Double KO: $693\pm41*10^3$ µm^2). Statistically significant difference **p<0.01, ***p<0.001.

atherosclerosis. Combined deletion of ABCA1 and SR-BI in bone marrow-derived cells resulted in a more dramatic 2.0-fold ($p<0.001$) increase in the mean atherosclerotic lesion area compared to WT (Figure 2B). In addition, the lesion size in the ABCA1/SR-BI double KO transplanted animals was also significantly larger as compared to mice transplanted with single ABCA1 KO or SR-BI KO bone marrow (1.4-fold and 1.3-fold, respectively, $p<0.01$). Morphometric analysis of the composition of the lesions showed that the macrophage content of the lesions of LDLr KO mice transplanted with ABCA1/SR-BI double KO bone marrow [31±4%, n=9] was significantly reduced as compared to WT, single ABCA1 KO, and single SR-BI KO transplanted animals (46±6% [n=11$p<0.05$], 41±4% [n=8, $p<0.01$], and 49±5% [n=8, $p<0.01$], respectively). In addition, a significant increase in the necrotic core content of lesions of ABCA1/SR-BI double KO transplanted animals [21±2%, n=9] was observed as compared to WT, single ABCA1 KO, and single

SR-BI KO transplanted animals (8±2% [n=10, $p<0.01$], 15±3% [n=8, $p<0.05$], and 10±2% [n=8, $p<0.05$], respectively). No effect was observed on the collagen content of the lesions. The decreased macrophage content and increased necrotic area in atherosclerotic lesions of the ABCA1/SR-BI double KO transplanted animals are consistent with the presence of more advanced lesions.

In addition to the aortic root, lesion development was also determined in the aortic arch, thoracic aorta, and right coronary artery after 10 weeks WTD feeding (Supplementary Figure I). In WT and SR-BI KO transplanted mice 4.0±0.2% and 4.6±1.0%, respectively of the aortic arch was covered with lesion. Single deletion of ABCA1 and combined deletion of ABCA1 and SR-BI in bone marrow-derived induced a similar 2.3-fold increase ($p<0.01$) in the vessel area covered by lesion. In the thoracic aorta only 1.4±0.2% of the vessel was covered with lesion in WT transplanted mice. Deletion of SR-BI in bone marrow-derived cells resulted in a 3.5-fold decrease ($p<0.05$) in the area covered by lesion. These findings are in agreement with our earlier published studies showing that SR-BI in bone marrow-derived cells induces early lesion development, does not affect intermediate lesions, and protects against the development of advanced lesions (15). Also in the thoracic aorta no additional induction of lesion development was observed upon combined deletion of ABCA1 and SR-BI as compared to single deletion of ABCA1 (2.9±0.7% and 3.2±0.5%, respectively). The lesion size in the coronary artery was $3.6\pm0.3\times10^3$ μm^2 and $3.6\pm0.4\times10^3$ μm^2 in mice transplanted with WT and SR-BI KO bone marrow, respectively after 10 weeks WTD feeding. Deletion of ABCA1 induced a 2.2-fold increase in coronary artery lesion size to $8.0\pm1.6\times10^3$ μm^2 ($p<0.05$), while lesions in ABCA1/SR-BI dKO transplanted animals were $9.0\pm1.5\times10^3$ μm^2 ($p<0.05$).

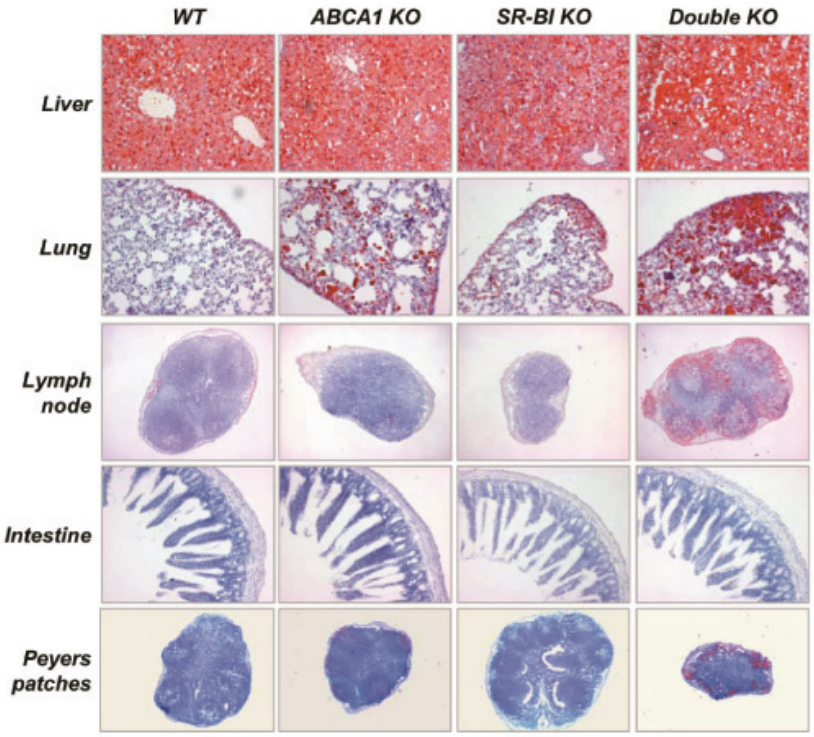

Figure 3. **Effect of combined deletion of ABCA1 and SR-BI in bone marrow-derived cells in LDLr KO mice on lipid accumulation in liver, lung, lymph node, small intestine, and Peyer's patches.**

At 18 weeks post transplant, including 10 weeks Western-type diet feeding, indicated organs were isolated from LDLr KO mice transplanted with WT, ABCA1 KO, SR-BI KO, and ABCA1/SR-BI double KO bone marrow. Cryostat sections were stained with oil-red-O to visualize lipid accumulation. Original magnification 5x10.

Massive foam cell formation in spleen and peritoneum by combined deletion of ABCA1 and SR-BI in bone marrow-derived cells

To assess potential morphological changes associated with combined ABCA1 and SR-BI deficiency in bone marrow-derived cells outside the vasculature, a necropsy of the transplanted mice was performed. Due to the WTD feeding period, massive lipid accumulation was induced in livers of the transplanted animals (Figure 3). However, quantitative lipid analysis revealed no differences in lipid accumulation in the livers of the different groups of transplanted mice (data not shown). Microscopically no heavily lipid-laden foam cells were evident in the liver. Furthermore, no foam cells were found in the lamina propria of the intestines, the largest reservoir of macrophages in the body, of either of the transplanted groups. The Peyer's patches, lungs, and lymph nodes of the ABCA1/SR-BI double knockout transplanted mice showed slightly enhanced lipid accumulation (Figure 3). Most striking differences, however, were observed on spleen morphology. No significant effect of leukocyte SR-BI deficiency was observed on spleen weight (3.7±0.4 mg/g bodyweight [n=9] as compared to 3.8±0.3 mg/g [n=9] for WT transplanted mice, $p>0.05$). ABCA1 and combined deletion of ABCA1 and SR-BI, however, induced a 1.6-fold (6.0±0.9 mg/g, n=9, $p<0.05$) and a 4.5-fold (17.1±3.1 mg/g, n=9, $p<0.001$) increase in

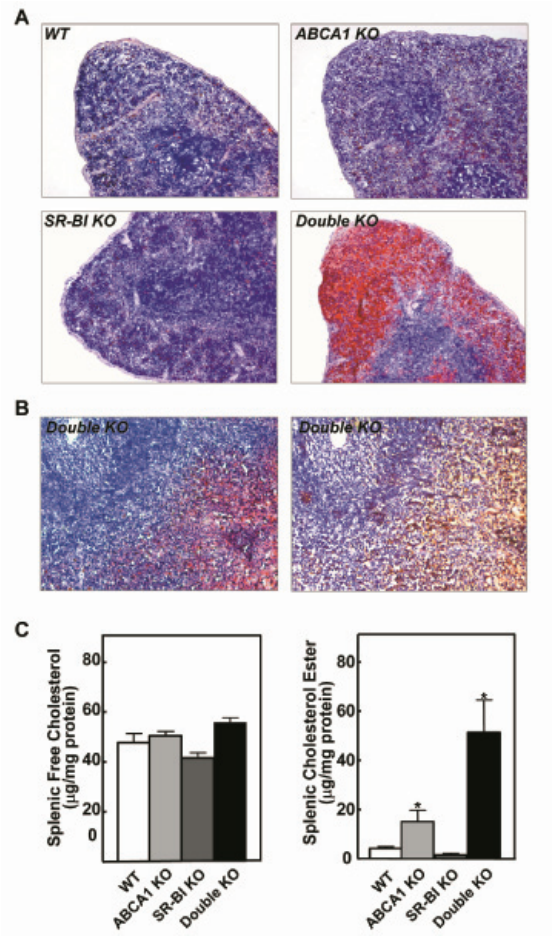

Figure 4. **Massive lipid accumulation in the red pulp of spleens of LDLr KO mice transplanted with ABCA1/SR-BI double KO bone marrow.**

At 18 weeks post transplant, including 10 weeks Western-type diet feeding, spleens were isolated from LDLr KO mice transplanted with WT, ABCA1 KO, SR-BI KO, and ABCA1/SR-BI double KO bone marrow. (**A**) Cryostat sections were stained with oil-red-O to visualize lipid accumulation. Original magnification 5x10. (**B**) Co-localization of oil-red-O (left) and the macrophage marker F4/80 (right) in spleen sections of ABCA1/SR-BI double KO transplanted mice. Original magnification 20x10. (**C**) Quantification of free and cholesterol ester content of spleens of WT (open bars), ABCA1 KO (grey bars), SR-BI KO (dark grey bars), and ABCA1/SR-BI double KO (black bars) transplanted mice. Values are means±SEM (n=5). Statistically significant difference *$p<0.05$.

spleen weight, respectively. Analysis of oil-red-O stained sections of the spleen indicated that WT and SR-BI knockout transplanted animals displayed only a few lipid-laden cells in the spleen (Figure 4A). Deletion of ABCA1 in bone marrow-derived cells resulted in slightly enhanced accumulation of lipid-laden cells. However, spleens of the mice

transplanted with ABCA1/SR-BI double KO bone marrow displayed massive lipid loading. The lipid loading was especially evident in the red pulp of the spleen, constituting the reticulo-endothelial system of the spleen, where it co-localized with macrophages (Figure 4B). Analyses of the lipid content of the spleens showed no significant effect of combined ABCA1 and SR-BI deletion in bone marrow on phospholipid, triglyceride, and free cholesterol concentrations. However, substantial effects were observed on cholesteryl ester accumulation. Single ABCA1 deletion induced a 3.7-fold (n=5, $p<0.05$) increase in the cholesteryl ester content of the spleen as compared to WT transplanted animals, while single SR-BI deficiency in bone marrow resulted in 3-fold (n=5) lower splenic cholesteryl ester levels, which failed to reach statistical significance (Figure 4C). Combined deletion of bone marrow ABCA1 and SR-BI, however, induced a dramatic 12.5-fold (n=5, $p<0.05$) increase in cholesteryl ester accumulation in spleens.

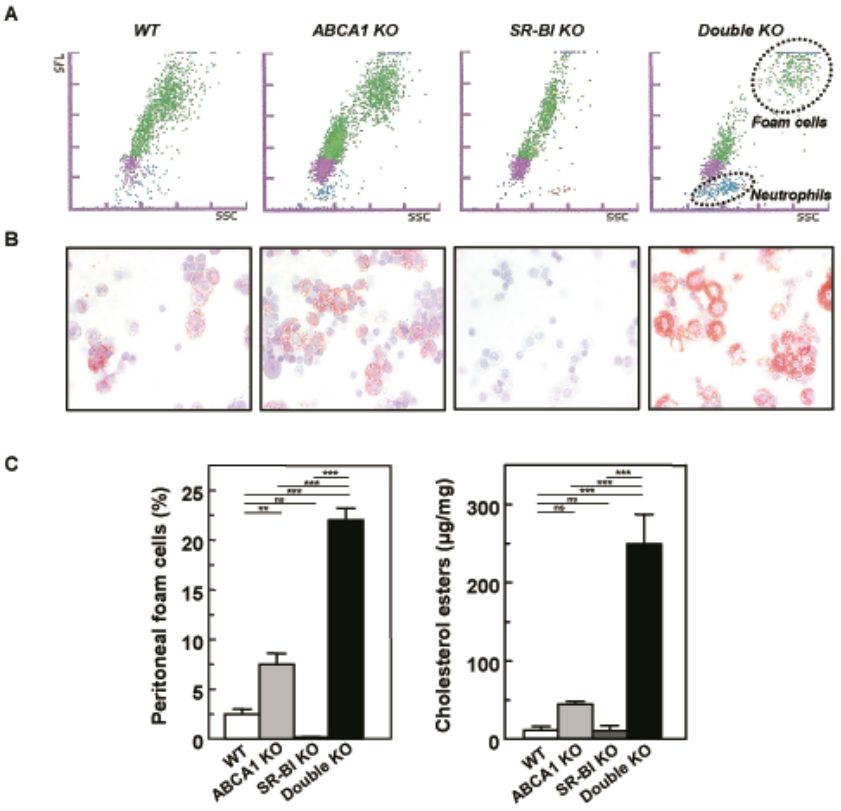

Figure 5. **Identification of heavily lipid-laden macrophage foam cells in peritoneal cavity of LDLr KO mice transplanted with ABCA1/SR-BI double KO bone marrow.**

At 18 weeks post transplant, including 10 weeks Western-type diet feeding, the peritoneal cavity of the LDLr KO mice transplanted with WT (open bar), ABCA1 KO (grey bar), SR-BI KO (dark grey bar), and ABCA1/SR-BI double KO (black bar) bone marrow was lavaged, and the collected peritoneal leukocytes were analyzed using an automated Veterinary Hematology analyzer. (**A**) Scattergrams of peritoneal leukocytes isolated from LDLr KO mice reconstituted with WT, ABCA1 KO, SR-BI KO, or ABCA1/SR-BI double KO bone marrow. Side scattered light (SSC), indicating the complexity of the cells, is plotted against side fluorescent light (SFL), determining the nucleic acid content of the cells. (**B**) Photomicrographs of cytospins of peritoneal cells of the corresponding animals after oil-red-O lipid staining. Original magnification 40x10. (**C**) Quantification of the number of macrophage foam cells as percentage of the total amount of isolated cells by gating of the cells in the upper right hand corner of panel A (left, n=8-12 per group) and quantification of the cholesterol ester content of the cells (right, n=4 per group). Note the massive lipid-accumulation in peritoneal leukocytes of LDLr KO mice transplanted with ABCA1/SR-BI double KO bone marrow. Values are means±SEM. Statistically significant difference **$p<0.01$, ***$p<0.001$, and ns for non-significant.

Interestingly, in addition to the observed increase in spleen size also more lipid-laden macrophages were present in the peritoneum of mice reconstituted with ABCA1/SR-BI double KO bone marrow (22±1.2%, n=11, $p<0.001$), compared to the WT reconstituted animals (2.5±0.5%, n=12) (Figure 5). In the peritoneum also increased numbers lipid-laden cells were observed in single ABCA1 KO transplanted animals (7.5±1.1%, n=8, $p<0.01$), but the effect was less severe as compared to combined deletion of ABCA1 and SR-BI. In addition, a tendency to reduced lipid-loading was observed in peritoneal macrophages from mice reconstituted with SR-BI KO bone marrow (0.2±0.04%, n=9, $p>0.05$), in line with the dual function of SR-BI in macrophage foam cell formation and atherosclerotic lesion development (15). Quantitative analysis of the lipid content of the peritoneal leukocytes confirmed that combined deletion of ABCA1 and SR-BI resulted in a highly significant ($p<0.001$) increase in cholesterol ester accumulation in peritoneal macrophages as compared to single deletion of ABCA1 (WT: 11±5 (n=4), SR-BI KO:10±7 (n=4), ABCA1 KO:44±4 (n=4), ABCA1/SR-BI dKO:249±38 μg/mg (n=4)).

Combined deletion of ABCA1 and SR-BI leads to reduced cholesterol efflux capacity from macrophages to both apoAI and HDL

To get more insight in the mechanism behind the massive lipid accumulation in peritoneal leukocytes and macrophages of the spleen, in vitro cholesterol efflux experiments were performed (Figure 6A). As previously shown (15), macrophage SR-BI deficiency resulted in 24% (n=8, $p<0.01$) lower cholesterol efflux to HDL. Combined deletion of ABCA1 and SR-BI resulted in a similar 20% (n=8, $p<0.05$) decrease in cholesterol efflux to HDL. In addition, macrophages lacking both ABCA1 and SR-BI showed an almost complete absence of apoAI-induced cholesterol efflux, similar to ABCA1-deficient macrophages. To exclude that the observed effects on cholesterol efflux might be the consequence of down-regulation of ABCG1, the expression of the major cholesterol transporters was analysed by Western blotting (Figure 6B). As expected, in cells from ABCA1 deficient mice ABCA1 was absent, while cells from the SR-BI knockout mice lacked SR-BI expression. ABCG1 expression was similarly upregulated in all 3 groups as compared to WT macrophages, indicating that differences in HDL cholesterol efflux were not due differences in ABCG1 expression.

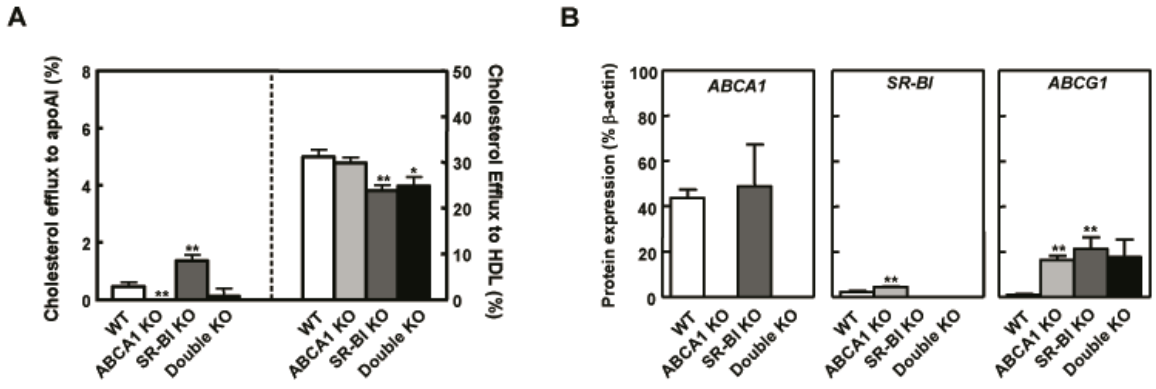

Figure 6. **Impaired cholesterol efflux from macrophages lacking ABCA1 and SR-BI.** (**A**) Cellular cholesterol efflux to apoAI (10 μg/mL) and HDL (50 μg/mL) from in vivo ^{3}H-cholesterol-labeled peritoneal macrophages. (**B**) Quantification of ABCA1, SR-BI, and ABCG1 protein expression in the peritoneal macrophages by Western blotting. Values are means±SEM (n=3-4). Statistically significant difference of *$p<0.05$ and **$p<0.01$.

Cholesterol efflux experiments were also performed using macrophages laden with acetylated LDL. Under these conditions, however, no additional effect of combined deletion of ABCA1 and SR-BI over single deletion of ABCA1 was observed on cholesterol mass and ^{3}H-label efflux due to absence of SR-BI expression in all groups examined (Supplementary Figure II).

Increased inflammation by combined deletion of ABCA1 and SR-BI in bone marrow-derived cells

Studies in patients with Tangier disease have suggested a dual function for ABCA1 in both lipid metabolism and inflammation (23). Furthermore, we have shown that disruption of ABCA1 in bone marrow-derived cells results in an enhanced recruitment of leukocytes into peripheral tissues (4). In agreement with our earlier data, ABCA1-deficiency in bone marrow-derived cells resulted in a 2-fold ($p<0.01$) increase in the number of resident leukocytes in the peritoneal cavity ($6.17\pm0.96*10^6$ cells [n=8] as compared to $3.15\pm0.33*10^6$ cells [n=12] for WT transplanted animals, Figure 7). No effect of single SR-BI deficiency was observed on peritoneal leukocyte counts ($2.69\pm0.21*10^6$ cells). Interestingly, combined deletion of ABCA1 and SR-BI in bone marrow-derived cells resulted in a more dramatic increase in peritoneal leukocyte accumulation ($8.79\pm0.71*10^6$ cells; n=11, $p<0.001$ as compared to WT and SR-BI KO transplanted animals and $p<0.01$ as compared to ABCA1 KO reconstituted mice). As indicated in Figure 7, the increased peritoneal leukocyte counts in the single ABCA1 KO reconstituted animals were the result of a 1.6-fold increase (n=8, $p<0.05$) in macrophage counts and a 3.2-fold increase (n=8, $p<0.01$) in lymphocytes. In the ABCA1/SR-BI double KO transplanted animals a similar increase in macrophage counts was observed. The lymphocyte counts, however, were more dramatically increased (5.4-fold, n=11, $p<0.001$).

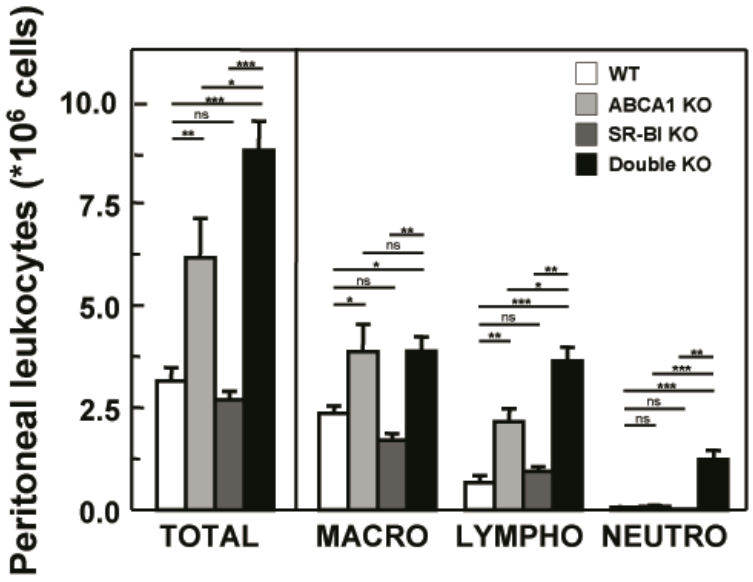

Figure 7. Enhanced leukocyte accumulation in the peritoneal cavity of LDLr KO mice transplanted with ABCA1/SR-BI double KO bone marrow.

At 18 weeks post transplant including 10 weeks Western-type diet feeding, the peritoneal cavity of the LDLr KO mice transplanted with WT (open bar), ABCA1 KO (grey bar), SR-BI KO (dark grey bar), and ABCA1/SR-BI double KO (black bar) bone marrow was lavaged, and the collected peritoneal leukocytes were analyzed using an automated Sysmex XT-2000iV Veterinary Hematology analyzer for total cell (TOTAL), macrophage (MACRO), lymphocyte (LYMPHO), and neutrophil (NEUTRO) counts. Values are means±SEM (n=8-12). Statistically significant difference *$p<0.05$, **$p<0.01$, ***$p<0.001$, and ns for non-significant.

In addition, a striking accumulation of neutrophilic granulocytes was observed in the peritoneal cavity, accounting for 20% of the increase in the peritoneal leukocyte count in mice transplanted with ABCA1/SR-BI double KO bone marrow. Combined deletion of ABCA1 and SR-BI did not affect the peripheral WBC counts ($5.6\pm0.6*10^9$ cells/L, n=12 as compared to $5.8\pm0.8*10^9$ cells/L, n=11 for WT transplanted animals), nor the percentile composition of the blood cells (data not shown). The increased neutrophil counts in the peritoneal cavity were thus primarily the result of increased recruitment of neutrophils. Since no thioglycollate or other additional trigger was used to elicit the recruitment of neutrophils, an endogenous trigger inside the peritoneal cavity most likely has caused the recruitment of the cells. It is interesting to speculate that this is the consequence of the extensive foam cell accumulation inside the peritoneal cavity. Next, live neutrophils inside the lesions were visualized using a naphthol AS-D chloroacetate esterase activity kit. Surprisingly, based on this esterase activity assay no significantly higher neutrophil counts were observed within the atherosclerotic lesions of ABCA1/SR-BI double KO transplanted mice (49±15 [n=8] versus 39±6 for WT transplanted mice [n=10], p=0.51) or in the adventitia surrounding the lesion (134±18 [n=8] versus 93±14 [n=10] for WT transplanted mice, p=0.08). In addition to the esterase activity assay, an immunohistochemical staining for the neutrophil specific marker Ly-6G was performed. Interestingly, using this staining we did find a highly significant increase in the Ly-6G positive area of lesions of ABCA1/SR-BI double KO (5.2±0.8% [n=5], p<0.0001) versus WT (0.2±0.04% [n=5]) transplanted animals. Ly-6G staining was primarily localized in acellular regions of the corners of the necrotic areas of the lesions, indicating the increased presence of residues of neutrophils that had infiltrated the lesion.

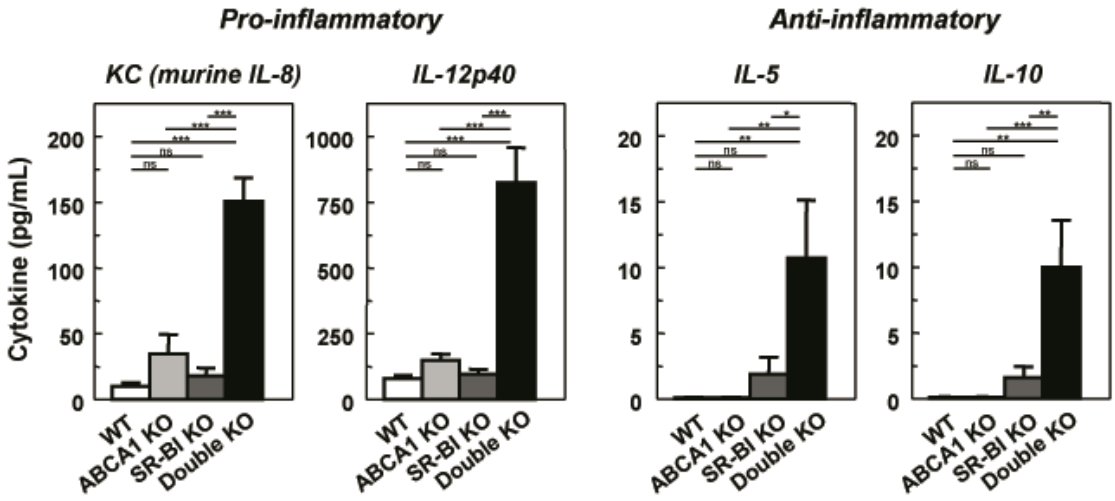

Figure 8. **Increased circulating cytokine levels in LDLr KO mice transplanted with ABCA1/SR-BI double KO bone marrow.**

Serum from the transplanted LDLr KO mice was collected at 18 weeks after transplantation including 10 weeks Western-type diet feeding. A Bio-Plex suspension array was used to measure 8 different cytokines, including IL-1β, IL-5, IL-6, KC (murine IL-8), IL-10, IL-12, TNF-α, and RANTES. The concentrations of IL-5, KC (murine IL-8), IL-10, and IL-12 in WT (open bars), ABCA1 KO (grey bars), SR-BI KO (dark grey bars) and ABCA1/SR-BI double KO (black bars) transplanted mice are shown. No significant differences were observed in the concentrations of IL-1β, IL-6, TNF-α, or RANTES between the four groups of mice. Values are means±SEM (n=5-10). Statistically significant difference *p<0.05, **p<0.01, ***p<0.001, and ns for non-significant.

An inflammatory response involves a complex set of events that, in addition to rearrangements of innate immune cell populations, include changes in the cytokine

profiles. Therefore, also the serum cytokine levels were examined in the different groups of transplanted animals using a Bio-Plex suspension array. On chow diet, no effect on cytokine levels was observed (data not shown). After 4 weeks WTD feeding, however, a significant 1.8-fold increase (n=6, $p<0.01$) in the pro-inflammatory cytokine KC (murine ortholog of IL-8) was observed in mice reconstituted with ABCA1/SR-BI double KO bone marrow, while no significant effect was observed on the other cytokines tested (IL-1β, IL-6, IL-5, IL-10, IL-12, TNF-α, or RANTES). After 10 weeks WTD feeding, an even more dramatic 17-fold (n=5, $p<0.001$) increase in KC levels was observed in the ABCA1/SR-BI double KO transplanted animals, while under these conditions also IL-12p40 levels were highly increased (11-fold, n=5, $p<0.001$). (Figure 8). In addition, an increase in the anti-inflammatory cytokines IL-5 and IL-10 was observed in the ABCA1/SR-BI double KO reconstituted animals. The levels of the anti-inflammatory cytokines, however, remained substantially lower as compared to the pro-inflammatory cytokines (7.2±3.7 and 10.0±3.7 pg/ml for IL-5 and IL-10 as compared to 139±16 pg/ml and 858±192 pg/ml for KC and IL-12p40, respectively). The effects on the cytokine levels thus increase with a prolonged duration of the WTD feeding period.

No increased foam cell formation and atherosclerosis in the aortic root as a result of combined deletion of ABCA1 and SR-BI in bone marrow-derived cells in LDL receptor knockout mice on chow diet.

To investigate if the WTD-induced increase in pro-inflammatory cytokines is required to induce massive foam cell formation and promote atherosclerotic lesion development in the aortic root upon combined disruption of ABCA1 and SR-BI in bone marrow-derived cells of LDLr KO mice, a bone marrow transplantation experiment was performed and atherosclerotic lesion development was analysed at 14 and 20 weeks after transplantation while maintaining the mice on regular chow diet. At 14 weeks, WT transplanted animals developed small foam cell-rich lesions with an average size of $85\pm8x10^3$ μm^2 (n=11). Consistent with our previously published pro-atherogenic role of SR-BI in small foam cell-rich lesions, disruption of SR-BI in bone marrow-derived cells in LDLr KO mice on chow diet resulted in slightly smaller atherosclerotic lesions ($62\pm7x10^3$ μm^2, n=12, $p<0.05$). Deletion of ABCA1 led to a significant 1.5-fold increase in lesion size ($127\pm18x10^3$ μm^2, n= 11, $p<0.05$). In contrast to the result obtained in mice fed WTD, no added effect of combined deletion of ABCA1 and SR-BI in bone marrow-derived cells was found in LDLr KO mice on chow ($140\pm22x10^3$ μm^2, n=11) as compared to single deletion of ABCA1. Also at 20 weeks after transplantation no added effect of combined ABCA1 and SR-BI deletion was found on chow as compared to single deletion of ABCA1 (data not shown).

Under chow conditions, also similarly increased foam cell accumulation was observed in the peritoneal cavity of ABCA1 KO and ABCA1/SR-BI dKO transplanted animals (1.1±0.11% [n=11] and 1.3±0.22% [n=10], respectively, as compared to 0.15±0.02% [$p<0.001$, n=11] and 0.25±0.07% [n=11, $p<0.001$] for WT and SR-BI knockout transplanted mice. Foam cell counts, however, were much less as compared to the levels in transplanted animals challenged with WTD. No effect on total peritoneal leukocyte counts was observed (data not shown) and neutrophil counts remained low (~5% in all groups). Furthermore, no lipid accumulation was observed in the spleens nor a change in spleen size was observed of ABCA1/SR-BI dKO transplanted animals. The WTD challenge is thus essential to induce the enhanced foam cell formation, atherosclerotic lesion development, and inflammation in LDLr KO mice upon combined deletion of ABCA1 and SR-BI in bone marrow-derived cells.

Discussion

In the current study we show that specific disruption of both ABCA1 and SR-BI in bone marrow-derived cells of LDLr KO mice led to an added increase in atherosclerotic lesion development in the aortic root upon challenge with WTD, compared to single ABCA1 KO or SR-BI KO reconstituted LDLr KO mice, despite lower serum cholesterol levels. Massive lipid accumulation was found in peritoneal macrophages as well as macrophages in the red pulp of the spleens of LDLr KO animals reconstituted with ABCA1/SR-BI double KO bone marrow. Furthermore, in addition to the lipid parameters a significant increase in inflammation markers was noticed in the ABCA1/SR-BI double KO transplanted mice on WTD, which is expected to have contributed to the observed dramatic increase in lesion development. In line, no enhanced foam cell formation and atherosclerotic lesion development was observed upon combined deletion of ABCA1 and SR-BI as compared to single deletion of ABCA1 in bone marrow-derived cells in LDLr KO mice fed regular chow diet that did not show enhanced inflammatory markers. Important to note is that this might also be the consequence of the less advanced stage of lesion development in the animals on chow. Furthermore, the site examined for atherosclerosis determines the outcome, as no additional effect of combined deletion of ABCA1/SR-BI over single ABCA1 deletion was observed in less advanced lesions in the aortic arch, thoracic aorta, and coronary arteries of LDLr KO mice challenged with WTD.

The massive lipid accumulation in peritoneal leukocytes and the red pulp of spleens upon combined deletion of ABCA1 and SR-BI in LDLr KO mice on WTD highlights the pivotal role of these transporters in cellular lipid homeostasis in vivo under high dietary lipid conditions. Furthermore, it is interesting to speculate that the presence of ABCG1 is not sufficient to compensate for the absence of these two cholesterol transporters under these conditions. ABCA1 stimulates the active transport of both cholesterol and phospholipids from the cell to lipid-poor apoAI, but only little to mature HDL (2). SR-BI and ABCG1 on the other hand require a phospholipid-containing acceptor, like mature HDL, to induce cholesterol efflux (2). In vitro studies showed that the transfer of lipids to apoAI mediated by ABCA1 activity is sufficient to generate an efficient acceptor for ABCG1-mediated cholesterol efflux (24,25). ABCA1 and ABCG1 thus function sequentially in the cholesterol efflux process in which ABCA1 first lipidates apoAI thereby forming a substrate for ABCG1 mediated efflux (2). The similarity in acceptor specificity between ABCG1 and SR-BI would suggest that SR-BI also cooperatively works with ABCA1 in cholesterol export. However, recent siRNA-mediated knockdown studies using the RAW macrophage cell line suggested that the interaction of lipid-free apoAI with ABCA1 generates a particle that interacts with ABCG1, but not with SR-BI (26). The observed massive in vivo lipid loading in peritoneal leukocytes and spleens as well as the increased atherosclerotic lesion development in the aortic root of ABCA1/SR-BI double knockout transplanted animals on WTD, however, indicate that combined deletion of ABCA1 and SR-BI in bone marrow-derived cells does have an added effect on foam cell formation in vivo. Cholesterol efflux studies showed that combined deletion of ABCA1 and SR-BI leads to a complete ablation of apoAI-induced cholesterol efflux, similar as observed upon single deletion of ABCA1. However, in addition, a moderate reduction in HDL cholesterol efflux could be observed. It is tempting to speculate that the increased foam cell formation observed in vivo is the result of the combined impairment of both apoAI and HDL-mediated efflux. However, since the effects observed on cholesterol efflux in vitro, were relatively small it cannot be excluded that in addition to effects on cholesterol efflux also other mechanisms contribute to the increased foam cell formation observed in the ABCA1/SR-BI double knockout transplanted animals. Remarkably, enhanced in vivo foam cell formation in the peritoneum and spleen was observed upon

combined deletion of ABCA1 and SR-BI in bone marrow-derived cells, despite the presence of ABCG1. On the other hand, in recent studies with ABCA1/ABCG1 double KO transplanted animals, we and others showed that combined deletion of ABCA1 and ABCG1 in bone marrow-derived cells also results in massive foam cell formation despite the presence of functional SR-BI (12-14). It can be anticipated that ABCG1 and SR-BI might have different roles in cholesterol homeostasis at different stages of macrophage foam cell formation. As previously shown, the role of macrophage SR-BI in atherosclerotic lesion development is dual: it accelerates early atherosclerotic development (15), while it slows down the progression of more advanced lesions (15-17). In agreement, in the current study the percentage of peritoneal macrophages with a single SR-BI deletion that are transformed into foam cells appear to be reduced. SR-BI is a multifunctional receptor capable of binding a wide array of native and modified lipoproteins as well as mediating the bidirectional flux of cholesterol. This leads to the unique function of macrophage SR-BI that it can facilitate initial lesion formation by inducing the uptake of pro-atherogenic lipoproteins by macrophages (15) and inhibit more advanced lesion formation by promoting cholesterol efflux when foam cells are heavily loaded with cholesterol.

Alternatively, SR-BI and ABCG1 might efflux cholesterol from different specific cellular compartments or functionally distinct cellular pools of cholesterol. Wang et al showed that LDL cholesterol is preferentially effluxed to HDL, whereas cholesterol from modified acetylated LDL (AcLDL) is primarily effluxed to lipid-poor apoAI in an ABCA1-dependent fashion (27). In agreement, SR-BI only mediated LDL-cholesterol efflux and not AcLDL-cholesterol efflux (28). It is currently, however, unknown if SR-BI and ABCG1 mediate efflux from distinct or similar cellular cholesterol pools. Upon combined deletion of ABCA1 and SR-BI massive foam cell formation was primarily observed in peritoneal leukocytes and macrophages of the red pulp in the spleen. Interestingly, combined deletion of ABCA1 and ABCG1 in bone marrow-derived cells of LDLr KO mice resulted not only in massive oil red O-positive lipid staining in peritoneal leukocytes and macrophages of the red pulp of the spleen, but also in other tissues rich in macrophages, including the liver, spleen, lymph nodes, lamina propria of the intestine, and Peyer's patches (12). Importantly, in contrast to ABCA1/SR-BI double knockout transplanted LDLr KO mice, ABCA1/ABCG1 transplanted animals did display foam cell accumulation in macrophage-rich organs on chow diet, although less extreme than when challenged with WTD (unpublished observation from our group). Thus, although the similarity in acceptor specificity of SR-BI and ABCG1 suggests possible redundancy of these transporters on macrophages for cholesterol efflux to HDL, apparently also the biological environment of the macrophage and possibly the availability of substrates influence their in vivo importance. Generation of ABCG1/SR-BI double knockout mice, ABCA1/ABCG1/SR-BI triple knockouts, and ABCA1/SR-BI double knockout mice, overexpressing ABCG1 is expected to shed further light on the (in)dependent roles of these cholesterol transporters in macrophage foam cell formation and atherosclerosis.

Atherosclerotic lesion development results from a combination of hyperlipidemia and an inflammatory response. In LDLr KO mice, reconstituted with ABCA1/SR-BI double knockout bone marrow, excessive atherosclerosis develops in the aortic root, despite largely reduced serum cholesterol levels. Interestingly, the pro-inflammatory cytokines KC (murine IL-8) and IL-12p40 were greatly elevated in LDLr KO mice transplanted with ABCA1/SR-BI double deficient bone marrow. Both IL-12 and IL-8 are important pro-atherogenic cytokines. Daily administration of IL-12 promotes atherosclerosis in young apoE KO mice (29), while targeted deletion of IL-12 and vaccination against IL-12 attenuates atherosclerotic lesion development in murine models of atherosclerosis (30,31). IL-8 is a powerful, independent predictor of cardiovascular

events (32). Furthermore, deletion of KC (murine IL-8) in LDLr KO mice attenuates atherosclerosis (33). Interestingly, IL-8 production is dose-dependently induced in human macrophage foam cells as a response to cholesterol loading with modified LDL, suggesting that the observed increase in KC (murine IL-8) levels are a direct effect of the massive foam cell formation in the ABCA1/SR-BI double KO transplanted animals (34,35). Excessive free cholesterol accumulation in macrophage foam cells induces cytokine secretion as a result of endoplasmic reticulum (ER) stress triggered by excess cholesterol in the ER (36). No effect of combined ABCA1/SR-BI deficiency was observed on free cholesterol loading. Therefore, it is unlikely that increased ER stress as a result of excess free cholesterol is the general cause for the increased cytokine production. Alternatively, KC (murine IL-8) secretion by macrophages could be induced as a result of increased accumulation of oxysterols, including 25-hydroxycholesterol, 7beta-hydroxycholesterol, and 7-ketocholesterol (37). KC (murine IL-8) triggers monocyte arrest on early atherosclerotic endothelium (38) and plays a central role in macrophage accumulation in established fatty streak lesions (39). Interestingly, IL-8 is also one of the most potent chemoattractants for neutrophils (40,41) and the increased levels of KC (murine IL-8) in the ABCA1/SR-BI double KO transplanted animals clearly parallel the increased accumulation of neutrophils in the peritoneal cavity. Neutrophils are short-lived phagocytic cells that serve as essential early cellular effectors of innate immunity and constitute the "first line of defense". The sequestration of neutrophils into the peritoneal cavity is thus most likely a protective response induced by the accumulation of heavily lipid-laden peritoneal macrophages in absence of both SR-BI and ABCA1. Interestingly, neutrophil activation is increased in patients with significant coronary stenosis (42) and enhanced neutrophil infiltration is observed in culprit lesions in acute coronary syndromes (43), suggesting an important role for neutrophils in atherosclerosis. In agreement, neutrophil depletion reduces atherosclerotic lesion development in apoE knockout mice (44). Although a clear increase in neutrophil accumulation was observed in the peritoneal cavity in ABCA1/SR-BI double knockout transplanted mice, within the atherosclerotic lesions and in the adventitia surrounding the lesion no significant increase in the amount of neutrophils was observed based on esterase activity. Immunohistochemical staining for the neutrophil specific marker Ly-6G did show a significant increase in the Ly-6G positive area of lesions of ABCA1/SR-BI double knockout versus WT transplanted animals. Ly-6G positive staining was primarily localized in acellular regions of the corners of the necrotic areas of the lesions, suggesting the increased presence of residues of neutrophils that had infiltrated the lesion. Necrotic core formation during lesion development can in turn elicit an inflammatory response, which could further increase the recruitment of neutrophils. Analysis of the potential contribution of neutrophils locally in the arterial wall to the excessive atherosclerotic lesion development in mice with a combined deletion of ABCA1 and SR-BI in bone marrow-derived cells forms an interesting future challenge.

In addition, to the observed increase in the pro-inflammatory cytokines KC (murine IL-8) and IL-12p40, we also observed an increase in the anti-inflammatory cytokines IL-5 and IL-10, probably as a feed-back reaction to control the inflammatory response. The absolute levels of the IL-5 and IL-10, however, remained substantially lower as compared to the KC (murine IL-8) and IL-12p40 levels, suggesting a pro-inflammatory balance. Interestingly, several lines of evidence suggest that pro- and anti-inflammatory cytokines can affect the amount of circulating lipids. Previously, we have shown that IL-10 overexpression in LDLr KO mice results in a significant reduction in plasma cholesterol levels (45). Interestingly, the ABCA1/SR-BI double KO transplanted animals with the highest IL-10 concentrations also had the lowest serum cholesterol levels. Furthermore, chronic inflammation is associated with reduced serum cholesterol levels (46). Although

the mechanism of the inflammation induced reduction in serum cholesterol levels is still largely unclear it might have contributed to the lower serum cholesterol levels observed in this study. A recent study by Lo et al. showed that disruption of the production of the potent pro-inflammatory cytokines LIGHT and lymphotoxin leading to reduced T cell numbers reduces serum cholesterol levels, which is associated with increased hepatic lipase levels (47). Combined disruption of ABCA1 and SR-BI in bone marrow-derived cells, however, did not affect T cell counts or hepatic lipase expression in the liver. In contrast, we showed that food intake, intestinal lipid absorption, and HMGCoA expression and VLDL production by the liver were reduced, all processes that are likely to have contributed to the observed reduction in serum cholesterol levels in de ABCA1/SR-BI double KO transplanted animals.

In conclusion, despite lower serum cholesterol levels, combined deletion of ABCA1 and SR-BI in bone marrow-derived cells induces massive foam cell formation and promotes inflammation and atherosclerotic lesion development in LDLr KO mice challenged with a WTD, indicating that both macrophage ABCA1 and SR-BI contribute significantly to healthy cholesterol homeostasis in the macrophage in vivo and are essential for reducing the risk for atherosclerosis.

Sources of funding

This work was supported by The Netherlands Organization of Scientific Research (grant 912-02-063 (M.P.) and VIDI grant 917.66.301 (M.V.E.)) and The Netherlands Heart Foundation (grants 2001T4101 (Y.Z.), 2003B134 (R.O.), and 2008T070 (M.H.)). M.V.E. is an Established Investigator of The Netherlands Heart Foundation (grant 2007T056).

Disclosures: None.

References

1. Ross R. Atherosclerosis-An inflammatory disease. *N Engl J Med*. 1999;340:115-126
2. Jessup W, Gelissen IC, Gaus K, Kritharides L. Roles of ATP binding cassette transporters A1 and G1, scavenger receptor BI and membrane lipid domains in cholesterol export from macrophages. *Curr Opin Lipidol.* 2006;17:247-257.
3. Van Eck M, Pennings M, Hoekstra M, Out R, Van Berkel TJ. Scavenger receptor BI and ATP-binding cassette transporter A1 in reverse cholesterol transport and atherosclerosis. *Curr Opin Lipidol.* 2005;16:307-315.
4. Van Eck M, Bos IS, Kaminski WE, Orsó E, Rothe G, Twisk J, Böttcher A, Van Amersfoort ES, Christiansen-Weber TA, Fung-Leung WP, Van Berkel TJ, Schmitz G. Leukocyte ABCA1 controls susceptibility to atherosclerosis and macrophage recruitment into tissues. *Proc Natl Acad Sci. USA*. 2002;99:6298-6303.
5. Aiello RJ, Brees D, Bourassa PA, Royer L, Lindsey S, Coskran T, Haghpassand M, Francone OL. Increased atherosclerosis in hyperlipidemic mice with inactivation of ABCA1 in macrophages. *Arterioscler Thromb Vasc Biol.* 2002;22:630-637.
6. Van Eck M, Singaraja RR, Ye D, Hildebrand RB, James ER, Hayden MR, Van Berkel TJ. Macrophage ATP-binding cassette transporter A1 overexpression inhibits atherosclerotic lesion progression in low-density lipoprotein receptor knockout mice. *Arterioscler Thromb Vasc Biol.* 2006;26:929-934.
7. Klucken J, Büchler C, Orsó E, Kaminski WE, Porsch-Ozcürümez M, Liebisch G, Kapinsky M, Diederich W, Drobnik W, Dean M, Allikmets R, Schmitz G. ABCG1 (ABC8), the human homolog of the Drosophila white gene, is a regulator of macrophage cholesterol and phospholipid transport. *Proc Natl Acad Sci USA*. 2000;97:817-822.
8. Kennedy MA, Barrera GC, Nakamura K, Baldan A, Tarr P, Fishbein MC, Frank J, Francone OL, Edwards PA. ABCG1 has a critical role in mediating cholesterol efflux to HDL and preventing cellular lipid accumulation. *Cell Metab.* 2005;1:121-131.
9. Out R, Hoekstra M, Hildebrand RB, Kruit JK, Meurs I, Li Z, Kuipers F, Van Berkel TJ, Van Eck M. Macrophage ABCG1 deletion disrupts lipid homeostasis in alveolar macrophages and moderately

influences atherosclerotic lesion development in LDL receptor-deficient mice. *Arterioscler Thromb Vasc Biol.* 2006;26:2295-2300.

10. Baldan A, Pei L, Lee R, Tarr P, Tangirala RK, Weinstein MM, Frank J, Li AC, Tontonoz P, Edwards PA. Impaired development of atherosclerosis in hyperlipidemic Ldlr-/- and ApoE-/- mice transplanted with Abcg1-/- bone marrow. *Arterioscler Thromb Vasc Biol.* 2006;26:2301-2307.
11. Ranalletta M, Wang N, Han S, Yvan-Charvet L, Welch C, Tall AR. Decreased atherosclerosis in low-density lipoprotein receptor knockout mice transplanted with Abcg1-/- bone marrow. *Arterioscler Thromb Vasc Biol*. 2006;26:2308-2315.
12. Out R, Hoekstra M, Habets K, Meurs I, de Waard V, Hildebrand RB, Wang Y, Chimini G, Kuiper J, Van Berkel TJ, Van Eck M. Combined deletion of macrophage ABCA1 and ABCG1 leads to massive lipid accumulation in tissue macrophages and distinct atherosclerosis at relatively low plasma cholesterol levels. *Arterioscler Thromb Vasc Biol.* 2008;28:258-264.
13. Out R, Jessup W, Le Goff W, Hoekstra M, Gelissen IC, Zhao Y, Kritharides L, Chimini G, Kuiper J, Chapman MJ, Huby T, Van Berkel TJ, Van Eck M. Coexistence of foam cells and hypocholesterolemia in mice lacking the ABC transporters A1 and G1. *Circ Res.* 2008;102:113-120.
14. Yvan-Charvet L, Ranalletta M, Wang N, Han S, Terasaka N, Li R, Welch C, Tall AR. Combined deficiency of ABCA1 and ABCG1 promotes foam cell accumulation and accelerates atherosclerosis in mice. *J Clin Invest.* 2007;117:3900-3908.
15. Van Eck M, Bos IS, Hildebrand RB, Van Rij BT, Van Berkel TJC. Dual role for scavenger receptor class B type I on bone marrow-derived cells in atherosclerotic lesion development. *Am J Pathol.* 2004;165:785-794.
16. Covey SD, Krieger M, Wang W, Penman M, Trigatti BL. Scavenger receptor class B type I-mediated protection against atherosclerosis in LDL receptor-negative mice involves its expression in bone marrow-derived cells. *Arterioscler Thromb Vasc Biol.* 2003;23:1589-1594.
17. Zhang W, Yancey PG, Su YR, Babaev VR, Zhang Y, Fazio S, Linton MF. Inactivation of macrophage scavenger receptor class B type I promotes atherosclerotic lesion development in apolipoprotein E-deficient mice. *Circulation.* 2003;108:2258-2263.
18. Adorni MP, Zimetti F, Billheimer JT, Wang N, Rader DJ, Phillips MC, Rothblat GH. The roles of different pathways in the release of cholesterol from macrophages. *J Lipid Res.* 2007;48:2453-2462.
19. Wang X, Collins HL, Ranalletta M, Fuki IV, Billheimer JT, Rothblat GH, Tall AR, Rader DJ. Macrophage ABCA1 and ABCG1, but not SR-BI, promote macrophage reverse cholesterol transport in vivo. *J Clin Invest.* 2007;117:2216-2224.
20. Yancey PG, Jerome WG, Yu H, Griffin EE, Cox BE, Babaev VR, Fazio S, Linton MF. Severely altered cholesterol homeostasis in macrophages lacking apoE and SR-BI. J Lipid Res. 2007;48:1140-1149.
21. Cuchel M, Lund-Katz S, Llera-Moya M, Millar JS, Chang D, Fuki I, Rothblat GH, Phillips MC, Rader DJ. Pathways by which reconstituted high-density lipoprotein mobilizes free cholesterol from whole body and from macrophages. Arterioscler Thromb Vasc Biol 2010; 30:526-532.
22. Yvan-Charvet L, Pagler T, Gautier EL, Avagyan S, Siry RL, Han S, Welch CL, Wang N, Randolph GJ, Snoeck HW, Tall AR. ATP-Binding Cassette Transporters and HDL Suppress Hematopoietic Stem Cell Proliferation. Science 2010; May 20. [Epub ahead of print]
23. Schmitz G, Kaminski WE, Porsch-Ozcurumez M, Klucken J, Orsó E, Bodzioch M, Buchler C, Drobnik W. ATP-binding cassette transporter A1 (ABCA1) in macrophages: a dual function in inflammation and lipid metabolism? *Pathobiology*. 1999;67:236-240.
24. Gelissen IC, Harris M, Rye KA, Quinn C, Brown AJ, Kockx M, Cartland S, Packianathan M, Kritharides L, Jessup W. ABCA1 and ABCG1 synergize to mediate cholesterol export to apoA-I. *Arterioscler Thromb Vasc Biol.* 2006;26:534-540.
25. Vaughan AM, Oram JF. ABCA1 and ABCG1 or ABCG4 act sequentially to remove cellular cholesterol and generate cholesterol-rich HDL. *J Lipid Res.* 2006;47:2433-2443.
26. Lorenzi I, von Eckardstein A, Radosavljevic S, Rohrer L. Lipidation of apolipoprotein A-I by ATP-binding cassette transporter (ABC) A1 generates an interaction partner for ABCG1 but not for scavenger receptor BI. *Biochim Biophys Acta.* 2008;781:306-313.
27. Wang MD, Kiss RS, Franklin V, McBride HM, Whitman SC, Marcel YL. Different cellular traffic of LDL-cholesterol and acetylated LDL-cholesterol leads to distinct reverse cholesterol transport pathways. *J Lipid Res.* 2007;48:633-645.
28. Wang MD, Franklin V, Gallant M, Marcel YL. ABCA1 and SR-BI are significant contributors to in vivo reverse cholesterol transport from macrophages. *Arterioscler. Thromb. Vasc. Biol.* 2007;27:e122. (Abstr.)
29. Lee TS, Yen HC, Pan CC, Chau LY. The role of interleukin 12 in the development of atherosclerosis in ApoE-deficient mice. *Arterioscler Thromb Vasc Biol.* 1999;19:734-742.

30. Davenport P, Tipping PG. The role of interleukin-4 and interleukin-12 in the progression of atherosclerosis in apolipoprotein E-deficient mice. *Am J Pathol*. 2003;163:1117-1125.
31. Hauer AD, Uyttenhove C, de Vos P, Stroobant V, Renauld JC, Van Berkel TJ, van Snick J, Kuiper J. Blockade of interleukin-12 function by protein vaccination attenuates atherosclerosis. *Circulation.* 2005;112:1054-1062.
32. Inoue T, Komoda H, Nonaka M, Kameda M, Uchida T, Node K. Interleukin-8 as an independent predictor of long-term clinical outcome in patients with coronary artery disease. *Int J Cardiol.* 2008;124:319-325.
33. Boisvert WA, Rose DM, Johnson KA, Fuentes ME, Lira SA, Curtiss LK, Terkeltaub RA. Up-regulated expression of the CXCR2 ligand KC/GRO-α in atherosclerotic lesions plays a central role in macrophage accumulation and lesion progression. *Am J Pathol.* 2006 ;168:1385-1395.
34. Wang N, Tabas I, Winchester R, Ravalli S, Rabbani LE, Tall A. Interleukin 8 is induced by cholesterol loading of macrophages and expressed by macrophage foam cells in human atheroma. *J Biol Chem.* 1996;271:8837-8842.
35. Terkeltaub R, Banka CL, Solan J, Santoro D, Brand K, Curtiss LK. Oxidized LDL induces monocytic cell expression of interleukin-8, a chemokine with T-lymphocyte chemotactic activity. *Arterioscler Thromb.* 1994;14:47-53.
36. Li Y, Schwabe RF, DeVries-Seimon T, Yao PM, Gerbod-Giannone MC, Tall AR, Davis RJ, Flavell R, Brenner DA, Tabas I. Free cholesterol-loaded macrophages are an abundant source of tumor necrosis factor-alpha and interleukin-6: model of NF-kappaB- and map kinase-dependent inflammation in advanced atherosclerosis. *J Biol Chem.* 2005;280:21763-21772.
37. Erridge C, Webb DJ, Spickett CM. 25-Hydroxycholesterol, 7beta-hydroxycholesterol and 7-ketocholesterol upregulate interleukin-8 expression independently of Toll-like receptor 1, 2, 4 or 6 signalling in human macrophages. *Free Radic Res*. 2007;41:260-266.
38. Huo Y, Weber C, Forlow SB, Sperandio M, Thatte J, Mack M, Jung S, Littman DR, Ley K. The chemokine KC, but not monocytes chemoattractant protein-1, triggers monocytes arrest on early atherosclerotic endothelium. *J Clin Invest.* 2001;108:1307-1314.
39. Schröder JM, Christophers E. Secretion of novel and homologous neutrophil-activating peptides by LPS-stimulated human endothelial cells. *J Immunol*. 1989;142:244-251.
40. Peveri P, Walz A, Dewald B, Baggiolini M. A novel neutrophil-activating factor produced by human mononuclear phagocytes. *J Exp Med.* 1988;167:1547-1559.
41. Molad Y, Haines KA, Anderson DC, Buyon JP, Cronstein BN. Immunocomplexes stimulate different signalling events to chemoattractants in the neutrophil and regulate L-selectin and beta 2-integrin expression differently. *Biochem J.* 1994;299:881-887.
42. Videm V, Wiseth R, Gunnes S, Madsen HO, Garred P. Multiple inflammatory markers in patients with significant coronary artery disease. *Int. J. Cardiol.* 2007;118:81-87.
43. Naruko T, Ueda M, Haze K, van der Wal AC, van der Loos CM, Itoh A, Komatsu R, Ikura Y, Ogami M, Shimada Y, Ehara S, Yoshiyama M, Takeuchi K, Yoshikawa J, Becker AE. Neutrophil infiltration of culprit lesions in acute coronary syndromes. *Circulation.* 2002;106:2894-2900.
44. Zernecke A, Bot I, Djalali-Talab Y, Shagdarsuren E, Bidzhekov K, Meiler S, Krohn R, Schober A, Sperandio M, Soehnlein O, Bornemann J, Tacke F, Biessen EA, Weber C. Protective role of CXC receptor 4/CXC ligand 12 unveils the importance of neutrophils in atherosclerosis. *Circ Res.* 2008;102:209-217.
45. Von Der Thüsen JH, Kuiper J, Fekkes ML, De Vos P, Van Berkel TJ, Biessen EA. Attenuation of atherogenesis by systemic and local adenovirus-mediated gene transfer of interleukin-10 in LDLr-/- mice. *FASEB J*. 2001;15:2730-2732.
46. Tous M, Ribas V, Escolà-Gil JC, Blanco-Vaca F, Calpe-Berdiel L, Coll B, Ferré N, Alonso-Villaverde C, Rull A, Camps J, Joven J. Manipulation of inflammation modulates hyperlipidemia in apolipoprotein E-deficient mice: a possible role for interleukin-6. *Cytokine.* 2006;34:224-232.
47. Lo JC, Wang Y, Tumanov AV, Bamji M, Yao Z, Reardon CA, Getz GS, Fu YX. Lymphotoxin beta receptor-dependent control of lipid homeostasis. *Science.* 2007;316:285-288.

Supplementary methods and figures

Detailed Methods

Mice

ABCA1 knockout (ABCA1 KO) mice were a kind gift of Dr. G. Chimini (14) and SR-BI knockout (SR-BI KO) mice were obtained from Dr. M. Krieger (21). The ABCA1 KO and SR-BI KO mice (both at least 8 generations backcrossed to the C57Bl/6 background) were cross-bred to generate double heterozygous offspring, which were subsequently intercrossed to obtain the ABCA1/SR-BI double knockout (double KO) mice, and single ABCA1 KO, SR-BI KO, and wildtype (WT) littermates. LDL receptor knock out (LDLr KO) mice were obtained from the Jackson Laboratory (Bar Habor, USA). All mice were housed in a light and temperature controlled environment. Food and water were supplied ad libitum. Mice were maintained on regular chow (RM3, Special Diet Services, Whitham, UK), or were fed a Western-type diet, containing 15% (w/w) total fat and 0.25% (w/w) cholesterol (Diet W, Special Diet Services, Whitham, UK). Drinking water was supplied with antibiotics (83 mg/L ciprofloxacin and 67 mg/L polymyxin B sulphate) and 6.5 g/L sucrose. Animal experiments were performed at the Gorlaeus laboratories of the Leiden/Amsterdam Center for Drug Research in accordance with the National Laws. All experimental protocols were approved by the Ethics Committee for Animal Experiments of Leiden University.

Bone Marrow Transplantation

Female LDLr KO mice (n=20/group), age 11 weeks, were lethally irradiated with a single dose of 9 Gy (0.19 Gy/min, 200 kV, 4 mA), 1 day before transplantation. Bone marrow was harvested by flushing the femurs and tibias from male ABCA1/SR-BI double KO mice, single ABCA1 KO littermates, single SR-BI KO littermates or non transgenic (WT) littermates. Irradiated recipients received 5 x 106 bone marrow cells by intravenous injection into the tail vein.

Assessment of Chimerism

The reconstitution of the transplanted bone marrow was determined using PCR on genomic DNA from bone marrow. The wildtype ABCA1 gene was detected using a forward primer (5'-TgggAACTCCTgCTAAAAT-3') and a reverse primer (5'-CCATgTggTgTgTAgACA-3') resulting in a 751 bp PCR-fragment. The mutant ABCA1 gene was detected using a forward primer (5'-TTTCTCATAgggTTggTCA-3') and a reverse primer (5'-TgCAATCCATCTTgTTCAAT-3') resulting in a 540 bp PCR-fragment. The wildtype and mutant SR-BI gene were detected using a forward primer (5'-gATgggACATgggACACgAAgCCATTCT-3') and a reverse primer (5'-CTgTCTCCgTCTCCTTCAggTCCTgA-3') resulting in a 1000 bp PCR-fragment for the wildtype allele and a 1500 bp PCR-fragment for the mutant allelle. Primers were obtained from Eurogentec (Liege, Belgium).

Lipid Analyses

After an overnight fasting-period, 100 µl of blood was drawn from the mice (n=10/group) by tail bleeding. Triglycerides in serum were determined using a standard enzymatic colorimetric assay (Roche Diagnostics, Mannheim, Germany). The concentrations of cholesterol in serum were determined by incubation with 0.025 U/mL cholesterol oxidase (Sigma) and 0.065 U/mL peroxidase and 15 µg/mL cholesteryl esterase (Roche Diagnostics, Mannheim, Germany) in reaction buffer (1.0 KPi buffer, pH=7.7 containing 0.01 M phenol, 1 mM 4-amino-antipyrine, 1% polyoxyethylene-9-laurylether, and 7.5% methanol). Absorbance was read at 490 nm. The distribution of cholesterol over the different lipoproteins in serum was determined by fractionation of 30 µL serum of 2 individual mice using a Superose 6 column (3.2 x 300 mm, Smart-system; Pharmacia, Uppsala, Sweden). Cholesterol content of the effluent was determined as indicated. Splenic free cholesterol, cholesterol ester and triglyceride content were determined as described above after extraction according to Bligh and Dyer (1) and dissolving the lipids in 2% Triton X-

100. Phospholipid content of the spleens was determined using a standard enzymatic colorimetric assay (Wako chemicals GmbH, Neuss, Germany).

Intestinal lipid absorption

The intestinal absorption of cholesterol and triglycerides was determined by a dual isotope ratio method 16 weeks post-transplant after 8 weeks Western-type diet feeding. Briefly, mice were fasted overnight and lipoprotein lipase activity was inhibited by intravenous injection of 500 mg/kg Triton WR1339 as a 15 g/dL solution in 0.9% NaCl (Sigma) to inhibit the clearance of chylomicrons. Subsequently, mice were dosed intragastrically with a bolus of 200µl olive oil containing 1 g/L cholesterol, 2 µCi of [14C] cholesterol (Amersham) and 2 µCi of [3H] triolein (Amersham). Blood was collected at 1,2,3, and 4h after gavage and serum was isolated for scintillation counting to determine the 14C and 3H activity. The percentage of cholesterol and triglyceride absorption was expressed as percentage of administered dose absorbed.

In vivo VLDL production

VLDL production was measured 16 weeks post-transplant after 8 weeks Western-type diet feeding. Hereto, mice were injected intravenously with 500 mg of Triton WR-1339 (Sigma) per kg body weight as described above after an overnight fast to inhibit plasma VLDL clearance. Mice were fasted throughout the experiment. Blood samples were taken at 0, 1, 2, 3, and 4 hours after Triton WR1339 injection. Plasma triglycerides were analysed enzymatically and were related to the body mass of the animals. The hepatic VLDL production rate was calculated from the slope of the curve and expressed as g/h/kg body weight.

Analysis of gene expression by Real-Time Quantitative PCR

Total RNA was extracted from livers of transplanted animals at 18 weeks post-transplant after 10 weeks Western-type diet feeding by the acid guanidium thiocyanate-phenol chloroform extraction method according to Chomczynski et al. (2). cDNA was synthesised from 0.5–1 µg of total RNA using RevertAid™ M-MuLV Reverse Transcriptase according to manufacturer's instructions. mRNA levels were quantitatively determined on an ABI Prism® 7700 Sequence Detection system (Applied Biosystems, Foster City, CA) using SYBR-green technology. PCR primers were designed using Primer Express 1.5 Software with the manufacturer's default settings (Applied Biosystems). For detection of hepatic lipase 5'-CAGCCTGGGAGCGCAC-3' and 5'-CAATCTTGTTCTTCCCGTCCA-3' were used as forward and reverse primers, respectively. mRNA expression levels are indicated relative to the average of the housekeeping genes hypoxanthine phosphoribosyltransferase (HPRT), glyceraldehyde-3-phosphate dehydrogenase (GAPDH), ribosomal protein 36B4, and 18Sr-RNA.

Histological Analysis of the Atherosclerosis

To analyze the development of atherosclerosis at the aortic root, the transplanted LDLr KO mice (n=20/group) were sacrificed at 18 weeks after bone marrow transplantation (age 29 weeks). All mice were fed the Western-type diet for 10 weeks before sacrifice. The arterial tree was perfused *in situ* with PBS and the heart was excised and stored in 3.7% neutral-buffered formalin (Formal-fixx; Shandon Scientific Ltd., UK) until use. The hearts were bisected just below the atria, and the base of the hearts plus aortic roots were taken for analysis. The hearts were then sectioned perpendicular to the axis of the aorta, starting within the heart and working in the direction of the aortic arch as described by Paigen et al. (3). Once the aortic root was identified by the appearance of aortic valve leaflets, alternate 10-µm sections were taken and mounted on gelatinized slides and stained with oil-red-O. The atherosclerotic lesion area in the sections was quantified by using a Leica image analysis system, consisting of a Leica DMRE microscope coupled to a camera and Leica QWin Imaging software (Leica Ltd., Cambridge, UK). Mean lesion area was calculated (in µm2) from 10 sections, starting at the appearance of the tricuspid valves. Cryostat sections of the aortic root were stained immunofluorescently with primary antibodies specific for murine ABCA1 (Santa Cruz, Santa Cruz, USA) or SR-BI (Abcam, Cambridge, UK) to visualize the ABCA1 and/or SR-BI expression in the lesions. Photomicrographs of sections immunofluorescently labeled for ABCA1

or SR-BI were taken using a Bio-Rad Radiance 2100 MP confocal laser scanning system equipped with a Nikon Eclipse TE2000-U inverted fluorescence microscope. For morphological analysis, sections were stained with Masson's Trichrome Accustain according to manufacturer's instructions (Sigma). Neutrophils were visualized using a naphthol AS-D chloroacetate esterase activity kit (Sigma-Aldrich, Zwijndrecht, The Netherlands) according to manufacturer's instructions. Where indicated atherosclerosis was also analysed in oil-red-O stained cross sections of the right coronary artery near the aortic root and en face in the aortic arch and thoracic aorta. All analyses were performed blinded.

Peritoneal leukocyte analysis

Upon sacrifice of the transplanted LDLr KO mice at 18 weeks after transplantation (including 10 weeks Western-type diet), the peritoneal cavity of the mice was lavaged with 10 ml cold PBS to collect peritoneal leukocytes for quantification of neutrophil, lymphocyte, and macrophage counts using an automated Sysmex XT-2000iV Veterinary Hematology analyzer (Sysmex Corporation, Kobe, Japan). The XT-2000iV employs a fluorescent flow cytometry method using a fluorescent dye staining cellular DNA and RNA and a semiconductor laser to detect forward-, side-scattered, and fluorescent light. Corresponding samples were cytospun for manual confirmation and stained with oil-red-O for detection of lipid accumulation.

Macrophage cholesterol efflux studies

Macrophage cholesterol efflux studies were performed using bone marrow-derived macrophages (BMDM) and thioglycollate-elicited peritoneal macrophages (PM) isolated from WT, SR-BI KO, ABCA1 KO, and SR-BI/ABCA1 dKO mice fed chow diet. To label PM with 3H-cholesterol the in vivo method was used that was previously developed in our lab (4), allowing the study of cholesterol efflux with minimal culture times. Briefly, PM were elicited by intraperitoneal injection with 1 ml 3% Brewer's thioglycollate medium (Difco, Detroit, USA). After five days, the elicited PM were labelled in vivo by intraperitoneal injection of 3H-cholesterol. The injection sample was prepared by dissolving 6.25 μCi of 3H-cholesterol in 6.25 μL ethanol and subsequent addition of 500 μl PBS of 37oC. At 3.5 hours after injection, PM were harvested and seeded on 24-well plates at a density of 0.5 x 106 cells in 500 μL Dulbecco's modified Eagle's medium (DMEM)/0.2% free fatty acid free BSA. After 1 hour, nonadherent cells were removed by washing. The cholesterol mass of the cells was 60.4±3.0, 64.6±2.2, 60.3±2.7, and 60.3±1.7 μg/mg cell protein for WT, ABCA1 KO, SR-BI KO, and ABCA1/SR-BI double knockout macrophages, respectively.

For culture of BMDM, bone marrow cells were isolated from both femurs and tibias, plated, and differentiated in DMEM supplemented with 10% fetal bovine serum, 2 mmol/L glutamine, 20% L929 cell-conditioned media (as a source of M-CSF), and penicillin-streptomycin for 6 days. Subsequently, cells were loaded with cholesterol for 48 hours with acetylated LDL (50 μg/mL) and 0.5 μCi/mL 3H-cholesterol in DMEM/BSA. The loading medium was removed and the cells washed twice in PBS, then incubated overnight (16 hours) with DMEM/BSA, supplemented with 22-hydroxycholesterol (10 μmol/L) and 9-cis retinoic acid (1 μmol/L).

Cholesterol efflux from in vivo labeled PM and cholesterol-loaded BMDM was subsequently studied by incubation of the cells with DMEM/BSA alone, or supplemented with either 10 μg/ml apoAI (Calbiochem) or 10 or 50 μg/ml human HDL (isolated according to Redgrave et al. (5)). After a 24-hours efflux period, radioactivity in the cells and medium was determined by liquid scintillation counting. Efflux of 3H-cholesterol label is defined as (dpmmedium/ dpmcell +dpmmedium) x 100%. When indicated cell and media samples were also extracted and analyzed for free and esterified cholesterol mass by HLPC, as previously described (6). Cell proteins were measured using the BCA assay (Pierce). For mass analysis, HDL samples were separately analyzed to allow correction for HDL cholesterol present in relevant media samples. Mass cholesterol efflux is expressed as the percentage of total cell cholesterol present in the medium. Basal efflux to media (in the absence of added acceptors) has been subtracted from the data shown.

Western blot analysis

Macrophages (peritoneal and BMDM) were generated as described above and scraped in 50 mM Tris-HCL, 100 mM NaCl, and 0.5% Triton X-100 in the presence of protease inhibitors (Roche Molecular Biochemicals). The protein content was determined by the Bio-Rad protein assay. Aliquots of 20 µg (for BMDM) or 40 µg of protein (for peritoneal macrophages) were separated by 6% SDS-PAGE electrophoresis and transferred onto nitrocellulose membranes. Immunolabelling was performed using polyclonal antibodies directed against SR-BI (Santa Cruz Biotechnology Inc) or ABCG1 (Novus) or a murine monoclonal antibody against ABCA1 (AC-10, kindly provided by Dr M. R. Hayden (Vancouver, Canada)).

Cytokine serum levels

At 8 (chow diet), 12 weeks (4 weeks Western-type diet), and 18 weeks (10 weeks Western-type diet) post-transplant blood was collected from the transplanted animals. Serum was separated by centrifugation and stored at -80°C until analysis. The mouse Bio-Plex suspension array (Bio-Rad Laboratories AB, Sundbyberg, Sweden) was used to measure 8 different cytokines: interleukin (IL) 1β, IL-5, IL-6, KC (murine ortholog of IL-8), IL-10, IL-12, tumor necrosis factor (TNF)-α, and RANTES (regulated on activation and normally T cell expressed and secreted). The assay was performed according to the protocol of the manufacturer. In brief, serum samples were thawed on ice and centrifuged at 4500 rpm for 3 min at 4°C. After this initial step, serum was incubated with microbeads labeled with specific antibodies to one of the indicated cytokines for 30 min. Samples were washed after the incubation and were then incubated with the detection antibody cocktail. This step was followed by another wash step, and the beads were incubated with streptavidin-phycoerythrin for 10 min, again washed, and the concentration of each cytokine was determined using the array reader.

Statistical analysis

Values are expressed as mean±SEM. A one way ANOVA and the Student Newman Keuls posttest were used to compare means after confirming normal distribution by the method Kolmogorov and Smirnov using Graphpad Instat Software (San Diego, USA). A p value of <0.05 was considered significant.

Supplementary Figures

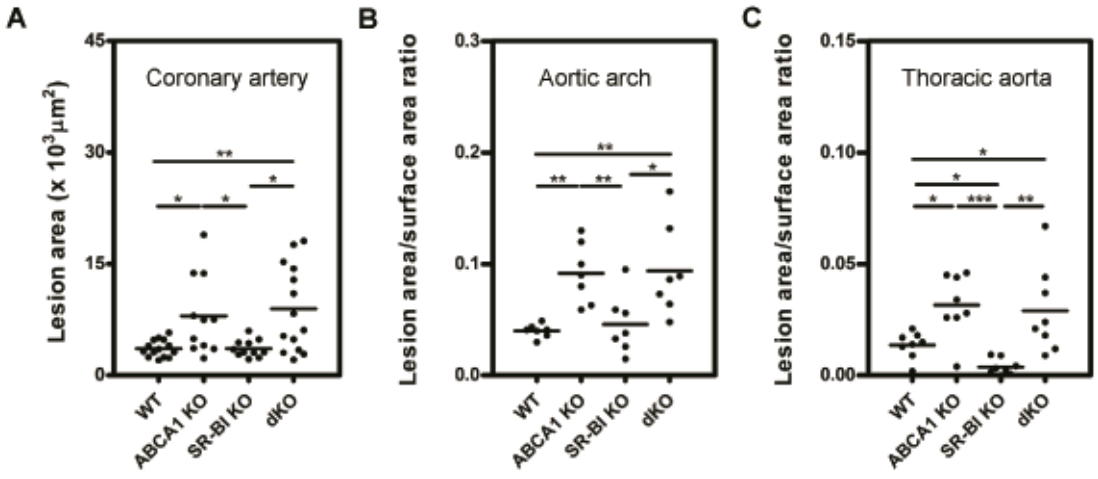

Supplementary Figure I. Atherosclerotic lesion quantification in the right coronary artery (A), the aortic arch (B), and the thoracic aorta (C) of LDLr KO mice, transplanted with WT, ABCA1 KO, SR-BI KO, or ABCA1/SR-BI double KO (dKO) bone marrow. Each symbol represents the mean lesion area in the coronary artery of single mouse, or the ratio of lesion area to surface area in the aortic arch and thoracic aorta of single mouse. The horizontal bar indicates the mean value for the group. Statistically significant difference *p<0.05, **p<0.01 and ***p<0.001.

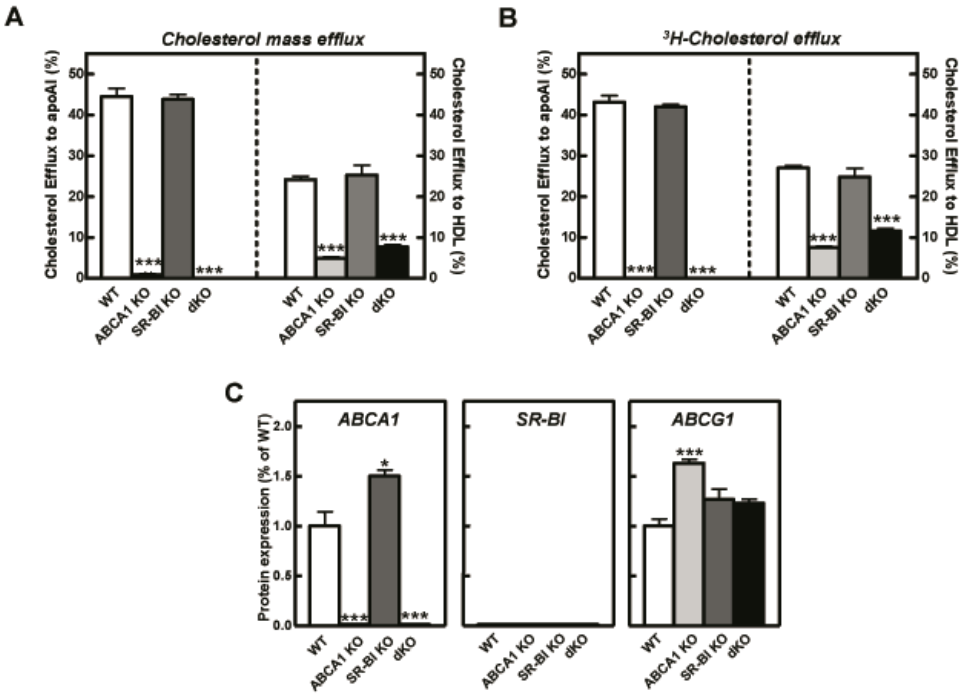

Supplementary Figure II. Cholesterol mass (A) and 3H-label (B) efflux from acetylated LDL-loaded macrophages to apoAI (10 µg/mL) and HDL (10 µg/mL). (C) Quantification of ABCA1, SR-BI, and ABCG1 protein by Western blotting. Values are means±SEM. Statistically significant difference *p<0.05 and ***p<0.001. Note that no additional effect of combined deletion of ABCA1 and SR-BI over single deletion of ABCA1 was observed on cholesterol mass and 3H-label efflux due to absence of SR-BI expression under this condition where macrophages are loaded with acetylated LDL.

Supplemental References

1. Bligh, E.G., and Dyer, W.J. 1959. A rapid method of total lipid extraction and purification. *Can. J. Med. Sci.* **37**: 911-917.
2. Chomczynski, P., and Sacchi, N. 1987. Single-step method of RNA isolation by acid guanidinium thiocyanate-phenol-chloroform extraction. *Anal. Biochem.* **162**:156-159.
3. Paigen, B., Morrow, A., Holmes, P.A., Mitchell, D., and Williams, R.A. 1987. Quantitative assessment of atherosclerotic lesions in mice. *Atherosclerosis.* **68**:231-40.
4. Van Eck, M., Bos, I.S., Hildebrand, RB., Van Rij, B.T., and Van Berkel, T.J.C. 2004. Dual role for scavenger receptor class B type I on bone marrow-derived cells in
atherosclerotic lesion development. *Am. J. Pathol.* **165**:785-794.
5. Redgrave, T.G., Roberts, D.C.K., and West, C.E. 1975. Separation of plasma lipoproteins by density-gradient ultracentrifugation. *Anal. Biochem.* **65**:42-49.
6. Gelissen, I.C., Brown, A.J., Mander, E.L., Kritharides, L., Dean, R.T., and Jessup, W. 1996. Sterol efflux is impaired from macrophage foam cells selectively enriched with 7-ketocholesterol. *J Biol Chem.* **271**: 17852–17860.

CHAPTER 6

Leukocyte ABC-transporter A1 and LDL receptor play independent roles in atherosclerosis: the potential contribution of T cells

Ying Zhao[1], Laura Calpe-Berdiel[1], Jun Wang[2], Amanda C. Foks[1], Bart Lammers, Johan Kuiper[1], Theo J.C. Van Berkel[1], Miranda Van Eck[1]

[1] Division of Biopharmaceutics, Leiden/Amsterdam Center for Drug Research, Leiden University, Einsteinweg 55, 2333 CC Leiden, The Netherlands
[2] Department of Human Genetics, Leiden University Medical Center, Leiden, The Netherlands

Abstract

Objective: The present study aims to investigate whether LDL receptor (LDLr) deficiency influences the atheroprotective effects of leukocyte ABC-transporter A1 (ABCA1) *in vivo*.

Methods and Results: LDLr-/- mice were transplanted with bone marrow from $LDLr^{-/-}$ /$ABCA1^{-/-}$ mice, $LDLr^{+/+}$/$ABCA1^{-/-}$ mice, and their respective controls. Plasma cholesterol levels were significantly reduced upon deletion of leukocyte ABCA1 after 8 weeks of Western-type diet feeding. Also, leukocyte ABCA1 deficiency led to increased monocytosis, recruitment of macrophages into peripheral tissues, and macrophage foam cell formation. None of these effects was influenced by the deletion of the leukocyte LDLr. Despite relatively low plasma cholesterol levels, animals transplanted with $LDLr^{-/-}$ /$ABCA1^{-/-}$ and $LDLr^{+/+}$/$ABCA1^{-/-}$ bone marrow developed 1.6-fold ($p<0.01$) and 1.4-fold ($p<0.05$) larger lesions, compared to their respective controls. Two-way ANOVA analysis also demonstrated that deletion of the leukocyte LDLr reduced lesion development ($p<0.001$). Interestingly, in $LDLr^{-/-}$/$ABCA1^{-/-}$ transplanted mice, the reduced lesion size was associated with reduced lymphocytosis and recruitment of T cells into the adventitia of lesions.

Conclusions: Leukocyte LDLr deficiency does not affect the atheroprotective effects of leukocyte ABCA1. Furthermore, in addition to promoting macrophage cholesterol efflux, leukocyte ABCA1 also protects against atherosclerosis through inhibiting lymphocytosis and recruitment of T cells into the adventitia of lesions.

--- submitted ---

Introduction

Macrophage foam cell formation is a hallmark of atherosclerosis. Since macrophages cannot limit lipid uptake, cholesterol efflux is crucial for prevention of macrophage foam cell formation and atherosclerosis. ABC-transporter A1 (ABCA1) facilitates cholesterol efflux to lipid-free or lipid-poor apoAI [1]. Patients with Tangier disease, due to loss-of-function mutations in the ABCA1 gene, display macrophage foam cell accumulation in peripheral tissues and premature atherosclerosis [2]. Bone marrow transplantation (BMT) studies in LDL receptor knockout ($LDLr^{-/-}$) mice indicate that leukocyte ABCA1 is atheroprotective. Leukocyte ABCA1 deficiency accelerates atherosclerosis [3], while overexpression of ABCA1 in leukocytes prevents the progression of atherosclerosis [4]. The atheroprotective effects of leukocyte ABCA1 have been primarily attributed to ABCA1 in macrophages. Mice that specifically lack ABCA1 in macrophages and neutrophils were generated in the group of Dr. Parks by crossing *ABCA1* floxed mice with mice expressing *Cre* recombinase under the control of the macrophage/neutrophil-specific lysozyme M promoter [5]. Surprisingly, specific deletion of macrophage ABCA1 on $LDLr^{-/-}$ background does not promote atherosclerosis [6]. BMT studies in $LDLr^{-/-}$ mice were performed using bone marrow from single $ABCA1^{-/-}$ mice and thus, in contrast to the LDLr-/- mice with specific knockdown of macrophage ABCA1, the leukocytes in the BMT animals do express the LDLr. Interestingly, a direct link between macrophage LDLr and ABCA1 expression has been suggested. Macrophages lacking the LDLr display reduced expression of ABCA1 [7]. In these macrophages, oxysterols cannot inactivate sterol regulatory element-binding protein 1 (SREBP1), which suppresses ABCA1 expression via microRNA33 [8]. Thus, impaired induction of ABCA1 in macrophages lacking the LDLr in response to oxysterol loading might explain why no effect was observed of specific deletion of macrophage ABCA1 on atherosclerosis.

To test if absence or presence of the LDLr determines the effects of leukocyte ABCA1 deficiency on atherosclerosis, bone marrow from $LDLr^{-/-}/ABCA1^{-/-}$, $LDLr^{+/+}/ABCA1^{-/-}$, and their respective controls was transplanted into $LDLr^{-/-}$ mice. After 8 weeks recovery, the animals were fed Western-type diet (WTD) for an additional 8 weeks before determination of atherosclerotic lesion formation. Our results clearly demonstrate that leukocyte ABCA1 deficiency led to an increased susceptibility to atherosclerotic lesion development both in the absence and presence of the LDLr. Importantly, the present study also for the first time provides evidence that suppression of lymphocytosis and T-cell recruitment into the adventitia of lesions contributes to the atheroprotective function of leukocyte ABCA1.

Methods

For detailed methodology, please see the data supplement, available online at http://atvb.ahajournals.org. Briefly, bone marrow transplantations were performed with $LDLr^{-/-}/ABCA1^{-/-}$, $LDLr^{-/-}/ABCA1^{-/-}$, and respective control mice as donors and $LDLr^{-/-}$ mice as recipients. Plasma lipids were determined by enzymatic colorimetric assays. Atherosclerotic lesion area and lesion composition in cryostat sections of the aortic root were quantified using the Leica image analysis system. Peritoneal leukocytes and white blood cells were analyzed with hematology cell analyzer. Macrophages ($CD11b^{+}Ly6G^{-}$) in the spleen were quantified using flow cytometry. Macrophages in the liver and T cells in atherosclerotic lesions were detected by immunolabelling with anti-F4/80 and anti-CD3 antibody, respectively.

Results

Leukocyte ABCA1 deficiency inhibited the WTD-induced increase in plasma cholesterol independently of LDL receptor expression

To investigate the effects of combined deficiency of leukocyte ABCA1 and LDLr on foam cell formation and atherogenesis, bone marrow from LDLr$^{-/-}$/ABCA1$^{-/-}$, LDLr$^{+/+}$/ABCA1$^{-/-}$, LDLr$^{-/-}$/ABCA1$^{+/+}$, and LDLr$^{+/+}$/ABCA1$^{+/+}$ mice was transplanted into LDLr$^{-/-}$ mice, which represent an established model for the development of atherosclerosis. Successful reconstitution of the recipient mice with donor bone marrow was confirmed by analysis of LDLr and ABCA1 transcripts in genomic DNA from bone marrow of transplanted mice as described previously [3, 9] (data not shown). Deletion of ABCA1, LDLr, or both ABCA1 and LDLr in bone marrow-derived cells did not affect plasma total cholesterol levels when fed regular chow diet (277±8, 263±7, 286±5, and 289±8 mg/dL for LDLr$^{+/+}$/ABCA1$^{+/+}$, LDLr$^{+/+}$/ABCA1$^{-/-}$, LDLr$^{-/-}$/ABCA1$^{+/+}$, and LDLr$^{-/-}$/ABCA1$^{-/-}$ transplanted animals, respectively), as shown in Figure 1A. At 8 weeks after BMT, the animals were switched from regular chow diet to WTD to induce atherosclerotic lesion formation. After 8 weeks on WTD, the total plasma cholesterol levels in both LDLr$^{+/+}$/ABCA1$^{+/+}$ and LDLr$^{-/-}$/ABCA1$^{+/+}$ transplanted mice increased approximately 4-fold (1108±72 mg/dL) and 3.6-fold (1017±63 mg/dL) (Figure 1A), respectively. In line with previous studies [10, 11], deletion of ABCA1 in bone marrow cells resulted in lower plasma cholesterol levels upon challenge with WTD (568±14, $p<0.001$ *vs* LDLr$^{+/+}$/ABCA1$^{+/+}$ and LDLr$^{-/-}$/ABCA1$^{+/+}$ transplanted mice). Like LDLr$^{+/+}$/ABCA1$^{-/-}$ transplanted animals, LDLr$^{-/-}$/ABCA1$^{-/-}$ transplanted animals showed lower plasma cholesterol levels (611±16, $p<0.001$ *vs* LDLr$^{+/+}$/ABCA1$^{+/+}$ and LDLr$^{-/-}$/ABCA1$^{+/+}$ transplanted mice), indicating that the effect of leukocyte ABCA1 on plasma cholesterol levels is independent of LDLr expression (Figure 1A). The lower levels of plasma cholesterol in the LDLr$^{+/+}$/ABCA1$^{-/-}$ and LDLr$^{-/-}$/ABCA1$^{-/-}$ transplanted animals were mainly due to reduced VLDL and LDL levels (Figure 1B).

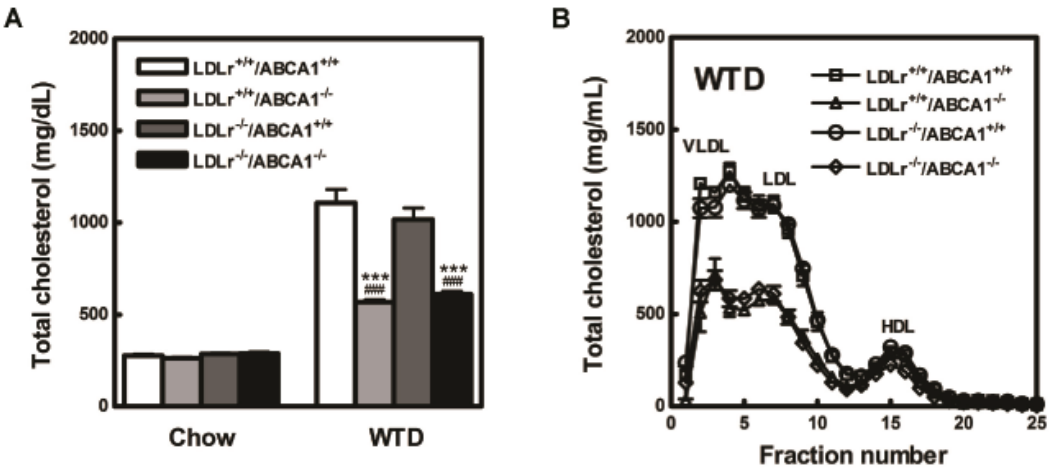

Figure 1. Plasma cholesterol levels on chow and Western-type diet (A) and lipoprotein cholesterol distribution profile on Western-type diet (B) in LDLr$^{-/-}$ mice reconstituted with LDLr$^{+/+}$/ABCA1$^{+/+}$, LDLr$^{+/+}$/ABCA1$^{-/-}$, LDLr$^{-/-}$/ABCA1$^{+/+}$, and LDLr$^{-/-}$/ABCA1$^{-/-}$ bone marrow. Values are mean±SEM. Statistically significant difference $^{***}P<0.001$ *vs* LDLr$^{+/+}$/ABCA1$^{+/+}$ group; $^{###}P<0.001$ *vs* LDLr$^{-/-}$/ABCA1$^{+/+}$ group.

Leukocyte ABCA1 and LDLr deficiency independently affected atherosclerotic lesion development

The development of atherosclerotic lesions was analyzed at the aortic root. After 8 weeks on WTD, atherosclerotic lesion size in the aortic root was $475\pm73\times10^3$ μm^2 in $LDLr^{+/+}/ABCA1^{+/+}$ and $359\pm41\times10^3$ μm^2 in $LDLr^{-/-}/ABCA1^{+/+}$ transplanted mice (Figure 2A and 2B). In line with previous studies [3, 10, 11], despite the lower plasma cholesterol levels, selective disruption of ABCA1 in bone marrow-derived cells resulted in a 1.4-fold increase ($681\pm33\times10^3$ μm^2, $p<0.05$) in the mean atherosclerotic lesion size as compared to $LDLr^{+/+}/ABCA1^{+/+}$ transplanted mice. Notably, $LDLr^{-/-}/ABCA1^{-/-}$ transplanted mice also developed 1.6-fold ($563\pm41\times10^3$ μm^2, $p<0.01$) larger atherosclerotic lesions as compared to $LDLr^{-/-}/ABCA1^{+/+}$ transplanted mice, indicating that leukocyte ABCA1 could protect against atherosclerosis even in the absence of LDLr expression (Figure 2A). Interestingly, two-way ANOVA analysis demonstrated not only the atheroprotective effect of leukocyte ABCA1 ($p<0.001$) but also a pro-atherogenic effect of LDLr expression on leukocytes ($p<0.001$). No interaction between the effect of leukocyte ABCA1 and LDLr deletion on atherosclerosis was observed ($p=0.93$) (Figure 2B).

Quantitative morphological analysis of the atherosclerotic lesions showed that the macrophage content in the lesions was significantly reduced in $LDLr^{+/+}/ABCA1^{-/-}$ (19.6±2.5%, $p<0.001$) and $LDLr^{-/-}/ABCA1^{-/-}$ (14.6±3.3%, $p<0.001$) transplanted mice as compared to $LDLr^{+/+}/ABCA1^{+/+}$ (35.8±3.3%) and $LDLr^{-/-}/ABCA1^{+/+}$ (41.3±3.8%) transplanted mice, respectively (Figure 2C and 2D). As determined by Masson's Trichrome staining, ABCA1 deficiency and combined deficiency of ABCA1 and LDLr in bone marrow-derived cells led to a 2.8-fold (9.5±1.4%, $P<0.001$) and 4.6-fold (11.8±1.0%, $p<0.001$) increase in collagen deposition in lesions as compared to $LDLr^{+/+}/ABCA1^{+/+}$ (3.4±0.7%) and $LDLr^{-/-}/ABCA1^{+/+}$ (2.6±0.4%) transplanted animals, respectively (Figure 2C and 2D). Furthermore, an increased necrotic core content was also evident in lesions of $LDLr^{+/+}/ABCA1^{-/-}$ (4.5-fold, $P<0.01$ *vs* $LDLr^{+/+}/ABCA1^{+/+}$) and $LDLr^{-/-}/ABCA1^{-/-}$ (5.0-fold, $P<0.001$ *vs* $LDLr^{-/-}/ABCA1^{+/+}$) transplanted animals (Figure 2D). Taken together, leukocyte ABCA1 deficiency led to more advanced lesion formation even in the absence of LDLr expression.

Leukocyte ABCA1 deficiency impaired cellular cholesterol efflux *in vitro* and increased foam cell formation *in vivo* independently of LDLr expression

Next, we determined the combined effect of leukocyte ABCA1 and LDLr deficiency on cellular cholesterol efflux using bone marrow-derived macrophages. As shown in Figure 3, LDLr deficiency did not influence cholesterol efflux from macrophages to apoAI, while ABCA1 deficiency, as expected, diminished macrophage cholesterol efflux to apoAI in both the absence and presence of the LDLr (>90% decrease, $p<0.001$). In contrast, macrophage cholesterol efflux to HDL was not affected by deletion of ABCA1, LDLr, or both (Figure 3). Moreover, cholesterol loading with LDL (Figure 3A) or oxidized LDL (Figure 3B) did not influence the effect of macrophage ABCA1 deficiency on cholesterol efflux. In line with the cholesterol efflux data, foam cells within the peritoneal cavity of both $LDLr^{+/+}/ABCA1^{-/-}$ (11.9±1.0%, $p<0.001$) and $LDLr^{-/-}/ABCA1^{-/-}$ (11.1±0.7%, $p<0.001$) transplanted mice were similarly increased as compared to $LDLr^{+/+}/ABCA1^{+/+}$ (1.1±0.3%) and $LDLr^{-/-}/ABCA1^{+/+}$ (1.5±0.4%) transplanted mice (Figure 4A). This was also evident from peritoneal cells stained for neutral lipids with oil-red-O (Figure 4B). These data indicate that the essential role of macrophage ABCA1 in prevention from foam cell formation is independent of LDLr expression.

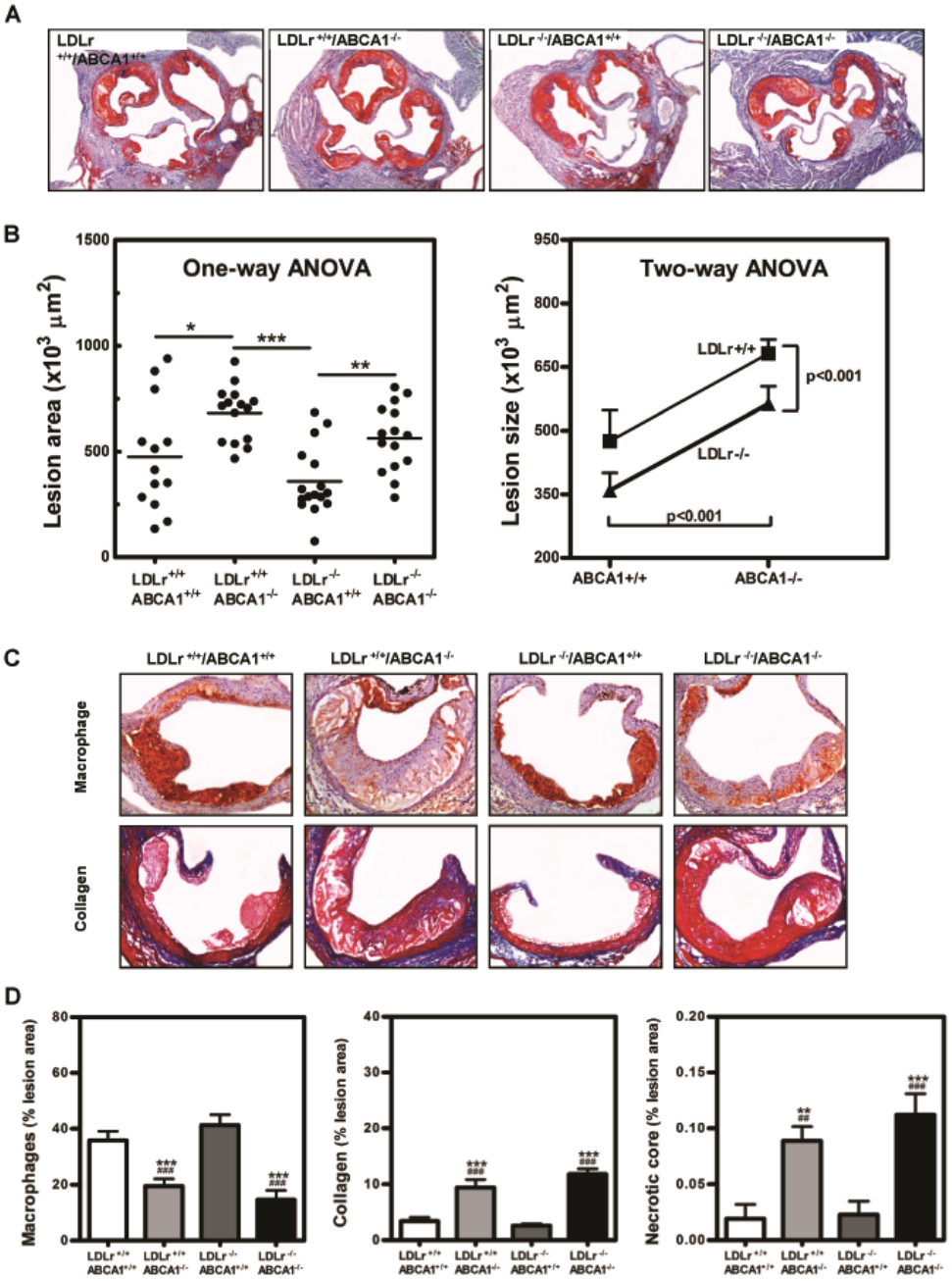

Figure 2. Atherosclerosis in the aortic root of LDLr$^{-/-}$ mice reconstituted with LDLr$^{+/+}$/ABCA1$^{+/+}$, LDLr$^{+/+}$/ABCA1$^{-/-}$, LDLr$^{-/-}$/ABCA1$^{+/+}$, and LDLr$^{-/-}$/ABCA1$^{-/-}$ bone marrow at 8 weeks on WTD. A, Photomicrographs showing representative oil-red-O-stained sections (50x). B, Mean atherosclerotic lesion size in the aortic root of mice. Each symbol (Left panel) represents the mean lesion area in a single mouse. The horizontal line represents the mean of the group. Statistically significant difference $^{*}P<0.05$, $^{**}P<0.01$, $^{***}P<0.001$. Two-way ANOVA analysis (right panel) of the effect of ABCA1 and LDLr on mean atherosclerotic lesion size in the aortic root of mice. C, Photomicrographs showing the lesion compositions in the aortic root of mice. Sections of the aortic roots were stained with antibody against Moma-2 to visualize macrophages (100x). Morphological staining of atherosclerotic lesions in the aortic root with Masson's Trichrome Accustain, which stains cytoplasma and muscle fiber red and collagen blue (100x). D, Bar graphs showing the quantification of macrophages, collagen, and necrotic core content of lesions in the aortic root of mice, transplanted with LDLr$^{+/+}$/ABCA1$^{+/+}$ (open bar), LDLr$^{+/+}$/ABCA1$^{-/-}$ (gray bar), LDLr$^{-/-}$/ABCA1$^{+/+}$ (dark gray bar), and LDLr$^{-/-}$/ABCA1$^{-/-}$ (black bar) bone marrow. Values represent the mean±SEM. Statistically significant difference **P<0.01 and ***P<0.001 *vs* LDLr$^{+/+}$/ABCA1$^{+/+}$ group; $^{\#\#}$P<0.01 and $^{\#\#\#}$P<0.01 *vs* LDLr$^{-/-}$/ABCA1$^{+/+}$ group.

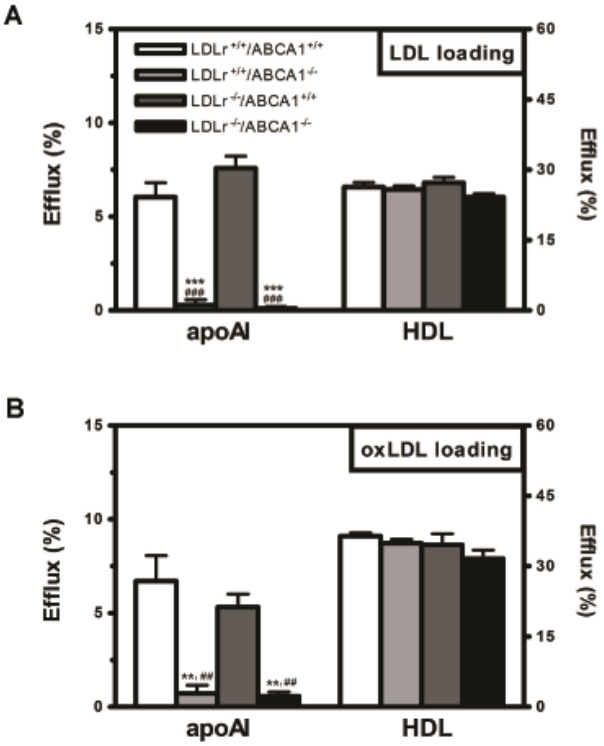

Figure 3. Cholesterol efflux from LDL-loaded (A) and oxidized LDL-loaded macrophages to apoAI and HDL. Bone marrow macrophages from LDLr$^{+/+}$/ABCA1$^{+/+}$ (open bar), LDLr$^{+/+}$/ABCA1$^{-/-}$ (gray bar), LDLr$^{-/-}$/ABCA1$^{+/+}$ (dark gray bar), and LDLr$^{-/-}$/ABCA1$^{-/-}$ (black bar) transplanted mice were labeled for cholesterol efflux as described in the materials and methods. Basal efflux to media (in the absence of added acceptors) has been substracted from the data shown. Values are mean±SEM (n=3 mice/group). Statistically significant difference $^{**}P<0.01$, $^{***}P<0.001$ *vs* LDLr$^{+/+}$/ABCA1$^{+/+}$ group; $^{\#\#}P<0.01$, $^{\#\#\#}P<0.001$ *vs* LDLr$^{-/-}$/ABCA1$^{+/+}$ group.

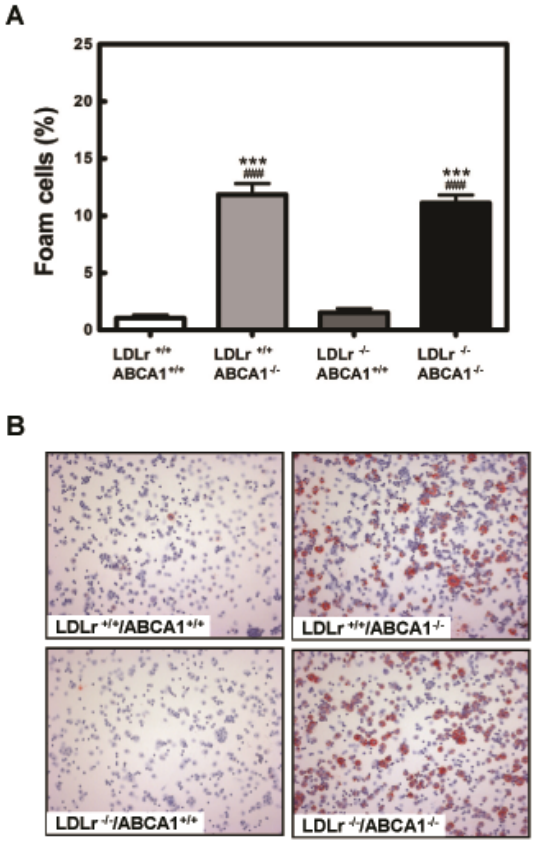

Figure 4. Macrophage foam cell formation in the peritoneal cavity of LDLr$^{-/-}$ mice reconstituted with LDLr$^{+/+}$/ABCA1$^{+/+}$ (open bar), LDLr$^{+/+}$/ABCA1$^{-/-}$ (gray bar), LDLr$^{-/-}$/ABCA1$^{+/+}$ (dark gray bar), and LDLr$^{-/-}$/ABCA1$^{-/-}$ (black bar) bone marrow at 8 weeks on WTD.
A, Quantification of macrophage foam cells as percentage of the total amount of macrophages. Values are mean±SEM. Statistically significant difference $^{***}P<0.001$ *vs* LDLr$^{+/+}$/ABCA1$^{+/+}$ group; $^{\#\#\#}P<0.001$ *vs* LDLr$^{-/-}$/ABCA1$^{+/+}$ group. B, Photomicrographs of oil-red-O-stained cytospins of peritoneal cells.

The deletion of leukocyte LDLr reduced lymphocytosis and inhibited the recruitment of T cells into the adventitia underlying the lesions of animals transplanted with ABCA1 KO bone marrow.

Deletion of ABCA1 in bone marrow-derived cells has been shown to enhance leukocytosis [3]. In line, also in the current study, the concentration of monocytes in the blood was

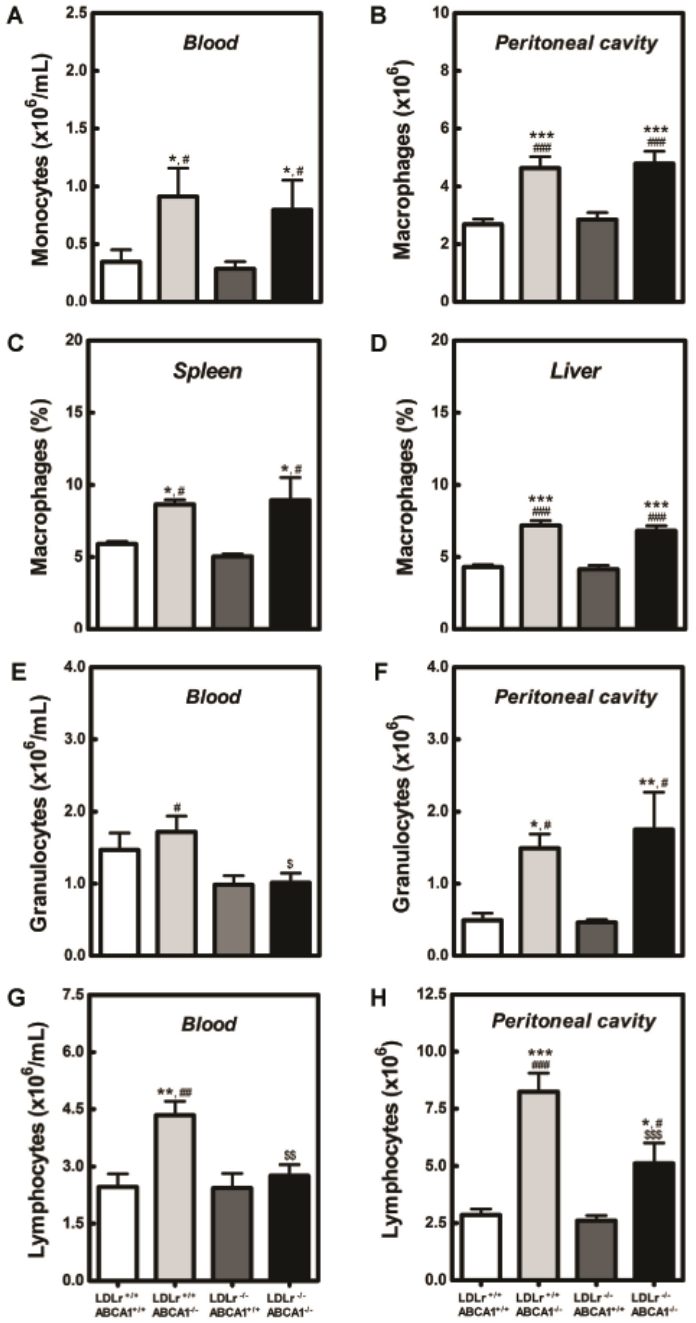

Figure 5. Leukocytosis and recruitment of leukocytes into peripheral tissues in the LDLr$^{-/-}$ mice reconstituted with LDLr$^{+/+}$/ABCA1$^{+/+}$ (open bar), LDLr$^{+/+}$/ABCA1$^{-/-}$ (gray bar), LDLr$^{-/-}$/ABCA1$^{+/+}$ (dark gray bar), and LDLr$^{-/-}$/ABCA1$^{-/-}$ (black bar) bone marrow at 8 weeks on WTD.

Monocytes/macrophages, granulocytes, and Lymphocytes, in the blood (A, E, G) and peritoneal cavity (B, F, H) were analyzed using a hematology analyzer. Macrophages in the spleen (C) were quantified using flow cytometry as CD11b+Ly6G- cells. In the liver (D), the macrophage content was determined by immunohistochemistry by using F4/80, a specific marker for mature tissue macrophages. Values represent the mean±SEM. Statistically significant difference *P<0.05, **P<0.01, and ***P<0.001 *vs* LDLr$^{+/+}$/ABCA1$^{+/+}$ group; $^{\#}$P<0.05, $^{\#\#}$P<0.01, and $^{\#\#\#}$P<0.01 *vs* LDLr$^{-/-}$/ABCA1$^{+/+}$ group; $^{\$}$P<0.05, $^{\$\$}$P<0.01, and $^{\$\$\$}$P<0.001 *vs* LDLr$^{+/+}$/ABCA1$^{-/-}$ group.

increased ~2-fold in LDLr$^{+/+}$/ABCA1$^{-/-}$ (0.50±0.10×10^6/mL, p<0.05) as compared to LDLr$^{+/+}$/ABCA1$^{+/+}$ (0.23±0.03×10^6/mL) transplanted mice. A similar increase was observed in LDLr$^{-/-}$/ABCA1$^{-/-}$ (0.44±0.07×10^6/mL, p<0.05) transplanted mice as compared to LDLr$^{-/-}$/ABCA1$^{+/+}$ (0.22±0.04×10^6/mL) (Figure 5A). Moreover, in line with our previous study [3], leukocyte ABCA1 deficiency also resulted in increased numbers of macrophages in the peritoneal cavity (1.7-fold, p<0.001 *vs* WT), the spleen (1.5-fold,

p<0.05 *vs* WT), and the liver (1.7-fold, p<0.001 *vs* LDLr$^{+/+}$/ABCA1$^{+/+}$) (Figure 5B, C, and D). In contrast, leukocyte LDLr deficiency did not affect the recruitment of macrophages into the organs studied. Also, LDLr$^{-/-}$/ABCA1$^{-/-}$ transplanted animals showed increased macrophage recruitment in the peritoneal cavity (1.7-fold, p<0.001), the spleen (1.8-fold, p<0.05), and liver (1.6-fold, p<0.001) as compared to LDLr$^{-/-}$/ABCA1$^{+/+}$ transplanted animals (Figure 5B, C, and D). Taken together, the effects of leukocyte ABCA1 on monocytosis and recruitment of macrophages into peripheral tissues are independent of leukocyte LDLr expression.

As shown in Figure 5E, single deletion of either leukocyte ABCA1 or leukocyte LDLr did not significantly affect circulating granulocytes, as compared to LDLr$^{+/+}$/ABCA1$^{+/+}$ transplanted animals. However, as compared to LDLr$^{+/+}$/ABCA1$^{-/-}$ transplanted mice, both LDLr$^{-/-}$/ABCA1$^{-/-}$ and LDLr$^{-/-}$/ABCA1$^{+/+}$ transplanted animals displayed a similar 1.7-fold reduction (p<0.05) in the circulating levels of granulocytes. Strikingly, despite the lower amount of circulating granulocytes, combined deletion of leukocyte LDLr and ABCA1 resulted in enhanced recruitment of granulocytes into the peritoneal cavity (3.8-fold, p<0.05 *vs* LDLr$^{-/-}$/ABCA1$^{+/+}$), similar to the effect of single ABCA1 deficiency (3.0-fold, p<0.05 *vs* LDLr$^{+/+}$/ABCA1$^{+/+}$) (Figure 5F).

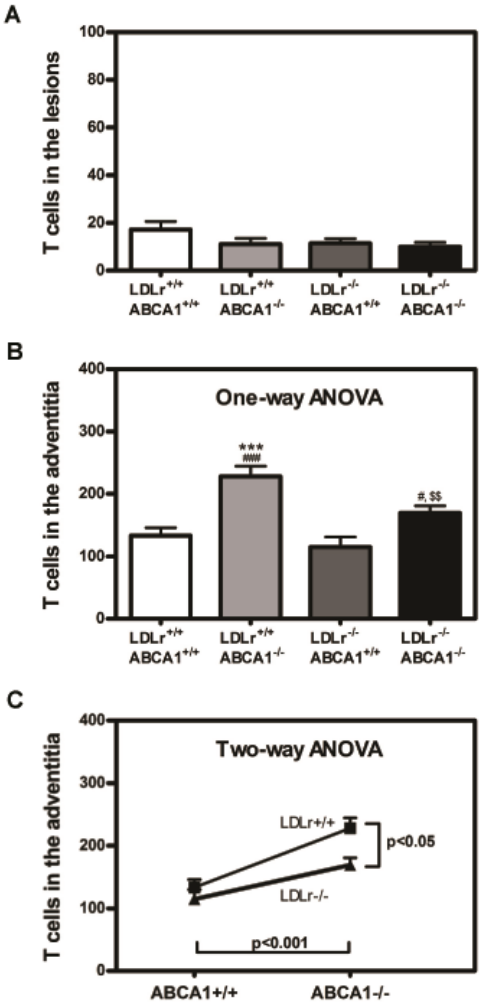

Figure 6. Recruitment of T cells into the lesions (A) and adventitia (B) of the LDLr$^{-/-}$ mice reconstituted with LDLr$^{+/+}$/ABCA1$^{+/+}$ (open bar), LDLr$^{+/+}$/ABCA1$^{-/-}$ (gray bar), LDLr$^{-/-}$/ABCA1$^{+/+}$ (dark gray bar), and LDLr$^{-/-}$/ABCA1$^{-/-}$ (black bar) bone marrow at 8 weeks on WTD.
Values are mean±SEM. Statistically significant difference $^{***}P$<0.001 *vs* LDLr$^{+/+}$/ABCA1$^{+/+}$ group; $^{\#}P$<0.05 *vs* LDLr$^{-/-}$/ABCA1$^{+/+}$ group; $^{\$\$}$P<0.01 *vs* LDLr$^{+/+}$/ABCA1$^{-/-}$ group. Two-way ANOVA analysis (C) of the effect of ABCA1 and LDLr on the recruitment of T cells into the adventitia underlying atherosclerotic lesions in the aortic root of mice.

In addition to increased monocytosis, leukocyte ABCA1 also led to increased lymphocytosis as evidenced by increased levels of circulating lymphocytes (1.8-fold, p<0.05 *vs* WT) (Figure 5G). Although deletion of the leukocyte LDLr alone did not significantly affect lymphocyte counts in the circulation, combined deletion of leukocyte

LDLr and ABCA1 resulted in a 1.6-fold reduction ($p<0.01$) as compared to single leukocyte ABCA1 deficiency. In the peritoneal cavity lymphocyte counts were increased in $LDLr^{+/+}/ABCA1^{-/-}$ (2.9-fold, $p<0.001$ *vs* $LDLr^{+/+}/ABCA1^{+/+}$) transplanted mice and $LDLr^{-/-}/ABCA1^{-/-}$ (2.0-fold, $p<0.05$ *vs* $LDLr^{-/-}/ABCA1^{+/+}$) transplanted animals. Of note, the counts in the peritoneal cavity of $LDLr^{-/-}/ABCA1^{-/-}$ transplanted animals were 1.6-fold lower ($p<0.001$) as compared to $LDLr^{+/+}/ABCA1^{-/-}$ transplanted animals (Figure 5H). Single deletion of the leukocyte LDLr did not affect the already low amount of peritoneal lymphocytes as compared to $LDLr^{+/+}/ABCA1^{+/+}$ transplanted mice.

T lymphocytes are important players in the progression of atherosclerotic lesions [12]. We next analyzed the number of T cells in the lesions and underlying adventitias. As shown in Figure 6A, the number of T cells was limited inside the lesions, and no significant difference in the number of T cells was observed in the lesions of the different groups. In contrast, more T cells were visible in the underlying adventitia (Figure 6B). Leukocyte ABCA1 deficiency resulted in a 1.7-fold increase ($p<0.001$ *vs* $LDLr^{+/+}/ABCA1^{+/+}$) in the recruitment of T cells into the adventitia. Also, $LDLr^{-/-}/ABCA1^{-/-}$ transplanted animals showed 1.5-fold ($p<0.05$) more T cells in the adventitia as compared to $LDLr^{-/-}/ABCA1^{+/+}$ transplanted animals. Deletion of the leukocyte LDLr resulted in 1.2-fold lower amount of T cells in the adventitia, which however failed to reach the statistical significance. Combined deletion of leukocyte LDLr and ABCA1 did lead to a significant reduction in recruitment of T cells into the adventitia (1.3-fold, $p<0.01$) as compared to single leukocyte ABCA1 deficiency. Of note, two-way ANOVA analysis demonstrated that leukocyte ABCA1 deficiency ($p<0.001$) increased, while leukocyte LDLr deficiency decreased ($p<0.05$) the recruitment of T cells into the adventitia of the atherosclerotic lesions. No interaction of leukocyte ABCA1 and LDLr on recruitment of T cells into the adventitia was observed ($p=0.16$) (Figure 6C). Interestingly, pearson correlation analyses demonstrated that the size of lesions was highly correlated with the number of T cells ($r=0.72$, $p<0.0001$) in the adventitia.

Discussion

Using bone marrow transplantation, we investigated the combined effects of leukocyte ABCA1 and LDLr deficiency on foam cell formation and atherosclerosis. In line with previous studies [3, 10, 11], transplantation of $ABCA1^{-/-}/ LDLr^{+/+}$ bone marrow into $LDLr^{-/-}$ mice led to increased foam cell formation and atherosclerosis. Importantly, $ABCA1^{-/-}/LDLr^{-/-}$ transplanted animals also showed more foam cell formation and increased lesion development as compared to $ABCA1^{+/+}/LDLr^{-/-}$ transplanted animals, clearly demonstrating that LDLr deficiency did not affect the atheroprotective function of leukocyte ABCA1. Interestingly, $ABCA1^{-/-}/LDLr^{-/-}$ transplanted animals showed reduced lymphocytosis and less atherosclerotic lesion formation as compared to $ABCA1^{-/-}/LDLr^{+/+}$ transplanted animals, indicating a pro-atherogenic role of LDLr on leukocytes.

Zhou et al demonstrated that deletion of the LDLr in peritoneal macrophages impairs sterol-induced ABCA1 expression and ABCA1-mediated cholesterol efflux [7]. However, in our studies, cholesterol efflux from bone marrow-derived macrophages lacking the LDLr to either apoAI or HDL was not affected. Importantly, in line with our cholesterol efflux studies, absence of the LDLr in bone marrow-derived cells also did not enhance foam cell formation upon WTD challenge *in vivo*. Interestingly, deletion of the LDLr in bone marrow-derived cells did lead to a small but significant reduction in atherosclerosis susceptibility in both the presence and absence of ABCA1. The transcription of the LDLr on macrophages is quickly downregulated after cholesterol loading [13], which leads to the previously published limited contribution of the

macrophage LDLr to foam cell formation and atherosclerosis in $LDLr^{-/-}$ mice upon transplantation with $LDLr^{+/+}$ bone marrow [9, 14]. In agreement, we found no effect of leukocyte LDLr deletion on macrophage foam cell formation *in vivo*. In contrast, the presence of the LDLr on lymphocytes is crucial for the proliferation of lymphocytes [15]. In the present study, the circulating lymphocyte count was reduced in $ABCA1^{-/-}/LDLr^{-/-}$ transplanted animals as compared to $ABCA1^{-/-}/LDLr^{+/+}$ transplanted mice. Therefore, we speculate that the effect of leukocyte LDLr deficiency on atherosclerosis in the present study might be rather due to its effect on the proliferation of lymphocytes, which becomes evident under conditions where lymphocyte counts are highly elevated due to the absence of ABCA1.

Hypercholesterolemia induces leukocytosis, in particular monocytosis [16] and neutrophilia [17], which promotes the development of atherosclerosis. The cholesterol efflux transporters ABCA1 and ABCG1 inhibit hypercholesterolemia-induced leukocytosis by suppressing bone marrow myeloid cell proliferation [18]. In line, increased leukocytosis and monocytosis was observed in ABCA1-/- transplanted $LDLr^{-/-}$ animals upon WTD challenge in previous [3] and present studies. Of note, the absence of LDLr did not influence the effects of leukocyte ABCA1 deficiency on monocytosis. In addition, in agreement with our previous study [3], also elevated circulating lymphocyte counts were observed in animals transplanted with $ABCA1^{-/-}$ bone marrow. Cholesterol accumulation in T lymphocytes is associated with increased proliferation [19]. Increased lymphocytosis in $ABCA1^{-/-}$ transplanted animals might thus be the consequence of the impaired cholesterol efflux from lymphocytes via ABCA1. Interestingly, blockade of cholesterol uptake via LDLr could reverse it, indicating the importance of the LDLr-mediated cholesterol uptake pathway for the induction of lymphocytosis.

Extensive evidence suggests an atheroprotective role for macrophage ABCA1. First, bone marrow transplantation studies showed that deficiency of leukocyte ABCA1 results in increased atherosclerotic lesion formation [3] while overexpression of leukocyte ABCA1 prevents the progression of atherosclerosis [4]. Second, ABCA1-mediated cholesterol efflux is crucial for the prevention of macrophage foam cell formation *in vitro and in vivo* [3, 10, 11]. Third, macrophage ABCA1 functions as an anti-inflammatory molecule [5, 20, 21]. Fourth, ABCA1 deficiency impairs the migration of macrophages [22], which might lead to the retention of macrophages in lesions. However, Brunham et al recently showed that macrophage-specific inactivation of ABCA1 on the LDLr KO background did not change the susceptibility to atherosclerosis [6]. The authors hypothesized that the failure to pick up the effect of macrophage ABCA1 on atherosclerosis might be due to the $LDLr^{-/-}$ background, as $LDLr^{-/-}$ macrophages were shown to have significantly less ABCA1 expression compared to wild-type macrophages [7]. In the present study, we excluded this possibility by clearly showing that absence of the LDLr did not affect the effects of leukocyte ABCA1 deficiency on macrophage foam cell formation *in vivo* nor atherosclerotic lesion development. Brunham et al also hypothesized that the enhanced lymphocytosis observed in ABCA1 KO transplanted animals might contribute to the increased lesion formation upon deletion of ABCA1 in bone marrow-derived cells of $LDLr^{-/-}$ mice. Interestingly, in the present study, we found that absence of the leukocyte LDLr did reduce the circulating lymphocyte counts and T cell recruitment into the adventitia of lesions in $ABCA1^{-/-}$ transplanted animals. Importantly, the number of T cells in the adventitia underlying lesions was highly associated with the lesion size. Our data thus indicate that enhanced lymphocytosis and T cell infiltration into the adventitia might contribute to the effects of leukocyte ABCA1 deficiency on atherosclerosis. Generation of T cell-specific $ABCA1^{-/-}$ mice is needed in the future to elucidate the extent of the atheroprotective effects of ABCA1 on T cells. Of note,

despite that ABCA1$^{-/-}$/LDLr$^{-/-}$ transplanted animals developed less lesions as compared to ABCA1$^{-/-}$/LDLr$^{+/+}$ transplanted animals, lesions of both types of animals contained more necrotic core material. Therefore, the effects of macrophage ABCA1 on the vulnerability of lesions also warrants further investigation.

In conclusion, deletion of the leukocyte LDLr does not affect the atheroprotective effect of leukocyte ABCA1. Furthermore, in addition to promoting macrophage cholesterol efflux, leukocyte ABCA1 also protects against atherosclerosis probably through inhibiting lymphocytosis and recruitment of T cells into the adventitia of lesions.

Acknowledgement

This work was supported by grants from the Netherlands Heart Foundation (#2001T4101 to M.V.E. and Y.Z., and the Established Investigator grant 2007T056 to M.V.E.), the Catalan University and Research Grants Management Agency (Beatriu de Pinós Postdoctoral Grant to L.C-B), and the Netherlands Organization for Scientific Research (VIDI grant 917.66.301 to M.V.E.).

References

1. Oram JF, Lawn RM, Garvin MR, Wade DP. ABCA1 is the cAMP-inducible apolipoprotein receptor that mediates cholesterol secretion from macrophages. *J Biol Chem.* 2000; 275: 34508-34511.
2. Van Eck M, Pennings M, Hoekstra M, Out R, Van Berkel TJ. Scavenger receptor BI and ATP-binding cassette transporter A1 in reverse cholesterol transport and atherosclerosis. *Curr Opin Lipidol.* 2005; 16: 307-315.
3. Van Eck M, Bos IS, Kaminski WE, Orsó E, Rothe G, Twisk J, Böttcher A, Van Amersfoort ES, Christiansen-Weber TA, Fung-Leung WP, Van Berkel TJ, Schmitz G. Leukocyte ABCA1 controls susceptibility to atherosclerosis and macrophage recruitment into tissues. *Proc Natl Acad Sci U S A.* 2002; 99: 6298-6303.
4. Van Eck M, Singaraja RR, Ye D, Hildebrand RB, James ER, Hayden MR, Van Berkel TJ. Macrophage ATP-binding cassette transporter A1 overexpression inhibits atherosclerotic lesion progression in low-density lipoprotein receptor knockout mice. *Arterioscler Thromb Vasc Biol.* 2006; 26: 929-934.
5. Zhu X, Lee JY, Timmins JM, Brown JM, Boudyguina E, Mulya A, Gebre AK, Willingham MC, Hiltbold EM, Mishra N, Maeda N, Parks JS. Increased cellular free cholesterol in macrophage-specific Abca1 knock-out mice enhances pro-inflammatory response of macrophages. *J Biol Chem.* 2008; 283: 22930-22941.
6. Brunham LR, Singaraja RR, Duong M, Timmins JM, Fievet C, Bissada N, Kang MH, Samra A, Fruchart JC, McManus B, Staels B, Parks JS, Hayden MR. Tissue-specific roles of ABCA1 influence susceptibility to atherosclerosis. *Arterioscler Thromb Vasc Biol.* 2009; 29: 548-554.
7. Zhou X, He W, Huang Z, Gotto AM Jr, Hajjar DP, Han J. Genetic deletion of low density lipoprotein receptor impairs sterol-induced mouse macrophage ABCA1 expression. A new SREBP1-dependent mechanism. *J Biol Chem.* 2008; 283: 2129-2138.
8. Najafi-Shoushtari SH, Kristo F, Li Y, Shioda T, Cohen DE, Gerszten RE, Näär AM. MicroRNA-33 and the SREBP host genes cooperate to control cholesterol homeostasis. *Science.* 2010; 328: 1566-1569.
9. Herijgers N, Van Eck M, Groot PH, Hoogerbrugge PM, Van Berkel TJ. Effect of bone marrow transplantation on lipoprotein metabolism and atherosclerosis in LDL receptor-knockout mice. *Arterioscler Thromb Vasc Biol.* 1997; 17: 1995-2003.
10. Out R, Hoekstra M, Habets K, Meurs I, de Waard V, Hildebrand RB, Wang Y, Chimini G, Kuiper J, Van Berkel TJ, Van Eck M. Combined deletion of macrophage ABCA1 and ABCG1 leads to massive lipid accumulation in tissue macrophages and distinct atherosclerosis at relatively low plasma cholesterol levels. *Arterioscler Thromb Vasc Biol.* 2008; 28: 258-264.
11. Zhao Y, Pennings M, Hildebrand RB, Ye D, Calpe-Berdiel L, Out R, Kjerrulf M, Hurt-Camejo E, Groen AK, Hoekstra M, Jessup W, Chimini G, Van Berkel TJ, Van Eck M. Enhanced foam cell formation, atherosclerotic lesion development, and inflammation by combined deletion of ABCA1 and SR-BI in

Bone marrow-derived cells in LDL receptor knockout mice on western-type diet. *Circ Res.* 2010; 107: e20-e31.

12. Hansson GK, Jonasson L. The discovery of cellular immunity in the atherosclerotic plaque. *Arterioscler Thromb Vasc Biol.* 2009; 29: 1714-1717.
13. Goldstein JL, Brown MS. The low-density lipoprotein pathway and its relation to atherosclerosis. *Annu Rev Biochem.* 1977; 46: 897-930.
14. Linton MF, Babaev VR, Gleaves LA, Fazio S. A direct role for the macrophage low density lipoprotein receptor in atherosclerotic lesion formation. *J Biol Chem.* 1999; 274:19204-19210.
15. Cuthbert JA, Lipsky PE. Modulation of human lymphocyte responses by low density lipoproteins (LDL): enhancement but not immunosuppression is mediated by LDL receptors. *Proc Natl Acad Sci U S A.* 1984; 81: 4539-4543.
16. Swirski FK, Libby P, Aikawa E, Alcaide P, Luscinskas FW, Weissleder R, Pittet MJ. Ly-6Chi monocytes dominate hypercholesterolemia-associated monocytosis and give rise to macrophages in atheromata. *J Clin Invest.* 2007; 117: 195-205.
17. Drechsler M, Megens RT, van Zandvoort M, Weber C, Soehnlein O. Hyperlipidemia-triggered neutrophilia promotes early atherosclerosis. *Circulation.* 2010; 122: 1837-1845.
18. Yvan-Charvet L, Pagler T, Gautier EL, Avagyan S, Siry RL, Han S, Welch CL, Wang N, Randolph GJ, Snoeck HW, Tall AR. ATP-binding cassette transporters and HDL suppress hematopoietic stem cell proliferation. *Science.* 2010; 328: 1689-1693.
19. Wilhelm AJ, Zabalawi M, Grayson JM, Weant AE, Major AS, Owen J, Bharadwaj M, Walzem R, Chan L, Oka K, Thomas MJ, Sorci-Thomas MG. Apolipoprotein A-I and its role in lymphocyte cholesterol homeostasis and autoimmunity. *Arterioscler Thromb Vasc Biol.* 2009; 29: 843-849.
20. Francone OL, Royer L, Boucher G, Haghpassand M, Freeman A, Brees D, Aiello RJ. Increased cholesterol deposition, expression of scavenger receptors, and response to chemotactic factors in Abca1-deficient macrophages. *Arterioscler Thromb Vasc Biol.* 2005; 25: 1198-1205.
21. Tang C, Liu Y, Kessler PS, Vaughan AM, Oram JF. The macrophage cholesterol exporter ABCA1 functions as an anti-inflammatory receptor. *J Biol Chem.* 2009; 284: 32336-32343.
22. Adorni MP, Favari E, Ronda N, Granata A, Bellosta S, Arnaboldi L, Corsini A, Gatti R, Bernini F. Free cholesterol alters macrophage morphology and mobility by an ABCA1 dependent mechanism. *Atherosclerosis.* 2011; 215: 70-76.

Supplementary methods

Mice

$LDLr^{-/-}$ mice were obtained from the Jackson Laboratory (Bar Habor, USA). $ABCA1^{-/-}$ mice, a kind gift of Dr. G. Chimini [1] were backcrossed to the C57Bl/6 background for at least 8 generations. $LDLr^{+/-}/ABCA1^{+/-}$ offsprings, which were generated from cross-breeding, were intercrossed to obtain the $LDLr^{-/-}/ABCA1^{-/-}$ mice, $LDLr^{+/+}/ABCA1^{-/-}$, $LDLr^{-/-}/ABCA1^{+/+}$, and $LDLr^{+/+}/ABCA1^{+/+}$ littermates. All mice were housed in a light and temperature controlled environment. Food and water were supplied ad libitum. Mice were maintained on regular chow (RM3, Special Diet Services, Whitham, UK), or were fed a Western-type diet, containing 15% (w/w) total fat and 0.25% (w/w) cholesterol (Diet W, Special Diet Services, Whitham, UK). Drinking water was supplied with antibiotics (83 mg/L ciprofloxacin and 67 mg/L polymyxin B sulphate) and 6.5 g/L sucrose. Animal experiments were performed at the Gorlaeus Laboratories of the Leiden/Amsterdam Center for Drug Research in accordance with the National Laws. All experimental protocols were approved by the Ethics Committee for Animal Experiments of Leiden University.

Bone Marrow Transplantation

Female $LDLr^{-/-}$ mice were lethally irradiated with a single dose of 9 Gy (0.19 Gy/min, 200 kV, 4 mA) at the age of 12 weeks. Bone marrow was harvested by flushing the femurs and tibias from male $LDLr^{-/-}/ABCA1^{-/-}$ mice, $LDLr^{+/+}/ABCA1^{-/-}$, $LDLr^{-/-}/ABCA1^{+/+}$, and $LDLr^{+/+}/ABCA1^{+/+}$

littermates. Irradiated recipients received 5 x 10^6 bone marrow cells by intravenous injection into the tail vein at 1 day after irradiation.

Plasma cholesterol analyses

After an overnight fasting-period, 100 μL of blood was drawn from the mice by tail bleeding. The concentrations of cholesterol in serum were determined by incubation with 0.025 U/mL cholesterol oxidase (Sigma) and 0.065 U/mL peroxidase and 15 μg/mL cholesteryl esterase (Roche Diagnostics, Mannheim, Germany) in reaction buffer (1.0 KPi buffer, pH=7.7 containing 0.01 M phenol, 1 mM 4-amino-antipyrine, 1% polyoxyethylene-9-laurylether, and 7.5% methanol). Absorbance was read at 490 nm. The distribution of cholesterol over the different lipoproteins in serum was determined by fractionation of 30 μL serum of individual mice using a Superose 6 column (3.2 x 300 mm, Smart-system; Pharmacia, Uppsala, Sweden). Cholesterol content of the effluent was determined as indicated.

Histological Analysis of the Aortic Root

To analyze the development of atherosclerosis at the aortic root, the transplanted LDLr$^{-/-}$mice (n=13-16/group) were sacrificed at 16 weeks after bone marrow transplantation. All mice were fed the Western-type diet for 8 weeks before sacrifice. The arterial tree was perfused *in situ* with PBS and the heart was excised and stored in 3.7% neutral-buffered formalin (Formal-fixx; Shandon Scientific Ltd., UK) until use. The hearts were bisected just below the atria, and the base of the hearts plus aortic roots were taken for analysis. The hearts were then sectioned perpendicular to the axis of the aorta, starting within the heart and working in the direction of the aortic arch as described by Paigen et al. [2]. Once the aortic root was identified by the appearance of aortic valve leaflets, alternate 10-μm sections were taken and mounted on gelatinized slides and stained with oil-red-O. The atherosclerotic lesion area in the sections was quantified by using a Leica image analysis system, consisting of a Leica DMRE microscope coupled to a camera and Leica QWin Imaging software (Leica Ltd., UK). Mean lesion area was calculated (in μm^2) from 10 sections, starting at the appearance of the tricuspid valves. Macrophages and T cells were detected by incubation of consecutive sections with α-MOMA-2 (Research diagnostics, USA) and α-CD3 (Neomarkers, USA), respectively. For morphological analysis, sections were stained with Masson's Trichrome Accustain according to manufacturer's instructions (Sigma). All analyses were performed blinded.

White blood cells and peritoneal leukocyte analysis

Upon sacrifice of the transplanted LDLr$^{-/-}$ mice at 16 weeks after transplantation, the blood and peritoneal leukocytes were collected as before [3]. Lymphocyte, monocyte/macrophage, and granulocyte counts were quantified using an automated Sysmex XT-2000iV Veterinary Hematology analyzer (Sysmex Corporation, Kobe, Japan). The XT-2000iV employs a fluorescent flow cytometry method using a fluorescent dye staining cellular DNA and RNA and a semiconductor laser to detect forward-, side-scattered, and fluorescent light. Corresponding samples were cytospun for manual confirmation and stained with oil-red-O for detection of lipid accumulation.

Macrophage cholesterol efflux studies

Macrophage cholesterol efflux studies were performed using bone marrow-derived macrophages (BMDM). For culture of BMDM, bone marrow cells were isolated from both femurs and tibias, plated, and differentiated in Dulbecco's modified Eagle's medium (DMEM) supplemented with 10% fetal bovine serum, 2 mmol/L glutamine, 20% L929 cell-conditioned media (as a source of M-CSF), and penicillin-streptomycin for 6 days. BMDM were subsequently harvested and plated at 0.5 x 10^6 cells/well in 24-well plates in medium without L cell-conditioned medium. The next day, the cells were washed and incubated with either 100 μg/mL LDL or 20 μg/mL oxidized LDL and 0.5 μCi/mL ^{3}H-cholesterol in DMEM/0.2% BSA for 24 hours at 37°C to load the cells with

cholesterol. Cholesterol efflux from BMDM was subsequently studied by incubation of the cells with DMEM/0.2% free fatty acid-free BSA alone, or supplemented with either 10 μg/mL apoAI (Calbiochem) or 50 μg/mL human HDL. After a 24-hours efflux period, radioactivity in the cells and medium was determined by liquid scintillation counting. Cholesterol efflux is defined as (dpm_{medium}/ dpm_{cell} +dpm_{medium}) x 100%.

Quantification of macrophages in the spleen and liver

Splenocytes were isolated and stained with fluorochrome-conjugate combinations of the following monoclonal antibodies aganist CD11b and Ly6G from eBioscience at 4^{o}C for 30 min in labeling buffer (1% mouse serum in PBS). Flow cytometry was performed with FacsCalibur and then analyzed with CellQuest software (Becton-Dickinson, San Jose), correcting for nonspecific staining with isotype antibody controls.

Cryostat sections of the liver (6 μm) were collected and immunolabeled with rat anti-mouse F4/80 (BMA Biomedicals) for detection of macrophages. The positive area in liver was quantified by using the Leica image analysis system.

Statistical Analysis

Statistical analysis was performed using ANOVA and the Student-Newman-Keuls post-test (GraphPad InStat and Prism software). A Pearson r test was used to perform correlation analysis. A level of $p<0.05$ was considered significant.

Supplemental References

1. McNeish J, Aiello RJ, Guyot D, Turi T, Gabel C, Aldinger C, Hoppe KL, Roach ML, Royer LJ, de Wet J, Broccardo C, Chimini G, Francone OL. High density lipoprotein deficiency and foam cell accumulation in mice with targeted disruption of ATP-binding cassette transporter-1. *Proc Natl Acad Sci U S A.* 2000; 97: 4245-4250.
2. Paigen B, Morrow A, Holmes PA, Mitchell D, Williams RA. Quantitative assessment of atherosclerotic lesions in mice. *Atherosclerosis.* 1987; 68: 231-240.
3. Zhao Y, Pennings M, Hildebrand RB, Ye D, Calpe-Berdiel L, Out R, Kjerrulf M, Hurt-Camejo E, Groen AK, Hoekstra M, Jessup W, Chimini G, Van Berkel TJ, Van Eck M. Enhanced foam cell formation, atherosclerotic lesion development, and inflammation by combined deletion of ABCA1 and SR-BI in Bone marrow-derived cells in LDL receptor knockout mice on western-type diet. *Circ Res.* 2010; 107: e20-e31.

CHAPTER 7

Leukocyte ABC-transporter A1 is atheroprotective in absence of apolipoprotein AI

Ying Zhao[1*], Laura Calpe-Berdiel[1*], Josep Julve[2], Joan Carles Escolà-Gil[2], Amanda Foks[1], Ronald J. van der Sluis[1], Johan Kuiper[1], Francisco Blanco-Vaca[2,3], Theo J.C. Van Berkel[1], Jan-Albert Kuivenhoven[4], Miranda Van Eck[1]

[1] Division of Biopharmaceutics, Leiden/Amsterdam Center for Drug Research, Gorlaeus Laboratories, Leiden University, Leiden, The Netherlands
[2] IIB Sant Pau and CIBER de Diabetes y Enfermedades Metabólicas Asociadas, CIBERDEM, Barcelona, Spain
[3] Departament de Bioquímica i Biologia Molecular, Universitat Autònoma de Barcelona, Barcelona, Spain
[4] Department of Vascular Medicine, Academic Medical Center, University of Amsterdam, Amsterdam, The Netherlands

*** These two authors contributed equally**

Abstract

Objective: ABC-transporter A1 (ABCA1) facilitates macrophage cholesterol efflux to lipid-free/poor apolipoprotein AI (ApoAI). The aim of the present study was to investigate the importance of ApoAI for macrophage ABCA1-mediated reverse cholesterol transport (RCT) and the atheroprotective effects of leukocyte ABCA1.

Methods and Results: Deletion of ABCA1 on macrophages did not impair cellular cholesterol efflux to HDL and lipoprotein-depleted serum of ApoAI$^{-/-}$/LDLr$^{-/-}$ mice nor radiolabeled cholesterol excretion into feces in ApoAI$^{-/-}$/LDLr$^{-/-}$ mice. However, leukocyte ABCA1 deficiency in ApoAI$^{-/-}$/LDLr$^{-/-}$ mice did promote atherosclerotic lesion development at both the aortic root and aortic arch. This coincided with enhanced neutrophilia and monocytosis in the circulation, increased plasma levels of pro-inflammatory chemoattractants KC and MCP-1, and augmented neutrophil accumulation in lesions.

Conclusion: ApoAI and macrophage ABCA1 are identified as functional partners in macrophage RCT. Nevertheless, leukocyte ABCA1 protects against atherosclerosis in absence of circulating ApoAI, probably through its anti-inflammatory function.

--- submitted ---

Introduction

Atherosclerosis is the principle cause of coronary artery disease and stroke. A growing body of evidence indicates that induction of the levels of high-density lipoprotein (HDL) inhibits the progression of atherosclerosis in mice and humans [1, 2]. HDL protects against atherosclerosis through several mechanisms, such as preserving the endothelial integrity and its anti-inflammatory and anti-oxidative properties [3-6]. However, the most important atheroprotective function of HDL is facilitation of reverse cholesterol transport (RCT), a process in which excess cholesterol from peripheral tissues is transferred to the liver via HDL for bile acid synthesis and excretion into the feces [7]. Macrophage-derived foam cells are major cellular components of early and advanced lesions which contribute to the initiation, development, and rupture of atherosclerotic lesions. Macrophages cannot limit the uptake of lipids. Removal of cholesterol from macrophage foam cells by RCT is thus crucial for inhibition of atherosclerosis [8]. ABC-transporter A1 (ABCA1) is an important facilitator of macrophage cholesterol efflux to lipid-free/poor apolipoproteins, including apolipoprotein AI (ApoAI) [8]. Bone marrow transplantation studies have demonstrated that leukocyte ABCA1 protects against atherosclerosis, probably by inhibiting macrophage foam cell formation [9]. The importance of ApoAI for macrophage ABCA1-facilitated RCT and the atheroprotective effects of leukocyte ABCA1, however, are still unknown.

The current study investigated the interrelationship between ApoAI and macrophage ABCA1 in RCT and the effects of hematopoietic ABCA1 deficiency on atherosclerosis in mice lacking ApoAI. Our results show that macrophage ABCA1 and ApoAI are functional partners in RCT. Interestingly, leukocyte ABCA1 protects against atherosclerosis even in the absence of circulating ApoAI.

Methods

Animals

Homozygous low-density lipoprotein receptor (LDLr) knockout ($^{-/-}$) mice were obtained from The Jackson Laboratory (Bar Harbor, Me, USA) as mating pairs and bred at the Gorlaeus Laboratory (Leiden, The Netherlands). ApoAI/LDLr double $^{-/-}$ ($ApoAI^{-/-}/LDLr^{-/-}$) mice were kindly provided by Amsterdam Molecular Therapeutics (AMT, Amsterdam, The Netherlands). $ABCA1^{-/-}$ mice were a kind gift of Dr. G. Chimini (Centre d'Immunologie de Marseille Luminy, France). The $ABCA1^{-/-}$ mice were at least 8 generations backcrossed to the C57bl/6 wild-type background. Mice were housed in sterilized filter-top cages in a temperature-controlled room with a 12-h light/dark cycle and food and water were provided *ad libitum*. Mice were maintained on sterilized regular chow containing 4.3% (w/w) fat and no added cholesterol (RM3, Special Diet Services, Witham, UK) or fed Western-type diet (WTD) containing 15% (w/w) cacao butter and 0.25% (w/w) cholesterol (Diet W, Ab diets, Woerden, The Netherlands). Drinking water was supplied with antibiotics (83 mg/L ciprofloxacin and 67 mg/L polymyxin B sulfate) and 6.5 g/L sucrose. Animal experiments were performed at the Gorlaeus Laboratories of the Leiden/Amsterdam Center for Drug Research in accordance with the National Laws. All experimental protocols were approved by the Ethics Committee for Animal Experiments of Leiden University and carried out in compliance with the Dutch government guidelines.

Lipoprotein isolation and characterization

Non-HDL, HDL and lipoprotein-depleted serum (LPDS) were isolated from serum of $ApoAI^{+/+}/LDLr^{-/-}$ and $ApoAI^{-/-}/LDLr^{-/-}$ mice on WTD by sequential ultracentrifugation at

100,000 *g* for 24 h at densities <1.063, 1.063-1.21 and >1.21 g/mL, respectively [10]. After dialysis to PBS/1mM EDTA, the volume of the isolated fractions was adjusted to the original amount of serum from which it was isolated. HDL total and free cholesterol were determined using enzymatic colorimetric assays (Roche Diagnostics, Mannheim, Germany), with 0.03 U/mL cholesterol oxidase (Sigma Diagnostics, St. Louis, MO, USA), 0.065 U/mL peroxidase, and 15 μg/mL cholesteryl esterase (Seikagaku, Tokyo, Japan) in reaction buffer (1.0 KPi buffer, pH=7.7 containing 0.01 M phenol, 1 mM 4-amino-antipyrine, 1% polyoxyethylene-9-laurylether, and 7.5% methanol). The concentrations of phospholipids and triglycerides in HDL were determined using enzymatic colorimetric assays (Spinreact S.A., Girona, Spain and Roche Diagnostics, Mannheim, Germany, respectively). Protein concentrations were determined by the BCA method (Pierce, Brebières, France).

For analysis of the ApoAI and ApoE content of HDL and LPDS, 10 μL HDL or LPDS, isolated from ApoAI$^{+/+}$/LDLr$^{-/-}$ and ApoAI$^{-/-}$/LDLr$^{-/-}$ mice (corresponding to the amount of HDL in 10 μL serum) were mixed with 10 μL Laemli sample buffer (Bio-Rad, California, US) and incubated for 5 min at 100°C in the presence of β-mercaptoethanol (Sigma-Aldrich, St. Louis, MO, USA). Murine ApoAI and ApoE were separated by 10%-SDS polyacrylamide electrophoresis and detected by Western blot analysis with specific antibodies. Antiserum to mouse ApoAI was produced by subcutaneous immunization of a rabbit with the purified protein as previously described [11], whereas for detection of ApoE a commercial goat polyclonal anti-ApoE antibody was used (Santa Cruz Biotechnology, Inc., Heidelberg, Germany*)*. Mouse ApoAI and ApoE bands were evaluated with a Chemidoc 2000 densitometer and Quantity One software (Bio-Rad, California, USA) [10].

Macrophage cholesterol efflux studies

Bone marrow (BM) cells, isolated from ABCA1$^{+/+}$ and ABCA1$^{-/-}$ mice, were cultured for 7 days in complete RPMI medium supplemented with 20% fetal calf serum (FCS) and 30% L929 cell-conditioned medium, as the source of macrophage colony-stimulating factor (M-CSF), to generate BM-derived macrophages (BMDM).

Subsequently, cells were incubated with 2.5% endogenous non-HDL lipoproteins isolated from LDLr$^{-/-}$ and ApoAI$^{-/-}$/LDLr$^{-/-}$ serum in the presence of 0.5 μCi/mL [1α,2α(n)-^{3}H]-cholesterol in DMEM/0.2% BSA (fatty acid free) for 24 hours at 37°C. Cholesterol efflux was studied by incubation of the cells with DMEM/0.2% BSA supplemented with either 2.5% LPDS or 15 μg/mL HDL (protein concentration of HDL) isolated from the plasma of LDLr$^{-/-}$ and ApoAI$^{-/-}$/LDLr$^{-/-}$ mice. Radioactivity in the medium and the cells was determined by scintillation counting (Beckman Coulter, Woerden, the Netherlands) after 24 hours of incubation. Cholesterol efflux was calculated as the amount of radioactivity in the medium compared to the total amount of radioactivity measured in the medium plus cells.

In vivo macrophage-specific reverse cholesterol transport assay

BMDM from WT and ABCA1$^{-/-}$ mice were generated as described above. Subsequently, macrophages were loaded with 5 μCi/mL [1α,2α(n)-^{3}H]-cholesterol (Amersham Biosciences Europe GmbH, Germany) and 50 μg/mL of acetylated LDL (acLDL) in DMEM/0.2% BSA for 48 hours at 37^{o}C. The cells were washed, equilibrated and harvested by treatment with 4 mM EDTA for 15 min at 37^{o}C. Radioactivity incorporated in the macrophages was determined by liquid scintillation counting (Beckman). LDLr$^{-/-}$ and ApoAI$^{-/-}$/LDLr$^{-/-}$ mice fed WTD for 4 weeks were injected intraperitoneally with 2×10^{6}

^{3}H-cholesterol labeled-macrophages in 0.5 mL PBS (cell viability was above 75% in all cases, measured by trypan blue exclusion). Similar amounts of radioactivity were injected for ABCA1$^{+/+}$ and ABCA1$^{-/-}$ macrophages (with means of 13×10^{6} *vs* 10×10^{6} dpm/mouse, respectively). Blood was collected at 24 hours after injection and plasma was used for liquid scintillation counting (Beckman). Feces were collected, dried at 50^{o}C, weighed and rehydrated in 10 mL milliQ water overnight. Fecal samples were then homogenized and radioactivity was determined by liquid scintillation counting. The amount of ^{3}H-tracer in plasma and feces was expressed as a percent of the injected dose.

Bone marrow transplantation

To induce BM aplasia, male LDLr$^{-/-}$ and ApoAI$^{-/-}$/LDLr$^{-/-}$ recipient mice of 10-12 weeks old were exposed to a single dose of 9 Gy (0.19 Gy/min, 200 kV, 4 mA) total body irradiation using an Andrex Smart 225 Röntgen source (YXLON International, Hamburg, Germany) with a 6-mm aluminum filter 1 day before the transplantation (n=17-20 per group). BM was isolated by flushing the femurs and tibias from the donor ABCA1$^{+/+}$ and ABCA1$^{-/-}$ mice with phosphate-buffered saline (PBS). Single-cell suspensions were obtained by passing the cells through a 70-µm cell strainer (Falcon, The Netherlands). Irradiated recipients received $5x10^{6}$ BM cells by intravenous injection into the tail vein. After that, the transplanted LDLr$^{-/-}$ and ApoAI$^{-/-}$/LDLr$^{-/-}$ mice were maintained on regular chow diet for 8 weeks, to allow repopulation with donor-derived cells. To induce atherosclerosis, the transplanted mice were fed high fat WTD for an additional 6 weeks.

Blood and lipoprotein analyses

After an overnight fast, ~100 µL of blood was drawn from each mouse by tail bleeding. The concentrations of total cholesterol (TC) in serum were determined as described above. HDL cholesterol was measured after precipitation with phosphotungstic acid and magnesium ions (Roche Diagnostics GmbH, Mannheim, Germany). For this purpose, lipidemic plasmas were diluted 1:2 with saline prior to precipitation of ApoB-containing lipoproteins and, in all cases, the supernatant was clear. Non-HDL cholesterol was calculated as the difference between TC and HDL cholesterol [12]. Precipath I (Roche Diagnostics, Mannheim, Germany) was used as an internal standard.

Histological analysis of the aortic root and arch

Upon sacrifice, hearts and descending aortas were excised and stored in 3.7% neutral-buffered formalin (Formal-fixx; Shandon Scientific Ltd, UK) after *in situ* perfusion. Next, 10-µm cross-sections were made of the aortic roots using a cryostate, while aortic arches were cut longitudinally. Mean atherosclerotic lesion area (in μm^{2}) was calculated from 10 oil-red-O/hematoxylin-stained sections of the aortic root, starting at the appearance of the tricuspid valves, and from 10 sections with maximal lesion area of the aortic arch.

The collagen content of the lesions was visualized by a Masson's Trichrome staining according to the manufacturer's instructions (Sigma Diagnostics, St. Louis, MO, USA). Macrophages, T cells, and neutrophils in the atherosclerotic lesions were stained by immunohistochemistry with antibodies directed against the macrophage specific antigen MOMA2 (monoclonal rat IgG2b, Research Diagnostics Inc, NJ), CD3 (polyclonal rabbit IgG, Neomarkers, USA) and Ly6G (monoclonal rat IgG2b, eBioscience, Austria), respectively. The collagen, macrophage, and neutrophil positive area of the lesions were quantified and expressed as percentage of total lesion area (five sections from each mouse). All quantifications were performed blinded by using the Leica image analysis system,

consisting of a Leica DMRE microscope coupled to a video camera and Leica Qwin Imaging software (Leica Ltd., Cambridge, UK).

Quantification of macrophage and neutrophil recruitment into liver and spleen

At sacrifice, spleen and liver were isolated and single cell suspension were obtained by squeezing the organs through a 70-μm cell strainer (Falcon). Red blood cells were removed from the splenocyte suspension using erythrocyte lysis buffer (0.15 M NH_4Cl, 10 mM $NaHCO_3$, 0.1 mM EDTA, pH 7.3). Leukocytes in spleen and liver were stained using antibodies directed against CD11b and Ly6G according to the manufacturer's protocol (eBioscience). Neutrophils ($CD11b^+Ly6G^+$) and macrophages ($CD11b^+Ly6G^-$) were quantified by Flow cytometry (FACSCantoII, Beckton Dickinson, CA). Data were analyzed using FACSDiva software (Beckton Dickinson).

White blood cell analysis

Upon sacrifice of the transplanted mice at 14 weeks after transplantation, the blood was collected as before [13]. Lymphocyte, monocyte, and neutrophil counts were quantified using an automated Sysmex XT-2000iV Veterinary Hematology analyzer (Sysmex Corporation, Kobe, Japan). The XT-2000iV employs a fluorescent flow cytometry method using a fluorescent dye staining cellular DNA and RNA and a semiconductor laser to detect forward-, side-scattered, and fluorescent light.

Determination of plasma levels of MCP-1 and KC

Commercial ELISA kits were used for determination of monocyte chemotactic protein-1 (MCP-1) (eBioscences) and keratinocyte-derived chemokine (KC) (Invitrogen) according to manufacturer's instructions.

Data analyses

Data are expressed as mean ± S.E.M. A one way ANOVA and the Student Newman Keuls posttest were used to compare means after confirming normal distribution by the method of Kolmogorov and Smirnov using Graphpad Instat Software (San Diego, USA). *P* value <0.05 was considered statistically significant.

Results

ApoAI was required for macrophage ABCA1-facilitated reverse cholesterol transport

To determine the interrelationship between macrophage ABCA1 and ApoAI in RCT, the cholesterol efflux rate from $ABCA1^{+/+}$ and $ABCA1^{-/-}$ BMDM to 2.5% endogenous LPDS and 15 μg/mL HDL, isolated from WTD-fed $ApoAI^{+/+}/LDLr^{-/-}$ and $ApoAI^{-/-}/LDLr^{-/-}$ mice, was analyzed (Figure 1A). Deletion of ABCA1 in macrophages led to a 1.7-fold ($p<0.01$) and 1.6-fold ($p<0.001$) reduction in cholesterol efflux to LPDS and HDL of $ApoAI^{+/+}/LDLr^{-/-}$ mice, respectively. Also, absence of ApoAI impaired the cholesterol efflux capacity of LPDS (1.3-fold, $p<0.05$) and HDL (1.6-fold, $p<0.001$) from $ABCA1^{+/+}$ macrophages. Interestingly, no further decrease in efflux was observed from $ABCA1^{-/-}$ macrophages to LPDS and HDL of $ApoAI^{-/-}/LDLr^{-/-}$ mice (Figure 1A), indicating that ApoAI is essential for ABCA1-mediated cholesterol efflux from macrophages. As shown in Supplementary Figure 1A, HDL of $ApoAI^{-/-}/LDLr^{-/-}$ mice contains more free cholesterol (7% *vs* 3%) and triglycerides (4% *vs* 1%) and less protein (41% *vs* 47%) as compared to

that of LDLr$^{-/-}$ mice. However, the main difference is that ApoE is the major apolipoprotein of HDL in ApoAI$^{-/-}$/LDLr$^{-/-}$ mice instead of ApoAI in ApoAI$^{+/+}$/LDLr$^{-/-}$ mice (Supplementary Figure 1B). The finding that macrophage ABCA1 deficiency did not affect cholesterol efflux to HDL of ApoAI$^{-/-}$/LDLr$^{-/-}$ mice thus indicates that the ApoE-rich HDL from these animals does not serve as an acceptor for ABCA1-mediated efflux. Of note, ApoE was not detectable in LPDS of either ApoAI$^{+/+}$/LDLr$^{-/-}$ or ApoAI$^{-/-}$/LDLr$^{-/-}$ mice (data not shown).

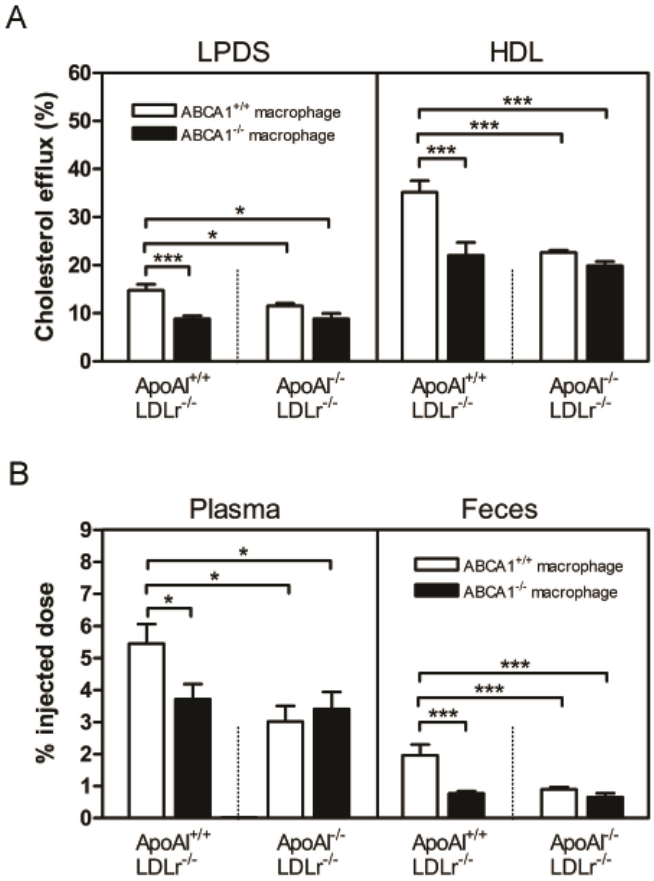

Figure 1. Macrophage ABCA1 deficiency does not impair macrophage RCT in absence of ApoAI. **(A)** Cholesterol efflux was studied by incubation of cholesterol labelled ABCA1$^{+/+}$ (open bar) and ABCA1$^{-/-}$ (close bar) BMDM with DMEM/0.2% BSA alone or supplemented with either 2.5% LPDS or 15 µg/mL HDL from either LDLr$^{-/-}$ or ApoAI$^{-/-}$/LDLr$^{-/-}$ plasmas. **(B)** ^{3}H-cholesterol return to the circulation and feces from ABCA1$^{+/+}$ (open bar) or ABCA1$^{-/-}$ (close bar) macrophage foam cells loaded with acLDL was measured at 24 hours after injection into peritoneal cavity of either LDLr$^{-/-}$ or ApoAI$^{-/-}$ /LDLr$^{-/-}$ mice. Values represent the mean ± SEM. Statistically significant difference **P*<0.05 and ****P*<0.001.

Next, the importance of circulating ApoAI for macrophage ABCA1-facilitated *in vivo* RCT was investigated. Hereto, ApoAI$^{+/+}$/LDLr$^{-/-}$ and ApoAI$^{-/-}$/LDLr$^{-/-}$ mice fed WTD were injected intraperitoneally with ^{3}H-cholesterol labeled/acLDL loaded ABCA1$^{+/+}$ or ABCA1$^{-/-}$ BMDM. Transport of labeled cholesterol from the macrophages to the circulation and feces was assessed after 24 hours (Figure 1B). In agreement with previous studies [14], transport of radiolabeled tracer into the circulation and the feces was reduced 1.5-fold ($p<0.05$) and 2.6-fold ($p<0.001$) by macrophage ABCA1 deficiency in ApoAI$^{+/+}$/LDLr$^{-/-}$ mice, respectively. Also, absence of circulating ApoAI led to a 1.8-fold ($p<0.05$) and 2.2-fold ($p<0.001$) decreased recovery of the tracer in plasma and feces,

respectively upon injection of ABCA1$^{+/+}$ macrophages into ApoAI$^{-/-}$/LDLr$^{-/-}$ mice. Interestingly, when ABCA1$^{-/-}$ macrophages were injected into ApoAI$^{-/-}$/LDLr$^{-/-}$ mice, a similar reduction of tracer cholesterol was detected in both plasma (1.6-fold, $p<0.05$) and feces (3.0-fold, $p<0.001$). Thus, in agreement with the *in vitro* cholesterol efflux studies, deletion of macrophage ABCA1 did not further impair *in vivo* macrophage-specific RCT in absence of circulating ApoAI.

Leukocyte ABCA1 deficiency reduced non-HDL cholesterol in absence of circulating ApoAI

To investigate the importance of ApoAI for the atheroprotective effects of leukocyte ABCA1, ApoAI$^{+/+}$/LDLr$^{-/-}$ or ApoAI$^{-/-}$/LDLr$^{-/-}$ mice were transplanted with bone marrow from ABCA1$^{+/+}$ and ABCA1$^{-/-}$ mice. During the first 8 weeks after bone marrow transplantation, animals were fed regular chow. As shown in Table 1, leukocyte ABCA1 deficiency did not affect plasma cholesterol levels in ApoAI$^{+/+}$/LDLr$^{-/-}$ or ApoAI$^{-/-}$/LDLr$^{-/-}$ mice on chow. In line with previous observations [15], ApoAI$^{-/-}$/LDLr$^{-/-}$ mice on chow did show reduced (~1.3-fold, $p<0.01$) total plasma cholesterol levels, mainly due to a virtual absence of HDL cholesterol (Table 1). To induce atherosclerotic lesion development, animals were fed WTD for an additional 6 weeks. As previously shown [13, 16], upon challenge with WTD, leukocyte ABCA1 deficiency resulted in lower total (1.2-fold, $p<0.05$) and non-HDL cholesterol (1.3-fold, $p<0.05$) levels in ApoAI$^{+/+}$/LDLr$^{-/-}$ mice (Table 1). Also, ApoAI$^{-/-}$/LDLr$^{-/-}$ mice reconstituted with ABCA1$^{-/-}$ bone marrow showed a 1.7-fold ($p<0.001$) reduction in both total and non-HDL cholesterol levels as compared to ApoAI$^{-/-}$/LDLr$^{-/-}$ mice transplanted with ABCA1$^{+/+}$ bone marrow. The effect of leukocyte ABCA1 deficiency on plasma cholesterol levels is thus independent of the presence of ApoAI.

Table 1. Plasma cholesterol levels in ApoAI$^{+/+}$/LDLr$^{-/-}$ and ApoAI$^{-/-}$/LDLr$^{-/-}$ mice transplanted with ABCA1$^{+/+}$ or ABCA1$^{-/-}$ bone marrow after 8 weeks on chow diet and 6 weeks on WTD.

Diet	Experimental group	Total cholesterol (mg/dL)	Non-HDL cholesterol (mg/dL)	HDL cholesterol (mg/dL)
Chow	ABCA1 $^{BM+/+}$ → ApoAI$^{+/+}$/LDLr$^{-/-}$	232.9 ± 8.6	148.2 ± 16.2	84.7 ± 15.9
	ABCA1 $^{BM-/-}$ → ApoAI$^{+/+}$/LDLr$^{-/-}$	213.1 ± 3.8	115.2 ± 14.3	99.7 ± 14.5
	ABCA1 $^{BM+/+}$ → ApoAI$^{-/-}$/LDLr$^{-/-}$	180.1 ± 7.5 **	173.4 ± 9.2	6.0 ± 2.6 $^{***, \#\#\#}$
	ABCA1 $^{BM-/-}$ → ApoAI$^{-/-}$/LDLr$^{-/-}$	174.7 ± 15.7 **	170.4 ± 16.1	4.2 ± 1.3 $^{***, \#\#\#}$
WTD	ABCA1 $^{BM+/+}$ → ApoAI$^{+/+}$/LDLr$^{-/-}$	587.5 ± 47.3	546.6 ± 46.8	40.8 ± 6.2
	ABCA1 $^{BM-/-}$ → ApoAI$^{+/+}$/LDLr$^{-/-}$	471.6 ± 16.3 *	436.7 ± 17.7 *	34.9 ± 4.3
	ABCA1 $^{BM+/+}$ → ApoAI$^{-/-}$/LDLr$^{-/-}$	652.5 ± 42.2 $^{\#\#}$	647.1 ± 42.8 $^{\#\#\#}$	5.3 ± 0.8 $^{***, \#\#\#}$
	ABCA1 $^{BM-/-}$ → ApoAI$^{-/-}$/LDLr$^{-/-}$	388.8 ± 32.5 $^{**, \partial\partial\partial}$	383.9 ± 32.7 $^{**, \partial\partial\partial}$	4.8 ± 1.4 $^{***, \#\#\#}$

Values represent the mean ± SEM. Statistically significant difference *$p<0.05$, **$p<0.01$, ***$p<0.001$ *vs* ABCA1 $^{BM+/+}$ → ApoAI$^{+/+}$/LDLr$^{-/-}$. $^{\#}p<0.05$, $^{\#\#}p<0.01$, $^{\#\#\#}p<0.001$ *vs* ABCA1 $^{BM-/-}$ → ApoAI$^{+/+}$/LDLr$^{-/-}$. $^{\partial}p<0.05$, $^{\partial\partial}p<0.01$, $^{\partial\partial\partial}p<0.001$ *vs* ABCA1 $^{BM+/+}$ → ApoAI$^{-/-}$/LDLr$^{-/-}$.

Leukocyte ABCA1 deficiency enhances atherosclerotic lesion development and promotes the recruitment of neutrophils into lesions in absence of circulating ApoAI

Atherosclerotic lesion development was evaluated at the aortic root and aortic arch of the transplanted animals after 6 weeks WTD feeding. At the aortic root, leukocyte ABCA1 deficiency in ApoAI$^{+/+}$/LDLr$^{-/-}$ mice resulted in a ~2.8-fold ($p<0.05$) increase in lesion size

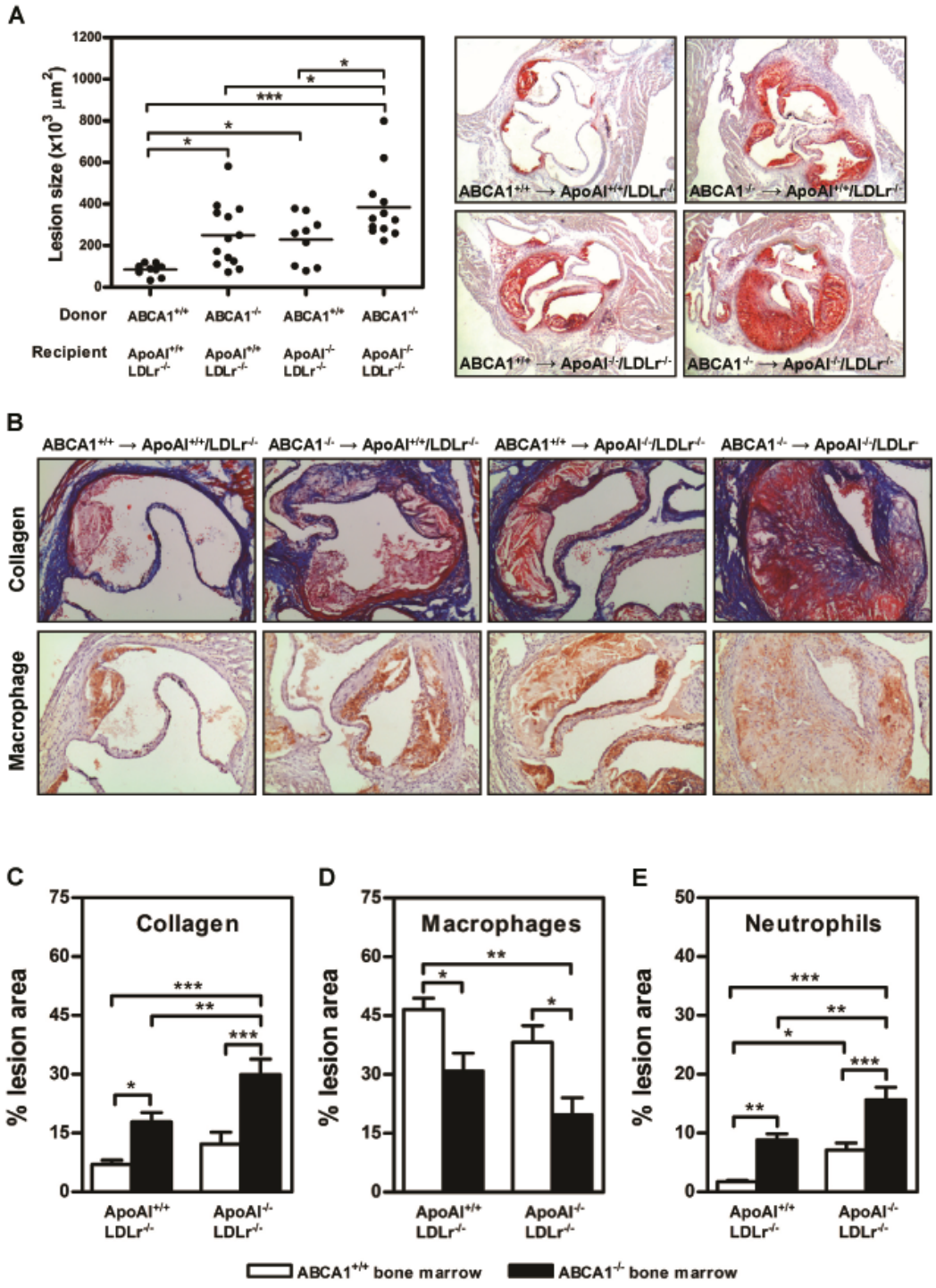

Figure 2. Enhanced atherosclerotic lesion development in the aortic root of ApoAI$^{-/-}$/LDLr$^{-/-}$ mice reconstituted with ABCA1$^{-/-}$ bone marrow after 6 weeks on WTD. (A) Photomicrographs showing a scatter dot plot of atherosclerotic lesion quantification (left panel) and representative Oil-red-O stained sections (right panel, original magnification 40x). Each symbol represents the mean lesion area in a single mouse. The horizontal line represents the mean of the group. (B) Photomicrographs showing the lesion compositions in the aortic root of mice. Sections of the aortic roots were stained with antibody against Moma-2 to visualize macrophages (100x). Morphological staining of atherosclerotic lesions in the aortic root with Masson's Trichrome Accustain, which stains cytoplasma and muscle fiber red and collagen blue (100x). Bar graphs showing the amount of collagen (C), macrophages (D), and neutrophils (E) in the lesion. Neutrophils were visualized by immunohistochemistry staining using antibody against Ly6G. Values represent the mean ± SEM of ≥11 (root) and 6 (arch) mice per group. Statistically significant difference *P<0.05, **P<0.01, and ***P<0.001.

(Figure 2A). Similarly, circulating ApoAI deficiency increased the lesion size 2.7-fold ($p<0.05$) in mice transplanted with $ABCA^{+/+}$ bone marrow. Interestingly, deletion of leukocyte ABCA1 in $ApoAI^{-/-}/LDLr^{-/-}$ mice aggravated atherosclerotic lesion development an additional 1.6-fold ($P<0.05$) (Figure 2A). This clearly indicates that leukocyte ABCA1 protects against atherosclerosis even in absence of circulating ApoAI. Quantification of lesion composition showed that leukocyte ABCA1 deficiency was associated with more collagen (2.6-fold, $p<0.05$, in $ApoAI^{+/+}/LDLr^{-/-}$ mice; 2.5-fold, $p<0.001$, in $ApoAI^{-/-}/LDLr^{-/-}$ mice) and less macrophages (1.5-fold, $p<0.05$, in $ApoAI^{+/+}/LDLr^{-/-}$ mice; 1.9-fold, $p<0.05$, in $ApoAI^{-/-}/LDLr^{-/-}$ mice) in lesions (Figure 2B, 2C and 2D). It must be noted that $ApoAI^{-/-}/LDLr^{-/-}$ mice transplanted with $ABCA1^{-/-}$ bone marrow showed 1.7-fold ($p<0.01$) higher collagen and 1.6-fold ($p=0.10$) lower macrophage content of lesions as compared to $ApoAI^{+/+}/LDLr^{-/-}$ mice transplanted with $ABCA1^{-/-}$ bone marrow (Figure 2B, 2C and 2D). Thus, in absence of circulating ApoAI, leukocyte ABCA1 deficiency led to the formation of more advanced lesions in the aortic root.

In addition, other inflammatory cells, including T cells and neutrophils, were analysed in lesions at the aortic root. Only a limited amount of T cells was visible in lesions and there was no difference between the different groups of transplanted animals (data not shown). Neutrophils in lesions of $ApoAI^{+/+}/LDLr^{-/-}$ mice transplanted with $ABCA1^{-/-}$ bone marrow, however, were increased 5.1-fold ($p<0.01$ *vs* $ApoAI^{+/+}/LDLr^{-/-}$ mice transplanted with $ABCA1^{+/+}$ bone marrow) (Figure 2E). Also, a similar 4.1-fold ($p<0.05$) increase in neutrophils was evident as a result of circulating ApoAI deficiency in mice transplanted with $ABCA1^{+/+}$ bone marrow. Strikingly, deletion of leukocyte ABCA1 in $ApoAI^{-/-}/LDLr^{-/-}$ mice promoted neutrophil recruitment into lesions an additional 2.2-fold ($p<0.001$ *vs* $ApoAI^{-/-}/LDLr^{-/-}$ mice transplanted with $ABCA1^{+/+}$ bone marrow).

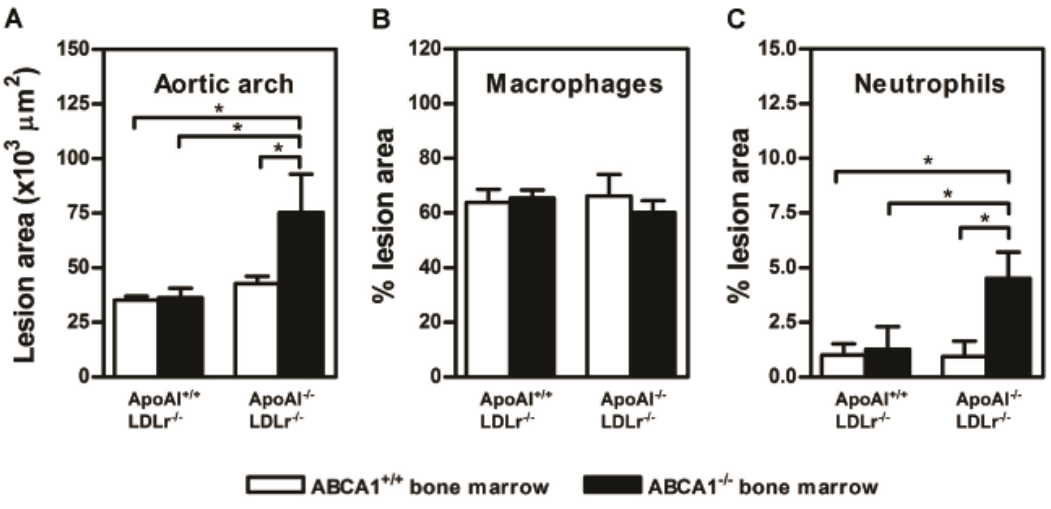

Figure 3. Enhanced atherosclerotic lesion development in the aortic arch of $ApoAI^{-/-}/LDLr^{-/-}$ mice reconstituted with $ABCA1^{-/-}$ bone marrow after 6 weeks on WTD. Bar graphs showing the mean lesion area (A) developed in the aortic arch, and relative amount of macrophages (B) and neutrophils (C) in lesions of aortic arch. Values represent the mean ± SEM. Statistically significant difference **P*<0.05.

In mouse models of atherosclerosis, the aortic root is the site most susceptible to lesion development. In line, much smaller lesions were observed in the aortic arch of the transplanted animals after 6 weeks WTD challenge. The mean lesion size at the aortic arch of $ApoAI^{+/+}/LDLr^{-/-}$ mice transplanted with $ABCA1^{+/+}$ bone marrow was only 35±2 $x10^3$

μm^2, as compared to 86±9 $x10^3$ μm^2 in the aortic root (Figure 3A). Strikingly, leukocyte ABCA1 deficiency in $ApoAI^{+/+}/LDLr^{-/-}$ mice did not enhance lesion development at this site; neither did deficiency of circulating ApoAI in animals transplanted with $ABCA1^{+/+}$ bone marrow. However, leukocyte ABCA1 deficiency in $ApoAI^{-/-}/LDLr^{-/-}$ mice did lead to a 1.8-fold ($p<0.05$) increase in lesion size in the aortic arch, demonstrating again that leukocyte ABCA1 deficiency enhances atherosclerosis susceptibility in absence of ApoAI (Figure 3A). The enlarged lesions at the aortic arch of $ApoAI^{-/-}/LDLr^{-/-}$ mice transplanted with $ABCA1^{-/-}$ bone marrow were fatty streak lesions, primarily composed of macrophages (Figure 3B). However, also in these early lesions, neutrophils were increased 4.8-fold ($p<0.05$) upon deletion of leukocyte ABCA1 in $ApoAI^{-/-}/LDLr^{-/-}$ mice (Figure 3C). Taken together, leukocyte ABCA1 prevented the development of atherosclerotic lesions and inhibited recruitment of neutrophils into lesions in absence of circulating ApoAI.

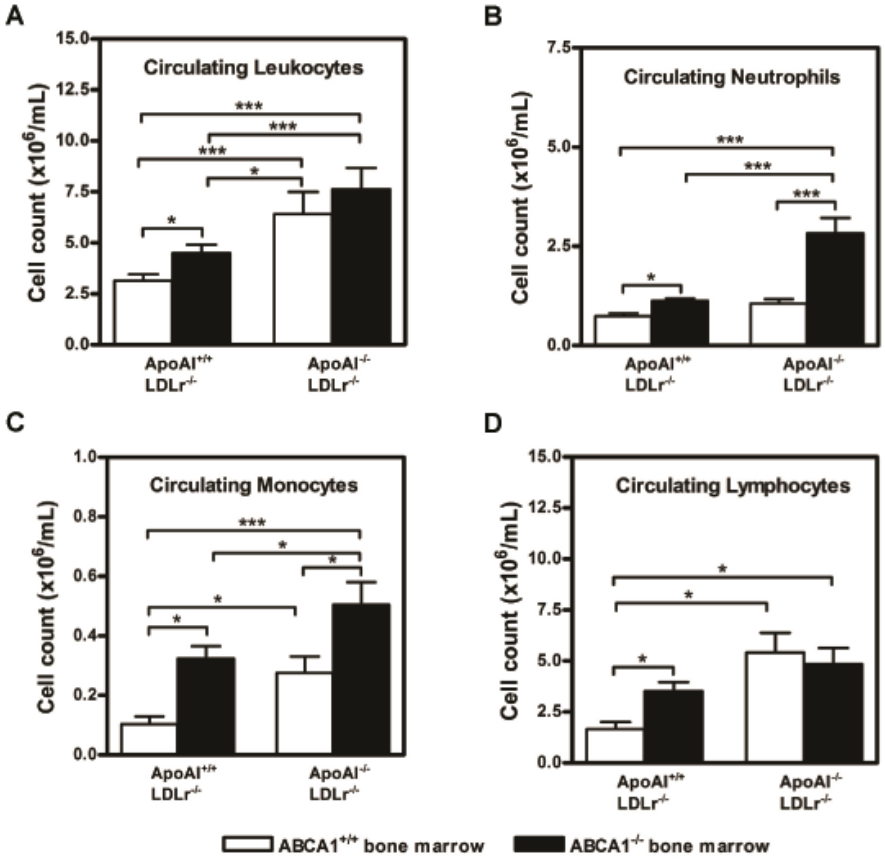

Figure 4. Increased leukocytosis in $ApoAI^{-/-}/LDLr^{-/-}$ mice reconstituted with $ABCA1^{-/-}$ bone marrow after 6 weeks on WTD. Leukocytes (A), neutrophils (B), monocytes (C), and lymphocytes (D) in whole blood were analyzed using a Sysmex XT-2000iV Hematology Analyzer. Values represent the mean ± SEM. Statistically significant difference **P*<0.05 and ****P*<0.001.

Leukocyte ABCA1 deficiency increases neutrophilia and monocytosis in absence of circulating ApoAI

To investigate if the enhanced neutrophil infiltration observed in atherosclerotic lesions and peripheral tissues was the consequence of neutrophilia in the circulation, blood leukocyte counts were analyzed. As previously described [9], disruption of leukocyte ABCA1 in $ApoAI^{+/+}/LDLr^{-/-}$ mice led to leukocytosis (1.6-fold, $p<0.05$), including neutrophilia (1.7-fold, $p<0.05$), monocytosis (1.9-fold, $p<0.05$), and lymphocytosis (Figure

4A-D). Leukocytosis was more severe in ApoAI$^{-/-}$/LDLr$^{-/-}$ mice with functional ABCA1 (2.2-fold increase, p<0.001). However, only a trend towards increased neutrophil counts (1.4-fold, p=0.0605) was observed in ApoAI$^{-/-}$/LDLr$^{-/-}$ mice reconstituted with ABCA1$^{+/+}$ bone marrow as compared to ApoAI$^{+/+}$/LDLr$^{-/-}$ mice transplanted with ABCA1$^{+/+}$ bone marrow (Figure 4B). Leukocytosis induced by absence of circulating ApoAI in animals transplanted with ABCA1$^{+/+}$ bone marrow was mainly due to increased amounts of monocytes (2.7-fold, p<0.05) (Figure 4C) and lymphocytes (3.3-fold, p<0.05) (Figure 4D). Interestingly, despite no further induction of leukocytosis and lymphocytosis, leukocyte ABCA1 deficiency in ApoAI$^{-/-}$/LDLr$^{-/-}$ mice led to higher neutrophil (2.7-fold, p<0.001) (Figure 4B) and, to a lesser extent, monocyte (1.8-fold, p<0.05) counts (Figure 4C). Leukocyte ABCA1 thus inhibits monocytosis and neutrophilia even in absence of circulating ApoAI.

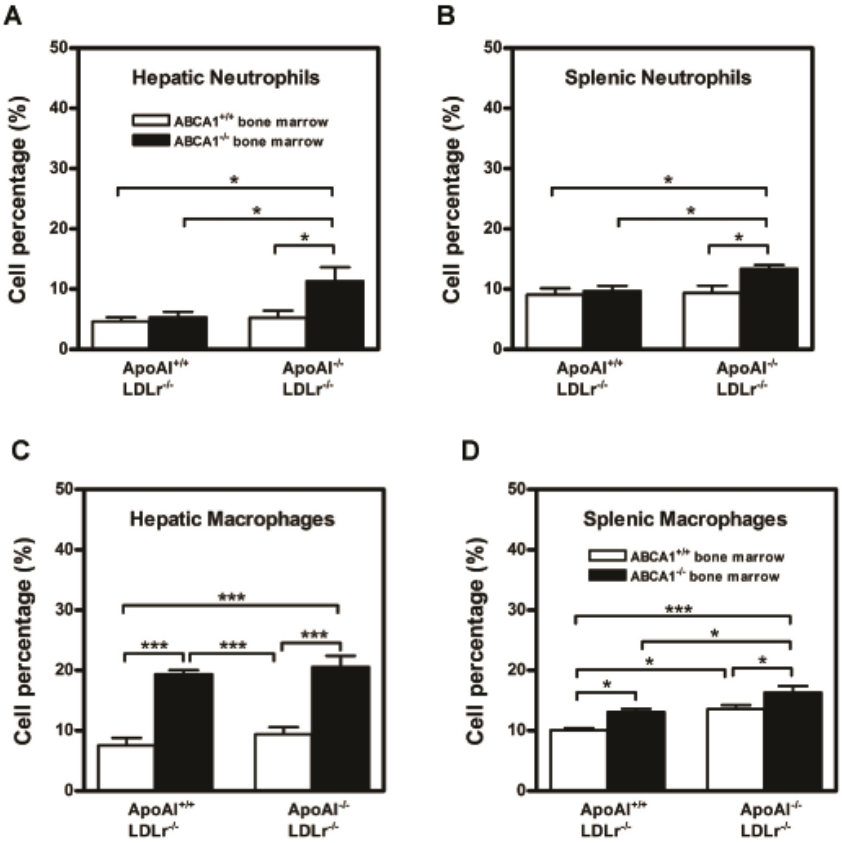

Figure 5. Enhanced recruitment of neutrophils and monocytes into the liver and spleen of ApoAI$^{-/-}$/LDLr$^{-/-}$ mice reconstituted with ABCA1$^{-/-}$ bone marrow after 6 weeks on WTD. Neutrophils and macrophages in the liver (A and C) and spleen (B and D) were quantified by flowcytometry as described in methods. Values represent the mean ± SEM. Statistically significant difference *P<0.05 and ***P<0.001.

Leukocyte ABCA1 deficiency promotes recruitment of neutrophils and monocytes into peripheral tissues in absence of circulating ApoAI

To investigate whether the observed increase in neutrophilia and monocytosis could lead to enhanced recruitment of neutrophils and monocytes into peripheral tissues, the amount of macrophages in liver and spleen was evaluated next. Accumulation of neutrophils in liver and spleen was not influenced by either leukocyte ABCA1 deficiency in ApoAI$^{+/+}$/LDLr$^{-/-}$ mice or absence of circulating apoAI in animals transplanted with ABCA1$^{+/+}$ bone marrow (Figure 5A and 5B). However, similar as observed in lesions, leukocyte ABCA1

deficiency in ApoAI$^{-/-}$/LDLr$^{-/-}$ mice increased neutrophil accumulation in both the liver (~2.0-fold, $p<0.05$) and the spleen (~1.5-fold, $p<0.05$). As previously shown [14], the amount of macrophages was elevated in liver (2.6-fold, $p<0.001$) and spleen (1.3-fold, $p<0.05$) upon disruption of leukocyte ABCA1 in ApoAI$^{+/+}$/LDLr$^{-/-}$ mice (Figure 5C and 5D). Also, leukocyte ABCA1 deficiency in ApoAI$^{-/-}$/LDLr$^{-/-}$ mice induced macrophage recruitment into liver (2.2-fold, $p<0.05$) and spleen (1.2-fold, $p<0.05$) (Figure 5C and 5D). However, absence of circulating apoAI in mice transplanted with ABCA1$^{+/+}$ bone marrow only led to a slight increase in macrophage accumulation in spleen (1.3-fold, $p<0.05$) but not liver.

Leukocyte ABCA1 deficiency increases the plasma levels of MCP-1 and KC

Pro-inflammatory chemokines MCP-1 and KC are known inducers of monocytosis and neutrophilia, respectively [17, 18]. Therefore, the plasma levels of MCP-1 and KC were determined. The concentrations of MCP-1 and KC in plasma were increased ~3.0-fold ($p<0.05$) and ~2.5-fold ($p<0.05$), respectively by deletion of leukocyte ABCA1 in both ApoAI$^{+/+}$/LDLr$^{-/-}$ and ApoAI$^{-/-}$/LDLr$^{-/-}$ mice (Figure 7A and 6B). However, absence of circulating ApoAI in the transplanted animals did not affect the plasma levels of MCP-1 and KC, indicating that the effects of leukocyte ABCA1 deficiency on plasma levels of MCP-1 and KC are independent of the presence of circulating ApoAI.

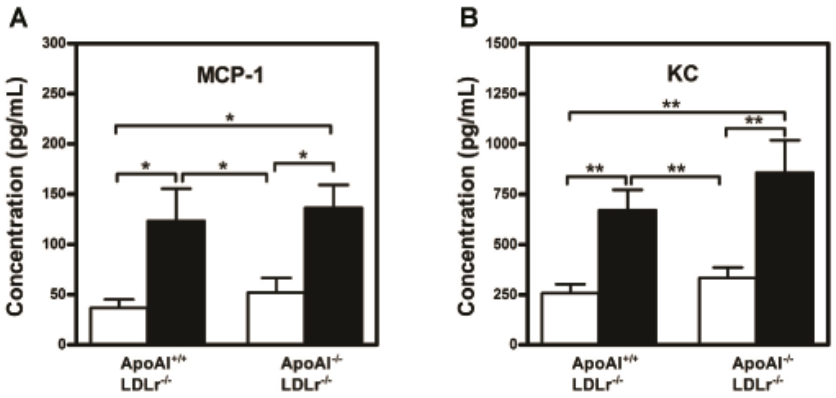

Figure 6. Increased plasma levels of MCP-1 and KC in the ApoAI$^{-/-}$/LDLr$^{-/-}$ mice reconstituted with ABCA1$^{-/-}$ bone marrow after 6 weeks on WTD. MCP-1 (A) and KC (B) were determined by ELISA. Values represent the mean ± SEM. Statistically significant difference *$P<0.05$ and **$P<0.01$.

Discussion

The present study for the first time assessed the importance of circulating ApoAI for macrophage ABCA1-facilitated RCT and the atheroprotective effects of leukocyte ABCA1. *In-vitro* cholesterol efflux and *in-vivo* macrophage RCT studies demonstrated the functional partnership of macrophage ABCA1 and ApoAI for these processes. Unexpectedly, our studies also established that leukocyte ABCA1 ameliorates atherosclerotic lesion development in absence of circulating ApoAI. These ApoAI-independent atheroprotective effects of leukocyte ABCA1 were associated with suppression of monocytosis and neutrophilia in the circulation and reduction of plasma levels of MCP-1 and KC, important chemoattractants of these cell types.

Functional macrophage RCT is regarded crucial for prevention of atherosclerosis [19]. Previously, the importance of ABCA1 for macrophage RCT has been unequivocally established both *in vitro* [20] and *in vivo* [14, 21]. In agreement, in the current study we show

that macrophage ABCA1 deficiency inhibited cholesterol efflux to LPDS and HDL from ApoAI$^{+/+}$/LDLr$^{-/-}$ mice and led to impaired macrophage RCT *in vivo*. Moreover, in line with a previous study [22], absence of ApoAI in LDLr$^{-/-}$ mice reduced RCT from macrophages with functional ABCA1 expression. This can likely be attributed to the virtual absence of HDL in these animals. In addition, we showed that the HDL that circulates in ApoAI$^{-/-}$/LDLr$^{-/-}$ mice, which is rich in apoE, has a reduced cholesterol efflux capacity. ABCA1 mediates cholesterol efflux from macrophages not only to ApoAI, but also to other lipid-free/poor apolipoproteins, including ApoE [23]. Deletion of macrophage ABCA1, however, did not reduce cholesterol efflux to HDL of ApoAI$^{-/-}$/LDLr$^{-/-}$ mice. Also using LPDS from ApoAI$^{-/-}$/LDLr$^{-/-}$ mice as a lipid acceptor, the primary source of lipid-free apolipoproteins, no effect of macrophage ABCA1 deficiency was found. Of note, no ApoE was found in the LPDS that was added as acceptor. Also, endogenous ApoE secreted by the macrophages was apparently not sufficient to induce ABCA1-mediated efflux under these conditions.

The effects of leukocyte ABCA1 on atherosclerosis have been investigated using bone marrow transplantation studies. Selective inactivation of leukocyte ABCA1 accelerates atherosclerosis [9, 24], while overexpression of leukocyte ABCA1 inhibits atherosclerotic lesion progression [25]. ABCA1-faciliated macrophage cholesterol efflux and RCT were considered the primary contributors to the atheroprotective effects of leukocyte ABCA1. In the present study, we found that leukocyte ABCA1 deficiency induced atherosclerotic lesion development even in absence of circulating ApoAI, despite the fact that macrophage RCT in ApoAI$^{-/-}$/LDLr$^{-/-}$ mice was not further impaired by deletion of macrophage ABCA1. Thus, the atheroprotective effects of leukocyte ABCA1 cannot be solely attributed to induction of macrophage cholesterol efflux and RCT, especially under conditions in which circulating ApoAI is absent. Atherosclerotic lesion development results from a combination of hypercholesterolemia and an inflammatory response. In addition to their roles in macrophage RCT, both ABCA1 and ApoAI also have anti-inflammatory functions [22, 26]. Importantly, in absence of circulating ApoAI, leukocyte ABCA1 deficiency induced neutrophilia and monocytosis in the circulation, enhanced the recruitment of neutrophils and monocytes into peripheral tissues, as well as increased the plasma levels of pro-inflammatory chemokines MCP-1 and KC. Furthermore, neutrophil accumulation in lesions of ApoAI$^{-/-}$/LDLr$^{-/-}$ mice transplanted with ABCA1$^{-/-}$ bone marrow was largely increased. These ApoAI-independent anti-inflammatory properties of leukocyte ABCA1 could thus contribute to its atheroprotective effects.

Hypercholesterolemia induces monocytosis [27] and neutrophilia [30], mainly due to increased proliferation of bone marrow cells [27, 30]. In the current study, leukocytosis was evident in ApoAI$^{-/-}$/LDLr$^{-/-}$ mice transplanted with ABCA1$^{+/+}$ bone marrow. Moreover, consistent with our previous findings [9], deletion of leukocyte ABCA1 in ApoAI$^{+/+}$/LDLr$^{-/-}$ mice was associated with elevated levels of leukocytes. Interestingly, in absence of circulating ApoAI, leukocyte ABCA1 deficiency further enhanced monocytosis and neutrophilia, indicating that the effects of ApoAI and leukocyte ABCA1 on these processes are, at least partly, independent. In agreement, Yvan-Charvet et al. recently demonstrated that overexpression of ApoAI suppresses the proliferation of hematopoietic stem cells (HSC) deficient of ABCA1 and ABCG1 [29]. In addition, important inducers of monocytosis [17] and neutrophilia [18] include not only growth factors GM-CSF (granulocyte-macrophage colony-stimulating factor) [30] and G-CSF [31] but also pro-inflammatory chemokines MCP-1 and KC. Deletion of ABCA1 induces the secretion of MCP-1 [32] and KC [Zhao Y, unpublished data] by macrophages. In line, the plasma levels of MCP-1 and KC were elevated upon deletion of leukocyte ABCA1 in both ApoAI$^{+/+}$/LDLr$^{-/-}$ and ApoAI$^{-/-}$/LDLr$^{-/-}$

mice. No effect was observed of ApoAI deficiency, indicating that leukocyte ABCA1 does not require ApoAI to maintain low levels of MPC-1 and KC secretion.

Epidemiological observations showed that leukocytosis, especially monocytosis and neutrophilia, is strongly associated with the progression of atherosclerosis [33]. Monocytes are widely regarded as key cellular protagonists of atherosclerosis [34, 35]. Accumulation of monocytes in atherosclerotic lesions is progressive and correlates with lesion size [36]. Deficiency of MCP-1, an important chemoattractant of monocytes, inhibits monocyte recruitment into lesions and hence reduces atherosclerotic lesion formation [37]. The observed increase in plasma levels of MCP-1 upon deletion of leukocyte ABCA1 might thus have aided the increase in lesion development in ApoAI$^{+/+}$/LDLr$^{-/-}$ and ApoAI$^{-/-}$/LDLr$^{-/-}$ mice. Moreover, deletion of ABCA1 on macrophages increases their migratory capacity in response to chemotactic factors [32]. In line, enhanced macrophage accumulation in the liver and spleen was evident in animals transplanted with ABCA1$^{-/-}$ bone marrow. Similar effects on MCP-1 and macrophage accumulation in tissues were observed in both ApoAI$^{+/+}$/LDLr$^{-/-}$ and ApoAI$^{-/-}$/LDLr$^{-/-}$ recipients, indicating that these are not the causative factors for the increased lesion development in the latter. The level of monocytosis, however, was higher in ApoAI$^{-/-}$/LDLr$^{-/-}$ recipients, suggesting that increased monocyte pressure from the circulation might have contributed to the enhanced atherosclerotic lesion development in ApoAI$^{-/-}$/LDLr$^{-/-}$ mice transplanted with ABCA1$^{-/-}$ bone marrow. Lately, several animal studies unveiled a prominent role of neutrophils in atherogenesis [28, 38-40, 41]. Upon activation, neutrophils release mediators that have been implicated in the pathogenesis of coronary artery disease, such as oxygen radicals, cytokines and matrix metalloproteinases [30, 38-40]. Drechsler et al demonstrated that neutrophils infiltrate early lesions of apoE-/- mice on a high fat diet (HFD; 21% fat), while numbers decline in more advanced lesions. Furthermore, depletion of neutrophils inhibited the development of early lesions after 4 weeks HFD feeding, but not of advanced lesions (>16 weeks HFD feeding) [28]. In the current study we found massive infiltration of neutrophils in advanced lesions of ApoAI$^{-/-}$/LDLr$^{-/-}$ mice transplanted with ABCA1$^{-/-}$ bone marrow fed WTD for 6 weeks. It is thus likely that in this model neutrophil accumulation will also have contributed to the development of advanced lesions. In agreement we previously showed that LDLr$^{-/-}$ mice transplanted with ABCA1/SR-BI dKO bone marrow, when fed WTD for 10 weeks, displayed enhanced neutrophil accumulation in advanced lesions [13]. KC is one of the most potent chemoattractant for neutrophils. Plasma KC levels were induced by deletion of leukocyte ABCA1. However, neutrophil accumulation in the liver, spleen, and lesions of aortic arch was only promoted by leukocyte ABCA1 deficiency in ApoAI$^{-/-}$/LDLr$^{-/-}$ mice. Therefore, the induction of neutrophil infiltration in these animals might be the combined consequence of the severe neutrophilia in the circulation and the elevated KC levels in plasma.

In conclusion, macrophage ABCA1 and ApoAI are functional partners in cellular cholesterol efflux and RCT. However, leukocyte ABCA1 remains atheroprotective in absence of circulating ApoAI. The ApoAI-independent atheroprotective effects of ABCA1 might be attributed to its anti-inflammatory function in suppression of monocytosis and neutrophilia and reduction of the secretion of MCP-1 and KC.

Acknowledgement

ABCA1$^{-/-}$ mice and ApoAI$^{-/-}$/LDLr$^{-/-}$ mice were kindly provided by Dr. G. Chimini (Centre d'Immunologie de Marseille Luminy) and Amsterdam Molecular Therapeutics (AMT), respectively.

Sources of funding

This work was supported by the Catalan University and Research Grants Management Agency (Beatriu de Pinós Postdoctoral Grant to LC-B), by the Netherlands Heart Foundation (2001T4101 to Y.Z.). This project was done under the framework of Top Institute Pharma T2-110, with Partners MSD, Radboud University Nijmegen, University Medical Center Groningen, University of Leiden, the Academic Medical Center Amsterdam, and TI Pharma. J.J. was recipient of funds from ISCIII (FIS10-00277). CIBER de Diabetes y Enfermedades Metabólicas Asociadas is an Instituto Carlos III Project. M. Van Eck is an Established Investigator of the Netherlands Heart Foundation (Grant 2007T056).

Disclosures

Nothing to disclose.

References

1. Plump AS, Scott CJ, Breslow JL. Human apolipoprotein A-I gene expression increases high density lipoprotein and suppresses atherosclerosis in the apolipoprotein E-deficient mouse. *Proc Natl Acad Sci U S A.* Sep 27 1994;91(20):9607-9611.
2. Tardif JC, Gregoire J, L'Allier PL, et al. Effects of reconstituted high-density lipoprotein infusions on coronary atherosclerosis: a randomized controlled trial. *Jama.* Apr 18 2007;297(15):1675-1682.
3. Meurs I, Van Eck M, Van Berkel TJ. High-density lipoprotein: key molecule in cholesterol efflux and the prevention of atherosclerosis. *Curr Pharm Des.* May 2010;16(13):1445-1467.
4. Escola-Gil JC, Calpe-Berdiel L, Palomer X, et al. Antiatherogenic role of high-density lipoproteins: insights from genetically engineered-mice. *Front Biosci.* May 1 2006;11:1328-1348.
5. Feig JE, Shamir R, Fisher EA. Atheroprotective effects of HDL: beyond reverse cholesterol transport. *Curr Drug Targets.* Mar 2008;9(3):196-203.
6. Barter PJ, Nicholls S, Rye KA, et al. Antiinflammatory properties of HDL. *Circ Res.* Oct 15 2004;95(8):764-772.
7. Lewis GF, Rader DJ. New insights into the regulation of HDL metabolism and reverse cholesterol transport. *Circ Res.* Jun 24 2005;96(12):1221-1232.
8. Zhao Y, Van Berkel TJ, Van Eck M. Relative roles of various efflux pathways in net cholesterol efflux from macrophage foam cells in atherosclerotic lesions. *Curr Opin Lipidol.* Oct 2010;21(5):441-453.
9. van Eck M, Bos IS, Kaminski WE, et al. Leukocyte ABCA1 controls susceptibility to atherosclerosis and macrophage recruitment into tissues. *Proc Natl Acad Sci U S A.* Apr 30 2002;99(9):6298-6303.
10. Julve J, Escola-Gil JC, Rotllan N, et al. Human apolipoprotein A-II determines plasma triglycerides by regulating lipoprotein lipase activity and high-density lipoprotein proteome. *Arterioscler Thromb Vasc Biol.* Feb 2010;30(2):232-238.
11. Marzal-Casacuberta A, Blanco-Vaca F, Ishida BY, et al. Functional lecithin:cholesterol acyltransferase deficiency and high density lipoprotein deficiency in transgenic mice overexpressing human apolipoprotein A-II. *J Biol Chem.* Mar 22 1996;271(12):6720-6728.
12. Escola-Gil JC, Julve J, Marzal-Casacuberta A, et al. Expression of human apolipoprotein A-II in apolipoprotein E-deficient mice induces features of familial combined hyperlipidemia. *J Lipid Res.* Aug 2000;41(8):1328-1338.
13. Zhao Y, Pennings M, Hildebrand RB, et al. Enhanced foam cell formation, atherosclerotic lesion development, and inflammation by combined deletion of ABCA1 and SR-BI in Bone marrow-derived cells in LDL receptor knockout mice on western-type diet. *Circ Res.* Dec 10 2010;107(12):e20-31.
14. Wang MD, Franklin V, Marcel YL. In vivo reverse cholesterol transport from macrophages lacking ABCA1 expression is impaired. *Arterioscler Thromb Vasc Biol.* Aug 2007;27(8):1837-1842.
15. Zabalawi M, Bhat S, Loughlin T, et al. Induction of fatal inflammation in LDL receptor and ApoA-I double-knockout mice fed dietary fat and cholesterol. *Am J Pathol.* Sep 2003;163(3):1201-1213.
16. Out R, Hoekstra M, Habets K, et al. Combined deletion of macrophage ABCA1 and ABCG1 leads to massive lipid accumulation in tissue macrophages and distinct atherosclerosis at relatively low plasma cholesterol levels. *Arterioscler Thromb Vasc Biol.* Feb 2008;28(2):258-264.

17. Combadiere C, Potteaux S, Rodero M, et al. Combined inhibition of CCL2, CX3CR1, and CCR5 abrogates Ly6C(hi) and Ly6C(lo) monocytosis and almost abolishes atherosclerosis in hypercholesterolemic mice. *Circulation.* Apr 1 2008;117(13):1649-1657.

18. Terashima T, English D, Hogg JC, et al. Release of polymorphonuclear leukocytes from the bone marrow by interleukin-8. *Blood.* Aug 1 1998;92(3):1062-1069.

19. Khera AV, Cuchel M, de la Llera-Moya M, et al. Cholesterol efflux capacity, high-density lipoprotein function, and atherosclerosis. *N Engl J Med.* Jan 13 2010;364(2):127-135.

20. Bodzioch M, Orso E, Klucken J, et al. The gene encoding ATP-binding cassette transporter 1 is mutated in Tangier disease. *Nat Genet.* Aug 1999;22(4):347-351.

21. Wang X, Collins HL, Ranalletta M, et al. Macrophage ABCA1 and ABCG1, but not SR-BI, promote macrophage reverse cholesterol transport in vivo. *J Clin Invest.* Aug 2007;117(8):2216-2224.

22. Moore RE, Navab M, Millar JS, et al. Increased atherosclerosis in mice lacking apolipoprotein A-I attributable to both impaired reverse cholesterol transport and increased inflammation. *Circ Res.* Oct 14 2005;97(8):763-771.

23. Remaley AT, Stonik JA, Demosky SJ, et al. Apolipoprotein specificity for lipid efflux by the human ABCAI transporter. *Biochem Biophys Res Commun.* Jan 26 2001;280(3):818-823.

24. Aiello RJ, Brees D, Bourassa PA, et al. Increased atherosclerosis in hyperlipidemic mice with inactivation of ABCA1 in macrophages. *Arterioscler Thromb Vasc Biol.* Apr 1 2002;22(4):630-637.

25. Van Eck M, Singaraja RR, Ye D, et al. Macrophage ATP-binding cassette transporter A1 overexpression inhibits atherosclerotic lesion progression in low-density lipoprotein receptor knockout mice. *Arterioscler Thromb Vasc Biol.* Apr 2006;26(4):929-934.

26. Tang C, Liu Y, Kessler PS, et al. The macrophage cholesterol exporter ABCA1 functions as an anti-inflammatory receptor. *J Biol Chem.* Nov 20 2009;284(47):32336-32343.

27. Swirski FK, Libby P, Aikawa E, et al. Ly-6Chi monocytes dominate hypercholesterolemia-associated monocytosis and give rise to macrophages in atheromata. *J Clin Invest.* Jan 2007;117(1):195-205.

28. Drechsler M, Megens RT, van Zandvoort M, et al. Hyperlipidemia-triggered neutrophilia promotes early atherosclerosis. *Circulation.* Nov 2 2010;122(18):1837-1845.

29. Yvan-Charvet L, Pagler T, Gautier EL, Avagyan S, Siry RL, Han S, Welch CL, Wang N, Randolph GJ, Snoeck HW, Tall AR. ATP-binding cassette transporters and HDL suppress hematopoietic stem cell proliferation. *Science.* 2010;328:1689-1693.

30. Shang XZ, Issekutz AC. Enhancement of monocyte transendothelial migration by granulocyte-macrophage colony-stimulating factor: requirement for chemoattractant and CD11a/CD18 mechanisms. *Eur J Immunol.* Nov 1999;29(11):3571-3582.

31. Basu S, Hodgson G, Katz M, et al. Evaluation of role of G-CSF in the production, survival, and release of neutrophils from bone marrow into circulation. *Blood.* Aug 1 2002;100(3):854-861.

32. Francone OL, Royer L, Boucher G, et al. Increased cholesterol deposition, expression of scavenger receptors, and response to chemotactic factors in Abca1-deficient macrophages. *Arterioscler Thromb Vasc Biol.* Jun 2005;25(6):1198-1205.

33. Loimaala A, Rontu R, Vuori I, et al. Blood leukocyte count is a risk factor for intima-media thickening and subclinical carotid atherosclerosis in middle-aged men. *Atherosclerosis.* Oct 2006;188(2):363-369.

34. Smith JD, Trogan E, Ginsberg M, et al. Decreased atherosclerosis in mice deficient in both macrophage colony-stimulating factor (op) and apolipoprotein E. *Proc Natl Acad Sci U S A.* Aug 29 1995;92(18):8264-8268.

35. Stoneman V, Braganza D, Figg N, et al. Monocyte/macrophage suppression in CD11b diphtheria toxin receptor transgenic mice differentially affects atherogenesis and established plaques. *Circ Res.* Mar 30 2007;100(6):884-893.

36. Swirski FK, Pittet MJ, Kircher MF, et al. Monocyte accumulation in mouse atherogenesis is progressive and proportional to extent of disease. *Proc Natl Acad Sci U S A.* Jul 5 2006;103(27):10340-10345.

37. Gosling J, Slaymaker S, Gu L, et al. MCP-1 deficiency reduces susceptibility to atherosclerosis in mice that overexpress human apolipoprotein B. *J Clin Invest.* Mar 1999;103(6):773-778.

38. van Leeuwen M, Gijbels MJ, Duijvestijn A, et al. Accumulation of myeloperoxidase-positive neutrophils in atherosclerotic lesions in LDLR-/- mice. *Arterioscler Thromb Vasc Biol.* Jan 2008;28(1):84-89.

39. Zernecke A, Bot I, Djalali-Talab Y, et al. Protective role of CXC receptor 4/CXC ligand 12 unveils the importance of neutrophils in atherosclerosis. *Circ Res.* Feb 1 2008;102(2):209-217.

40. Baetta R, Corsini A. Role of polymorphonuclear neutrophils in atherosclerosis: current state and future perspectives. *Atherosclerosis.* May 2010;210(1):1-13.

41. Boisvert WA, Rose DM, Johnson KA, et al. Up-regulated expression of the CXCR2 ligand KC/GRO-alpha in atherosclerotic lesions plays a central role in macrophage accumulation and lesion progression. *Am J Pathol.* Apr 2006;168(4):1385-1395.

Supplementary Figures

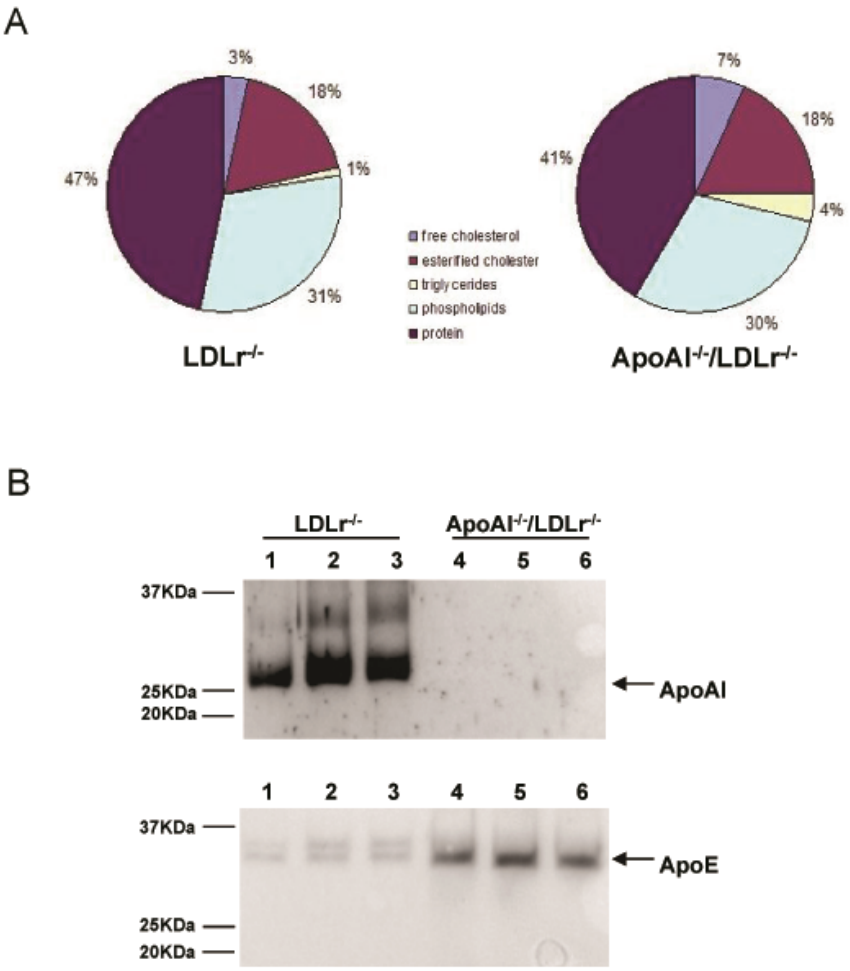

Supplemental Figure 1. Characterization of HDL lipoprotein from LDLr$^{-/-}$ and ApoAI$^{-/-}$/LDLr$^{-/-}$ mice. (A) Relative weight of free cholesterol, cholesteryl ester, phospholipids, triglycerides, and protein in HDL particles from both types of mice expressed as the percentage of total HDL mass. (B) Western blot analysis of HDL lipoproteins. Murine ApoAI and ApoE were determined after 10%-SDS polyacrylamide electrophoresis and detected with specific antibodies.

CHAPTER 8

Stage-specific remodelling of atherosclerotic lesions upon cholesterol lowering in LDL receptor knockout mice

Ying Zhao[1], Dan Ye [1], Jun Wang[2], Laura Calpe-Berdiel[1], Saaleha B.R.N. Azzis[1], Theo J.C. Van Berkel[1], Miranda Van Eck[1]

[1] Division of Biopharmaceutics, Leiden/Amsterdam Center for Drug Research, Leiden University, The Netherlands

[2] Department of Human Genetics, Leiden University Medical Center, Leiden, The Netherlands

Abstract

Lipid lowering reduces cardiovascular morbidity and mortality. However, the dynamic remodeling of established atherosclerotic lesions upon lipid lowering is poorly understood. Early and advanced lesions in the aortic root were induced by feeding LDL receptor knockout mice a high fat/high cholesterol Western-type diet for 5 and 9 weeks, respectively. Lipid lowering was achieved by switching mice to chow diet. In the first week after the diet switch, plasma total cholesterol (TC) levels dropped 70%, but both early and advanced lesions increased in size. Early lesions grew due to an increase in smooth muscle cells while advanced lesions showed an enlargement of the absolute macrophage area. From 1 to 3 weeks, plasma TC levels were completely normalized. This did not influence the size of early lesions. However, advanced lesions became smaller due to a reduction of the absolute macrophage area. From 3 to 6 weeks, both early and advanced lesions progressed further as a result of expansion of the absolute collagen and necrotic core area. In contrast, early lesions became proinflammatory as evidenced by the increased infiltration of neutrophils, increased oxidative stress, probably caused by the activation of mast cells in the adventitia.

In conclusion, the severity of the atherosclerotic lesion affects its dynamic response to lipid lowering, indicating the importance of establishing stage-specific therapeutic protocols for the treatment of atherosclerosis.

--- *Am. J. Pathol.* 2011; 179(3):1522-32---

Introduction

Atherosclerosis, the leading cause of morbidity and mortality in the Westernized society, is a multifactorial complex disease with numerous etiologies that work synergistically to promote lesion development [1]. Among the many cardiovascular risk factors, hypercholesterolemia, especially due to elevated levels of very-low-density lipoprotein cholesterol (VLDL-C) and LDL-C, is sufficient to initiate and promote atherogenesis even in the absence of other known risk facors [2]. Clinical trials have shown that the extent of LDL-C lowering is negatively associated with the rate of atherosclerosis progression [3-5]. However, after normalization of hypercholesterolemia by lipid lowering therapy, a considerable proportion of patients still showed continued progression of atherosclerosis and the occurrence of clinical events, such as myocardial infarction [6-7]. In the ASTEROID trial, after intensive LDL-C lowering by rosuvastatin, approximately 35% of the patients still showed atherosclerotic lesion progression in the coronary artery [3,8]. Also the recent METEOR study showed that intensive LDL-C lowering by rosuvastatin only reduced rather than stopped the progression of carotid atherosclerosis in asymptomatic subjects with low risk of cardiovascular disease [9]. Thus, there is a clear need for a better insight into the mechanisms underlying the effects of plasma lipid lowering on atherogenesis.

The progression of an atherosclerotic lesion is a dynamic process, involving the influx and efflux of lipids, cell migration and emigration, cell proliferation and death, and matrix synthesis and degradation [10]. Identification of lesion dynamics is expected to have important implications for the treatment of atherosclerosis, as it will allow establishment of the optimal timing for modulating specific cellular or acelluar components of the lesion to induce lesion stabilization or regression. In the current study, we for the first time addressed the effects of plasma lipid lowering on the dynamic remodeling of atherosclerotic lesions with different degrees of severity in LDL receptor knockout (LDLr KO) mice by applying a dietary switch from a high fat/high cholesterol Western-type diet (WTD) to regular chow diet. Evidence is provided that the complexity of the initial lesion determines its dynamic response to lipid lowering.

Methods

Mice

LDL receptor knockout (LDLr KO) mice, obtained from the Jackson Laboratory (Bar Habor, USA) were bred at the Gorlaeus Laboratories and maintained on sterilized regular chow, containing 4.3% (w/w) fat and no added cholesterol (RM3; Special Diet Service, Witham, UK). Mice at the age of 12 weeks received a Western-type diet containing 15% (w/w) total fat and 0.25% (w/w) cholesterol (Diet W, Special Diet Services, Whitham, UK) for 5 weeks (n= 32) and 9 weeks (n= 32) to induce the development of early and advanced atherosclerotic lesions, respectively. Subsequently, 8 animals were euthanized (control group). The remaining animals were divided into 3 groups (n=8/group) and fed a regular chow for 1 (W1 group), 3 (W3 group), and 6 (W6 group) weeks, respectively. Animal experiments were performed at the Gorlaeus Laboratories of the Leiden/Amsterdam Center for Drug Research in accordance with the National Laws. All experimental protocols were approved by the Ethics Committee for Animal Experiments of Leiden University.

Lipids Analysis

After an overnight fasting-period, blood was collected by retro-orbital puncture under anesthesia. Hepatic lipids were extracted according to the method of Bligh & Dyer [11] and dissolved in 2% Triton X-100. Triglycerides (TG) and Phospholipids (PL) in serum and liver were determined using a standard enzymatic colorimetric assay (TG: Roche Diagnostics, Mannheim, Germany; PL: Spinreact, Girona, Spain). The concentrations of cholesterol in serum and liver were determined by incubation with 0.025

U/mL cholesterol oxidase (Sigma) and 0.065 U/mL peroxidase and 15 μg/mL cholesteryl esterase (Roche Diagnostics, Mannheim, Germany) in reaction buffer (1.0 KPi buffer, pH=7.7 containing 0.01 M phenol, 1 mM 4-amino-antipyrine, 1% polyoxyethylene-9-laurylether, and 7.5% methanol). Absorbance was read at 490 nm. The hepatic lipids levels were normalized to their protein concentrations determined using the BCA™ protein assay (Pierce Biotechnology, Rockford, USA). The distribution of cholesterol over the different lipoproteins in serum was determined by fractionation of 30 μL of serum of individual mice using a Superpose 6 column (3.2 x 300 mm, Smart system; Pharmacia, Uppsala, Sweden).

Circulating leukocyte analysis

Upon sacrifice, blood was collected by retro-orbital puncture under anesthesia. Total white blood cells, neutrophil, lymphocyte, and monocyte counts in the blood were analyzed using an automated Sysmex XT-2000iV Veterinary Hematology analyzer (Sysmex Corporation, Kobe, Japan).

Histological Analysis of the Aortic Root

On sacrifice the arterial tree was perfused *in situ* with phosphate buffer solution (PBS) and the heart was excised and stored in 3.7% neutral-buffered formalin (Formal-fixx; Shandon Scientific Ltd., UK) until use. 10-μm sections were taken once the aortic root was identified by the appearance of aortic valve leaflets. The aortic arches were frozen and longitudinal 8-μm cryosections were taken. Atherosclerotic lesion development was quantified in the aortic root and aortic arch from oil red O/hematoxylin-stained cryostat sections using the Leica image analysis system, consisting of a Leica DMRE microscope coupled to a video camera and Leica Qwin Imaging software (Leica Ltd). Mean lesion area (in μm^2) was calculated from 10 oil red O/hematoxylin-stained sections in the aortic root and 15 of the sections with maximal lesion area in the aortic arch. Sections were immunolabeled against MOMA-2 (monoclonal rat IgG2b, dilution 1:50, Research diagnostics), α-smooth muscle actin (monoclonal mouse IgG2a, dilution 1:500, Sigma), CD3 (polyclonal Rabbit IgG, dilution 1:150, Neomarkers), and Ly6G (monoclonal rat IgG2b, dilution 1:100, eBiosciences) for detection of monocytes/macrophages, smooth muscle cells, T lymphocytes, and neutrophils, respectively. Collagen content of the lesions was visualized with aniline blue by using Masson's Trichrome accustain according to the manufacturer's instructions (Sigma). TUNEL staining of lesions was performed to visualize apoptotic cells using the in Situ Cell Death Detection kit (Roche Diagnostics). Mast cells were stained with naphthol AS-D chloroacetate esterase (Sigma). Histochemical stainings were subsequently quantified in 5 consecutive sections by computer-aided morphometric analysis using the Leica image analysis system. Furthermore, quantifications of necrotic core area were performed on oil red O/hematoxylin and Masson's Trichrome stained sections. Oxidative stress was quantified by using α-nitrotyrosine (IgG2b, dilution 1:100, Abcam) and α-8-hydroxy-2'-deoxyguanosine (8-OHdG) (IgG2a, dilution 1:100, QED Bioscience) monoclonal mouse antibodies. All analyses were performed blinded.

Flow cytometry

White blood cell suspensions from whole blood were prepared by lysis of red blood cells. Cell surface immunolabelling of monocytes and neutrophils was performed according to the manufacturer's instructions (eBioscience & BD Biosciences). Briefly, fluorochrome-conjugated monoclonal antibodies to CD11b (Biosciences) and to Ly6G and Ly6C (BD Biosciences) were incubated with the white blood cell suspensions for 30 min at 4^oC in labeling buffer (1% mouse serum in PBS). Flow cytometric analysis was performed with FacsCalibur and then analyzed with CellQuest software (Becton Dickinson, San Jose), correcting for nonspecific staining with isotype antibody controls.

Statistical Analysis

Statistical analysis was performed using ANOVA and the Student-Newman-Keuls post-test (GraphPad InStat and Prism software). A Pearson r test was used to perform correlation analysis. A level of $p<0.05$ was considered significant.

Results

Dietary lipid lowering led to decreased lipid levels in plasma and liver

LDLr KO mice were fed WTD for 5 weeks to induce atherosclerotic lesion formation. Thereafter the diet was switched to regular chow to lower plasma cholesterol levels. As shown in Table 1, once the diet was switched to chow, plasma free cholesterol and total cholesterol levels dropped approximately 60% from 357±36 mg/dL to 156±2 mg/dL ($p<0.001$) and 70% from 1347±78 mg/dL to 438±13 mg/dL ($p<0.001$) at 1 week and decreased further to 84±3 and 222±6 mg/dL, respectively, at 6 weeks after the diet switch. The reduced plasma total cholesterol levels were mainly due to decreased VLDL/LDL-C levels (supplementary Figure S1). Moreover, an around 45% reduction in plasma triglycerides ($p<0.001$) and phospholipids ($p<0.001$) was observed at 1 week after the diet switch, which remained low during the remaining period of the experiment (Table 1). The reduction of plasma lipids thus mainly occurred in the first week after the dietary lipid withdrawal. In contrast, livers showed delayed cholesterol lowering upon switch of WTD to chow with the major effects seen at 3 weeks. After 3 weeks on regular chow, hepatic free and esterifed cholesterol levels decreased approximately 35% ($p<0.001$) and 75% ($p<0.001$), respectively (Table 1). Dietary lipid lowering did not affect the hepatic triglyceride and phospholipid content (Table 1). Of note, dietary lipid lowering did normalize both plasma and hepatic lipid levels at 6 weeks after the diet switch to similar levels as in LDLr KO mice of the same age without WTD challenge (Table 1).

Table 1: Effect of dietary cholesterol lowering on plasma and hepatic lipids

Groups	C	W1	W3	W6		LDLr KO Control
Diet	WTD	Chow	Chow	Chow		Chow
Plasma FC (mg/dL)	357±36	156±2***	96±4***,ǂ	84±3***,ǂ		85±3
Plasma TC (mg/dL)	1347±78	438±13***	232±7***,#	222±6***,#		237±7
Plasma TG (mg/dL)	216±21	104±14***	120±10***	115±7***		106±10
Plasma PL (mg/dL)	748±50	489±17***	447±23***	405±19***		425±15
Hepatic FC (ug/mg protein)	26±1	23±1*	17±1***,#	17±1***,#		16±1
Hepatic CE (ug/mg protein)	41±3	31±4*	11±1***,#	9±1***,#		8±1
Hepatic TG (ug/mg protein)	67±2	77±7	73±3	77±4		64±9
Hepatic PL (ug/mg protein)	74±4	73±4	65±3	68±2		75±5

LDLr KO mice were fed WTD for 5 weeks. Thereafter, the animals were switched to regular chow and euthanized at 0 (group C), 1 (group W1), 3 (group W3) and 6 (group W6) weeks after the diet switch. LDLr KO control mice were kept on chow diet all the time during the experiment. Plasma and hepatic lipids were measured. FC, free cholesterol; TC, total cholesterol; CE, cholesteryl ester; TG, triglycerides; PL, phospholipids. Data represent mean ± SEM of 8 mice. Statistically significant difference ***$P<0.001$ and *$P<0.05$ versus group C; #$P<0.01$ and ǂ$P<0.05$ versus group W1.

Decreased circulating neutrophils and monocytes upon dietary lipid lowering

Next, we examined the effect of dietary lipid lowering on circulating leukocytes. The amount of total white blood cells was 4.0±0.7 x10^6/mL at baseline and had a tendency to decrease to 3.1±0.5 x10^6/mL at 3 weeks and remained low (3.3±0.4 x10^6/mL) until 6 weeks after the WTD withdrawal. Dietary lipid lowering did not affect the mount of lymphocytes in the circulation (~2.5x10^6/mL). As shown in Figure 1A and B, the tendency to a reduction in white blood cells by dietary lipid lowering can be attributed to reduced levels of circulating monocytes and neutrophils. Neutrophils in the circulation were reduced about 2-fold ($p<0.05$) after 1 week on chow, while monocytes did not change at this time point. In contrast, at 3 weeks after the dietary lipid withdrawal circulating monocytes were reduced ~3-fold ($p<0.05$).

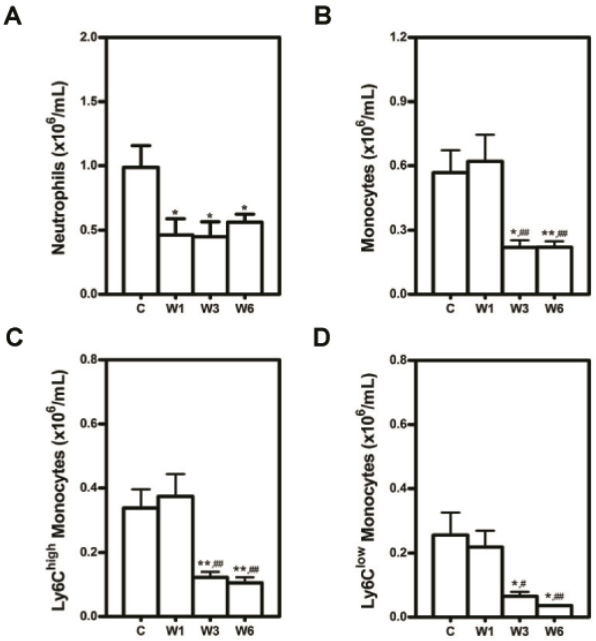

Figure 1. Decreased circulating neutrophils and monocytes upon dietary lipid lowering. LDLr KO mice were fed Western-type diet (WTD) for 5 weeks and thereafter switched to regular chow for 0 (C), 1 (W1), 3 (W3), and 6 (W6) weeks. At each time point, circulating neutrophils and monocytes were analyzed by using flow cytometry. Neutrophils and monocytes were defined as $CD11b^+Ly6G^+$ cells and $CD11b^+Ly6G^-$ cells, respectively. $CD11b^+Ly6G^-$ monocytes were separated further according to their Ly6C expression into $Ly6C^{high}$ and $Ly6C^{low}$ monocyte subsets. Values represent the mean±SEM of 8 mice. Statistically significant difference $^*P<0.05$ and $^{**}P<0.01$ versus group C; $^{\#}P<0.05$ and $^{\#\#}P<0.01$ versus group W1.

Two specific monocyte subsets that vary in their capacity to infiltrate into atherosclerotic lesions are characterized by different expression levels of Ly6C. $Ly6C^{high}$ monocytes preferentially accumulate in the growing atheroma in hyperlipidemic mice, while $Ly6C^{low}$ monocytes do not [12]. Therefore, $Ly6C^{high}$ and $Ly6C^{low}$ monocyte subsets were further analyzed. Both $Ly6C^{high}$ (3.1-fold, $p<0.01$) and $Ly6C^{low}$ (3.3-fold, $p<0.05$) monocytes were reduced after 3 weeks on chow (Figure 1C and 1D). Moreover, the percentage of $Ly6C^{high}$ monocytes decreased from 60±2% at baseline to 47±2% (1.3-fold, $P<0.001$) at 6 weeks after the diet switch.

Dynamic remodeling of established early atherosclerotic lesions upon dietary lipid lowering

Feeding LDLr KO mice the WTD for 5 weeks induced the development of early atherosclerotic lesions in the aortic root, characterized by fatty streaks and accumulation of macrophage foam cells (Figure 2C and 3A). The dynamic remodeling of these established early lesions following dietary lipid lowering was investigated by analyzing the effects on lesion size and lesion compositions at 0 (group C), 1 (group W1), 3 (group W3) and 6 (group W6) weeks after the diet switch to regular chow.

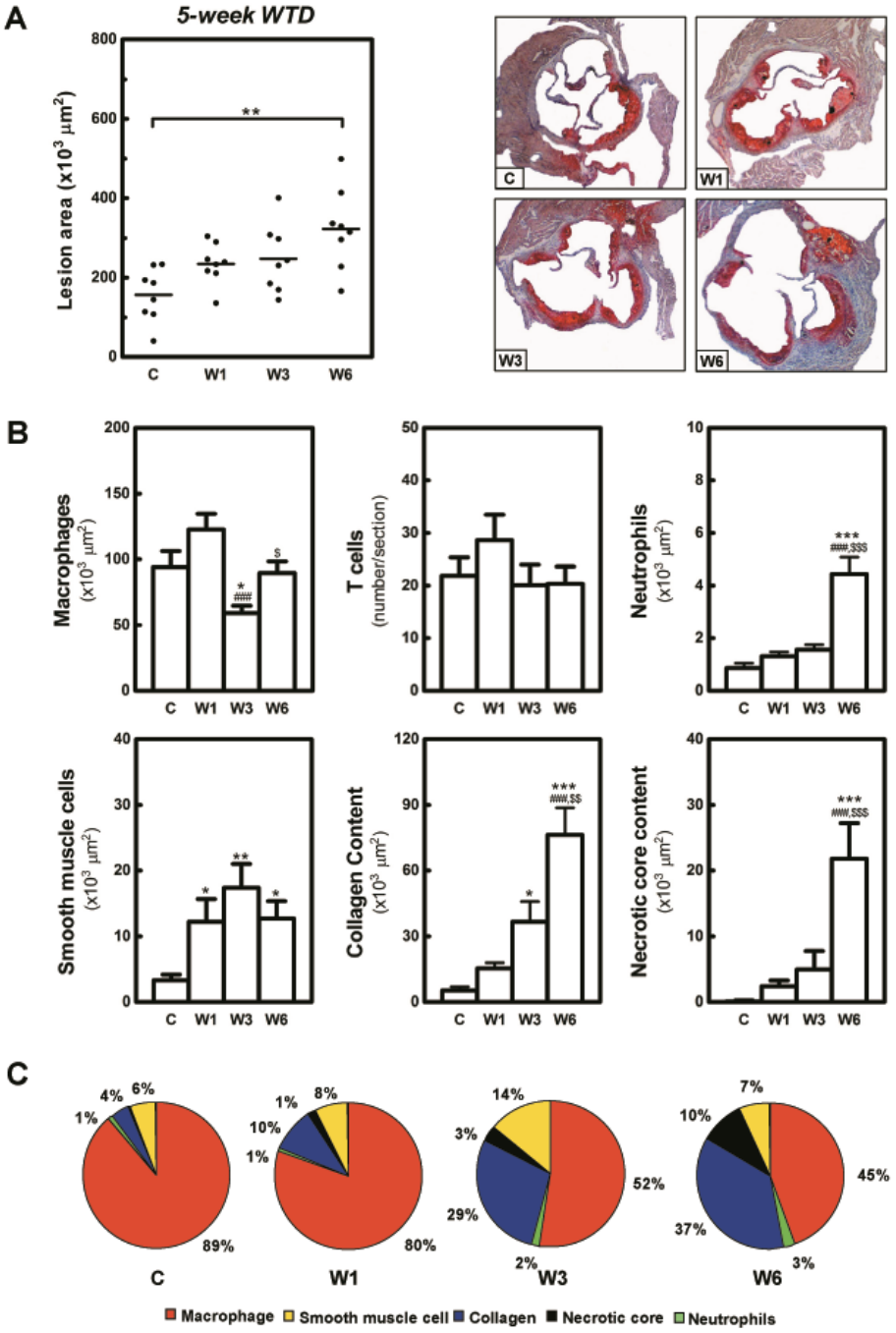

Figure 2. **Dynamic remodeling of established early lesions upon dietary lipid lowering.** Feeding LDLr KO mice WTD for 5 weeks induced early atherosclerotic lesion formation in the arotic root. Atherosclerotic lesion development was analyzed at the aortic root at 0 (C), 1 (W1), 3 (W3), and 6 (W6) weeks after the switch of the mice to regular chow. (A) Photomicrographs showing a scatter dot plot of atherosclerotic lesion quantification and representative oil-red-O stained sections (original magnification 10x2.5). Each symbol represents the mean lesion area in a single mouse. The horizontal bar indicates the mean value for the group. (B) Bar graphs showing the dynamic changes in macrophages, T cells, neutrophils, smooth muscle cells, collagen content and necrotic core area of early lesions after the diet switch. Statistically significant difference *P<0.05, **P<0.01, and ***P<0.001 versus group C; $^{\#\#\#}$P<0.001 versus group W1; $^{\$}$P<0.05 and $^{\$\$\$}$P<0.001 versus group W3. (C) Pie graph showing the relative abundance of macrophage (red), smooth muscle cell (yellow), collagen (blue), necrotic core (black) and neutrophils (green) in the early lesions during the remodeling upon dietary lipid lowering. The relative percentage of each lesion component was normalized to sum to 100%.

In the initial phase (the first week after the dietary lipid withdrawal), the lesions still progressed from 157±24 $\times 10^3$ μm^2 to 235±18 $\times 10^3$ μm^2, despite the 70% decrease in plasma total cholesterol levels to 438±13 mg/dL (Figure 2A). Quantification of the lesioncomposition indicated a 3.7-fold increase of smooth muscle cells ($p<0.05$) but no significant change in macrophages, T cells or neutrophils or collagen content of lesions (Figure 2B). The percentage of apoptotic cells in the lesions was only 1.3±0.3% (Supplementary Figure S2). Morphological analysis of the lesions also revealed the appearance of a necrotic core at 1 week after the diet switch. However, the mean size of the necrotic core area was only 2.4±0.9 $\times 10^3$ μm^2 (Figure 2B). As shown in Figure 2C, after 1 week chow diet feeding, the early lesions were still mainly composed of macrophage foam cells (Figure 2C).

In the second phase (from 1 to 3 weeks on chow), the plasma total cholesterol levels decreased further to around 232±7 mg/dL. Interestingly, no change in the lesion size was detected as compared to 1 week chow feeding (W3: 248±18 $\times 10^3$ μm^2 *vs* W1: 235±18 $\times 10^3$ μm^2) (Figure 2A). Of note, dietary lipid lowering for 3 weeks did lead to a reduction in macrophages (2.1-fold, $p<0.001$ *vs* W1; 1.6-fold, $p<0.05$ *vs* C) (Figure 2B and 3B), while the average size of macrophage foam cells remained unchanged (data not shown). The smooth muscle cells (7.4-fold, $p<0.05$) (Figure 3C and 3D) and collagen content (7.0-fold, $p<0.05$) increased further as compared to baseline (Figure 2B), which formed the subluminal fibrous cap (Figure 3D). Also the percentage of apoptotic cells increased ~2.3-fold ($p<0.05$ *vs* C and W1) to 2.9±0.4% (Supplementary Figure S2). Although the buildup of necrotic material inside the lesions was augmented (5.0±2.8 $\times 10^3$ μm^2), the collagen to necrotic core ratio was increased 3.3-fold to 16.2±5.8, indicating that dietary lipid lowering induced lesion stabilization. Moreover, T cells (Figure 3E and 3F) and neutrophils of the lesions were not significantly changed (Figure 2B and 2C). In line, the lesion contains more collagen and smooth muscle cells, and fewer macrophage foam cells after dietary lipid lowering for 3 weeks (Figure 2C).

In the third phase (from 3 to 6 weeks on chow), the size of the lesions reached a value of 323±36 $\times 10^3$ μm^2 ($p<0.01$ *vs* C) (Figure 2A), although the plasma total cholesterol levels remained low (222±6 mg/dL). The lesional macrophage area of mice kept on chow for 6 weeks increased 1.5-fold ($p<0.05$) as compared to the lesions of mice fed chow for 3 weeks and became similar to baseline levels (Figure 2B). The amount of smooth muscle cells in the lesions remained relatively high, 3.9-fold ($p<0.05$) higher as compared to baseline. Moreover, the collagen content of the lesions was further increased (2.1-fold *vs* W3, 14.5-fold *vs* C, $p<0.001$) (Figure 2B and 3H), indicating that the rate of collagen synthesis was still higher than that of its degradation. Importantly, in the 3 additional weeks chow diet feeding, also a dramatic enlargement of necrotic core (4.4-fold, $p<0.001$ *vs* W3) was observed (Figure 2B and 2C). The ratio of collagen to necrotic core was thus reduced 5.5-fold to 2.9±0.4 ($p<0.05$ *vs* W3). A further increase in the percentage of apoptotic cells was also found (4.7±0.6%, 1.6-fold *vs* W3, $P<0.05$; 3.7-fold *vs* C and W1, $p<0.001$) (Supplementary Figure S2). In addition, the neutrophil content of the lesions was increased 2.8-fold ($p<0.001$ *vs* W3) (Figure 2B and 3J). The enhanced infiltration of neutrophils and a decreased ratio of collagen to necrotic core suggested a proinflammatory phenotype of the lesions. Strikingly, the T cell content still remained the same as baseline (Figure 2B).

After 6 week chow diet feeding, as shown in Figure 2C, the early lesions mainly consisted of macrophages, collagen and necrotic core. Interestingly, pearson correlation analyses demonstrated that after normalization of hypercholesterolemia, the size of early

lesions was highly correlated with the macrophage (r=0.67, p=0.0048, n=16), collagen (r=0.85, p<0.0001, n=16), and necrotic core (r=0.66, p=0.0055, n=16) area.

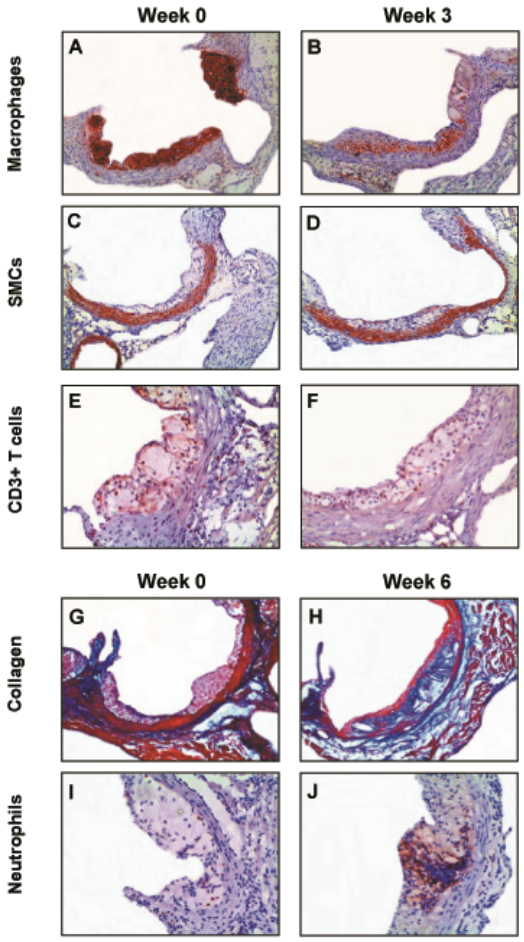

Figure 3. Photomicrographs showing morphometric changes of early lesions upon dietary lipid lowering. Sections of the aortic roots were stained with antibodies against Moma-2, α-actin, CD3, and Ly6G to visualize macrophages (A, B, 50x), smooth muscle cells (SMCs) (C, D, 50x), T cells (E, F, 100x), and neutrophils (I, J, 100x), respectively. Morphological staining of atherosclerotic lesions in the aortic root with Masson's Trichrome Accustain, which stains cytoplasma and muscle fiber red and collagen blue (G, H, 50x).

Dynamic remodeling of established advanced atherosclerotic lesions upon dietary lipid lowering

We next examined whether the dynamic remodeling of established advanced atherosclerotic lesions differs from the response of early lesions upon dietary lipid lowering. Advanced lesions in the aortic roots were induced by feeding LDLr KO mice WTD for 9 weeks. The lesion size and composition were again examined at 0 (group C), 1 (group W1), 3 (group W3) and 6 (group W6) weeks after the diet switch to regular chow. When the mice were fed WTD for 9 weeks prior to the switch to chow diet, dietary lipid lowering led to a similar reduction in plasma and hepatic lipid levels as compared to 5 weeks WTD feeding prior to the diet switch (data not shown). As compared to early lesions, advanced lesions displayed a markedly lower macrophage content, increased smooth muscle cell content and collagen deposition (Figure 2C and 4C), while also a necrotic core and a fibrous cap can be distinguished. In addition, advanced lesions contained 2-fold more T cells (p=0.0013) and 49-fold more neutrophils (p=0.0011), respectively as compared to early lesions. The percentage of apoptotic cells in advanced lesions was also largely increased (8. 5±0.8%, 6.7-fold, p<0.001) (Supplementary Figure S2). Interestingly, the neutrophil content of advanced lesions was about 5-fold (p=0.0003) higher as compared to the level in early lesions after 6 weeks WTD withdrawal (Figure 2B and 4B).

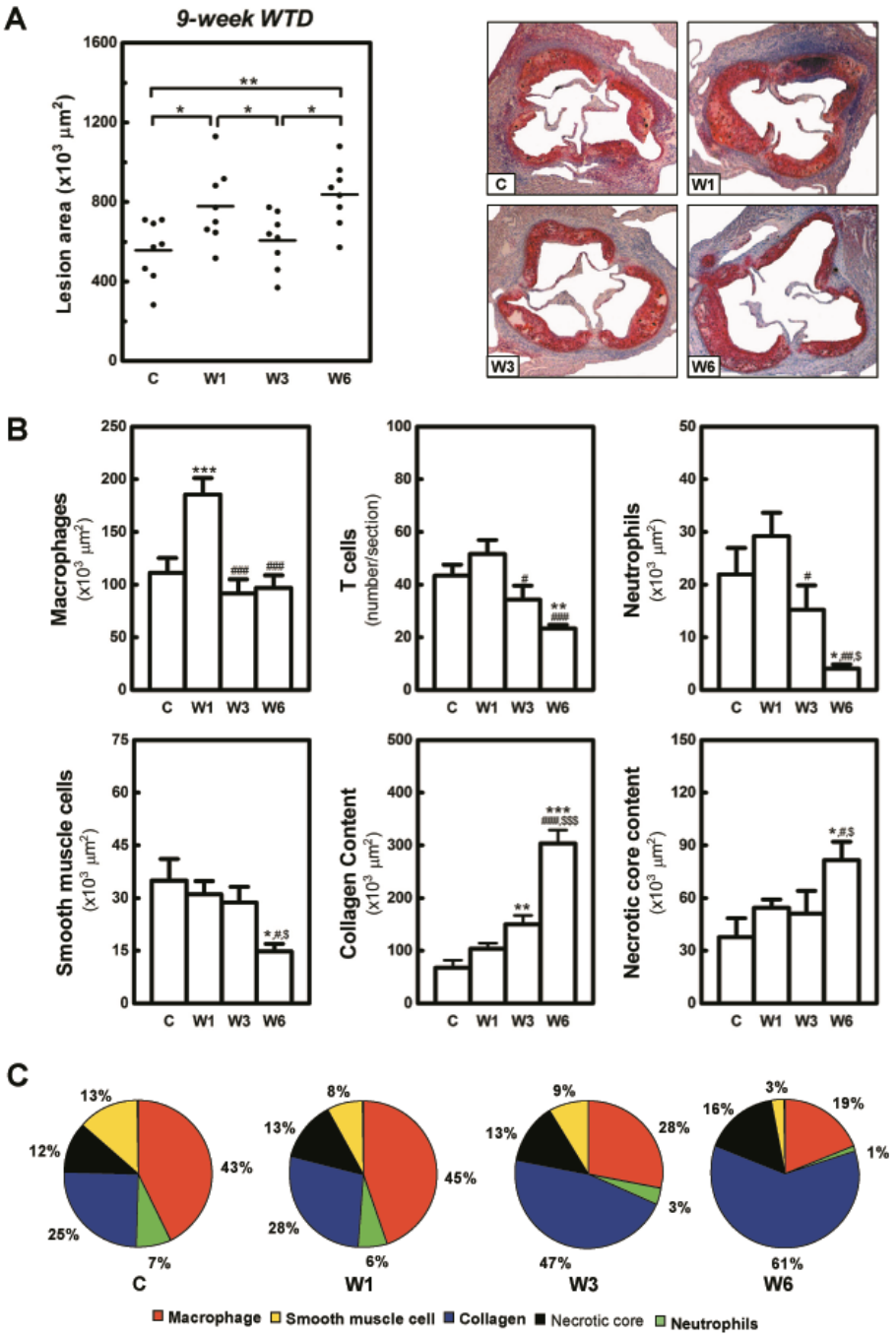

Figure 4. Dynamic remodeling of established advanced lesions upon dietary lipid lowering. Feeding LDLr KO mice WTD for 9 weeks induced advanced atherosclerotic lesion formation in the aortic root. Atherosclerotic lesion development was analyzed at the aortic root at 0 (C), 1 (W1), 3 (W3), and 6 (W6) weeks after the switch of the mice to regular chow. (A) Photomicrographs showing a scatter dot plot of atherosclerotic lesion quantification and representative oil-red-O stained sections (original magnification 10x2.5). Each symbol represents the mean lesion area in a single mouse. The horizontal bar indicates the mean value for the group. (B) Bar graphs showing the dynamic changes in macrophages, T cells, neutrophils, smooth muscle cells, collagen content and necrotic core area of advanced lesions after the diet switch. Statistically significant difference $^{*}P<0.05$, $^{**}P<0.01$, and $^{***}P<0.001$ versus group C; $^{\#}P<0.05$, $^{\#\#}P<0.01$, and $^{\#\#\#}P<0.001$ versus group W1; $^{\$}P<0.05$ and $^{\$\$\$}P<0.001$ versus group W3. (C) Pie graph showing the relative abundance of macrophage (red), smooth muscle cell (yellow), collagen (blue), necrotic core (black) and neutrophils (green) in the advanced lesions during the remodeling upon dietary lipid lowering. The relative percentage of each lesion component was normalized to sum to 100%.

In the initial phase upon WTD withdrawal, advanced lesions, increased 1.4-fold in size (778±68 $\times 10^3$ μm^2 *vs* 557±54 $\times 10^3$ μm^2, $p<0.05$) (Figure 4A). In contrast to early lesions, this was associated with a 1.7-fold ($p<0.001$) increase of macrophage content in advanced lesions (Figure 4B). No significant change was observed in the other lesion components. Notably, in the second phase from 1 to 3 weeks on chow, a significant 1.3-fold reduction in the size of advanced lesions was observed (606±50 $\times 10^3$ μm^2, $p<0.05$ *vs* W1) (Figure 3A), which was primarily the consequence of a 2-fold reduction in the macrophage content of the lesions (Figure 4B and 5B). In addition, T cells (1.5-fold, $p<0.05$ *vs* W1) and neutrophils (1.9-fold, $p<0.05$ *vs* W1) were decreased to baseline. Increased fibrous cap area in the subluminal Moma-2 negative region (Figure 5B) was correlated with increased collagen accumulation (2.2-fold, $p<0.01$ as compared to baseline), but smooth muscle cells and the necrotic core remained the same (Figure 4B and 4C). The collagen to necrotic core ratio was thus increased 1.8-fold to 3.7±0.6 ($p<0.05$, *vs* C and W1). The percentage of apoptotic cells remained unchanged (8.6±0.6%) (Supplementary Figure S2). All these changes indicated that advanced lesions became stabilized after dietary lipid lowering for 3 weeks. In line, collagen became the major component of advanced lesions after 3 weeks chow diet feeding (Figure 4C).

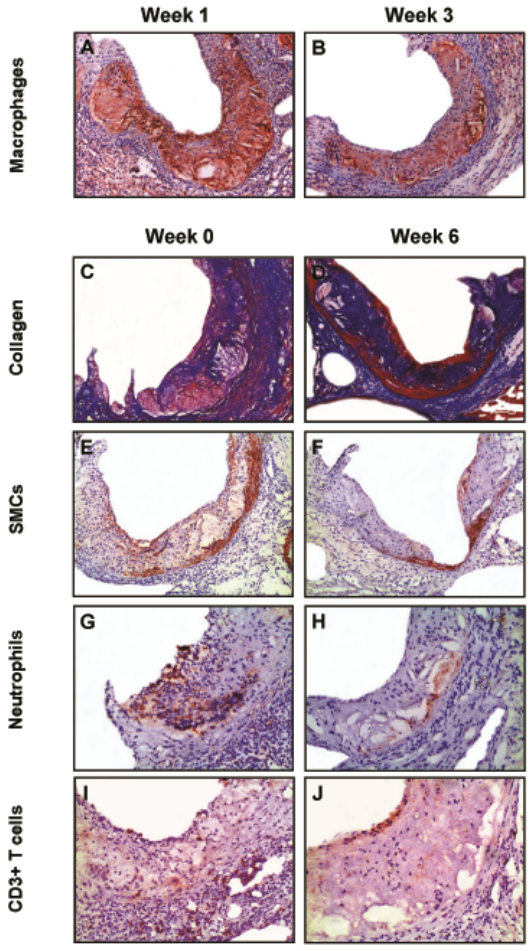

Figure 5. Photomicrographs showing morphometric changes of advanced lesions in response to dietary lipid lowering. Sections of the aortic roots were stained with antibodies against Moma-2, α-actin, Ly6G, and CD3 to visualize macrophages (A, B, 50x), smooth muscle cells (SMCs) (E, F, 50x), neutrophils (G, H, 100x), and T cells (I, J, 100x), respectively. Morphological staining of atherosclerotic lesions in the aortic root with Masson's Trichrome Accustain, which stains cytoplasma and muscle fiber red and collagen blue (C, D, 50x).

In the third phase, advanced lesions, like the early lesions, progressed to 838±56 $\times 10^3$ μm^2 (1.4-fold, $p<0.05$ *vs* W3) (Figure 4A). This was primarily the consequence of an increase (2.0-fold, $p<0.001$) in collagen content of advanced lesions and to a lesser extent of an enhanced buildup of necrotic core material (1.7-fold, $p<0.001$) (Figure 4B and 5D). The macrophage area of advanced lesions did not change while smooth muscle cells

(Figure 5E and 5F) decreased 1.9-fold ($p<0.05$ *vs* W3; 2.4-fold, $p<0.05$ *vs* C) after the 3 additional weeks chow diet feeding (Figure 4B). The ratio of collagen to necrotic core remained stably high (4.0±0.4, $p<0.01$ *vs* C). The percentage of apoptotic cells in the lesions was even slightly decreased to 7.1±0.6% ($p<0.05$ *vs* W1) (Supplementary Figure S2). Moreover, neutrophils of advanced lesions (Figure 5G and 5H) were dramatically reduced (3.7-fold, $p<0.05$ *vs* W3, 5.4-fold, $p<0.05$ *vs* C) at 6 weeks (Figure 4B). T cells of advanced lesions (Figure 5I and 5J) decreased further (1.9-fold, $p<0.01$ *vs* C) to the similar levels of early lesions (Figure 4B). In line, advanced lesions became the collagen-rich lesions after dietary lipid lowering for 6 weeks (Figure 4C). Interestingly, pearson correlation analyses demonstrated that after normalization of hypercholesterolemia, the size of advanced lesions was also highly correlated with collagen ($r=0.91$, $p=0.0002$, $n=16$) and necrotic core ($r=0.80$, $p=0.0003$, $n=16$) content, but not correlated with macrophage content ($r=0.39$, $p=0.14$, $n=16$).

Effects of dietary lipid lowering on inflammatory cells in the adventitia of mice with early and advanced lesions

Adventitial inflammatory cells also play a critical role in the progression of atherosclerotic lesions [13]. The response of inflammatory cells in the adventitia to dietary lipid lowering might thus influence the progression of established lesions. Therefore, total and degranulated mast cells, neutrophils, and T cells in the adventitia underlying the early and advanced lesions were analyzed following WTD withdrawal. Upon dietary lipid lowering, total and degranulated mast cells in the adventitia of early lesions increased 2.1-fold ($p<0.05$ *vs* C and W1) and 3.8-fold ($p<0.05$), respectively at 3 weeks and remained stably high (total: 2.8-fold, $p<0.01$ *vs* C; degranulated: 3.9-fold, $p<0.05$ *vs* C) at 6 weeks (Figure 6B&C). Degranulated mast cells can recruit neutrophils by secretion of KC, the murine ortholog of IL-8 [14]. In line, also a significant increase of neutrophils (1.9-fold, $p<0.01$ *vs* C; 1.2-fold, $p<0.05$ *vs* W1) was observed in the adventitia of early lesions at 3 weeks after WTD withdrawal. Unexpectedly, at 6 weeks, neutrophils declined 2-fold to approximately the levels at baseline ($p<0.05$ *vs* W3) (Figure 6D). As compared to early lesions, the adventitia of advanced lesions contained more total (1.7-fold, $p=0.0251$) and degranulated (5.2-fold, $p=0.0072$) mast cells and neutrophils (3.6-fold, $p=0.0008$) before the diet switch. While total mast cells did not change in the adventitia of advanced lesion after the WTD withdrawal, dietary lipid lowering did lead to a reduction of degranulated mast cells (3.1-fold, $p<0.001$ *vs* C) after 1 week on chow, which remained stably low during the remainder of the experiment (Figure 6B and 6C). Neutrophils in the adventitia of advanced lesions declined in time (6.8-fold, $p<0.001$, W6 *vs* C) to the baseline levels of early lesions at 6 weeks on chow (Figure 6D).

As an important component of adaptive immunity, T cells are critical for the progression rather than initiation of atherosclerosis [15]. In line, 16-fold more T cells ($p=0.0004$) were observed in the adventitia of advanced lesions as compared to early lesions. As shown in Figure 6E, T cells in the adventitia of early lesions increased approximately 2-fold ($p<0.01$ vs C) in the first week after the WTD withdrawal and did not significantly change afterwards, while a 1.7-fold ($p<0.05$ *vs* W1) reduction of T cells was detected in the adventitia of advanced lesions from 1 to 3 weeks, which remained low (1.9-fold, $p<0.01$ vs W1) at 6 weeks on chow. The amount of T cells in the adventitia of advanced lesions, however, remained 7.9-fold ($p=0.0003$) higher as compared to the levels in early lesions at 6 weeks on chow.

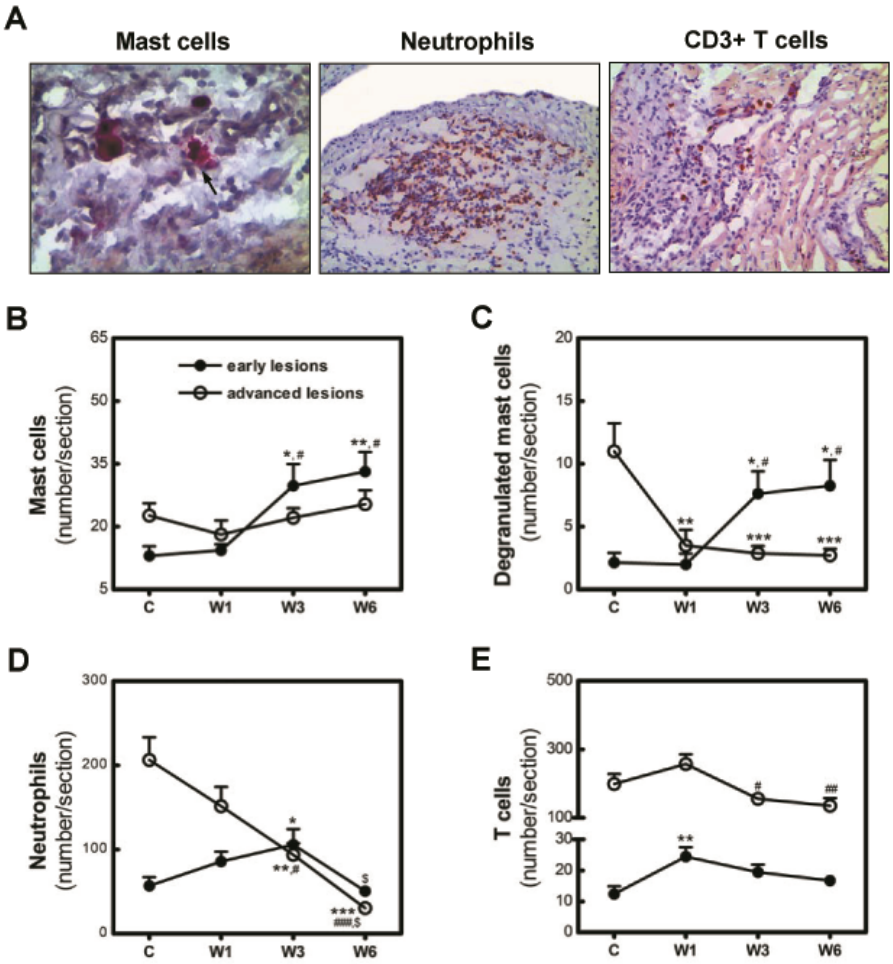

Figure 6. **Effect of dietary lipid lowering on inflammatory cells in the adventitia of early and advanced lesions.** (A) Representative photomicrographs of mast cells (200x), degranulated mast cells (arrow, 200x), neutrophils (100x) and T cells (100x) in the adventitia. Bar graphs showing the dynamic changes of total mast cells (B), degranulated mast cells (C), neutrophils (D) and T cells (D) in the adventitia of early (closed circles) and advanced (open circles) lesions after the switch of WTD to chow diet. Values are means±SEM (n=8). Statistically significant difference *P<0.05, **P<0.01, and ***P<0.001 versus group C; $^{\#}$P<0.05, $^{\#\#}$P<0.01, and $^{\#\#\#}$P<0.01 versus group W1; $^{\$}$P<0.05 versus group W3.

Effects of dietary lipid lowering on oxidative stress in early and advanced lesions

To study the effect of dietary lipid lowering on oxidative stress in the established lesions, the mount of nitrotyrosine and 8-hydroxy-2'-deoxyguanosine (8-OHdG) in the lesions were quantified after the diet switch. Although the plasma cholesterol decreased after 6 weeks on chow, the amount of nitrotyrosine and 8-OHdG in the early lesions was significantly increased 17-fold (p=0.009) and 3.3-fold (p=0.043), respectively in the early lesions (Supplementary Figure S3A). In contrast, the oxidative stress was reduced in advanced lesions as evidenced by the reduction of nitrotyrosine (13-fold, p=0.005) and 8-OHdG (5.0-fold, p=0.0003) (Supplementary Figure S3B).

Effects of dietary lipid lowering on the established atherosclerotic lesion development in the coronary artery and aortic arch

The lesion development in the coronary artery and aortic arch was next analyzed. In line with the fact that the aortic root is the most susceptible site for atherosclerosis in murine

models, no lesion formation was visible in the coronary artery of LDLr KO mice after 5 weeks WTD feeding. Even after 9 weeks on WTD, only 2 out of 8 mice displayed very small lesions (lesion size: 5.6 x 10^3 μm^2 and 7.2 x 10^3 μm^2). Moreover, LDLr KO mice did not develop any atherosclerotic lesions in the aortic arch after 5 weeks on WTD (data not shown). After 9-week WTD feeding, macrophage-rich fatty streak lesions had formed in the aortic arch with a mean lesion area of 86.5±16.4 x 10^3 μm^2 (Supplementary Figure S4A). The ratio of collagen to macrophages in the aortic arch after 9 weeks on WTD (0.053±0.021) was similar to the established early lesions in the aortic root (0.051±0.015) after 5 weeks WTD feeding. No necrotic core was visible in these established lesions of the aortic arch (Supplementary Figure S4D). After the first week on the chow, no significant change was found in the lesion size (97.8±13.4 x 10^3 μm^2) and composition (Supplementary Figure S4). Three weeks chow diet feeding led to a ~2.0-fold ($p<0.05$ *vs* C and W1) and ~7.5-fold ($p<0.01$ *vs* C and W1) increase in size and collagen content, respectively (Supplementary Figure S4A and C). In addition, a small necrotic core became evident. However, the mean size was only 2.5 × 10^3 μm^2 ($p<0.05$ *vs* C and W1) (Supplementary Figure S4D). The lesion increased further in size (1.5-fold, $p<0.05$ *vs* W3; ~3-fold, $p<0.001$ *vs* C and W1) and collagen content (2.4-fold, $p<0.001$ vs W3; ~20-fold *vs* C and W1) after an additional 3 weeks on chow, i.e. total 6 weeks on chow (Supplementary Figure S4A and C). Also, an enlargement of the necrotic core was observed (5.5-fold, $p<0.001$ *vs* W3). The ratio of collagen to necrotic core was thereby reduced 5.2-fold to 5.8±1.3 ($P<0.05$ *vs* W3) (Supplementary Figure S4D). Meanwhile, dietary lipid lowering did not significantly affect the macrophage content, although a tendency to a similar profile was observed as established early lesions in the aortic root (Supplementary Figure S4B). Taken together, dietary lipid lowering did lead to similar changes on early lesions in both arotic root and aortic arch.

Discussion

The present study for the first time investigated the dynamic remodeling of established early and advanced atherosclerotic lesions upon dietary lipid lowering. Strikingly, both established early and advanced atherosclerotic lesions continued to progress after the withdrawal of dietary lipids, which was strongly correlated with the induction of collagen and necrotic core content of the lesions. However, after normalization of hypercholesterolemia, early lesions exhibited a proinflammatory phenotype while advanced lesions became less inflammatory. The clear differences in the response of early and advanced lesions to dietary lipid lowering indicate that the severity of the lesions affected their dynamic response to lipid lowering.

Dietary lipid lowering, as expected, induced a decrease in plasma and hepatic cholesterol levels. However, both established early and advanced lesions in LDLr KO mice could further increase in size when the plasma cholesterol levels of the animals was normalized to around 220 mg/dL, i.e. lower than 300 mg/dL that is prerequisite for initiation of lesion development [16]. This finding indicates that the plasma cholesterol levels required for lesion progression are lower than those for lesion initiation. This might also explain why progression of atherosclerotic lesions can occur in patients with normal LDL-C levels (< 90 mg/dL) after lipid lowering treatment with statins [3]. In line, a robust reduction of the plasma LDL-C levels (<70 mg/dL) is required to halt the progression of established atherosclerotic lesions in humans [3, 4]. However, it should be noted that some patients cannot reach this threshold level of LDL-C even after intensive lipid lowering treatment. Combined therapy that targets multiple pathogenic mechanisms involved in lesion progression is thus needed for efficient treatment of this group of patients.

Consistent with previous findings in rabbits [17] and miniature pigs [18], dietary lipid lowering also led to massive collagen accumulation in the lesion of LDLr KO mice. Importantly, we observed that the collagen content was highly correlated with the size of both early and advanced lesions from 3 to 6 weeks after normalization of hypercholesterolemia. Despite being important for providing mechanical stability to the lesion, excessive collagen may also stimulate lesion development by serving as a depot for proatherogenic molecules (modified lipoproteins, growth factors and glycation end-products) and by promoting foam cell formation [19]. Moreover, massive collagen accumulation might obstruct the access of healthy phagocytotic cells to clear apoptotic cells in the lesions, thereby leading to the increased necrotic core formation. Necrotic core areas are sites of active inflammation and oxidative stress [20, 21], which could thus further promote the progression of lesions. In agreement, we found that necrotic core formation increased in time upon dietary lipid lowering. It should thus be carefully investigated if inhibition of collagen synthesis in combination with lipid lowering might be a potential therapeutic strategy for the treatment of atherosclerosis.

Recruitment of monocytes into atherogenic foci is central to the initiation and progression of atherosclerosis. Hypercholesterolemia induces Ly6C^{high} monocytosis [22, 23], subsequently contributing to atherogenesis [12]. Reduction of plasma cholesterol levels by statins could reduce Ly6C^{high} monocytosis [22]. However, the anti-inflammatory effects of statins beyond cholesterol lowering could also contribute to these alterations. In the present study, we showed that cholesterol lowering alone by dietary lipid withdrawal could not only decrease circulating monocytes, but also normalize the increased levels of Ly6C^{high} monocytes in LDLr KO mice. Of note, these effects were mainly observed at 3 weeks after the diet switch. Therefore, both early and advanced lesions continued to accumulate macrophages in the first week after dietary lipid lowering, probably as a result of monocyte recruitment from the circulation. Swirski et al demonstrated that apart from the bone marrow, spleen is another reservoir for a large number of monocytes [24]. These splenic monocytes can be recruited to inflammatory sites. Interestingly, reduced monocytes in the subcapsular red pulp of spleen was also observed after 1 week on chow (unpublished data), indicating that splenic monocytes might account for the increased macrophage accumulation in lesions within the first week after the diet switch. However, more experiments remain to be done to test this hypothesis. From 1 to 3 weeks after the diet switch, dietary lipid lowering reduced the macrophage content of both early and advanced lesions. Meanwhile, the size of macrophage foam cells and necrotic core was not significantly changed. Moreover, the rate of apoptosis was either very low in the early lesions or remain stable in the advanced lesions, we thus speculate that the reduction of macrophages is mainly the consequence of their emigration. Emigration of monocyte-derived foam cells from atherosclerotic lesions and regression of established atherosclerotic lesions has been elegantly shown by transplantation of a region of the aorta with atherosclerotic lesions from hypercholesterolemic apoE KO mice to normocholesterolemic wildtype mice [25]. From 1 to 3 weeks after WTD withdrawal, the lesion size was not increased in early lesions and even reduced in advanced lesions, indicating that dietary lipid lowering can inhibit the progression and/or induce the regression of established lesions. However, despite the reduced Ly6C^{high} monocytosis upon dietary lipid lowering, macrophage accumulation in the early lesions was enhanced again from 3 to 6 weeks after the diet switch. Interestingly, the macrophage area was highly correlated with the lesion size of early lesions but not of advanced lesions at this time point after WTD withdrawal. In agreement, using bone marrow transplantation we recently demonstrated that the growth of established early lesions under hypercholesterolemia is mainly caused by the continuous recruitment of monocyte-derived cells, while this process

is largely impaired in established advanced lesions [26]. Thus, inhibition of monocyte infiltration combined with lipid lowering might be a more efficient therapeutic strategy for the treatment of established early lesions than advanced lesions.

Another important finding is that early and advanced lesions showed a different inflammatory phenotype after normalization of hypercholesterolemia. Early lesions became proinflammatory, as evidenced by a decreased ratio of collagen to necrotic core, an elevated neutrophil content, and increased oxidative stress, while advanced lesions became less inflammatory. Zernecke et al demonstrated that an expansion of circulating neutrophils leads to more neutrophil infiltration into lesions [27]. However, dietary lipid lowering did reduce the levels of circulating neutrophils. This thus cannot contribute to the increased neutrophil infiltration in the lesions upon dietary lipid lowering. Moreover, in line with previous study [28], the area of necrosis did not correlate with neutrophil accumulation. Actually, almost no neutrophil was found in close proximity of the necrotic core in the atherosclerotic lesion. Interestingly, quantification of inflammatory cells in the adventitia of early lesions revealed increased numbers of degranulated mast cells. Activation of mast cells not only recruits monocytes, neutrophils and other mast cells by secreting their respective chemoattractant MCP-1, KC and eotaxin [14, 29], but also promotes macrophage apoptosis, probably thereby leading to the augmented buildup of necrotic core material [30]. In line, the enhanced infiltration of monocytes and neutrophils into the lesions, the increased recruitment of mast cells into the adventitia, and a dramatic enlargement of necrotic core were observed upon progression of the early lesions after normalization of hypercholesterolemia. Increased macrophages and neutrophils in early lesions could generate more reactive oxygen species through NADPH oxidase and myeloperoxidase [31], thereby leading to the enhanced oxidative stress. Therefore, the proinflammatory phenotype of early lesions might be the consequence of mast cell activation in the adventitia. Importantly, Sun et al recently demonstrated that mast cells promote atherogenesis by promoting the secretion of the proinflammatory cytokine IL-6 and IFN-γ [32]. Also, the activation of mast cells is involved in induction of rupture of advanced lesions [30]. Targeting mast cell activation might thus be a promising strategy for combination with lipid lowering therapies for treatment of established atherosclerotic lesions.

We recognize the limitations of the current study. Dietary lipid lowering might not be as effective as the use of statins in the treatment of atheroclerosis, due to their many pleiotropic effects beyond their cholesterol lowering capacity [33]. Also mice have no cholesterol ester transport protein (CETP) while humans do [34]. Moreover, in contrast to humans, LDLr KO used in our study developed atherosclerosis at the aortic root and descending aorta rather than coronary artery. In addition, mice seldom show signs of myocardial infarction or stroke [35] as murine atherosclerotic lesions are not prone to plaque rupture. Therefore, it is clear that findings based on mouse models must be carefully evaluated in larger animal models and in humans.

In summary, our study provides important insights into the dynamic remodeling of established atherosclerotic lesions upon dietary lipid lowering. Progression of established atherosclerotic lesions after dietary lipid lowering indicates that more effective therapeutic strategies are needed for the treatment of atherosclerosis. The dynamics of lesion remodeling upon dietary lipid lowering are complex and depend on the stage of atherosclerotic lesion development. Establishment of stage-specific therapeutic protocols might thus improve the eventual outcome. However, the requirement of stage-specific therapy for atherosclerosis calls for the development of better molecular imaging tools to characterize lesion compositions *in vivo*.

Acknowledgements

This work was supported by grants from the Netherlands Heart Foundation (#2001T4101 to M.V.E. and Y.Z., and the Established Investigator grant 2007T056 to M.V.E.), the Catalan University and Research Grants Management Agency (Beatriu de Pinós Postdoctoral Grant to L.C-B), the Top Institute Pharma (TI Pharma project T2-110 to Y.Z. and L.C-B), and the Netherlands Organization for Scientific Research (VIDI grant 917.66.301 to M.V.E.).

Dr. Theo Reijmers from the Division of Analytical Biosciences is gratefully acknowledged for his help with statistical analysis.

References

1. Zadelaar S, Kleemann R, Verschuren L, de Vries-Van der Weij J, van der Hoorn J, Princen HM, Kooistra T. Mouse models for atherosclerosis and pharmaceutical modifiers. *Arterioscler Thromb Vasc Biol.* 2007; 27(8):1706-21.
2. Falk E. Pathogenesis of atherosclerosis. *J Am Coll Cardiol.* 2006; 47(8 Suppl):C7-12.
3. Nissen SE, Tuzcu EM, Schoenhagen P, Brown BG, Ganz P, Vogel RA, Crowe T, Howard G, Cooper CJ, Brodie B, Grines CL, DeMaria AN. Effect of intensive compared with moderate lipid-lowering therapy on progression of coronary atherosclerosis: a randomized controlled trial. *JAMA.* 2004; 291(9):1071-80.
4. Sipahi I, Nicholls SJ, Tuzcu EM, Nissen SE. Coronary atherosclerosis can regress with very intensive statin therapy. *Cleve Clin J Med.* 2006; 73(10):937-44.
5. Chhatriwalla AK, Nicholls SJ, Wang TH, Wolski K, Sipahi I, Crowe T, Schoenhagen P, Kapadia S, Tuzcu EM, Nissen SE. Low levels of low-density lipoprotein cholesterol and blood pressure and progression of coronary atherosclerosis. *J Am Coll Cardiol.* 2009; 53(13):1110-5.
6. Brown BG, Zhao XQ, Sacco DE, Albers JJ. Lipid lowering and plaque regression: New insights into prevention of plaque disruption and clinical events in coronary disease. *Circulation.* 1993; 87(6):1781-91.
7. Bucher HC, Griffith LE, Guyatt GH. Systematic review on the risk and benefit of different cholesterol-lowering interventions. *Arterioscler Thromb Vasc Biol*. 1999; 19(2):187-95.
8. Nissen SE, Nicholls SJ, Sipahi I, Libby P, Raichlen JS, Ballantyne CM, Davignon J, Erbel R, Fruchart JC, Tardif JC, Schoenhagen P, Crowe T, Cain V, Wolski K, Goormastic M, Tuzcu EM. ASTEROID Investigators.Effect of very high-intensity statin therapy on regression of coronary atherosclerosis: the ASTEROID trial. *JAMA*. 2006; 295(13):1556-65.
9. Bots ML, Palmer MK, Dogan S, Plantinga Y, Raichlen JS, Evans GW, O'Leary DH, Grobbee DE, Crouse JR. Intensive lipid lowering may reduce progression of carotid atherosclerosis within 12 months of treatment: the METEOR study. *J Intern Med.* 2009; 265(6):698-707.
10. Bennett MR. The atherosclerotic plaque was not built in a day: the dynamic nature of plaque progression and instability. *Heart Metab.* 2007; 36:5-7
11. Bligh EG, Dyer WJ. A rapid method of total lipid extraction and purification. *Can J Biochem Physiol.* 1959; **37**: 911-917.
12. Tacke F, Alvarez D, Kaplan TJ, Jakubzick C, Spanbroek R, Llodra J, Garin A, Liu J, Mack M, van Rooijen N, Lira SA, Habenicht AJ, Randolph GJ. Monocyte subsets differentially employ CCR2, CCR5, and CX3CR1 to accumulate within atherosclerotic plaques. *J Clin Invest.* 2007; 117(1):185-94.
13. Maiellaro K, Taylor WR. The role of the adventitia in vascular inflammation. *Cardiovasc Res.* 2007; 75(4):640-8.
14. Bot I, de Jager SC, Zernecke A, Weber C, van Berkel TJ, Biessen EA. Mast cell activation promotes leukocyte recruitment and adhesion to the atherosclerotic plaque. *Circulation.* 2007; 116:II_242.
15. Weber, C., A. Zernecke, and P. Libby. The multifaceted contributions of leukocyte subsets to atherosclerosis: lessons from mouse models. *Nat. Rev. Immunol.* 2008; 8**:**802–815.
16. Getz GS, Reardon CA. Diet and murine atherosclerosis. *Arterioscler Thromb Vasc Biol.* 2006; 26(2):242-9.

17. Aikawa M, Rabkin E, Okada Y, Voglic SJ, Clinton SK, Brinckerhoff CE, Sukhova GK, Libby P. Lipid lowering by diet reduces matrix metalloproteinase activity and increases collagen content of rabbit atheroma: a potential mechanism of lesion stabilization. *Circulation.* 1998; 97(24):2433-44.

18. Verhamme P, Quarck R, Hao H, Knaapen M, et al. Dietary cholesterol withdrawal reduces vascular inflammation and induces coronary plaque stabilization in miniature pigs. *Cardiovasc Res.* 2002; 56(1):135-44.

19. Rekhter MD. Collagen synthesis in atherosclerosis: too much and not enough. *Cardiovasc Res.* 1999; 41(2):376-84.

20. Schrijvers DM, De Meyer GR, Kockx MM, Herman AG, Martinet W. Phagocytosis of apoptotic cells by macrophages is impaired in atherosclerosis. *Arterioscler Thromb Vasc Biol.* 2005; 25(6):1256-61.

21. Clarke MC, Talib S, Figg NL, Bennett MR. Vascular smooth muscle cell apoptosis induces interleukin-1-directed inflammation: effects of hyperlipidemia-mediated inhibition of phagocytosis. *Circ Res.* 2010; 106(2):363-72.

22. Swirski, F.K., et al. 2007. Ly-6C^{hi} monocytes dominate hypercholesterolemia-associated monocytosis and give rise to macrophages in atheromata. *J. Clin. Invest.* **117:**195-205.

23. Combadière C, Potteaux S, Rodero M, Simon T, Pezard A, Esposito B, Merval R, Proudfoot A, Tedgui A, Mallat Z. Combined inhibition of CCL2, CX3CR1, and CCR5 abrogates Ly6C(hi) and Ly6C(lo) monocytosis and almost abolishes atherosclerosis in hypercholesterolemic mice. *Circulation.* 2008; 117(13):1649-1657.

24. Swirski FK, Nahrendorf M, Etzrodt M, Wildgruber M, Cortez-Retamozo V, Panizzi P, Figueiredo JL, Kohler RH, Chudnovskiy A, Waterman P, Aikawa E, Mempel TR, Libby P, Weissleder R, Pittet MJ. Identification of splenic reservoir monocytes and their deployment to inflammatory sites. *Science.* 2009; 325(5940):612-616.

25. Llodrá J, Angeli V, Liu J, Trogan E, Fisher EA, Randolph GJ. Emigration of monocyte-derived cells from atherosclerotic lesions characterizes regressive, but not progressive, plaques. *Proc Natl Acad Sci U S A.* 2004; 101(32):11779-84.

26. Ye D, Zhao Y, Hildebrand RB, Singaraja RR, Hayden MR, Van Berkel TJC, Van Eck M. The dynamics of macrophage infiltration into the arterial wall during atherosclerotic lesion development in LDL receptor knockout mice. *Am J Pathol.* 2010; 178(1):413-22.

27. Zernecke A, Bot I, Djalali-Talab Y, Shagdarsuren E, Bidzhekov K, Meiler S, Krohn R, Schober A, Sperandio M, Soehnlein O, Bornemann J, Tacke F, Biessen EA, Weber C. Protective role of CXC receptor 4/CXC ligand 12 unveils the importance of neutrophils in atherosclerosis. *Circ Res.* 2008; 102(2):209-17.

28. van Leeuwen M, Gijbels MJ, Duijvestijn A, Smook M, van de Gaar MJ, Heeringa P, de Winther MP, Tervaert JW. Accumulation of myeloperoxidase-positive neutrophils in atherosclerotic lesions in LDLR-/- mice. *Arterioscler Thromb Vasc Biol.* 2008; 28(1):84-89.

29. Libby P, Shi GP. Mast Cells as Mediators and Modulators of Atherogenesis. *Circulation.* 2007; 115:2471-2473

30. Bot I, de Jager SC, Zernecke A, Lindstedt KA, van Berkel TJ, Weber C, Biessen EA. Perivascular mast cells promote atherogenesis and induce laque destabilization in apolipoprotein E-deficient mice. *Circulation.* 2007; 115(19):2516-25.

31. Parthasarathy S, Santanam N. Mechanisms of oxidation, antioxidants, and atherosclerosis. *Curr Opin Lipidol.* 1994; 5(5):371-375.

32. Sun J, Sukhova GK, Wolters PJ, Yang M, Kitamoto S, Libby P, MacFarlane LA, Mallen-St Clair J, Shi GP. Mast cells promote atherosclerosis by releasing proinflammatory cytokines. *Nat Med.* 2007; 13(6):719-24.

33. Blum A, Shamburek R. The pleiotropic effects of statins on endothelial function, vascular inflammation, immunomodulation and thrombogenesis. *Atherosclerosis.* 2009; 203(2):325-330.

34. Breslow JL. Transgenic mouse models of lipoprotein metabolism and atherosclerosis. *Proc Natl Acad Sci U S A.* 1993; 90(18):8314-8318.

35. Cullen P, Baetta R, Bellosta S, Bernini F, Chinetti G, Cignarella A, von Eckardstein A, Exley A, Goddard M, Hofker M, Hurt-Camejo E, Kanters E, Kovanen P, Lorkowski S, McPheat W, Pentikäinen M, Rauterberg J, Ritchie A, Staels B, Weitkamp B, de Winther M; MAFAPS Consortium. Rupture of the atherosclerotic plaque: does a good animal model exist? *Arterioscler Thromb Vasc Biol.* 2003; 23(4):535-42.

Supplementary Figures

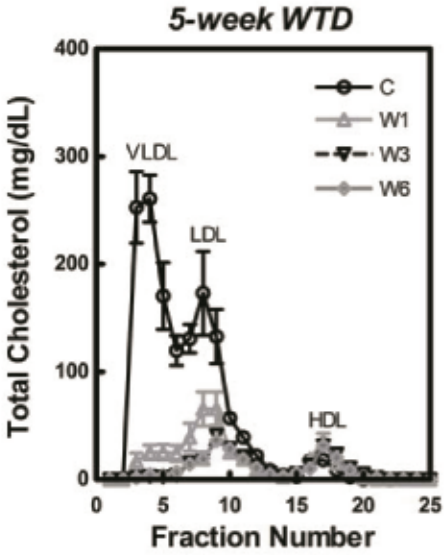

Supplementary Figure S1. **Effect of dietary cholesterol lowering on lipoprotein distribution of total cholesterol (TC).** LDLr-/- mice were fed WTD for 5 weeks to induce the lesion formation. Thereafter, the animals were switched to regular chow and euthanized at 0 (C), 1 (W1), 3 (W3), and 6 weeks after the diet switch. 30 μL aliquot of serum was fractionated by a Pharmacia Smart column and TC of each fraction was determined. Fractions 3 to 6 represent VLDL, fractions 8 to 12 represent LDL, and fractions 16 to 20 represent HDL. Values represent the mean±SEM of 8 mice.

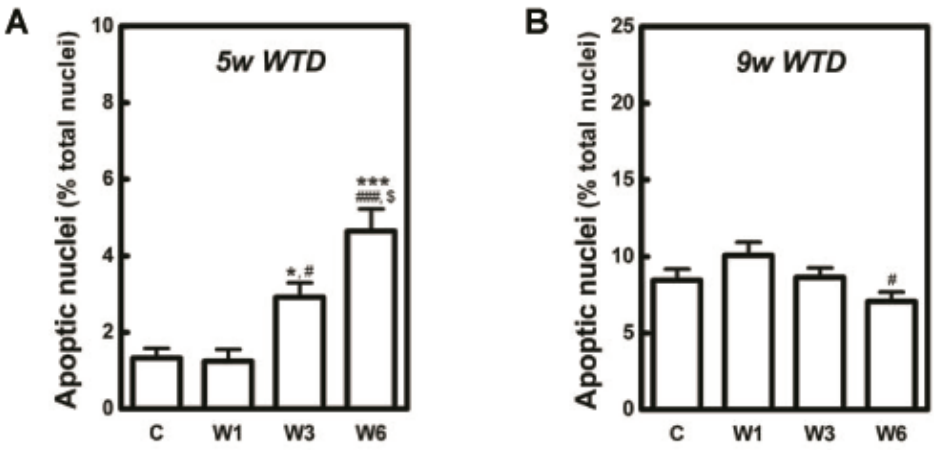

Supplementary Figure S2. **Effect of dietary cholesterol lowering on the cell apoptosis in the established lesions.** LDLr-/- mice were fed WTD for 5 and 9 weeks to induce the lesion formation. Thereafter, the animals were switched to regular chow and euthanized at 0 (C), 1 (W1), 3 (W3), and 6 weeks after the diet switch. Apoptosis is expressed as the percentage TUNEL-positive to total nuclei in the atherosclerotic lesions. Values represent the mean±SEM of 8 mice. Statistically significant difference $^{*}P<0.05$ and $^{***}P<0.001$ versus group C; $^{\#}P<0.05$ and $^{\#\#\#}P<0.001$ versus group W1; $^{\$}P<0.05$ versus group W3.

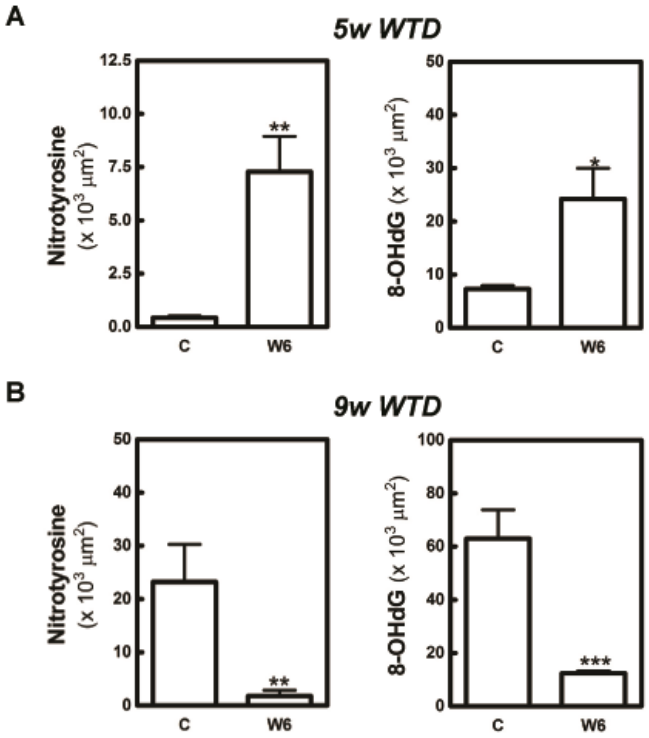

Supplementary Figure S3. **Effect of dietary cholesterol lowering on oxidative stress in the established lesions.** LDLr-/- mice were fed WTD for 5 and 9 weeks to induce the lesion formation. Thereafter, the animals were switched to regular chow and euthanized at 0 (C), 1 (W1), 3 (W3), and 6 weeks after the diet switch. Oxidative stress is expressed as the mount of nitrotyrosine and 8-hydroxy-2'-deoxyguanosine (oh^8dG) in the atherosclerotic lesions. Values represent the mean±SEM of 5 mice. Statistically significant difference $^{*}P<0.05$, $^{**}P<0.01$, and $^{***}P<0.001$ versus group C.

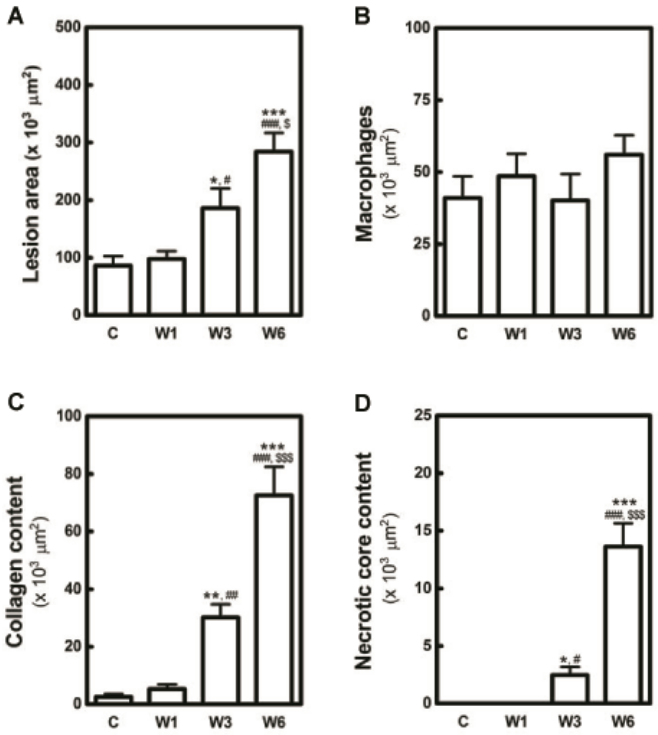

Supplementary Figure S4. Effect of dietary cholesterol lowering on the development of established lesions in the aortic arch. LDLr-/- mice were fed WTD for 9 weeks to induce the lesion formation. Thereafter, the animals were switched to regular chow and euthanized at 0 (C), 1 (W1), 3 (W3), and 6 weeks after the diet switch. Mean lesion area (A) and macrophage (B), collagen (C) and necrotic core (D) content were quantified as mentioned in the materials and methods. Values represent the mean±SEM of 8 mice. Statistically significant difference $^{*}P<0.05$, $^{**}P<0.01$, and $^{***}P<0.001$ versus group C; $^{\#}P<0.05$, $^{\#\#}P<0.01$, and $^{\#\#\#}P<0.001$ versus group W1; $^{\$}P<0.05$ and $^{\$\$\$}P<0.001$ versus group W3.

CHAPTER 9

The dynamics of macrophage infiltration into the arterial wall during atherosclerotic lesion development in LDL receptor knockout mice

Dan Ye[1], Ying Zhao[1], Reeni B. Hildebrand[1], Roshni R. Singaraja[2], Michael R. Hayden[2], Theo J.C. Van Berkel[1], Miranda Van Eck[1]

[1] Division of Biopharmaceutics, Leiden/Amsterdam Center for Drug Research, Leiden University, The Netherlands
[2] Centre for Molecular Medicine and Therapeutics, Children's and Women's Hospital, University of British Columbia, Vancouver, Canada.

Abstract

Atherosclerosis is a progressive disease in which macrophages play an essential role. Macrophage infiltration into the arterial wall induces the development of an early atherosclerotic lesion. However, the dynamics of macrophage infiltration into the arterial wall during lesion progression remains poorly understood.

In this study, low-density lipoprotein receptor knockout ($LDLr^{-/-}$) mice were fed a Western-type diet (WTD) for 3, 6, 9, and 12 weeks to induce the formation of atherosclerotic lesions with different degrees of complexity. Subsequently, these mice were transplanted with bone marrow overexpressing enhanced green fluorescent protein (EGFP) to track donor-derived cells, including macrophages. After 8 weeks WTD feeding post-transplant, macrophage infiltration was evaluated by immunohistochemical staining of donor-derived macrophages ($EGFP^{+}F4/80^{+}$) in the aortic roots. We found that the growth of pre-existing initial lesions was mainly caused by continued recruitment of donor-derived macrophages into the arterial wall. Interestingly, macrophage infiltration into pre-existing more advanced lesions was largely impaired, likely due to the formation of fibrous caps. In addition, interference with the expression of macrophage ATP-binding cassette transporter 1 (ABCA1), an ABC-transporter involved in cellular cholesterol efflux and macrophage recruitment into tissues, affects the infiltration of macrophages into pre-existing early lesions, but not into advanced lesions.

In conclusion, our data suggest that the dynamics of macrophage infiltration into the arterial wall varies greatly during atherogenesis, and thus may affect the efficiency of pharmaceutical interventions aimed at targeting macrophage infiltration into the arterial wall.

--- *Am. J. Pathol.* 2011; 178(1): 413-422 ---

Introduction

Atherosclerosis is a progressive disease characterized by the accumulation of lipid-laden macrophages and fibrous elements within the large arteries. Recent studies have suggested that atherosclerosis is a dynamic vascular disease, displaying both progression and regression of atherosclerotic lesions, as well as marked changes in composition that affect plaque stability [1]. Hypercholesterolemia, especially that resulting from high levels of very low-density lipoprotein and low-density lipoprotein cholesterol (VLDL/LDL-C), is one of the key risk factors in the development of atherosclerotic lesions [2]. However, hypercholesterolemic mice become resistant to atherosclerosis when bred to a macrophage-deficient background [3], illustrating the crucial role of macrophages in promoting lesion initiation and progression. Macrophages are transformed into foam cells upon accumulation of (modified) lipoproteins, resulting in the formation of fatty streaks which represent the earliest detectable atherosclerotic lesions. Macrophages also play important roles in innate and acquired immune responses [4]. They mediate inflammatory response by secreting various cytokines, chemokines, and growth factors, thus encouraging the recruitment of other cell types (e.g., monocytes, T cells, fibroblasts, and smooth muscle cells) which promote atherogenesis. Moreover, macrophages produce a variety of matrix-degrading proteases that can affect plaque stability by inducing weakening of the fibrous cap [5,6]. Thus, macrophages play essential roles in all stages of atherosclerotic lesion development. Although the critical role of macrophage infiltration in the initiation of atherosclerosis is generally accepted, the dynamics of macrophage infiltration into the arterial wall during atherosclerosis progression remains an open question.

The accumulation of macrophages in atherosclerotic lesions primarily depends on the infiltration of bone marrow-derived monocytes into the arterial wall. In this study, to clarify the dynamics of macrophage infiltration into the arterial wall during atherogenesis, low-density lipoprotein receptor knockout ($LDLr^{-/-}$) mice with pre-existing initial or more advanced atherosclerotic lesions were transplanted with bone marrow overexpressing enhanced green fluorescent protein (EGFP) to track donor-derived cells, including macrophages. We show that the ability of donor-derived macrophages to infiltrate into the arterial wall is influenced by the severity of the pre-existing lesions. This may have important implications for the design of pharmaceutical interventions aimed at targeting macrophage infiltration into the arterial wall. ATP-binding cassette transporter 1 (ABCA1)-dependent cholesterol efflux is a crucial factor in prevention of excessive cholesterol accumulation in macrophages of the arterial wall and their transformation into foam cells [7-10]. Therefore, the concept that promotion of macrophage cholesterol efflux by up-regulating ABCA1 might prevent progression or even induce regression of atherosclerosis is remarkably attractive. Moreover, ABCA1 has also been implicated as a factor which is important for the recruitment of macrophages into tissues [9]. For the design of new therapeutic strategies aimed at up-regulating ABCA1, it is essential to quantify the effect of ABCA1 on macrophage infiltration into lesions. Hence, studies were performed in which $LDLr^{-/-}$ mice with pre-existing initial or advanced lesions were transplanted with ABCA1 knockout (KO) or ABCA1 overexpressing bone marrow, also co-expressing EGFP. We find that overexpression of ABCA1 decreases macrophage recruitment specifically into early lesions, resulting in reduced lesion sizes. Our data suggest that preventing macrophage recruitment into very early lesions provides a therapeutic strategy to reduce atherosclerosis burden. Increasing macrophage ABCA1 may be one avenue of doing so.

Methods

Mice

C57BL/6 mice that express a transgene coding for enhanced green fluorescent protein (EGFP) under control of the human ubiquitin C promoter were obtained from the Jackson Laboratory (Bar Harbor, ME, USA). These mice, called UBC-EGFP/BL6, express GFP in all tissues examined, with high levels of GFP expression observed in hematopoietic cells (henceforth called EGFP/WT) [11]. Mice homozygous for the null mutant ABCA1 gene and expressing EGFP (henceforth called EGFP/ABCA1 KO), and mice overexpressing human ABCA1 bacterial artificial chromosome (BAC) and EGFP (henceforth called EGFP/hABCA1) were generated by crossbreeding. All the transgenic mice are on the C57BL/6J background. Homozygous LDLr$^{-/-}$ mice (C57BL/6 background) were purchased from the Jackson Laboratory (Bar Harbor, ME, USA) as mating pairs and bred at the Gorlaeus Laboratory, Leiden, The Netherlands. Mice were maintained on regular chow (4.3 % w/w fat and no added cholesterol; RM3, Special Diet Services, Witham, UK) until the beginning of the study (8 - 10 weeks of age), at which time LDLr$^{-/-}$ mice were fed a Western-type diet (WTD) (15% w/w cacao butter and 0.25% w/w cholesterol; Diet W, Ab diets, Woerden, The Netherlands) to induce hypercholesterolemia and atherosclerosis. Animal experiments were performed at the Gorlaeus laboratory in accordance with National Laws. All experimental protocols were approved by the Ethics Committee for Animal Experiments of Leiden University.

Generation of chimeras by bone marrow transplantation (BMT)

To induce bone marrow aplasia, female LDLr$^{-/-}$ mice without or with pre-existing atherosclerotic lesions were exposed to a single dose of 9 Gy (0.19 Gy/min, 200 kV, 4 mA), using an Andrex Smart 225 Röntgen source (YXLON International, Copenhagen, Denmark) with a 6-mm aluminium filter 1 day before BMT. Bone marrow was harvested by flushing the femurs and tibias from the donor mice with phosphate-buffered saline (PBS). Single-cell suspensions were prepared by passing the cells through a 30-μm nylon gauze. Irradiated recipients received 0.5 x 10^7 bone marrow cells by intravenous injection into the tail vein. Drinking water was supplied with antibiotics (83 mg/L ciprofloxacin and 67 mg/L polymyxin B sulfate) and 6.5 g/L sucrose.

Flow cytometry

In order to determine the extent of repopulation of circulating blood cells with donor cells post-transplant, whole blood was collected each week after BMT. Blood cell suspension in PBS was subjected to flow cytometric analysis (FACS) to detect EGFP fluorescence.

8 weeks after BMT, transplanted mice were euthanized and the spleen and intestinal lymph nodes were harvested. Single-cell suspensions were prepared by passing the spleen and lymph nodes through a 30-μm nylon gauze. Leukocytes from the spleen were isolated by density gradient centrifugation with Lympholyte (Cedarlane Laboratories, Hornby, Ontario, Canada) according to manufacturer's protocol. Cell suspensions from the spleen and lymph nodes were incubated with 1% normal mouse serum in PBS and stained for surface markers (0.5 μg Ab/300 000 cells). All antibodies were purchased from eBiosciences (Belgium). Samples were analyzed by flow cytometry. All data was acquired on a FACSCalibur and was analyzed with CELLQuest software (BD Biosciences).

Serum lipid analyses

After an overnight fast, ≈100 μL of blood was drawn from each mouse by tail bleeding. Serum levels of total cholesterol (TC), free cholesterol (FC), and esterified cholesterol (CE) were determined using enzymatic colorimetric assays (Roche Diagnostics, Mannheim, Germany), with 0.03 U/ml cholesterol oxidase (Sigma Chemical Co., USA), 0.065 U/ml peroxidase, and 15 μg/ml cholesteryl esterase (Seikagaku, Tokyo, Japan) in reaction buffer (1.0 KPi buffer, pH=7.7 containing 0.01 M phenol, 1 mM 4-amino-antipyrine, 1% polyoxyethylene-9-laurylether, and 7.5% methanol). The concentrations of phospholipids (PL) and triglycerides (TG) in serum were determined using enzymatic colorimetric assays (Spinreact S.A. and Roche Diagnostics, respectively). Precipath I (Roche Diagnostics) was used as an internal standard. Absorbance was read at 490 nm. The distribution of lipids over the different lipoproteins was determined by fractionation of 30 μl serum of each mouse using a Superose 6 column

(3.2x300mm, Smart-system, Pharmacia, Uppsala, Sweden). TC, TG, and PL contents in the effluent were determined as described above.

Histological and immunocytochemical analysis of the aortic root

To analyze atherosclerosis development, transplanted mice were euthanized, hearts and aortas were perfused in situ with PBS for 20 to 30 minutes via a cannula in the left ventricle, and subsequently stored in 3.7% neutral-buffered formalin (Formal-Fixx, Shandon Scientific Ltd, UK). Cryostat sections of the aortic root (10 μm) were collected and stained with Oil-Red-O/hematoxylin (Sigma Diagnostics, St. Louis, MO). Mean lesion area (in μm^2) was calculated from 10 consecutive sections, starting at the appearance of the tricuspid valves. Moreover, sections on separate slides were stained with a primary monoclonal antibody to MOMA-2 (Rat anti-mouse IgG2b, dilution 1:50; Research diagnostics), and a secondary antibody conjugated to alkaline phosphates (Goat anti-rat IgG-AP, dilution 1:200; Sigma). MOMA-2 is a useful marker for broad detection of monocytes and macrophages. BCIP/NBT (Sigma) was used as enzyme substrates. In addition, sections were immunolabeled with a primary monoclonal antibody to F4/80 (Rat anti-mouse, dilution 1:200; BMA Biomedicals) for detection of mature macrophages, and a peroxidase-conjugated secondary antibody (Jackson ImmunoResearch Laboratories, Suffolk, UK). Masson trichrome staining (Sigma Diagnostics, St Louis, Mo) was used to visualize collagen (blue staining). The macrophage and collagen contents of lesions were subsequently calculated as the percentage of mean positive area versus mean total lesion area using 5 consecutive sections per mouse by computer-aided morphometric analysis. A histological classification of atherosclerotic lesions in the aortic root was performed on Oil-Red-O/hematoxylin and Masson's Trichrome stained sections according to the recommendations of the American Heart Association [12]. Images were obtained with a Leica image analysis system, consisting of a Leica DMRE microscope coupled to a camera and Leica Qwin Imaging software (Leica Ltd., Cambridge, UK).

To track donor-derived macrophages, cryostat sections of the aortic root were double-immunolabeled with the primary monoclonal antibodies, rat anti-mouse F4/80 for detection of macrophages, and goat anti-mouse JL-8 (CLONTECH Laboratories, Inc., Palo Alto, CA; dilution 1:2000) for detection of EGFP. Secondary antibodies were conjugated to Cy3 and FITC (Jackson ImmunoResearch Laboratories, Suffolk, UK), respectively. Nuclei were stained with 4,6-diamidino-2-phenylindole (DAPI) (Serva Feinbiochemica, Heidelberg, Germany). Photomicrographs were taken using a Bio-Rad Radiance 2100 MP confocal laser scanning system equipped with a Nikon Eclipse TE2000-U inverted fluorescence microscope (Melville, NY). The acquisition of images and analysis of lesions were performed in a blinded fashion.

Hepatic lipid composition and liver histology/immunohistology

Hepatic lipids were extracted according to Bligh and Dyer [13]. After dissolving the lipids in 2% Triton X-100, contents of FC, CE, PL, and TG in liver tissue were determined as described above and expressed as micrograms per milligram (μg/mg) of protein.

Cryostat sections of the liver (8 μm) were collected and routinely stained with Oil-Red-O/hematoxylin (Sigma Diagnostics, St. Louis, MO) for lipid visualization. In addition, to investigate the replacement of Kupffer cells post-transplant, liver sections were also double-immunolabeled to detect macrophages and EGFP as described above.

Statistical Analyses

Data were presented as means±SEM. Statistical analyses were performed using one- and two-way ANOVA using Graphpad Prism Software (Graphpad Software, Inc.; http://www.graphpad.com). The level of statistical significance was set at $p<0.05$.

Results

Generation of LDLr$^{-/-}$ mice with pre-existing atherosclerotic lesions by WTD feeding

To induce the development of atherosclerotic lesions with different degrees of complexity, LDLr$^{-/-}$ mice were maintained on regular chow diet or fed a Western-type diet (WTD) for 3, 6, 9, and 12 weeks. On chow, the majority of serum cholesterol in LDLr$^{-/-}$ mice is

transported by LDL and HDL (data not shown). Serum TC was increased by ~2-fold ($p<0.01$) and ~5-fold ($p<0.001$) after 3 and 6 weeks WTD feeding, respectively, and the increases in TC were primarily due to in the VLDL/LDL-C fractions (data not shown). As shown in **Table 1**, serum levels of FC and CE were induced by 3 and 6 weeks WTD feeding. No further increases in serum FC and CE were observed after 9 and 12 weeks WTD feeding, indicating that a steady-state serum cholesterol level was reached after 6 weeks WTD feeding. Serum levels of PL, but not TG, were also induced by WTD feeding (**Table 1**). The elevated PL levels were primarily due to increases in the VLDL/LDL fractions (data not shown).

Table 1: Effect of WTD feeding on serum and hepatic lipids in $LDLr^{-/-}$ mice

Groups	***Time on WTD (weeks)***	***n***	***Serum FC (mg/dL)***	***Serum CE (mg/dL)***	***Serum PL (mg/dL)***	***Serum TG (mg/dL)***
1	0	6	78±4	338±18	497±18	143±13
2	3	6	221±14*	732±11**	687±13*	154±19
3	6	6	362±25***	1712±74***	985±45**	164±38
4	9	6	216±36*	1643±58***	1023±64**	147±29
5	12	6	251±20**	1937±46***	1136±78**	124±23
Groups	**Time on WTD (weeks)**	**n**	**Hepatic FC (μg/mg)**	**Hepatic CE (μg/mg)**	**Hepatic PL (μg/mg)**	**Hepatic TG (μg/mg)**
1	0	6	16±1	8±2	70±4	156±6
2	3	6	21±2*	32±5**	74±3	134±9
3	6	6	28±2**	47±3**	77±4	130±7
4	9	6	36±2$^{***,\#}$	60±7$^{***,\#}$	83±8*	114±5
5	12	6	39±1$^{***,\#}$	68±3$^{***,\#}$	81±6	113±7

Serum levels of free cholesterol (FC), cholesterol ester (CE), phospholipids (PL), and triglycerides (TG) were determined in $LDLr^{-/-}$ mice fed on regular chow diet (baseline, group 1) or a high-cholesterol Western-type diet (WTD) for 3, 6, 9, and 12 weeks (group 2-5). Moreover, hepatic lipids were extracted from these WTD-fed $LDLr^{-/-}$ mice, and hepatic levels of FC, CE, PL, and TG were determined. Data represent mean±SEM of 6 mice per group. Statistically significant differences $^{*}p<0.05$, $^{**}p<0.01$, $^{***}p<0.001$ vs. $LDLr^{-/-}$ mice on chow (group 1); $^{\#}p<0.05$ vs. $LDLr^{-/-}$ mice on WTD for 6 weeks (group 3).

The liver of WTD-fed $LDLr^{-/-}$ mice displayed massive accumulation of lipids, as examined by Oil-red-O staining (data not shown) and hepatic lipid composition analysis (**Table 1**). Of note, $LDLr^{-/-}$ mice which had been challenged with WTD for a longer period (i.e., 9 and 12 weeks WTD fed mice) displayed higher levels of intrahepatic cholesterol, mainly FC and CE.

Next, atherosclerotic lesion development was analyzed in the aortic root of $LDLr^{-/-}$ mice at different time points after initiation of the WTD challenge. No atherosclerotic lesions were found in $LDLr^{-/-}$ mice on chow. After 3 week WTD feeding, small initial lesions ($31\pm7x10^3$ μm^2, n=6) were formed, primarily composed of macrophage-derived foam cells. The lesion size increased further after 6, 9, and 12 weeks WTD feeding ($190\pm43x10^3$ μm^2, n=6, $505\pm51x10^3$ μm^2, n=6, and $600\pm11x10^3$ μm^2, n=6, respectively) (**Fig. 1**). Based on the lesion composition, plaques were classified as fatty streak lesions (58±4.2% for the macrophage content, and 5±1.4% for the collagen content), more advanced lesions (24±3.1% for the macrophage content, and 16±2.0% for the collagen content), and advanced fibroatheroma lesions (22±2.5% for the macrophage content, and 21±3.5% for the collagen content) after 6, 9, and 12 weeks WTD feeding, respectively.

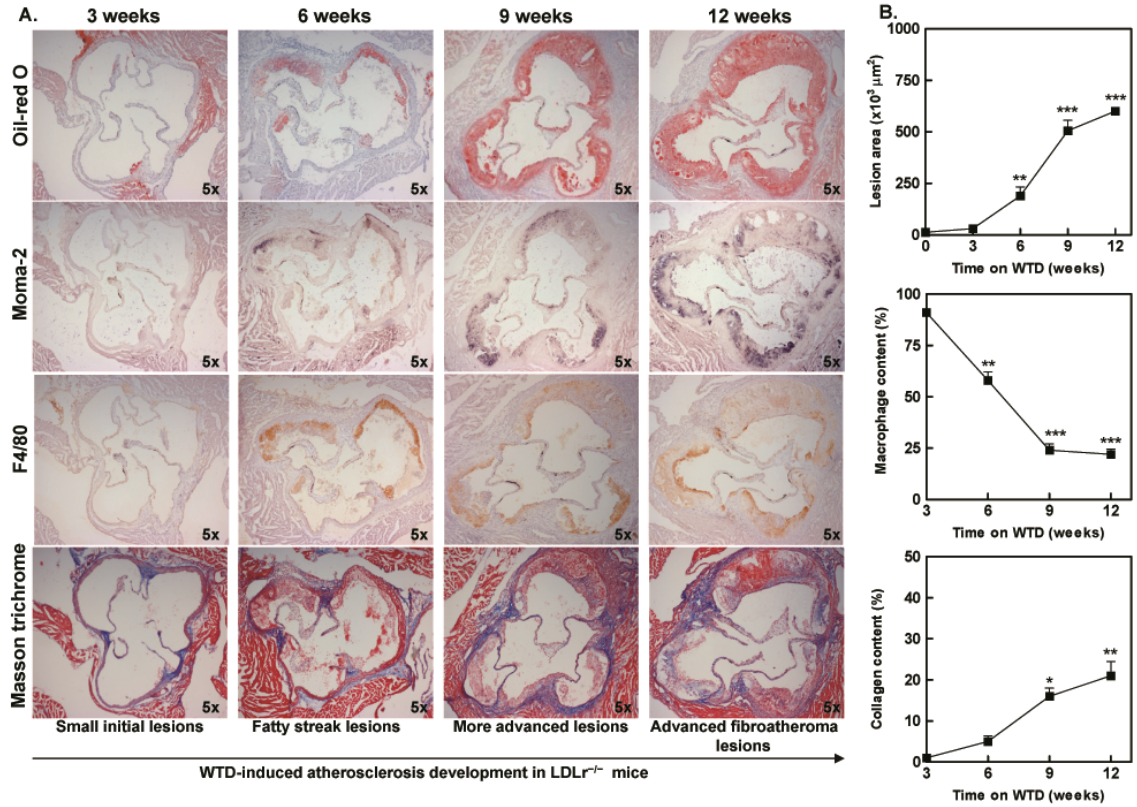

Fig. 1: Western-type diet induces atherosclerosis development in LDLr$^{-/-}$ mice. A: Atherosclerotic lesion development was analyzed in the aortic root of LDLr$^{-/-}$ mice after 0, 3, 6, 9, and 12 weeks WTD feeding. Representative images for Oil-Red-O, MOMA-2 (monocytes and macrophages), F4/80 (macrophages), and Masson trichrome (collagen) staining. Original magnification 50x. **B:** The mean lesion area was calculated from Oil-Red-O/hematoxylin-stained cross-sections of the aortic root at the level of the tricuspid valves. The macrophage and collagen contents of the lesions were quantified in 5 consecutive sections. Values represent the mean of 6 mice per group. *p<0.05, **p<0.01 and ***p<0.001 vs. on chow.

Generation of LDLr$^{-/-}$ mice with pre-existing atherosclerotic lesions and over-expressing EGFP in macrophages

To assess the dynamics of macrophage infiltration into the arterial wall during atherosclerosis development, we performed a BMT where bone marrow from EGFP/WT mice was transplanted into LDLr$^{-/-}$ mice that had been fed WTD for 0, 3, 6, 9, and 12 weeks prior to BMT (EGFP/WT → LDLr$^{-/-}$). The transplanted animals were sacrificed after 8, 11, 14, 17, and 20 weeks WTD feeding in total (i.e., 8 weeks WTD feeding after BMT) (**Fig. 2A**). To exclude potential direct effects of irradiation on plaque morphology, we have compared initial lesions and advanced lesions in LDL receptor knockout mice before irradiation and 3 days after irradiation. Neither lesion size nor lesion composition was significantly changed as a result of the irradiation (data not shown).

Regardless of the duration of WTD feeding prior to BMT, circulating whole blood cells were quantitatively replaced by donor-derived cells (EGFP-positive, EGFP^{+}), starting at 6 days after BMT, and reaching a level of 99±0.2% at 8 weeks post-transplant (see Supplemental **Fig. S1**). This indicated that the bone marrow transfers were successful.

Independently of the duration of WTD feeding prior to transplantation, BMT resulted in a temporary decrease in serum TC levels (22~35%), primarily due to significantly reduced VLDL/LDL-C levels, as well as moderately decreased HDL-C levels (data not shown). Of note, this effect is specific for mice on WTD, as it was not observed

in mice that had been transplanted while being fed regular chow diet in our previous studies [9,10]. Nevertheless, the new steady-state serum cholesterol levels were still adequately high to induce further progression of the pre-existing atherosclerotic lesions. At the time of sacrifice EGFP/WT → $LDLr^{-/-}$ mice without established lesions (i.e., 0+8 weeks WTD fed mice) and the transplanted mice with pre-existing initial lesions (i.e., 3+8 or 6+8 weeks WTD fed mice) had similar serum levels of FC and CE. However, the transplanted mice with pre-existing more advanced lesions (i.e., 9+8 or 12+8 weeks WTD fed mice) displayed significantly ($p<0.05$) higher levels of serum CE, but not FC (**Table 2**). PL and TG levels were similar in all groups, except for the transplanted group which had been fed WTD for 6 weeks prior to BMT (i.e., 6+8 weeks WTD fed mice), showing slightly lower PL and TG levels.

Table 2: Serum lipid levels in the transplanted $LDLr^{-/-}$ mice with pre-existing atherosclerotic lesions and over-expressing EGFP in macrophages

Groups	*Time on WTD (weeks)*	*n*	*FC (mg/dL)*	*CE (mg/dL)*	*PL (mg/dL)*	*TG (mg/dL)*
1	0+8	10	653±9	870±30	702±39	326±58
2	3+8	10	625±9	913±14	642±31	270±49
3	6+8	10	658±14	1056±51	529±31**	144±7**
4	9+8	10	671±17	1264±74*	614±33	193±25
5	12+8	10	680±18	1303±68*	620±30	193±29

Prior to BMT, $LDLr^{-/-}$ mice had been fed a high-cholesterol Western-type diet (WTD) for 0, 3, 6, 9, and 12 weeks. Serum levels of free cholesterol (FC), cholesterol ester (CE), phospholipids (PL), and triglycerides (TG) were determined in the transplanted $LDLr^{-/-}$ mice after 8, 11, 14, 17, and 20 weeks WTD feeding in total, that is, 8 weeks WTD feeding after BMT. Data represent mean±SEM of 10 mice per group. Statistically significant differences *P<0.05, **P<0.01 vs. transplanted $LDLr^{-/-}$ mice without pre-existing lesions (group 1).

Macrophage infiltration into pre-existing atherosclerotic lesions with different degrees of complexity

Next, atherosclerotic lesion development was analyzed in the aortic root of EGFP/WT → $LDLr^{-/-}$ mice after 8, 11, 14, 17, and 20 weeks WTD feeding in total (i.e., 8 weeks WTD feeding after BMT) (**Fig. 2B** and **2C**). In the transplanted mice without pre-existing lesions (i.e., 0+8 weeks WTD fed mice), fatty streak lesions were formed ($304\pm20x10^3$ μm^2, n=10), mostly composed of macrophage-derived foam cells and no fibrous cap. In the transplanted mice which had been fed WTD for 3 and 6 weeks prior to BMT, pre-existing initial lesions had formed before transplantation ($31\pm7x10^3$ μm^2, n=4 and $190\pm43x10^3$, n=4, respectively), and they progressed into larger sized lesions ($336\pm34x10^3$ μm^2, n=10 and $480\pm68x10^3$ μm^2, n=10) at 8 weeks after BMT (i.e., 3+8 and 6+8 weeks WTD feeding, respectively). Moreover, in the transplanted mice which had been fed WTD for 9 and 12 weeks prior to BMT, pre-existing more advanced lesions had formed ($505\pm51x10^3$ μm^2, n=4 and $600\pm11x10^3$ μm^2, n=4, respectively), characterized by a low macrophage content, an increased collagen content, and fibrous cap formation. These pre-existing more advanced lesions increased only slightly in size ($696\pm46x10^3$ μm^2, n=10 and $720\pm82x10^3$ μm^2, n=10, respectively) at 8 weeks after BMT (i.e., 9+8 and 12+8 weeks WTD feeding, respectively). Immunohistochemical staining was performed to distinguish between the pre-existing lesions (EGFP-negative, $EGFP^-$) and the newly formed lesions (EGFP-positive, $EGFP^+$). As shown, in EGFP/WT → $LDLr^{-/-}$ mice without pre-existing lesions (i.e., 0+8 weeks

WTD fed mice), the aortic lesions were exclusively composed of donor-derived EGFP expressing cells, which were primarily F4/80$^+$ macrophages (**Fig. 2B-1**). In contrast, in

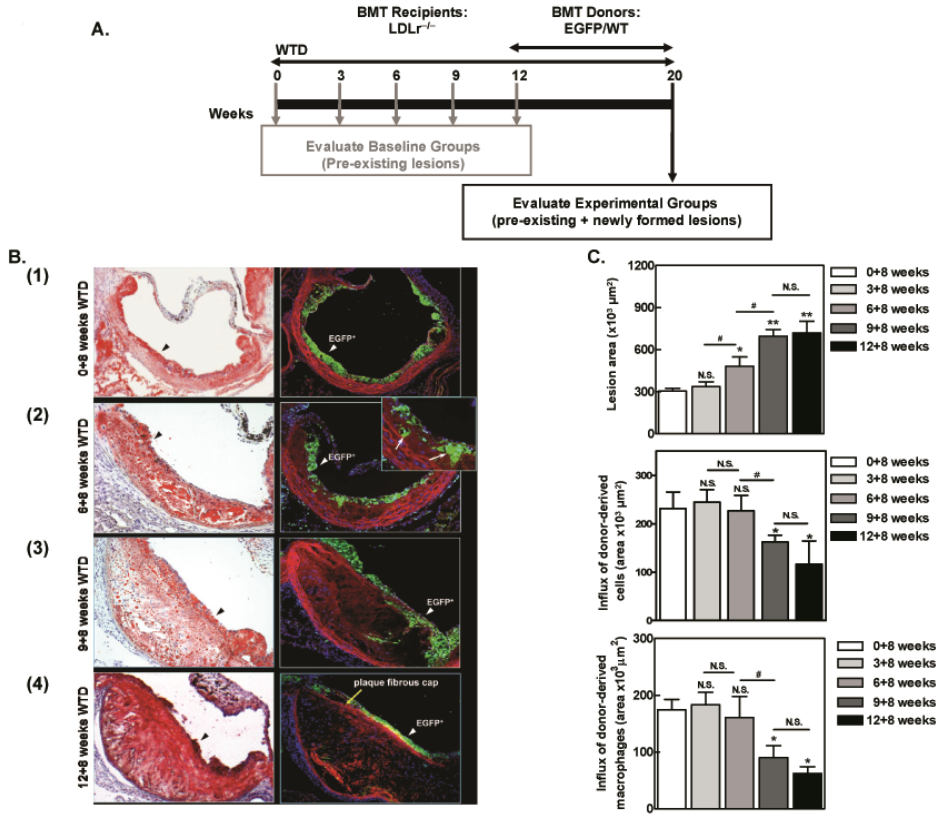

Fig. 2: Generation of LDLr$^{-/-}$ mice with pre-existing atherosclerotic lesions and overexpressing EGFP in macrophages. A: The experimental setup is demonstrated. Bone marrow from EGFP/WT donors was transplanted into LDLr$^{-/-}$ mice that had been fed WTD for 0, 3, 6, 9, and 12 weeks prior to BMT (EGFP/WT → LDLr$^{-/-}$). The transplanted animals were sacrificed after 8, 11, 14, 17, and 20 weeks WTD feeding in total (i.e., 8 weeks WTD feeding after BMT). Subsequently, the pre-existing and newly formed atherosclerotic lesions were analyzed. B: Representative images for Oil-Red-O staining of the atherosclerotic lesions with freshly infiltrated donor-derived macrophages showing massive lipid accumulation (black arrows). Corresponding merged photomicrographs of EGFP (green), F4/80 (red) for macrophages, and DAPI for nuclei (blue) in the aortic root lesions. Co-localization of macrophages with EGFP fluorescence is yellow-green (white arrows). A fibrous cap (yellow arrow) was clearly observed in pre-existing advanced fibroatheroma lesions, and almost no donor-derived macrophages were detected within these lesions. Original magnification 200x. **C:** The mean lesion area was calculated from Oil-Red-O/hematoxylin-stained cross-sections of the aortic root of EGFP-WT → LDLr$^{-/-}$ mice at the level of the tricuspid valves. The influx of donor-derived cells and donor-derived macrophages was evaluated by quantifying the total EGFP$^+$ and EGFP$^+$F4/80$^+$ areas in the aortic root of EGFP-WT → LDLr$^{-/-}$ mice, respectively. Values represent the mean of 10 mice per group. *p<0.05 and **p<0.01 vs. transplanted mice without pre-existing lesions (i.e., 0+8 weeks WTD fed mice). $^{\#}$p<0.05 vs the indicated group. N.S. = non-significant.

EGFP/WT → LDLr$^{-/-}$ mice with pre-existing initial lesions (i.e., 6+8 weeks WTD fed mice), the fatty streak lesions had grown partly by forming a new layer of EGFP$^+$F4/80$^+$ donor-derived macrophages above the pre-existing EGFP$^-$ lesions. Furthermore, a few donor-derived macrophages had infiltrated inside the pre-existing initial lesions (**Fig. 2B-2**). Interestingly, in EGFP/WT → LDLr$^{-/-}$ mice with pre-existing more advanced lesions (i.e., 9+8 weeks WTD fed mice), influx of donor-derived cells, including F4/80$^+$ macrophages, into the arterial wall was largely blocked, as only a very thin layer of newly infiltrated cells had accumulated on top of the fibrous cap of the established complex

lesions (**Fig. 2B-3**). Furthermore, almost no donor-derived cells were detected within the pre-existing advanced fibroatheroma lesions (i.e., 12+8 weeks WTD fed mice) (**Fig. 2B-4**). By quantifying the $EGFP^+F4/80^+$ areas, we did not find a significant difference in the influx of donor-derived macrophages into the arterial wall of the transplanted mice without pre-existing lesions (i.e., 0+8 weeks WTD fed mice) as compared to those with pre-existing initial lesions (i.e., 3+8 or 6+8 weeks WTD fed mice) (**Fig. 2C**). In total 78±22% of the infiltrated $EGFP^+$ cells were $F4/80^+$ macrophages. The remainder percentage will include F4/80-negative macrophages, as well as dendritic cell, T cells, neutrophils, and mast cells. Interestingly, significantly ($p<0.05$) lower influx of donor-derived macrophages into the arterial wall was observed in the transplanted mice with pre-existing more advanced lesions (i.e., 9+8 or 12+8 weeks WTD fed mice). Under these conditions, the percentage of $EGFP^+$ cells that also expressed F4/80 had decreased to 55±7% and 52±24 of the total amount of $EGFP^+$ cells, respectively. These results suggest that the dynamics of cellular infiltration and more specific macrophage infiltration into the arterial wall is largely impaired in more advanced atherosclerotic lesions.

Replacement of liver, spleen and lymph node resident macrophages in transplanted $LDLr^{-/-}$ mice

The liver contains the most abundant macrophage population in the body. At 8 weeks after BMT, a large amount of the F4/80-positive ($F4/80^+$) resident macrophages in the liver, Kupffer cells, expressed EGFP, and were thus of donor-origin (**Fig. 3**). Calculation of the

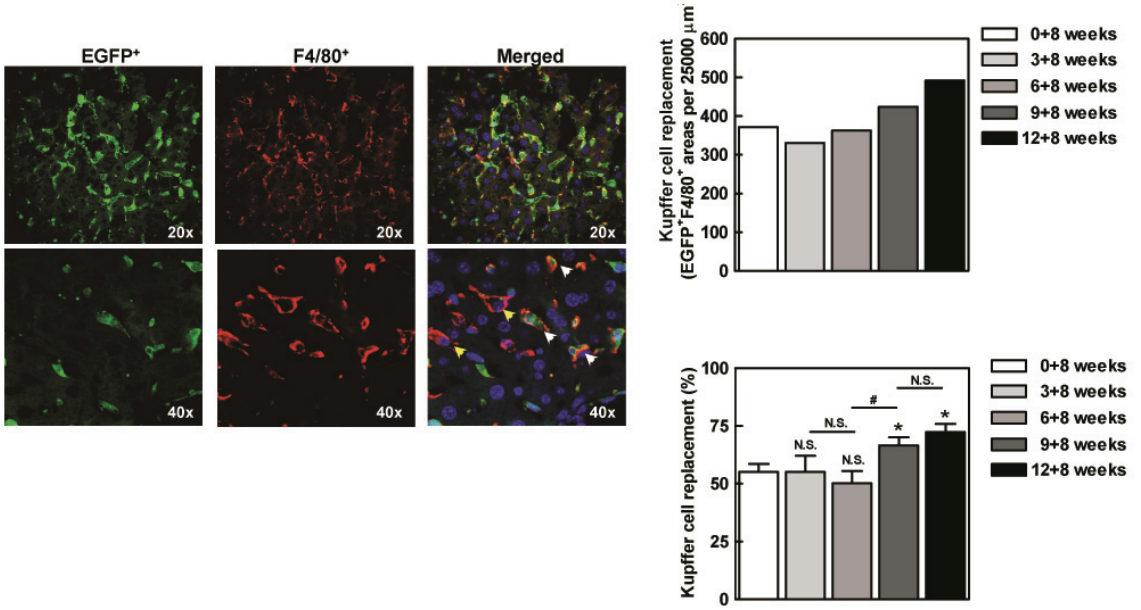

Fig. 3: Replacement of Kupffer cells in the liver of transplanted $LDLr^{-/-}$ mice with pre-existing atherosclerotic lesions with different degrees of complexity. Representative merged photomicrographs of EGFP (green), F4/80 (red) for Kupffer cells (hepatic resident macrophages), and DAPI for nuclei (blue) in the liver of EGFP-WT → $LDLr^{-/-}$ mice. Co-localization of Kupffer cells with EGFP fluorescence (thus of donor-origin) is yellow-green (white arrows). Kupffer cells without EGFP fluorescence (thus of recipient-origin) are red (yellow arrows). Original magnification 400x. The density of $F4/80^+$ and $EGFP^+F4/80^+$ cells was calculated as the number of stained cells per 25000 μm^2 in the liver of EGFP-WT → $LDLr^{-/-}$ mice. Regions of interest were selected blindly using DAPI staining as a reference. Values represent the average from at least 5 adjacent sections. We further determined the ratio $EGFP^+F4/80^+$cells/$F4/80^+$cells, indicative for the replacement of Kupffer cells. Values represent the mean of 10 mice per group. *$p<0.05$ vs. transplanted mice without pre-existing lesions (i.e., 0+8 weeks WTD fed mice). $^{\#}p<0.05$ *vs.* the indicated group. N.S. = non-significant.

ratio $EGFP^+F4/80^+$cells/$F4/80^+$cells, indicative for the replacement of Kupffer cells, showed that >50% of the Kupffer cells were replaced. Interestingly, significantly ($p<0.05$) higher replacement of Kupffer cells was observed in the liver of EGFP-WT → $LDLr^{-/-}$ mice with pre-existing more advanced lesions (i.e., 9+8 or 12+8 weeks WTD fed mice) than those without pre-existing lesions (i.e., 0+8 weeks WTD fed mice) or with pre-existing initial lesions (i.e., 3+8 or 6+8 weeks WTD fed mice).

In addition, higher replacement of resident macrophages in the spleen and lymph nodes was found in the transplanted mice with pre-existing more advanced lesions than those without pre-existing lesions or with pre-existing initial lesions, as determined by FACS analysis (see Supplemental **Fig. S2**). Thus, the observed impaired infiltration of macrophages into more advanced atherosclerotic lesions is not a consequence of a generally impaired macrophage infiltration into tissues. Actually, macrophage infiltration into other organs was increased, probably as a result of an enhanced inflammatory status in those transplanted animals with pre-existing more advanced lesions.

The effect of macrophage ABCA1 expression on the development of pre-existing atherosclerotic lesions in $LDLr^{-/-}$ mice

Previously, we demonstrated a protective role for macrophage ABCA1 in atherosclerosis development in $LDLr^{-/-}$ mice without pre-existing lesions [9,10], and disruption of ABCA1 in hematopoietic cells resulted in enhanced recruitment of macrophages into multiple tissues (e.g. the liver and spleen) [9]. To reveal the effect of ABCA1 expression on the infiltration of macrophages into pre-existing atherosclerotic lesions, bone marrow from EGFP/ABCA1 KO, EGFP/hABCA1, and EGFP/WT mice was transplanted into $LDLr^{-/-}$ mice that had been fed WTD for 6 and 9 weeks prior to BMT (EGFP/ABCA1 KO → $LDLr^{-/-}$, EGFP/hABCA1 → $LDLr^{-/-}$, and EGFP/WT → $LDLr^{-/-}$), and subsequently challenged for another 15 and 12 weeks with WTD, respectively (**Fig. 4A**).

Successful reconstitution of recipients with donor-derived cells was established at 12 or 15 weeks after BMT. Genomic DNA isolated from the EGFP/ABCA1 KO → $LDLr^{-/-}$, EGFP/hABCA1 → $LDLr^{-/-}$, and EGFP/WT → $LDLr^{-/-}$ mice contained the ABCA1 null mutant, the human ABCA1, and only the murine ABCA1 gene, respectively (see Supplemental **Fig. S3**). Independently of the presence of pre-existing lesions, macrophage ABCA1 expression did not significantly affect serum HDL-C levels (data not shown), which is in line with our previous findings [9,10].

Atherosclerotic lesion development was analyzed in the aortic root of EGFP/WT → $LDLr^{-/-}$, EGFP/hABCA1 → $LDLr^{-/-}$, and EGFP/ABCA1 KO → $LDLr^{-/-}$ mice after 21 weeks WTD feeding in total (i.e., 15 and 12 weeks WTD feeding after BMT). As shown in **Fig. 4B**, macrophage ABCA1 deficiency did not significantly affect the development of pre-existing initial lesions (mean lesion areas: $803\pm113x10^3$ μm^2, n=12 and $758\pm86x10^3$ μm^2, n=12 for EGFP/ABCA1 KO → $LDLr^{-/-}$ mice and EGFP/WT → $LDLr^{-/-}$ controls, respectively, P=0.13), while macrophage ABCA1 overexpression moderately (p=0.05) inhibited the progression of pre-existing initial lesions (mean lesion area: $631\pm42x10^3$ μm^2, n=8 for EGFP/hABCA1 → $LDLr^{-/-}$ mice)**.** On pre-existing advanced lesions, no effect of deletion or overexpression of macrophage ABCA1 was observed (mean lesion areas: $783\pm42x10^3$ μm^2, n=12, $807\pm63x10^3$ μm^2, n=8, and $742\pm60x10^3$ μm^2, n=10 for EGFP/ABCA1 KO → $LDLr^{-/-}$ mice, EGFP/hABCA1 → $LDLr^{-/-}$ mice, and EGFP/WT → $LDLr^{-/-}$ controls, respectively).

By quantifying the EGFP$^+$F4/80$^+$ areas in the lesions, we observed that influx of ABCA1 deficient macrophages into the pre-existing initial lesions was not significantly

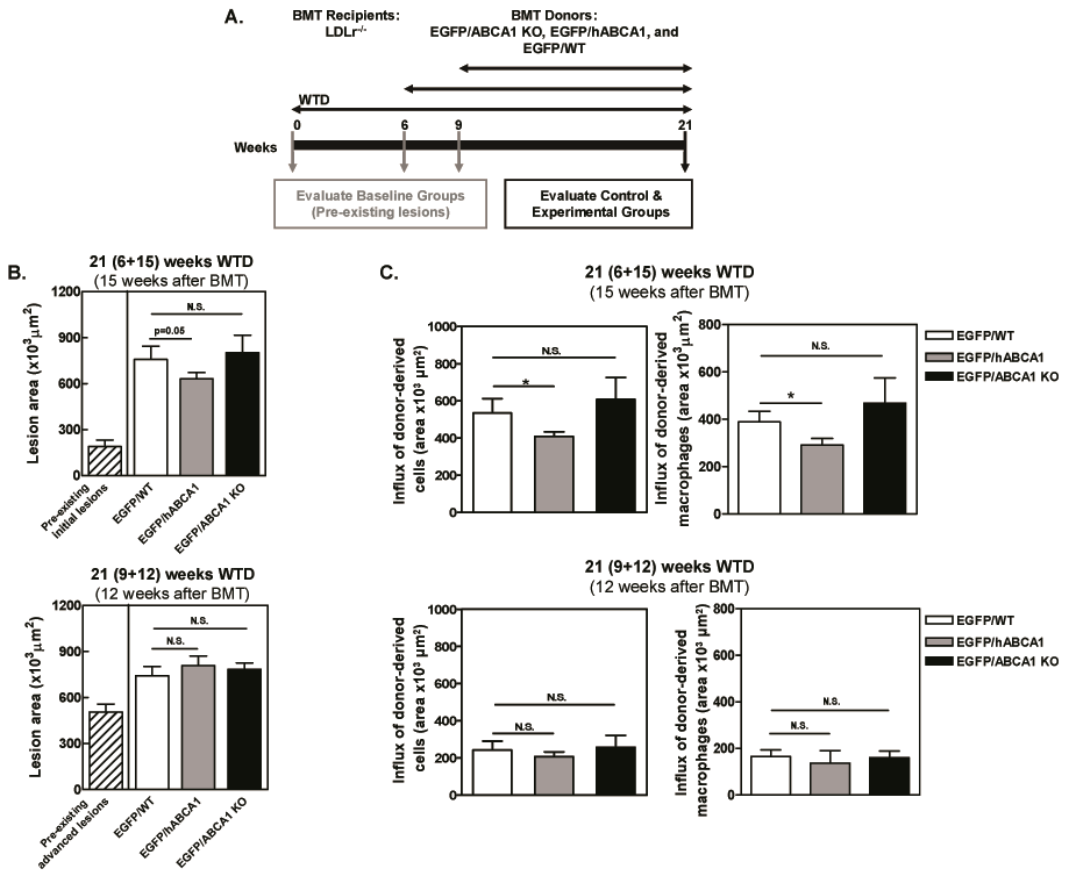

Figure 4: The effect of macrophage ABCA1 expression on the development of pre-existing atherosclerotic lesions in LDLr$^{-/-}$ mice. **A:** The experimental setup is demonstrated. Bone marrow from EGFP/ABCA1 KO, EGFP/hABCA1, and EGFP/WT mice was transplanted into LDLr$^{-/-}$ mice that had been fed WTD for 6 and 9 weeks prior to BMT (EGFP/ABCA1 KO → LDLr$^{-/-}$, EGFP/hABCA1 → LDLr$^{-/-}$, and EGFP/WT → LDLr$^{-/-}$), and subsequently challenged for another 15 and 12 weeks with WTD, respectively. **B:** The mean lesion area was calculated from Oil-Red-O/hematoxylin-stained cross-sections of the aortic root of transplanted mice with pre-existing initial lesions or with pre-existing more advanced lesions. **C:** The influx of donor-derived cells and macrophages was evaluated by quantifying the total EGFP$^+$ and EGFP$^+$F4/80$^+$ areas in the aortic root of transplanted animals. Values represent the mean of 8-12 mice per group. *p<0.05 vs. EGFP/WT transplanted mice. N.S. = non-significant.

changed (mean EGFP$^+$F4/80$^+$ areas: 468±107x10^3 µm^2, n=12 and 389±44x10^3 µm^2, n=12 for EGFP/ABCA1 KO → LDLr$^{-/-}$ mice and EGFP/WT → LDLr$^{-/-}$ controls, respectively), while influx of ABCA1 overexpressing macrophages into the pre-existing initial lesions was significantly (p<0.05) impaired (mean EGFP$^+$F4/80$^+$ area: 291±28x10^3 µm^2, n=8 for EGFP/hABCA1 → LDLr$^{-/-}$ mice) (**Fig. 4C**). Independent of the type of donor bone marrow used, EGFP$^+$F4/80$^+$ cells comprised ~75% of the total amount of EGFP$^+$ infiltrated cells. As expected, the infiltration of bone marrow-derived macrophages into the pre-existing more advanced lesions was substantially lower than that into the pre-existing initial lesions. Importantly, the influx of donor-derived macrophages into the established more advanced lesions was not affected by macrophage ABCA1 expression (mean EGFP$^+$F4/80$^+$ areas: 161±28x10^3 µm^2, n=12 and 165±29x10^3 µm^2, n=8, and 137±54x10^3 µm^2, n=10 for EGFP/ABCA1 KO → LDLr$^{-/-}$ mice, EGFP/hABCA1 → LDLr$^{-/-}$ mice, and

EGFP/WT → LDLr$^{-/-}$ controls, respectively). Moreover, total amount of EGFP^{+} cells that had infiltrated the lesions was not affected.

Discussion

In this study, bone marrow transplantation was utilized to investigate the dynamics of macrophage infiltration into the arterial wall during the pathogenesis of atherosclerosis. By tracking donor-derived macrophages (EGFP^{+}F4/80^{+}), we demonstrate that (1) the growth of pre-existing early lesions is mainly caused by continued infiltration of macrophages into the arterial wall, (2) macrophage infiltration into pre-existing more advanced lesions is largely impaired, most likely due to the formation of a fibrous cap, and (3) macrophage ABCA1 expression affects the infiltration of macrophage into pre-existing early lesions, but not into more advanced lesions.

After transplantation, pre-existing fatty streak lesions largely increased in size, which was mainly caused by continued infiltration of donor-derived macrophages into the arterial wall. Moreover, we found that influx of ABCA1 overexpressing macrophages into the pre-existing fatty streak lesions was significantly impaired. ABCA1-mediated cholesterol efflux is a key factor to prevent the accumulation of macrophage foam cells in the arterial wall. In addition, ABCA1 modulates cholesterol content both on the cell surface and within intracellular compartments, and thereby impacts macrophage function via influencing cellular inflammatory cytokine secretion [14-18]. However, it was also suggested that not all of the anti-inflammatory properties of ABCA1 are a consequence of its lipid transport activity. ABCA1 interacts with its acceptor (i.e., apoAI its mimetic peptides), and activates signaling molecules (i.e., Janis kinase 2) [19-22]. Macrophage ABCA1 thus exerts multiple anti-atherogenic functions, which may explain the inhibitory effect of ABCA1 overexpression on the infiltration of macrophages into pre-existing fatty streak lesions, resulting in reduced lesion size. These findings suggest that preventing macrophage recruitment into early stages of lesion development provides a promising therapeutic strategy to reduce atherosclerosis burden, and increasing macrophage ABCA1 expression may be one avenue of doing so. Surprisingly, no significant effect of ABCA1 deficiency was observed on macrophage recruitment into pre-existing early lesions. Bone marrow transplantation has been shown to affect atherosclerotic lesion development [23]. Therefore, the lack of an effect of macrophage ABCA1 knock out on lesion progression and macrophage infiltration may be due to BMT-dependent effects on lesion progression.

Pre-existing more advanced lesions increased only slightly in size after transplantation, and the infiltration of donor-derived macrophages into these lesions was largely impaired. In mice with pre-existing advanced lesions, we did observe a significantly higher replacement of tissue macrophages, as compared to mice without pre-existing lesions or with pre-existing early lesions. Wouters et al. demonstrated that dietary cholesterol can provoke hepatic inflammation in hyperlipidemic mice, possibly due to the direct activation of Kupffer cells upon scavenging remnant lipoproteins [24]. Recently, the effect of dietary cholesterol on hepatic inflammation was further elucidated by the same group, and it was suggested that intrahepatic cholesterol influences progression, inhibition and reversal of non-alcoholic steatohepatitis in hyperlipidemic mice [25]. In this study, we found that LDLr$^{-/-}$ mice with pre-existing more advanced lesions displayed higher levels of intrahepatic cholesterol, which may trigger an inflammatory response in the liver of these animals. Our findings also indicate that the impaired influx of macrophages into atherosclerotic lesions of mice with pre-existing more advanced lesions is not the consequence of a reduced capacity of macrophage to infiltrate into tissues under these conditions. Lesion progression coincides with the formation of a fibrous cap, which is

essential for the stability of the plaque. Currently, it is most likely that the formation of fibrous caps in pre-existing advanced lesions directly prevents further influx of macrophages into the arterial wall. Importantly, our results indicate that therapeutic modulation of macrophage infiltration would not be expected to have beneficial effects on more advanced lesions. In line, we show that neither disruption nor up-regulation of macrophage ABCA1 expression significantly influences the development of atherosclerotic lesion in mice with pre-existing more advanced lesions.

In conclusion, we have established a new model for studying the dynamic changes in lesion development using the technique of bone marrow transplantation. It must be noted that the bone marrow transplantation procedure, and in particular the irradiation required to eliminate the endogenous bone marrow cells, might impact on the atherogenic process. However, using this model we for the first time have been able to show that the dynamics of macrophage infiltration into the arterial wall largely differs during atherosclerotic lesion development. This may affect the efficiency of pharmaceutical interventions aimed at targeting macrophage infiltration into the arterial wall.

Acknowledgements

This work was supported by the Netherlands Heart Foundation (Grants 2007T056 to D. Y., 2001T4101 to Y.Z.), the Netherlands Organization for Scientific Research (VIDI Grant 917.66.301 to M.V.E.), and the Canadian Institutes of Health Research. M. Van Eck is an Established Investigator of the Netherlands Heart Foundation (Grant 2007T056). M. R. Hayden is a University Killam Professor and holds a Canada Research Chair in Human Genetics and Molecular Medicine.

References

1. Martin R. Bennett. The atherosclerotic plaque was not built in a day: the dynamic nature of plaque progression and instability. *Heart Metab.* 2007; 36:5-7.
2. Blood Cholesterol Consensus Conference: Lowering blood cholesterol to prevent heart disease. *JAMA.* 1985; 253:2080-2086.
3. Smith JD, Trogan E, Ginsberg M, Grigaux C, Tian J, Miyata M. Decreased atherosclerosis in mice deficient in both macrophage colony-stimulating factor (op) and apolipoprotein E. *Proc Natl Acad Sci U S A.* 1995; 92(18):8264-8268.
4. McKnight AJ, Gordon S. Membrane molecules as differentiation antigens of murine macrophages. *Adv Immunol.* 1998; 68:271-314.
5. Vu TH, Werb Z. Matrix metalloproteinases: effectors of development and normal physiology. *Genes Dev.* 2000; 14:2123-2133.
6. Galis ZS, Sukhova GK, Lark MW, Libby P. Increased expression of matrix metalloproteinases and matrix degrading activity in vulnerable regions of human atherosclerotic plaques. *J Clin Invest*. 1994; 94:2493-2503.
7. Oram JF. HDL apolipoproteins and ABCA1: partners in the removal of excess cellular cholesterol. *Arterioscler Thromb Vasc Biol.* 2003; 23(5):720-727.
8. Francis GA, Knopp RH, Oram JF. Defective removal of cellular cholesterol and phospholipids by apolipoprotein A-I in Tangier Disease. *J Clin Invest.* 1995; 96:78-87.
9. Van Eck M, Bos IS, Kaminski WE. Leukocyte ABCA1 controls susceptibility to atherosclerosis and macrophage recruitment into tissues. *Proc Natl Acad Sci USA.* 2002; 99:6298-6303.
10. Van Eck M, Singaraja RR, Ye D, Hildebrand RB, James ER, Hayden MR, Van Berkel TJ. Macrophage ATP-binding cassette transporter A1 overexpression inhibits atherosclerotic lesion progression in low-density lipoprotein receptor knockout mice. *Arterioscler Thromb Vasc Biol.* 2006; 26(4):929-934.
11. Schaefer BC, Schaefer ML, Kappler JW, Marrack P, Kedl RM. Observation of antigen-dependent CD8+ T-cell/ dendritic cell interactions in vivo. *Cell Immunol.* 2001; 214(2):110-122.

12. Stary HC, Chandler AB, Glagov S, Guyton JR, Insull W Jr, Rosenfeld ME, Schaffer SA, Schwartz CJ, Wagner WD, Wissler RW. A definition of initial, fatty streak, and intermediate lesions of atherosclerosis. A report from the Committee on Vascular Lesions of the Council on Arteriosclerosis, American Heart Association. *Circulation.* 1994; 89(5):2462-2478.
13. Bligh EG, Dyer WJ. A rapid method of total lipid extraction and purification. *Can. J. Biochem. Physiol.* 1959; 37(8):911-917.
14. Zhu X, Lee JY, Timmins JM, Brown JM, Boudyguina E, Mulya A, Gebre AK, Willingham MC, Hiltbold EM, Mishra N, Maeda N, Parks JS. Increased cellular free cholesterol in macrophage-specific Abca1 knock-out mice enhances pro-inflammatory response of macrophages. *J Biol Chem.* 2008; 283(34):22930-22941.
15. Koseki M, Hirano K, Masuda D, Ikegami C, Tanaka M, Ota A, Sandoval JC, Nakagawa-Toyama Y, Sato SB, Kobayashi T, Shimada Y, Ohno-Iwashita Y, Matsuura F, Shimomura I, Yamashita S. Increased lipid rafts and accelerated lipopolysaccharide-induced tumor necrosis factor-alpha secretion in Abca1-deficient macrophages. *J. Lipid Res.* 2007; 48:299-306.
16. Sun Y, Ishibashi M, Seimon T, Lee M, Sharma SM, Fitzgerald KA, Samokhin AO, Wang Y, Sayers S, Aikawa M, Jerome WG, Ostrowski MC, Bromme D, Libby P, Tabas IA, Welch CL, Tall AR. Free cholesterol accumulation in macrophage membranes activates Toll-like receptors and p38 mitogen-activated protein kinase and induces cathepsin K. *Circ Res*. 2009; 104:455-465.
17. Lajoie P, Goetz JG, Dennis JW, Nabi IR. Lattices, rafts, and scaffolds: domain regulation of receptor signaling at the plasma membrane. *J Cell Biol*. 2009; 185:381-385.
18. Strauss JF 3rd, Liu P, Christenson LK, Watari H. Sterols and intracellular vesicular trafficking: lessons from the study of NPC1. *Steroids.* 2002; 67(12):947-951.
19. Tang C, Vaughan AM, Anantharamaiah GM, Oram JF. Janus kinase 2 modulates the lipid-removing but not protein-stabilizing interactions of amphipathic helices with ABCA1. *J Lipid Res.* 2006; 47:107-114.
20. Tang C, Vaughan AM, Oram J F. Janus kinase 2 modulates the apolipoprotein interactions with ABCA1 required for removing cellular cholesterol. *J Biol Chem.* 2004; 279:7622-7628.
21. Aaronson DS, Horvath CM. A road map for those who don't know JAK-STAT. *Science.* 2002; 296:1653-1655.
22. Tang C, Liu Y, Kessler PS, Vaughan AM, Oram JF. The macrophage cholesterol exporter ABCA1 functions as an anti-inflammatory receptor. *J Biol Chem*. 2009; 20;284(47):32336-32343.
23. Schiller NK, Kubo N, Boisvert WA, Curtiss LK. Effect of gamma-irradiation and bone marrow transplantation on atherosclerosis in LDL receptor-deficient mice. *Arterioscler Thromb Vasc Biol.* 2001; 21(10):1674-1680.
24. Wouters K, van Gorp PJ, Bieghs V, Gijbels MJ, Duimel H, Lütjohann D, Kerksiek A, van Kruchten R, Maeda N, Staels B, van Bilsen M, Shiri-Sverdlov R, Hofker MH. Dietary cholesterol, rather than liver steatosis, leads to hepatic inflammation in hyperlipidemic mouse models of nonalcoholic steatohepatitis. *Hepatology.* 2008; 48(2):474-486.
25. Wouters K, van Bilsen M, van Gorp PJ, Bieghs V, Lütjohann D, Kerksiek A, Staels B, Hofker MH, Shiri-Sverdlov R. Intrahepatic cholesterol influences progression, inhibition and reversal of non-alcoholic steatohepatitis in hyperlipidemic mice. *FEBS Lett.* 2010; 584(5):1001-1005.

Supplementary Figures

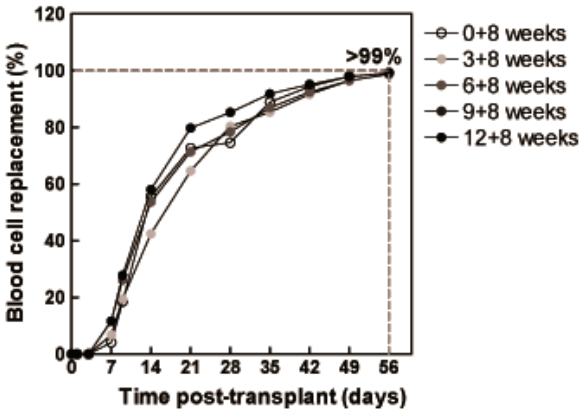

Fig. S1: Verification of success of bone marrow transplantation. The appearance of donor-derived EGFP-expressing blood cells in the circulation was determined by FACS analysis at different time points after transplantation.

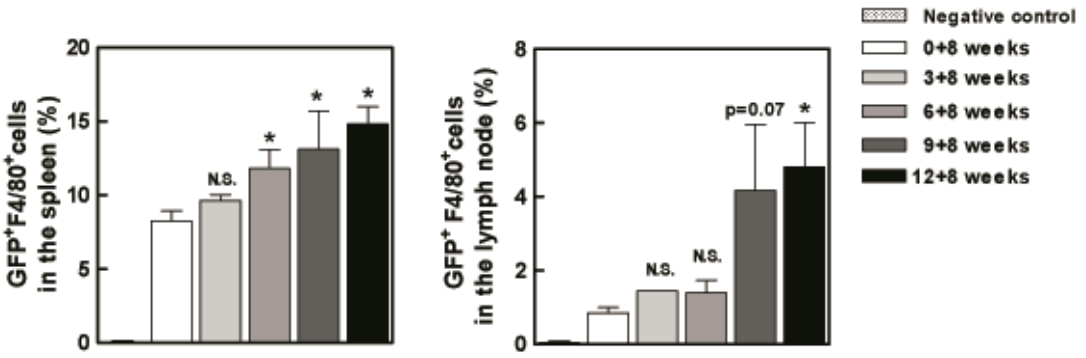

Fig. S2: Replacement of spleen and lymph node resident macrophages in transplanted LDLr$^{-/-}$ mice. At 8 weeks post-transplant, the proportion of EGFP labeled cells that were immunoreactive for F4/80 (i.e., the percentage of EGFP^{+}F4/80^{+}cells from F4/80^{+}cells) in the spleen and intestinal lymph node of EGFP-WT → LDLr$^{-/-}$ mice with pre-existing lesions was determined by FACS analysis. Values represent the mean of 10 mice per group. Data are presented as mean±SEM. *p<0.05 vs. transplanted animals without pre-existing lesions (i.e., 0+8 weeks WTD fed mice). N.S. = non-significant.

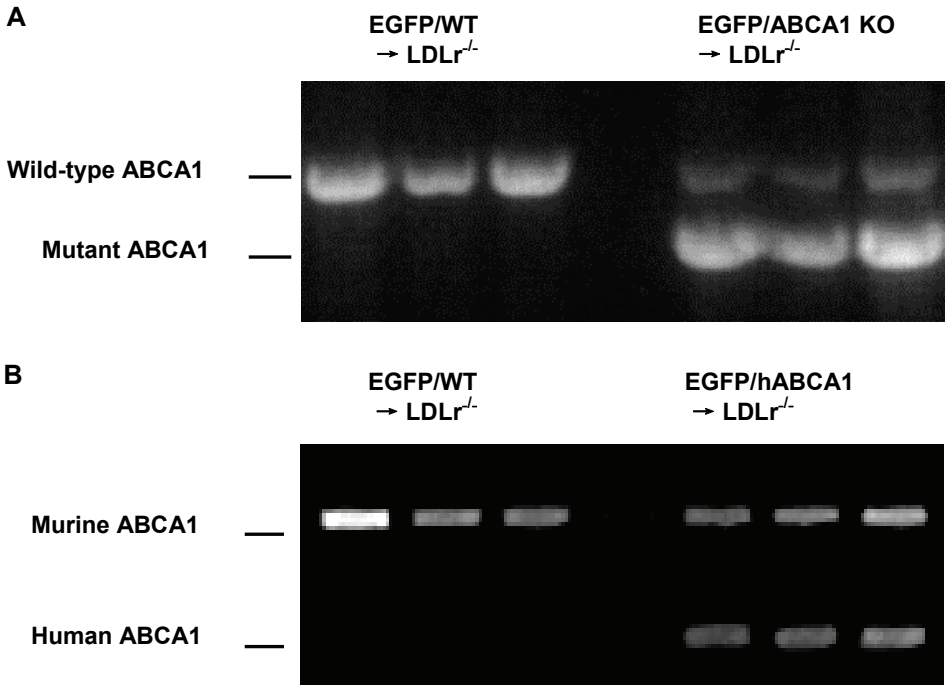

Fig. S3: Verification of success of bone marrow transplantation. The hematologic chimerism of the transplanted LDLr$^{-/-}$ mice was determined using genomic DNA from bone marrow by polymerase chain reaction (PCR) at 12 or 15 weeks post-transplant. The forward and reverse primers 5'-TTTCTCATAGGGTTGGTCA-3' and 5'-TGCAATCCATCTTGTTCAAT-3' for the null mutant ABCA1, 5'-TGGGAACTCCTGCTAAAAT-3' and 5'-CCATGTGGTGTGTAGACA-3' for the wild-type gene, and the forward and reverse primers 5'-GGCTGGATTAGCAGTCCTCA-3' and 5'-ATCCCCAACTCAAAACCACA-3' for the human ABCA1 were used. **A:** Amplification of the ABCA1 null mutant gene resulted in a 1.0kb PCR band, whereas the wild-type ABCA1 gene yielded a 1.3kb band. **B:** Amplification of the human ABCA1 gene resulted in a ~304bp PCR band, whereas the murine ABCA1 gene yielded a ~900bp band.

CHAPTER 10

High-dose phosphatidylcholine particle mobilizes free cholesterol and rapidly stabilizes established atherosclerotic lesions

Ying Zhao[1], Reeni B. Hildebrand[1], Theo J.C. Van Berkel[1], Miranda Van Eck[1]

[1] Division of Biopharmaceutics, Leiden/Amsterdam Center for Drug Research, Leiden University, Einsteinweg 55, 2333 CC Leiden, The Netherlands

Abstract

Objective: The beneficial effect of reconstituted HDL (rHDL), composed of human apolipoprotein AI (apoAI) and phosphatidylcholine (PC), on atherosclerosis might be attributed to both its capacities to induce cholesterol efflux from macrophage foam cells and suppress inflammation. The aim of the present study is to investigate whether promotion of macrophage cholesterol efflux alone by phosphatidylcholone (PC) infusion could modify established atherosclerotic lesions.

Methods and Results: *In-vitro* cholesterol efflux studies demonstrated that at high concentrations (>84 μg/mL), PC particles induced cholesterol efflux from macrophage foam cells as efficiently as rHDL containing the same amount of PC. Also, a single intravenous injection of 1680 mg/kg PC increased plasma free and total cholesterol levels in female LDL receptor knockout mice on Western-type diet. Importantly, PC infusion rapidly decreased the macrophage content and increased the amount of collagen in both established early and advanced lesions.

Conclusions: Promotion of macrophage cholesterol efflux by PC infusion does lead to the stabilization of established atherosclerotic lesions.

--- submitted---

Introduction

Numerous studies have demonstrated that HDL is an inverse predictor of cardiovascular disease [1]. Elevating the plasma levels of HDL is therefore regarded as a promising therapeutic strategy for atherosclerosis. The atheroprotective properties of HDL might be attributed to its role in prevention of foam cell formation, oxidative stress, inflammation, and thrombosis [2]. It is hypothesized that HDL induces cholesterol efflux from macrophage foam cells and subsequently promote reverse cholesterol transport, thereby inhibiting atherogenesis [3]. Recent human studies have shown that the cholesterol efflux capacity of HDL in humans has a strong inverse association with both carotid intima-media thickness and the likelihood of angiographic coronary artery disease [4]. However, it is still unclear whether enhancement of the efflux capacity of HDL alone could stabilize established atherosclerotic lesions and protect against the development of atherosclerosis.

A promising approach to increase the circulating levels of HDL is infusion of reconstituted HDL (rHDL), composed of human apolipoprotein AI (apoAI) and phosphatidylcholine (PC). rHDL infusion increases the cholesterol efflux capacity and anti-inflammatory properties of plasma HDL and modifies atherosclerotic lesions in both mice [5,6] and humans [7, 8]. The atheroprotective effects of rHDL are mainly attributed to apoAI, its main protein component, as apoAI induces cellular cholesterol efflux via ABC-transporter A1 (ABCA1) [9] and suppresses inflammation [10, 11]. PC particles are also acceptors for cholesterol effluxed via ABC-transporter G1 (ABCG1), scavenger receptor class B type I (SR-BI), and aqueous diffusion [13]. Infusion of large amounts of PC is thus expected to have substantial effects. Also repeated infusion of large unilamellar vesicles composed of egg PC, removes cholesterol and regresses the atheroma in cholesterol-fed rabbit [14]. However, studies investigating rHDL do not include PC particles as controls [7, 8, 15]. Our present study clearly demonstrates that the PC component of rHDL is sufficient to induce cholesterol efflux and stabilize atherosclerotic lesions in mice.

Methods

Preparation of PC particles and rHDL

3.08 g cholic acid sodium salt (Sigma) was dissolved in 25 mL of buffer containing 10 mmol/L Tris-HCl, 10 mmol/L NaCl, 1 mmol/L EDTA, pH 8.0. In this buffer 4.2 g soybean phosphatidylcholine (Phospholipon 90, Nattermann Phospholipid, Germany) was dissolved for 6 hours at room temperature. After dialysis against 1% sucrose solution, the concentration of PC in the solution was determined (Spinreact, Girona, Spain) and adjusted to 84 mg/mL. Sucrose was added to a final concentration of 10%. PC particles were prepared freshly and sterile-filtered before use. The particle size was determined by dynamic light scattering (ZetaSizer Nano, Malvern Instruments, U. K.). The mean diameter of two main populations of PC particles (Peak 1 and 2) is 4.4±0.6 nm and 24.7±2.4 nm, respectively (Supplementary Figure 1).

rHDL (CSL-111, Behring AG, Switzerland) consists of apoAI isolated from human plasma and PC from soybean (Phospholipon 90, Nattermann Phospholipid, Germany) with a molar ratio of 1:150. Before use, rHDL was reconstituted with 50 mL of sterile water to yield a clear, pale-yellow solution containing 20 mg/mL apoAI and 84 mg/mL PC in 10% (w/v) sucrose. The size of the rHDL particles was 12.6±2.8 nm [16].

Mice

LDL receptor knockout (LDLr KO) female mice, obtained from the Jackson Laboratory (Bar Habor, USA) were bred at the Gorlaeus Laboratories and maintained on sterilized regular chow, containing 4.3% (w/w) fat and no added cholesterol (RM3; Special Diet Service, Witham, UK). At the age of 12 weeks the LDLr KO mice were challenged with a Western-type diet (WTD) containing 15% (w/w) total fat and 0.25% (w/w) cholesterol (Diet W, Special Diet Services, Whitham, UK) for 5 weeks (n= 32) or 9 weeks (n= 32) to induce the development of early and advanced atherosclerotic lesions, respectively. Subsequently, animals received a single intravenous injection of 1680 mg/kg PC or vehicle (control group). After 48 hours, animals were sacrificed under full anesthesia. Animal experiments were performed at the Gorlaeus Laboratories of the Leiden/Amsterdam Center for Drug Research in accordance with the National Laws. All experimental protocols were approved by the Ethics Committee for Animal Experiments of Leiden University.

Cholesterol efflux studies

Thioglycollate-elicited peritoneal macrophages, harvested from LDLr KO mice, were loaded with 0.5 μCi/mL ^{3}H-cholesterol and 2.5% serum from LDLr KO mice on chow diet in DMEM/0.2% BSA for 24 h at 37^{o}C. Cholesterol efflux was studied by incubation of cells with DMEM/0.2%BSA supplemented with reconstituted HDL containg 10, 20, or 50 μg/mL apoAI (CSL Behring AG, Switzerland) or 42, 84, or 210 μg/mL soybean phosphatidylcholine. After a 6- or 24-hours efflux period, radioactivity in the cells and medium was determined by liquid scintillation counting. Cholesterol efflux is defined as (dpm_{medium}/ dpm_{cell} +dpm_{medium}) x 100%.

Lipids Analysis

The concentrations of cholesterol in serum were determined by incubation with 0.025 U/mL cholesterol oxidase (Sigma) and 0.065 U/mL peroxidase and 15 μg/mL cholesteryl esterase (Roche Diagnostics, Mannheim, Germany) in reaction buffer (1.0 KPi buffer, pH=7.7 containing 0.01 M phenol, 1 mM 4-amino-antipyrine, 1% polyoxyethylene-9-laurylether, and 7.5% methanol). Phospholipids (PL) in serum were determined using a standard enzymatic colorimetric assay (Spinreact, Girona, Spain).

Histological Analysis of the Aortic Root

On sacrifice the arterial tree was perfused *in situ* with phosphate buffer solution (PBS) and the heart was excised and stored in 3.7% neutral-buffered formalin (Formal-fixx; Shandon Scientific Ltd., UK) until use. Atherosclerotic lesion development was quantified in oil red O/hematoxylin-stained cryostat sections of the aortic root from using the Leica image analysis system, consisting of a Leica DMRE microscope coupled to a video camera and Leica Qwin Imaging software (Leica Ltd). Mean lesion area (in μm^2) was calculated from 10 oil red O/hematoxylin-stained sections, starting at the appearance of the tricuspid valves. Sections were immunolabeled against MOMA-2 (monoclonal rat IgG2b, dilution 1:50, Research diagnostics) for detection of monocytes/macrophages. Collagen content of the lesions was visualized with aniline blue by using Masson's Trichrome accustain according to the manufacturer's instructions (Sigma). Histochemical stainings were subsequently quantified in 5 consecutive sections by computer-aided morphometric analysis using the Leica image analysis system. All analyses were performed blinded.

Statistical Analysis

Statistical analysis was performed using ANOVA and the Student-Newman-Keuls post-test (GraphPad InStat and Prism software). A level of $p<0.05$ was considered significant.

Results and Discussion

PC particle induced cholesterol efflux from macrophage foam cells

Reconstituted HDL (rHDL), composed of apoAI and phospholipids, is an efficient cholesterol acceptor *in vitro* and *in vivo* [17, 18]. ApoAI induces cholesterol efflux via ABCA1 while particles rich in phospholipid accept cholesterol transported by SR-BI, ABCG1 and aqueous diffusion [17, 19]. To test the efficiency of PC particles in induction of cholesterol efflux, PC and rHDL particles were incubated with [^{3}H]-cholesterol labeled macrophage foam cells for 6 or 24 hours. As shown in Figure 1, after 6-hour incubation, at the concentration of 42 μg/mL (the concentration of PC in rHDL containing 10 μg/mL apoAI), rHDL induced 1.6-fold ($P<0.05$) more cholesterol efflux as compared to PC particles, which might be attributed to apoAI-mediated cholesterol efflux. Interestingly, with the increase of the concentration of rHDL, the difference between rHDL and a comparable amount of PC in particles lacking apoAI diminished and finally was completely absent at the concentration of 210 μg/mL PC. Similar results were also found after 24 hours in the presence of rHDL and PC particles (data not shown). These data indicate that PC could induce cholesterol efflux as efficiently as rHDL at concentrations above 84 μg/mL. Since small PC particles are more efficient in inducing cholesterol efflux from macrophages as compared to larger ones [17, 20], it is likely athat the smallest PC particles in the PC solution with a mean diameter of 4.4±0.6 nm (Supplementary Figure 1) greatly contributed to the PC-mediated cholesterol efflux.

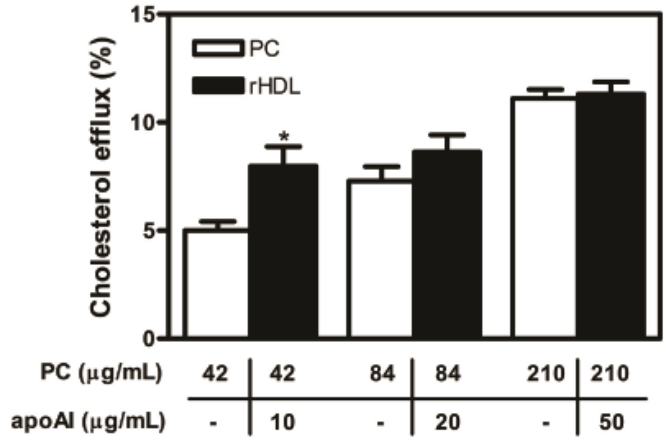

Figure 1. PC promotes cholesterol efflux from serum-loaded macrophages. Peritoneal macrophages from wildtype mice were labeled for cholesterol efflux as described in the materials and methods. Basal efflux to media (in the absence of added acceptors) has been subtracted from the data shown. Values are mean±SEM (n=3 mice). Statistically significant difference $^*P<0.05$ *vs* PC.

PC particles mobilized FC *in vivo* and modified the composition of established early and advanced atherosclerotic lesions

Previous studies showed that infusion of rHDL containing 400 mg/kg $apoAI_{milano}$ quickly modulates the stability of atherosclerotic lesions in apoE KO mice [6]. Thus, in the present study, 1680 mg/kg of PC particles, comparable to the amount of PC in rHDL at

concentration of 400 mg/kg apoAI, or control vehicle were intraveneously injected into female LDLr KO mice fed WTD for 5 weeks. This allowed us to determine whether augmentation of macrophage cholesterol efflux alone could modulate established early lesions. The plasma lipid levels were determined at 1 and 48 hours after infusion. As shown in Figure 2A, at 1 hour after infusion, a dramatic increase (4.3-fold, $p<0.001$) of plasma phospholipid (PL) levels was observed in PC-treated animals as compared to controls, indicating successful infusion. PC-treated animals also showed increased levels of plasma free cholesterol (FC) (1.4-fold, $p<0.001$) and total cholesterol (TC) (1.1-fold, $p<0.05$) levels. At 48 hours after infusion, the levels of plasma PL in PC-treated mice were declined to the levels of control mice. In contrast, slight increases in plasma FC (1.2-fold, $p<0.01$) and TC (1.2-fold, $p<0.01$) levels were still evident in PC-treated mice (Figure 2B). In line with our *in-vitro* efflux data, PC could thus also mobilize FC *in vivo*, similar to rHDL [18].

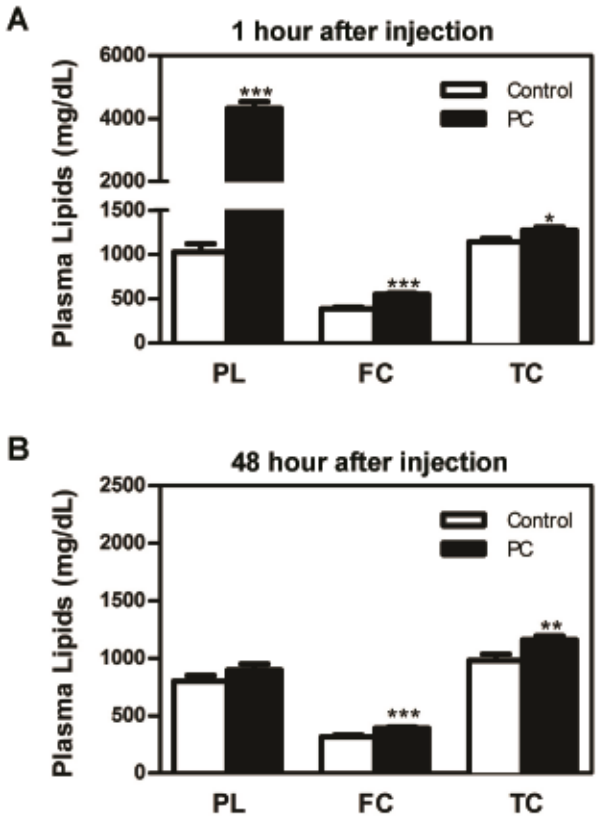

Figure 2. PC infusion increased plasma free and total cholesterol, and phospholipid levels. Animals were put on WTD for 5 weeks and were separated into two groups with equal plasma cholesterol levels. At 1 (A) and 48 (B) hours after infusion with PC or control vehicle, plasma was collected for lipid analysis. Values are means±SEM. Statistically significant difference $^{*}P<0.05$, $^{**}P<0.01$, and $^{***}P<0.05$ *vs* control.

Next, the effects of PC infusion on the established early atherosclerotic lesions were evaluated at the aortic root. As shown in Figure 3A and 3B, infusion of a large dose of PC did not affect the size of established early lesions. However, PC infusion did lead to a 1.3-fold ($p=0.053$) reduction of the macrophage content and a 1.8-fold ($p=0.023$) increase in the amount of collagen in early lesions (Figure 3B and 3C).

To further determine the effects of PC particle infusion on established advanced lesions, female LDLr-/- mice were fed WTD for 9 weeks prior to the treatment with PC particles. Infusion of PC also increased the plasma FC and TC levels in mice with advanced lesions at 1 and 48 hours after infusion (data not shown). As shown in Figure 4A, strikingly, the size of advanced lesions at the aortic root of PC-treated mice was 1.4-fold ($p=0.0369$) smaller than that of control mice at 48 hours after infusion of PC particles. Similar to early lesions, PC infusion also led to a reduced macrophage (1.4-fold, $p=0.085$) and an increased collagen (1.4-fold, $p=0.0238$) content of advanced lesions.

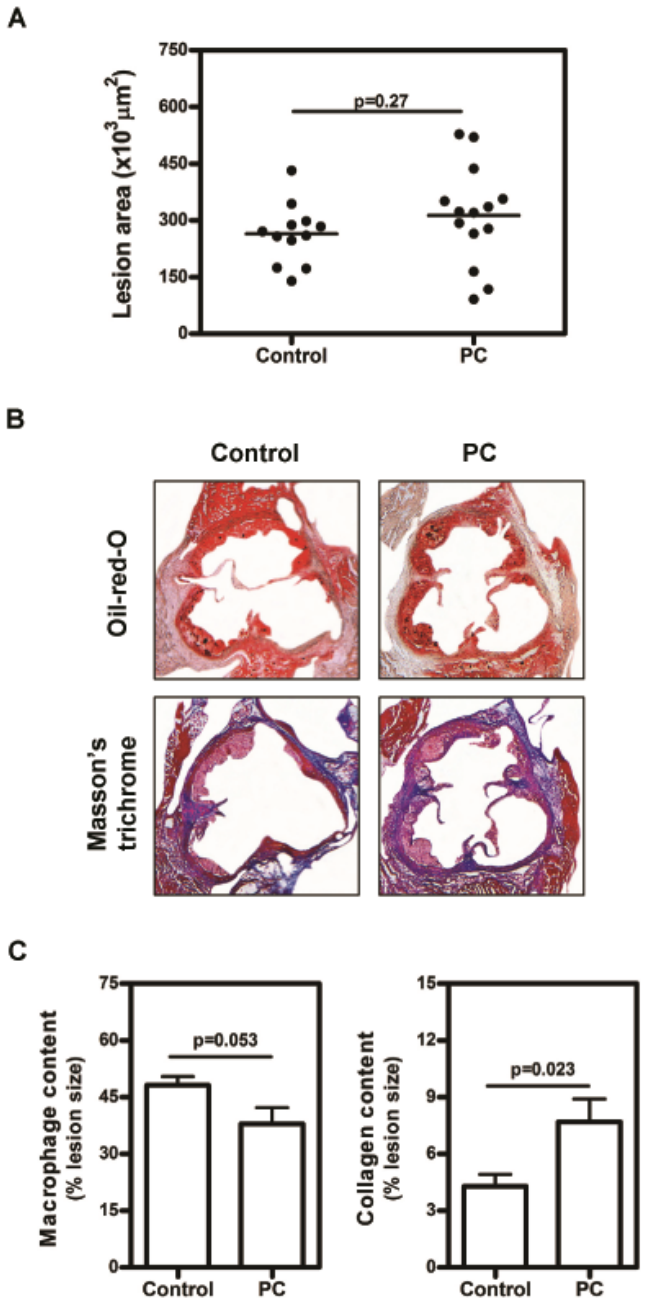

Figure 3. PC modulates the composition of the established early lesions. Animals were put on WTD for 5 weeks to induce the established early lesions at the aortic root. At 48 hours after infusion of PC, animals were euthanized. (A) Photomicrographs showing a scatter dot plot of atherosclerotic lesion quantification. Each symbol represents the mean lesion area in a single mouse. The horizontal line represents the mean of the group. (B) Representative photomicrographs showing oil-red-O and Masson's Trichrome stained sections (original magnification 10x4). (C) Bar graphs showing quantification of macrophage and collagen content in the lesions. Values represent the mean±SEM.

Augmentation of cholesterol efflux by PC particles infusion leads to lesion stabilization as evidenced by reduced macrophage content and increased collagen accumulation in both established early and advanced lesions. Lesion stabilization is crucial for prevention of acute luminal thrombosis [21]. Increased macrophage content and decreased collagen content are associated with the vulnerable lesion phenotype. Colesterol loading impairs the migration capacity of macrophages [22], which probably leads to the retention of foam cells in atherosclerotic lesions. Moreover, macrophage foam cells are the main producer of MMPs in the lesions [23]. The present study as well as pevious studies [14, 24] clearly show that PC particles can promote cellular cholesterol efflux *in vitro* and FC mobilization *in vivo*. Thus, augmentation of cholesterol efflux from cells in lesions might stabilize the plaque by restoring the migration capacity of macrophages and decreasing the production of MMPs.

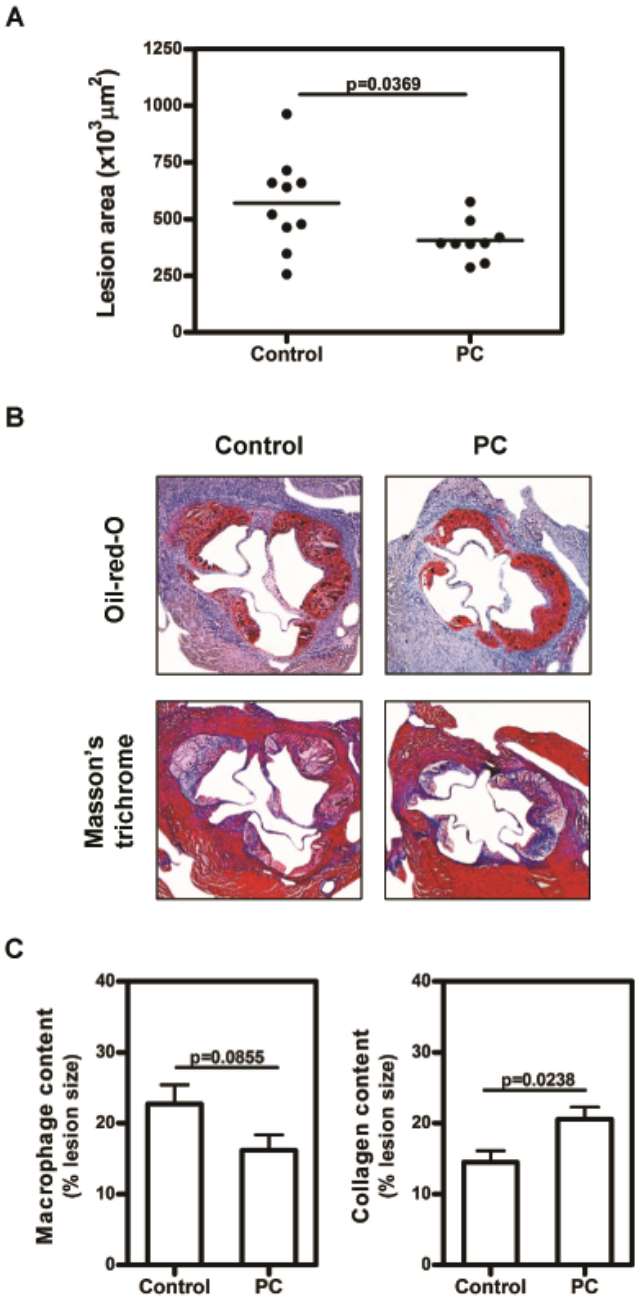

Figure 4. PC modulates the composition of the established advanced lesions. Animals were put on WTD for 9 weeks to induce the established advanced lesions in the aortic root. At 48 hours after infusion of PC, animals were euthanized. (A) Photomicrographs showing a scatter dot plot of atherosclerotic lesion quantification. Each symbol represents the mean lesion area in a single mouse. The horizontal line represents the mean of the group. (B) Representative photomicrographs showing oil-red-O and Masson's Trichrome stained sections (original magnification 10x4). (C) Bar graphs showing quantification of macrophage and collagen content in the lesions. Values represent the mean±SEM.

In conclusion, we provide evidence that promoting macrophage cholesterol efflux by infusion of PC particles stabilizes established atherosclerotic lesions. Apart from apoAI mediated efflux, it is thus likely that the PC component of rHDL contributes to its cholesterol efflux inducing capacity and exerts beneficial effects on atherosclerosis. Studies on rHDL are thus recommended to include PC alone as control.

Acknowledgements

This work was supported by grants from the Netherlands Heart Foundation (#2001T4101 to M.V.E. and Y.Z., and the Established Investigator grant 2007T056 to M.V.E.).

References

1. Khera AV, Rader DJ. Future therapeutic directions in reverse cholesterol transport. *Curr Atheroscler Rep.* 2010; 12(1):73-81.
2. Feig JE, Quick JS, Fisher EA. The role of a murine transplantation model of atherosclerosis regression in drug discovery. *Curr Opin Investig Drugs.* 2009; 10(3):232-8.
3. Schmitz G, Brüning T, Williamson E, Nowicka G. The role of HDL in reverse cholesterol transport and its disturbances in Tangier disease and HDL deficiency with xanthomas. *Eur Heart J.* 1990; 11 Suppl E:197-211.
4. Khera AV, Cuchel M, de la Llera-Moya M, Rodrigues A, Burke MF, Jafri K, French BC, Phillips JA, Mucksavage ML, Wilensky RL, Mohler ER, Rothblat GH, Rader DJ. Cholesterol efflux capacity, high-density lipoprotein function, and atherosclerosis. *N Engl J Med.* 2011; 364(2):127-35.
5. Shah PK, Nilsson J, Kaul S, Fishbein MC, Ageland H, Hamsten A, Johansson J, Karpe F, Cercek B. Effects of recombinant apolipoprotein A-I(Milano) on aortic atherosclerosis in apolipoprotein E-deficient mice. *Circulation.* 1998; 97(8):780-5.
6. Shah PK, Yano J, Reyes O, Chyu KY, Kaul S, Bisgaier CL, Drake S, Cercek B. High-dose recombinant apolipoprotein A-I(milano) mobilizes tissue cholesterol and rapidly reduces plaque lipid and macrophage content in apolipoprotein e-deficient mice. Potential implications for acute plaque stabilization. *Circulation.* 2001; 103(25):3047-50.
7. Tardif JC, Grégoire J, L'Allier PL, Ibrahim R, Lespérance J, Heinonen TM, Kouz S, Berry C, Basser R, Lavoie MA, Guertin MC, Rodés-Cabau J; Effect of rHDL on Atherosclerosis-Safety and Efficacy (ERASE) Investigators. Effects of reconstituted high-density lipoprotein infusions on coronary atherosclerosis: a randomized controlled trial. *JAMA.* 2007; 297(15):1675-82.
8. Shaw JA, Bobik A, Murphy A, Kanellakis P, Blombery P, Mukhamedova N, Woollard K, Lyon S, Sviridov D, Dart AM. Infusion of reconstituted high-density lipoprotein leads to acute changes in human atherosclerotic plaque. *Circ Res.* 2008; 103(10):1084-91.
9. Oram JF, Lawn RM, Garvin MR, Wade DP. ABCA1 is the cAMP-inducible apolipoprotein receptor that mediates cholesterol secretion from macrophages. *J Biol Chem.* 2000; 275(44):34508-11.
10. Pajkrt D, Doran JE, Koster F, Lerch PG, Arnet B, van der Poll T, ten Cate JW, van Deventer SJ. Antiinflammatory effects of reconstituted high-density lipoprotein during human endotoxemia. *J Exp Med.* 1996; 184(5):1601-8.
11. Zabalawi M, Bhat S, Loughlin T, Thomas MJ, Alexander E, Cline M, Bullock B, Willingham M, Sorci-Thomas MG. Induction of fatal inflammation in LDL receptor and ApoA-I double-knockout mice fed dietary fat and cholesterol. *Am J Pathol.* 2003; 163(3):1201-13.
12. Patel S, Di Bartolo BA, Nakhla S, Heather AK, Mitchell TW, Jessup W, Celermajer DS, Barter PJ, Rye KA. Anti-inflammatory effects of apolipoprotein A-I in the rabbit. *Atherosclerosis.* 2010; 212(2):392-7.
13. Jessup W, Gelissen IC, Gaus K, Kritharides L. Roles of ATP binding cassette transporters A1 and G1, scavenger receptor BI and membrane lipid domains in cholesterol export from macrophages. *Curr Opin Lipidol.* 2006; 17(3):247-57.
14. Rodrigueza WV, Klimuk SK, Pritchard PH, Hope MJ. Cholesterol mobilization and regression of atheroma in cholesterol-fed rabbits induced by large unilamellar vesicles. *Biochim Biophys Acta.* 1998; 1368(2):306-20.
15. Patel S, Drew BG, Nakhla S, Duffy SJ, Murphy AJ, Barter PJ, Rye KA, Chin-Dusting J, Hoang A, Sviridov D, Celermajer DS, Kingwell BA. Reconstituted high-density lipoprotein increases plasma high-density lipoprotein anti-inflammatory properties and cholesterol efflux capacity in patients with type 2 diabetes. *J Am Coll Cardiol.* 2009; 53(11):962-71.
16. Lerch PG, Förtsch V, Hodler G, Bolli R. Production and characterization of a reconstituted high density lipoprotein for therapeutic applications. *Vox Sang.* 1996; 71(3):155-64.
17. Sankaranarayanan S, Oram JF, Asztalos BF, Vaughan AM, Lund-Katz S, Adorni MP, Phillips MC, Rothblat GH. Effects of acceptor composition and mechanism of ABCG1-mediated cellular free cholesterol efflux. *J Lipid Res.* 2009; 50(2):275-84.
18. Cuchel M, Lund-Katz S, de la Llera-Moya M, Millar JS, Chang D, Fuki I, Rothblat GH, Phillips MC, Rader DJ. Pathways by which reconstituted high-density lipoprotein mobilizes free cholesterol from whole body and from macrophages. *Arterioscler Thromb Vasc Biol.* 2010; 30(3):526-32.
19. Yancey PG, Bortnick AE, Kellner-Weibel G, de la Llera-Moya M, Phillips MC, Rothblat GH. Importance of different pathways of cellular cholesterol efflux. *Arterioscler Thromb Vasc Biol.* 2003; 23(5):712-9.
20. Davidson WS, Rodrigueza WV, Lund-Katz S, Johnson WJ, Rothblat GH, Phillips MC. Effects of acceptor particle size on the efflux of cellular free cholesterol. *J Biol Chem.* 1995; 270(29):17106-113.

21. Gutstein DE, Fuster V. Pathophysiology and clinical significance of atherosclerotic plaque rupture. *Cardiovasc Res.* 1999; 41(2):323-33.
22. Nagao T, Qin C, Grosheva I, Maxfield FR, Pierini LM. Elevated cholesterol levels in the plasma membranes of macrophages inhibit migration by disrupting RhoA regulation. *Arterioscler Thromb Vasc Biol.* 2007; 27(7):1596-602.
23. Galis ZS, Sukhova GK, Kranzhöfer R, Clark S, Libby P. Macrophage foam cells from experimental atheroma constitutively produce matrix-degrading proteinases. *Proc Natl Acad Sci U S A.* 1995; 92(2):402-6.
24. Yau-Young AO, Rothblat GH, Small DM. Mobilization of cholesterol from cholesterol ester-enriched tissue culture cells by phospholipid dispersions. *Biochim Biophys Acta.* 1982; 710(2):181-7.

Supplementary Figure 1. Size of PC particles

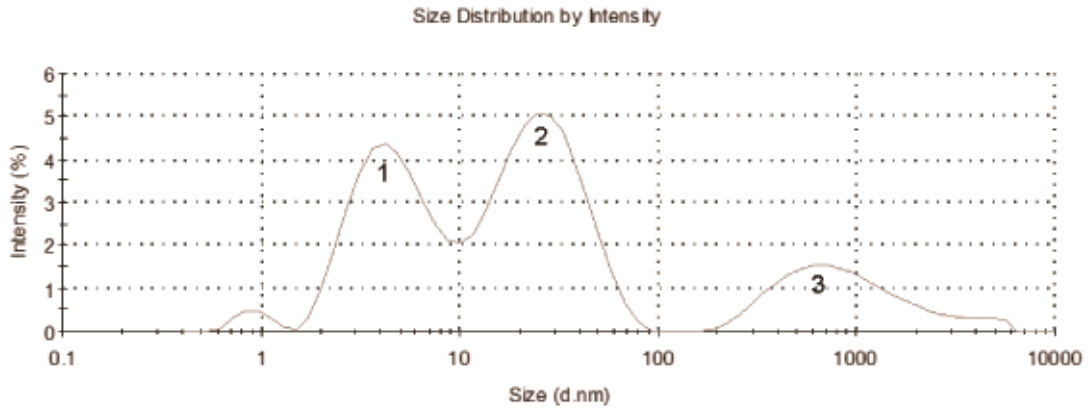

Samples		Intensity (%)	Mean diameter (nm)
PC	Peak 1	34.5±1.0	4.4±0.6
	Peak 2	43.5±0.4	24.7±2.4
	Peak 3	16.5±1.6	627.3±81.1

Supplementary Figure 1. Determination of the size of PC particles. The upper graph showing the size distribution by intensity. The lower table summarizing the quantification of mean diameter of different population of particles.

CHAPTER 11

Summary and General discussion

11.1 English Summary

11.2 Concluding remarks and future perspectives

11.3 Dutch Summary

11.4 中文摘要

11.5 References

11.1 English Summary

Atherosclerosis is the major cause of death in the Western society due to the development of acute clinical events such as myocardial infarction and cerebral stroke. Currently, lowering plasma LDL cholesterol (LDL-C) levels using statins, inhibitors of de-novo cholesterol synthesis, is the main therapeutic strategy to prevent the progression of atherosclerosis. The remaining high incidence of cardiovascular disease indicates a clear need for new therapies. Numerous epidemiological studies have established HDL cholesterol (HDL-C) levels as an inverse predictor for atherosclerosis. HDL has important anti-oxidative and anti-inflammatory properties. The most important atheroprotective function of HDL is, however, facilitation of reverse cholesterol transport (RCT), a process in which HDL removes excess cholesterol from peripheral tissues and subsequently delivers it to the liver for biliary excretion. In this thesis, the importance of RCT for prevention of atherosclerosis and the potential of RCT augmentation for the treatment of atherosclerosis were evaluated.

11.1.1 The importance of reverse cholesterol transport for prevention of atherosclerosis

Key regulators of HDL metabolism are ABC-transporter A1 (ABCA1) and scavenger receptor BI (SR-BI). ABCA1 is the rate-limiting factor for HDL biogenesis, while SR-BI delivers cholesteryl ester (CE) from HDL to the liver. To get insight in the putative synergistic role of ABCA1 and SR-BI in RCT and atherosclerosis, ABCA1/SR-BI double knockout (dKO) mice were generated. In **Chapter 2**, ABCA1/SR-BI dKO mice on chow diet were phenotypically characterized. On one hand, dKO mice displayed a complete blockade of selective cholesterol ester (CE) uptake by the liver, similar as observed previously for single SR-BI KO mice. On the other hand, dKO mice resembled ABCA1 KO mice with respect to hypocholesterolemia and HDL loss. Deletion of ABCA1, SR-BI, or both impaired RCT from wildtype (WT) macrophages to a similar extend. However, dKO mice did accumulate enlarged macrophage foam cells in the lung and Peyer's patches, clearly illustrating the importance of ABCA1 and SR-BI for cellular cholesterol homeostasis. Due to the lack of pro-atherogenic lipoproteins, no atherosclerotic lesions were evident in the aortic root of dKO mice. In **Chapter 3**, the effect of combined deficiency of ABCA1 and SR-BI on atherogenesis was further determined by feeding dKO mice an atherogenic diet (ATD), containing 15% cocoa butter, 1% cholesterol, and 0.5% cholate for 10 weeks. DKO mice displayed lower plasma total cholesterol levels than WT mice, mainly due to the absence of HDL. Plasma non-HDL-C levels in dKO mice were higher than ABCA1 KO mice but much lower than SR-BI KO mice. Enhanced macrophage foam cell accumulation was again observed in the peritoneal cavity of dKO mice on ATD. As compared to WT mice, HDL deficiency in ABCA1 KO mice and dKO mice induced leukocytosis and promoted atherosclerotic lesion development by recruitment of leukocytes into lesions and adventitia. Also, SR-BI KO mice displayed elevated levels of non-HDL and abnormally large HDL, increased leukocyte infiltration into lesions and surrounding adventitia, and enhanced atherosclerosis. These findings clearly indicate the crucial role of HDL-mediated RCT for prevention of atherosclerosis. Strikingly, disruption of ABCA1 in SR-BI KO mice attenuated atherosclerotic lesion development. This coincided with reduced plasma levels of monocyte chemoattractant MCP-1 and expression of the adhesion molecule ICAM-1 in the arterial wall, which probably led to reduced infiltration of monocytes from the circulation into the arterial wall. Evidence is accumulating that not only proatherogenic lipoproteins, like LDL and VLDL, but also dysfunctional HDL can induce secretion of MCP-1 from the arterial wall and

upregulates the expression of ICAM-1 on arterial endothelial cells [1]. The observed reduced atherosclerotic lesion development in dKO mice is thus probably the result of diminished dysfunctional HDL and reduced plasma levels of pro-atherogenic lipoproteins upon inactivation of ABCA1, leading to reduced infiltration of monocytes into the arterial wall.

11.1.2 The importance of cellular cholesterol efflux mechanisms for prevention of atherosclerosis

As a hallmark of atherosclerosis, macrophage-derived foam cells are an early and persistent component of atherosclerotic lesions. They play a key role in disease progression, as both lipid scavengers and inflammatory mediators. Cholesterol efflux mechanisms in macrophages, the first step of RCT, are essential for prevention of foam cell formation. The relative roles of various efflux pathways in net cholesterol efflux from macrophage foam cells in atherosclerotic lesions were reviewed in **Chapter 4**. In addition to their essential role in HDL metabolism, ABCA1 and SR-BI are important modulators of cellular cholesterol efflux to lipid-poor apolipoprotein AI (ApoAI) and mature HDL, respectively. In **Chapter 5**, the combined effect of macrophage ABCA1 and SR-BI deficiency on foam cell formation and atherosclerotic lesion development was investigated by transplantation of bone marrow from ABCA1/SR-BI dKO mice into LDL receptor (LDLr) KO mice. Upon challenge with Western-type diet (WTD), dKO transplanted mice showed lower plasma cholesterol levels compared to respective controls, probably due to less food intake, impaired intestinal absorption, and reduced VLDL production. However, massive foam cell formation was evident in the peritoneal cavity and spleen of dKO mice. Importantly, combined deletion of macrophage ABCA1 and SR-BI also increased circulating levels of pro-inflammatory KC (murine IL-8) and IL-12, and accelerated atherosclerosis. Under high-dietary lipid conditions, both ABCA1 and SR-BI in bone marrow-derived cells are thus essential for prevention of macrophage foam cell formation and atherosclerosis, and other cholesterol efflux mechanisms cannot compensate for the absence of these two cholesterol transporters.

Strikingly, Brunham et al. showed that specific deletion of ABCA1 in macrophages did not affect atherogenesis in LDLr KO mice [2]. This was suggested to be the consequence of the fact that deletion of the LDLr on macrophages impairs the sterol-induced upregulation of macrophage ABCA1 expression and macrophage cholesterol efflux [3]. In **Chapter 6**, bone marrow from LDLr/ABCA1 dKO mice and respective controls was transplanted into LDLr KO mice to investigate the interaction between the LDLr and ABCA1 on leukocytes and the consequences for atherosclerotic lesion development. Deletion of the macrophage LDLr did not affect cholesterol efflux from bone marrow-derived macrophages *in vitro* or macrophage foam cell formation *in vivo*. Of note, leukocyte ABCA1 deficiency resulted in increased foam cell formation and promoted atherosclerosis both in the presence and absence of the LDLr, clearly indicating that the atheroprotective effect of leukocyte ABCA1 is independent of LDLr expression. Interestingly, LDLr/ABCA1 dKO transplanted animals displayed less lymphocytosis, reduced recruitment of T cells into adventitia underlying lesions, and smaller lesions as compared to single ABCA1 KO transplanted animals. These findings suggest that in addition to the role ABCA1 in cholesterol efflux, leukocyte ABCA1 might protect against atherosclerosis by inhibiting the proliferation and recruitment of T cells.

ABCA1 facilitates cholesterol efflux from macrophages to lipid-free/poor apolipoproteins, including ApoAI [4]. In **Chapter 7**, the importance of circulating ApoAI

for macrophage ABCA1-faciliated RCT and the atheroprotective effects of leukocyte ABCA1 was evaluated. Lipoprotein-depleted serum (LPDS) and HDL of LDLr/ApoAI dKO mice showed reduced cholesterol efflux capacity from WT macrophages as compared to the counterparts of LDLr KO mice. However, macrophage ABCA1 deficiency did not lead to further reduced cholesterol efflux to LPDS and HDL of LDLr/ApoAI dKO mice or radio-labeled cholesterol excretion into feces in LDLr/ApoAI dKO mice. Therefore, ApoAI and macrophage ABCA1 are identified as functional partners in macrophage RCT. Next, LDLr/ApoAI dKO mice were transplanted with bone marrow from ABCA1 KO mice and WT controls. Upon challenge with WTD, ABCA1 deficiency accelerated atherosclerosis in LDLr/ApoAI dKO mice, despite reduced non-HDL cholesterol levels. This clearly indicates that leukocyte ABCA1 can protect against atherosclerosis even in absence of circulating ApoAI. Thus, in addition to macrophage RCT, other mechanisms are involved in the atheroprotective effects of leukocyte ABCA1, especially under conditions in which circulating ApoAI is absent. Interestingly, the accelerated atherosclerosis in LDLr/ApoAI dKO mice with ABCA1 deficiency in bone marrow-derived cells coincided with enhanced monocytosis and neutrophilia in the circulation, induced plasma levels of important chemoattractants of monocytes and neutrophils MCP-1 and KC, and augmented neutrophil accumulation in lesions. These findings suggest that, in addition to its essential role as a facilitator of cellular cholesterol efflux, the atheroprotective effects of leukocyte ABCA1 could also be attributed to its anti-inflammatory function.

11.1.3 The potential of augmentation of reverse cholesterol transport from macrophage for the treatment of atherosclerosis

To evaluate the potential of augmentation of RCT from macrophages to reduce established atherosclerotic lesions, different strategies, including dietary lipid lowering, overexpression of ABCA1 on macrophages, and infusion of synthetic cholesterol-free phosphatidylcholine (PC) discs, were tested. In **Chapter 8**, LDLr KO mice were fed WTD for 5 and 9 weeks to induce early and advanced lesion development. Thereafter, the animals were switched to a chow diet to lower plasma cholesterol levels and the dynamic response of the lesions was investigated. Dietary lipid lowering reduced the macrophage content of both early and advanced established lesions. However, progression of lesion development continued as a result of expansion of collagen and the necrotic core. Importantly, early lesions became more pro-inflammatory, while inflammation was reduced in advanced lesions. The severity of the established lesions thus determined the dynamics of lesion remodeling upon lowering of plasma cholesterol, indicating the importance of establishing stage-specific therapeutic protocols for the treatment of atherosclerosis.

In **Chapter 9**, BMT experiments in LDLr KO mice with established lesions were used to study the potential of ABCA1 overexpression in bone marrow-derived cells, including macrophages, for the treatment of atherosclerosis. Overexpression of ABCA1 inhibited macrophage infiltration into early, but not into advanced lesions. The latter is likely the consequence of the fact that macrophage infiltration into established advanced lesions was largely impaired, due to the presence of fibrous caps. Therefore, the severity of the pre-existing lesions could influence the therapeutic potential of ABCA1 overexpression in bone marrow-derived cells.

Infusion of reconstituted HDL (rHDL), composed of human ApoAI and phosphatidylcholine (PC), protects against atherosclerosis probably by induction of

cholesterol efflux from macrophage foam cells and inhibition of inflammation [5,6]. PC discs, like rHDL, can accept cholesterol transported via SR-BI, ABCG1, and aqueous diffusion. Infusion of large amounts of PC is therefore expected to positively affect cellular cholesterol efflux and thus atherosclerosis. In **Chapter 10**, the effect of PC discs on macrophage cholesterol efflux *in vitro* and the progression of established atherosclerotic lesions in LDLr KO mice was evaluated. First, as expected, PC particles at high concentrations (>84 μg/mL) induced cholesterol efflux from macrophages as efficiently as rHDL containing the same amount of PC. Importantly, augmentation of macrophage cholesterol removal by a single infusion of high-dose PC discs rapidly led to stabilization of established lesions in LDLr KO mice on WTD. The PC component of rHDL thus contributes to its cholesterol efflux-inducing capacity and exerts beneficial effects on atherosclerosis.

11.2 Concluding remarks and future perspectives

Using our unique transgenic animals and the technique of bone marrow transplantation we investigated the importance of HDL-mediated RCT for prevention of atherosclerotic lesion development. Although many other molecules are also involved in RCT, ABCA1, ApoAI, and SR-BI are considered good candidates for pharmaceutical intervention to elevate HDL-C, facilitate cholesterol efflux from lesions, promote the delivery of cholesterol to the liver, and thus prevent or even regress atherosclerosis. Combined therapeutic targeting of these molecules in RCT is expected to greatly improve the efficacy of the treatment for atherosclerosis.

The potential of overexpression of SR-BI and ABCA1 for treatment of atherosclerosis has been investigated in animal models. Overexpression of hepatic SR-BI reduces atherosclerosis in LDLr KO mice [7]. In contrast, overexpression of ABCA1 in the liver of LDLr KO mice [8] and apoE KO mice [9] induces not only HDL but also proatherogenic apoB-containing lipoproteins, thereby accelerating the development of atherosclerotic lesions. Lately, Brunham et al. demonstrated that moderate overexpression (2-fold instead of 20-fold) of hepatic ABCA1 does confer atheroprotection in LDLr KO mice [2]. Interestingly, the expression of hepatic SR-BI is important for preserving the beneficial effects of HDL on both endothelial progenitor cells (EPCs) and endothelial cells (EC) [10]. Hepatocyte-specific ABCA1 overexpression via adenoviral vectors increases HDL-C, but decreases SR-BI protein in liver and abrogates the beneficial effects of HDL on EC function [10]. Therefore, combined overexpression of ABCA1 and SR-BI in the liver may prove more successful in the prevention of atherosclerosis.

Augmentation of cholesterol efflux from macrophage foam cells in atherosclerotic lesions, the first step of RCT, is considered to be an attractive approach to prevent or even regress established lesions. Established transporters facilitating cellular cholesterol efflux are ABCA1, ABCG1, and SR-BI [11]. Combined deletion of ABCA1 and ABCG1 [12] or ABCA1 and SR-BI [13] on bone marrow-derived cells induces extreme macrophage foam cell formation and accelerates atherosclerosis. These findings highlight the potential of these cholesterol transporters as therapeutic targets. A therapeutic strategy to up-regulate ABCA1 and ABCG1 in macrophages is pharmacological activation of the liver X receptors (LXRs) [14]. Activation of LXRs on macrophages is required for regression of atherosclerotic lesions [15]. Systemic application of LXR agonists, however, induces off-target effects in liver, including increased lipogenesis and production of TG [16]. This therapeutic strategy may be improved by specific targeting of LXR agonists to

macrophages inside the atherosclerotic lesion. In addition, the expression of the cholesterol transporters ABCA1 and SR-BI in lesions is upregulated during atherosclerosis regression [17]. It is thus worthwhile to investigate if therapeutic upregulation of ABCA1 and SR-BI in atherosclerotic lesions might be a potential new strategy for induction of atherosclerotic lesion regression.

For decades, elevation of HDL-C is believed to be a promising strategy for treatment of atherosclerosis as levels of HDL correlate inversely with cardiovascular risk. Elevation of circulating ApoAI and HDL indeed induces rapid atherosclerosis regression in ApoE KO mice [18]. Clinical approaches to raise HDL-C include oral administration of cholesterol ester transfer protein (CETP) inhibitors and intravenous administration of rHDL (ApoAI-PC complex). CETP is an enzyme that exchanges cholesterol esters in HDL for triglycerides in VLDL [19]. The CETP inhibitor torcetrapib efficiently elevates HDL-C and enhances the cholesterol efflux capacity of HDL in treated patients [20]. It, however, failed in a clinic trial with 15067 patients at high cardiovascular risk, owing to off-target effects on blood pressure, and increased levels of aldosterone [21]. Two other CETP inhibitors, dalcetrapib and anacetrapib, have entered clinical evaluation. The safety of dalcetrapib and anacetrapib was recently affirmed in clinical trials [22, 23]. The results of continuing large end-point trials will prove if the inhibition of CETP is a good therapeutic target for reducing cardiovascular risk by elevation of HDL.

Moreover, infusion of rHDL has been proven to be a promising therapy for atherosclerosis [24, 25, 26]. Although we show that PC, the phospholipid component of rHDL, has beneficial effects on atherosclerosis at high doses, the ApoAI in rHDL might augment cholesterol efflux by facilitating cholesterol efflux via ABCA1. In addition, ApoAI has other atheroprotective properties, such as anti-oxidation and anti-inflammation [11]. Interestingly, the induction of FC mobilization by rHDL infusion is dependent on the expression of SR-BI [27]. Thus, overexperssion of SR-BI might enhance the beneficial effect of rHDL infusion.

Recent findings also indicate that anti-inflammatory strategies or inhibition of monocyte infiltration are crucial for inducing regression of atherosclerosis [28]. Atherosclerotic lesion development results from a combination of hypercholesterolemia and an inflammatory response. We demonstrated in this thesis, that in addition to their importance for macrophage RCT, the atheroprotective effects of ABCA1 and ApoAI could also be attributed to their anti-inflammatory function. This highlights the enormous therapeutic potential of targeting these factors for the treatment of atherosclerosis.

Increasing evidence is accumulating that the steady-state levels of HDL cholesterol in plasma poorly reflect HDL function. HDL can be modified by atherogenic factors, like oxidative stress and inflammation, and turn into a dysfunctional particle with decreased cholesterol efflux capacity [11]. It should, however, be noted that a preserved cholesterol efflux capacity of HDL does not necessarily reflect the functionality of the other atheroprotective properties of HDL, such as its anti-inflammatory and endothelial preservation properties [29]. It is thus important to monitor all anti-atheroprotective properties of HDL during the treatment of atherosclerosis. Laboratory assessments of HDL function includes evaluation of cholesterol efflux capacity, its PON1 (paraoxonase) activity for its anti-oxidant capacity, the expression of endothelial adhesion molecules for its anti-inflammatory function, sphingosine-1-phosphate mass for its nitric oxide-promoting capacity, and the coagulation system for its anti-coagulant property [30]. Development and validation of assays that can be easily used in a clinical setting will be of great importance for prediction of cardiovascular risk and assessment of the success of

therapeutic interventions.

In addition to macrophages, cellular cholesterol homeostasis might also be crucial for the function of other cell types involved in the pathogenesis of atherosclerosis. Increased cholesterol content in T lymphocytes is associated with augmented activation and proliferation [31]. Recruitment of these activated T cells into the arterial wall could accelerate atherosclerosis. Also, secretion of insulin is impaired by increased accumulation of cholesterol in islet β-cells [20463468]. Subsequent hyperglycemia due to low levels of insulin in patients with type 2 diabetes could also modify HDL leading to a cholesterol efflux capacity and accelerated development of atherosclerosis [11]. Therefore, the role of cellular cholesterol homeostasis in these cell types warrants future investigation. These studies will highlight the importance of systemic augmentation of RCT for treatment of atherosclerosis at different levels.

In conclusion, as described in this thesis, the importance of RCT in atherosclerosis has been established and augmentation of RCT is a promising target for the treatment of atherosclerosis and reducing cardiovascular risk.

11.3 Dutch Samenvatting

Hart- en vaatziekten vormen de voornaamste doodsoorzaak in de westerse wereld. Een belangrijke oorzaak voor de ontwikkeling van hart- en vaatziekten is de vorming van vernauwingen in de bloedvaten, de zogenaamde atherosclerose ofwel aderverkalking genoemd. Een belangrijke risicofactor voor het ontstaan van atherosclerose is een te hoog cholesterolgehalte. Huidige therapieën richten zich voornamelijk op het verlagen van het (slechte) cholesterol in lage-dichtheids lipoproteïnen (LDL) en zeer-lage-dichtheids lipoproteïnen (VLDL). Hoewel de incidentie van atherosclerose sterk is verminderd blijft het aantal patiënten dat lijdt aan hart- en vaatziekten hoog. Veel klinische onderzoeken laten zien dat het cholesterol in (goede) hoge-dichtheids lipoproteïnen (HDL) een beschermende rol kan spelen bij de ontwikkeling van atherosclerose. De belangrijkste functie van HDL richt zich op de verwijdering van cholesterol uit perifere weefsels, welke vervolgens via de lever wordt uitgescheiden (omgekeerd cholesterol transport, ofwel RCT). In dit proefschrift is het belang van RCT voor de bescherming tegen atherosclerose onderzocht. Daarnaast zijn de effecten van RCT stimulatie als een mogelijk nieuwe behandeling van atherosclerose geëvalueerd.

11.3.1 Het belang van RCT ter bescherming tegen atherosclerose

ABC-transporter A1 (ABCA1) en scavenger receptor BI (SR-BI) spelen een belangrijke rol in het HDL metabolisme. ABCA1 is essentieel voor de productie van HDL, terwijl SR-BI zorgt voor het transport van cholesteryl esters (CE) van HDL naar de lever. Om inzicht te krijgen in de veronderstelde rol van ABCA1 en SR-BI in RCT en atherosclerose, zijn er muizen gecreëerd die ABCA1 en SR-BI missen (dubbele knockout muizen, ofwel dKO). In **Hoofdstuk 2** zijn deze muizen gekarakteriseerd. Net als SR-BI deficiënte muizen, vertoonden dKO muizen geen opname van CE uit HDL door de lever. Aan de andere kant hadden ze, in overeenstemming met ABCA1 deficiëntie, hypocholesterolemie en weinig tot geen HDL. Deficiëntie van ABCA1, SR-BI of beide zorgde voor een identieke reductie in RCT vanuit wildtype (WT) macrofagen. dKO muizen vertoonden stapeling van macrofaag schuimcellen in de long en Peyer's patches. Dit suggereert een functie van ABCA1 en SR-BI in cellulaire cholesterol homeostase. Vanwege de afwezigheid van pro-atherogene lipoproteïnen ontwikkelden dKO muizen echter geen atherosclerotische lesies. In **Hoofdstuk 3** is het effect van gecombineerde deficiëntie van ABCA1 en SR-BI op atherogenese verder onderzocht door deze muizen voor een periode van 10 weken een atherogeen dieet te voeren. Dit dieet bevat 15% cacaoboter, 1% cholesterol en 0.5 cholaat. Voornamelijk door de afwezigheid van HDL hadden dKO muizen lagere cholesterol waarden dan de WT muizen. VLDL en LDL concentraties in dKO muizen waren hoger dan in ABCA1 KO muizen, maar veel lager dan in SR-BI KO muizen. Ook na het atherogene dieet vertoonden dKO muizen verhoogde macrofaag schuimcel vorming in het peritoneum. Vergeleken met WT muizen resulteert de HDL deficiëntie in ABCA1 KO en dKO muizen in verhoogde leukocytose en meer atherosclerose door verhoogde rekrutering van leukocyten naar de atherosclerotische lesie en de adventitia. Daarnaast vertoonden SR-BI KO muizen verhoogd VLDL/LDL en abnormaal groot HDL, verhoogde leukocyt infiltratie in de lesies en omringende adventitia en toegenomen vorming van atherosclerose. Deze resultaten onderstrepen de cruciale beschermende rol van HDL afhankelijke RCT met betrekking tot atherosclerose. Het is opmerkelijk dat ABCA1 deficiëntie in SR-BI KO muizen atherosclerose vermindert. Verlaagde plasma concentraties van monocyt chemoattractant MCP-1 en verlaagde expressie van het adhesie molecuul ICAM-1 in de vaatwand, leidt waarschijnlijk tot verminderde infiltratie van monocyten vanuit de circulatie in de vaatwand. Niet alleen de proatherogene lipoproteïnen LDL en VLDL, maar

ook niet-functioneel HDL induceert MCP-1 secretie en verhoogt ICAM-1 expressie in endotheelcellen in de vaatwand [17941290]. De verminderde atherosclerose ontwikkeling in dKO muizen is dus waarschijnlijk veroorzaakt door de verlaging van de hoeveelheid niet-functioneel HDL en proatherogene lipoproteïnen in het plasma als gevolg van ABCA1 deficiëntie.

11.3.2. Het belang van cellulaire cholesterol efflux mechanismen ter preventie van atherosclerose

Macrofagen spelen een belangrijke rol bij de initiatie en de progressie van atherosclerose. Deze cellen fungeren als de opruimcellen voor vetten en produceren grote hoeveelheden ontstekingsfactoren die het ziekteproces beïnvloeden. Cholesterol efflux mechanismen in macrofagen, de eerste stap van het RCT, zijn essentieel om stapeling van cholesterol en dus schuimcel vorming te voorkomen. In **Hoofdstuk 4** is het relatieve belang van verschillende cholesterol efflux routes van macrofaag schuimcellen in atherosclerotische lesies samengevat. Naast hun belangrijke rol in het metabolisme van HDL zijn ABCA1 en SR-BI ook betrokken bij efflux van cholesterol vanuit macrofagen naar apolipoproteïne AI (ApoAI) en HDL. In **Hoofdstuk 5** is gebruik gemaakt van de beenmergtransplantatie (BMT) techniek. Het effect van gecombineerde uitschakeling van ABCA1 en SR-BI in macrofagen op schuimcel vorming en atherosclerose werd onderzocht door middel van transplantatie van ABCA1/SR-BI dKO beenmerg naar LDL receptor (LDLr) KO muizen. Het voeren van een Western-type dieet (WTD) resulteerde in de dKO getransplanteerde muizen tot een verminderde verhoging van de concentraties cholesterol in het bloed. Dit kwam waarschijnlijk door verlaagde voedselinname, aangetaste absorptie in de darmen en verminderde VLDL productie. Desondanks vertoonden deze dKO getransplanteerde muizen extreme schuimcel vorming in het peritoneum en de milt. Gecombineerde deficiëntie van macrofaag ABCA1 en SR-BI resulteerde ook in verhoogde concentraties pro-inflammatoir KC (muizen IL-8) en IL-12 en versnelde atherosclerose. Onder condities van hoge, dieet-geïnduceerde, concentraties vetten zijn zowel ABCA1 als SR-BI in beenmerg afgeleide cellen dus essentieel voor de preventie van macrofaag schuimcel vorming en atherosclerose. Andere cholesterol efflux mechanismen kunnen niet compenseren voor de afwezigheid van deze cholesterol transporters.

Een opvallende bevinding van Brunham et al. is dat specifieke genetische uitschakeling van ABCA1 op macrofagen geen effect had op atherogenese in LDLr KO muizen [17322896]. Dit zou veroorzaakt kunnen worden doordat macrofaag LDLr deficiëntie de vet geïnduceerde opregulatie van ABCA1 op macrofagen en daarmee macrofaag cholesterol efflux uit macrofagen verhinderd [18029360]. In **Hoofdstuk 6** zijn LDLr KO muizen getransplanteerd met beenmerg van LDLr/ABCA1 dKO muizen en hun respectievelijke controles om de interactie tussen de LDLr en ABCA1 op leukocyten en de gevolgen voor de ontwikkeling van atherosclerotische lesies te onderzoeken. Macrofaag LDLr deficiëntie had geen invloed op de cholesterol efflux van beenmerg afgeleide macrofagen *in vitro* of macrofaag schuimcel vorming *in vivo*. Leukocyt ABCA1 deficiëntie resulteerde echter in een verhoogde schuimcel vorming en meer atherosclerose, zowel in de aanwezigheid als afwezigheid van LDLr expressie. Hieruit blijkt duidelijk dat het beschermende effect van leukocyt ABCA1 op atherosclerose onafhankelijk is van LDLr expressie. LDLr/ABCA1 dKO getransplanteerde muizen vertoonden minder lymfocytose, verminderde rekrutering van T-cellen naar de adventitia van het bloedvat met atherosclerotische lesies, en kleinere lesies in vergelijking met ABCA1 KO getransplanteerde dieren. Deze bevindingen suggereren dat ABCA1 in leukocyten, naast een rol in cholesterol efflux, ook tegen atherosclerose beschermt door het remmen van de

proliferatie en de rekrutering van T-cellen.

ABCA1 bevordert cholesterol efflux van macrofagen naar apolipoproteïnen, waaronder ApoAI [11162594]. In **Hoofdstuk 7** is het belang van circulerend ApoAI voor macrofaag ABCA1 afhankelijke RCT en het beschermende effect van leukocyt ABCA1 op atherosclerose onderzocht. Lipoproteïnen-deficiënt serum (LPDS) en HDL van LDLr/ApoAI dKO muizen vertoonden een verminderde capaciteit om cholesterol efflux te induceren vanuit WT macrofagen in vergelijking met die van LDLr KO muizen. Echter, macrofaag ABCA1 deficiëntie leidde niet tot een verder gereduceerde cholesterol efflux naar LPDS en HDL van LDLR/ApoAI dKO muizen noch tot verminderde uitscheiding van radioactief gemerkt cholesterol vanuit WT macrofagen in de ontlasting van LDLR/ApoAI dKO muizen. Daarom worden ApoAI en macrofaag ABCA1 gezien als functionele partners in macrofaag RCT. Vervolgens werden LDLr/ApoAI dKO muizen getransplanteerd met beenmerg van ABCA1 KO muizen of WT controles. Het voeren van WTD aan deze muizen resulteerde, ondanks de verlaging van cholesterol in VLDL en LDL, bij ABCA1 deficiëntie in versnelde ontwikkeling van atherosclerose in LDLr/ApoAI dKO muizen Hieruit blijkt duidelijk dat leukocyt ABCA1, zelfs in de afwezigheid van circulerend ApoAI, beschermt tegen atherosclerose. Naast macrofaag RCT dragen dus ook andere mechanismen bij aan de beschermende effecten van leukocyt ABCA1, vooral onder omstandigheden waarin circulerend ApoAI afwezig is. De versnelde atherosclerose in LDLr/ApoAI dKO muizen met macrofaag ABCA1 deficiëntie viel samen met een verhoogde monocytose en neutrofilie in het bloed, verhoogde plasmaspiegels van de belangrijke monocyt en neutrofiel chemoattractants van monocyten en neutrofielen; MCP-1 en KC, en verhoogde neutrofiel accumulatie in de lesies. Deze bevindingen suggereren dat de beschermende effecten van leukocyt ABCA1, naast cholesterol efflux, ook kunnen worden toegeschreven aan een anti-inflammatoire werking.

11.3.3 Bevordering van RCT vanuit macrofagen ter bescherming tegen atherosclerose

Om te onderzoeken of een mogelijke toename van de macrofaag RCT capaciteit beschermt tegen de ontwikkeling van atherosclerose zijn verschillende strategieën getest, waaronder dieet afhankelijke verlaging van cholesterol in het bloed, macrofaag ABCA1 overexpressie en infusie van synthetische cholesterol-vrije fosfatidylcholine (PC) deeltjes. In **Hoofdstuk 8** werden LDLr KO muizen gedurende 5 of 9 weken WTD gevoerd om de vorming van beginnende en vergevorderde atherosclerotische lesies te stimuleren. Daarna kregen de dieren chow dieet om lagere plasma cholesterol spiegels te verkrijgen. De dynamische respons van de gevestigde lesies werd onderzocht. Dieet geïnduceerde verlaging van cholesterol verminderde de hoeveelheid macrofagen in de vergevorderde lesies. Echter, de lesie ontwikkeling werd voortgezet als gevolg van de uitbreiding van collageen en de necrotische gebieden. Het is opvallend dat beginnende lesies meer pro-inflammatoir werden, terwijl de ontsteking was verminderd in vergevorderde lesies. De ernst van de lesies bepaalde dus de effecten van de verlaging van het plasma cholesterol op de lesie. Dit onderstreept het belang van het stadium van atherosclerotische lesie ontwikkeling voor onderzoek naar nieuwe therapeutische strategieën gericht op vermindering van atherosclerose.

In **Hoofdstuk 9** werden BMT experimenten in LDLr KO muizen met vergevorderde lesies gebruikt om de mogelijkheden van ABCA1 overexpressie in beenmerg-afgeleide cellen voor de behandeling van al aanwezige atherosclerose te bestuderen. ABCA1 overexpressie remde macrofaag infiltratie in beginnende, maar niet in vergevorderde lesies. Dat laatste is waarschijnlijk het gevolg van het feit dat infiltratie van macrofagen in bestaande lesies in een vergevorderd stadium van ontwikkeling grotendeels werd verminderd als gevolg van de aanwezigheid van een fibrotische laag. De ernst van de

al bestaande lesies bepaalt dus de therapeutische mogelijkheden van ABCA1 overexpressie in beenmerg-afgeleide cellen.

Infusie van artificieel HDL (rHDL), bestaande uit menselijk ApoAI en PC, beschermt tegen atherosclerose door cholesterol efflux uit macrofaag schuimcellen stimuleren en de ontstekingsreactie te remmen [10918070, 12937162, 20609437]. PC deeltjes, zoals rHDL, kunnen cholesterol opnemen dat uit cellen wordt getransporteerd via SR-BI, ABCG1 en diffusie. Infusie van grote hoeveelheden PC zou dan ook naar verwachting een positief effect kunnen hebben op efflux van cholesterol uit cellen en dus atherosclerose. In Hoofdstuk 10 werd het effect van PC deeltjes op macrofaag cholesterol efflux in vitro en de ontwikkeling van al aanwezige atherosclerotische lesies in LDLr KO muizen geëvalueerd. Zoals verwacht zorgden hoge concentraties PC deeltjes (>84 μg/ml) voor een inductie van cholesterol efflux uit macrofagen. De PC deeltjes bleken net zo efficiënt als rHDL met dezelfde hoeveelheid PC. De verhoging van macrofaag cholesterol verwijdering door een enkele infusie van een hoge dosis PC deeltjes leidde tot een snelle stabilisatie/regressie van de aanwezige lesies in LDLr KO muizen op WTD. De PC component van het rHDL draagt dus bij aan de cholesterol efflux inducerende capaciteit en oefent een gunstig effect uit op de ontwikkeling van atherosclerose.

Samengevat toont dit proefschrift het belang van RCT aan voor het remmen van atherosclerotische lesie ontwikkeling. ABCA1 en SR-BI, zowel in de lever als de macrofagen kunnen worden beschouwd als kandidaten voor farmaceutische interventie om HDL te verhogen, macrofaag cholesterol efflux te bevorderen, cholesterol transport naar de lever te stimuleren, en zo te beschermen tegen atherosclerose. Verscheidene mogelijkheden voor het verhogen van macrofaag cholesterol efflux zijn geëvalueerd, welke hopelijk zullen leiden tot nieuwe behandelingen die zich richten op stimulering van RCT. De verworven kennis over de effecten van de ernst van de bestaande lesies op lesie transformatie en monocyt infiltratie na interventie helpen bij de ontwikkeling van stadiumspecifieke therapieën tegen atherosclerose. Daarnaast suggereren de nieuwe bevindingen van ABCA1 en HDL niveaus op leukocytose dat cholesterol homeostase van leukocyten de immuunrespons beïnvloedt, wat een verband aangeeft tussen hypercholesterolemie en systemische inflammatie tijdens atherogenese.

11.4 中文摘要

在西方社会， 动脉粥样硬化是引发急性心肌梗死和脑卒的重要原因。目前主要的治疗策略是使用他汀类（statins）药物通过抑制人体内胆固醇合成酶来降低血浆中低密度脂蛋白胆固醇（LDL-C）的水平, 以此防止动脉粥样硬化的进展。然而，在广泛的使用 stains 以来，心血管疾病的发病率仍然很高，这表明需要新的治疗方法。大量的流行病学研究表明血清中高密度脂蛋白胆固醇（HDL-C）的水平是与动脉粥样硬化发展呈反相关的关系。高密度脂蛋白，具有重要的抗氧化和抗炎特性。然而最重要的高密度脂蛋白对动脉粥样硬化的保护功能是促进胆固醇的逆向转运（RCT）。高密度脂蛋白可从外周组织中移除多余的胆固醇，并随后把它们传送到肝脏通过胆汁排出体外。本论文研究了 RCT 在预防动脉粥样硬化中的重要性并对其在治疗动脉粥样硬化中的潜力进行了评估。

11.4.1 胆固醇的逆向转运在预防动脉粥样硬化中的重要性

高密度脂蛋白代谢的关键调节分子是 ABC 转运体 A1（ABCA1）和清道夫受体 BI（SR-BI）。 ABCA1 是高密度脂蛋白生物合成的限速因素，而 SR-BI 介导肝脏从高密度脂蛋白中摄入胆固醇酯（CE）。为了研究 ABCA1 和 SR–BI 在 RCT 和预防动脉粥样硬化中的协同作用，ABCA1/SR-BI 双敲除（dKO）小鼠被制造出来。首先，我们在**第一章**研究了 ABCA1/SR-BI dKO 小鼠在普通的 chow 饮食条件下的表型特征。一方面，dKO 小鼠类似 SR-BI KO 小鼠，它们的肝脏无法从高密度脂蛋白中选择性的摄取胆固醇酯（CE）。另一方面，dKO 小鼠又相似 ABCA1 KO 小鼠显示了低胆固醇血症和血清中高密度脂蛋白的缺失。从野生型（WT）的巨噬细胞中流出的胆固醇逆向转运在 dKO 小鼠体内是减少的， 其减少的程度类似 ABCA1 和 SR–BI 单基因敲除小鼠。然而，dKO 小鼠在肺和 Peyer 氏斑积聚了增大的巨噬细胞源的泡沫细胞，清楚地说明了 ABCA1 和 SR–BI 在细胞胆固醇平衡中的重要性。由于血液中缺乏促动脉粥样硬化的脂蛋白，dKO 小鼠的主动脉根部并没有动脉粥样硬化病变。为了近一步研究 ABCA1 和 SR-BI 共同缺乏对动脉粥样硬化的影响，在**第二章**，dKO 小鼠被给予含有 15％的可可脂，1％胆固醇，和 0.5％胆盐的致动脉粥样硬化的饮食（ATD）为期 10 个星期。 DKO 小鼠的血浆总胆固醇水平依然比 WT 小鼠低下，其主要是由于高密度脂蛋白的缺失。dKO 小鼠血浆中非高密度脂蛋白的胆固醇的水平是高于 ABCA1 KO 小鼠，但比 SR-BI KO 小鼠低很多。增强的巨噬细胞源性的泡沫细胞再次在 dKO 小鼠腹腔中堆积。与 WT 小鼠相比，高密度脂蛋白在 ABCA1 KO 小鼠和 dKO 小鼠中的缺乏引起了血中白细胞的增多，并促进白细胞浸润到动脉粥样硬化病变和其动脉外膜，以及增进了动脉粥样硬化病变在主动脉根部的发展。相比，SR-BI KO 小鼠显示了非高密度脂蛋白和异常大的高密度脂蛋白胆固醇水平的升高，增加了白细胞浸润到病变及其周围的外膜，和促进了动脉粥样硬化的发展。这些研究结果清楚地表明，高密度脂蛋白介导的 RCT 对于预防动脉粥样硬化是至关重要的。引人注目的是，ABCA1 的缺失阻止了动脉粥样硬化病变在 SR-BI KO 小鼠中的发展。ABCA1 的缺失还降低了 SR-BI KO 小鼠的血浆中单核细胞趋化因子 MCP-1 的水平和粘附分子 ICAM-1 在动脉壁上的表达水平，这很可能导致了单核细胞浸润到病变中的减少。不断积累的证据显示不仅引发动脉粥样硬化的非高密度脂蛋白，如 LDL 和极低密度脂蛋白（VLDL），而且功能失调的高密度脂蛋白也可诱导动脉壁 MCP-1 的分泌和上调动脉内皮细胞上 ICAM-1 的表达[1]。因此，dKO 小鼠动脉粥样硬化病变的减少很可能是由于 ABCA1 的缺失降低了血浆中致动脉粥

样硬化的脂蛋白以及功能失调的高密度脂蛋白水平，从而减少单核细胞浸润到动脉壁。

11.4.2 细胞胆固醇流出机制对预防动脉粥样硬化的重要性

巨噬细胞源性泡沫细胞的形成是动脉粥样硬化的标志。这些巨噬细胞源性泡沫细胞是动脉粥样硬化病变中的重要组成部分。作为脂剂和炎症介质，他们在疾病的进展中发挥了关键作用。促进胆固醇从巨噬细胞的流出作为RCT的第一步，对预防泡沫细胞形成是很重要的。巨噬细胞源性泡沫细胞可以通过多种途径将多余的胆固醇流出。**第四章**对这些流出途径在动脉粥样硬化病变中泡沫细胞胆固醇的净流出中的相对作用的进行了综述。

ABCA1和SR-BI除了在高密度脂蛋白胆固醇代谢中的重要作用，他们还分别调节细胞胆固醇流出至贫脂的载脂蛋白AI（apoAI）和成熟的高密度脂蛋白。为了研究ABCA1和SR-BI在骨髓细胞上的共同缺失对泡沫细胞形成和动脉粥样硬化病变发展的影响，在**第五章**，ABCA1/SR-BI dKO小鼠的骨髓被移植入低密度脂蛋白受体（LDLr）KO的小鼠。在喂食含胆固醇的西式饮食（WTD）后，相对于其他对照小鼠，移植dKO骨髓的小鼠表现出了低下的血浆胆固醇水平。这可能是由于他们食物摄入量，肠道吸收，以及肝脏VLDL产出的减少。然而，在移植dKO骨髓的小鼠的腹腔和脾脏中呈现了巨大的泡沫细胞。更重要的是，ABCA1和SR–BI在骨髓细胞上的共同缺失还增加了促炎性细胞因子KC（小鼠的白细胞间素IL-8）和白细胞间素IL-12在血清中的水平以及加速了动脉粥样硬化的发展。因此，在高脂质膳食条件下，ABCA1和SR-BI在骨髓衍生的细胞上的表达对于预防巨噬细胞泡沫细胞形成和动脉粥样硬化是至关重要的。其他胆固醇流出的机制是无法弥补这两种胆固醇转运机制的共同缺失。

Brunham 等最近发现 ABCA1 在巨噬细胞上的特异缺失并不影响 LDLr KO 小鼠动脉粥样硬化的发展[2]。他们认为这是由于删除巨噬细胞上 LDLr 下调甾醇诱导的巨噬细胞 ABCA1 的表达和巨噬细胞胆固醇流出[3]的后果。为了验证这一假设，在**第六章**，LDLr/ABCA1 dKO 小鼠和其对照小鼠的骨髓被移植到 LDLr KO 小鼠内。LDLr 缺失并不影响从骨髓来源的巨噬细胞在体外胆固醇流出或体内的巨噬细胞源性泡沫细胞的形成。值得注意的是， 无论 LDLr 的存在与否, ABCA1 在骨髓细胞上的缺乏都促进了泡沫细胞的形成和动脉粥样硬化的增加。这明确表示骨髓细胞上 ABCA1 对动脉粥样硬化的保护作用是不需要 LDLr 的存在。有趣的是，LDLr/ABCA1 dKO 移植动物与 ABCA1 KO 移植动物相比显示了减少的血液淋巴细胞，降低了 T 细胞在动脉外膜的浸润，和较小的动脉粥样硬化病灶的形成。这些结果表明除了在胆固醇流出中的作用，骨髓细胞上 ABCA1 很可能也通过抑制 T 细胞的增殖和转移来防止动脉粥样硬化。

ABCA1促进巨噬细胞胆固醇流出到贫脂的载脂蛋白，其中也包括载脂蛋白AI[4]。本论文**第七章**的研究目的是评估血液中载脂蛋白AI在巨噬细胞ABCA1促进胆固醇逆向转运和骨髓细胞ABCA1预防动脉粥样硬化中的重要性。LDLr/ApoAI dKO小鼠与LDLR KO小鼠相比，其去脂蛋白的血清（LPDS）和高密度脂蛋白（HDL）显示了减弱的在体外诱导胆固醇从野生型巨噬细胞中流出的能力。然而，巨噬细胞ABCA1的缺失并没有进一步降低胆固醇流出到dKO小鼠的LPDS和HDL。而且，在dKO小鼠体内， 巨噬细胞上ABCA1的缺失也没有减少放射性标记的巨噬细胞内的胆固醇的流出和排泄到粪便中。因此，载脂蛋白AI和巨噬细胞ABCA1被认定为在巨噬

细胞的胆固醇逆向转运中是合作伙伴。接下来，ABCA1存在与缺失的骨髓被移植到dKO体内。在喂食西式食物后，尽管血清中非高密度脂蛋白胆固醇的水平更低，骨髓细胞上ABCA1的缺乏在dKO小鼠体内加速了动脉粥样硬化的发展。这清楚地表明，在缺乏循环载脂蛋白AI的情况下，骨髓细胞上ABCA1对动脉粥样硬化仍有保护作用。因此，除了促进巨噬细胞胆固醇逆向转运，骨髓细胞上ABCA1也可通过其他机制预防动脉粥样硬化。这些保护机制在循环载脂蛋白AI缺席的条件下尤其重要。有趣的是，在dKO小鼠体内，骨髓衍生的细胞上ABCA1的缺乏增加了血液中单核细胞和中性粒细胞的数量，提高了单核细胞和中性粒细胞的重要趋化因子MCP-1和KC的血浆水平，还增强中性粒细胞在动脉粥样硬化病变中的聚集。这些结果表明，除了促进细胞胆固醇流出，骨髓衍生的细胞上的ABCA1还可以通过的抗炎作用来预防动脉粥样硬化的发展。

11.4.3 促进逆向巨噬细胞胆固醇转运在动脉粥样硬化中的治疗前景

不同的策略，包括降低饮食中的脂含量，增加巨噬细胞 ABCA1 的表达，以及静脉滴注不含胆固醇的合成磷脂酰胆碱（PC）颗粒悬液被采用来评估是否增强巨噬细胞胆固醇转运可以减少已建立的动脉粥样硬化病变。首先，在**第八章**，西式食物喂养 LDLr KO 小鼠 5 和 9 周用于诱导在主动脉根部形成早期和晚期的动脉粥样硬化病变。此后，动物给与低脂的饮食用于观察其对降低血浆胆固醇水平和病灶动态重塑的影响。降低膳食脂质减少了在已形成的早期和晚期病变中巨噬细胞的含量。但是，病变的依然增大，这主要是由于胶原蛋白的不断沉积的和坏死核的不断扩大。更重要的是，早期病变变得更加炎症化，而晚期病变的炎症随着血浆胆固醇水平的降低而减弱。因此，已形成的病变的严重程度影响了降低血浆胆固醇对病灶的动态重塑，说明建立阶段，具体的治疗方案在治疗动脉粥样硬化中的重要性。

在**第九章**，ABCA1 过度表达骨髓细胞被移植入已有病变的 LDLr KO 小鼠体内用于观察增强 ABCA1 介导的巨噬细胞胆固醇流出在治疗动脉粥样硬化中的前景。ABCA1 的过度表达抑制巨噬细胞浸润到早期而不是晚期的病变里。后者很可能是由于晚期的病变存在纤维帽阻碍巨噬细胞渗透的结果。因此，已形成的病变的严重程度是可能影响增强骨髓细胞上 ABCA1 的表达的治疗疗效。

人载脂蛋白 AI 和卵磷脂（PC）组成的重组高密度脂蛋白（rHDL）输液可以阻止动脉粥样硬化的发展。这很可能是通过诱导巨噬细胞源的泡沫细胞胆固醇流出和抑制炎症来起作用的[5,6]。 PC 颗粒与 rHDL 颗粒一样，可以接受通过 SR-BI，ABCG1，和水扩散转运出的胆固醇。输注大量的 PC 颗粒悬液因此很可能积极影响到细胞内胆固醇流出，从而改善动脉粥样硬化病变。因此，**第十章**评估了 PC 颗粒在体外对巨噬细胞胆固醇流出和 LDLR KO 小鼠动脉粥样硬化病变的进展的影响。首先，正如所料，在高浓度（> 84 g/mL）PC 诱导巨噬细胞胆固醇流出的能力等同于含有相同数量的 PC 的 rHDL。重要的是，单次高剂量的 PC 颗粒的输注可以迅速稳定在 LDLR KO 小鼠体内已成立的病变。因此，rHDL 的 PC 组分是有助于 rHDL 诱导的胆固醇流出和改善动脉粥样硬化的。

综上所述，本论文探讨了 RCT 对抑制动脉粥样硬化病变形成中的重要性。肝脏和巨噬细胞上 ABCA1 和 SR-BI 都可以称为为医药干预的靶点。他们增加高密度脂蛋白的合成和巨噬细胞胆固醇的流出以促进胆固醇运送到肝脏，从而防止动脉粥样硬化。对增加巨噬细胞胆固醇流出在治疗动脉粥样硬化病变中的评估将有望刺激 RCT 成为新的疗法。动脉粥样硬化病变的严重性对降脂治疗和单核细胞浸润程度的

影响将帮助动脉粥样硬化阶段特异性疗法的建立。此外，有关 ABCA1 和高密度脂蛋白在白细胞的胆固醇平衡和增生中的新作用也将为动脉粥样硬化发展中高胆固醇血症和全身炎症之间提供新的联系。

11.5 References

1. Ansell BJ. The two faces of the 'good' cholesterol. *Cleve Clin J Med.* 2007; 74(10):697-700, 703-5.
2. Brunham LR, Singaraja RR, Duong M, Timmins JM, Fievet C, Bissada N, Kang MH, Samra A, Fruchart JC, McManus B, Staels B, Parks JS, Hayden MR. Tissue-specific roles of ABCA1 influence susceptibility to atherosclerosis. *Arterioscler Thromb Vasc Biol.* 2009; 29(4):548-54.
3. Zhou X, He W, Huang Z, Gotto AM Jr, Hajjar DP, Han J. Genetic deletion of low density lipoprotein receptor impairs sterol-induced mouse macrophage ABCA1 expression. A new SREBP1-dependent mechanism. *J Biol Chem.* 2008; 283(4):2129-38.
4. Remaley AT, Stonik JA, Demosky SJ, Neufeld EB, Bocharov AV, Vishnyakova TG, Eggerman TL, Patterson AP, Duverger NJ, Santamarina-Fojo S, Brewer HB Jr. Apolipoprotein specificity for lipid efflux by the human ABCAI transporter. *Biochem Biophys Res Commun.* 2001; 280(3):818-23.
5. Oram JF, Lawn RM, Garvin MR, Wade DP. ABCA1 is the cAMP-inducible apolipoprotein receptor that mediates cholesterol secretion from macrophages. *J Biol Chem*. 2000; 275(44):34508-11.
6. Patel S, Di Bartolo BA, Nakhla S, Heather AK, Mitchell TW, Jessup W, Celermajer DS, Barter PJ, Rye KA. Anti-inflammatory effects of apolipoprotein A-I in the rabbit. *Atherosclerosis.* 2010; 212(2):392-7.
7. Kozarsky KF, Donahee MH, Glick JM, Krieger M, Rader DJ. Gene transfer and hepatic overexpression of the HDL receptor SR-BI reduces atherosclerosis in the cholesterol-fed LDL receptor-deficient mouse. *Arterioscler Thromb Vasc Biol.* 2000; 20(3):721-7.
8. Joyce CW, Wagner EM, Basso F, Amar MJ, Freeman LA, Shamburek RD, Knapper CL, Syed J, Wu J, Vaisman BL, Fruchart-Najib J, Billings EM, Paigen B, Remaley AT, Santamarina-Fojo S, Brewer HB Jr. ABCA1 overexpression in the liver of LDLr-KO mice leads to accumulation of pro-atherogenic lipoproteins and enhanced atherosclerosis. *J Biol Chem.* 2006; 281(44):33053-65.
9. Joyce CW, Amar MJ, Lambert G, Vaisman BL, Paigen B, Najib-Fruchart J, Hoyt RF Jr, Neufeld ED, Remaley AT, Fredrickson DS, Brewer HB Jr, Santamarina-Fojo S. The ATP binding cassette transporter A1 (ABCA1) modulates the development of aortic atherosclerosis in C57BL/6 and apoE-knockout mice. *Proc Natl Acad Sci U S A.* 2002; 99(1):407-12.
10. Feng Y, Lievens J, Jacobs F, Hoekstra M, Van Craeyveld E, Gordts SC, Snoeys J, De Geest B. atocyte-specific ABCA1 transfer increases HDL cholesterol but impairs HDL function and accelerates atherosclerosis. *Cardiovasc Res.* 2010; 88(2):376-85.
11. Zhao Y, Van Berkel TJ, Van Eck M. Relative roles of various efflux pathways in net cholesterol efflux from macrophage foam cells in atherosclerotic lesions. *Curr Opin Lipidol.* 2010; 21(5):441-53.
12. Yvan-Charvet L, Ranalletta M, Wang N, Han S, Terasaka N, Li R, Welch C, Tall AR. Combined deficiency of ABCA1 and ABCG1 promotes foam cell accumulation and accelerates atherosclerosis in mice. *J Clin Invest.* 2007; 117(12):3900-8.
13. Zhao Y, Pennings M, Hildebrand RB, Ye D, Calpe-Berdiel L, Out R, Kjerrulf M, Hurt-Camejo E, Groen AK, Hoekstra M, Jessup W, Chimini G, Van Berkel TJ, Van Eck M. Enhanced foam cell formation, atherosclerotic lesion development, and inflammation by combined deletion of ABCA1 and SR-BI in Bone marrow-derived cells in LDL receptor knockout mice on western-type diet. *Circ Res.* 2010; 107(12):e20-31.
14. Jaye M. LXR agonists for the treatment of atherosclerosis. *Curr Opin Investig Drugs.* 2003; 4(9):1053-8.
15. Feig JE, Pineda-Torra I, Sanson M, Bradley MN, Vengrenyuk Y, Bogunovic D, Gautier EL, Rubinstein D, Hong C, Liu J, Wu C, van Rooijen N, Bhardwaj N, Garabedian M, Tontonoz P, Fisher EA. LXR promotes the maximal egress of monocyte-derived cells from mouse aortic plaques during atherosclerosis regression. *J Clin Invest.* 2010; 120(12):4415-24.
16. Tontonoz P, Mangelsdorf DJ. Liver X receptor signaling pathways in cardiovascular disease. *Mol Endocrinol.* 2003; 17(6):985-93.
17. Trogan E, Feig JE, Dogan S, Rothblat GH, Angeli V, Tacke F, Randolph GJ, Fisher EA. Gene expression changes in foam cells and the role of chemokine receptor CCR7 during atherosclerosis regression in ApoE-deficient mice. *Proc Natl Acad Sci U S A.* 2006; 103(10):3781-6.

18. Feig JE, Rong JX, Shamir R, Sanson M, Vengrenyuk Y, Liu J, Rayner K, Moore K, Garabedian M, Fisher EA. HDL promotes rapid atherosclerosis regression in mice and alters inflammatory properties of plaque monocyte-derived cells. *Proc Natl Acad Sci U S A*. 2011; 108(17):7166-71.
19. Barter P. CETP and atherosclerosis. *Arterioscler Thromb Vasc Biol.* 2000; 20(9):2029-31.
20. Matsuura F, Wang N, Chen W, Jiang XC, Tall AR. HDL from CETP-deficient subjects shows enhanced ability to promote cholesterol efflux from macrophages in an apoE- and ABCG1-dependent pathway. *J Clin Invest.* 2006; 116(5):1435-42.
21. Barter PJ, Caulfield M, Eriksson M, Grundy SM, Kastelein JJ, Komajda M, Lopez-Sendon J, Mosca L, Tardif JC, Waters DD, Shear CL, Revkin JH, Buhr KA, Fisher MR, Tall AR, Brewer B; ILLUMINATE Investigators. Effects of torcetrapib in patients at high risk for coronary events. *N Engl J Med.* 2007; 357(21):2109-22. Epub 2007 Nov 5.
22. Cannon CP, Shah S, Dansky HM, Davidson M, Brinton EA, Gotto AM, Stepanavage M, Liu SX, Gibbons P, Ashraf TB, Zafarino J, Mitchel Y, Barter P; Determining the Efficacy and Tolerability Investigators. Safety of anacetrapib in patients with or at high risk for coronary heart disease. *N Engl J Med.* 2010; 363(25):2406-15.
23. Kastelein JJ, Duivenvoorden R, Deanfield J, de Groot E, Jukema JW, Kaski JC, Münzel T, Taddei S, Lehnert V, Burgess T, Kallend D, Lüscher TF. Rationale and design of dal-VESSEL: a study to assess the safety and efficacy of dalcetrapib on endothelial function using brachial artery flow-mediated vasodilatation. *Curr Med Res Opin.* 2011; 27(1):141-50.
24. Nissen SE, Tsunoda T, Tuzcu EM, Schoenhagen P, Cooper CJ, Yasin M, Eaton GM, Lauer MA, Sheldon WS, Grines CL, Halpern S, Crowe T, Blankenship JC, Kerensky R. Effect of recombinant ApoA-I Milano on coronary atherosclerosis in patients with acute coronary syndromes: a randomized controlled trial. *JAMA.* 2003; 290(17):2292-300.
25. Tardif JC, Grégoire J, L'Allier PL, Ibrahim R, Lespérance J, Heinonen TM, Kouz S, Berry C, Basser R, Lavoie MA, Guertin MC, Rodés-Cabau J; Effect of rHDL on Atherosclerosis-Safety and Efficacy (ERASE) Investigators. Effects of reconstituted high-density lipoprotein infusions on coronary atherosclerosis: a randomized controlled trial. *JAMA.* 2007; 297(15):1675-82.
26. Shaw JA, Bobik A, Murphy A, Kanellakis P, Blombery P, Mukhamedova N, Woollard K, Lyon S, Sviridov D, Dart AM. Infusion of reconstituted high-density lipoprotein leads to acute changes in human atherosclerotic plaque. *Circ Res.* 2008; 103(10):1084-91.
27. Cuchel M, Lund-Katz S, de la Llera-Moya M, Millar JS, Chang D, Fuki I, Rothblat GH, Phillips MC, Rader DJ. Pathways by which reconstituted high-density lipoprotein mobilizes free cholesterol from whole body and from macrophages. *Arterioscler Thromb Vasc Biol.* 2010; 30(3):526-32.
28. Potteaux S, Gautier EL, Hutchison SB, van Rooijen N, Rader DJ, Thomas MJ, Sorci-Thomas MG, Randolph GJ. Suppressed monocyte recruitment drives macrophage removal from atherosclerotic plaques of Apoe-/- mice during disease regression. *J Clin Invest.* 2011; 121(5):2025-36.
29. Undurti A, Huang Y, Lupica JA, Smith JD, DiDonato JA, Hazen SL. Modification of high density lipoprotein by myeloperoxidase generates a pro-inflammatory particle. *J Biol Chem.* 2009; 284(45):30825-35.
30. Movva R, Rader DJ. Laboratory assessment of HDL heterogeneity and function. *Clin Chem.* 2008; 54(5):788-800.
31. Wilhelm AJ, Zabalawi M, Grayson JM, Weant AE, Major AS, Owen J, Bharadwaj M, Walzem R, Chan L, Oka K, Thomas MJ, Sorci-Thomas MG. Apolipoprotein A-I and its role in lymphocyte cholesterol homeostasis and autoimmunity. *Arterioscler Thromb Vasc Biol.* 2009; 29(6):843-9.
32. Kruit JK, Brunham LR, Verchere CB, Hayden MR. HDL and LDL cholesterol significantly influence beta-cell function in type 2 diabetes mellitus. *Curr Opin Lipidol.* 2010; 21(3):178-85.

Curriculum vitae

Name:	Ying Zhao
Date of Birth:	August 25, 1978
Place of Birth:	Nanjing, Jiangsu Province, **P.R. China**
Sep 1993 - Jul 1996	Second Affiliated High School of Nanjing Normal University, Yizheng, **P.R. China**
Sep 1996 - Jul 2001	**B.Sc.** Dept. of Pharmacology for Chinese Materia Medica, China Pharmaceutical University, **P.R. China** (Graduation: July 1st, 2001)
Sep 2001 - Jun 2004	**M.Sc.**, Dept. of Biological Science & Technology, Nanjing University, **P.R. China** (Graduation: Jun 15th, 2004) **Supervisor: Prof. Dr. Qiang Xu**
Sep 2004 - May 2005	**Ph.D** student, Dept. of Biology and Chemistry, City University of Hong Kong, **P.R. China** **Supervisor: Prof. Dr. Wang-Fun Fong**
Jun 2005 - Jun 2006	**Mphil student**, Dept. of Immunohematology and Blood Transfusion, Leiden University Medical Center, **The Netherlands** **Supervisor: Prof. Dr. Bart Roep** **Co-Supervisor: Prof. Dr. Rene R.R.P. de Vires**
Aug 2006 - Nov 2010	**Ph.D** student at Division of Biopharmaceutics, LACDR, Leiden University, **The Netherlands** (Promotion: Nov 1st, 2011) **Supervisor: Dr. Miranda van Eck** **Promoter: Prof. Dr. Theo J.C. van Berkel**
Dec 2010 -	**Postdoctoral fellow** at Division of Biopharmaceutics, LACDR, Leiden University, **The Netherlands**

Award and Honors

1996-1999	**Undergraduate Scholarships (7 times)**
2001	**Outstanding Thesis of Bachelor's Degree** of China Pharmaceutical University
2004	**BASF Scholarship** of Nanjing University
2004	**UGC Scholarship** provided by Hong Kong Government
2005-2006	**Leiden University Scholarship**
2006	**Best poster presentation** at the LACDR Spring Symposium

Publications

Accepted manuscripts

Lammers B, **Zhao Y**, Hoekstra M, Hildebrand RB, Ye D, Meurs I, Van Berkel TJC, Van Eck M. Augmented atherogensis in LDL receptor deficiënt mice lacking both macrophage ABCA1 and apoE. ***PLoS One.*** 2011; *in press*

Zhao Y, Pennings M, Vrins CLJ, Calpe-Berdiel L, Hoekstra M, Kruijt JK, Ottenhoff R, Hildebrand RB, Van der Sluis R, Jessup W, Le Goff W, Chapman J, Huby T, Groen AK, Van Berkel TJC, Van Eck M. Hypocholestrolemia, foam cell formation, but no atherosclerosis in mice lack ABC-transporter A1 and scavenger receptor class B type I. ***Atherosclerosis***. 2011; 218: 314-322 (**accompany by an editorial comment**).

Foks AC, Frodermann V, Ter Borg M, Habets KL, Bot I, **Zhao Y**, van Eck M, van Berkel TJ, Kuiper J, van Puijvelde GH. Differential effects of regulatory T cells on the initiation and regression of atherosclerosis. ***Atherosclerosis.*** 2011; 218: 53-60.

Zhao Y, Ye D, Wang J, Calpe-Berdiel L, Azzis SB, Van Berkel TJ, Van Eck M. Stage-Specific Remodeling of Atherosclerotic Lesions on Cholesterol Lowering in LDL Receptor Knockout Mice. ***Am J Pathol.*** 2011; 179(3):1522-1532.

Ye D, **Zhao Y**, Hildebrand RB, Singaraja RR, Hayden MR, Van Berkel TJ, Van Eck M. The dynamics of macrophage infiltration into the arterial wall during atherosclerotic lesion development in low-density lipoprotein receptor knockout mice. ***Am J Pathol.*** 2011; 178 (1): 413-22.

Ye D, Lammers B, **Zhao Y**, Meurs I, Van Berkel TJ, Van Eck M. ATP-binding cassette transporters A1 and G1, HDL metabolism, cholesterol efflux, and inflammation: important targets for the treatment of atherosclerosis. ***Curr Drug Targets.*** 2011; 12 (5): 647-60.

Zhao Y, Pennings M, Hildebrand RB, Ye D, Calpe-Berdiel L, Out R, Kjerrulf M, Hurt-Camejo E, Groen AK, Hoekstra M, Jessup W, Chimini G, Van Berkel TJ, Van Eck M. Enhanced foam cell formation, atherosclerotic lesion development, and inflammation by combined deletion of ABCA1 and SR-BI in Bone marrow-derived cells in LDL receptor knockout mice on western-type diet. ***Circ Res.*** 2010; 107 (12): e20-31 (**Cover Story**).

Zhao Y, Van Berkel TJ, Van Eck M. Relative roles of various efflux pathways in net cholesterol efflux from macrophage foam cells in atherosclerotic lesions. ***Curr Opin Lipidol.*** 2010; 21 (5): 441-53.

Hoekstra M, Korporaal SJ, Li Z, **Zhao Y**, Van Eck M, Van Berkel TJ. Plasma lipoproteins are required for both basal and stress-induced adrenal glucocorticoid synthesis and protection against endotoxemia in mice. ***Am J Physiol Endocrinol Metab.*** 2010; 299 (6): E1038-43.

Hildebrand RB, Lammers B, Meurs I, Korporaal SJ, De Haan W, **Zhao Y**, Kruijt JK, Praticò D, Schimmel AW, Holleboom AG, Hoekstra M, Kuivenhoven JA, Van Berkel TJ, Rensen PC, Van Eck M. Restoration of high-density lipoprotein levels by cholesteryl ester transfer protein expression in scavenger receptor class B type I (SR-BI) knockout mice

does not normalize pathologies associated with SR-BI deficiency. ***Arterioscler Thromb Vasc Biol.*** 2010; 30 (7): 1439-45.

Ye D, Meurs I, Ohigashi M, Calpe-Berdiel L, Habets KL, **Zhao Y**, Kubo Y, Yamaguchi A, Van Berkel TJ, Nishi T, Van Eck M. Macrophage ABCA5 deficiency influences cellular cholesterol efflux and increases susceptibility to atherosclerosis in female LDLr knockout mice. ***Biochem Biophys Res Commun.*** 2010; 395 (3): 387-94.

Hoekstra M, Ye D, Hildebrand RB, **Zhao Y**, Lammers B, Stitzinger M, Kuiper J, Van Berkel TJ, Van Eck M. Scavenger receptor class B type I-mediated uptake of serum cholesterol is essential for optimal adrenal glucocorticoid production. ***J Lipid Res.*** 2009; 50 (6): 1039-46.

Out R, Jessup W, Le Goff W, Hoekstra M, Gelissen IC, **Zhao Y**, Kritharides L, Chimini G, Kuiper J, Chapman MJ, Huby T, Van Berkel TJ, Van Eck M. Coexistence of foam cells and hypocholesterolemia in mice lacking the ABC transporters A1 and G1. ***Circ Res.*** 2008; 102 (1): 113-20.

Xu L, **Zhao Y**, Qin Y, Xu Q. A novel model of acute liver injury in mice induced by T cell-mediated immune response to lactosylated bovine serum albumin. ***Clin Exp Immunol.*** 2006; 144 (1): 125-33.

Zhao Y, Liu J, Wang J, Wang L, Yin H, Tan R, Xu Q. Fumigaclavine C improves concanavalin A-induced liver injury in mice mainly via inhibiting TNF-alpha production and lymphocyte adhesion to extracellular matrices. ***J Pharm Pharmacol.*** 2004; 56 (6): 775-82.

Wu X, Zeng H, Zhang X, **Zhao Y**, Sha H, Ge X, Zhang M, Gao X, Xu Q. Phosphatase of regenerating liver-3 promotes motility and metastasis of mouse melanoma cells. ***Am J Pathol.*** 2004; 164 (6): 2039-54.

Wang J, **Zhao Y**, Xu Q. Astilbin prevents concanavalin A-induced liver injury by reducing TNF-alpha production and T lymphocytes adhesion. ***J Pharm Pharmacol.*** 2004; 56 (4): 495-502.

Submitted manuscripts

Zhao Y, Wang J, Out R, Ye D, Van Berkel TJ, Van Eck M. ABCA1 deficiency induces macrophage foam cell formation and leukocytosis but inhibits early atheorsclerotic lesion development in SR-BI knockout mice.

Zhao Y, Calpe-Berdiel L, Wang J, Lammers B, Foks A, Van der Sluis R, Hildebrand RB, Van Berkel TJ, Van Eck M. Leukocyte ABCA1 and LDL receptor play independent roles in atherosclerosis: the potential contribution of T cells.

Zhao Y*, Calpe-Berdiel L*, Julve J, Escolà-Gil JC, Foks A, Van der Sluis RJ, Kuiper J, Blanco-Vaca F, Van Berkel TJC, Kuivenhoven JA, Van Eck M. Leukocyte ABC-transporter A1 is atheroprotective in absence of apolipoprotien AI (* These two authors contributed equally)

Zhao Y, Hildebrand RB, Van Berkel TJ, Van Eck M. High-Dose phosphatidylcholine particle mobilizes free cholesterol and rapidly stabilizes established atherosclerotic lesions. Calpe-Berdiel L, **Zhao Y**, de Graauw M, Ye D, Van Santbrink PJ, Mommaas AM, Foks A, Bot M, Meurs I, Kuiper J, Mack JT, Van Eck M, Tew KD, Van Berkel TJC. Macrophage ABCA2 deletion modulates intracellular cholesterol deposition, affects macrophage apoptosis, and decreases early atherosclerosis in LDL receptor knockout mice.

Meurs I, Lammers B, **Zhao Y**, Out R, Hildebrand RB, Hoekstra M, Van Berkel TJC, Van Eck M. The effect of ABCG1 deficiency on atherosclerotic lesion development in LDL receptor knockout mice depends on the stage of atherosclerosis.

Habets KLL, Van Puijvelde GHM, Frodermann V, **Zhao Y**, de Vos P, Van Eck M, Van Berkel TJC, Kuiper J. Adoptive transfer of immature dentritic cells prevents progression of established atherosclerosis in LDL receptor knockout mice.

Meurs I, Calpe-Berdiel L, Habets KLL, **Zhao Y**, Korporaal SJA, Josselin E, Hildebrand RB, Ye D, Out R, Kuiper J, Van Berkel TJ, Chimini G, Van Eck M. Effects of deletion of macrophage ABCA7 on lipid metabolism and the development of atherosclerosis in the presence and absence of ABCA1.

Published abstract

Hildebrand RB, Lammers B, **Zhao Y**, Jauhiainen M, Van Berkel TJC, **Van Eck M**. Deletion of PLTP in SR-BI knockout mice shifts lipids from HDL to VLDL/LDL and reduces atherosclerosis. ***Circulation.*** 2010; 122: A15213.

Van Berkel TJC, **Zhao Y**, Hildebrand RB, Out R, Hoekstra M, Meurs I, Van Eck M. Macrophage cholesterol homeostasis and atherosclerosis. ***Atherosclerosis Supp.*** 2009; 10(2): e140

Zhao Y, Out R, Ye D, Van Berkel TJC, **Van Eck M**. ABCA1 deficiency diminishes dysfunctional HDL and inhibits early atherosclerotic lesion development in SR-BI knockout mice. ***Circulation.*** 2008; 118: S_411.

Out R, Jessup W, Le Goff W, Hoekstra M, Gelissen IC, **Zhao Y**, Kritharides L, Chimini G, Kuiper J, Chapman MJ, Huby T, Van Berkel TJ, Van Eck M. The ABCs in foam cell formation. ***Arterioscler Thromb Vasc Biol.*** 2008; 28(6): E131

Van Eck M, Pennings M, **Zhao Y**, Hildebrand RB, Chimini G, Van Berkel TJC. Enhanced foam cell formation, inflammation, and atherosclerosis in LDL receptor knockout mice with a combined deletion of macrophage SR-BI and ABCA1. ***Circulation.*** 2007; 116: II-298.